

Summer 8-1-2013

# Shoreline Dynamics and Environmental Change Under the Modern Marine Transgression: St. Catherines Island, Georgia

Brian K. Meyer  
*Georgia State University*

Follow this and additional works at: [https://scholarworks.gsu.edu/geosciences\\_diss](https://scholarworks.gsu.edu/geosciences_diss)

---

## Recommended Citation

Meyer, Brian K., "Shoreline Dynamics and Environmental Change Under the Modern Marine Transgression: St. Catherines Island, Georgia." Dissertation, Georgia State University, 2013.  
[https://scholarworks.gsu.edu/geosciences\\_diss/5](https://scholarworks.gsu.edu/geosciences_diss/5)

This Dissertation is brought to you for free and open access by the Department of Geosciences at ScholarWorks @ Georgia State University. It has been accepted for inclusion in Geosciences Dissertations by an authorized administrator of ScholarWorks @ Georgia State University. For more information, please contact [scholarworks@gsu.edu](mailto:scholarworks@gsu.edu).

SHORELINE DYNAMICS AND ENVIRONMENTAL CHANGE UNDER THE MODERN  
MARINE TRANSGRESSION: ST. CATHERINES ISLAND, GEORGIA

by

BRIAN K. MEYER

Under the Direction of Daniel M. Deocampo

ABSTRACT

The current study has evaluated shoreline dynamics and environmental change at St. Catherines Island, Georgia, with attention to the two major controls of barrier island formation and modification processes. These major controls include the increase in accommodation space, or the rate of sea level rise for the Georgia Bight which has remained constant in 20<sup>th</sup> and 21<sup>st</sup> century tide gauge data and dynamically changing rates of sediment supply based on anthropogenic modifications to land cover (Trimble, 1974) that are reflected in sediment transport (McCarney-Castle et al., 2010). Vibracoring and radiocarbon data provided valuable insights into the stratigraphy and development of St. Catherines Island. A stratigraphic model has been developed for the sediments associated with the Late Holocene accretional terrains where multiple small scale fluctuations in sea level have resulted in the formation of a sedimentary veneer punctuated with transgressive surfaces and regressive sequences. A working model for an interpolated Late Holocene sea level curve has been constructed using direct evidence from vibracore data as constraining points and indirect evidence from other regional sea level studies to provide additional structure. The relationship between the timing of the regressions versus periods of beach ridge formation and implications from the current shoreline dynamics study regarding the role of sediment supply complement each other. The



ages of beach ridge formation strongly correlate to periods that are associated with regressions in sea level based on the sedimentary record and an evaluation of Late Holocene sea level conditions. The evaluation of anthropogenic modifications to the rate of sediment supply performed under the current study indicates that in spite of significant changes in sediment flux rates of +300% (pre-dam era) and -20% (post-dam era), shoreline retreat was continuous during the study period with an acceleration noted in the rates of shoreline retreat associated with spit and berm landforms during the post-dam or modern era. The two associations indicate strongly that the rate of sediment supply plays a secondary role to the major control of the rate of sea level rise in the formation and modification processes at St. Catherines Island.

**INDEX WORDS:** Shoreline dynamics, Barrier island, Late Holocene, Stratigraphy

SHORELINE DYNAMICS AND ENVIRONMENTAL CHANGE UNDER THE MODERN  
MARINE TRANSGRESSION: ST. CATHERINES ISLAND, GEORGIA

by

BRIAN K. MEYER

A Dissertation Submitted in Partial Fulfillment of the Requirements for the Degree of

Doctor of Philosophy

in the College of Arts and Sciences

Georgia State University

2013



Copyright by  
Brian Kevin Meyer  
2013

SHORELINE DYNAMICS AND ENVIRONMENTAL CHANGE UNDER THE MODERN  
MARINE TRANSGRESSION: ST. CATHERINES ISLAND, GEORGIA

by

BRIAN K. MEYER

Committee Chair: Daniel M. Deocampo

Committee: Gale A. Bishop

Dajun Dai

Lawrence M. Kiage

Robert Kelly Vance

Electronic Version Approved:

Office of Graduate Studies

College of Arts and Sciences

Georgia State University

August 2013

## ACKNOWLEDGEMENTS

I would like to acknowledge and extend my gratitude to the entire Department of Geosciences at Georgia State University for the opportunities and support that everyone has provided. Thank you to all my committee members for balancing their multiple commitments and helping make the research sound and improving the quality of the dissertation: Drs. Gale Bishop, Dajun Dai, Daniel Deocampo, Larry Kiage, and Kelly Vance.

I would like to directly thank the St. Catherines Island Scientific Research Committee for their financial and logistical support and the opportunity to perform research on one of the most unique places on our planet. Thanks are especially extended to Royce Hayes for his support as superintendent of the island and incredible knowledge of the setting. I'm extremely grateful for the support during the field work portion of the project, especially the staff of St. Catherines Island (Richard Bew, Spyder Crews, Alan Dean, Mike Halderson, Capt. Lee Thompson and Jeff Woods) and my fellow vibracoring enthusiast Kelly Vance who was there for practically every core collected during the project under incredible weather extremes. I would be remiss to not also recognize Andreas Shoredits for his vibracoring support and being a great sounding board, and Sam Kennedy for his vibracoring support, fellowship and incredible ability to repair mechanical devices with minimal tools and resources. The vibracoring team that supported me also included Brock Nelson, Mehmet Samiratedu, Fred Rich, Jim Reichard, Carolyn Smith, Brent Leggett, Semir Sarajlic, Shawn Huckins and Amber Skiles.

I'm appreciative for the collaboration that I have enjoyed with David Hurst Thomas and the entire staff from the American Museum of Natural History over the years, especially Elliot Blair, Rachel Cajigas, Ginessa Maher, Matt Napolitano, Lorrie Pendleton, Matt Sanger and Anna Semon. And I've also enjoyed the I look forward to more stimulating conversations at Bradford Hall with everyone and opportunities to collaborate in the future.

I'm thankful for Jacob and Joshua and the inspiration that they have provided since they joined this journey. But there would have never been a journey without the support and encouragement of my wife Jennifer, who is my companion in life and my favorite companion in the field. Our entire family is indebted for the opportunities offered to the citizens of our State by the University System of Georgia and I will always be grateful to all of my science teachers but especially Gale Bishop who has been a teacher, a colleague and a friend through the years. Gale took a chance on me as a field geologist allowing me to grow as a geologist in the Black Hills of South Dakota. Gale also initiated my interest in the modern depositional environments of barrier island systems via direct immersion in the *Marshes of Glynn* just a "few" short years ago. It's ironic that after a lot of travels, opportunities and professional endeavors that I came right back to where it all started, albeit this time in the *Marshes of Liberty*.

Thanks to all,

Brian K. Meyer  
Cabin 1 (Button)  
St. Catherines Island, Georgia  
June 2013

## TABLE OF CONTENTS

<b>ACKNOWLEDGEMENTS</b> .....		<b>iv</b>
<b>LIST OF TABLES</b> .....		<b>xi</b>
<b>LIST OF FIGURES</b> .....		<b>xii</b>
<b>1 INTRODUCTION</b> .....		<b>1</b>
<b>1.1 Research Objective</b> .....		<b>3</b>
<b>2 STUDY AREA PHYSICAL SETTING</b> .....		<b>6</b>
<b>3 BARRIER ISLAND SYSTEMS AND DEPOSITIONAL ENVIRONMENTS</b> .....		<b>11</b>
<b>3.1 Marsh and Tidal Creek Depositional System</b> .....		<b>11</b>
<b>3.2 Estuaries and Inlets</b> .....		<b>16</b>
<b>3.3 Beach and Nearshore Depositional Systems</b> .....		<b>19</b>
3.3.1 <i>Offshore - Bioturbated Facies</i> .....		<i>19</i>
3.3.2 <i>Transition Zone – Bioturbated and Laminated Facies</i> .....		<i>20</i>
3.3.3 <i>Shoreface (Lower Forebeach) – Burrowed and Laminated Facies</i> ...		<i>20</i>
3.3.4 <i>Foreshore (Upper Forebeach) – Laminated Facies</i> .....		<i>21</i>
3.3.5 <i>Backshore (Backbeach) – Laminated and Bioturbated Facies</i> .....		<i>21</i>
3.3.6 <i>Dunes – Eolian Laminated and Bioturbated Facies</i> .....		<i>23</i>
3.3.7 <i>Washover Fans</i> .....		<i>24</i>
<b>3.4 Barrier Island Models - Response to Rising Sea Level</b> .....		<b>30</b>
<b>3.5 Facies Successions – Walther’s Law of Facies</b> .....		<b>34</b>
<b>4 GEOLOGICAL SETTING</b> .....		<b>36</b>
<b>4.1 Regional Geological Setting</b> .....		<b>36</b>
<b>4.2 Study Area Geological Setting</b> .....		<b>42</b>



4.2.1	<i>Island Core</i> .....	45
4.2.2	<i>Northern Accretional Terrains</i> .....	46
4.2.3	<i>Southeastern Accretional Terrains</i> .....	50
<b>4.3</b>	<b>Island Development Model</b> .....	<b>51</b>
<b>5</b>	<b>RESEARCH METHODS</b> .....	<b>56</b>
<b>5.1</b>	<b>Shoreline Dynamics Methods</b> .....	<b>56</b>
5.1.1	<i>Methodology</i> .....	57
5.1.2	<i>Error/Uncertainty Analysis</i> .....	59
5.1.3	<i>Data Sources</i> .....	66
<b>5.2</b>	<b>Vibracoring Methods</b> .....	<b>67</b>
5.2.1	<i>Methodology</i> .....	69
5.2.2	<i>Data Processing</i> .....	72
<b>5.3</b>	<b>XRF Methods</b> .....	<b>73</b>
5.3.1	<i>Methodology</i> .....	73
5.3.2	<i>Data Collection</i> .....	74
5.3.3	<i>Data Processing and Analysis</i> .....	76
5.3.4	<i>Current Study Approach</i> .....	79
<b>5.4</b>	<b>Evaluation of Late Holocene Sea Level</b> .....	<b>80</b>
5.4.1	<i>Background</i> .....	81
5.4.2	<i>Methodology</i> .....	83
5.4.3	<i>Radiocarbon Data Calibration Methods</i> .....	83
<b>6</b>	<b>RESULTS</b> .....	<b>86</b>
<b>6.1</b>	<b>Shoreline Dynamics</b> .....	<b>86</b>

6.1.1	<i>Island Shoreface Dynamics</i> .....	86
6.1.2	<i>Mission Santa Catalina de Guale Landform Dynamics</i> .....	93
<b>6.2</b>	<b>Vibracoring</b> .....	<b>102</b>
6.2.1	<i>Seaside Spit Study Area</i> .....	105
6.2.2	<i>Beach Pond Study Area</i> .....	109
6.2.3	<i>Flag Pond Study Area</i> .....	112
6.2.4	<i>North Beach Study Area</i> .....	114
6.2.5	<i>St. Catherines Shell Ring - High Marsh Core</i> .....	119
6.2.6	<i>Mission Santa Catalina de Guale</i> .....	121
<b>6.3</b>	<b>XRF Results</b> .....	<b>124</b>
6.3.1	<i>Correlation Analysis</i> .....	125
6.3.2	<i>Cluster Analysis</i> .....	128
6.3.3	<i>Facies/Depositional Subenvironment Evaluation</i> .....	132
6.3.4	<i>Quality Assurance/Quality Control</i> .....	138
<b>6.4</b>	<b>Lithostratigraphic and Chemostratigraphic Results</b> .....	<b>141</b>
6.4.1	<i>Seaside Spit Study Area</i> .....	141
6.4.2	<i>Beach Pond Study Area</i> .....	143
6.4.3	<i>Flag Pond Study Area</i> .....	146
6.4.4	<i>North Beach Study Area</i> .....	151
6.4.5	<i>Mission Santa Catalina de Guale</i> .....	154
6.4.6	<i>Southeastern Accretional Terrains</i> .....	155
<b>6.5</b>	<b>Evaluation of Late Holocene Sea Level Conditions</b> .....	<b>163</b>
6.5.1	<i>Radiocarbon Data</i> .....	166

	6.5.2	<i>Calibrated Radiocarbon Data</i> .....	168
<b>7</b>		<b>DISCUSSIONS</b> .....	<b>172</b>
	7.1	<b>Chemofacies of Barrier Island Sediments</b> .....	<b>172</b>
	7.2	<b>Shoreline Dynamics and Anthropogenic Mods to Sediment Supply</b> .....	<b>174</b>
	7.3	<b>Environmental Change</b> .....	<b>188</b>
	7.4	<b>Stratigraphic Models</b> .....	<b>198</b>
	7.5	<b>Stratigraphy and Development of St. Catherines Island</b> .....	<b>199</b>
	7.5.1	<i>Southeastern Accretional Terrains</i> .....	199
	7.5.2	<i>Northern Accretional Terrains</i> .....	200
	7.5.3	<i>Northeastern Accretional Terrains</i> .....	205
	7.5.5	<i>St. Catherines Island – Holocene Developmental Mode</i> .....	207
	7.6	<b>Evaluation of Late Holocene Sea Level</b> .....	<b>215</b>
	7.6.1	<i>Late Holocene Sea Level - Radiocarbon Data</i> .....	215
	7.6.2	<i>Late Holocene Sea Level - Calibrated Radiocarbon Data</i> .....	217
	7.6.3	<i>Late Holocene Sea Level - Interpolated Sea Level Curve</i> .....	221
	7.7	<b>Limitations and Uncertainties of Data</b> .....	<b>227</b>
<b>8</b>		<b>CONCLUSIONS AND RECOMENDATIONS</b> .....	<b>231</b>
	8.1	<b>Conclusions</b> .....	<b>231</b>
	8.2	<b>Recommendations</b> .....	<b>234</b>
	8.2.1	<i>Future Scenarios - Implications to the SCISTP and AMNH Archaeology Program</i> .....	234
	8.2.2	<i>Opportunities for Research - “Coastal Change” Program</i> .....	235
		<b>REFERENCES</b> .....	<b>238</b>

**APPENDICES .....261**

**Appendix A: Shoreline Dynamics Model Results.....261**

**Appendix B: Vibracore Boring Logs .....270**

**Appendix C: XRF Results .....315**

**Appendix D: Chemostratigraphic Logs .....333**

**Appendix E: Shoreline Forecasting Results .....353**

**LIST OF TABLES**

<b>Table 1: Mineralogy of Heavy Mineral Sands, Selected Localities from Southeast Georgia and Northeast Florida.....</b>	<b>43</b>
<b>Table 2: Shoreline Uncertainty Evaluation, Shoreline Dynamics Study.....</b>	<b>64</b>
<b>Table 3: Shoreline Uncertainty Evaluation, <i>Mission Santa Catalina de Guale</i> Landform Dynamics Study.....</b>	<b>66</b>
<b>Table 4: <i>Mission Santa Catalina de Guale</i>, Landform Dynamics Results .....</b>	<b>100</b>
<b>Table 5: Vibracore Boring Information .....</b>	<b>105</b>
<b>Table 6: Chemofacies, Descriptive Statistics and Lithofacies.....</b>	<b>131</b>
<b>Table 7: Lithofacies and Chemofacies Evaluation.....</b>	<b>136</b>
<b>Table 8: Evaluation of Late Holocene Sea Level Conditions, Radiocarbon Sample Metadata and Age/Depth Relationship Data .....</b>	<b>164</b>
<b>Table 9: Mineralogy of Heavy Mineral Sands and FPXRF Results for the Most Commonly Detected Analytes.....</b>	<b>173</b>

## LIST OF FIGURES

Figure 1-1: Index map of Coastal Georgia and South Carolina .....	2
Figure 1-2: Global occurrence of barrier islands in mesotidal settings .....	5
Figure 2-1: St. Catherines Island Location Map.....	7
Figure 2-2: Topography and land cover of St. Catherines Island, GA. ....	10
Figure 3-1: Elements of the marsh and tidal creek depositional environments of St. Catherines Island, GA. ....	13
Figure 3-2: Elements of inlets and sounds associated with St. Catherines Island, GA.....	18
Figure 3-3: Elements of supratidal and intertidal beach environments associated with St. Catherines Island, GA. ....	22
Figure 3-4: Elements of eolian/dune and washover depositional environments associated with St. Catherines Island, GA. ....	25
Figure 3-5: Washover fan generalized facies stratigraphic models.....	29
Figure 3-6: Barrier islands and associated depositional environments response to sea level .....	32
Figure 3-7: Transitional stages of washover fans .....	33
Figure 3-8: Facies associated with subtidal, intertidal and supratidal depositional environments of St. Catherines Island, GA. ....	35
Figure 4-1: Development of successive shorelines on the Georgia Coast .....	37
Figure 4-2: Geology and Geomorphology of St. Catherines Island .....	44
Figure 4-3: Holocene accretional terrains of St. Catherines Island .....	47
Figure 4-4: Comparison of the Sapelo/Blackbeard Island Doublet with the hypothesized St. Catherines/Guale Island Doublet .....	52
Figure 4-5: Developmental Model for St. Catherines Island.....	54

Figure 5-1: Shoreline dynamics study process flowchart .....	68
Figure 5-2: Equipment and methods in vibracoring .....	70
Figure 5-3: Equipment and methods in XRF analysis of cores and reference samples.....	75
Figure 5-4: Vibracore and XRF data process flowchart .....	77
Figure 5-5: Application of facies and mean sea level constraining data.....	84
Figure 6-1: Shoreline dynamics results.....	89
Figure 6-2: Dynamics of McQueen Dune Field .....	91
Figure 6-3: Shoreline dynamic rates vs. landforms: Pre-Dam Era (1859-1951).....	94
Figure 6-4: Shoreline dynamic rates vs. landforms: Post-Dam Era (1968-2011) .....	95
Figure 6-5: Framework for the DSAS Model - <i>Mission Santa Catalina de Guale</i> .....	97
Figure 6-6: WLR rates (1951-2013): <i>Mission Santa Catalina de Guale</i> .....	99
Figure 6-7: Landform changes - <i>Mission Santa Catalina de Guale</i> .....	101
Figure 6-8: WLR rates by landform - <i>Mission Santa Catalina de Guale</i> .....	103
Figure 6-9: Location maps for vibracores .....	104
Figure 6-10: Vibracore locations associated with <i>Mission Santa Catalina de Guale</i> , St. Catherines Island, GA. ....	122
Figure 6-11: XRF Results - Frequency of Detections.....	126
Figure 6-12: XRF Results - Intercorrelations .....	127
Figure 6-13: Chemofacies Results - Relative elemental abundances .....	131
Figure 6-14: Chemofacies Results - Depositional Environments.....	133
Figure 6-15: XRF Results - Quality Control .....	139
Figure 6-16: Vibracore data and interpreted section - Seaside Spit Study Area .....	142
Figure 6-17: Chemostratigraphy - Seaside Spit Study Area .....	144

Figure 6-18: Vibracore data and interpreted section - Beach Pond Study Area.....	145
Figure 6-19: Chemostratigraphy - Beach Pond Study Area.....	147
Figure 6-20: Vibracore data and interpreted section - Flag Pond Study Area .....	148
Figure 6-21: Chemostratigraphy - Flag Pond Study Area.....	150
Figure 6-22: Vibracore data and interpreted section - North Beach Study Area.....	152
Figure 6-23: Vibracore data and interpreted section - <i>Mission Santa Catalina de Guale</i> .....	156
Figure 6-24: SE Accretional Terrains Interpreted Section .....	157
Figure 6-25: Cracker Tom Transect Details .....	159
Figure 6-26: Beach and Flag Pond Transect Details.....	161
Figure 6-27: Late Holocene conceptual sea level curve .....	165
Figure 6-28: Sea level envelope for St. Catherines Island in radiocarbon years .....	169
Figure 6-29: Sea level envelope for St. Catherines Island in calibrated years .....	171
Figure 7-1: Tide gauge data from Ft. Pulaski, Georgia.....	176
Figure 7-2: Timeline of modifications to the Savannah River system.....	177
Figure 7-3: Pre-dam and post-dam sediment flux rates for five major watersheds in the southeastern U.S. ....	179
Figure 7-4: Quantitative and qualitative indications of an acceleration in shoreline retreat for the spit/berm landforms associated with Seaside Spit, Middle Beach and South Beach .....	181
Figure 7-5: Comparison of shoreline retreat at St, Catherines Island, GA to barrier islands of the Georgia Bight.....	183
Figure 7-6: Barrier island schematic model .....	185
Figure 7-7: Environmental change at the Seaside Spit Study Area .....	189
Figure 7-8: Environmental change at the Seaside Spit Study Area interpreted section .....	190



Figure 7-9: Environmental change at the Beach Pond Study Area .....	192
Figure 7-10: Environmental change at the Beach Pond Study Area interpreted section.....	193
Figure 7-11: Evaluation of shoreline dynamics as an agent of environmental change on sea turtle habitat.....	195
Figure 7-12: Developmental model for the southeastern accretional terrains.....	201
Figure 7-13: Holocene cover materials – vertical accretion model.....	209
Figure 7-14: Revised Island Developmental Model .....	213
Figure 7-15: Plotted sea level envelope in radiocarbon years before present (B.P.) for St. Catherines Island, Georgia compared to previous radiocarbon sea level curves .....	216
Figure 7-16: Plotted sea level envelope in calibrated years before present (Cal B.P.) for St. Catherines Island, Georgia compared to previous calibrated sea level curves.....	218
Figure 7-17: Working model for sea level conditions (St. Catherines Island, GA) .....	226
Figure 7-18: Comparison of SCI sea level envelope and Gulf of Mexico/Global sea level data and Bond events.....	228
Figure A-1: Framework for the DSAS Shoreline Model (St. Catherines Island, GA) .....	261
Figure A-2: Index map to detailed study areas .....	262
Figure A-3: Shoreline dynamics modeling results for the north end of St. Catherines Island, GA.....	263
Figure A-4: Shoreline dynamics modeling results for the Yellow Banks Bluff area .....	264
Figure A-5: Shoreline dynamics modeling results for the south end of Seaside Spit.....	265
Figure A-6: Shoreline dynamics modeling results for the area located to the south of McQueen Inlet .....	266
Figure A-7: Shoreline dynamics modeling results for the area located near Beach Pond.....	267

Figure A-8: Shoreline dynamics modeling results for the area located near Flag Pond.....	268
Figure A-9: Shoreline dynamics modeling results for the north end of St. Catherines Island, GA.....	269
Figure E-1: Shoreline Forecasting Exercise Results North - Scenario I.....	353
Figure E-2: Shoreline Forecasting Exercise Results North - Scenario II.....	354
Figure E-3: Shoreline Forecasting Exercise Results Middle Beach - South Beach (North).....	355
Figure E-4: Shoreline Forecasting Exercise Results South Beach (Central) .....	356
Figure E-5: Shoreline Forecasting Exercise Results South Beach (South).....	357

## 1 INTRODUCTION

St. Catherines Island is one of twelve barrier islands located on the Georgia Coast, situated approximately 32 kilometers (20 miles) south of Savannah, Georgia (Figure 1-1). St. Catherines Island is a privately owned island that has been dedicated to research, education and conservation efforts with programs administered under the Edward John Noble Foundation. The island was purchased by Edward John Noble in 1943 and transferred to the foundation bearing his name in 1968. Previous land use of the island since European colonization included the production of cotton, rice and cattle. The focus of the current programs include an island archaeological research program conducted by the American Museum of Natural History (David Hurst Thomas, Director), a sea turtle conservation program (Gale A. Bishop, Director), educational programs administered by Georgia Southern University, and Sewanee: The University of the South and supporting research programs by other entities.

A major emphasis of sedimentary geology is the comparison of ancient depositional facies and modern analogues. St. Catherines Island, Georgia offers a unique study opportunity in that the major or more common mesotidal barrier island depositional environments and sub-environments exist in a natural setting with minimal modern anthropogenic modifications on a local scale. Progradation of the modern beach depositional environment and subenvironments (beach ridge, backbeach, foreshore, shoreface, etc.) is currently occurring within a limited area in the northeastern portion of the island. Aggradational features such as Holocene salt marshes and tidal creeks and associated drainages border the western, southern, and eastern portions of the island. These modern depositional environments are also reflected in the geology of the island as the sediments that compose the island are dominated by facies associated with shallow subtidal,



Figure 1-1: Index map of Coastal Georgia and South Carolina, showing the location of St. Catherines Island, Georgia. Note that St. Catherines Island is located approximately equidistant from the Savannah and Altamaha Rivers, the major tributaries and sources of sediment to the Georgia Coast.

intertidal and supratidal depositional environments. The island is comprised of three major geomorphic components consisting of an older Pleistocene Island Core, Holocene accretional terrains consisting of beach ridge and swale systems and Holocene marsh sediments. Therefore, St. Catherines Island offers a unique field setting in that the modern depositional environments and sub-environments associated with barrier island systems are situated in close proximity to the older Holocene and Pleistocene sedimentary deposits, allowing for direct comparisons between the physical, chemical and biogenic features from the recent rock record with modern analogues.

### **1.1 Research Objective**

The current study has evaluated modifications to the barrier island system under the modern marine transgression with attention on the two major controls of barrier island formation. Attempts have also been made to continue to develop an understanding of the stratigraphy of St. Catherines Island and to evaluate Late Holocene sea level conditions. The current study supplements and expands upon the geoarchaeological efforts that culminated in the “Geoarchaeology of St. Catherines Island”, published in the Anthropological Papers of the American Museum of Natural History, Number 94 (Bishop, Rollins and Thomas, 2011). Specifically, the current study addresses questions including how did sea level and landforms change during the 5,000 years of human occupation of St. Catherines Island? In addition, what is the relative role of the two major controls on barrier island formation and modification processes in the mesotidal setting of the Georgia Bight and what are the implications to barrier systems in similar settings? To facilitate an understanding of the initial question, a shoreline dynamics model has been created to depict shoreline and landform changes associated with the

modern transgression where modern sea level dynamics are established from historical tide gauge data (1930s to present) and anthropogenic modifications to sediment supply. This baseline model of shoreline dynamics was created with attention to changes in the rates of sediment supply and sea level rise or the primary controls on barrier island formation and modification processes. Based on an existing qualitative understanding that the rate of sediment supply has been modified in the modern era by anthropogenic activities, an initial hypothesis was formed that the rate of sediment supply would be the major control on the barrier island system. This assumption was extended and tested by quantifying the magnitude and timing of modifications to the rate of sediment supply and comparing the change in sediment supply rates to changes in the shoreline and associated landforms at St. Catherines Island. The baseline model of shoreline dynamics was then used with evidence from the sedimentary record of St. Catherines Island to evaluate the relative role of sea level rise versus sediment supply in the development of the island during the Holocene. The results of the current study have direct implications to sea level and landform changes during human occupation of St. Catherines Island as well as to other Holocene barrier islands in similar mesotidal settings throughout the world (Figure 1-2).

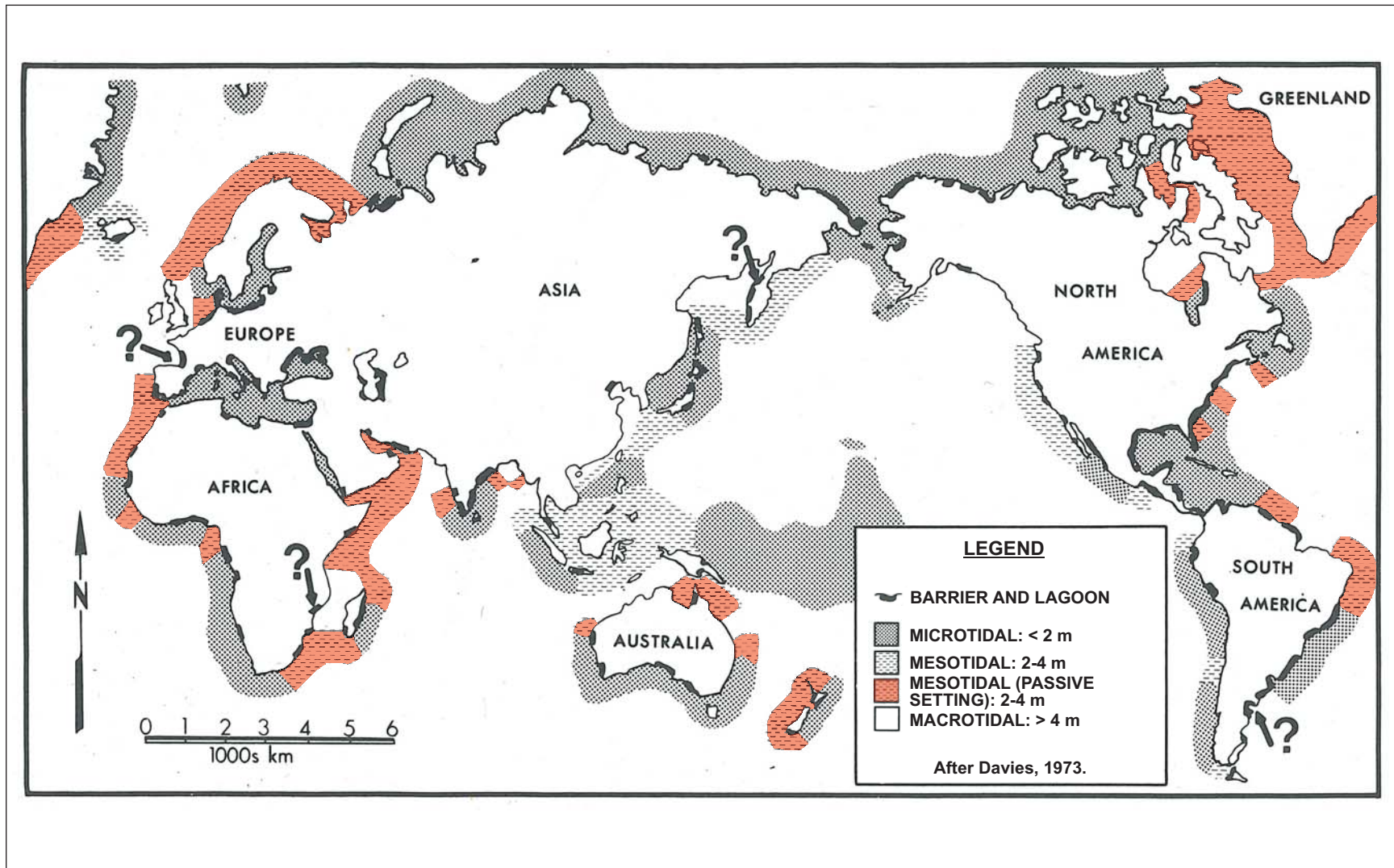


Figure 1-2: Results from the current study regarding the relative roles of the rate of sediment supply and the rate of increase in accommodation space (sea level rise) and the corresponding stratigraphic models for washover fans and barrier island response to sea level rise have implications on barrier island systems in similar physical or mesotidal settings worldwide. Figure adapted from Leatherman, 1979.



## 2 STUDY AREA PHYSICAL SETTING

St. Catherines Island is bordered by the Atlantic Ocean to the east, tidal marshes to the west, Sapelo Sound to the south and St. Catherines Sound to the north (Figure 2-1). These sounds are the lower reaches of salt water estuaries or marine embayments that are devoid of significant fluvial input or discharge (Wadsworth, 1981). St. Catherines Island is dependent upon net longshore transport of sand from north to south along the Georgia Coast (Hails and Hoyt, 1969, Clayton et al., 1992) and short term storage in tidal deltas. Landforms associated with the net longshore transport include the chenier-like deltas with notable southward accretion located at the Savannah River and Altamaha River Deltas (Alexander and Henry, 2007). Recent sea-level trends are documented on *The NOAA Sea Levels Online* site (NOAA, 2013) for the region including a current sea level rising rate of 2.98 millimeters per year (mm/yr) at Fort Pulaski near Savannah, Georgia and a rate of 2 mm/yr (1897-1999) at Fernandina Beach, Florida. An estimated sea level rise rate of 2.7 mm/yr is interpolated from these values for the study area of St. Catherines Island. The combination of factors, including the starving of longshore transport or flow of sand by damming rivers to the north, dredging the Savannah Ship Channel across the Savannah River Delta (U.S. Army Corps of Engineers, or USACE, 1991, 1996), and rising sea level have accumulated to make St. Catherines one of Georgia's most erosional barrier islands (Griffin and Henry, 1984). The significance of this setting is that the changes in shoreline, succession of depositional environments, and associated ecological effects observed on St. Catherines Island will eventually be reflected along the entire barrier island suite of the southeastern coast as sea level continues to rise under the modern transgression. Under



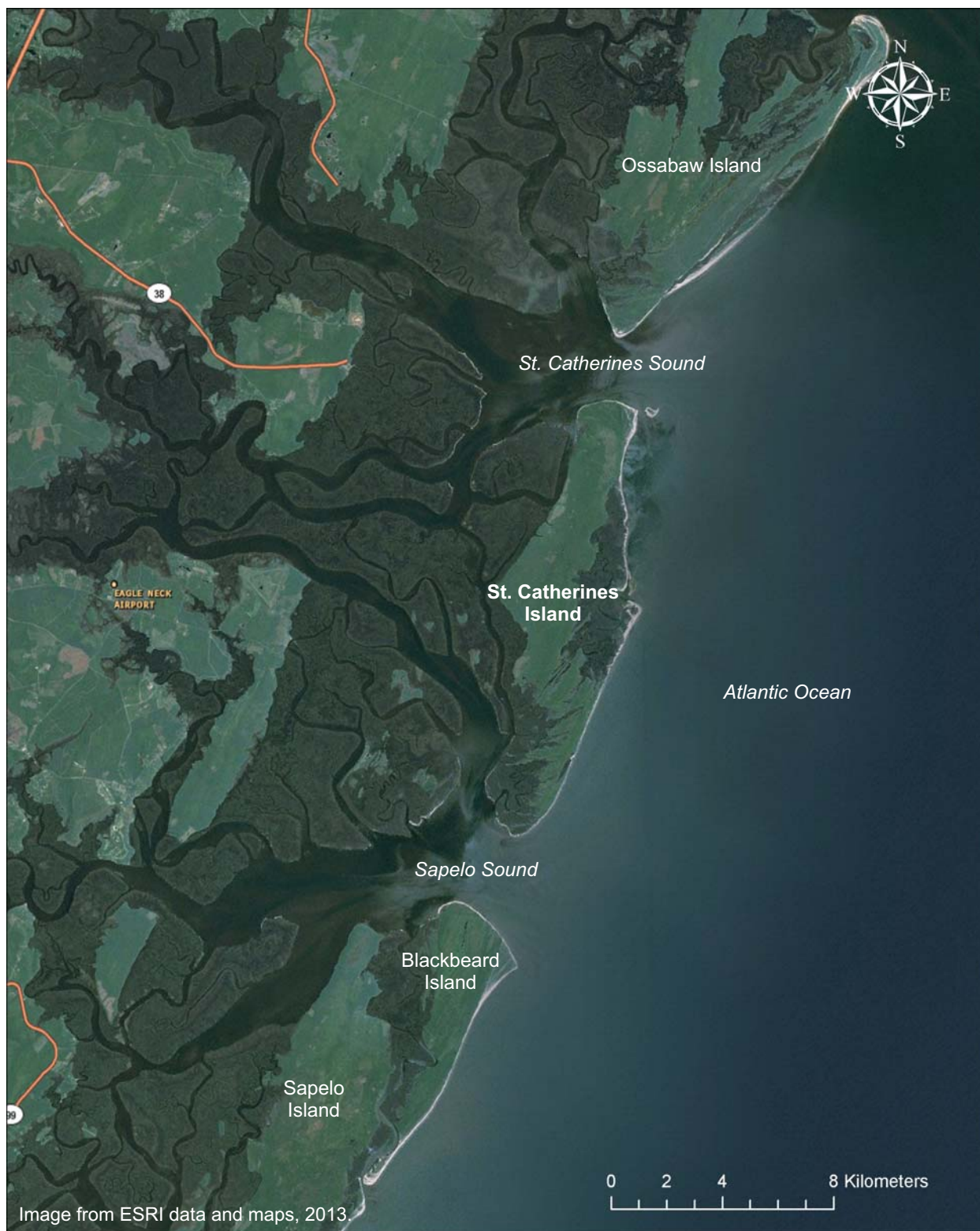


Figure 2-1: St. Catherines Island is separated from Ossabaw Island by St. Catherines Sound to the north and from Sapelo Island by Sapelo Sound to the south. The great distance to an appreciable sediment source, relatively high rate of sea level rise and other anthropogenic factors have accumulated to make St. Catherines Island Georgia's most erosional barrier island.

this premise, St. Catherines Island may be considered as a sentinel island for the barrier islands of the Georgia Bight (Bishop et al., 2007).

The island may be subdivided into four physiographic areas: 1) the island core, 2) the northern ridges and swale area composed of Holocene accretional beach ridges, 3) the marshes located west, east and south of the island core, and 4) the southeastern ridges and swales composed of Holocene accretional beach ridges. The island core is situated between 3 and 9 meters above mean sea level MSL and is approximately 8 km long and 2 km wide, with a long axis oriented north-northeast (N20°E to N25°E). There is little relief on the western portion of the island core, whereas the eastern portion rises to over 9 m MSL with little to moderate relief. The island core is heavily vegetated with maritime forest (Bellis, 1995) dominated by longleaf pine (*Pinus palustris*), live oak (*Quercus virginiana*) and palmetto (*Serenoa repens*).

The northern beach ridges are linear in shape and occur in three different orientations in the north-central, northwestern, and northeastern portions of the island. The beach ridges in the north-central portion of the island extend to 1,600 meters in length with a N55°W to N65°W trend and are truncated on the western and northwestern portions by the modern beach. The ridges rise to approximately 3.3 meters (11 feet) above the high tide elevation with the intervening swales varying from 1.5 meters (5 ft.) to 2.1 meters (7 ft.) above the high tide interval. A linear dune ridge set of appreciable height (25 ft. to 27 ft. MSL) and bearing north-south truncates the north-central beach ridges on the east and denotes the approximate location of the shoreline on the 1859 US Coast and Geodetic Survey Navigational Chart.

The southeastern beach ridges are linear in shape, extend to 5,000 meters in length with a N20°E to N25°E trend and are truncated on the eastern and southern portions of the ridges by Sapelo Sound and the Atlantic Ocean. Select ridges rise to approximately 3.3 meters (11 feet)

above the high tide elevation with the intervening swales varying from 1.5 meters (5 ft.) to 2.1 meters (7 ft.) above the high tide interval. The ridges occur in a series of packages with two distinct orientations that are generally oriented parallel to the modern shoreline and parallel to Sapelo Sound.

The modern marshes occupy the intertidal portions of the eastern, western, and southern margins of the island (Figure 2-2). The low marsh zone lies between neap high tide and mean high tide at approximately 0.6 meters to 1.1 meters above the mean low tide line and the high marsh is situated between the mean tide and spring high tide elevations and typically occurs from 1.1 meters to 2.0 meters above the mean low tide interval. Grasses dominate the land cover vegetation associated with the marshes and include *Spartina alterniflora* (Smooth Cordgrass or Saltmarsh Cordgrass) and salt tolerant plants or halophytes such as *Salicornia* (glasswort), *Distichlis* (salt grass), *Juncus* (needlerush) and *Spartina patens* (short marsh grass). Additional information regarding the interactions of plants, animals and the modern environments of St. Catherines Island follows in Section 3.

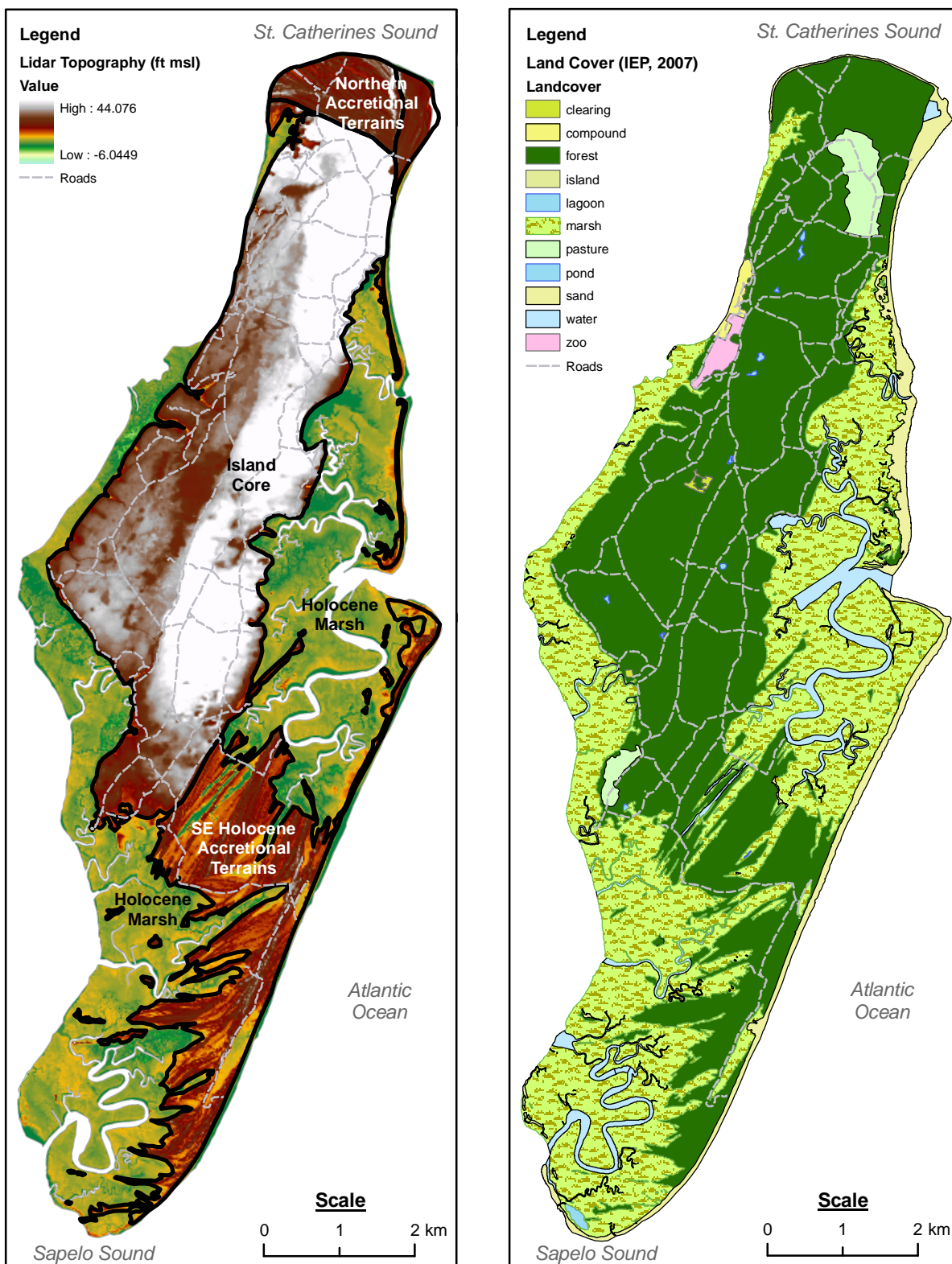


Figure 2-2: Comparison of the island topography (left) and island land cover (right) showing the strong relationships between the two data sets where lower topographic areas are dominated by intertidal marshes and the higher island core is vegetated by maritime forests. Data from Meyer et al., 2009.

### **3 BARRIER ISLAND SYSTEMS AND MODERN DEPOSITIONAL ENVIRONMENTS**

The following sections provide an overview of the predominant barrier island depositional environments and associated facies that are present on St. Catherines Island and common to the Georgia Bight. Specific attention is given to the most common physical sedimentary structures and the primary biogenic sedimentary structures as well as the modifying biogenic processes that are readily identifiable in vibracore samples and limited outcrops that are available within the study area.

Barrier islands are defined by six major sedimentary environments that are interactive in nature (Oertel, 1985) and impart the term “barrier island” on a littoral sand body and are defined as the 1) mainland, 2) backbarrier lagoon (or marsh), 3) inlet and inlet deltas, 4) barrier island, 5) barrier platform, and 6) shoreface. The following sections provide descriptions of the depositional elements of barrier islands including the marsh and tidal creeks, estuaries and inlets, beach, and nearshore depositional environments with a focus on the diagnostic physical and biogenic sedimentary structures that occur within each environment.

#### **3.1 Marsh and Tidal Creek Depositional System**

The intertidal salt marsh system and associated drainages (tidal creeks) form a complex and dynamic depositional system. Facies are dominated by fine grained sediments (clays/silts), with variations in the amount of coarse grained sediments (sand, granules, pebbles) being dependent upon numerous factors including the distance to the shoreline and proximity to upland areas where erosion may contribute coarse grained materials via erosion and surface water

runoff. Sedimentation in the marsh environment occurs as a surface process (Howard and Frey, 1985) in the form of peat development due to the accumulation of organic detritus and the deposition of fine grained inorganic sediment transported into the system by flood tides. The maximum depth of the modern marsh system may be defined by the erosion or scour depth of the meandering tidal stream channels. This scour depth is a function of the size and discharge of the tidal creeks or rivers. St. Catherines and Sapelo Sounds extend to depths of 15 meters below Mean Low Tide (MLT), the Medway River reaches a depth of 12 meters MLT, Walburg Creek extends to a depth of 6 meters MLT, and the tidal creeks located to the east of the island extend to 3-5 meters MLT. The smaller tidal creeks and rivers are typically less than 50 meters in width produce landforms that are typical of meandering streams. These landforms include meanders, levees, meander cutoffs, oxbows, point bars, cut banks and lateral stream capture of other tidal creeks (Figure 3-1).

Flow in these intertidal streams is dominated by tidal forces and has been described as asymmetrical bimodal flow (Oertel, 1975), with ebb flow being slightly more dominant. Point bars tend to migrate in the direction of flow, producing an upstream migration of point bars during flood tides and a downstream migration under ebb flow regimes. Due to the bimodal flow, cut banks develop as double cut banks with erosion occurring on the upstream and downstream portions of the features, depending upon the flood and ebb tidal conditions (Figure 3-1b). The lateral migration of tidal creeks has been estimated at 1-2 m per year (Letzsch and Frey, 1980) with the depth of erosion dependent on the aforementioned characteristics of the channel. The lateral migration and associated channel fill processes by point bars is a complex system whereby marsh sediments are aggressively reworked, producing a myriad of facies and associated range of absolute dates.





Figure 3-1: Elements of the marsh and tidal creek depositional environments of St. Catherines Island, GA. a) Low marsh environment with extensive meanders of tidal creeks, stream capture is typically promoted by lateral meanders rather than headward erosion of streams, b) sandy facies of point bar (left) and muddy facies of cut bank (right) of Fish Creek in Seaside Marsh, c) low marsh and high marsh surfaces inundated with water at spring tide high level in Seaside Marsh, d) muddy substrate of the low marsh environment near South End Plantation with tall marsh grass (*Spartina alterniflora*) and marsh periwinkle snails (*Littorina irrorata*), e) “clumping” habit of *Crassostrea virginica* in creek meander adjacent to the island core, and f) low marsh to high marsh transition in former Holocene beach ridge swales near Cracker Tom Causeway. Photographs by B. Meyer.

Within the marsh system, the depositional and biotic environments may best be described in terms of elevation, which is a direct result of the tidal reach. The highest elevation environment directly affected by tidal flux, rather than only storm surge or washover events is the flat-lying area covered by the marsh grass, *Spartina alterniflora*. This low marsh zone lies between neap high tide and mean high tide at an elevation between 0.6-1.1 m above MLT. Common biota in this zone include both tall and short *Spartina*, a semi-infaunal bivalve, *Geukensia demissa*, a gastropod *Littorina irrorata*, lives on the *Spartina*, and the fiddler crabs *Uca pugnax* and *Uca pugilator*. *Uca pugnax* tends to live on sandy substrates at higher elevations (high marsh) and *Uca pugilator* at lower elevations on muddy substrates. The high marsh interval from 1.1-2.0 m is situated between the mean tide and spring high tide elevations and is typically associated with more coarse grained sediments than the lower marsh environment. Flora include more salt tolerant plants or halophytes such as *Salicornia* (glasswort), *Distichlis* (salt grass), *Juncus* (needlerush) and *Spartina patens* (short marsh grass) in lower elevations of the high marsh. The high marsh environment is typically located adjacent to upland areas such as the island core (and/or mainland), but may also occur in close proximity to the backbeach environment on washover fans, and within dune ridge swales (Figure 3-1f). Erosion of the upland materials, washover fans and dune ridges contribute coarse grained materials via erosion and surface water runoff to the high marsh and storm activity provides an input of coarse grained materials from the backbeach environment. Facies associated with the high marsh include muddy sands and laminated sands and muds.

The barrier islands and associated marsh systems located along the Georgia Coast are dependent upon the net longshore transport of sediments or material from a northeastern to southwestern direction along the Georgia Coast with temporary storage in tidal deltas (Hails and



Hoyt, 1969, Clayton et al., 1992). This longshore current, and the inland transport of sediment as a result of flood tidal action, also provides a source of sediments to the marsh systems that are rich in illite and montmorillonite clays (Meade, 1969). Clay sediments of the outer shelf of Georgia that are susceptible to inland transport are dominated by illite-montmorillonite and contain as little as 10% kaolinite (Pinet and Morgan, 1979). The kaolinite rich suspended load from the larger Piedmont Rivers is mixed with the marine load of illite-montmorillonite clay in the tidally influenced estuaries. Previous work (Neiheisel and Weaver, 1969) has shown that the Coastal Plain Rivers with relatively lower flow regimes or discharge rates typically do not exhibit as strong of a kaolinite signature as the larger Piedmont Rivers.

Within the estuary or depositional basin near the mouth of the river, the clays are settled as a result of decreasing water velocity as the rivers approach base level as well as flocculation induced by contact with saline waters (Pevear, 1988). The greater ionic strength of the marine water produces a decrease in the surface charge allowing the clays to aggregate and settle from the suspended load. Sedimentation rates in marshes adjacent to the Savannah River estuary were estimated at 1.0 cm/yr by Goldberg et al. (1977). In addition to the physical settling of flocculated mud from suspension, biogenic pelletization is promoted by the filtering of sea water by organisms (Pryor, 1975). The most important of the filter-feeding organisms with regards to volumetric contribution of muds to the marsh system (Frey and Basan, 1985; Smith and Frey, 1985; Pryor, 1975) are the ribbed mussel (*Geukensia demissa*) and the Atlantic Oyster (*Crassostrea virginica*). Secondary contributions of muds to the marsh include ghost shrimp fecal matter that may be transported via washover processes or flood tide transport (Frey and Basan, 1985). Stability of the muds through biogenic pelletization by fiddler crabs (*Uca* spp.)

and mud snails (*Ilyanassa obsoleta*) also prevents re-suspension, as well as algal mats that trap muds within the marsh system (Frey and Basan, 1985).

### 3.2 Estuaries and Inlets

Barrier lagoons or marshes and the open oceans are connected via inlets that serve as the orifices or pathways through which sediment and water transport and exchange occur between the lagoon and shoreface of the barrier island system (Oertel, 1985). A bivariate relationship exists (O'Brien, 1969 and Jarrett, 1976) between the cross-sectional area of the tidal inlets ( $A_i$ ) and the tidal prisms of the backbarrier lagoon or marsh ( $P$ ):

$$A_i = nP^K$$

where  $n$  and  $K$  are constants

This relationship predicts that as lagoon or marsh flooding increases as expected under a marine transgression, a proportional increase in the cross-sectional inlet surface area occurs most commonly via erosion. Conversely, a decrease in lagoonal flooding under a marine regression will result in constriction of the inlet through expansion of the bounding barrier islands. Superimposed on the simple bivariate relationship are factors that complicate the process including anthropogenic modifications and areas where sediment supply and morphology (i.e. bedrock substrate) are not in equilibrium (Oertel, 1985).

A portion of the inlet throat area is typically scoured at depth forming an inlet trough. The trough slopes upward in both a seaward and landward direction over "ramps" to more shallow waters (Oertel, 1973). In barrier island systems, these features are designated as inlet-lagoon and inlet-shoreface ramps. When the inland or onshore flow through a tidal inlet is greater than the outflow volume, "flood-tidal delta" sedimentation tends to occur on the

landward side of the barrier island and associated inlet (Hayes, 1975). In contrast, ebb-tidal deltas are formed on the ocean side of an inlet and are commonly associated with the inlets and sounds in the mesotidal setting of the Georgia Bight. The inlet shoreface ramps associated with ebb-tidal deltas are typically covered with current structures that consist, in a landward to seaward direction, of sand waves, megaripples and ripples near the distal shoals of the ebb-tidal delta. Inlet ramps have distinct physical sedimentary structures and sediments associated with the transition from shoreface sands to muddy lagoonal or marsh sediments (Kumar et al., 1974).

St. Catherines Sound is located between St. Catherines Island and Ossabaw Island to the north and is the discharge estuary for the Medway River, Bear River, North Newport River, Timmons River and Walburg Creek. Sapelo Sound is located to the south of St. Catherines Island and is formed by the confluence of the Sapelo River, Todd River, Barbour Island River, Wahoo River, South Newport River, Johnson Creek and Blackbeard Creek. Box cores collected by Howard and Frey (1985) indicate significant variations in the sedimentary facies associated with St. Catherines Sound and Sapelo Sound. St. Catherines Sound sediments are described as being predominately bioturbated muddy fine sand with gravel in the upper reaches, and coarse, graded, planar and trough-crossbedded sands near Pleistocene aged sediment sources. A significant ebb-delta system is associated with St. Catherines Sound that includes St. Catherines Shoal (aka St. Catherines Bar) and a well-developed marginal shoal that extends onto the northern shores of the island. This margin shoal is composed of muddy sands and exhibits many of the characteristics of ebb deltas including sand ripples, scour pools, and *Skolithos* ichnofacies (Figures 3-2a, 3-2b and 3-2c). Sapelo Sound sediments are characterized as being coarser grained, graded sands with trough-crossbedded sands and local gravel in the upper reaches of the estuary, and bioturbated fine sand with shell materials in the lower reaches of the estuary.

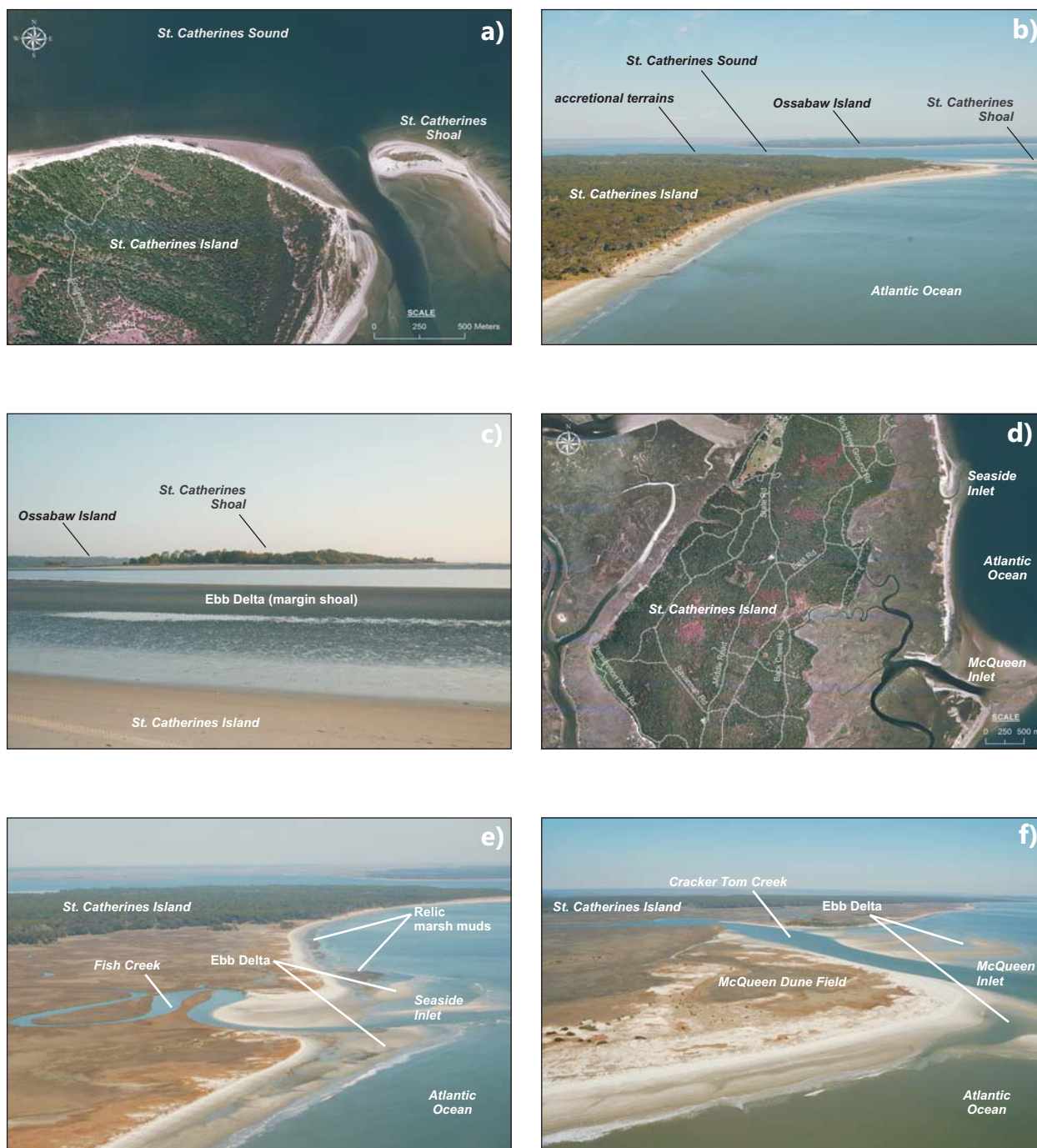


Figure 3-2: Elements of inlets and sounds associated with St. Catherines Island, GA. a) Location of St. Catherines Sound and St. Catherines Shoal that has developed as a portion of the ebb delta complex, b) Oblique view of St. Catherines Sound, ebb delta, St. Catherines Shoal and active accretional terrains, c) the marginal shoal of the ebb delta forms a muddy sand flat adjacent to St. Catherines Island with sand ripples, scour pools, and *Skolithos* ichnofacies, d) Location of tidal inlets and associated ebb tidal deltas at Seaside Inlet (discharge point of Fish Creek) and McQueen Inlet (discharge point of Cracker Tom Creek), e) oblique view of Seaside Inlet ebb delta and relic marsh muds on North Beach, f) oblique view of McQueen Inlet ebb delta and McQueen Dune Field. Map images in A and D are 2009 true color imagery from USDA NAIP, photographs by B. Meyer.

Two additional tidal inlets are formed on the eastern portion of St. Catherines Island by the discharges of Cracker Tom Creek (McQueen Inlet) and Fish Creek (Seaside Inlet). These inlets receive discharge from tidal creeks that are situated within the eastern marsh system on St. Catherines Island (Figure 3-2d). Small ebb deltas that function as sediment banks are located adjacent to these inlets and are exposed at low tide and associated with small areas of shoreline stability (Figures 3-2e and 3-2f).

### **3.3 Beach and Nearshore Depositional Systems**

The following sections describe the physical and biogenic sedimentary structures associated with the beach and nearshore depositional systems including offshore, transition zone, shoreface, foreshore (forebeach), backshore (backbeach), dune (eolian), and washover fan depositional environments.

#### *3.3.1 Offshore - Bioturbated Facies*

In water depths of 10 meters to 20 meters, the offshore facies below the average wave effective depth consists predominately of highly bioturbated muddy fine sands (Howard and Reineck, 1972 and Howard and Frey, 1980). This facies is dominated by biogenic structures due to the quiescent conditions that favor bioturbation over deposition except during extreme storm events. These sediments have been extensively re-worked where individual burrows may no longer be recognizable. In water depths greater than 10 meters the modern shelf is characterized by palimpsest (relict) sands.

### 3.3.2 Transition Zone – Bioturbated and Laminated Facies

Sediments from this depositional environment occur in water depths of 10 meters below MLT and extend upward into the intertidal zone and exhibit both physical and biogenic sedimentary structures. Physical sedimentary structures are observed in the form of muddy fine sands and mud layers with erosional contacts that truncate burrows. Hummocky style bedding may also be found with parallel-laminated and burrowed beds. Three distinct burrow types can be found, although all of them may not be present in one specific location. These biogenic structures include burrows of polychaete worms, *Callianassa* and *Thalassinoides*-type burrows. Howard and Scott (1983) observed this facies in a Pleistocene age outcrop on the St. Mary's River and noted an absence of physical sedimentary structures. The massive bioturbation that destroys physical sedimentary structures was attributed by Howard and Scott to indicate the minimal influence of storms in the transition zone.

### 3.3.3 Shoreface (Lower Forebeach) – Burrowed and Laminated Facies

The continuous effects of waves and currents in the intertidal zone results in extremely varied and well developed physical sedimentary structures in the lower forebeach or shoreface area. Sedimentary structures include ripple laminations in the lower or deeper sections with parallel laminae in the upper sections associated with the transition to the foreshore environment. Biogenic structures include *Ophiomorpha nodosa* mud-lined burrows attributed to *Callianassa major* (Say, 1818) or the Carolinian Ghost Shrimp that decrease in abundance or density with increasing elevation where the burrows are typically not observed above the mean water line. The burrows extend to depths of 2 meters and are noted by a small opening (0.4 cm) fringed with fecal pellets at the surface.

### 3.3.4 Foreshore (*Upper Forebeach*) – *Laminated Facies*

Sedimentary structures observed in upper forebeach sediments include subparallel, laminae dipping ( $< 5^\circ$ ) seaward, and laminae dipping ( $15^\circ - 20^\circ$ ) landward due to the development of ridge and runnels and ripple laminae may also be present in this facies due to runnels. This facies transitions into the backshore at the neap high tide interval although the exact boundary may be difficult to discern due to the transient or dynamic nature of the boundary. Examinations of forebeach deposits at St. Catherines Island under the current study indicate that the laminae may be faint or “ghostly” due to a lower relative abundance of the heavy mineral sands (HMS) that provide bedding definition and post-depositional bedding disturbance due to amphipod cryptobioturbation (Figure 3-3e). Heavy minerals were also observed to concentrate on a small or local scale via sorting in the troughs of ripple marks occurring in beach runnels (Figure 3-3f).

### 3.3.5 Backshore (*Backbeach*) – *Laminated and Bioturbated Facies*

Howard and Scott (1983) note that the main criteria used to differentiate the backshore or backbeach from the foreshore/forebeach at Sapelo Island, Georgia are: 1) absence of ridge and runnel structures, 2) higher concentrations of HMS and more distinct lamina, 3) more variations in physical sedimentary structures, and 4) presence of ghost crab and insect burrows. Examinations of backbeach deposits at St. Catherines Island under the current study indicate that extensive deposits of HMS occur in this depositional environment as a result of winnowing processes whereby quartz sands are preferentially transported via swash and backwash as the HMS concentrate as lag deposits forming a beach placer (Figure 3-3d).





Figure 3-3: Elements of supratidal and intertidal beach environments associated with St. Catherines Island, GA. a) inactive washovers, dunes, backbeach and forebeach environments, b) the storm high tide line is demarcated by vegetative debris or wrack, and corresponding spring tide high line, and neap tide high line. The sands of the backbeach are saturated during spring tides and exhibit higher albedo, c) heavy minerals in the backbeach occur as a placer where winnowing of less dense quartz sands results in the concentration of heavy minerals, d) backbeach sands, horizontal laminae or low angle ( $<2^{\circ}$ ) seaward dipping laminae of quartz and heavy minerals, e) forebeach sands with lower concentrations of heavy minerals and faint laminations due to amphipod cryptobioturbation, and f) asymmetrical ripple marks in a beach runnel. Photographs by B. Meyer.



Backbeach sediments may be distinguished from eolian sediments on the basis of primary physical sedimentary structures. The transition from marine (backbeach) to non-marine conditions may be observed at an elevation equal to or slightly above the modern spring tide high mark of 1.7 to 2.1 m (Figure 3-3a and 3-3b). This elevation is marked by a change from low angle bedding (backbeach) to higher angle bedding and represents the maximum elevation of wet sand and the lowest elevation at which eolian scour may occur (Roep and Beets, 1988).

### 3.3.6 Dunes (Eolian) - Laminated and Bioturbated Facies

Dunes are typically 0.5 to 2 meters high but may reach over six meters in height and denote supratidal conditions and the landward extent of the backbeach depositional environment. Wind is the dominant depositional agent with minor hydraulic modifications during spring tide and washover events. The saltation of sand across the dunes is a continuous process with plants providing local slope stability. Dunes may be classified as 1) straw dunes, that are the initial and small isolated dunes that are formed when sand is trapped by dead vegetation or marsh grasses, 2) foredunes that are intermediate dunes which are built upon straw dunes or by lateral migration of existing mature dunes, and 3) primary dunes that are mature, large and densely vegetated (Howard and Frey, 1980). Straw dunes are chiefly associated with salwort (*Salsola kali*) and spike grass (*Distichlis spicata*); secondary dunes are associated with beach hogwart (*Croton punctatus*), bitter panicgrass (*Panicum amarulum*) and occasionally salt meadow cordgrass (*Spartina patens*). Sea oats (*Uniola paniculata*) are most closely associated with primary dunes (Oertel and Larsen, 1976). Mature dunes associated with a prograding shoreline may become vegetated under a natural succession scheme whereby shrubs or bushes such as wax myrtle (*Myrica cerifera*) succeed grasses, and subsequently loblolly pine (*Pinus taeda*) become

established with initial topsoil development. Interdunal swales are commonly vegetated by sandbur (*Cenchrus paucifloras*) and species of the woody vine *Smilax* (Johnson et al., 1974). The natural succession of vegetation associated with a prograding dune field may be observed on North Beach at St. Catherines Island where the younger dunes in close proximity to the modern shoreline are vegetated with sea grasses, and the older beach ridges and dunes located landward are vegetated with shrubs and trees such as loblolly pine (Figures 3-4a, 3-4b and 3-4c).

Facies in this depositional environment are dominated by fine to very fine sands lacking significant mud content. Heavy mineral laminae are observed in festoon cross bedding with beds of up to 10 cm in thickness and dips greater than  $30^{\circ}$ ; however, these shallow sedimentary structures may be destroyed or disturbed by roots of the associated grasses, sea oats and trees or shrubs. In addition, bioturbation by insects and mammals is common in the upper 3-4 meters (Howard and Scott, 1983; Martin and Rindsberg, 2011).

### 3.3.7 Washover Fans

Washovers have been described as depositional units that result as a continuation of swash over the top of the beach berm or dunes during a storm or high energy event (Leatherman and Williams, 1977). A body of sediment is deposited as the washover flow velocity decreases in areas typically located landward of a spit or barrier beach. The combination of overwash processes, physical and biogenic modification of the washover fan, and compaction determine the final washover stratigraphy. The composition of washover deposits vary with the provenance of the sediment, but typically consist of alternating layers of sands, heavy minerals and shell fragments that are the result of changing hydraulic regimes under storm and tidal conditions (Kochel and Dolan, 1986). The frequency of overwash events, degree of bioturbation, and the

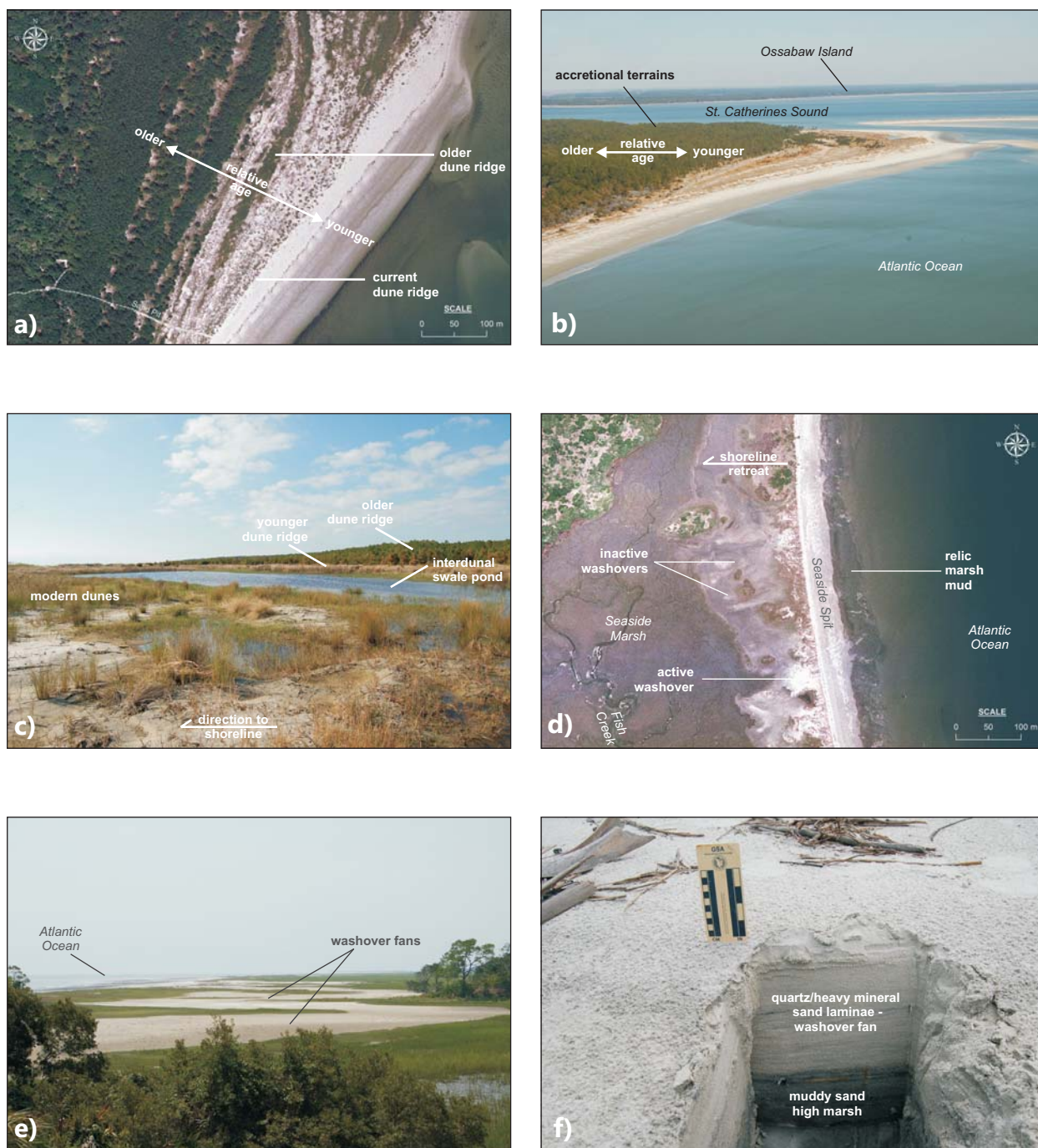


Figure 3-4: Elements of eolian/dune and washover depositional environments. a) aerial view of modern dune ridges prograding in the northeastern accretional terrains, b) oblique view of dune ridges, accretion occurs in this area due to protection from the erosion of waves by St. Catherines Bar/Shoal, c) view to the SW across progressively older dune ridges and location of a swale pond, a modern analog for Beach/Flag Ponds, d) aerial view of washovers in Seaside Marsh with retreating shoreline exposing relic marsh muds, e) oblique view of washover fans in Seaside Marsh, the washover fans occupy the low marsh environment and as a result are inundated during spring tide high events, and f) excavation in washover fan demonstrates laminated quartz and HMS overlying the high marsh muddy sand facies. Map images (2009 USDA NAIP), photographs by B. Meyer.

rate of sea level change determine the washover facies of the sedimentary units resulting from individual storm events and greatly affect the preservation potential. Reworking of sediments is common and compounds the challenges in the identification of individual storm events and subunits.

Although washover fans may be formed during marine regressions they are much more commonly observed in transgressive sequences (Deery and Howard, 1977) and are recognized generally as washover units overlying backbarrier facies such as marsh sediments (Figures 3-4d and 3-4f). The presence of foreset bedding structures is dependent on the antecedent water levels where foresets may be present on the distal portions of the fan as a result of the fan prograding into a bay or indicating high tide conditions during deposition in a marsh.

Examination of washover deposits at St. Catherines Island under the current study indicate appreciable levels of HMS occur in this depositional environment as a result of the washover sediments being dominated by a proximal source of backbeach and eolian quartz and HMS deposits. The washover facies and the laminated backbeach and forebeach sands are readily distinguished as laminae in the washover fans dip ( $< 20^\circ$ ) in a landward direction versus the lower dip angles and seaward dip direction associated with backbeach and forebeach sands. The washover deposits are lobate in plan view and wedge-shaped in longitudinal cross section, and thin in a landward direction with a long axis normal to the coast. Foreset laminations occur on the leading edge of washover fans, with sets and cosets up to 50 cm thick that dip up to  $30^\circ$  landward. During periods of storm inactivity, small ( $< 1$  m) eolian dunes, wind ripples and blowouts may form on the sparsely vegetated and unstable surfaces. Shell lags may also develop on some of the high washover surfaces. Small-scale crossbedding occurs with ripple laminae that form in areas of low water velocity, and trough crossbedding occurs in large washover channels.

Washovers represent episodic deposition associated with significant storms such as hurricanes and nor'easters and prograde in a landward direction. Individual washovers are typically 50 to 150 meters in length (parallel to flow direction) and 50 to 100 meters in width (parallel to shore). Individual washover fans may exhibit lobes superimposed on the greater fan morphology and multiple washovers can merge to form nearly continuous aprons. A continuous apron of superimposed washover fans was observed along Seaside Spit in May 2013 following a nor'easter storm event. Following deposition, washovers may be significantly modified by erosion associated with rainfall and surface water runoff or coupled spring tide/storm events.

Washover fans typically form in the low marsh or high marsh environments adjacent to the beach and eolian environments and as a result contain many of the same biogenic features of the marsh system such as burrows from fiddler crabs (*Uca pugilator*) and ghost crabs (*Ocypode quadrata*) and various insects including beetles (Martin and Rindsberg, 2011). Botanical colonization of distal fan margins by glasswort (*Salicornia*) and bioturbation by fiddler crabs is rapid and extensive. If washover fans form in the lower marsh and are inundated during tidal cycles, smooth cordgrass (*Spartina alterniflora*) or other marsh grasses may vegetate the surface, resulting in the accumulation of peat materials and root mottling obscuring the primary physical sedimentary structures.

Most washover fans generally form in a similar manner and therefore share physical and biogenic sedimentary structures that may be grouped into active and passive phases of activity (Deery and Howard, 1977). Active phase elements are created during the initial washover and as a result are dominated by physical sedimentary structures with minimal biogenic structures and modifications (Howard and Frey, 1980). Sub-horizontal stratification, consisting of parallel, gently dipping, laminated to thinly bedded (1-2 mm) quartz and heavy mineral sands are formed

during maximum washover conditions. Ripple laminations form small-scale crossbedding during low velocity flow regimes, foreset laminae form at the leading edge of the washover fans, and trough crossbedding forms in washover channels. Passive phase structures form during quiescent conditions, when wind and biologic activity are prevalent. Eolian dunes may form with crossbeds and lamina angles up to 30°, at the backbeach to washover margin. Wind ripples, less than 5 cm high, with more coarse grained materials in the crests, are also associated with blowouts (typically less than 10 cm deep) resulting from wind erosion. Climbing ripple laminations may also occur on the distal margins of the washover fan where thin veneers of loose sand are eroded and re-deposited by significant rainfall and surface water runoff.

Stratigraphic models depicting the generalized facies associated with washover fans have been produced for supratidal and microtidal settings (Figures 3-5a and 3-5b) and the preservation potential of the facies has been evaluated in microtidal (Sedgewick and Davis, 2003) and mesotidal settings (Deery and Howard, 1977). However, a stratigraphic model for washover fan facies has not been developed for a mesotidal setting. Based on field observations and vibracore samples collected under the current study, a general facies model for mesotidal washover fans has been developed and refined under the current study (Figure 3-5c). A distinction is made in this model for the mesotidal setting, where the distal edge or limits of the washover are controlled by the height or elevation of the tide at the time of deposition. For example, a washover emplaced in a mesotidal setting at a low tide stage will share many of the same physical sedimentary structures with a microtidal washover fan. In contrast, microtidal washover fans deposited at high tide stages are typically shorter with respect to their long axis than mesotidal washover fans deposited under lower tidal stage conditions. The development of peat

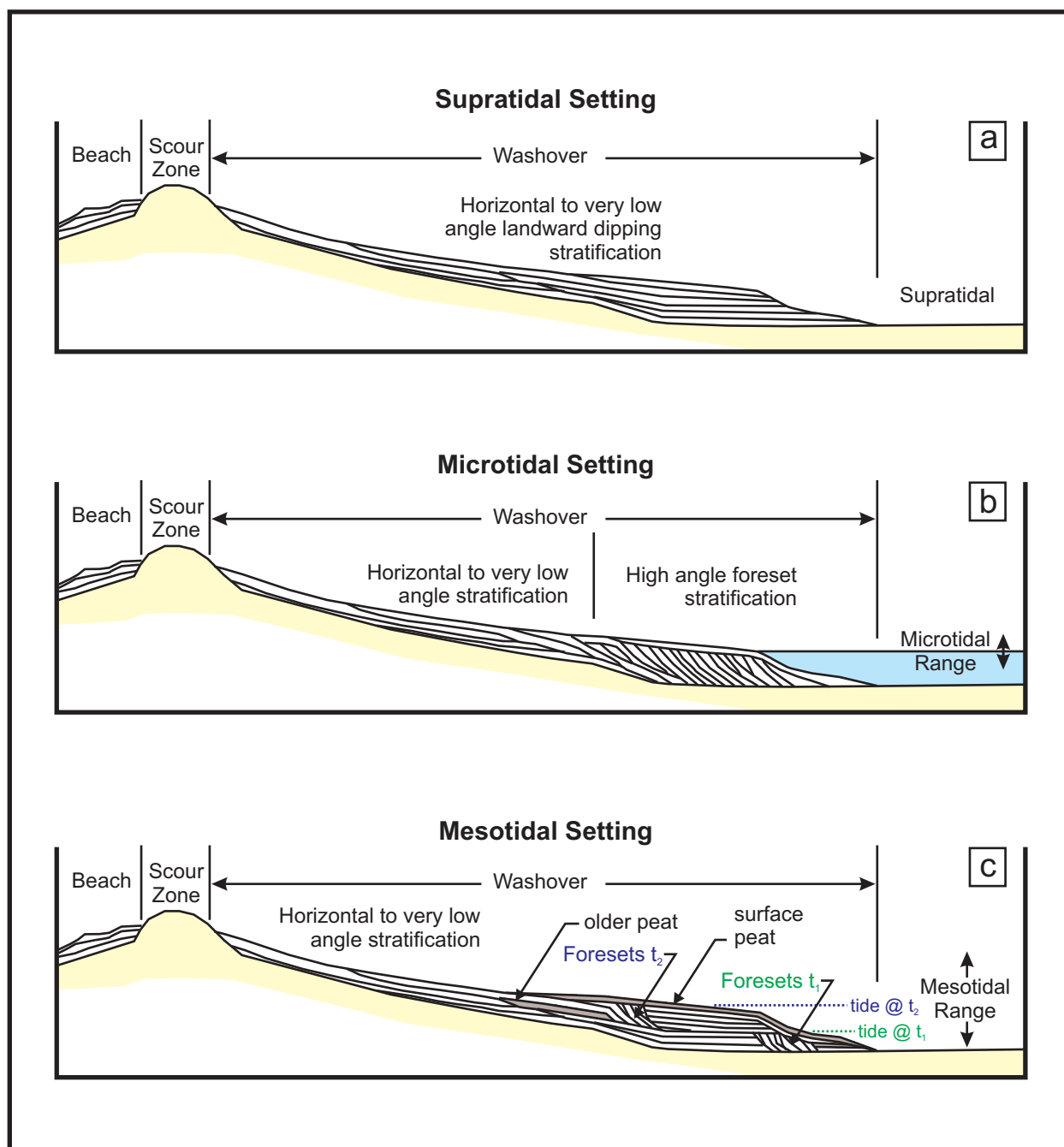


Figure 3-5: Washover fan facies stratigraphic models (a) supratidal setting: planar-laminated sand with no tidal influence, (b) microtidal setting: foreset laminae forming at distal/leading edge of washover fan indicating moderate tidal influence, and (c) mesotidal setting: due to the variable tidal levels, the facies and relationships are complicated versus the microtidal or supratidal setting. The tidal level influences the location of the distal edge of the washover fan under this scenario where the lower tidal level ( $H_2O t_1$ ) at time  $t_1$  has influenced the location of foresets assoc. with  $t_1$  versus a higher tidal stage ( $H_2O t_2$ ) at time  $t_2$ . Model b) would also apply to the high marsh depositional environment in a mesotidal setting. Models in a) and b) are adapted from Schwartz, 1975, and the stratigraphic model for the mesotidal setting (c) has been developed and tested/refined under the current study.

materials is also more likely due to the mesotidal setting and associated tidal range where the reworking of sediments produces discontinuous peat surfaces.

### **3.4 Barrier Island Models - Response to Rising Sea Level**

Barrier islands and associated depositional environments such as washover fans respond to sea level in a manner similar to salt marshes or coral reefs. The three major responses are designated as ‘catch up, keep up, and give up’ (Neumann and MacIntyre, 1985). The response of the barrier island and washover fans is dependent on the rate of sediment supply and the nature of sea level rise or the increase in accommodation space (Coe, 2005). Under conditions of sea level rise and tectonic stability, there is an inclination for overwash conditions to dominate unless vertical accretion balances or “keeps up” with the increase in sea level. When a low rate of sea level rise is coupled with a low rate of sediment supply or conversely when a rapid rate of sea level rise is associated with a high rate of sediment supply, the barrier island should sustain itself and washover fans will produce the dominant facies associated within this setting (“keeps up”). In contrast, a large sediment supply paired with a low rate of sea level rise will produce a progradational barrier island system with significant eolian conditions driving dune development. These dunes would produce a decrease in washover events and washover fan deposition resulting in the “catch up” scenario. If a high rate of sea-level rise is accompanied by a low rate of sediment supply, washover fan deposition lessens as inlets form, the barrier island deteriorates (‘give up’) into swashover deposition and the island is overcome or submerged by the rising sea level. By employing these models, the recognition of washover sequences in the ancient rock record can provide insights into the relative nature of sea level rise and sediment supply (Sedgwick and Davis, 2003). A graphical representation of the ‘catch up, keep up, and



give up' concepts for washover fan and barrier island response to rising sea level has been prepared under the current study and is presented as Figure 3-6.

Transitional stages of barrier islands and washover fans from the "keep up" to "give up" stages of Neumann and MacIntyre (1985) have also been observed under the current study at St. Catherines Island. A model has been constructed to capture these transitional or intermediate stages under a constant storm intensity scenario. If the rate of sediment supply is equal or balanced with the rate of increase in accommodation space (rate of sea level rise), the barrier island and washover fans should be laterally stable and vertical accretion will be the depositional pattern or "keep up" occurs (Figure 3-7a). When the rate of sediment supply is slightly less than the increase in accommodation space, shoreline retreat is initiated and the washover fan complex migrates and progrades in a landward direction due to the decrease in the distance from the distal edge of the washover fan to the shoreline (Figure 3-7b). If the rate of sediment supply continues to be less than the increase in accommodation space, or the rate of sediment supply decreases, shoreline retreat continues and washover fans are eventually overcome by marine conditions and deteriorate into flood deltas (Figure 3-7c). These same transitional stages would be expected where the rate of sea level rise increases and the rate of sediment supply remain constant. These transitional stages have been observed at Seaside Spit, Flag Pond and Beach Pond at St. Catherines Island, Georgia where significant shoreline retreat, inlet formation, and the conversion of washover fans to tidal deltas is occurring. The responses of shoreline retreat, inlet formation and the conversion of washover fans to flood deltas will be documented in the current study and the model will be refined where necessary.

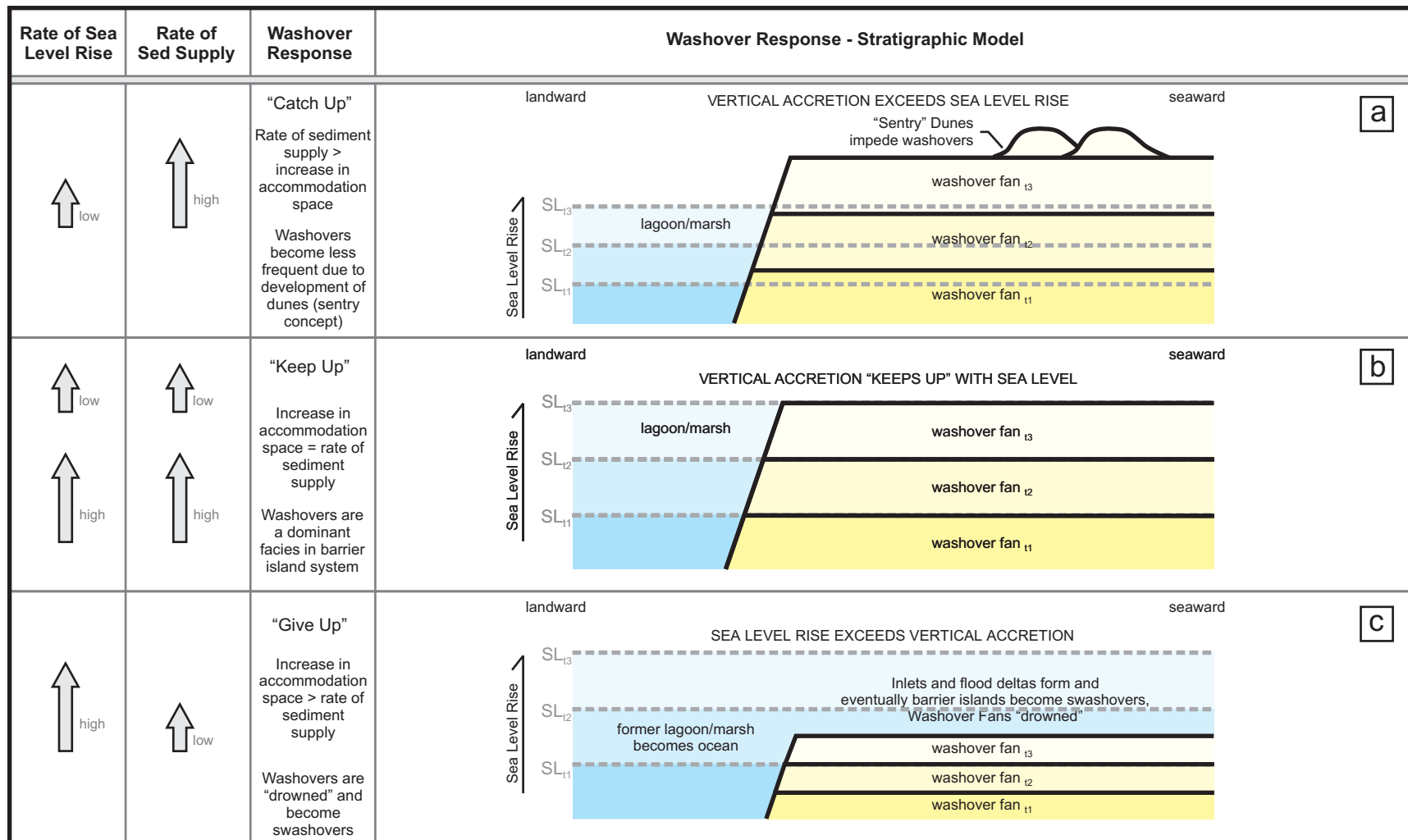


Figure 3-6: Barrier islands and associated depositional environments response to sea level. a) A large sediment supply with a low rate of sea level rise will produce a progradational barrier island system resulting in the “catch up” scenario. b) A low rate of sea level rise coupled with a low rate of sediment supply or a rapid rate of sea level rise is associated with a high rate of sediment supply, the barrier island “keeps up”. c) A high rate of sea-level rise accompanied by a low rate of sediment supply the barrier island deteriorates ('give up'). Concepts of reef response by Neumann and MacIntyre (1985) were originally applied to washovers by Sedgewick and Davis (2003), the stratigraphic model (above) has been developed under the current study.

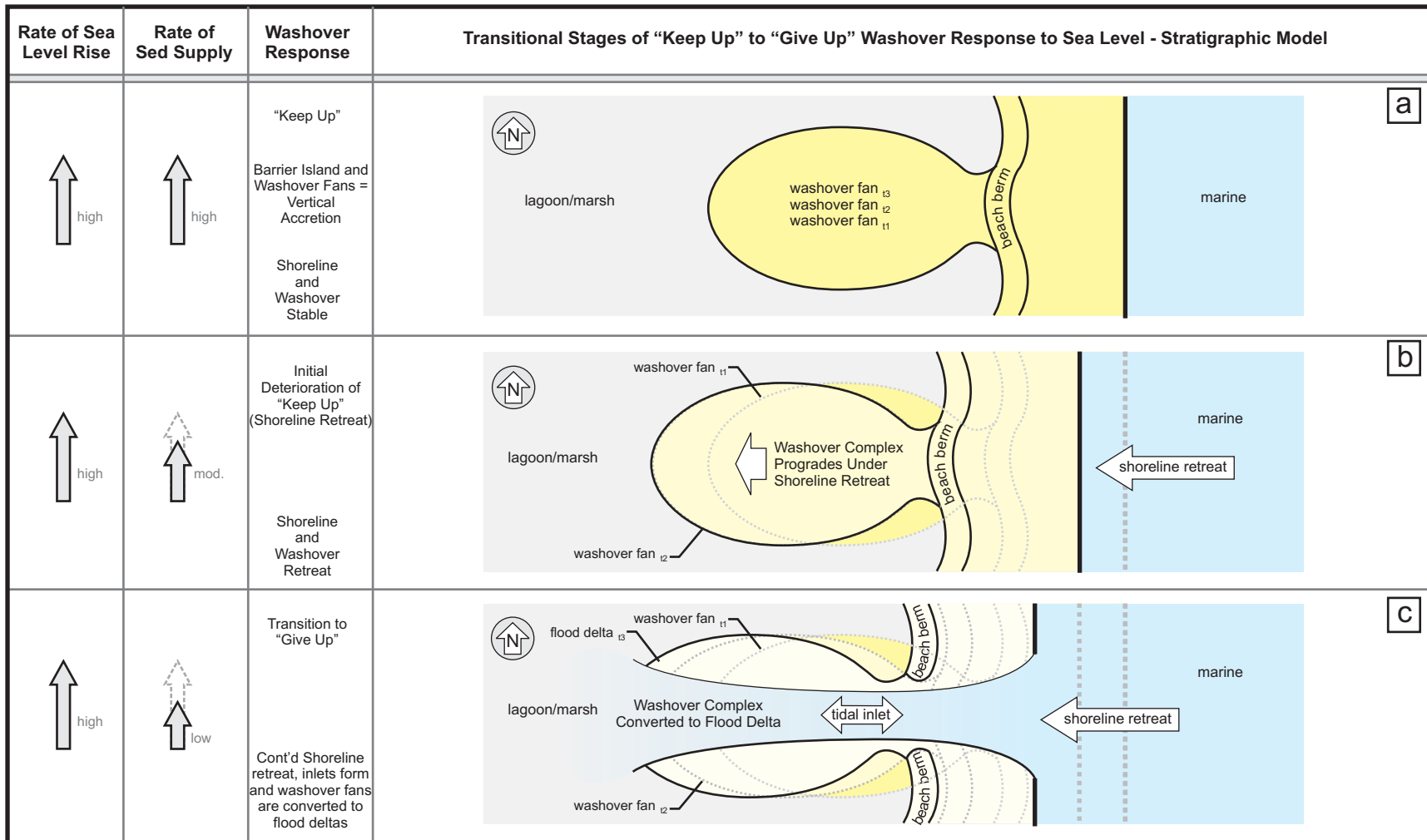


Figure 3-7: Transitional stages of washover fans from the “keep up” to “give up” stages of Neumann and MacIntyre (1985) under a constant storm intensity scenario. a) If the rate of sediment supply = increase in accommodation space, vertical accretion will be the depositional pattern or “keep up” occurs. b) When the rate of sediment supply is slightly less than the increase in accommodation space, shoreline retreat occurs and the washover fan complex migrates/progrades in a landward direction. c) As the rate of sediment supply continues to be less than the increase in accommodation space washover fans are eventually overcome by marine conditions and deteriorate into flood deltas.

### **3.5 Facies Successions – Walther’s Law of Facies**

Walther’s Law of Facies, or Walther’s Law, predicts that the vertical succession of facies observed in the rock record is a response to a lateral change or changes in the depositional environments. Another perspective of Walther’s Law states that as a depositional environment shifts laterally, sediments from adjacent depositional environments are deposited on top of one another, except where unconformities are present.

The various facies associated with the major subtidal to supratidal marine and marginal marine environments near St. Catherines Island have been compiled from field observations and literature sources, and an idealized vertical sequence has been constructed under a marine regression scenario (Figure 3-8). This model for the succession of environments and the inverse sequence or model under a marine transgression (Figure 3-8b) has been used to associate facies with depositional environments and to evaluate relative sea level dynamics under the current study.

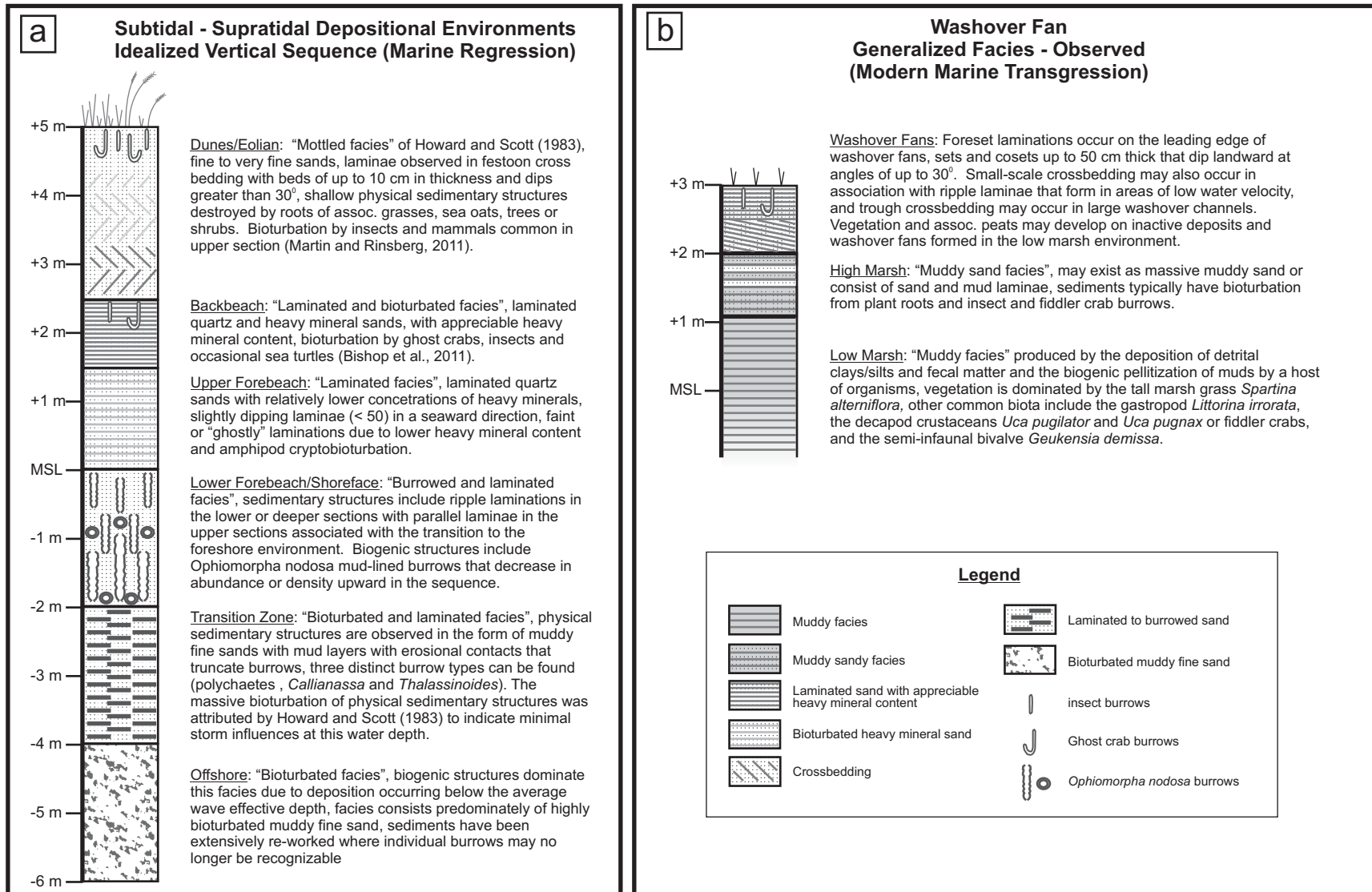


Figure 3-8: Facies associated with subtidal, intertidal and supratidal depositional environments of St. Catherines Island, GA. a) Idealized vertical succession of the major marine-terrestrial depositional environments of St. Catherines Island as predicted by Walther's Law under a marine regression, b) general facies observed for washover fans emplaced in the high and low marsh environments.

## 4 GEOLOGICAL SETTING

### 4.1 Regional Geological Setting

The marine terraces of the lower Coastal Plain of Georgia were initially described in a formal manner and mapped by LaForge and Cook (1925). MacNeil (1950) provided the first regional study and descriptions of the coastal stratigraphic units and recognized distinct terraces or paleoshorelines occurring between modern sea level and approximately 29-30 meters above MSL; Wicomico, ~29-30 m (~ 98 ft); Penholoway, ~23 m (~ 75 ft); Talbot, ~12-14 m (~39-46 ft); Pamlico, ~8 m (~ 26 ft); Princess Anne, ~4.5m (~ 14 ft); and Silver Bluff, ~1.5 m (~ 5 ft). The maximum elevation of Quaternary sea level in Georgia is considered to be the highest elevation of coastal sediments attributed to the Wicomico Terrace or paleoshoreline position (Figure 4-1a and 4-1c). MacNeil attributed the upper Okefenokee shorelines to the Yarmouth interglacial, the Wicomico shoreline to the Sangamon interglacial, the Pamlico shoreline to a mid-Wisconsin glacial retreat, and the Silver Bluff shoreline or the lowest paleoshoreline above modern sea level to a post-Wisconsin retreat.

Subsurface drilling data were linked with the surface deposit data and the Pleistocene deposits were presented as a thin veneer of sediments by Hoyt and Hails (1967), Hoyt, Henry, and Weimer (1968), and Hails and Hoyt (1969). Shoreline elevations were based on the elevations of fossil burrows of *Callichirus major* (Say, 1818; Rodrigues, 1983). This veneer of sediment and associated barrier island deposits were interpreted as the result of sea level fluctuations during the Pleistocene with each interglacial episode resulting in the formation of a paleoshoreline and associated barrier island complex. This interpretation was complicated by the condition that shorelines associated with glaciations were located below modern sea level

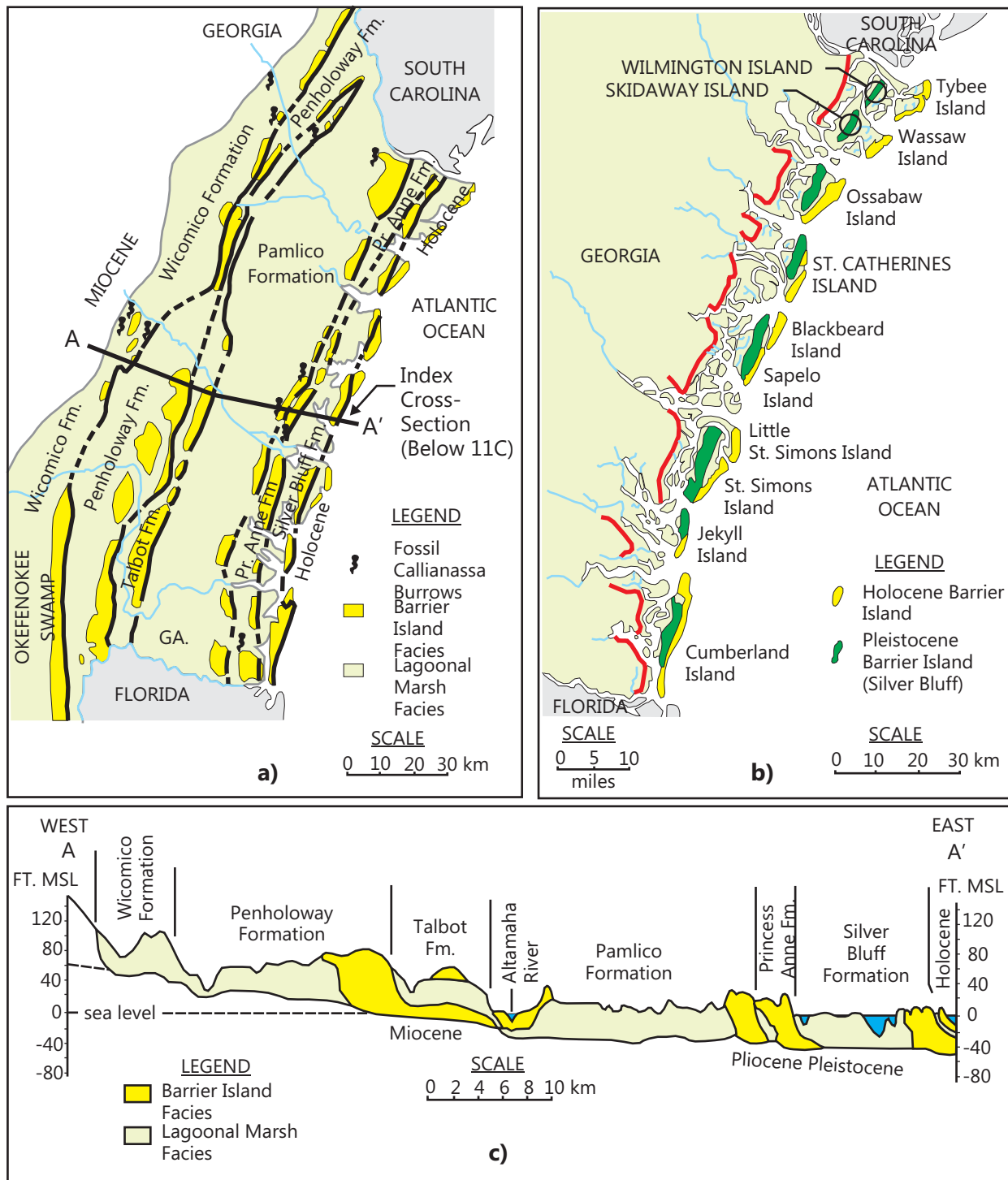


Figure 4-1: Development of successive shorelines on the Georgia Coast. a) Successive shorelines, headlands, and intervening marshes; b) Silver Bluff Pleistocene and Holocene Shorelines of Georgia forming the modern “Golden Isles”; and c) Cross-section of Pleistocene sediment veneer of Georgia Coastal Plain (after Hails and Hoyt (1969); Hoyt and Hails (1967)).

(Stapor and Mathews, 1983; Gayes et al., 1992). This condition was rectified when DePratter and Howard (1977) dated subtidal archaeological artifacts and vertebrate fossils and subsequently, when shallow continental shelf investigations allowed for partial reconstruction of low stands (Garrison, 2008). The analysis and direct dating of vibracore and hand collected samples from Gray's Reef National Marine Sanctuary and J-Reef have indicated a subaerial exposure of the coastal plain on the area occupied by the present continental shelf from MIS 3 through late MIS 2 (~ 60,000- 24,000 BP) with the subsequent, post- Last Glacial Maximum (LGM) transgression. DePratter and Howard recovered a bone antler tool and a projectile point that were typologically assigned to the early Middle Archaic Period (~ 8000 B.P.), indicating that sea level recovered to shallow subtidal conditions with respect to modern sea level by ~ 8000 BP. Based on the occurrence of ceramics, peats and submerged stumps, DePratter and Howard (1981) also indicate sea level on the Georgia and South Carolina coasts reached -1.5 to -2 meters MSL by 4500 B.P. At approximately 3000 B.P., a regression eventually decreased sea level to -3m to -4m MSL or greater. An ensuing transgression occurred, bringing sea level to its modern position by 2,400 B.P. A vibracore sample collected from the Cracker Tom Hammock area of St. Catherines Island corroborates this information, yielding a radiocarbon date of  $6020 \pm 50$  B.P for a charcoal sample that was preserved in intertidal to subtidal sediments above an unconformity at approximately -3.3 meters with respect to modern MSL. An underlying peat sample yielded a radiocarbon date of  $47,620 \pm 2500$  B.P. (Bishop et al., 2007). A Holocene transgression or small-scale high stand of sea level at approximately 1.5 meters below modern sea level is noted by Gayes et al. (1992) and Scott and Collins (1995) in a Murrells Inlet, South Carolina study area at ~ 4300 B.P.



Hails and Hoyt (1969), Hoyt and Hails (1967), Pickering et al., (1976), Linsley (1993), Linsley et al. (2008), Bishop et al. (2007), and Thomas et al. (2008) have noted that the outer or most recent sets of Georgia barrier islands typically consist of “doublets” with older Pleistocene sediments deposited 35,000-40,000 B.P. associated with the younger Holocene (4000-5000 B.P.) sediments situated or “docked” to the east (Figure 4-1b). The Pleistocene sediments of St. Catherines Island were examined in the limited exposures of the island core by Linsley (1993) who noted a marine origin for the sediments and that sea level was approximately 2.0 meters above modern mean sea level based on the occurrence of sedimentary structures and trace fossils. The oldest known Holocene sediments of St. Catherines Island are forebeach deposits that date to approximately 6020 B.P. overlying a peat that yields a date of  $47,620 \pm -2500$  B.P., representing a hiatus of over 41,000 years that resulted from the LGM and associated marine regression (Booth et al., 1999).

Variations in the elevations of the marine terraces and shoreline complexes indicate that in addition to eustatic controls, tectonic forces have also been a significant control in the lower coastal plain. Challenges to correlating the marine terraces and scarps were noted by Winker and Howard (1977) who adopted a new classification scheme (Chatham, Effingham, and Trail Ridge sequences) for the associated paleo-shorelines. Winker and Howard noted elevation changes along the Orangeburg-Trail Ridge shoreline of up to 50 meters indicating significant upwarping/downwarping, and changes in drainage patterns. West of the Talbot shoreline they noted well developed trellis-style drainage networks and landforms, whereas a dendritic pattern was noted to the east of the Talbot shoreline. Bartholomew and Rich (2012) also recognize significant tectonic influence on drainage systems of the southeastern Appalachian Piedmont and Coastal Plain.

Studies have also been conducted on the geology of the Georgia Coast to gain a better understanding of the depositional controls that concentrate heavy mineral sands, (Smith et al., 1968, Pirkle et al.1991, Pirkle et al. 2007) in order to improve prospecting and recovery operations for the economic deposits. Bishop (1990) studied heavy mineral sand deposits on St. Catherines Island and documented accumulation in the backbeach, backbeach dune fields, and mid-beach areas as a result of swash winnowing and eolian processes. Vance and Pirkle (2007) summarized the distribution, transport and provenance of heavy minerals on the Georgia Coast. The heavy mineral sands of the Atlantic Coastal Plain have been concentrated by various chemical and physical processes (Vance and Pirkle, 2007). Concentration of heavy minerals is initiated during chemical weathering of the parent rocks. Titanium is originally concentrated during weathering of the parent rock to saprolite, where the removal of iron from the primary hematite lamellae is initiated during weathering processes. Titanium is finally concentrated in heavy mineral sands through the leaching of iron and the alteration of ilmenite to leucoxene (Force, 1976; Force and Rich, 1989). The importance of the microfracturing of ilmenite grains and resulting increase in surface area whereby the removal of iron is facilitated by weathering was demonstrated by Lener (1997) in the Old Hickory Deposit of Sussex and Dinwiddie Counties in Virginia. While geochemical models exist for both reducing and oxidizing conditions that demonstrate the alteration of ilmenite and removal of iron, the process is more favorable under acidic and reducing conditions where the solubility of iron is greatly increased through the complexation with organic acids (Drever and Vance, 1994; Lener, 1997). The wet and acidic environmental conditions of the lower Atlantic Coastal Plain also favor this pathway with humates being commonly associated with the older Pliocene-aged Trail Ridge heavy mineral sands and the younger Pleistocene heavy mineral deposits. Carpenter and Carpenter

(1991) attributed decreasing TiO<sub>2</sub> concentrations with depth in heavy mineral sands of Virginia-North Carolina to a fluctuating water table and oxidizing conditions.

The gravity segregation of particles via sorting of the heavy minerals with greater specific gravity values versus quartz sands is the primary mechanism for the concentration of heavy minerals in detrital placer deposits. Marine regressions and seaward transport of heavy minerals were proposed as mechanisms for heavy mineral sands concentration by Garnar and Stanaway (1994). The combination of a marine transgression and winnowing by wind of heavy mineral lag deposits are also noted as possible scenarios for heavy mineral concentrations (Bishop and Marsh, 1998; Garnar and Stanaway, 1994).

The heavy mineral content in Pleistocene and Holocene sediments that comprise the lower Coastal Plain and barrier islands of Georgia are dominated by ilmenite, leucoxene, rutile, and zircon (Pirkle and Pirkle, 2007). Minor concentrations of kyanite/sillimanite, staurolite, spinel, corundum, tourmaline, monazite/xenotime, garnet, epidote, and hornblende are also found in the heavy mineral assemblages (Pirkle and Pirkle, 2007). HMS deposits are associated with the three major shoreline sequences identified by Winker and Howard (1977): 1) the Trail Ridge Shoreline Sequence; 2) the Effingham Shoreline Sequence; and 3) the Chatham Shoreline Sequence. The Trail Ridge Shoreline Sequence is associated with the Wicomico and Okefenokee terraces and an associated sea level stand of 29 to 31 meters above mean sea level (29-31 m), and is considered to represent the maximum transgression during the Pliocene. The Effingham Shoreline Sequence includes the Penholoway (21-23 m) and Talbot (12-14m) terraces and associated sea level stands and is designated as Pleistocene in age (Winker and Howard, 1977). The Chatham Shoreline Sequence includes the Pamlico (8 m), Princess Anne (4 m), and

Silver Bluff (1.4 m) Pleistocene aged deposits and Holocene sea level sediments on the eastern margin.

A summary of the mineral occurrence and weight percentages of the minerals (% of total heavy minerals) associated with the HMS deposits are included as Table 1. The heavy mineral assemblage in the samples is reasonably consistent except that garnet, monazite or epidote were not identified in Trail Ridge samples or were only reported in trace amounts. It was noted that the Okefenokee Terrace sediments were the local source material for the Trail Ridge materials and that no garnet, monazite or epidote occurs in the Okefenokee Terrace sediments (Pirkle and Yoho, 1970). Ilmenite ranged from 31.0% to 62.0% by weight, leucoxene ranged from 1.7% to 27.0%, and rutile ranged from 1.7% to 10.0% of the weight of the total heavy minerals in the selected samples from the Atlantic Coastal Plain. Zircon ranged from 4.9% to 20.6 %, kyanite/sillimanite ranged from 5.1% to 17.5%, and staurolite ranged from 3.7% to 19.5% in weight percentage of the total heavy minerals.

#### **4.2 Study Area Geological Setting**

The island is comprised of three major geomorphic components; 1) The Pleistocene Island Core, 2) Holocene Accretional Terrains, and 3) Holocene Marshes (Figure 4-2). The island core is a relatively high topographic feature with little relief that occupies the western portion of the island complex and was previously assigned to the Silver Bluff Shoreline Complex (Hails and Hoyt, 1969). The Holocene Accretional Terrains are situated on the northern and southeastern portions of the island and consist of progradational beach ridge and swale sediments. The beach ridges are parallel to subparallel sand ridges generally reaching 3 to 4 meters in elevation and separated by swales that are currently intertidal to supratidal. Beach

**Table 1:**  
**Mineralogy of Heavy Mineral Sands, Selected Localities from Southeast Georgia and Northeast Florida**

Heavy Minerals	Trail Ridge Shoreline Sequence: Pliocene			Effingham Shoreline Sequence: Pleistocene				Chatham Shoreline Sequence : Pleistocene-Holocene							
	Trail Ridge #1	Trail Ridge #2	Highland (Maxville)	Folkston	Boulougne	Green Cove Springs #1	Green Cove Springs #2	Jacksonville (min)	Jacksonville (max)	Yulee	Cabin Bluff	Altama	Little Talbot Island	Amelia Island	Mineral City
Ilmenite	34.7	36.8	32.8	31	35.2	47	33.8	38	40	52.7	62	54.6	31	37	47
Lecoxene	7.9	14.3	10.1	27	19.8	6.4	2.2	4	10	2.2	3	1.7	4.8	9.7	3
Rutile	3.4	1.7	1.8	7	6.8	4.6	7.4	7	10	7.4	5.6	6.9	3.4	4.6	5.4
Zircon	20.6	15	16.2	9	13	15.1	16	10	15	16	14.1	10.5	4.9	11.2	11.1
Kyanite/Sillimanite	17.5		12.3			6.7				6.7	5.1	8.4			
Staurolite	11		19.5			9.4				5.2	3.7	6			
Spinel	0		0.1			0.1						0			
Corundum	0.6		0.4			0.3					0.1	0.1			
Tourmaline	4.2		6.7			6.2				1.7	1.4	2.7			
Monazite/Xenotime	0.1	0.03	0.1	1	0.5	0.7	0.2	0.5	0.7		1.7	0.9	0.1	0.2	0.8
Garnet	0		0			0.5				0.4	0.8	0.3			
Epidote	0		0			3.1				6.6	1.8	7.3			
Hornblende	0		0			0.1				0.8	0.8	0.6			

Notes:

1) Percent of heavy minerals in HMS from selected localities, Southeast Georgia and Northeast Florida, data from Pirkle et al., 1991 and Elsner, 1997

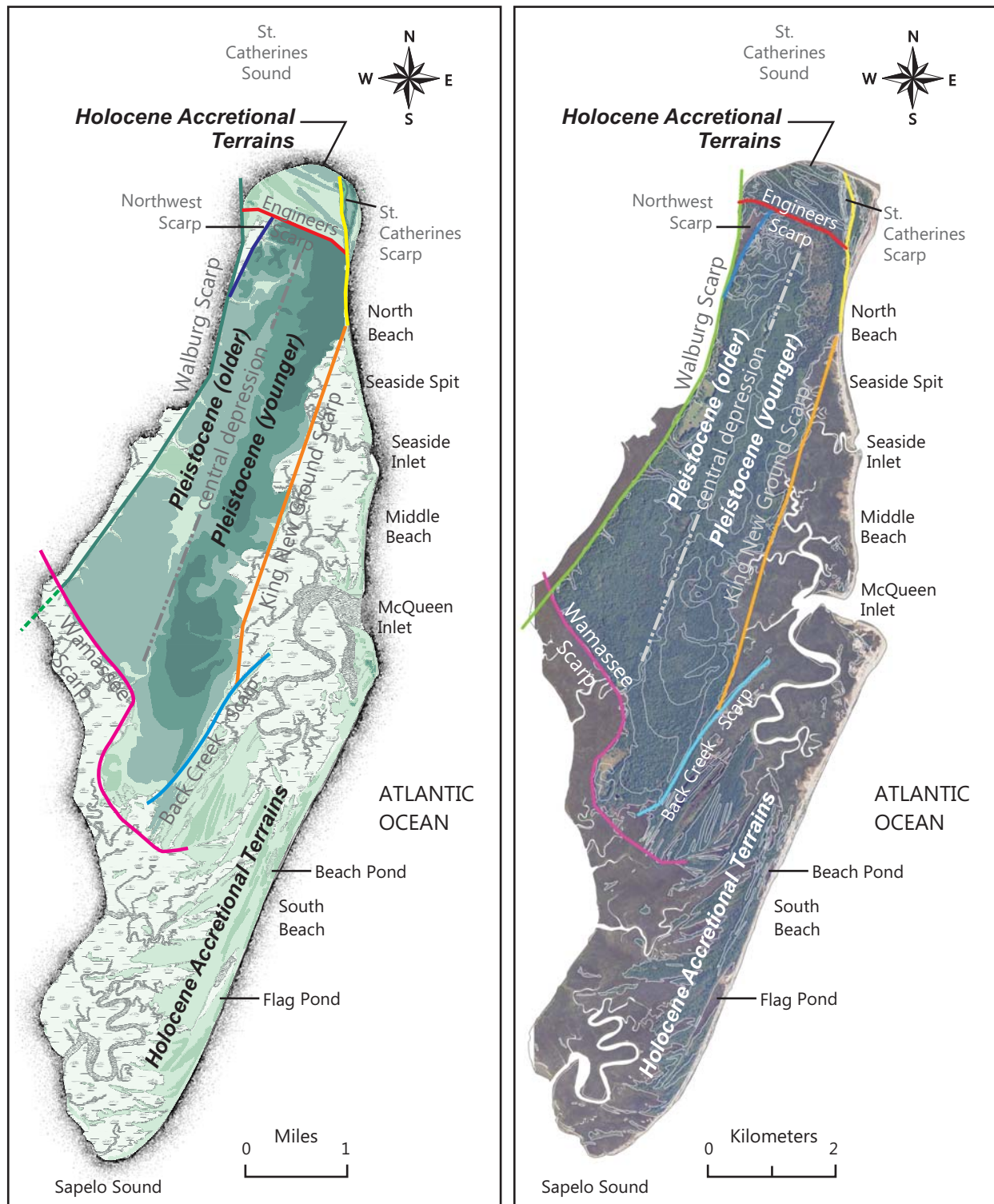


Figure 4-2: Geology and topography of St. Catherines Island showing the Pleistocene Island Core and Holocene Accretional Terrains. Beach Pond and Flag Pond are located in the Southeast Holocene Accretional terrains in sediments that were deposited as dune and swale complexes where the ponds were originally situated in former swales or topographic lower areas. After Bishop et al., (2007); Linsley, Bishop, and Rollins (2008); data from Meyer et al., (2009).

Pond and Flag Pond are former fresh water wetlands located in the southeastern Holocene Accretional Terrains and are situated in the topographically lower swales of the beach or dune ridge systems.

#### *4.2.1 Island Core*

Based on previous investigations, the island core is mostly composed of Late Pleistocene barrier island deposits initially assigned to the Silver Bluff Shoreline Complex (Hails and Hoyt, 1969). These deposits were reclassified as the Satilla Formation by Huddleston (1998) and are typically tan to light brown fine to medium grained sands that have been extensively bioturbated by modern vegetation to depths of two to three meters below the modern surface. The island core reaches elevations of five to seven meters above mean sea level with moderate to little relief and is slightly higher in elevation on the eastern portions of the core. A series of linear depressions can be traced along the middle of the island core trending in a north-northeast to south-southwest direction and are collectively referred to as the “Central Depression”. Ground penetrating radar investigations in the Central Depression reveal local subsurface features that have a synformal cross-sectional profile. The features are tentatively interpreted as sag structures that are the surface expressions of subsurface dissolution in the Eocene carbonates that comprise the upper Floridan Aquifer System (Vance, et al, 2011). Numerous Late Archaic archeological sites have been located in close proximity to the Central Depression and historical accounts describe spring-fed meadows and streams originating from the area (Hayes and Thomas, 2008). Palynological investigation of a vibracore sample extracted from a remnant fresh water marsh supports the former existence of these surface depressions as open fresh water wetlands (Ferguson et al., 2012). At the turn of the 19<sup>th</sup> century, artesian wells located on the

island had hydraulic heads ~ 45 feet above land surface: however, the current Floridan Aquifer potentiometric surface is located approximately 50 feet below land surface (Reichard, et al., 2012). Investigations into sediments that occur in the Central Depression and in exposures located on the eastern portion of the island have been performed by Vento and Stahlman (2011). However, these studies were limited in presenting the data in a spatial manner and elevation framework. This data will be evaluated in the current study and incorporated into the results and discussions where appropriate.

#### *4.2.2 Northern Accretional Terrains*

The northern accretional terrains are composed of three major sedimentary packages consisting of multiple beach ridges that have prograded into St. Catherines Sound as a result of sea level dynamics and responses of the inlet throats and adjustments to the tidal prism (Oertel, 1975). As these beach ridges prograded and filled the former southern extent of the inlet, shallowing upward sequences are expected within a facies succession representing subtidal to supratidal depositional environments. A minimal amount of vibracoring has been performed in this area but limited wave cut beach ridge exposures examined under the current project indicate backbeach deposits that are overlain by eolian sands and situated below the modern mean high water line. The three major packages of dune ridges in the northern accretional terrains appear in three distinct orientations indicating that separate processes or changing island-inlet configurations may be responsible for their formation (Figure 4-3). Oertel's studies (1975) of Holocene sediments associated with inlets stated that these accretional sediments are generally deposited in patterns that indicate semi-closed sedimentary cells, or that sediment is reworked in an area around the inlet, and the area is a function of the magnitude(s) and pattern of the



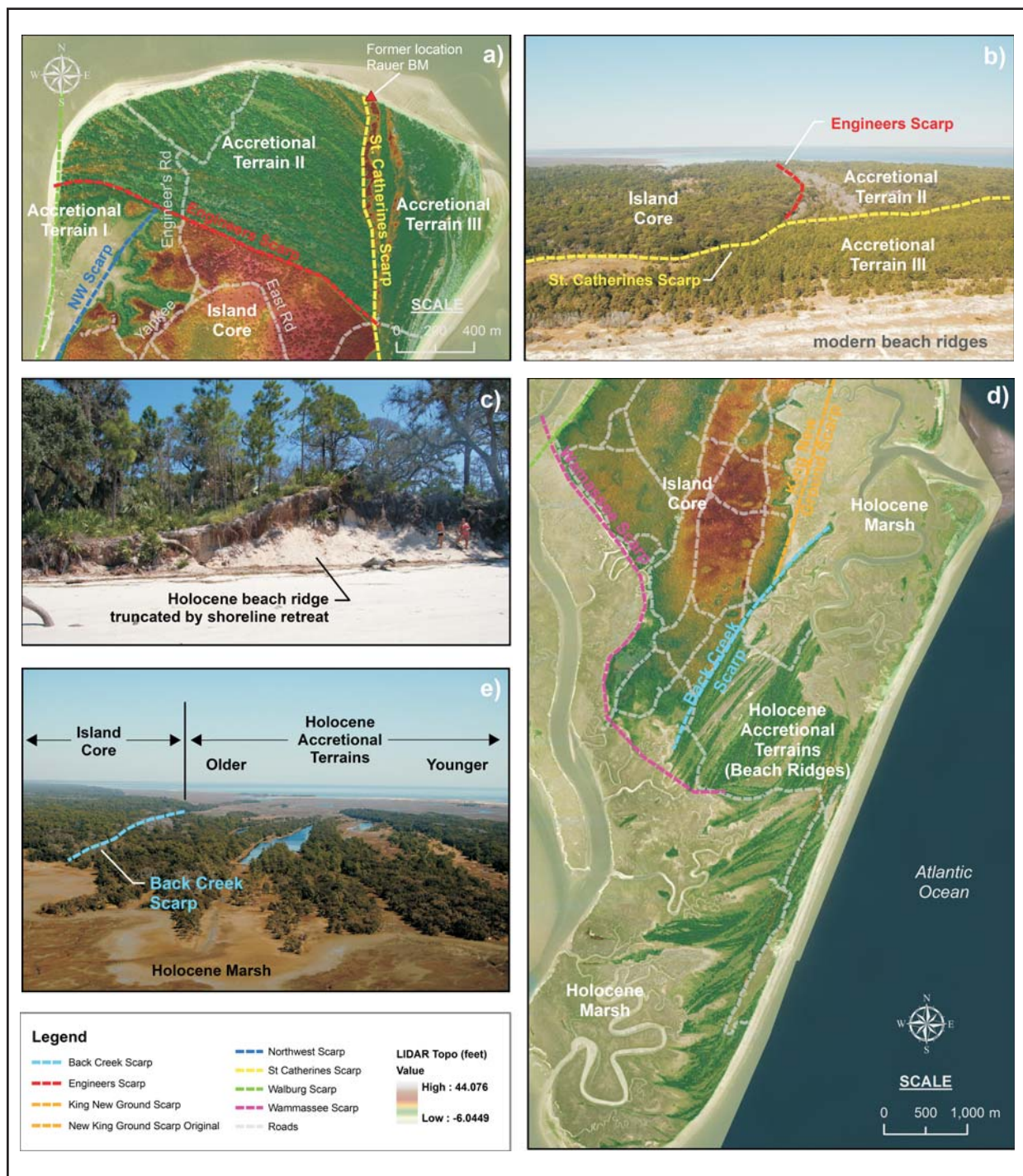


Figure 4-3: Holocene accretional terrains of St. Catherines Island. a) The three sediment packages that occur in the northern accretional terrains of St. Catherines Island are separated by three erosional scarps. The youngest accretional sediment package occurs in the NE portion of the island to the east of St. Catherines Scarp. b) oblique E-W view of the northern accretional terrains, c) truncated beach ridge located on the NW, d) Linear sets of beach ridges are also situated in the southeastern portion of the island and are separated from the island core by the Back Creek Scarp, and E) oblique SW-NE view of the SE terrains and relationship of Back Creek Scarp. LIDAR images in a) and d) from Meyer et al., 2009.

reversing tidal currents. In contrast, the traditional “river of sand” concept that is applied to many barrier island systems provides that sand or sediment is transported along the shoreline in the dominant current direction. Accretion in the downstream or down current direction is the result of the river of sand concept; however, this pattern is not observed at St. Catherines Island which has extensive shoreline retreat associated with the southern portion of the island. Oertel noted that the accretional terrains on the northern end of St. Catherines Island and southern portion of Ossabaw Island have formed with their long axis parallel to the throat of the inlet (St. Catherines Sound) as a result of inlet constriction. Inlet constriction and associated sedimentation is the response when an inlet has a larger throat size than the existing tidal prism. The conclusion is made by Oertel that the inlets have constricted as a result of shoreline retreat, seasonal reversals in longshore currents, and decreasing tidal prisms as a result of lagoonal or marsh deposition.

The three ridge and swale sediment packages that occur in the northern accretional terrains of St. Catherines Island are bounded or separated by three erosional boundaries or scarps (Figures 4-3a and 4-3b) designated as Northwest Scarp, Engineers Scarp, St. Catherines Scarp. The Northwest Scarp trends north-south and separates the oldest accretional sediment package (Accretional Terrain I, Figures 4-3a and 4-3b) from the island core. The Northwest Scarp is located in the northwestern portion of the island adjacent to Gator Creek Marsh. To the immediate north of the island core, Engineers Scarp bounds the southern limits of the second oldest accretional sediment package (Accretional Terrain II, Figures 4-3a and 4-3b) that consists of six sets or packages of beach ridge complexes that extend to the modern shoreline on St. Catherines Sound and is bound by St. Catherines Scarp to the east. The dune ridges located between Engineers Scarp and St. Catherines Scarp are linear in shape, extending to 1,600 feet in

length with a N55°W to N65°W trend and are truncated on the west and northwest by the modern beach (Figure 4-3c). The ridges rise to approximately 3.4 meters (11 feet) above the high tide elevation with the intervening swales varying from 1.5 meters (five feet) to 2.1 meters (seven feet) above the high tide interval. The youngest accretional sediment package (Accretional Terrain III, Figures 4-3a and 4-3b) occurs in the northeastern portion of the island to the east of St. Catherines Scarp. A linear dune ridge set of appreciable height (25 ft. to 27 ft. MSL) and bearing north-south is located to the immediate east of St. Catherines Scarp and denotes the approximate location of the shoreline on the 1867 US Coast and Geodetic Survey Navigational Chart that is based on 1859 planimetric data (Figure 4-3a). A depositional pattern is observed east of St. Catherines Scarp where subsequent beach ridges have prograded toward the east since the late 19<sup>th</sup> century, and beach ridges are currently accumulating along the northeastern shore of the island. Rollins et al. (2011) used historical imagery and demonstrated that three distinct beach ridges were established over a 5-year interval following Hurricane Hugo in 1989.

Vertical accretion has been documented in the northern accretional terrains adjacent to Engineers Road (east). Beach ridges form a small bluff that is four to five meters high along an erosional scarp adjacent to St. Catherines Sound. A charcoal-rich horizon delineates a former land surface and is observed at approximately 100 cm to 150 cm above the high tide elevation (Potter, 2011). Pine trees are also observed with lateral roots occupying positions below the charcoal horizon. A benchmark designated as “Rauer” by the US Coast and Geodetic Survey was originally placed in 1913 at 81.13677° west longitude and 31.69815° north latitude (Figure 4-3a). The benchmark location was recovered in 1933 and replaced with a new marker on the modern surface that was present until shoreline retreat or erosion of the bluff captured the marker

in June 2007. Increment borings obtained by Potter et al. (2011) in a pine tree near the modern benchmark showed 93 total rings and a burn scar on rings nine and ten, indicating a forest fire circa 1924. The current land surface is approximately three meters above the 1924 land surface indicating significant vertical accretion has occurred at an appreciable rate (approx. 3.5 cm/yr.). Detailed measurements have also been conducted in this area by faculty and students of Sewanee: The University of the South since the 1970s. The studies focused on shoreline dynamics and indicate cycles of erosion and relative shoreline stability over the study period. Vertical accretion has been attributed to mechanisms associated with washover and eolian processes.

#### *4.2.3 Southeastern Accretional Terrains*

The southeastern accretional terrains are separated from the island core by a series of scarps. The King New Ground Scarp separates the island core from the Holocene marsh deposits that are located to the east (Figures 4-3d and 4-3e). An emarginated boundary has been developed by meandering tidal creeks eroding into the island core and has been designated as the King New Ground Emarginate Scarp (Bishop et al., 2007). Linear sets of beach ridges are also situated in the southeastern portion of the island and are separated from the island core by the Back Creek Scarp (Figures 4-3d and 4-3e). The beach ridges situated between the island core and the modern shoreline exhibit a strong N35°E to N25°E trend, with selected ridge sets trending east-west or approximately parallel to Sapelo Sound. The ridges rise to approximately 3.4 meters (11 feet) above the high tide elevation with the intervening swales varying from 1.5 meters (five feet) to 2.1 meters (seven feet) above the high tide interval. Several of the beach ridge packages are truncated (bearings nearing N35°E) on their southern terminus. In addition,

numerous beach ridges are observed to the south with trends (N70°E) more closely paralleling Sapelo Sound. These may be analogous to the northern accretional terrains and be linked with accretional and erosional processes associated with the sound margin. A series of vibracores have been collected in the southeastern terrains by Chowens (2011), Bishop, Meyer and Vance (2007), Linsley (1993), and Bishop et al. (2011a). These vibracores yield radiocarbon and OSL dates for select terrains, and archeological materials collected by the AMNH yield dates on cultural materials that constrain the minimum age of formation of select beach ridges. The C<sup>14</sup> and OSL dates indicate shallow marine conditions adjacent to Back Creek Scarp in the Cracker Tom Causeway study area circa 6000 B.P. OSL dates from the beach ridge located to the immediate west of Beach Pond indicate beach ridge formation occurred at approximately 1200 B.P.

#### **4.3 Island Development Model**

A conceptual model for the development of the island was initially formulated by Bishop and refined by Meyer and Bishop during 2009 to 2010 (Bishop et al., 2011b). The model is based on 12 sequential steps that are framed on the relative sequences of scarps, absolute dates of sediments, regional information regarding sea level and several assumptions. Based on the occurrence of eastern marshes and associated relic marsh muds at St. Catherines Island, an assumption was made during the development of the model that a barrier island formerly existed to the east of the current location of St. Catherines Island. Island couplets are observed on the Georgia Coast (Figures 1-1 and 4-1b) such as the St. Simons–Sea Island or Sapelo–Blackbeard Island couplets, and it was assumed that a similar couplet with intervening salt marsh existed at St. Catherines Island prior to removal under the modern transgression (Figure 4-2). The

hypothesized portion of the couplet was designated as Guale Island (Figure 4-4) and incorporated into the island development model with the aforementioned scarps, absolute dates, results from local and regional studies and existing sea level information (Figure 4-5).

Information from previous local and regional studies have been compiled under the current study and supplemented with new vibracore, geochemical and radiocarbon data to better understand the nature of the accretional terrains and document environmental change under the modern marine transgression. Environmental change has been assessed in a horizontal and vertical manner, whereby the spatial changes have been evaluated by creating a shoreline dynamics model to depict the lateral changes in depositional environments. The corresponding vertical succession of depositional environments, as predicted by Walther's Law, were evaluated by collecting core and field observations. The facies, facies successions, and absolute dates that constrain the depositional environments and relative sea level conditions at the time of deposition were evaluated within the context of barrier island evolution under the modern transgression.

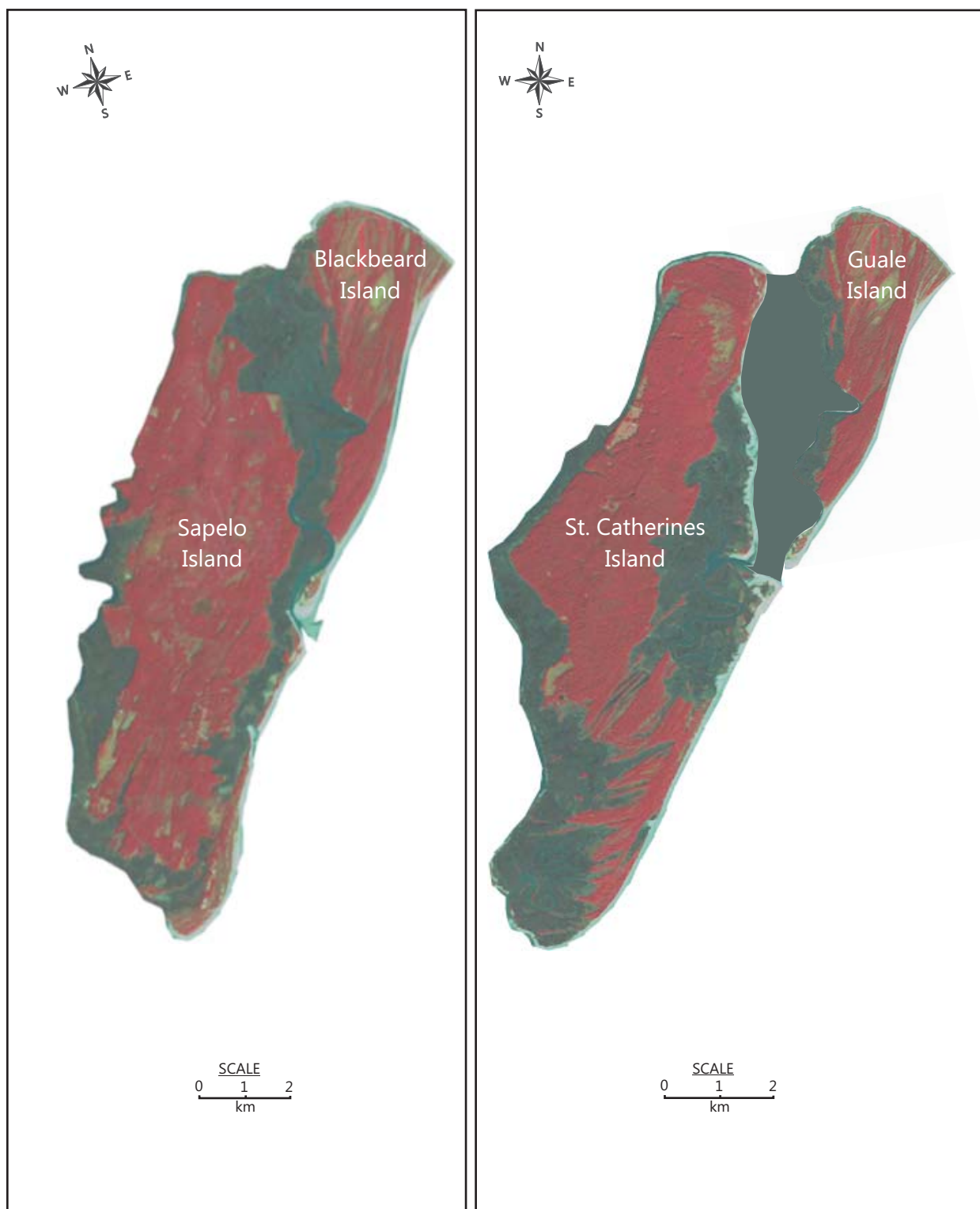


Figure 4-4: Comparison of the Sapelo/Blackbeard Island Doublet with the hypothesized St. Catherines/Guale Island Doublet. Images from 1999 USGS Landsat thematic mapper satellite data, Guale Island image modified from Blackbeard Island by B. Meyer.



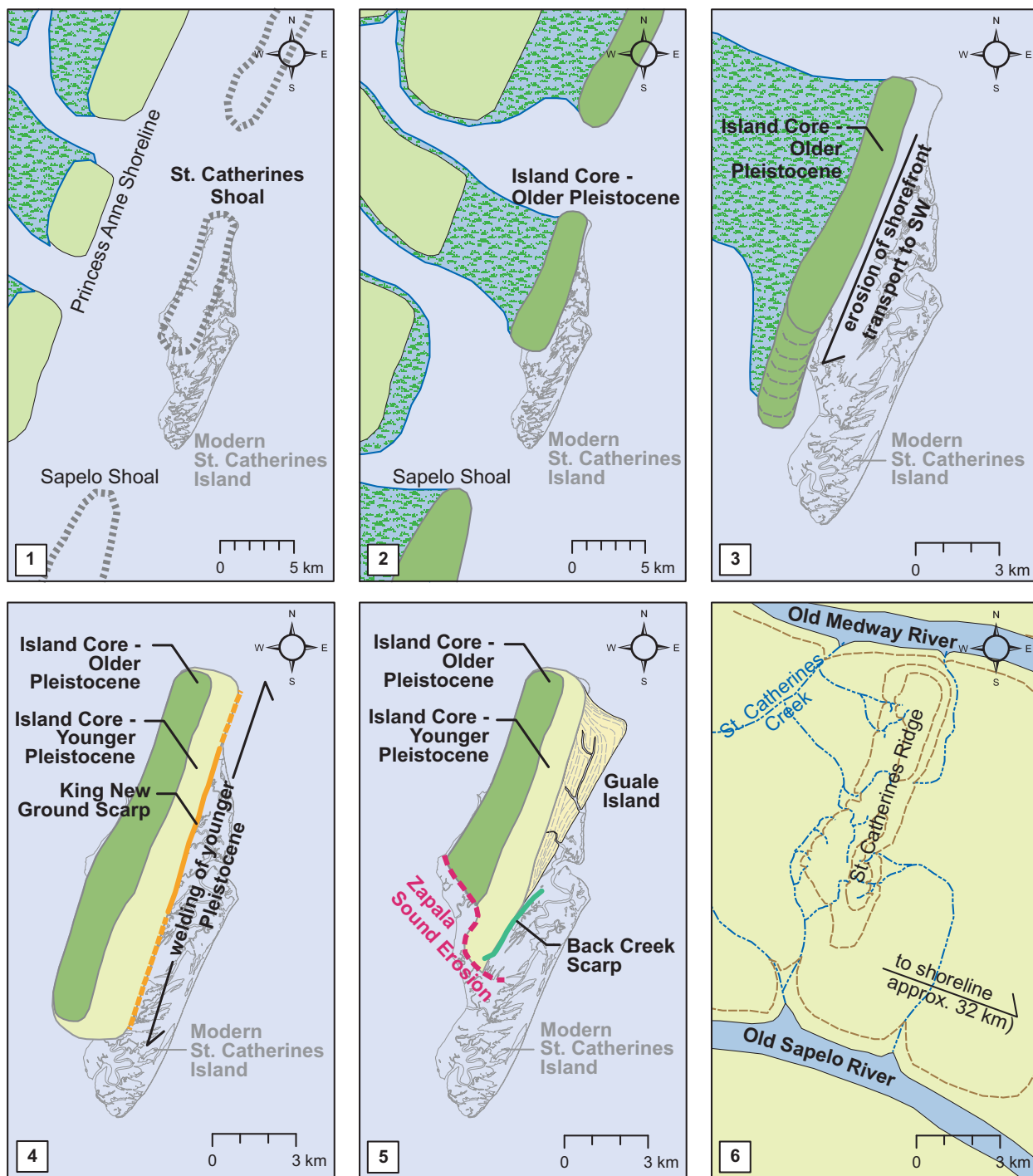


Figure 4-5: Development of St. Catherines Island depicted on background of geomorphology (Bishop et al. 2007) illustrates one possible scenario of Island evolution. 1) St. Catherines shoal at time of deposition of Princess Anne paleoshoreline; 2) Formation of initial Silver Bluff island; 3) Erosion of older Pleistocene results in long, narrow island and adds sediment to the south; 4) Welding of younger Pleistocene onto entire length of island; 5) Erosion meander of Zapala Sound cuts into older Pleistocene coupled with development of complex barrier island doublet St. Catherines/Guale Island; 6) Wisconsin low-stand, shoreline 32 km east near Grays Reef, where the island is part of a low-relief mainland (cont.),



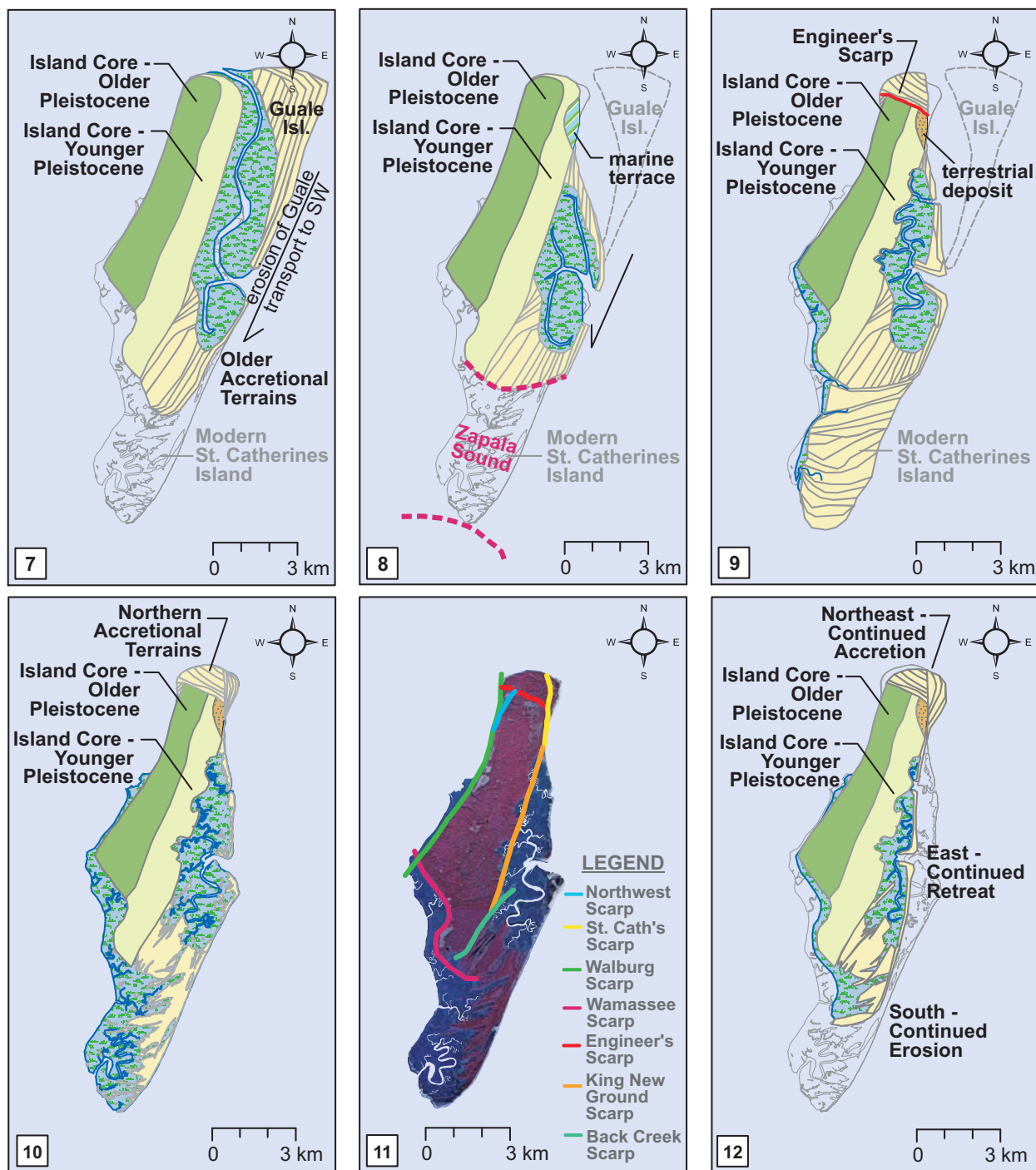


Figure 4-5 (cont.): 7) Sea level rises & new sedimentation pattern causes truncation of south end by northward migration of Zapala Sound as Guale erodes and sediment accumulates on south end, 8) destruction of Guale forms barriers protecting Seaside and McQueen Marshes, resulting in exposure of North Beach to ocean and erosion of a marine terrace as Zapala Sound migrates north, truncating accretional terrains and forming Terrain #6; 9) Sand from Guale continues south as accretional terrains are built on south end, meandering creeks erode emarginations into King New Ground Scarp, and blowing sand refills the terrace with terrestrial sediment, 10) Present configuration of the island as Native Americans found it; 11) Present day island with major scarps overlain, and 12) Future configuration of the island using current accretional/erosional areas.

## 5 RESEARCH METHODS

The methods in evaluating environmental change under the modern transgression and the stratigraphy of the study area include the creation of a shoreline dynamics model to depict the spatial response of the barrier island to rising sea level and the vibracoring of sediments to document and evaluate the vertical changes and successions in depositional environments. The vibracoring data were supplemented with x-ray fluorescence (XRF) scanning of the cores to provide insights into the bulk geochemistry of the sediments in an effort to apply the concept of chemofacies to barrier island sediments and associated depositional environments.

### 5.1 Shoreline Dynamics Methods

Previous studies of shoreline dynamics at St. Catherines Island have indicated significant erosion rates along the majority of the island with very limited areas of accretion (Griffin and Henry, 1984, Potter 2011). Traditional methods of evaluating shoreline dynamics were based on manual cartographic and calculation methods. These traditional methods employed by Griffin and Henry (1984) indicated a net shoreline retreat or erosion rate for 1859-1974 of 4.3 meters per year (m/yr.) along the north-central portion of the island, erosion rates of 2.5 m/yr. along the south central portion of the island, and a significant erosion rate of 8.2 m/yr. along the Sapelo Sound margin (Figure 2-1). More modern methods have employed the use of Geographic Information System (GIS) software to aid in determining shoreline dynamics (Langley, et al., 2003). A recent evaluation of shoreline dynamics by Meyer et al. (2011) used limited data sets and evaluated shoreline dynamics via transects located every 500 meters along the island.

Although statistical analysis was limited and a temporal evaluation was not performed, the study indicated rates on a comparable scale with Griffin and Henry (1984).

### *5.1.1 Methodology*

The United States Geological Survey (USGS) has recently developed and released (August 2010) a new software application, the Digital Shoreline Analysis System (DSAS) Version 4.2, which operates within the Environmental Systems Research Institute (ESRI) ArcGIS software as an extension. DSAS is a freely available or public domain software application that computes rate-of-change statistics for a time series of shoreline vector data. The current study used DSAS Version 4.2, generated statistics of shoreline change, and compared these results against the previous studies of Griffin and Henry (1984) and Meyer et al. (2011) and against the landform type that comprises the terrestrial-marine interface. In addition, the rates of erosion and accretion have been evaluated in a semi-quantitative manner with respect to the island's geology, topography and geomorphology and evaluated for temporal variations correlating to the timing of anthropogenic disruptions in sediment flux rates.

The results from the current study have been provided and reviewed with personnel from the St. Catherines Island conservation, education and research programs for strategic planning purposes. The Sea Turtle Conservation Program practices aggressive sea turtle nest relocation in areas of significant erosion in order to maximize the number of hatchlings for this endangered species. The results from the current study will assist the program in prioritizing nests for relocation and evaluating beaches for nest preservation and incubation success. In addition, the information has been provided to the archaeological research program to aid the American

Museum of Natural history (AMNH) in prioritizing and conserving archaeological and historical resources located on the island.

Shoreline data has been obtained from the various sources that follow and evaluated for statistics of shoreline change. The Shoreline Change (SC) calculation yields a linear distance of the displacement of the shoreline at a defined location. This value is calculated by subtracting the shoreline position at an older date from a younger shoreline position. The shoreline change and resulting rate statistics have been calculated for transects that were generated normal to or perpendicular to the shoreline. These transects were located on 200 meter spacings or centers for the shore normal transects. Given  $n$  shoreline samples, numbered in order from oldest to youngest date where  $Y$  denotes the shoreline position, the SC is:

$$SC = Y_n - Y_1$$

End Point Rates (EPR) have been calculated by dividing the shoreline change of two shorelines by the elapsed time between them to yield a distance-per-time rate. Therefore, the shoreline change rate yielded by the EPR method is the slope of the line between two points. Using  $X$  to denote the date of a shoreline, the EPR is:

$$EPR = (Y_n - Y_1)/(X_n - X_1)$$

Unlike the EPR method, the Linear Regression Rate (LRR) algorithm utilizes all shoreline positions instead of only two data points. The rate calculated by the LRR method is the slope of the line that is the least squares distance to the actual shoreline points and the equation is:

$$LRR = \sigma_{XY} / \sigma_{XX}$$

### 5.1.2 Error/Uncertainty Analysis

A degree of shoreline position error is expected due to internal factors or sources of error including digitizing techniques, image/map quality, GPS data accuracy, and analyst abilities (Anders and Byrnes, 1991; Crowell et al., 1991; Dolan et al, 1991). To facilitate an estimation of the shoreline error, the root mean square error (RMSE) was calculated by comparing predicted points from a registered map or image against points from a highly controlled digital image. As expected, the historical or older maps (prior to 1930) contain relatively higher RMSE values. Other sources of error include the interpretation of the high water line of demarcation, the width of plotted shorelines from maps, and the effects of scale (Dolan et al, 1980). These sources of error were evaluated by assigning a shoreline uncertainty value to each shoreline dataset in the DSAS Model based upon the expected errors inherent in the data source using calculated and published values.

The DSAS Model Version 4.2 allows for a weighted linear regression, whereby more reliable data are given a greater weight or emphasis in determining a best-fit line (Himmelstoss, 2009). In the computation of rate-of-change statistics for shorelines, greater emphasis is placed on data points for which the position uncertainty is smaller. The weight ( $w$ ) is defined as a function of the variance in the uncertainty of the measurement ( $e$ ):

$$w = 1 / (e^2) \quad \text{where } e = \text{shoreline uncertainty value}$$

The uncertainty field of the shoreline feature class is used to calculate a weight. In conjunction with the weighted linear regression rate, the standard error of the estimate (WSE), the standard

error of the slope with user-selected confidence interval (WCI), and the R-squared value (WR2) are reported (Himmelstoss, 2009).

A degree of shoreline position error was expected due to internal factors including digitizing techniques, image/map quality, GPS data accuracy, and analyst abilities (Anders and Byrnes, 1991; Crowell et al., 1991; Dolan et al, 1991). Based on the methods of Fletcher et al. (2003), Genz et al. (2007), and Rooney et al. (2003), seven different sources of uncertainty were evaluated including digitizing error ( $E_d$ ), pixel error ( $E_p$ ), seasonal error ( $E_s$ ), rectification error ( $E_r$ ) tidal fluctuation error ( $E_{td}$ ), T-sheet error ( $E_{ts}$ ), and the conversion error for T-sheets ( $E_{tc}$ ). An additional source of uncertainty is associated with the Positional Dilution of Precision (PDOP) resulting from the ground collected GPS data ( $E_{gps}$ ) as a result of satellite geometry at the time of data collection. The total positional uncertainty ( $E_T$ ) is the root sum of the squares of the individual errors.

- Digitizing Error ( $E_d$ ): Digitizing of the shoreline was performed by one analyst (B. Meyer) to promote consistency and as a result it is considered to be a constant for the various data sources and has been estimated at two meters as compared to literature values that range from 0.5 to 5.7 meters for scenarios using multiple analysts. The GPS point data (2009, 2010 and 2011) do not have a digitizing error associated with the data sets due to the ground collected nature of the data.
- Pixel Error ( $E_p$ ): The pixel error was calculated based upon the resolution of the raster data source and ranges up to 3.5 meters for older T-sheets and low resolution aerial images. The more modern aerial data sets (post-1993) have pixel errors of 1 meter due to the high resolution of the raster data. The GPS point data (2009, 2010 and

- 2011) do not have a raster pixel error associated with the data set due to the ground collected nature of the data.
- Seasonal Error ( $E_s$ ): The location of the shoreline may be influenced by seasonal variation in wind, waves and storms. The seasonal variation is minimized in the current study since the vast majority of the data sets were collected during the Spring to Fall seasons with the exception of the 1999 color infrared imagery (December 30, 1999). It is understood that seasonal error may be significant in microtidal settings where the seasonal variation may compose a significant portion of the tidal range and influence the shoreline position. However, the seasonal error or influence has been estimated to be minimal in the mesotidal setting of the Georgia Bight and therefore it has not been estimated or included in the subsequent uncertainty calculations.
  - Rectification Error ( $E_r$ ): The aerial photographs and images have been orthorectified in the ArcMap environment to reduce errors associated with optics (lens distortions and camera tilt), the Earth's curvature, and terrain relief. To facilitate an estimation of the rectification error, the root mean square error (RMSE) has been calculated for each raster data set by comparing predicted points from a registered map or image against points from a highly controlled digital image. The historical or older maps yield relatively higher RMSE values and these have been noted and considered in the shoreline dynamics evaluations.
  - Tidal Fluctuation Error ( $E_{td}$ ): As opposed to shoreline dynamics studies that use the mean water line or low water line, the current study utilizes the highest water mark that represents the extent of the spring high tides. This line is demarcated in the field and observed in aerial imagery by the location of the wrack line, or the linear feature

produced by the accumulation of vegetative debris at the backbeach to eolian transition zone and is not considered susceptible to small tidal fluctuations. Due to this condition, the tidal fluctuation error has not been estimated or included in the subsequent uncertainty calculations.

- T-sheet Error ( $E_{ts}$ ): T-sheets were produced by surveyors who mapped the high water mark (HWM) in the field using plane tables or transits. Shalowitz's (1964) analysis of topographic surveys identified three major sources of error associated with the T-sheet surveying methods: 1) measuring distances = +/- one meter, 2) plane table or transit position = +/- three meters, and 3) delineation of the high water line = +/- four meters. The total  $E_{ts}$  is the root sum of squares of the three different sources of errors, and equals +/- 5.1 meters. This uncertainty value has been included for the 1859, 1867, 1905, 1916 and 1926 historical navigation charts or T-sheets.
- Conversion Error for T-sheets ( $E_{tc}$ ): This uncertainty is encountered when the high water mark (HWM) is migrated from a T-sheet to a low water mark (LWM) using the surveyed horizontal distance between the HWM and LWM. The current study uses the HWM as the datum and as a result the conversion error for T-sheets error has not been estimated or included in the subsequent uncertainty calculations.
- Ground Collected GPS Error ( $E_{gps}$ ): GPS data accuracy is dependent on several factors including the number and location of satellite vehicles that are available during data collection. Positional Dilution of Precision (PDOP) is a calculated error that correlates to the satellite geometry at a given time and location. A Trimble GeoExplorer XM was used to collect the GPS data and PDOP values ranged from 2.1 to 2.3 meters.



The total positional uncertainty ( $E_T$ ) is the root sum of the squares of the individual errors (Romine et al., 2009; Fletcher et al., 2003).

$$U_T = \text{sqrt} (E_d^2 + E_p^2 + E_s^2 + E_r^2 + E_{td}^2 + E_{ts}^2 + E_{tc}^2 + E_{t_{gps}}^2)$$

$$\text{where } E_s = 0, E_{td} = 0 \text{ and } E_{tc} = 0$$

The total positional uncertainty ( $E_T$ ) has been calculated for each data source using the aforementioned assumptions and is provided in Table 2. The weight ( $w$ ) that is used for the weighted linear regression analysis in DSAS is defined as a function of the variance in the uncertainty of the measurement ( $e$ ):

$$w = 1 / (e^2) \quad \text{where } e = \text{shoreline uncertainty value or } U_T$$

The error inputs and the results of the shoreline uncertainty calculations are provided in Table 2 for the shoreface or eastern portion of the island.

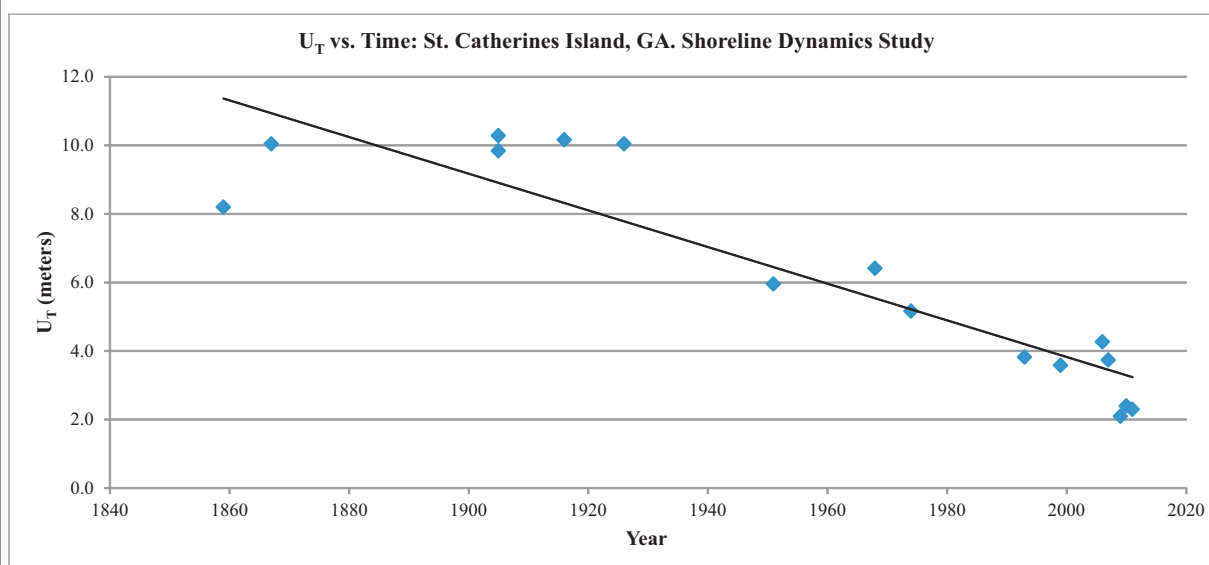
The uncertainty associated with the data sets decrease in general over time as a result of reductions in the errors associated with older data sets such as T-sheets (pre-1951), and the incorporation of more modern data such as higher resolution imagery and the 2009-2011 GPS data. The uncertainty values from Table 2 have been incorporated into the model for the weighted linear regression analysis whereby a greater emphasis is placed on shoreline data for which the positional uncertainty is smaller. In addition, uncertainty was also evaluated and incorporated into the data sets associated with *Mission Santa Catalina de Guale* using accuracy/precision metadata from the AMNH for the 2009-2013 GPS data. The error inputs and the results of the shoreline uncertainty calculations are provided in Table 3 for the *Mission Santa Catalina de Guale* landform dynamics study.

**Table 2:  
Shoreline Uncertainty Evaluation,  
Shoreline Dynamics Study**

Data Source	Scale	Rectification Error ( $E_r$ )	Digitizing Error ( $E_d$ )	Pixel Error ( $E_p$ )	T-sheet Error ( $E_{ts}$ )	Global Positioning System Error ( $E_{gpr}$ )	$U_t$	$w$
1859 Sapelo Sound	1:30,000	5.4	2.0	2.8	5.1	0.0	8.2	0.01
1867 St. Catherines Sound	1:40,000	7.7	2.0	3.5	5.1	0.0	10.0	0.01
1905 Sapelo Sound	1:30,000	8.5	2.0	1.9	5.1	0.0	10.3	0.01
1905 St. Catherines Sound	1:40,000	7.8	2.0	2.6	5.1	0.0	9.8	0.01
1916 Sapelo Sound	1:30,000	8.1	2.0	2.6	5.1	0.0	10.2	0.01
1926 St. Catherines Sound	1:40,000	8.0	2.0	2.6	5.1	0.0	10.0	0.01
1951 Black/White Images	1:32,800	5.5	2.0	1.0	0.0	0.0	6.0	0.03
1968 Black/White Images	1:40,000	5.2	2.0	3.2	0.0	0.0	6.4	0.02
1974 Black/White Images	1:20,500	4.4	2.0	1.8	0.0	0.0	5.2	0.04
1993 Black/White Images	1:6,000	3.1	2.0	1.0	0.0	0.0	3.8	0.07
1999 CIR	1:6,000	2.8	2.0	1.0	0.0	0.0	3.6	0.08
2006 True Color Image	1:6,000	3.2	2.0	2.0	0.0	0.0	4.3	0.05
2007 True Color Image	1:6,000	3.0	2.0	1.0	0.0	0.0	3.7	0.07
2009 GPS (Trimble GeoExplorer XM)	N/A	0.0	0.0	0.0	0.0	2.1	2.1	0.23
2010 GPS (Trimble GeoExplorer XM)	N/A	0.0	0.0	0.0	0.0	2.4	2.4	0.17
2011 GPS (Trimble GeoExplorer XM)	N/A	0.0	0.0	0.0	0.0	2.3	2.3	0.19

Notes:

- 1) Rectification Error: The root mean square error (RMSE) has been calculated for each raster data set by comparing predicted points from a registered map or image against points from a highly controlled digital image
- 2) Digitizing Error: Errors due to digitizing of the shoreline have been minimized by using one analyst.
- 3) Pixel Error: The pixel error was calculated based upon the resolution of the raster data source
- 4) T-Sheet Error: Shalowitz's (1964) analysis of topographic surveys identified three major sources of error associated with the T-sheet surveying methods: 1) measuring distances, 2) plane table or transit position, and 3) delineation of the high water line. The total  $E_{ts}$  is the root sum of squares and equals +/- 5.1 meters.
- 5) GPS Error: the PDOP has been included as a source of error.

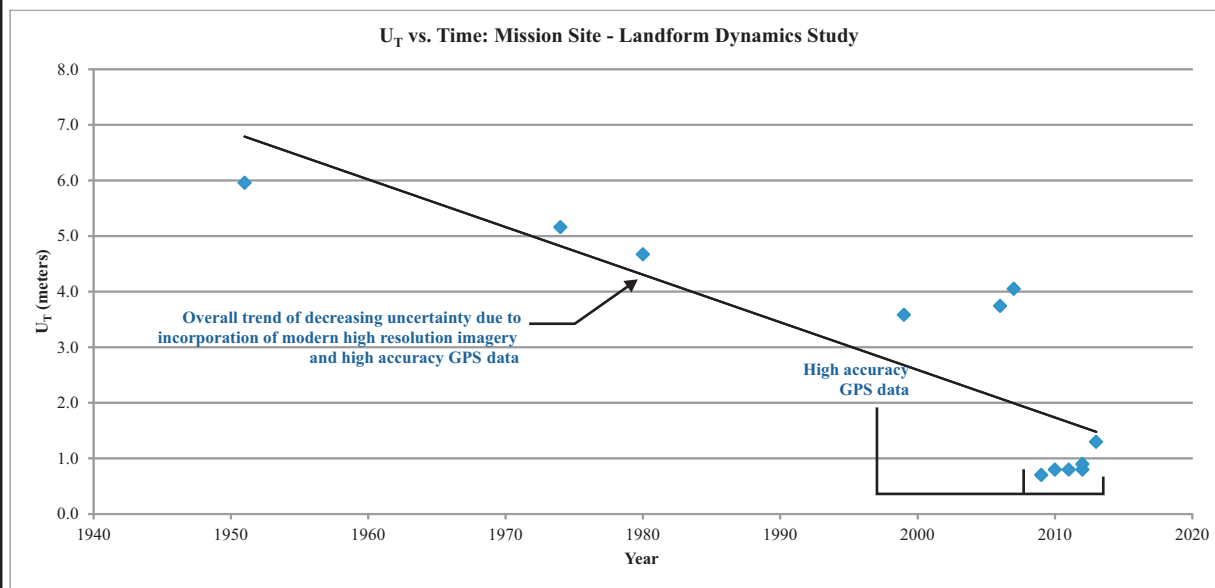


**Table 3:**  
**Shoreline Uncertainty Evaluation,**  
**Mission Santa Catalina de Guala Landform Dynamics Study**

Data Source	Scale	Rectification Error ( $E_r$ )	Digitizing Error ( $E_d$ )	Pixel Error ( $E_p$ )	T-sheet Error ( $E_{ts}$ )	Global Positioning System Error ( $E_{gps}$ )	$U_t$	$w$
1951 Black/White Images	1:32,800	5.5	2.0	1.0	0.0	0.0	6.0	0.03
1974 Black/White Images	1:20,500	4.4	2.0	1.8	0.0	0.0	5.2	0.04
1980 Field Map (AMNH)	1:1,000	4.1	2.0	1.0	0.0	0.0	4.7	0.05
1999 CIR	1:6,000	2.8	2.0	1.0	0.0	0.0	3.6	0.08
2006 True Color Image	1:6,000	3.0	2.0	1.0	0.0	0.0	3.7	0.07
2007 True Color Image	1:30,000	2.9	2.0	2.0	0.0	0.0	4.1	0.06
2009 Shoreline GPS (Trimble GeoExplorer XT)	N/A	0.0	0.0	0.0	0.0	0.7	0.7	2.04
2010 Shoreline GPS (Trimble GeoExplorer XT)	N/A	0.0	0.0	0.0	0.0	0.8	0.8	1.56
2011 Shoreline GPS (Trimble GeoExplorer XT)	N/A	0.0	0.0	0.0	0.0	0.8	0.8	1.56
2012 (Feb.) GPS (Trimble GeoExplorer XT)	N/A	0.0	0.0	0.0	0.0	0.8	0.8	1.56
2012 (May) GPS (Trimble GeoExplorer XT)	N/A	0.0	0.0	0.0	0.0	0.9	0.9	1.23
2013 GPS (Trimble GeoExplorer XT)	N/A	0.0	0.0	0.0	0.0	1.3	1.3	0.59

**Notes:**

- 1) Rectification Error: The root mean square error (RMSE) has been calculated for each raster data set by comparing predicted points from a registered map or image against points from a highly controlled digital image
- 2) Digitizing Error: Errors due to digitizing of the shoreline have been minimized by using one analyst.
- 3) Pixel Error: The pixel error was calculated based upon the resolution of the raster data source
- 4) T-Sheet Error: Shalowitz's (1964) analysis of topographic surveys identified three major sources of error associated with the T-sheet surveying methods: 1) measuring distances, 2) plane table or transit position, and 3) delineation of the high water line. The total  $E_{ts}$  is the root sum of squares and equals +/- 5.1 meters.
- 5) GPS Error: the PDOP has been included as a source of error.



### 5.1.3 Data Sources

Sources for shoreline data were identified including historical navigational charts from the Historical Maps and Images Collection of the National Oceanic and Atmospheric Administration (NOAA), digital orthoimagery from the USGS and USDA National Agricultural Inventory Program (NAIP), LIDAR data from the St. Catherine's Island Foundation (preprocessed by AMNH) and GPS data collected under the current study. Shorelines were digitized and generated from data sets including, but not limited to:

- 1859 Sapelo Sound Chart and 1867 St. Catherines Sound Navigational Chart (NOAA)
- 1899 Georgia Coast Navigational Chart (NOAA)
- 1916 Sapelo Sound Navigational Chart (NOAA)
- 1951 Black/White Aerial Imagery (USGS)
- 1968 Black/White Aerial Imagery (USGS)
- 1968 Ossabaw /St. Catherines Sound Navigational Chart (NOAA)
- 1971 Ossabaw /St. Catherines Sound Navigational Chart (NOAA)
- 1971 Sapelo and Doboy Sound Navigational Chart (NOAA)
- 1974 Black/White Aerial Imagery (USGS)
- 1979 Sapelo Sound and St. Catherines Sound USGS topographic maps (USGS)
- 1982 Color Infrared Imagery (USGS)
- 1993 Black/White Imagery (USDA NAIP)
- 1999 Color Infrared Imagery (USDA NAIP)
- 2005 True Color Imagery (USDA NAIP)
- 2006 True Color Imagery (USDA NAIP)
- 2007 True Color Imagery (USDA NAIP)

- LIDAR Data Personal Geodatabase (2008 Liberty County, GA)
- Global Positioning System (GPS) Data 2009 (B. Meyer)
- Global Positioning System (GPS) Data 2010 (B. Meyer)
- Global Positioning System (GPS) Data 2011 (B. Meyer)

The historical imagery was georeferenced and all imagery, shorelines and supporting data were assembled in a personal geodatabase. The Universal Transverse Mercator map projection (Snyder, 1987) was used for the data sets in Zone 17 North (UTM N17). This projection is appropriate for maps of the conterminous United States because of the visual presentation and equal-area characteristic, which facilitates areal analysis. This projection is frequently used for regional and local digital map data sets and was cast on the North American Datum of 1983 (NAD83).

A process flow chart that depicts the data processing for the shoreline dynamics study has been constructed and is provided in Figure 5-1. The current study used modern methods (DSAS Model) and applies historical and current data to evaluate shoreline dynamics associated with St. Catherines Island and provides an evaluation of more recent erosional/accretional rates with current or modern data, a greater spatial resolution of shoreline dynamics (more closely spaced transects), and a more robust analysis of potential sources of error enabled by the DSAS Model.

## **5.2 Vibracoring Methods**

Vibracoring is a subsurface sediment acquisition (sediment coring) technique that returns sediment preserved within its stratigraphic and sedimentological context (Howard and Frey, 1975). This process generates a continuous sediment sample at a location by vibrating an

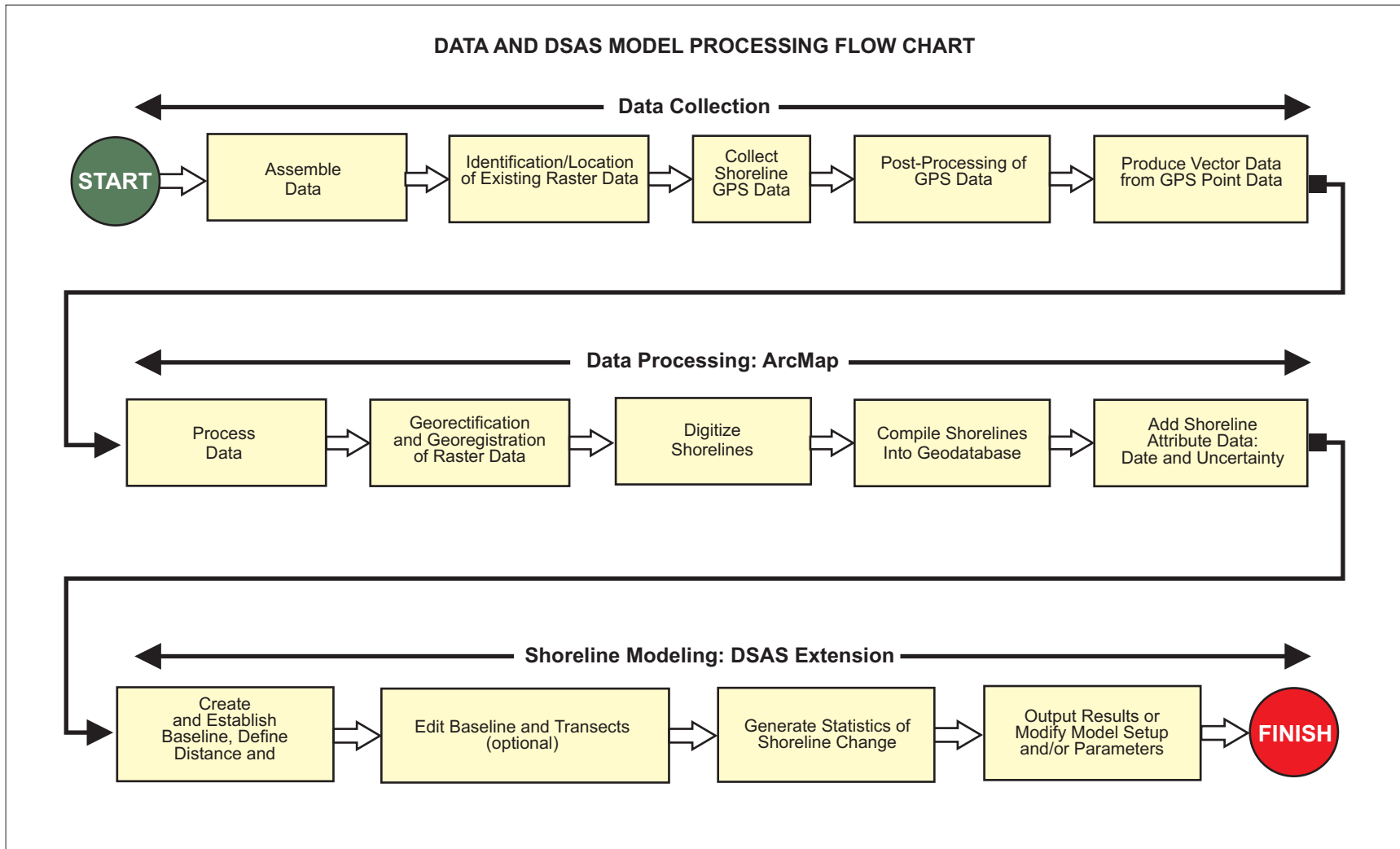


Figure 5-1: The current study utilized the Digital Shoreline Analysis System (DSAS) Version 4.2, that operates within the Environmental Systems Research Institute (ESRI) ArcGIS software as an extension. DSAS is a freely available software application that computes rate-of-change statistics for a time series of shoreline vector data. The current study used DSAS to generate statistics of shoreline change, and compared these results against the previous studies of Griffin and Henry (1984) and Bishop and Meyer (2009). In addition, the rates of erosion and accretion were evaluated with respect to the landforms that comprise the shoreline as an indicator of habitat quality.

aluminum core barrel vertically downward into the sediment. One advantage of vibracoring over more traditional incremental coring techniques is that core depths (up to ~ 7.5 m) can be extracted preserving stratigraphic layering, sedimentary structures, fossils, and lithology in their natural context.

### *5.2.1 Methodology*

The St. Catherines Island vibracoring (SCI VC) rig consists of a gasoline powered engine, a cement vibrator, a clamping device to attach the vibrator onto 20 feet (6.1 meters) long segments of aluminum irrigation pipe (3-inch inside diameter) and an aluminum tripod and a 2-ton endless chain hoist to extract the core barrel from the ground (Figure 5-2a).

The engine spins a flexible cable at high speed that causes the “cammed” or unevenly weighted head at the distal end to create a vibration. The head that clamps to the 3-inch aluminum core barrels causes the core pipe to vibrate and cut its way into the substrate. The vibration reduces the friction on the pipe-sediment interface as well as promoting liquefaction of saturated sediment at the leading edge of the core barrel. Penetration may be enhanced by sharpening or filing serrations into the end of the aluminum pipe, and producing a saw-toothed type of cutting edge. Because the adapter can easily be repositioned up the shaft as the core is vibrated into the substrate, the setup is capable of handling barrels of any length, although extraction of cores longer than 7.5 m becomes problematic. Commercially available twenty-foot core barrel lengths have been found to be optimal for coring operations on St. Catherines Island. Once maximum penetration is accomplished (the length of core barrel or until refusal) drilling is completed. At this point the depth to the sediment surface inside the core pipe is measured and the length of pipe remaining above the ground is measured, and the former is subtracted from the



Figure 5-2: Equipment and methods in vibracoring. a) rig assembly consisting of the tripod, gasoline engine that powers the concrete vibrator via the flexible cable assembly and the vibrator head assembly that connects the vibrator to the 3-inch aluminum pipe, b) worker safety is promoted by utilizing a 2-ton endless chain hoist with safety braking, a safety cable for redundant measure, and a swinging gate to protect against the loss of control of the pipe during advancement/retrieval, c) retrieval of the core using an expanding pipe plug to create a vacuum, a choker cable to grab the pipe, and a grommet cable/hoist connection, d) cores are opened using a circular saw and the assistance of a fabricated wooden box to serve as a jig in guiding a true and safe cut, e) cores are photographed using a fabricated copy stand, and f) a high resolution photographic image is produced using multiple images and a photographic log is produced. Photographs by B. Meyer.



latter to determine compaction of sediment in the core. The core's location and compaction and total depth measurements are recorded in a field notebook. The upper end of the pipe is plugged with an expandable cap such as a sewer plug prior to pulling the pipe section to create a vacuum inside the pipe. The core tube is then extracted using a tripod with an endless chain hoist and polypropylene choker straps or a wire rope choker (Figures 5-2b and 5-2c). The pipe is trimmed to approximately the core length (which is typically less than total depth due to sediment compaction) by cutting the pipe off with a hacksaw or rechargeable Sawzall® just above the top surface of sediment. The core is marked with catalog numbers and orientation indicated by placing consistent arrows and the word top (or up) directly on the aluminum pipe. The core may also be cut into two or three well marked sections in the field to facilitate handling, transport and processing. The location of the core is described in the notebook or on a logging form with global positioning system (GPS) data, longitude and latitude, and an elevation, if available.

Vibracoring is relatively easy to accomplish and the equipment is simple and easy to maintain and transport (Smith, 1984). Penetration success in the vibracoring process, however, is dependent on lithology and sediment pore water saturation; pure dry sands tend to attenuate the vibration of the barrel and slow its descent; saturated mud is easy to penetrate; and rock or semi-lithified sediment will typically stop penetration of the barrel (Hoyt and Demarest, 1981). The vibration of the pipe can be translated to the core sample itself, and may compact the sediments or disrupt laminations or bedding in the sediment, especially along the edges of the pipe surface, causing drag structures. Rapid penetration of the core barrel or pipe minimizes these effects.

### 5.2.2 Data Processing

The core is transported to a laboratory or shelter and opened for subsequent analyses. A wooden guide box that holds the core and allows for straight and true cuts is recommended to improve the quality of the process as well as provide additional safety precautions (Figure 5-2d). An electric circular saw with a carbide blade set to a slightly greater depth of the wall thickness is then used to saw along the straight line on one side of the core. The core tube is rotated 180° and cut a second time along its length. The core is removed from the box carefully to avoid separation and a cut is then made through the sediment with a thin knife, piano wire or a coping saw to separate the core into two hemicylinders. Holding the core with the cut vertical, the core is then allowed to split open laying each half with the cut surface horizontal and upward. The surface of the exposed sediment core is then gently shaved with a sharp knife, trowel or scraping tool to prepare the core for description and photographic purposes. A metric tape or folding metric scale is laid along the length of the core for scale or scaled marks can be placed directly on the core tube at 10 cm intervals. The core is then photographed in a commercially available or custom built photo stand (Figures 5-2e and 5-2f) and described on a logging form. The cores are normally logged from the surface downward, starting at the surface as "0" and logging downward to the total depth (TD) of the core. Logs typically include information such as sediment type, layering, and sedimentary structures and "fossils" if present. In the case of critically detailed work, the compaction of the sediment is proportioned along the length of the log to compensate for compaction. The vibracore data used in the Late Holocene sea level evaluation under the current study was corrected for compaction to provide accurate elevations for radiocarbon samples.

## 5.3 XRF Methods

### 5.3.1 Methodology

X-Ray Fluorescence (XRF) spectrometry is an analytical technique used to determine the elemental composition of a substance or sample. Elements are identified by the emission of characteristic radiation where the intensity of the emission is proportional to the concentration of the element. This is enabled by the generation of high-energy x-ray photons by a source that is typically an isotope or x-ray tube. These high-energy x-ray photons possess sufficient energy to displace electrons from the inner K or L shells, thereby ionizing the atoms. As the atom seeks stability, electrons from the outer shells move inward to occupy the vacant space and emit energy or secondary x-ray photons and the process of fluorescence occurs. The secondary x-ray is characteristic for each element since atoms of a specific element possess a fixed number of electrons with corresponding shells and associated energies. The difference in energy between the initial and final electron shells produces the energy of the x-ray photon and is described by the relationship:

$$E=hc/\lambda$$

where h = Planck's constant; c = the velocity of light; and  $\lambda$  = the characteristic wavelength of the photon.

The energies are inversely proportional to the wavelength and are characteristic for each element. The typical spectra for XRF are presented as a plot of Intensity (I) versus Energy (E). A Field Portable XRF (FPXRF) system is typically composed of three major parts; 1) the excitation source for the primary x-rays, 2) a detector/spectrometer, and 3) a data collection system. The advancement in electronics in the past 20 years have allowed for FPXRF units to be developed allowing for more rapid, precise and accurate XRF data collection (Thomsen and Schatzlein, 2002).

### 5.3.2 Data Collection

Data collection was performed using a field portable Innov-X Systems  $\alpha$ -4000 Model XRF unit (FPXRF). The FPXRF unit features a battery operated miniature x-ray tube (W anode, 10-40 kV, 10–50  $\mu$ A), a high-resolution silicon pin detector (Si PiN diode detector, < 230 eV FWHM at 5.95 keV Mn K-alpha line), high speed data acquisition circuitry, and a Compaq IPAQ Pocket PC handheld computer for data storage and retrieval. The unit is also accompanied by a fixed stand and stage or platform that allows for the scanning of bulk or bagged samples. A mounting unit has been constructed for the current research project that allows for the direct scanning of vibracore samples (Figure 5-3a).

The FPXRF provides analytical results for the elements Pb, Cr, Hg, Cd, Sb, Ti, Mn, Fe, Ni, Cu, Zn, Sn, Ag, As, Se, Ba, Co, Zr, Rb and also features a light element analytical package (LEAP) that provides results for Cr, Cl, P, Ba, Ti, S, Ca, and K (Forouzan et al., 2012). The data has been downloaded and archived at the conclusion of each sample run and reviewed for completeness. The data were imported into a database and the elemental results were joined with pertinent metadata such as the sample boring identification, location and depth to place the samples in the proper spatial locations. The Innov-X XRF analyzer is delivered with a factory calibration based upon the Compton Normalization (CN) method. The CN method provides a robust calibration generally independent of site-specific soil matrix chemistry. FPXRF is a valuable screening tool when benchmarked properly against fixed laboratory methods and results (Glanzman and Closs, 2007). Matrix interference, sample heterogeneity, particle size, interfering element spectra, and moisture content may affect FPXRF results. The U.S. EPA Office of Solid Waste SW-846 Method 6200 provides standard operating procedures for FPXRF including sample preparation, quality control (QC) and quality assurance (QA) processes. The QA

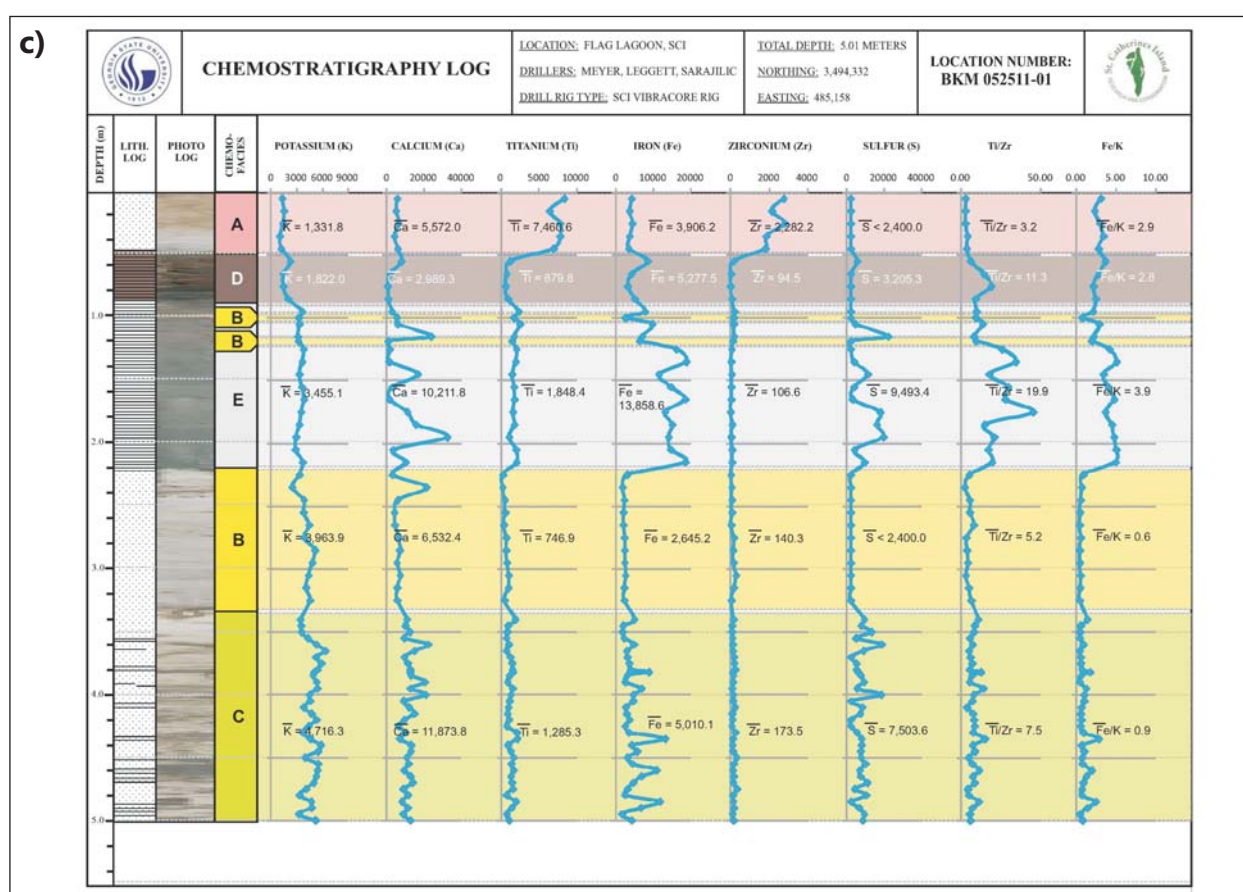
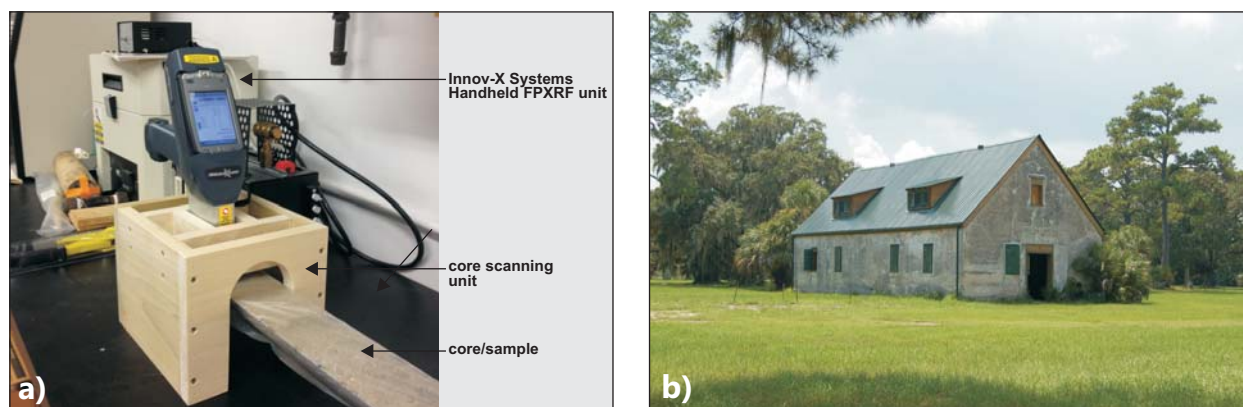


Figure 5-3: Equipment and methods in XRF analysis of cores and reference samples. a) a wooden structure has been fabricated to allow for the XRF scanning of cores, b) the restored 1830s horse barn at St. Catherine's Island that serves as the vibracore equipment/sample storage and core processing laboratory, c) typical chemostratigraphic log being generated by the assembly of lithologic, digital imaging, and XRF data from cores under the current project. Evaluating the FPXRF data in the format of a stratigraphic log with supporting lithological information constitutes a chemostratigraphic study, where the sedimentary sequence may be evaluated as geochemically distinct units. The FPXRF data has been subjected to a multivariate cluster analysis (CA). CA is a statistical tool used to organize, partition or group observed data into meaningful groups or homogenous classes based on independent variables.

procedures include instrument calibration verification, determination of instrument precision, accuracy & limits of detection (EPA, 2007). EPA Method 6200 recommends confirmation of 5-10% of the samples tested by FPXRF with fixed laboratory analysis (i.e. ICP, EDXRF). This is typically performed through the collection of duplicate samples that are analyzed via FPXRF and fixed laboratory methods and a comparison of target analyte results is performed to determine a correlation coefficient for each element of interest. If an acceptable correlation exists between the FPXRF and the fixed laboratory results this coefficient may then be applied to FPXRF results.

### *5.3.3 Data Processing and Analysis*

The elemental data has been used to generate log plots that were assembled with the high-resolution photographic logs and lithological descriptions to produce chemostratigraphic logs (Figure 5-4) and document changes in bulk geochemistry under the modern transgression. Evaluating the FPXRF data in the format of a stratigraphic log with supporting lithological information constitutes a chemostratigraphic study, whereby the sedimentary sequence may be evaluated as geochemically distinct units (Winchester and Max, 1996; Pearce et al., 1999; Reátegui et al., 2005).

The FPXRF data were subjected to a multivariate cluster analysis (CA). Cluster analysis (CA) is a statistical technique related to an analysis of variance, producing groups or clusters of data based on information that defines the groups and relationships (Tan et al., 2005), and is distinctly different from the cluster analysis of spatial data that evaluates the geographical similarities or differences in the attributes of spatial data. The goals of CA are to create groups that have similar variable relationships and to create groups that are different or more distinct

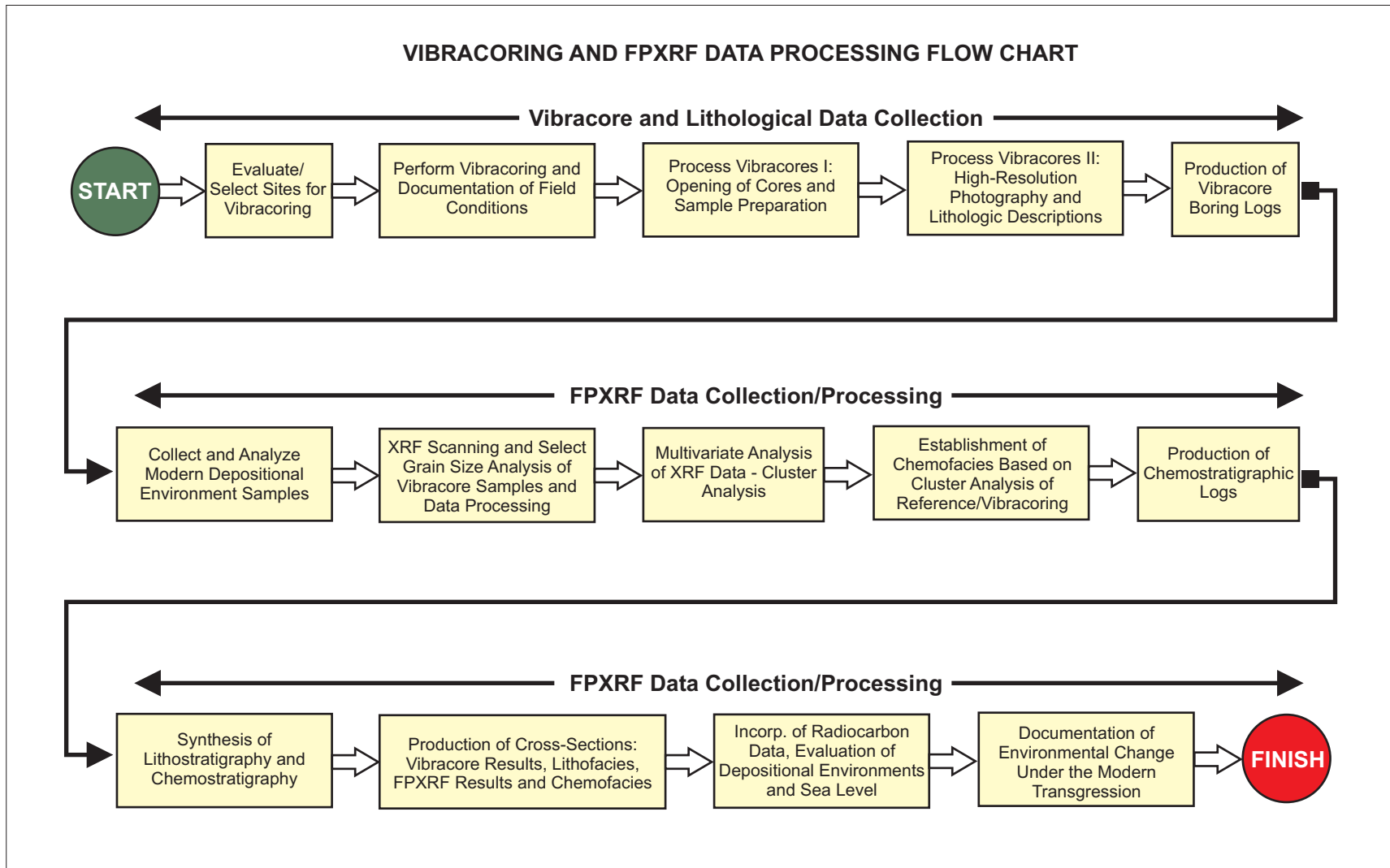


Figure 5-4: Vibracoring was performed to evaluate environmental change at Beach Pond, Flag Pond and Seaside Spit, to test/refine the mesotidal setting washover fan model and cores were collected on North Beach to evaluate timing/location of the hypothesized Guale Island. Cores were processed and supplemented with FPXRF data to determine the applicability of the concept of chemofacies to barrier island sediments. Radiocarbon data was used to determine the timing of events with respect to sea level conditions.

from other groups (Kachigan, 1991). The three most commonly used procedures for cluster analysis are the Two-Step, Hierarchical, and K-Means Cluster Analyses. Different algorithms are used for each procedure and each method has distinct strengths dependent on prior knowledge of the clusters, number of cases (samples), etc.

The hierarchical cluster procedure identifies homogenous groups of variables or cases (samples) based on similar characteristics and may be used for continuous, binary and count types of variables but limited to several hundreds of objects. Clusters are formed sequentially in a “nested” fashion under the hierarchical cluster analysis method. An algorithm is used where samples are considered as individual clusters in the initial step and the process continues through steps or stages until one cluster is produced. The output typically is produced as a dendrogram and statistics are generated at each step to evaluate the solution.

The Ward’s method of cluster analysis is typically used when there is no prior knowledge of the number of data clusters or which variables define the clusters. The Ward’s Method uses an analysis of variance approach (ANOVA) to determine the distances among the clusters. The inclusion in a cluster is evaluated by determining the total sum of squared deviations from a cluster mean. Clusters are joined or fused to produce the minimal increase in the error sum of the squares.

The k-means cluster method is used for continuous data when there is prior knowledge of the number of clusters, the variables that define the clusters are established, or to test hypotheses concerning the number of clusters.

The Two-Step procedure is a common approach to cluster analysis and allows the user to select from various cluster models and automatically determine the best quantity of clusters. The similarity in clusters can be evaluated by the Euclidean measure where the distance between



clusters is measured by a straight line, or by log likelihood measure that uses a probability distribution on variables, where variables are assumed to be normally distributed.

A common approach to cluster analysis is to utilize the hierarchical and the k-means techniques in succession. The hierarchical method is used to visualize the dendrogram and identify the number of clusters. A k-means cluster analysis is then performed where the selected number of clusters is used for the data set.

#### *5.3.4 Current Study Approach*

Initial attempts at performing cluster analysis using the entire FPXRF database and multiple variables were unproductive under the Two-Step approach. This approach resulted in more than 90% of the samples being placed into one cluster. A hybrid approach has been devised using the samples from single borings and five variables consisting of selected analytes (K, Fe, S, Ti and Zr). These are subjected to a hierarchical approach and three to five clusters are typically identified in XRF data from one core. A k-means cluster analysis is then performed on the data where the number of clusters indicated by the hierarchical approach is used for the analysis. These clusters are then separated from the data set and subjected to an additional step using the hybrid approach. This approach has generally resulted in sandy lithologies being separated from muddy lithologies under the initial step using the hybrid approach, and the subsequent hybrid approach results in the separation of these clusters into additional clusters. For examples, the initial hybrid approach identified a sandy facies dataset that was subsequently separated into a relatively higher concentration Ti and Zr cluster and a lower concentration Ti and Zr cluster. The relative abundance of Ti and Zr are controlled by the common minerals in HMS, or the abundance of ilmenite, leucoxene, rutile, and zircon (Pirkle and Pirkle, 2007).

Minor concentrations of kyanite/sillimanite, staurolite, spinel, corundum, tourmaline, monazite/xenotime, garnet, epidote, and hornblende are also found in the heavy mineral assemblages (Pirkle and Pirkle, 2007).

In addition to evaluating CA as a tool for partitioning FPXRF data and creating meaningful groups, the results were evaluated using the interpreted depositional environments from the vibracore data. Each sample was assigned a code based on the interpreted depositional environment, and descriptive statistics were generated. The interpreted depositional environment plots were compared to the chemofacies plots and are provided and described in the results section.

#### **5.4 Evaluation of Late Holocene Sea Level Conditions**

The relationship of the depositional environments and subenvironments with respect to mean sea level has been evaluated under the current study and by previous researchers (Howard and Scott, 1983; Howard and Frey, 1980). The vibracore data were evaluated with respect to facies and associated depositional environments/subenvironments using the relationship of the depositional environments and subenvironments with respect to mean sea level. The understanding of mean sea level based on the facies was used with radiocarbon data to evaluate sea level conditions at St. Catherines Island during the Late Holocene. Attempts were made to utilize marine shells from organisms that occur within the depositional environment associated with the sedimentary facies or to use indigenous versus exotic materials for radiocarbon analysis. In addition, marine shells were selected with minor abrasion to minimize the potential for reworked or transported materials. These objectives were applied to vibracore data and radiocarbon samples from low energy and high energy environments.

### 5.4.1 Background

Intertidal low energy sediments are directly connected to the tidal range and regime of the depositional environment. The use of intertidal environments in sea-level research stems from the fact that subenvironments can be distinguished on the basis of their sedimentary character (lithostratigraphy) and associated flora or fauna (biostratigraphy); and that these subenvironments can be linked to the tidal frame (van de Plassche, 1986). Since the depositional environments are located at the interface of the terrestrial and marine domains, significant physical and biogenic environmental gradients exist (Kemp et al., 2009). At the terrestrial extreme, marine organisms that can survive extended times of subaerial exposure exist, terrestrial organisms survive intermittent saturation with marine waters, and physical conditions reflect the transitional nature of the setting. With a decrease in elevation the depositional environments are modified where the physical conditions and organisms associated with marine conditions are dominant. These sediments may then be used for an indication of relative sea level based on the vertical zonation of the organisms and/or physical attributes of the sediments. The establishment or quantifying of the associations between elevation and the physical and biological characteristics of sediment has been termed the *indicative meaning* (van de Plassche, 1986). An advantage of performing sea level studies in low energy environments is that the sediments are less likely to be eroded and transported and may provide a continuous record of sea level change.

High energy environments may also be utilized using physical and biogenic sedimentary structures to interpret sedimentary subenvironments and associated tidal position. Descriptions of the major high energy depositional environments of barrier island systems and associated proxies for sea level are provided in the research proposal (Meyer, 2012). Examples of biogenic

structures such as *Ophiomorpha nodosa* mud-lined burrows attributed to ghost shrimp such as *Callichirus major* indicate the elevation of mean sea level and increase in density with increasing water depth (Howard and Scott, 1983). The transition from marine (backbeach) to non-marine conditions may be observed at an elevation equal to or slightly above the modern spring tide high mark of a study area. This elevation is marked by a change from low angle bedding (backbeach) to higher angle bedding and represents the maximum elevation of wet sand and the lowest elevation at which eolian scour may occur (Roep and Beets, 1988).

Macrofossils may be used in sea level studies including mollusks such as the Atlantic Oyster (*Crassostrea virginica*), and coral. The Atlantic Oyster is observed in the modern tidal creeks with an associated vertical range. Reef building corals exist near the sea surface, allowing them to be used as sea level indicators. Cores of coral are subsampled, radiocarbon dating is performed and age-depth relationships established to produce a sea level curve (Fairbanks, 1989). This method has been used extensively in tropical zones in determining sea level dynamics, however, there are disadvantages to coral proxies for sea level. Corals from sea level low stands may be difficult or expensive to locate due to logistics and drilling costs, and corals may contain gaps in sea level records due to erosion or other factors effecting growth, such as disease (Bard et al., 1996).

The presentation of sea level data has undergone a paradigm shift in the more recent high resolution and multi-proxy studies. Whereas the traditional studies produced sea level curves, the modern studies present sea level data points and associated uncertainties. The current study incorporates uncertainties in creating a sea level envelope to evaluate Late Holocene sea level conditions.

#### 5.4.2 Methodology

Radiocarbon data and associated facies were evaluated as constraining data on sea level conditions where facies occurring below mean sea level were used to constrain the lowest elevation for sea level and facies occurring above mean sea level were used to constrain the highest level or elevation for sea level. The associated facies and sample metadata were extracted from the vibracore logs and the reference stratigraphic section (Figure 3-8) was then used to verify facies and establish the vertical range of the depositional environment or *indicative meaning* of the data point. The results are plotted as constraining points based on the occurrence of the depositional environment with the elevation range plotted as a “window” in which sea level would have occurred. The windows of sea level may then be correlated to produce a sea level envelope that captures the range in which mean sea level would have most likely occurred, allowing for an evaluation of sea level trends (Figure 5-5).

#### 5.4.3 Radiocarbon Data Calibration

The radiocarbon data were calibrated to convert the radiocarbon ages into absolute or calibrated years (cal yrs) to account for variations in the specific activity of  $^{14}\text{C}$  in the atmosphere that were recognized early in radiocarbon dating (de Vries, 1958). The  $^{14}\text{C}$  data were initially corrected for fractionation of carbon isotopes ( $\delta^{13}\text{C}$ ) by normalizing to  $-25\text{‰}$  PeeDee Belemnite (PDB). Calibration databases have been constructed using radiocarbon data and absolute dates from dendrochronology and other independently dated samples. The radiocarbon samples in the current study were calibrated using CALIB 6.1.1 software (Reimer et al., 2005) against the IntCal04 database (Reimer et al. 2004) for terrestrial samples and marine samples were calibrated with the Marine04 dataset (Hughen et al., 2004). In addition, the local reservoir

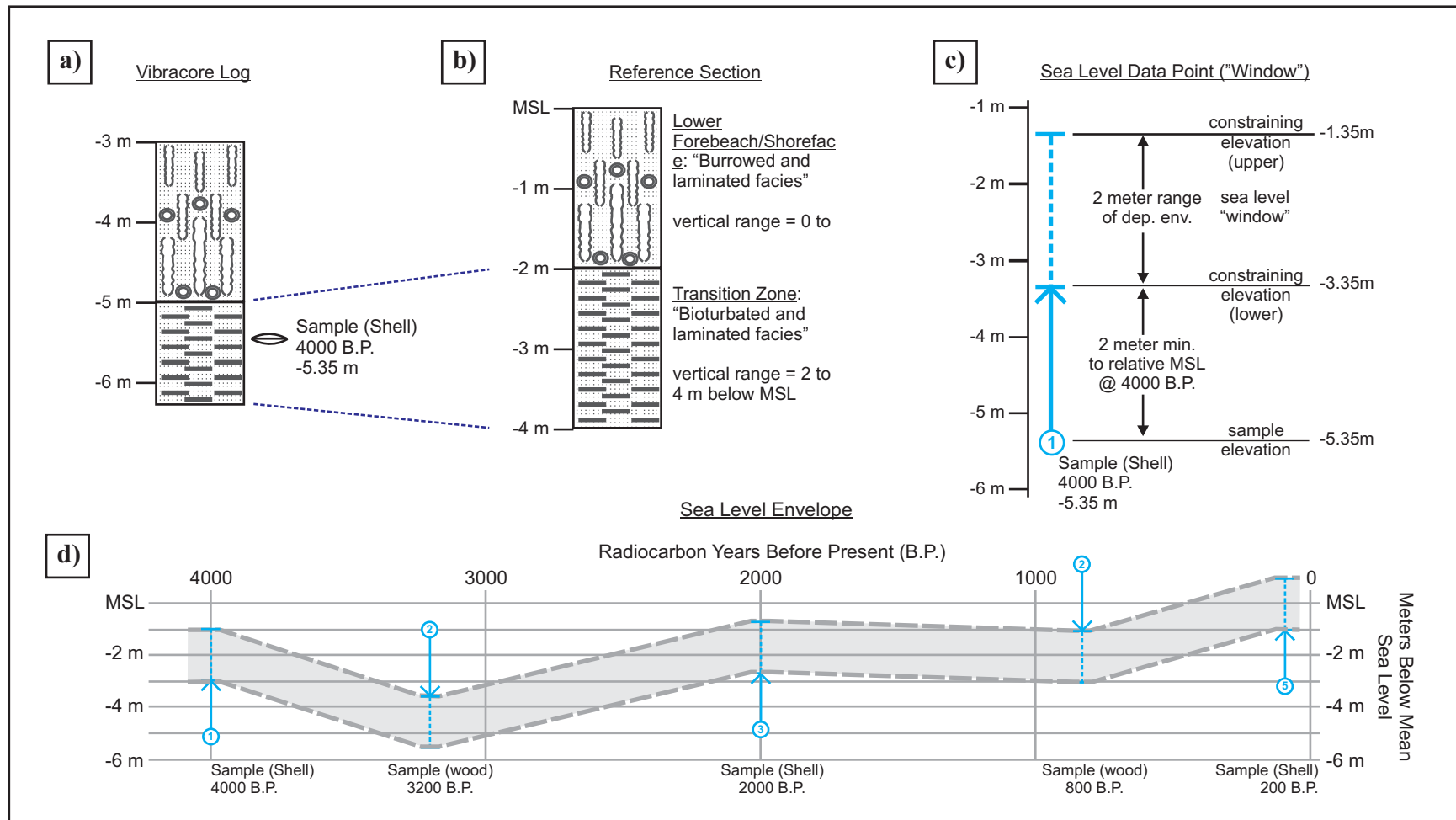


Figure 5-5: Radiocarbon data and associated facies were evaluated as constraining data on sea level conditions where facies occurring below mean sea level were used to constrain the lowest elevation for sea level and facies occurring above mean sea level were used to constrain the highest level or elevation for sea level. a) associated facies and sample metadata are extracted from the vibracore logs, b) the reference stratigraphic section is then used to verify facies and establish the vertical range of the depositional environment or indicative meaning, c) results are plotted as constraining points based on the occurrence of the depositional environment with the elevation range plotted as a "window" in which sea level would have occurred, d) the windows of sea level may then be correlated to produce a sea level envelope to evaluate sea level trends.

effects of St. Catherines Island on the calibrated data were integrated into the processing using the guidance established by Thomas, 2011. The local reservoir factor was evaluated by Thomas (2008) using harvested *Crassostrea virginica* associated with oyster boiling factories that operated from 1900 to 1920 on St. Catherines Island. The established known or absolute date of 1910 +/- 10 years was compared to radiocarbon data from the shell materials and resulted in a mean local reservoir factor ( $\Delta R$ ) of -134 +/- 26 that was incorporated into the CALIB datasets for processing. Data is presented in radiocarbon years and as calibrated data in the sea level evaluation and denoted as “B.P.” for measured or radiocarbon years and as “Cal B.P.” for calibrated years.

## 6 RESULTS

The following sections provide the results from the current study for the shoreline dynamics modeling, vibracore samples, XRF analyses, the synthesis of the data into lithostratigraphic and chemostratigraphic cross-sections, and an evaluation of Late Holocene sea level conditions.

### 6.1 Shoreline Dynamics

Results have been generated for both the shoreface portion of the island and the study area associated with *Mission Santa Catalina de Guale*. The results for the shoreface study were evaluated against the landforms that compose the terrestrial to marine transition (shoreline) within the study area and against changes in the rate of sediment supply where applicable. The results from the landform dynamics study for *Mission Santa Catalina de Guale* have been compared against the landform types occurring at the island core and marsh transition zone and the nature of three meanders of Wamassee Creek that cut into the island core adjacent to the mission site.

#### 6.1.1 Island Shoreface Dynamics

Imagery and GPS data for the eastern or shoreface portion of the island were imported into a personal geodatabase and processed from the following data sources: 1) 1859 Sapelo Sound Chart/St. Catherines Sound Navigational Chart (NOAA), 2) 1905 Sapelo Sound, 3) 1905 St. Catherines Sound, 4) 1916 Sapelo Sound Navigational Chart (NOAA), 5) 1926 St. Catherines Sound, 6) 1951 Black/White Aerial Imagery (USGS), 7) 1968 Black/White Aerial Imagery



(USGS), 8) 1974 Black/White Aerial Imagery (USGS), 9) 1993 Black/White Imagery (USDA NAIP), 10) 1999 Color Infrared Imagery (USDA NAIP), 11) 2005 True Color Imagery (USDA NAIP), 12) 2006 True Color Imagery (USDA NAIP), 13) 2007 True Color Imagery (USDA NAIP), 14) Global Positioning System (GPS) Data 2009 (B. Meyer), 15) Global Positioning System (GPS) Data 2010 (B. Meyer), and 16) Global Positioning System (GPS) Data 2011 (B. Meyer).

The 1899 Georgia Coast Navigational Chart (NOAA), 1982 Color Infrared Imagery (USGS), 1971 Ossabaw /St. Catherines Sound Navigational Chart (NOAA), and 1971 Sapelo and Dobby Sound Navigational Chart (NOAA) were not used in the current study to delineate the shoreline due to the low resolution of these raster data sets. The 1979 Sapelo Sound and St. Catherines Sound USGS topographic maps (USGS) were also not used due to the condition of redundancy because the topographic maps were based on the 1974 aerial imagery already included in the current study. In addition, the 1968 Ossabaw /St. Catherines Sound Navigational Chart (NOAA) was considered to be redundant with the 1968 Black/White imagery and was not used in the current study. Shorelines were digitized based on the wrack line position (backbeach environment) and compiled into the geodatabase with associated metadata. Transects were then cast at 200 meter spacings on the seaward portion of the island from St. Catherines Sound to Sapelo Sound.

The data and results were grouped into pre-dam (1858-1951) and post-dam (1968-2011) data sets and transects were assigned a landform type. The pre-dam and post-dam eras were selected to correlate with anthropogenic modifications to the rate of sediment supply associated with historical changes in land use associated with land clearing practices following colonization (increase in sediment flux) and impoundment of rivers (decrease in sediment flux) and are

described in detail in the discussions section. End Point Rates (EPR), Linear Regression Rates (LRR), and Weighted Linear Regression Rates (WLR) for shoreline dynamics were generated. A plot of the results for the various rates of change calculations for each of the time eras is provided for the shoreface portion of the island in Figure 6-1 and the results for the LRR method are provided in Appendix A. Mean values were generated for each shoreline compartment correlating to the landform type that encompasses the shoreline at a specific location in an effort to minimize local variances due to land slope, vegetative cover, etc. The shoreline compartments (from north to south) include: 1) the northeastern accretional terrains located on North Beach that are composed of sediments primarily deposited since 1859; 2) the island core that comprises the shoreline at Yellow Banks Bluff; 3) the shoreline spit at Seaside Spit; 4) the shoreline berm at Middle Beach; 5) the accretional dunes at McQueen Dune Field; 6) the shoreline spit located south of McQueen Dune Field; 7) the ridge and swale topography of the southeastern accretional terrains; and 8) the shoreline spit located on the extreme southern portion of South Beach in the vicinity of Beach Creek. Although not shown in Figure 6-1 due to presentation issues, the shoreline dynamics for the beach ridge/swale topography associated with the northern Holocene accretional terrains adjacent to St. Catherines Sound are described in the following text and are included in the landform analyses.

Shoreline dynamic rates for the beach ridge/swale topography associated with the northern Holocene accretional terrains adjacent to St. Catherines Sound that were calculated using the weighted linear regression (WLR) method for the pre-dam era range from -2.0 m/yr to -3.7 m/yr (mean value = -3.0 m/yr), and the post-dam era data indicate rates ranging from -1.0 to -2.0 m/yr (mean value = -1.6 m/yr). Rates for shoreline dynamics that were calculated in the actively accreting northeastern terrains for the pre-dam era range from -1.6 m/yr to 1.8 m/yr

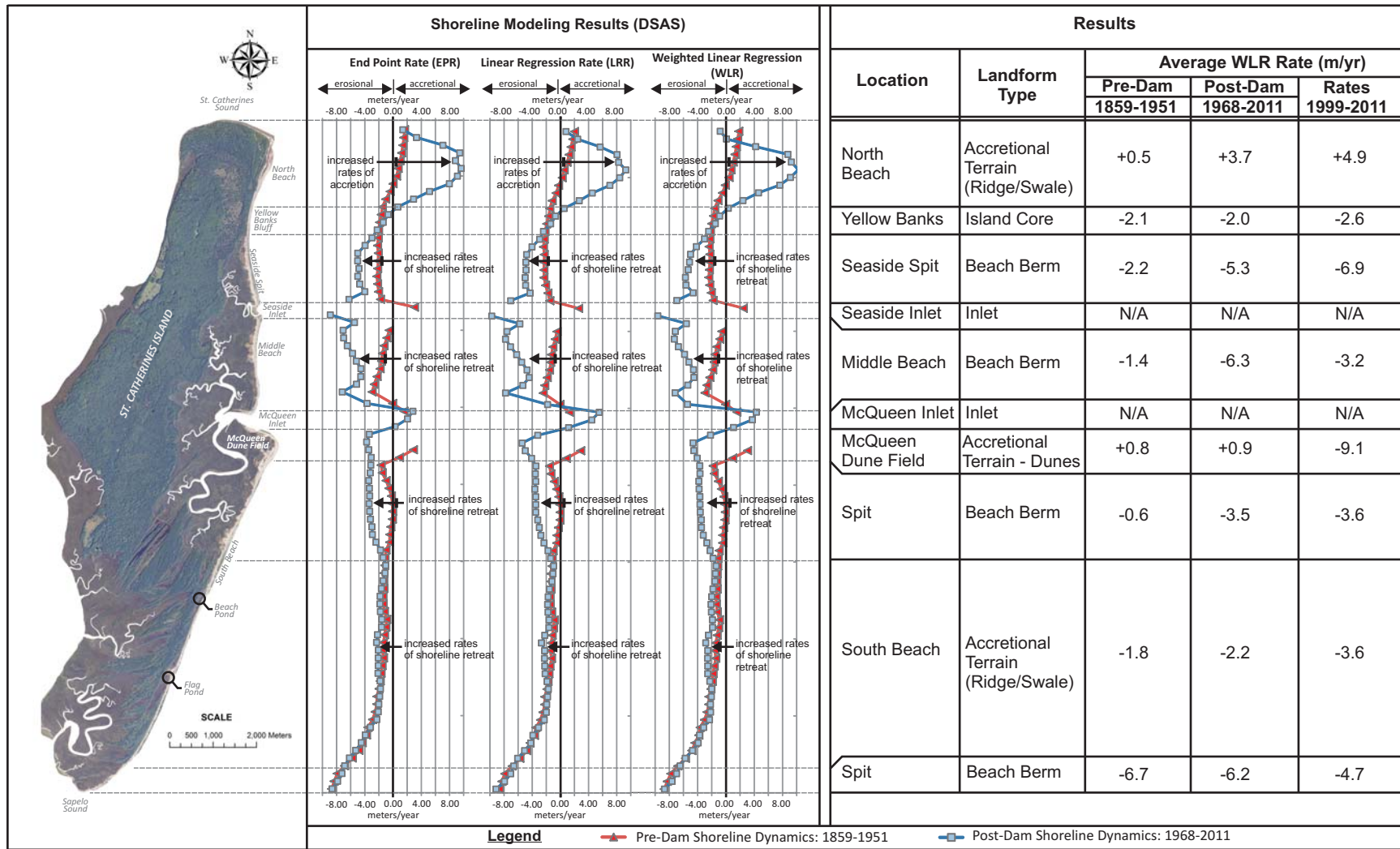


Figure 6-1: The pre-dam and post-dam shoreline results for the End Point Rate (EPR), Linear Regression Rate (LRR) and Weighted Linear Regression (WLR) algorithms were generated and plotted. Of particular note, the berm or spit landforms show an acceleration in shoreline retreat rates from the pre-dam to the post-dam results indicating that sediment supply plays a larger role in the shoreline dynamics associated with the spit and berm landforms.

(mean value = +0.5 m/yr), and the post-dam era data indicate rates ranging from -1.3 to +10.2 m/yr (mean value = +3.7 m/yr). The negative or erosional rates are associated with the northern margin of the northeastern terrains that bound St. Catherines Sound, indicating minor shoreline retreat in the northeastern terrains that is most likely associated with inlet dynamics. Shoreline retreat along Yellow Banks Bluff ranges from -1.8 m/yr to -2.3 m/yr (mean value = -2.1 m/yr) in the pre-dam data set, whereas shoreline retreat values range from -0.9 m/yr to -3.0 m/yr in the post-dam data (mean value = -2.0 m/yr) and the similarity in mean values may be interpreted as a constant rate of shoreline retreat. Shoreline retreat rates for the pre-dam era range from -1.8 m/yr to -2.4 m/yr (mean value = -2.2 m/yr) for the Seaside Spit portion of the island, and range from -4.2 m/yr to -6.9 m/yr (mean value = -5.3 m/yr) for the post-dam era data with notable increases in shoreline retreat values. Shoreline retreat on Middle Beach ranged from -0.6 to -2.3 m/yr (mean value = -1.4 m/yr) in pre-dam data and ranged from -4.5 m/yr to -9 m/yr (mean value = -6.3 m/yr) in post-dam data, also indicating significant increase in shoreline retreat values.

The dune field adjacent to McQueen Inlet has displayed tremendous dynamics over the study period, where McQueen Inlet previously occupied the current area of the dune field based on the 1859, 1905 and 1926 historical maps. In 1951 imagery the inlet has moved north and a spit had accreted to the north with initial dune accretion indicated in the imagery. In 1968 imagery an extensive dune field has accreted whereas more recent data sets and field observations, such as a prominent 1.0 to 2.0 meter high beach scarp, indicate modern or currently erosional conditions. In order to present and evaluate these dynamics, a time slicing method was used to evaluate temporal changes in the accretion and erosion rates associated with the McQueen Dune Field. End point rates (EPR) were calculated for the time intervals between each of the imagery and GPS data sets from 1951 to 2011 and are presented in Figure 6-2. The EPR

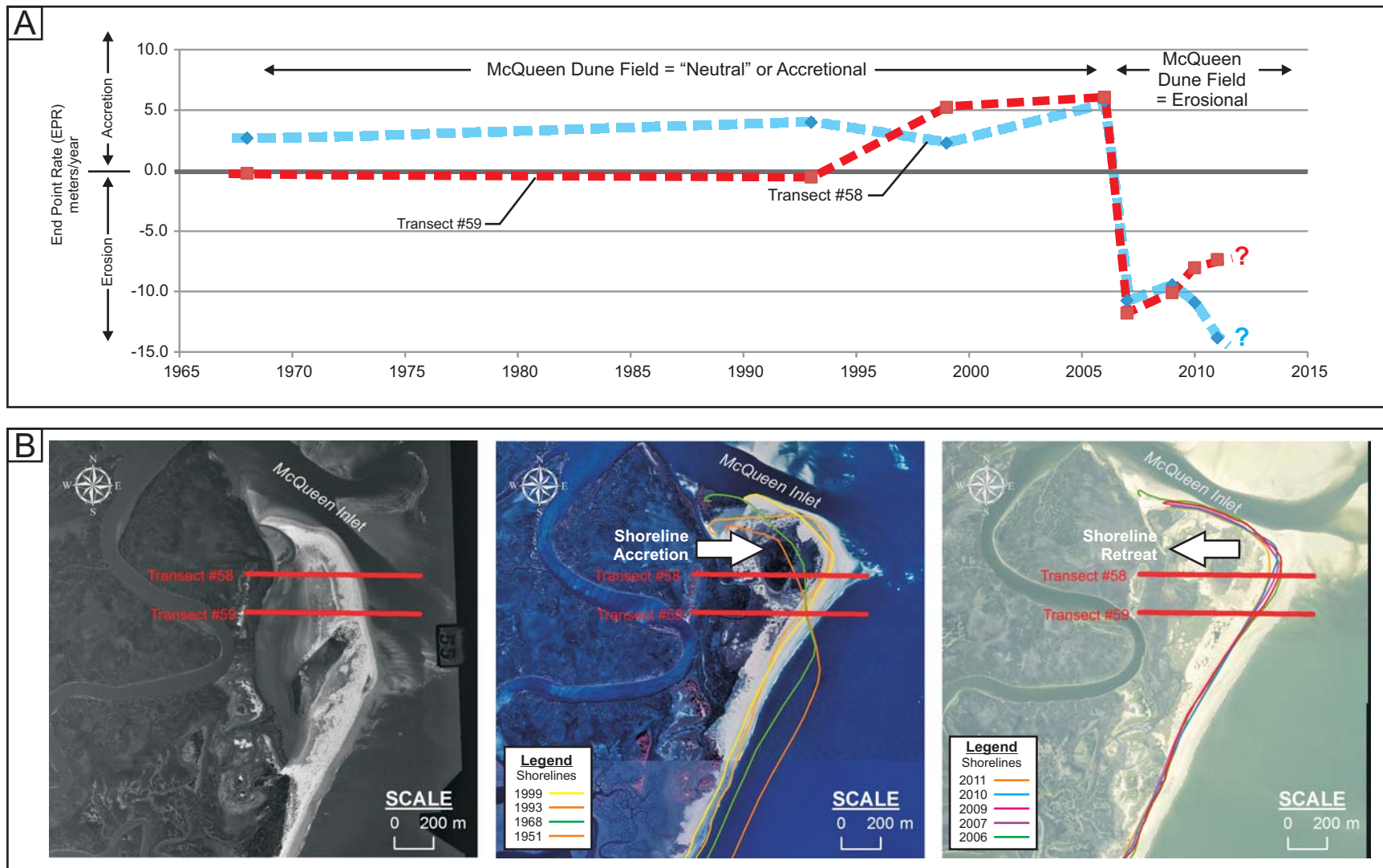


Figure 6-2: Dynamics of McQueen Dune Field. A) Time series plot of End Point Rates (EPR) calculated for aerial images and GPR data. The McQueen Dune Field initially began to form in the late 1940s (Shadroui, 1990) adjacent to McQueen Inlet. Since 2006 the dune field has been in a state of decline with significant shoreline retreat noted in imagery/GPS data and beach scarps observed in the field. B) Historical 1951 aerial image, 1999 color infrared image and 2008 image with historical shorelines plotted.

results indicate neutral to accretional conditions in the area from 1951 to 2005. These conditions appear to change in the time interval of 2005 to 2006 when EPR results indicate appreciable erosional rates or shoreline retreat conditions that continue through the 2011 data set and were confirmed with recent field observations in May 2013 including the presence of the aforementioned beach scarp and an increase in washover activity due to depletion of sentry dunes.

Shoreline retreat along the spit located to the south of the McQueen Inlet dune field ranges from -0.1 m/yr to -1.8 m/yr in the pre-dam data set (mean value = -0.6 m/yr), and shoreline retreat values range from -2.7 m/yr to -3.8 m/yr (mean value = -3.5 m/yr) in the post-dam data indicating increases in shoreline retreat. Shoreline retreat rates associated with the beach ridge/swale topography of the southeastern accretional terrains in the areas of Beach Pond and Flag Pond range from -0.9 m/yr to -3.8 m/yr (mean value = -1.8 m/yr) in the pre-dam data set, and shoreline retreat values range from -1.4 m/yr to -3.7 m/yr (mean value = -2.2 m/yr) in the post-dam data with no appreciable increase in shoreline retreat rates or acceleration noted. Shoreline retreat rates associated with the spit that occupies the beach in the areas south of Beach Pond and Flag Pond range from -4.4 m/yr to -8.8 m/yr (mean value = -6.7 m/yr) in the pre-dam data set, and shoreline retreat values range from -3.5 m/yr to -8.7 m/yr (mean value = -6.2 m/yr) in the post-dam data.

The shoreline compartments were then grouped by landform type to evaluate the influence of landform type on shoreline dynamics, where the five major landform types that comprise the shoreline at St. Catherines Island are 1) the active accretional terrains (northeast), 2), the McQueen dune field, 3) the island core, 4) the beach ridge/swale topography associated with Holocene beach ridge terrains, and 5) the spits/berms. Results indicate that shoreline

dynamics ranged from -1.6 m/yr to +1.8 m/yr (mean value = 0.5 m/yr) during the pre-dam era in the active accretional terrains (Figure 6-3 pre-dam) and ranged from -1.3 m/yr to +10.2 m/yr (mean value = +3.7 m/yr) in the post-dam data (Figure 6-4 post-dam) suggesting that shoreline accretion has increased in the active accretional terrains (northeast). Average WLR rates by landform ranged from -0.0 m/yr to +1.6 m/yr (mean value = +0.8 m/yr) during the pre-dam era in the McQueen dune field and ranged from +4.3 m/yr to -5.4 m/yr (mean value = +0.9 m/yr) in the post-dam data. Data from the island core in the area of Yellow Banks Bluff indicated pre-dam era rates ranging from -1.8 m/yr to -2.3 m/yr (mean value = -2.1 m/yr) and post-dam data indicate rates ranging from -0.9 m/yr to -3.0 m/yr (mean value = -2.0 m/yr), inferring that little to no change in the rate of shoreline retreat has occurred in the Yellow Banks Bluff area. Average WLR rates by landform ranged from -0.2 m/yr to -3.8 m/yr (mean value = -1.9 m/yr) during the pre-dam era in the ridge/swale landforms associated with Holocene beach ridge terrains and ranged from +0.4 m/yr to -7.3 m/yr (mean value = -1.9 m/yr) in the post-dam data. Results indicate that shoreline dynamics ranged from -0.1 m/yr to -8.8 m/yr (mean value = -2.8 m/yr) during the pre-dam era in the spit/berm landforms and ranged from -2.2 m/yr to -9.6 m/yr (mean value = -5.1 m/yr) in the post-dam data. The increase in the mean values from -2.8 m/yr (pre-dam era) to -5.1 m/yr (post-dam era) suggests that shoreline retreat has significantly increased in the spits and berm landforms associated with the shoreline at St. Catherines Island whereas other landform types appear to indicate a negligible acceleration in shoreline retreat rates.

### *6.1.2 Mission Santa Catalina de Guale Landform Dynamics*

Imagery and GPS data for the *Mission Santa Catalina de Guale* site have been imported into a personal geodatabase and processed from the following data sources: 1) 1951 Black/White

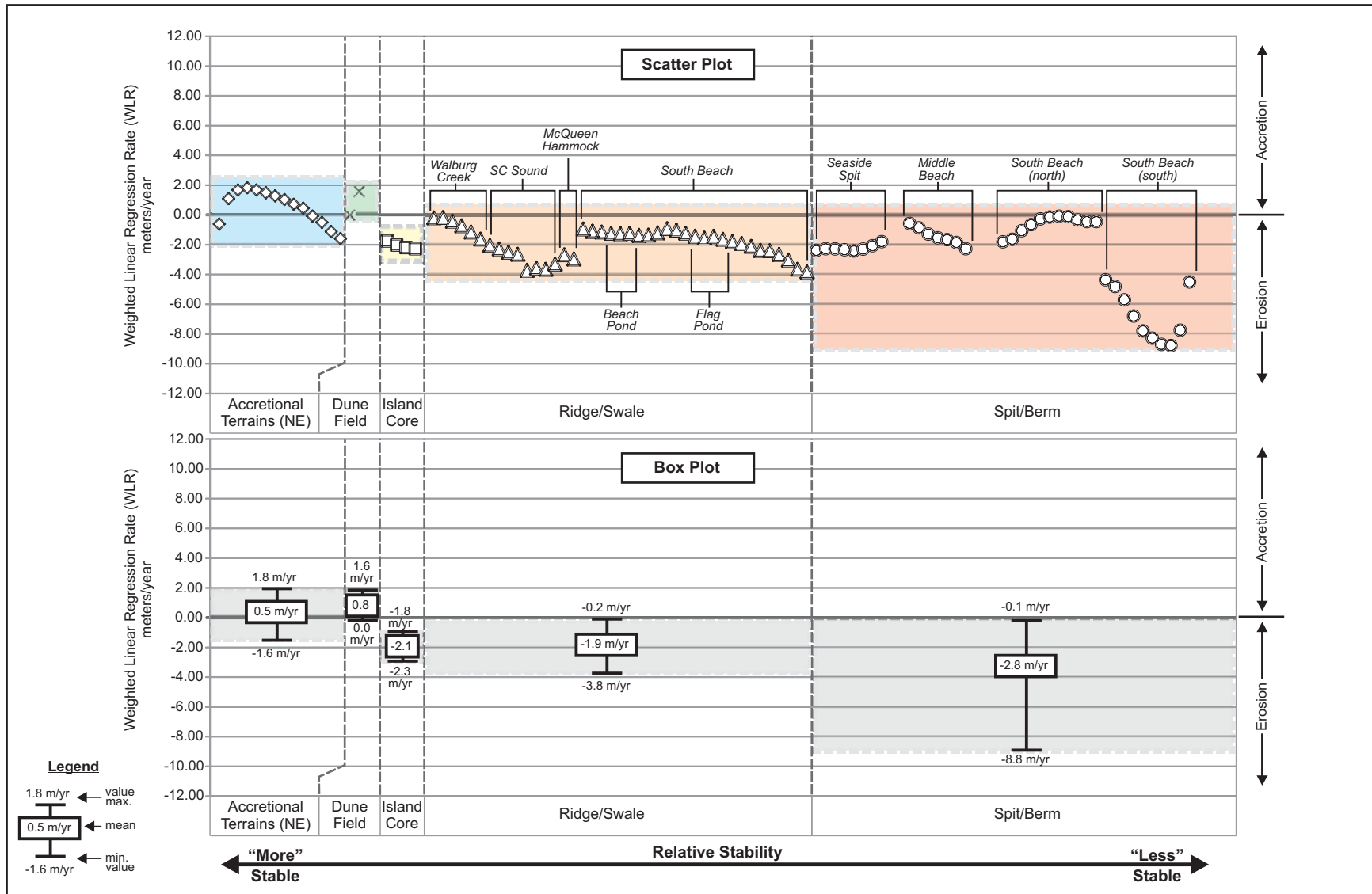


Figure 6-3: Shoreline dynamic rates are presented for the Pre-Dam Era (1859-1951) landforms that comprise the shoreline. Scatter plots of the WLR rates for each of the landforms and boxplots from descriptive statistics are presented. The landforms were sorted with respect to stability where the more stable landforms are shown on the left, and less stable landforms on the right.



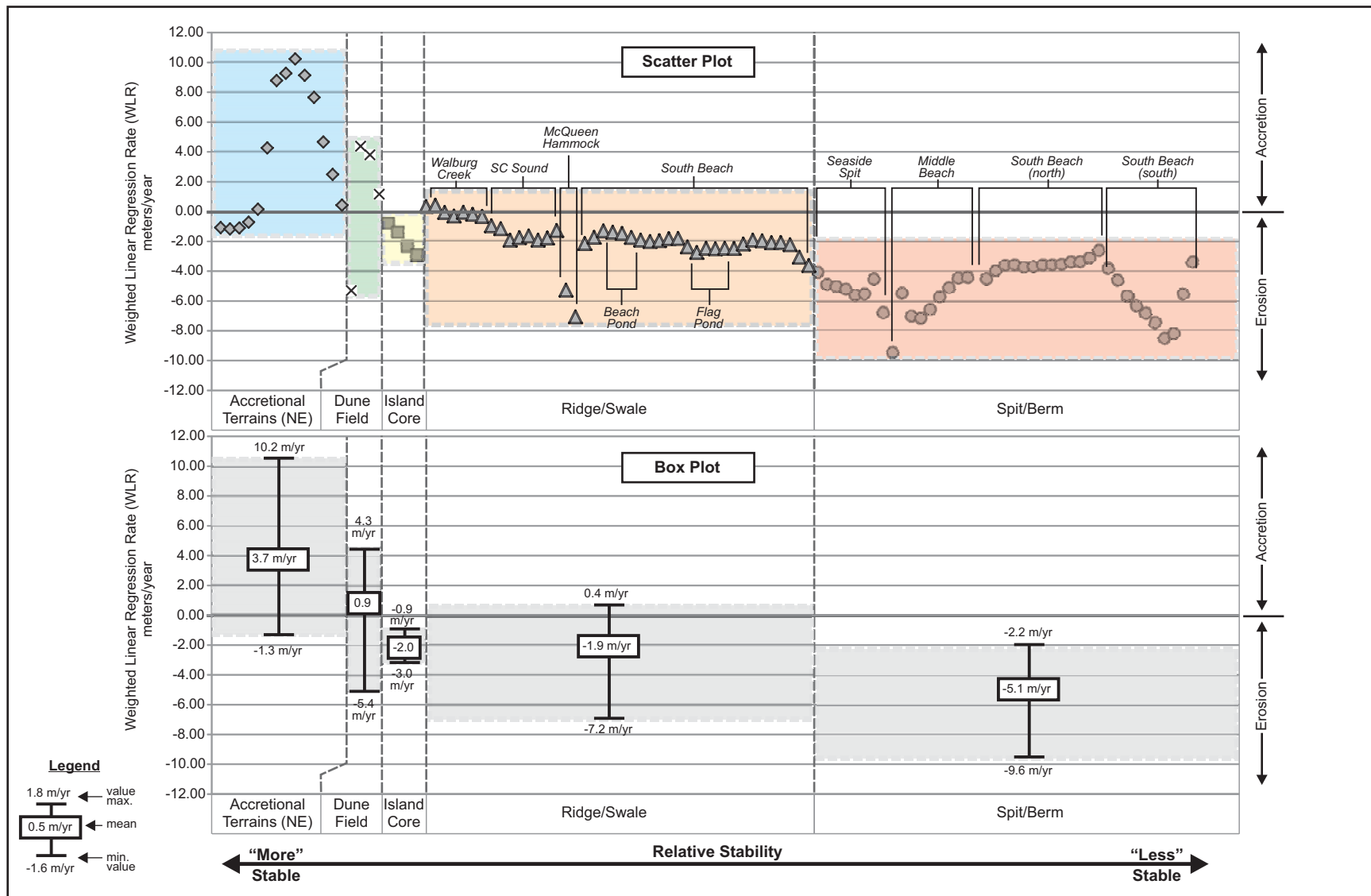


Figure 6-4: Shoreline dynamic rates are presented for the Post-Dam Era (1968-2011) landforms that comprise the shoreline. Scatter plots of the WLR rates for each of the landforms and boxplots from descriptive statistics are presented. The landforms were sorted with respect to stability where the more stable landforms are shown on the left, and less stable landforms on the right.

Aerial Imagery (USGS), 2) 1974 Black/White Aerial Imagery (USGS), 3) 1980 Field Conditions Map (AMNH), 4) 1999 Color Infrared Imagery (USDA NAIP), 5) 2005 True Color Imagery (USDA NAIP), 6) 2006 True Color Imagery (USDA NAIP), 7) 2009 Global Positioning System (GPS) Data (AMNH), 8) 2010 Global Positioning System (GPS) Data (AMNH), 9) 2011 Global Positioning System (GPS) Data (AMNH), 2012 Global Positioning System (GPS) Data (AMNH), and 10) 2013 Global Positioning System (GPS) Data (AMNH). The GPS data were provided by the American Museum of Natural History (AMNH).

Shorelines adjacent to the *Mission Santa Catalina de Guale* were digitized based on the position of the cut bank or bluff that bounds the island core, adjacent marsh and active meander cut banks of Wamassee Creek and compiled into the geodatabase with associated metadata. Transects were then cast at 20 meter spacings through the study area (Figure 6-5). In addition, Wamassee Creek was digitized from the 1951 and 2010 imagery to evaluate the direction and magnitude of the tidal creek meanders and the corresponding effect on the adjacent cut bank or bluff. Transects 1 to 12 were located along the bluff associated with the marsh and island core margin to the north of Meander #1 and transects 13 to 17 were located along a cutbank that occurs adjacent to Meander #1 (Figure 6-5). Transects 18 to 21 were located in the marsh and island core margin between Meanders #1 and #2, transects 22 to 25 were located on the cut bank associated with Meander #2, and transects 24 to 29 were located on the marsh located between Wamassee Creek and the island core adjacent to Structure 1/Iglesia. Transects 30 to 39 were located on the cut bank associated with Meander #3, and transects 40 and 41 were located on the marsh and island core margin immediately south of Meander #3.

Diagrams of the time series vector data (shorelines), transects and the Linear Regression Rate (LRR) and Weighted Linear Regression Rate (WLR) statistics have been generated. The

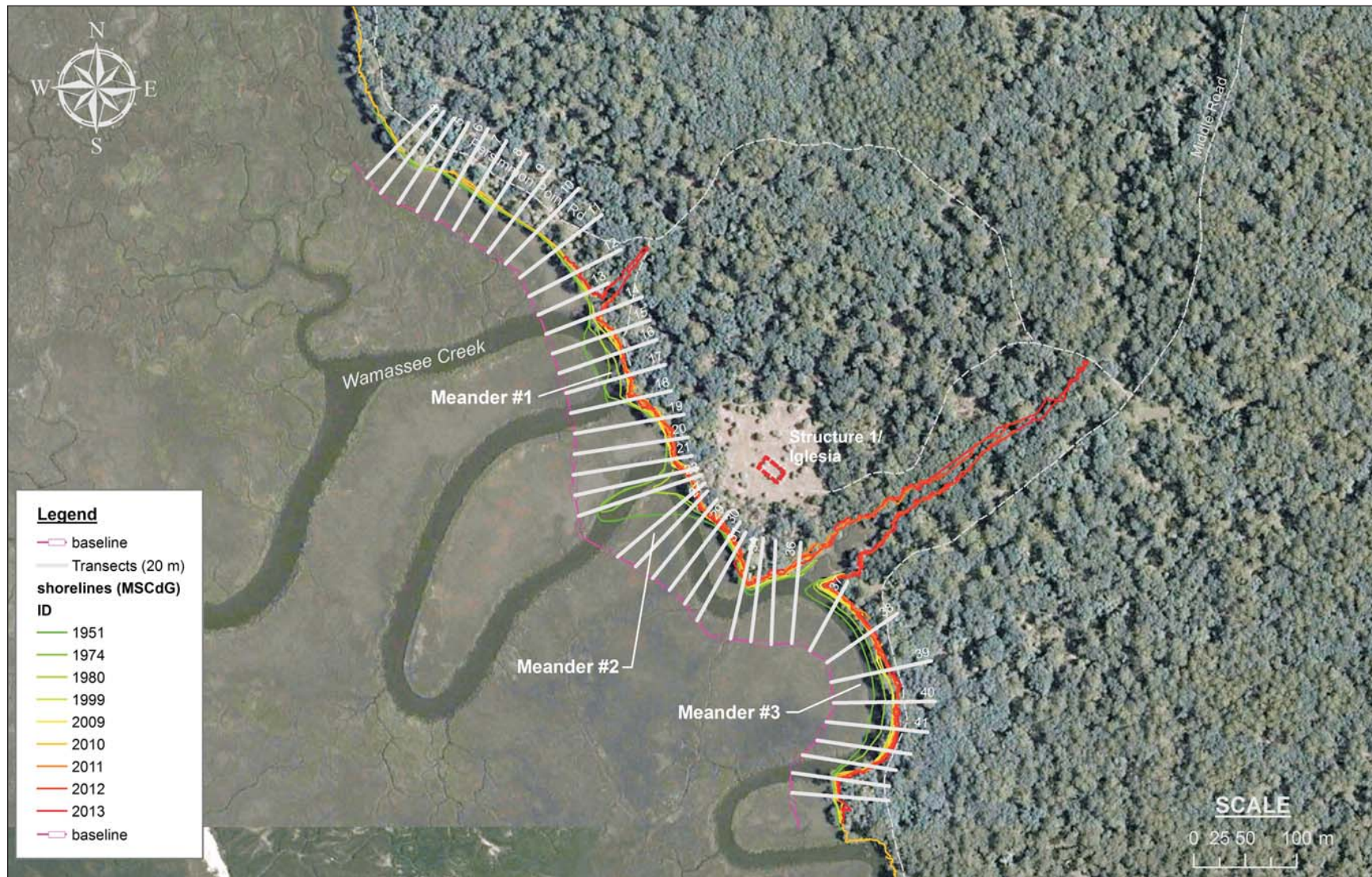


Figure 6-5: The framework for the DSAS Model was established to capture the landform dynamics associated with the three meanders of Wamassee Creek that form the emarginate portion of Wamassee Scarp. Shorelines were digitized from historical imagery (1951, 1968, 1974, 1980, and 1999) and ground collected GPS data (2009-2013) and imported into a geodatabase. A baseline was established parallel to the island/marsh interface and transects were cast at 20 meter spacings. Image from USDA NAIP, 2007.

data were partitioned into data sets corresponding to: 1) the 1951 to 2013 time period; and 2) the 1999 to 2013 time period. The 1951 to 2013 time period data set has been used to evaluate the landform dynamics over the entire study period, whereas the 1999 to 2013 data set has been used to forecast future landform and shoreline conditions.

Shoreline retreat and landform dynamics are primarily occurring as a result of fluvial (tidal creek) and marine forces. Three meanders of Wamassee Creek are currently eroding into the island core in the study area near the mission site (Figure 6-5) and the marine margins of the island are subject to erosion from the modern marine transgression. The marsh and island core margin associated with transects 1 to 12 appears to be relatively stable over the study period with WLR rates ranging from 0.01 to 0.20 m/yr, and a mean value of 0.06 m/yr (Figure 6-6; Table 4). Meander #1 has moved 27 meters in an east-northeast direction (Figure 6-7) and resulted in a net movement of the cut bank to the east. This condition has resulted in dynamics associated with the cut bank along transects 13 to 17, with moderate WLR rates ranging from 0.29 to 0.51 m/yr., and a mean value of 0.40 m/yr. The marsh located between Meanders #1 and #2 appears to be relatively stable over the study period with WLR rates for transects 18 to 20 ranging from 0.16 to 0.19 m/yr., and a mean value of 0.17 m/yr. Meander #2 has moved 52 meters in a northerly direction and resulted in a net movement of the cut bank or shoreline. The WLR rates for transects (21 to 23) ranged from 0.47 to 1.37 m/yr. with a mean value of 0.79 m/yr. as indicated. The highest erosion rate (1.37 m/yr.) was indicated at transect 22 where a peninsula of island core formerly extended west into the low marsh environment and existed until removal by Meander #2 in the late 20<sup>th</sup> century. The marsh located between Meanders #2 and #3 appears to be relatively stable over the study period with WLR rates for transects 24 to 29 ranging from 0.15 to 0.26 m/yr., and a mean value of 0.20 m/yr. Meander #3 has moved 21 meters in an



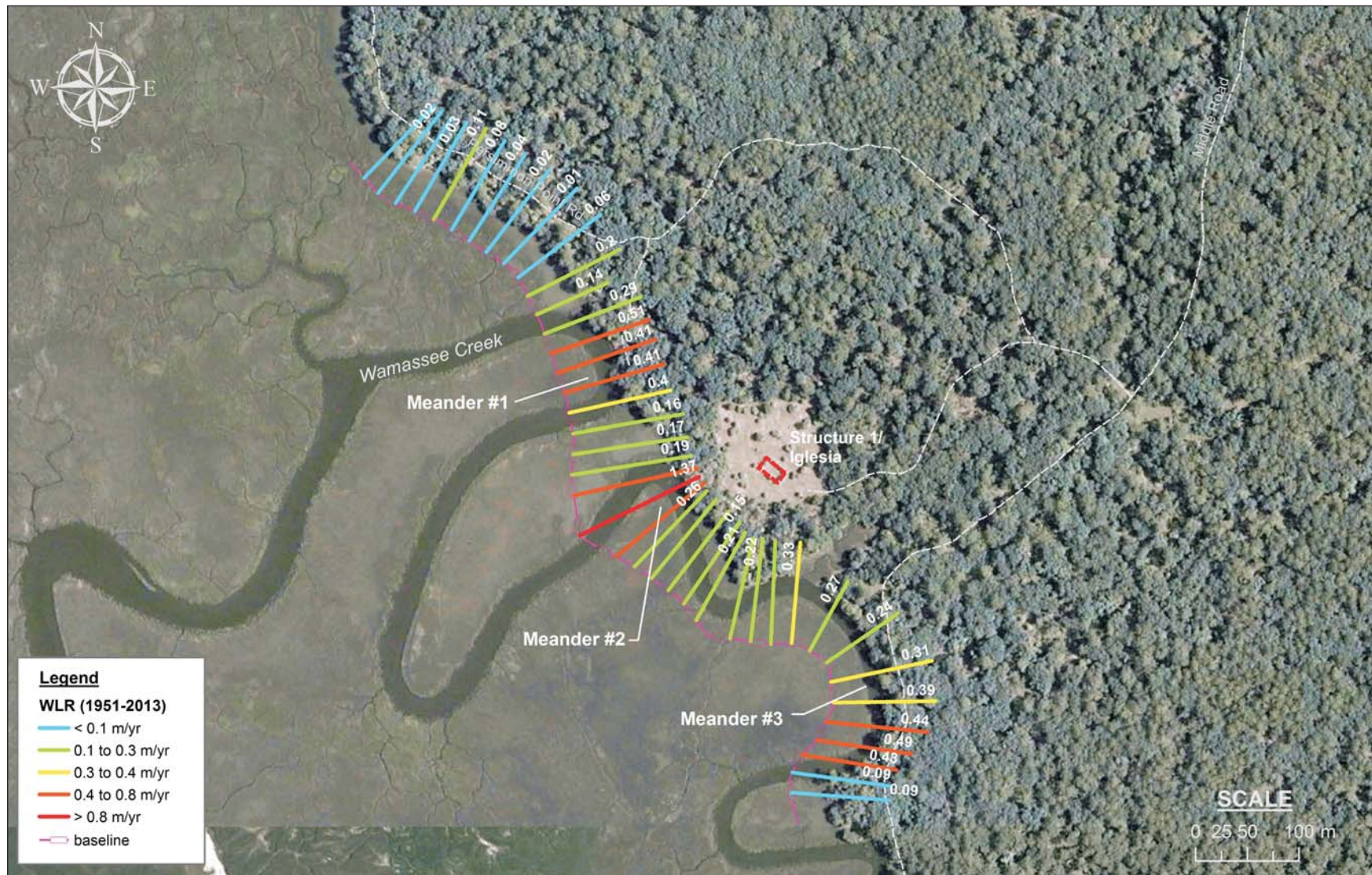


Figure 6-6: WLR rates (1951-2013) are provided in a thematic style where cool colors (blue/green) represent lower erosion rates versus hot colors (orange/red) represent higher erosion rate. "Hot spots" of erosion are observed to correlate with the three meanders of Wamassee Creek with an appreciable erosion rate of 1.37 m/yr in the area formerly occupied by a peninsula that was removed by Meander #2. Image from USDA NAIP, 2007.

**Table 4:  
Mission Santa Catalina de Guale,  
Landform Dynamics Results**

Transect ID	WLR Results: 1951-2013				Landform	Mean WLR by Landform (1951-2013)
	EPR	NSM	WLR	LRR		
1	0.01	0.40	0.01	0.01	Marsh	0.06
2	0.02	1.03	0.02	0.02		
3	0.04	2.10	0.02	0.03		
4	0.03	1.51	0.03	0.03		
5	0.09	5.34	0.11	0.07		
6	0.07	3.97	0.08	0.06		
7	0.06	3.63	0.04	0.03		
8	0.02	1.41	0.02	0.02		
9	0.01	0.88	0.01	0.01		
10	0.05	2.99	0.06	0.04		
11	0.14	8.87	0.20	0.11		
12	0.09	5.60	0.14	0.08		
13	0.18	11.15	0.29	0.20	Meander #1 Cut Bank	0.40
14	0.52	32.34	0.51	0.47		
15	0.49	30.36	0.41	0.46		
16	0.42	25.93	0.41	0.45		
17	0.30	18.30	0.40	0.36		
18	0.10	6.46	0.16	0.11	Marsh	0.17
19	0.04	2.71	0.17	0.07		
20	0.10	6.26	0.19	0.15		
21	0.41	25.34	0.52	0.53	Meander #2 Cut Bank	0.79
22	1.49	92.23	1.37	1.50		
23	0.56	34.67	0.47	0.53		
24	0.32	19.78	0.26	0.31	Marsh	0.20
25	0.17	10.33	0.16	0.15		
26	0.06	3.85	0.17	0.11		
27	0.10	6.01	0.15	0.10		
28	0.11	6.81	0.21	0.12		
29	0.10	6.28	0.23	0.16		
30	0.21	12.80	0.22	0.18		
31	0.15	9.25	0.17	0.11		
32	0.19	11.79	0.33	0.22		
33	0.27	16.75	0.27	0.26		
34	0.26	16.28	0.24	0.23		
35	0.34	20.83	0.31	0.28		
36	0.41	25.48	0.39	0.38		
37	0.48	29.68	0.44	0.42		
38	0.49	30.07	0.49	0.45		
39	0.42	26.24	0.43	0.45		
40	0.10	6.31	0.09	0.07	Marsh	0.09
41	0.07	4.54	0.09	0.03		



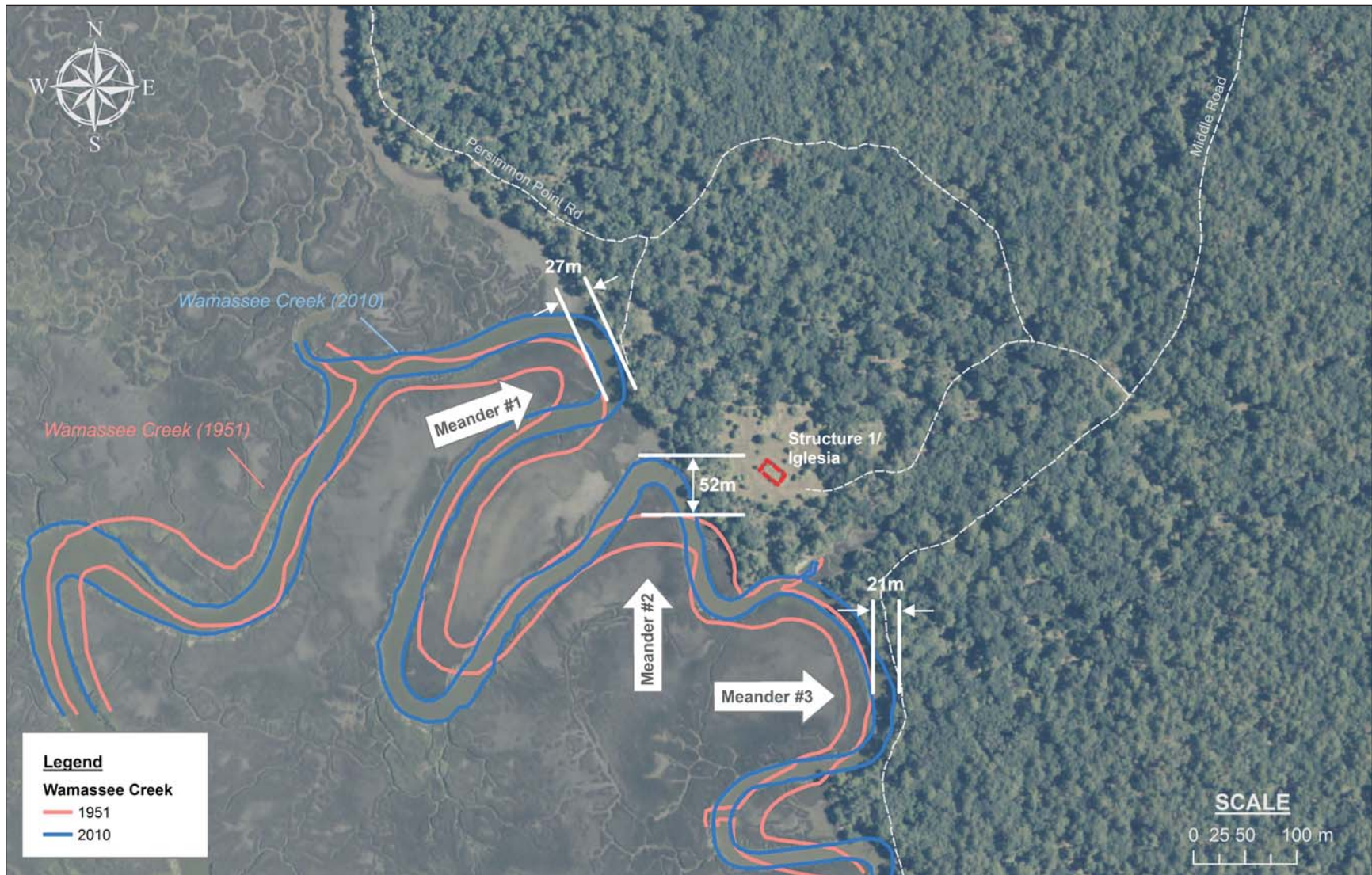


Figure 6-7: Landform changes may be observed in the historical imagery from 1951 until 2010. Meander #1 has moved 27 meters in an east-northeast direction and resulted in a net movement of the cut bank or shoreline of 0.29 m/yr. Meander #2 has moved 62 meters in a northerly direction and resulted in a net movement of the cut bank of 0.35 m/yr. Meander #3 has moved 21 meters in an eastern direction and resulted in a net movement of the cut bank or shoreline of 0.33 m/yr. Image from USDA NAIP, 2010.

eastern direction and resulted in a net movement of the cut bank or shoreline to the east. This condition has resulted in dynamics associated with the cut bank along transects 30 to 39, with moderate WLR rates ranging from 0.17 to 0.49 m/yr., and a mean value of 0.33 m/yr. The marsh and island margin located to the south of Meander #3 appears to be relatively stable with WLR rates observed at 0.09 m/yr. for the two transects.

The landforms associated with the shoreline transects were grouped or placed into compartments to minimize local variances and allow for a forecasting exercise to be performed. The WLR rates were averaged along each distinct landform and are presented using the thematic format (Figure 6-8). The results indicate that landform dynamics average 0.40 m/yr along Meander #1, 0.79 m/yr long Meander #2, and 0.33 m/yr at Meander #3. The marsh-island interface appears to be averaging < 0.5 m/yr to the north and south of the study area, with a mean rate of 0.17 m/yr between Meanders #1 and #2 and a mean rate of 0.20 m/yr between Meanders #2 and #3.

## **6.2 Vibracoring**

A total of 29 vibracores have been evaluated under the current study and an index map of the vibracoring locations is provided in Figure 6-9. A summary of the vibracore boring metadata and details is provided in Table 5, and the vibracore logs are included in Appendix B. Detailed lithological descriptions are provided within the individual vibracore logs, and a narrative follows to describe the lithological associations, interpreted depositional environments and the depositional framework of each study area. The vibracore locations were selected to evaluate the environmental change and island stratigraphy associated with Seaside Spit, Beach Pond, Flag Pond, the *Mission Santa Catalina de Guale*, the Central Depression and the North Beach area of



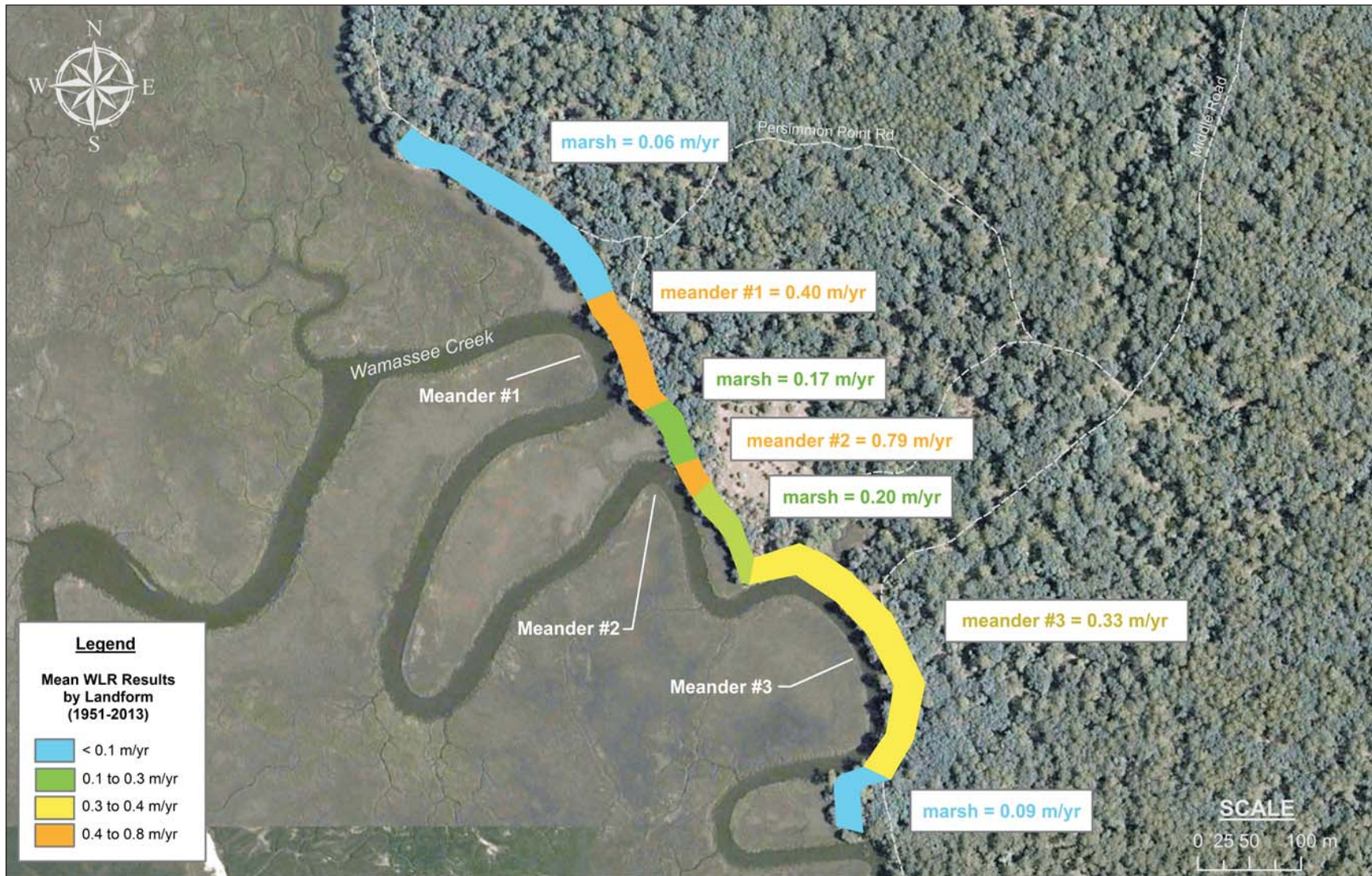


Figure 6-8: The WLR rates were averaged along each distinct landform and are presented using the thematic format. The results indicate that landform dynamics average 0.40 m/yr along Meander #1, 0.79 m/yr long Meander #2, and 0.33 m/yr at Meander #3. The marsh-island interface appears to be averaging < 1.0 m/yr to the north and south of the study area, with average rates of 0.17 m/yr between Meanders #1 and #2 and 0.20 m/yr between Meanders #2 and #3 respectively. Image from USDA NAIP, 2007.



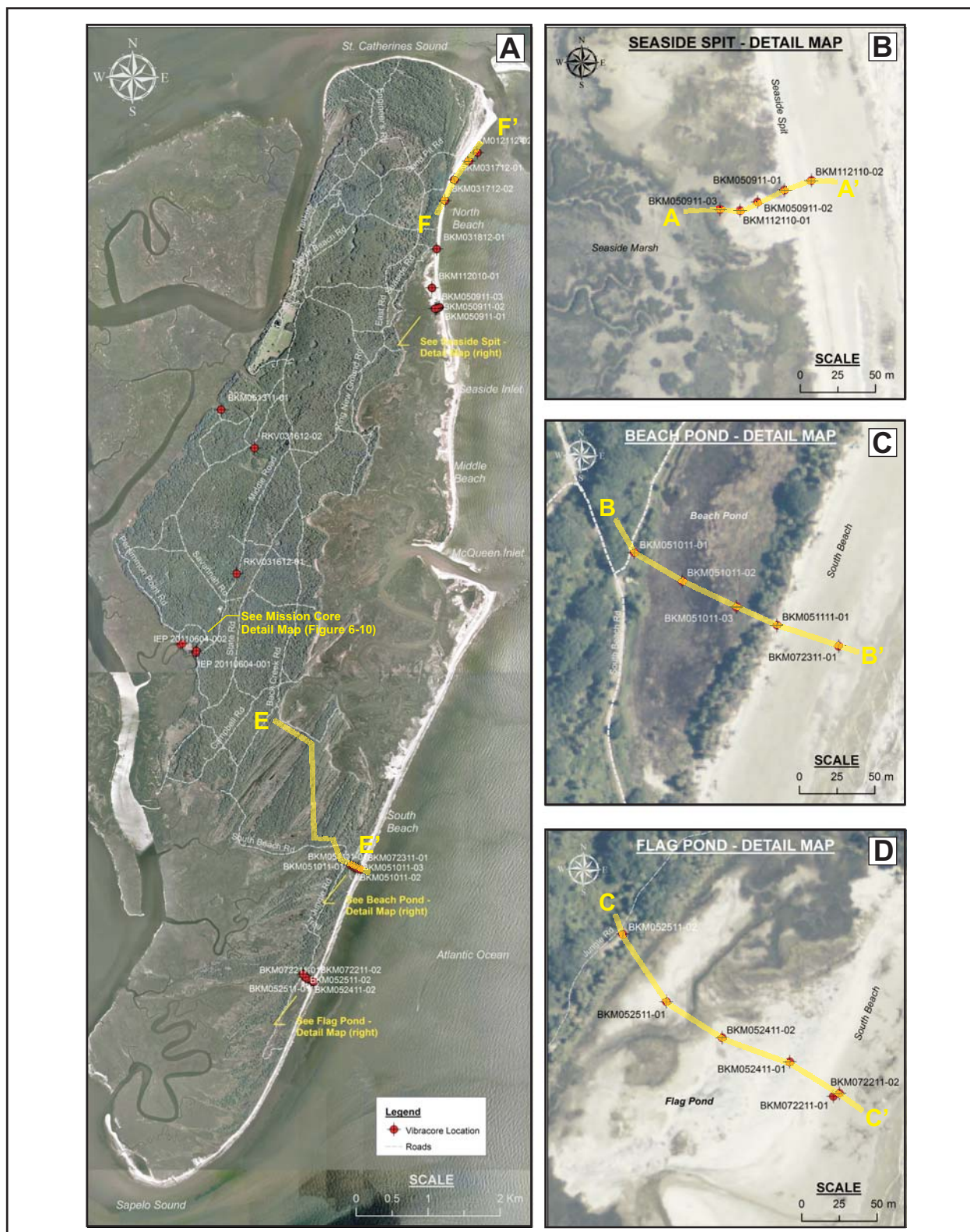


Figure 6-9: Location maps for vibracore locations. a) General location map for vibracores collected during 2010-2012. b) Detail map for Seaside Spit vibracore locations. c) Detail map for Beach Pond vibracore locations. d) Detail map for Flag Pond vibracore locations that are located on an active flood delta. Basemap image from USDA NAIP, 2010.

**Table 5  
Vibracore Boring Information**

No.	Boring ID	Date	Latitude	Longitude	Easting	Northing	Surface EL (ft)	Total Depth (cm) Recovered	Total Depth (cm) Original	Compaction (%)	Study Area	Location Description
1	BKM112010-01	11/20/2010	31.6705	-81.1380	486,918.23	3,503,920.19	6.05	478.0	536.0	10.9%	Seaside Spit	Seaside Spit, in washover south of hammock
2	BKM112110-01	11/21/2010	31.6679	-81.1374	486,975.32	3,503,630.37	3.41	490.0	530.0	7.5%	Seaside Spit	Seaside Spit transect, in washover
3	BKM112110-02	11/21/2010	31.6680	-81.1369	487,023.08	3,503,650.41	6.06	507.0	535.0	5.2%	Seaside Spit	Seaside Spit transect, on beach near relic marsh mud (backbeach/forebeach)
4	BKM050911-01	5/9/2011	31.6680	-81.1371	487,005.00	3,503,644.00	5.35	130.0	130.0	0.0%	Seaside Spit	dunes at top of berm, Seaside Spit
5	BKM050911-02	5/9/2011	31.6679	-81.1373	486,987.00	3,503,636.00	4.45	150.0	150.0	0.0%	Seaside Spit	washover fan, Seaside Spit
6	BKM050911-03	5/9/2011	31.6679	-81.1375	486,962.00	3,503,631.00	2.33	488.0	518.0	5.9%	Seaside Spit	marsh west of washover fan, Seaside Spit
7	BKM051011-01	5/10/2011	31.5981	-81.1498	485,792.00	3,495,895.00	6.95	137.0	147.0	6.9%	Beach Pond	Beach Pond transect, near trackhoe west of pond
8	BKM051011-02	5/10/2011	31.5979	-81.1494	485,824.00	3,495,876.00	2.89	476.5	563.0	15.3%	Beach Pond	Beach Pond transect, in pond - west
9	BKM051011-03	5/10/2011	31.5977	-81.1491	485,860.00	3,495,859.00	3.71	361.0	361.0	0.0%	Beach Pond	Beach Pond transect, in pond - east
10	BKM051111-01	5/11/2011	31.5976	-81.1488	485,887.00	3,495,847.00	7.56	392.0	403.0	2.8%	Beach Pond	Beach Pond transect, east side top of berm, backbeach
11	BKM051311-01	5/13/2011	31.6552	-81.1689	483,989.00	3,502,226.00	3.81	457.0	529.0	12.2%	SC Shell Ring	Marsh north of St Catherines Shell Ring (SCSR)
12	BKM052411-01	5/24/2011	31.5836	-81.1556	485,240.00	3,494,292.00	3.30	180.0	180.0	0.0%	Flag Pond	Flag Lagoon transect, eastern most point on beach berm
13	BKM052411-02	5/24/2011	31.5837	-81.1560	485,195.00	3,494,308.00	2.92	425.0	433.0	1.8%	Flag Pond	Flag Lagoon transect, in pond east
14	BKM052511-01	5/25/2011	31.5840	-81.1564	485,158.00	3,494,332.00	1.21	501.0	562.0	10.8%	Flag Pond	Flag Lagoon transect, in pond west
15	BKM052511-02	5/25/2011	31.5844	-81.1567	485,129.00	3,494,377.00	5.61	195.0	202.0	3.5%	Flag Pond	Flag Lagoon transect, western most point, on Jungle Road
16	IEP 060411-01	6/4/2011	31.6247	-81.1725	483,638.52	3,498,850.66	3.23	507.0	569.0	10.8%	<i>MSCdG</i>	Mission - Wamassee Creek
17	IEP 060411-02	6/4/2011	31.6249	-81.1724	483,647.10	3,498,877.25	2.68	538.0	568.0	5.3%	<i>MSCdG</i>	Mission - Wamassee Creek
18	BKM072211-01	7/22/2011	31.5834	-81.1553	485,269.00	3,494,269.00	N/A	N/A	N/A	N/A	Flag Pond	Flag Lagoon - on beach below MLS
19	BKM072211-02	7/22/2011	31.5834	-81.1552	485,273.00	3,494,271.00	1.71	275.0	549.0	6.5%	Flag Pond	Flag Lagoon - on beach below MLS
20	BKM072311-01	7/23/2011	31.5975	-81.1483	485,928.00	3,495,833.00	1.09	446.0	522.0	15%	Beach Pond	Beach Pond - on beach below MLS
21	BKM012112-01	1/21/2012	31.6864	-81.1326	487,431.00	3,505,686.00	1.19	577.0	526.0	8.8%	North Beach	North Beach at Sand Pit Road Entrance
22	BKM012112-02	1/21/2012	31.6875	-81.1314	487,549.00	3,505,804.00	0.20	527.0	575.0	8.2%	North Beach	North Beach north of Sand Pit Road Entrance
23	BKM031712-01	3/17/2012	31.6841	-81.1347	487,230.00	3,505,426.00	-0.42	488.0	529.0	7.7%	North Beach	North Beach north of YBB
24	BKM031712-02	3/17/2012	31.6814	-81.1361	487,099.00	3,505,135.00	1.08	515.0	568.0	9.4%	North Beach	North Beach at north end of YBB
25	BKM031812-01	3/18/2012	31.6754	-81.1373	486,985.00	3,504,460.00	3.68	466.0	468.5	3.7%	Seaside Spit	Seaside Ramp in peat layer
28	IEP-061112-01	6/11/2012	31.6257	-81.1748	483,425.60	3,498,963.70	2.78	380.0	545.0	30%	<i>MSCdG</i>	Mission - West Margin of Marsh
29	IEP-061112-02	6/11/2012	31.6259	-81.1745	483,454.10	3,498,978.40	9.09	150.0	179.0	16%	<i>MSCdG</i>	Mission - West Margin of Island Core

## Notes:

- 1) Date = date of initial boring
- 2) Latitude/Longitude in decimal degrees, datum is WGS 84
- 3) Easting/Northing = coordinates in meters, projection is UTM Zone 17 North, datum is NAD 83
- 4) Surface EL = elevation in feet above mean sea level (MSL) based on LIDAR data
- 5) Total Depth (cm) Recovered = total length of core recovered in cm, loss equals compaction and core lost during retrieval/recovery
- 6) Total Depth (cm) Original = total depth below land surface that core pipe was advanced in cm
- 7) Compaction = percent of compaction: (orig. core length - final core length)/orig. core length
- 8) *MSCdG* = Mission Santa Catalina de Guale

the island. Due to these study areas being associated with modern processes and depositional systems, many of the upper sections of the cores were used as reference data with the lower sections providing stratigraphic information. In addition, a select vibracore was collected in the high marsh depositional environment adjacent to the St. Catherines Shell Ring site as a vibracoring methods demonstration core and used in the current study. The interpretations of the facies and associated depositional environments were performed using field observations and reference data collected under the current study, local reference data from previous work on St. Catherines Island by other researchers (Linsley, 1993; Bishop et al, 2011), and regional reference data from local studies (Sapelo Island and adjacent continental shelf) consisting of sediment and core sampling results and interpretations of depositional environments (Howard and Frey, 1980; Howard and Scott, 1983; Howard and Frey, 1985).

### *6.2.1 Seaside Spit Study Area*

A series of five vibracores (BKM 112110-01, BKM 112110-02, BKM 050911-01, BKM 050911-02 and BKM 050911-03) were situated across an active washover fan at Seaside Spit and collected from November 2010 to May 2011 (Figure 6-9b). The eastern most core location was situated on the active beach near mean sea level, and the western most core was located in the marsh beyond the distal edge of the washover fan in May 2011. Three of the cores (BKM 112110-01, BKM 112110-02, and BKM 050911-03) were advanced to the maximum depth permissible by the length of the core pipe (20 feet or  $\pm 6.1$  meters) or approximately 5.5 meters (18 feet) below land surface (BLS), and two of the cores (BKM 050911-01 and BKM 050911-02) were advanced through the washover fan (approximately 2 meters) to evaluate the washover fan facies and stratigraphy. All three of the deeper cores penetrated an intensely bioturbated and

laminated sand and mud facies between 2.0 and 3.5 meters BLS. Laminae were composed of fine to very fine sands ranging from 2 to 13 cm in thickness, with dark gray (10YR 2/1) mud laminae ranging from 1 to 5 cm in thickness, containing mud clasts and rip-up clasts. Sand filled unlined burrows, approximately 1-3 cm in diameter (10YR 5/1) cut across or truncate mud laminae and are in turn truncated by erosional contacts and the mud laminae and clasts (clay with silt and little fine sand), that are dark gray-black (10YR 2/1). The sediments from this interval have been interpreted to represent the “bioturbated and laminated facies” of Howard and Scott (1983), and indicate sediments deposited in 2-5 meters of water depth. This laminated and burrowed interval is overlain in the three deeper cores by an abrupt or erosional contact, which is in turn overlain by approximately 50 cm of muddy sand. This muddy sand material is composed of a fine to very fine sand with appreciable mud content with no apparent bedding or sedimentary structures and it is associated with tidal creek processes. The muddy sand is overlain by a 1.6 to 3.1 meter thick mud unit in the three deeper cores, that is composed of dark gray-black mud (10YR 2/1), with abundant organic plant macromaterial and *Crassostrea* shells. The mud grades into a peaty material at 30 to 50 cm depth with increasing *Spartina* rhizomes and plant fragments and decreasing mud content in the upper section, culminating in a *Spartina* peat that ranges from 10 to 30 cm in thickness. The intertidal low energy marsh depositional environment is associated with the mud unit based on the observed similarities with modern analogues and reference data.

Washover fan facies are dominated by fine to very fine quartz sands with appreciable heavy mineral content based on visual observations and FPXRF results that are described in the results for the FPXRF data. Peat development is noted within the washover sands in several of the cores and appears to have been developed on inactive washovers and demarcate a minimum

of two separate washover events in cores BKM 112110-01 and BKM 112110-02. Peat development indicates the placement or deposition of the washover fan sediments within the low marsh environment (Deery and Howard, 1977). Cores BKM 050911-01 and BKM 050911-02 record evidence of one washover event based on limited peat development, and since these cores are located on the transect between BKM 112110-01 and BKM 112110-02, these conditions may indicate that reworking of washover materials has occurred, or that lateral discontinuities in the peat development or washover fan deposition exist.

Two samples for radiometric analysis were submitted from core BKM 112010-01 and one sample was collected and submitted for analysis from core BKM 050911-03. A sample of wood was collected from core BKM 112010-01 within the low marsh muddy facies interval at -90 cm BLS (Sample BKM 112010-01-90; percent modern carbon or pMC = 99.52%).

*Crassostrea* that appeared in living position were collected from the low marsh or tidal creek muddy facies at -155 cm BLS (Sample BKM 112010-01-155; AMS  $^{14}\text{C}$  = 677 +/- 28 B.P.), and a whole *Mulinia* shell was collected from the bioturbated and laminated facies at -440 cm BLS (Sample BKM 050911-03-440; AMS  $^{14}\text{C}$  = 6174 +/- 35 B.P.). The results from the Seaside Spit vibracores suggest an interpreted water depth of 2-4 meters below mean sea level based on the reference data of Howard and Scott (1983), indicating a shoreline that was located to the west of the modern shoreline at 6174 +/- 35 B.P. The subtidal sediments are unconformably overlain by a muddy sand facies associated with tidal creek processes, and low marsh or intertidal conditions are indicated by facies and radiocarbon data as occurring in Seaside Marsh from a time interval prior to 677 +/- 28 B.P. until recent. The wood sample collected from core BKM 112010-01 at -90 cm BLS constrains the overlying washover fans indicating that the two observed washover events occurred during the immediate recent or modern period.

### 6.2.2 Beach Pond Study Area

A series of five vibracores (BKM 051011-01, BKM 051011-02, BKM 051011-03, BKM 051111-01 and BKM 072311-01) were situated across an inactive washover fan at the Beach Pond study area and collected from May 2011 to July 2011 (Figure 6-9c). The eastern most core (BKM 072311-01) was located on the active beach at mean sea level, two of the cores were located within the footprint or extents of the pond (BKM 051011-02 and BKM 051011-03) and the western most core was located adjacent to a former beach ridge on the west side of the pond (BKM 051011-01). Four of the cores were advanced to the maximum depth permissible by the length of the core pipe (20 feet or  $\pm 6.1$  meters) or approximately 5.5 meters (18 feet) BLS, and two of the cores were advanced through the inactive washover fan to evaluate the washover fan facies and stratigraphy. Two of the cores penetrated an intensely bioturbated and laminated sand and mud facies between 3.15 and 3.62 meters BLS. Laminae were composed of fine to very fine sands ranging from 2 to 13 cm in thickness, with mud (clay/silt) laminae (10YR 2/1) ranging from 1 to 5 cm in thickness, containing mud clasts and rip-up clasts. Sand filled unlined and elliptical shaped burrows, approximately 1.5 to 2.0 cm in diameter (10YR 5/1) cut across or truncate mud laminae and are in turn truncated by erosional contacts. Fine sand sized shell fragments and whole disarticulated valves of *Mulinia* and *Donax* were observed. The sediments from this interval have been interpreted to represent the “bioturbated and laminated facies” of Howard and Scott (1983), and indicate sediments deposited in 2-4 meters of mean water depth or within the transition zone. The bioturbated and laminated facies grade abruptly into 80 cm of a fine to very fine quartz sand with faint laminations at 2.95 meters BLS in BKM 051011-02 that are interpreted to be forebeach sands or the “laminated facies” of Howard and Scott (1983), that

are in turn overlain by another 80 cm interval of laminated sands and muds assigned to the “bioturbated and laminated facies”. In BKM 051011-02 and BKM 072311-01 a second package of forebeach sand is situated above the uppermost bioturbated and laminated interval, whereas BKM 051011-03 and BKM 051111-01 terminated in the forebeach sands due to the relatively higher elevation or topography of the core location. All four of the eastern borings exhibit an upper interval of laminated mud and sands immediately overlying the forebeach sands, however this package of sediment is differentiated from the bioturbated and laminated facies observed in the lower section of the cores due to a much lower degree of burrowing, a relatively higher percentage of mud laminae, and a fining upward texture. This interval is interpreted as being deposited in the high marsh environment, or as fill material accumulating between adjacent dune ridges situated within a high marsh setting. This interpretation is substantiated by Booth et al. (1999), who noted an increasing percentage of terrestrial pollen (*Myrica*, *Poaceae*, *Asteroideae*, and *Iva*) near the top of the sequence in a core collected at Beach Pond. A marsh mud of approximately 80 to 90 cm in thickness is situated above the high marsh/swale fill material in the four eastern cores, and contains abundant *Poaceae*, *Myrica*, and Cheno-Am type pollen indicating a depositional environment similar to the modern marsh and hammock environments (Booth et al., 1999). Two of the cores (BKM 051011-03 and BKM 051111-01) penetrated the inactive washover fan and the development of peat (13 cm in thickness) was noted on the washover at core BKM 051011-03, whereas it appears to have been removed or non-existent at BKM 051111-01. A well developed, dark brownish black peat (5YR2/1) occurs near the surface at BKM 051011-02 and is attributed to deposition in a freshwater pond or lacustrine environment based on high abundance of *Myrica* (wax myrtle) pollen, a low percentage of broken *Pinus*



(pine) pollen indicating calm water conditions, and an absence of microforams and dinoflagellate cysts (Booth et al., 1999).

Three samples for radiometric analysis were submitted from core BKM 051011-02: 1) a *Mulinia* shell was collected from within the bioturbated and laminated facies interval at -350 cm BLS (Sample BKM 051011-02-350; AMS  $^{14}\text{C}$  = 1,632 +/- 30 B.P.); 2) a wood fragment was collected from the base of the high marsh/swale fill materials at -185 cm BLS (Sample BKM 051011-02-185; AMS  $^{14}\text{C}$  = 755 +/- 22 B.P.), and; 3) a wood fragment was collected from the base of the marsh mud at -90 cm BLS (Sample BKM 051011-02-90; AMS  $^{14}\text{C}$  = 777 +/- 30 B.P.). The results from sample BKM 051011-02-350 collected from within the subtidal sediments at 350 cm BLS suggest an interpreted water depth of 2-4 meters below mean sea level based on the reference data of Howard and Scott (1983) and indicate that the shoreline was located to the west of the modern shoreline at 1,632 +/- 30 B.P. Modern water depths of two to four meters are typically encountered at distances greater than one kilometer to the east of the current shoreline. A shallowing of water depth may be inferred from the facies succession to the overlying forebeach sands and indicate a change from subtidal to intertidal conditions. The radiometric samples from the high marsh/swale fill sediments (BKM 051011-02-185) and overlying marsh muds (BKM 051011-02-90) are rather congruent indicating a relatively rapid change in depositional environments. The high marsh to low marsh conversion of depositional environments is typically associated with a flooding scenario or an increase in relative sea level. A cyclical nature of deposition is indicated by the lower sections of cores BKM 051011-02 and BKM 072311-01 where two intervals of the subtidal sediments (bioturbated and laminated facies) alternate with two intervals of intertidal (laminated facies) sediments indicating multiple shallowing or progradational sequences.

### 6.2.3 Flag Pond Study Area

A series of five vibracores (BKM 052411-01, BKM 052411-02, BKM 052511-01, BKM 052511-02 and BKM 072211-02) were situated across an active flood delta and washover fan complex at Flag Pond and collected from May 2011 to July 2011 (Figure 6-9d). The eastern most core (BKM 072211-02) was located on the active beach at an elevation slightly higher than current mean sea level, one core was collected from the area occupied by the modern beach berm (BKM 052411-01), two of the cores were located within the tidally influenced pond or lagoon (BKM 052411-02 and BKM 052511-01) and the western most core was located within a former beach ridge on the west side of the pond (BKM 052511-02). Three of the cores were advanced to the maximum depth permissible by the length of the core pipe (20- feet or  $\pm 6.1$  meters) or approximately 5.5 meters (18 feet) BLS, and two of the cores met refusal at approximately 2 meters depth (BKM 052411-01 and BKM 052511-02). The three deeper cores penetrated an intensely bioturbated and laminated sand and mud facies between 2.4 and 3.7 meters BLS. Laminae were composed of fine to very fine sands ranging from 2 to 13 cm in thickness, with mud (clay/silt) laminae (10YR 2/1) ranging from 1 to 5 cm in thickness, containing mud clasts and rip-ups. Sand filled, unlined and elliptical shaped burrows, approximately 1.5 to 2.0 cm in diameter, and light grayish brown (10YR 5/1), cut across or truncate mud laminae and are in turn truncated by erosional contacts. Fine sand sized shell fragments and whole disarticulated valves of *Donax* are observed. The “bioturbated and laminated” sediments are overlain by a package of fine to very fine quartz sands with slight or faint quartz/HMS laminations and *Callianassa* burrows, indicating a lower forebeach depositional environment or the “burrowed and laminated” facies of Howard and Scott (1983). The “burrowed and laminated” facies grade into fine to very fine quartz sands with slight or faint quartz/HMS lamination above, but lacking *Callianassa*

burrows. This package is interpreted as the “laminated facies” of Howard and Scott (1983) indicating an upper forebeach depositional sub-environment. A marsh mud sequence overlies the forebeach sands with a well-developed peat material observed near the surface in cores BKM 052411-01, BKM 052411-02 and BKM 052511-01. The washover fan and flood delta complex completely covers the northern portions of Flag Pond and is prominent in cores BKM 052411-02 and BKM 052511-01, and consists of fine to very fine quartz sands with appreciable HMS content and small laminae (2-5 mm) that dip in opposite directions (N90°E/N90°W). Laminae that dip in opposite directions are indicative of bimodal flow regimes and are diagnostic features of flood deltas. Core BKM 052511-02 exhibits sediments and facies typically associated with forebeach and backbeach facies. The lower section of the core (195 cm to 110 cm BLS) has faint quartz/HMS laminations that become more pronounced at 100 cm BLS, however the primary physical structures were apparently destroyed by bioturbation (roots) in the upper 50 cm to 60 cm interval of the core. The lower section of BKM 052511-02 has been interpreted as forebeach in origin, and the upper portion of the core is attributed to the backbeach or beach berm environment.

Two samples were submitted for radiometric analysis from core BKM 052511-01 and one sample was submitted from core BKM 052411-02. A *Donax* shell was collected from the lower section of core BKM 052511-01 within the bioturbated and laminated facies at 496 cm BLS (AMS  $^{14}\text{C}$  = 5,831 +/- 35 B.P.) and a *Mulinia* shell was collected from near the top of the forebeach sands at 244 cm BLS (AMS  $^{14}\text{C}$  = 1,559 +/- 25 B.P.). A sample of wood was also collected from BKM 052411-02 near the top of the marsh mud at -79 cm BLS, however a radiocarbon date was not calculated for the specimen due to the high percentage of modern carbon (> 100 pMC), this date indicates very recent sedimentation in a low marsh environment.

Based on previous research (Bishop et al., 2011) and a review of historical imagery, an inlet initially formed through the eastern berm of Flag Pond as a result of the “Storm of the Century” in March 1993. The opening of the inlet resulted in the conversion of the washover fan into active flood deltas. The inlet has demonstrated a dynamic nature by moving over 75 meters from 1999 to 2009 in a southerly direction. Inlet fill facies were encountered in core BKM 072211-02 and are described as very fine quartz sands with abundant shell fragments, rippled laminations and peat materials associated with the abandoned inlet.

#### *6.2.4 North Beach Study Area*

A series of five vibracores (BKM 012112-01, BKM 012112-02, BKM 031712-01, BKM 031712-02 and BKM 031812-01) were collected in January and March 2012 from Seaside Ramp extending to the north of the Sand Pit Road entrance along North Beach (Figure 6-9a). All five cores were advanced to the maximum depth permissible by the length of the core pipe (20 feet or  $\pm 6.1$  meters) or approximately 5.5 meters (18 feet) BLS. Cores BKM 012112-01, BKM 012112-02, and BKM 031712-01 are located in the northeastern accretional terrains where active accretion is occurring, whereas the two cores to the south (BKM 031712-02 and BKM 031812-01) were located in areas where active shoreline retreat is occurring based on the results from the shoreline dynamics study.

Core BKM 012112-01 was situated due east of the Sand Pit Road entrance to North Beach at approximately 30 cm above MSL in the modern forebeach environment. The core location is situated in the northeastern accretional terrains where island progradation is occurring at the present. As a result of the location, the boring penetrated 150 cm of upper forebeach laminated sands with appreciable shell debris associated with the modern foreshore. At a depth

of 150 cm the material transitions to the laminated muds and sands associated with the “bioturbated and laminated facies”. From depths of 150 cm to 300 cm there is an increasing density in mud laminae and an abrupt contact with underlying muddy sands containing appreciable shell fragments observed at 300 cm BLS. At 340 cm BLS the muddy sand transitions to a dark gray brown (2.5Y 5/1) fine to very fine sand, with little mud content that is extensively burrowed with sand filled burrows, and the degree of bioturbation increases with depth to the total recovered length of the core (4.74 m). The lower 52.1 cm of sample material was lost upon retrieval and no carbon-dateable material of interest was observed or collected from the boring.

Core BKM 012112-02 was situated approximately 140 meters north of the Sand Pit Road entrance to North Beach near mean sea level in the modern forebeach environment. The core location is situated in the northeastern accretional terrains where island progradation is occurring at the present. As a result of the location the boring penetrated 180 cm of laminated upper forebeach sands with shell debris and peat stringers, where the latter are composed of plant macromaterial debris and appear to dip gently (10-15 degrees). The core was located in close proximity to a modern analogue where organic materials have accumulated within a beach runnel. The forebeach sequence was underlain by 90 cm of laminated sands and muds correlating to the bioturbated and laminated facies that is located at -2.0 to -2.7 meters below MSL. This facies succession is anticipated in an accretional terrain where the island is currently prograding and it would be predicted or expected that subtidal sediments would be succeeded or overlain by intertidal sediments as a result of island progradation. The laminated sands and muds (bioturbated and laminated facies) are underlain by a burrowed and abrupt contact and 45 cm of muddy sand containing whole disarticulated shells and shell fragments (*Mulinia*, *Ilyanassa*

and *Littoraria*). The muddy sand grades downward into a dark grayish-brown mud (2.5Y 3/1) with peat laminations that extends to 395 cm BLS. Another abrupt contact separates the muddy intervals from an underlying medium gray (2.5 6/1), fine to very fine quartz sand with mud clasts. The sand is heavily burrowed (sand filled burrows) with abundant shell fragments deposited in layers and is interpreted as a transgressive surface based on the shell lag facies and an unconformable sequence of facies. At 457 cm BLS a lower shell lag is situated on top of a lower marsh mud sequence and is also interpreted as a transgressive surface based on the shell lag facies and unconformable sequence of facies. The low marsh mud is 52 cm in thickness with a notable 8 mm peat lamination at 520 cm BLS. Four samples for radiometric analysis were submitted from core BKM 012112-02. An *Ilyanassa* shell was collected from the upper muddy sand interval at 315 cm BLS (AMS  $^{14}\text{C} = 2,614 \pm 27$  B.P.), a *Donax* shell was collected from the shell lag situated on the lower marsh mud at 465 cm BLS (Sample BKM 012112-02-465; AMS  $^{14}\text{C} = 39,124 \pm 377$  B.P.), a *Mulinia* shell was also collected from the shell lag situated on the lower marsh mud at 470 cm BLS (Sample BKM 012112-02-470; AMS  $^{14}\text{C} = 45,200 \pm 647$  B.P.), and the peat material located at 520 cm BLS was also sampled (Sample BKM 012112-02-520; AMS  $^{14}\text{C} = 50,376 \pm 1,020$  B.P.). Based on the results, the upper marsh mud is assigned a Late Holocene age and the lower marsh mud containing the peat material is assigned a Late Pleistocene age. The older radiocarbon dates ( $> 45,000$  B.P.) should be considered as minimum constraining dates for the age of the materials, as the age values are considered infinite using radiocarbon dating techniques.

Core BKM 031712-01 was situated on North Beach approximately 320 meters south of the Sand Pit Road entrance to North Beach near MSL in the modern forebeach environment. The core was situated in the northeastern accretional terrains where island progradation is

occurring at the present. As a result of the location, the boring penetrated 264 cm of faintly laminated fine to very fine sands with abundant shell fragments and whole disarticulated shells in layers at 94 cm, 100 cm, 117 cm, 145cm and 200 cm BLS. The mud content increased downward from 230 cm to 264 cm BLS where the sands transitioned abruptly into muddy sand with abundant shell fragments and whole disarticulated shells (*Mulinia*, *Donax* and *Littoraria*) in layers at 267 cm and 305 cm BLS. At 305 cm BLS the muddy sand is terminated abruptly by an erosive contact that is underlain by fine to very fine sands that are heavily burrowed with sand filled burrows (*Skolithos*). The boring was terminated at 4.18 meters BLS, or the practical extent of the core pipe. Three samples for radiometric analysis were submitted from core BKM 031712-01: 1) a *Mulinia* shell was collected from the upper sand with shell material at 117 cm BLS (Sample BKM 031712-01-117; AMS  $^{14}\text{C}$  = modern); 2) a *Mulinia* shell was collected from immediately above the muddy sand interval at 267 cm BLS (Sample BKM 031712-01-267; AMS  $^{14}\text{C}$  = modern), and; 3) a *Donax* shell was collected from the lower portion of the muddy sand interval at 305 cm BLS (Sample BKM 031712-01-305; AMS  $^{14}\text{C}$  = 295 +/- 24 B.P.). Rapid sedimentation and island progradation are inferred from the facies successions and the age-depth relationship indicates the rapid accumulation of more than three meters of sediment in less than 300 radiocarbon years.

Core BKM 031712-02 was situated on North Beach approximately 635 meters south of the Sand Pit Road entrance to North Beach near mean sea level in the modern forebeach environment. The core location is situated just north of Yellow Banks Bluff where island erosion or shoreline retreat is presently occurring and the core was positioned in an effort to penetrate the sediments associated with a former oxbow pond that is currently being removed via shoreline capture. The boring penetrated 55 cm of forebeach "laminated facies" consisting of

faintly laminated fine to very fine sands with abundant shell fragments and whole disarticulated shells. The sands were underlain by an abrupt contact with a brown peat containing abundant plant fragments that transitioned into a dark gray black (10YR 10YR 2/1) mud that extended to 120 cm BLS. The muds transition at 120 cm BLS to a fine to very fine sand with dark gray (2.5Y 4/1) mud laminae, with the mud laminations and clasts occurring in a light brown to gray (2.5Y 7/1) fine to very fine sand. Mud content increases upward from 180 cm to 120 cm BLS and the fining upward sequence is underlain by a shell lag at 410 cm to 425 cm BLS. The fining upward sediments from 120 cm to 425 cm BLS are interpreted as tidal creek facies with the overlying muds and peats from 55 cm to 120 cm interpreted as low marsh and oxbow pond sediments. The basal shell lag is situated above a dark gray brown (2.5Y 5/1) fine to very fine sand with some mud content from 425 cm to 477 cm BLS. The muddy sand is extensively burrowed with sand filled burrows and separated from the overlying tidal creek sequence by an abrupt erosional contact. One sample for radiometric analysis was submitted from core BKM 031712-02, which was a fragment of a *Mercenaria* shell that was collected from the shell lag at 410 cm BLS (Sample BKM 031712-02-410; AMS  $^{14}\text{C} = 2,829 \pm 29$  B.P.). No radiocarbon dateable materials were recovered from the lower burrowed muddy sand.

Core 031812-01 was situated on North Beach at the base of Seaside Ramp in the modern forebeach environment. The core was located at the southern terminus of Yellow Banks Bluff in an outcrop of brown peat on the active beach near mean sea level, where island erosion or shoreline retreat is occurring at the present. The boring penetrated 65 cm of a dark brown (2.5Y 8/2) peat with fine to very fine sand interbedded with organic material. The sandy peat was underlain by 65 cm of a dark brown (2.5Y 8/2) peat with some fine to very fine sand and transitioned at 130 cm to 135 cm BLS into a dark gray-black (10YR 2/1) sandy mud (clay and



silt) with some fine to very fine sand. At 170 cm BLS the sandy mud transitioned to a 65 cm thick dark gray-black (N3 to 10YR 2/1), organic mud (clay and silt and very little fine sand) with two sand stringers (5 mm to 10 mm) at 200 cm BLS. At 235 cm BLS the mud transitions to a fine to very fine sand with mud laminae, where the mud laminations and clasts (2.5Y 4/1) occur in a light brown to gray fine to very fine sand (2.5Y 7/1). The mud is terminated by an erosive contact that is underlain in turn by a medium to light gray (5Y 8/1) fine to very fine sand occurring from 260 cm to 322 cm, with brown mud-lined *Callianassa* burrows associated with the burrowed and laminated facies representing the lower forebeach environment. The forebeach sands are underlain by a dark gray brown (2.5Y 5/1) fine to very fine sand, with some to little mud that is extensively burrowed with sand filled burrows and is interpreted as being of a subtidal origin.

#### 6.2.5 *St. Catherines Shell Ring - High Marsh Core*

A core (BKM051311-01) was advanced in the high marsh located on the western margin of the island immediately north of the St. Catherines Shell Ring site in order to evaluate the facies associated with the high marsh environment (Figure 6-9a). The core was advanced to 4.57 meters BLS, or the practical extent of the 2-inch (505 mm) pipe. The upper 200 cm of sediment may be described as a gray fine to very fine quartz sand with dark gray mud laminae and clasts. The laminae are discontinuous, horizontal to gently dipping, and vary in thickness from 2 mm to > 20 mm and the sands have little HMS content. This unit is underlain by approximately 90 cm of a gray fine to very fine sand with appreciable HMS content, and the laminations are nearly horizontal and the HMS content appears to decrease with depth. An abrupt contact is noted at 295 cm BLS and the underlying sediment is described as a brown fine to very fine sand with

dark brown mud laminae and clasts. The mud laminae are discontinuous, horizontal to gently dipping, and vary in thickness from 2 mm to > 20 mm. Based on the location of the core and the nature of the facies observed in the upper portion of the core, the upper 200 cm of sediments are interpreted as high marsh sediments. The unit from 200 cm to 295 cm BLS is noted as being dominated by fine sands and is attributed to tidal creek processes. The high marsh adjacent to the St. Catherines Shell Ring site receives a substantial amount of runoff from streams that drain the island core. As a result of the island core sediments being composed primarily of marine sands, these materials would likely be transported into the marsh during significant rainfall or runoff events. The facies in the upper portion of the core (0 cm to 200 cm BLS) and the lower section of the core (295 cm to 457 cm BLS) are similar enough in terms of texture and bedding style such that the lower section is interpreted as representing the high marsh environment. However a distinction is made between the two units with respect to the dominant color of the mud laminae where gray laminae occur above 295 cm BLS and brown laminae occur below 295 cm BLS.

Two radiometric dating samples were collected from core BKM051311-01 and submitted for AMS  $^{14}\text{C}$  analysis: 1) a sample of wood/peat was collected from the lower section of the core in the brown laminated sand/mud interval (Sample BKM 051311-01-395; AMS  $^{14}\text{C}$  = 46,202 +/- 733 B.P.), and; 2) a sample of wood/peat was collected from the upper gray laminated sand/mud interval (Sample BKM 051311-01-133; AMS  $^{14}\text{C}$  = 298 +/- 23 B.P.). The older date of 46,202 +/- 733 B.P. is interpreted as being representative of radiocarbon infinity and should be considered as a minimal age for the sediments. The radiometric data indicates that the high marsh sequence occurring in the lower section of the core was deposited during the Late Pleistocene and the high marsh sequence in the upper portion of the core aggraded during the

Late Holocene or recent time period. The erosive contact noted by the distinct color change at 295 cm BLS is interpreted as a disconformity and the hiatus is most likely the result of the marine regression associated with the LGM. This interpretation is consistent with the occurrence of a regional disconformity between Late Pleistocene and Holocene marine sediments in the Atlantic and Gulf Coastal Plains. It is likely that the Late Pleistocene marine sediments correlate to the Sangamon Stage when sea level was equivalent or slightly greater than modern sea level (Vento and Stahlman, 2011). The subsequent regression of sea level (> 100 meters) during the Wisconsin Glacial Stage most likely resulted in the formation of the disconformity. Based on the age-depth relationship from the upper radiocarbon sample (BKM 051311-01-133), a derived sedimentation rate of 0.45 cm/yr is obtained for the upper sediments associated with the modern high marsh. This local rate of sedimentation has been evaluated against modern sedimentation studies in the high marsh of Sapelo Island and a narrative is provided in the discussions section.

#### *6.2.6 Mission Santa Catalina de Guale*

A series of four vibracores (IEP 060411-01, IEP 060411-02, IEP 061112-01, and IEP 061112-02) were collected at *Mission Santa Catalina de Guale* in June 2011 and June 2012 by students and faculty of the Island Ecology Program (IEP) from Sewanee: University of the South. The two cores that were collected in 2011 were situated within the floodplain of the tributary to Wamassee Creek (Figure 6-10), and the two that were collected in 2012 were situated between meanders of Wamassee Creek to the northwest of the mission site. One of the 2012 cores was located in the modern low marsh environment and one core was located on the topographically higher adjacent island core.

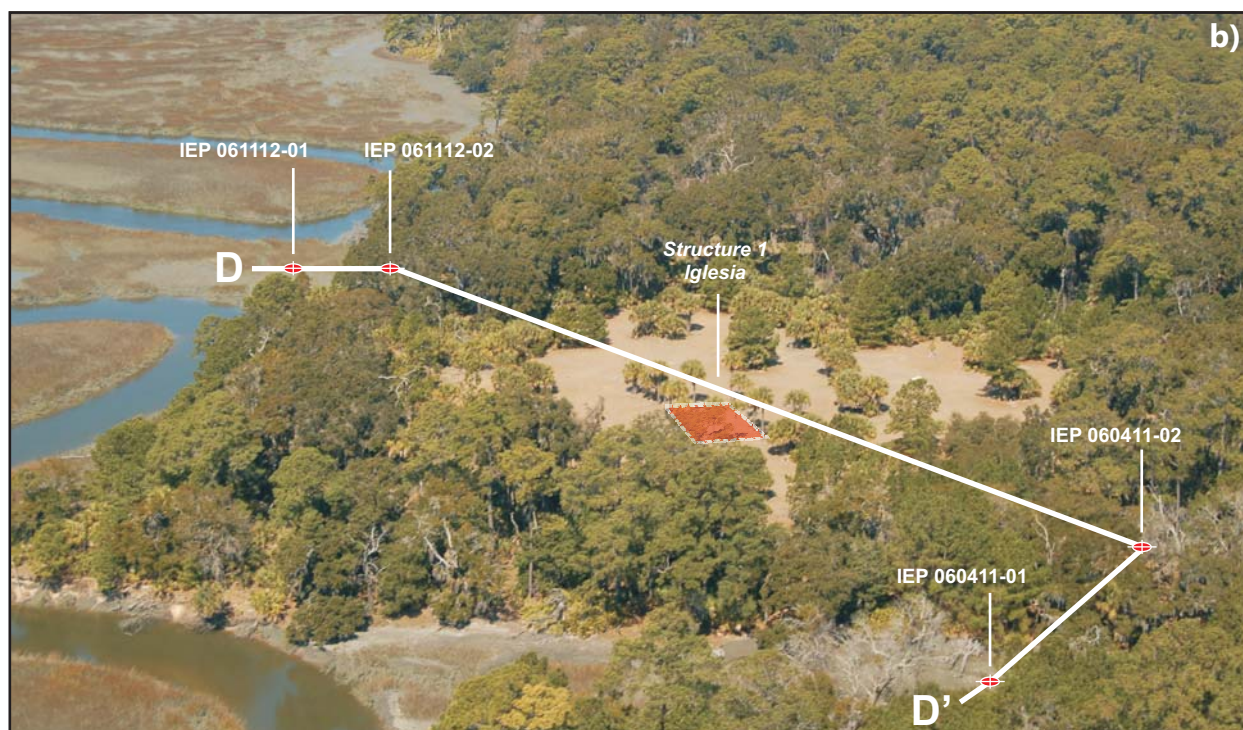


Figure 6-10. Vibracore locations associated with *Mission Santa Catalina de Guale*, St. Catherines Island, GA. a) Map view of four vibracores collected in 2011-2012 by the Island Ecology Program (IEP) of the University of the South. b) Oblique aerial view of the vibracore locations and the index line for vibracore transect D-D'. Photograph (lower) by B. Meyer, map image from USDA NAIP, 2008.



Core IEP 060411-01 was located to the south of the Wamassee Creek tributary and penetrated 50 cm of a dark brown peaty mud (silt/clay) with a noticeable sulfide odor. This unit transitions via a mottled and graded contact to a light brown lower sand with scattered heavy minerals and interbedded muddy sands and dark gray muds that extend to 180 cm BLS. From 180 cm to 320 cm BLS the light brown sand is interbedded with brown peat layers that vary in thickness to 35 cm. At 320 cm BLS this unit is underlain by an erosive contact and 55 cm of light brown fine to very fine sand with brown mud lined burrows, interpreted as the burrowed and laminated facies associated with the lower forebeach environment. This forebeach unit transitions at 375 cm to light brown fine to very fine sand with brown mud laminae and two burrowing styles. The burrow forms include both sand filled and mud lined burrows and the unit is interpreted as the subtidal bioturbated and laminated facies extending to the total depth of the core at 507 cm BLS.

Core IEP 060411-02 was located to the north of the Wamassee Creek tributary and initially penetrated 60 cm of a dark gray to brown, fine to very fine weathered sand, with appreciable organic and mud (clay/silt) content and is underlain by a highly erosive contact. From 60 cm to 170 cm BLS the core penetrated a fine to very fine brown sand with faint laminations and brown mud lined *Callianassa* burrows. The burrows are apparent from 170 cm to 420 cm and the brown mud laminae (< 1 cm) become more frequent from 300 cm to 420 cm BLS. At 460 cm BLS the unit transitions to a fine to very fine brown sand that is laminated with dark brown bioturbated muds and extends to 538 cm BLS. This lower unit is interpreted as the subtidal bioturbated and laminated facies.

Core IEP 061112-01 was located in the marsh between two meanders of Wamassee Creek, designated as Meanders #1 and #2 under the landform dynamics study (Figure 6-10). As

a result of the physical setting, the core penetrated 6 cm of dark brown organic detritus with some mud and sand. Below the surface organic materials, the boring penetrated dark gray mud with iron staining, with the percentage of plant detritus decreasing downward to 120 cm. A dark gray mud sequence occurs from 120 cm to 205 cm below land surface, and transitions into a laminated dark gray mud with light brown fine to very fine sand laminations with a fining upward appearance. This unit grades abruptly into a laminated sand and mud unit that occurs from 257 cm to 305 cm. The lower portion of the core from 305 cm to 380 cm consists of a laminated dark gray mud with light brown fine to very fine sand laminations. The upper section of the core from the surface to 205 cm BLS indicates facies associated with the low marsh depositional environment, and the lower section from 205 cm to 380 cm is interpreted as the high marsh or a tidal creek sequence.

Core IEP 061112-02 was located on the island core at an elevation of 2.77 m (9.09 ft) above MSL. The core penetrated 11 cm of a brown sandy organic top soil that transitioned to a light brown fine to very fine sand with little HMS yet extensive bioturbation (roots) that extended to 57 cm BLS. This unit transitioned to a very light brown fine to very fine sand with some HMS that extended to boring refusal at 150 cm BLS. Although quartz and HMS laminations were not apparent due to extensive bioturbation by plant roots, this unit is interpreted to represent upper forebeach sands due to the presence of some HMS and the lack of other diagnostic features such as mud-lined burrows, sand/mud laminations, etc.

### **6.3 XRF Results**

A total of 1,219 samples have been analyzed via FPXRF from twenty-one borings that were scanned at intervals ranging from five to ten centimeters. Analytes were detected at

concentrations above the detection limits in 100% of the samples for potassium (K), calcium (Ca), titanium (Ti), iron (Fe), strontium (Sr) and zirconium (Zr). Manganese (Mn) was detected in 90% of the samples analyzed and chlorine (Cl) and sulfur (S) were detected in 86% and 53%, of the samples analyzed respectively. A summary graph of the frequencies of analyte detections for the XRF results may be seen in Figure 6-11. The data were compiled into a database with sample metadata (Appendix C), descriptive statistics were generated for the elemental results and cluster analyses were performed.

### *6.3.1 Correlation Analysis*

Initially the XRF data were subjected to a correlation analysis where the intercorrelation for any number of variables (analytes) and for any number of observations (samples) per variable was calculated in order to determine elemental associations. The most commonly detected analytes (K, Ca, Ti, Mn, Fe, and Zr) were used as variables along with ratios for titanium/zirconium (Ti/Zr) and iron/potassium (Fe/K). In addition, sulfur was used for the analysis by substituting the average detection limit in each sample run for the non-detectable concentrations. The correlation evaluation was performed using the VassarStats intercorrelation tool (available at <http://www.vassarstats.net/>), and this analysis was performed on the results from all of the samples. The data were then sorted by general lithology (sands, muds/peats, and muddy sands) and a second intercorrelation of the elemental results was performed.

Strong correlations ( $r > 0.90$ ) are indicated in sandy facies between titanium, zirconium, iron, manganese and the Fe/K ratio as a result of the heavy mineral content and its associated minerals (ilmenite, leucoxene, rutile, garnet, epidote, etc.) as indicated in Figure 6-12. Moderately strong correlations ( $r > 0.70$ ) are indicated in the mud samples for iron and

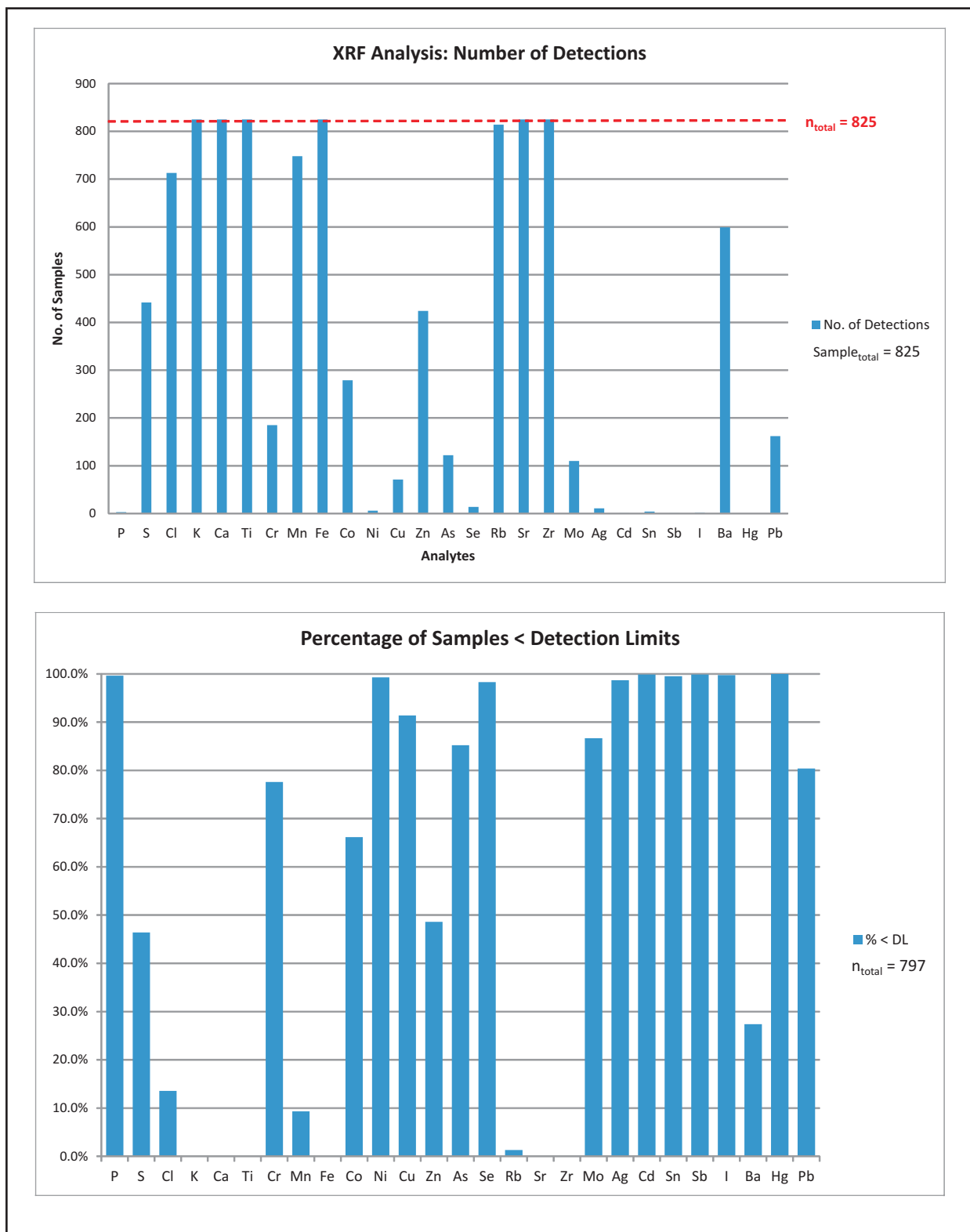


Figure 6-11: Analytes were detected above the detection limits in 100% of the samples for potassium (K), calcium (Ca), titanium (Ti), iron (Fe), strontium (Sr) and zirconium (Zr). Manganese (Mn) was detected in 90% of the samples analyzed using FPXRF. Chlorine (Cl) and sulfur (S) were detected in 86% and 53%, respectively, of the samples analyzed.



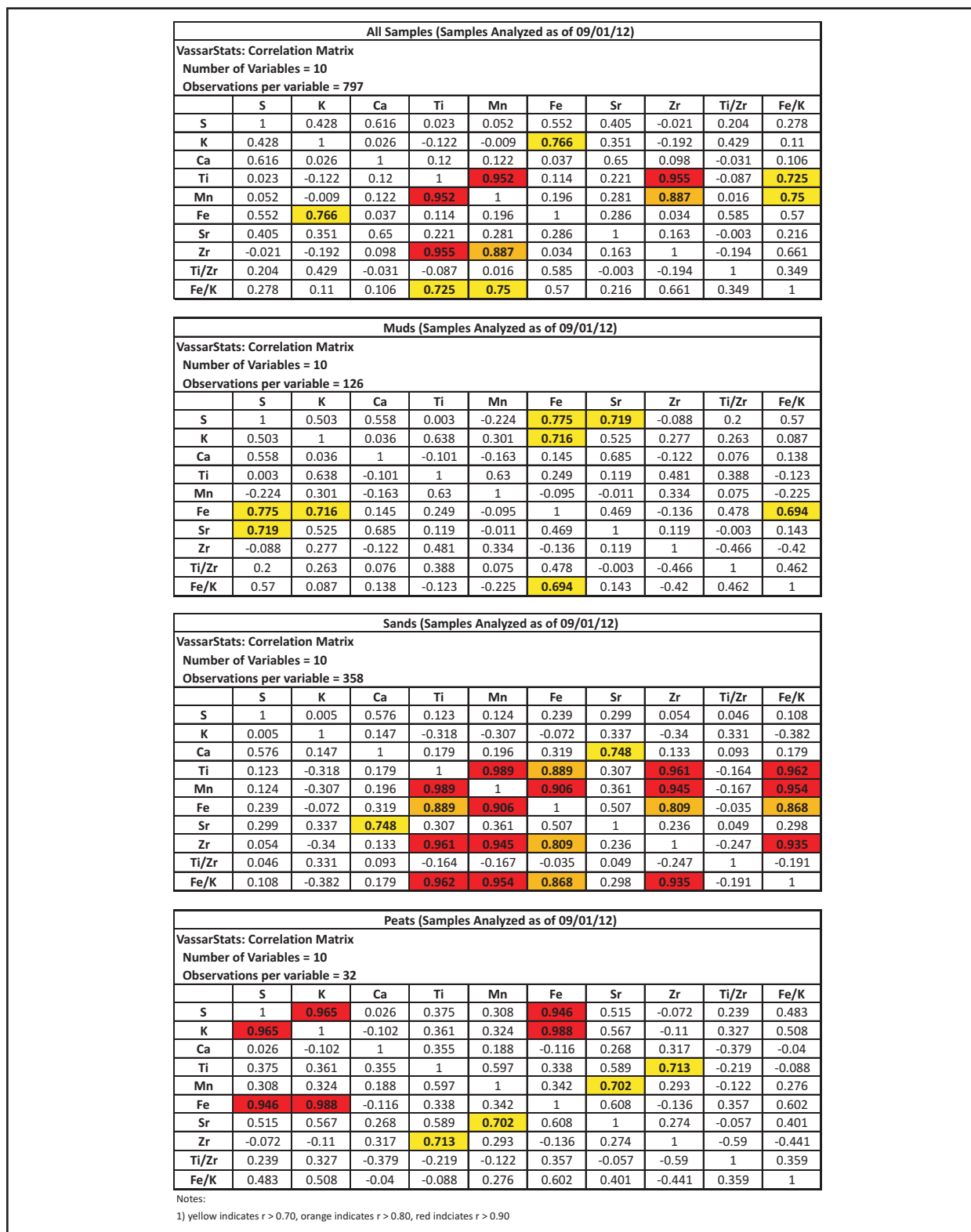


Figure 6-12: The XRF data were subjected to a correlation analysis where the intercorrelation for any number of variable and for any number of observations (samples) per variable were calculated in order to determine elemental associations. The most commonly detected analytes were used as variables with ratios for titanium/zirconium (Ti/Zr) and iron/potassium (Fe/K).

potassium and are most likely attributed to clay mineralogy and a combination of sorption processes and interlayer cation residence. It should be noted that select intervals of cores collected from the marsh muds exhibited strong correlations ( $r > 0.90$ ) in the muddy facies between calcium, sulfur and iron. This has been associated with the primary occurrence of calcareous shell material (*Ostrea virginica* and *Mercenaria mercenaria*) within the marsh mud samples, and secondary alteration to pyrite and/or marcasite of the primary calcareous materials under strongly reducing conditions that occur in the marsh subsurface.

Titanium (Ti) levels in the FPXRF data are controlled by the relative concentrations of ilmenite [(Fe,Mg,Mn,Ti)O<sub>3</sub>], leucoxene (variable chemical comp.) and rutile (TiO<sub>2</sub>). Zirconium (Zr) concentrations in the FPXRF data are controlled by the abundance of zircon (ZrSiO<sub>4</sub>). It is apparent that the concentration of Ti is controlled by the three titanium bearing minerals that occur in varying mineral abundance, and that Ti content also varies within ilmenite and leucoxene. While Ti and Zr were used in the subsequent cluster analysis to define Chemofacies A, appreciable iron and manganese are also present in the heavy minerals based on the FPXRF results and are most likely associated with the occurrence of almandine, hornblende, epidote, tourmaline and staurolite (Table 1).

### 6.3.2 Cluster Analysis

The results of the cluster analyses indicate five major groups that were designated as Chemofacies A through E. Initial cluster analysis results lumped or grouped Chemofacies A and B into one group; however, subsequent analysis using the data assigned to the original group was successful in splitting the data into two groups. Descriptive statistics were then generated for each of the chemofacies (A-E) and box plots were produced. The chemofacies were then

evaluated by plotting the results with the lithostratigraphic information in the form of a chemostratigraphic log, described in Section 6.4. A simple graphical representation of the chemofacies, relative elemental abundances, and associated lithofacies follows in Figure 6-13. The results of the descriptive statistics for the chemofacies and the associated depositional environments are provided in Table 6. The current interpretation of the chemofacies and associated lithologies and depositional environments are as follows:

- Chemofacies A: elevated titanium ( $q_1 = 1,470$  ppm), zirconium ( $q_1 = 254$  ppm) and calcium ( $q_1 = 3,932$  ppm), represented by laminated quartz sands, heavy mineral sands and shell debris, associated with backbeach, washover and eolian depositional environments.
- Chemofacies B: moderate to low levels of titanium ( $q_1 = 358$  ppm), zirconium ( $q_1 = 62$  ppm), and appreciable levels of calcium ( $q_1 = 2,857$  ppm), represented by quartz sands with little to trace amounts of heavy mineral sands, composed of the laminated facies and burrowed and laminated facies associated with the upper and lower forebeach subenvironments. Chemofacies B was originally grouped with Chemofacies A in the initial cluster analysis, a subsequent cluster analysis was performed using the hybrid approach to separate the groups.
- Chemofacies C: moderate levels of titanium ( $q_1 = 1,106$  ppm), zirconium ( $q_1 = 138$  ppm), and calcium ( $q_1 = 2,806$  ppm), appreciable levels of iron ( $q_1 = 2,573$  ppm) and potassium ( $q_1 = 2,524$  ppm), represented by laminated quartz sands (with some heavy mineral sand content) and muds (silt/clay), associated with transition zone subtidal facies (bioturbated and laminated), high marsh laminated muds and sands, and tidal creek depositional

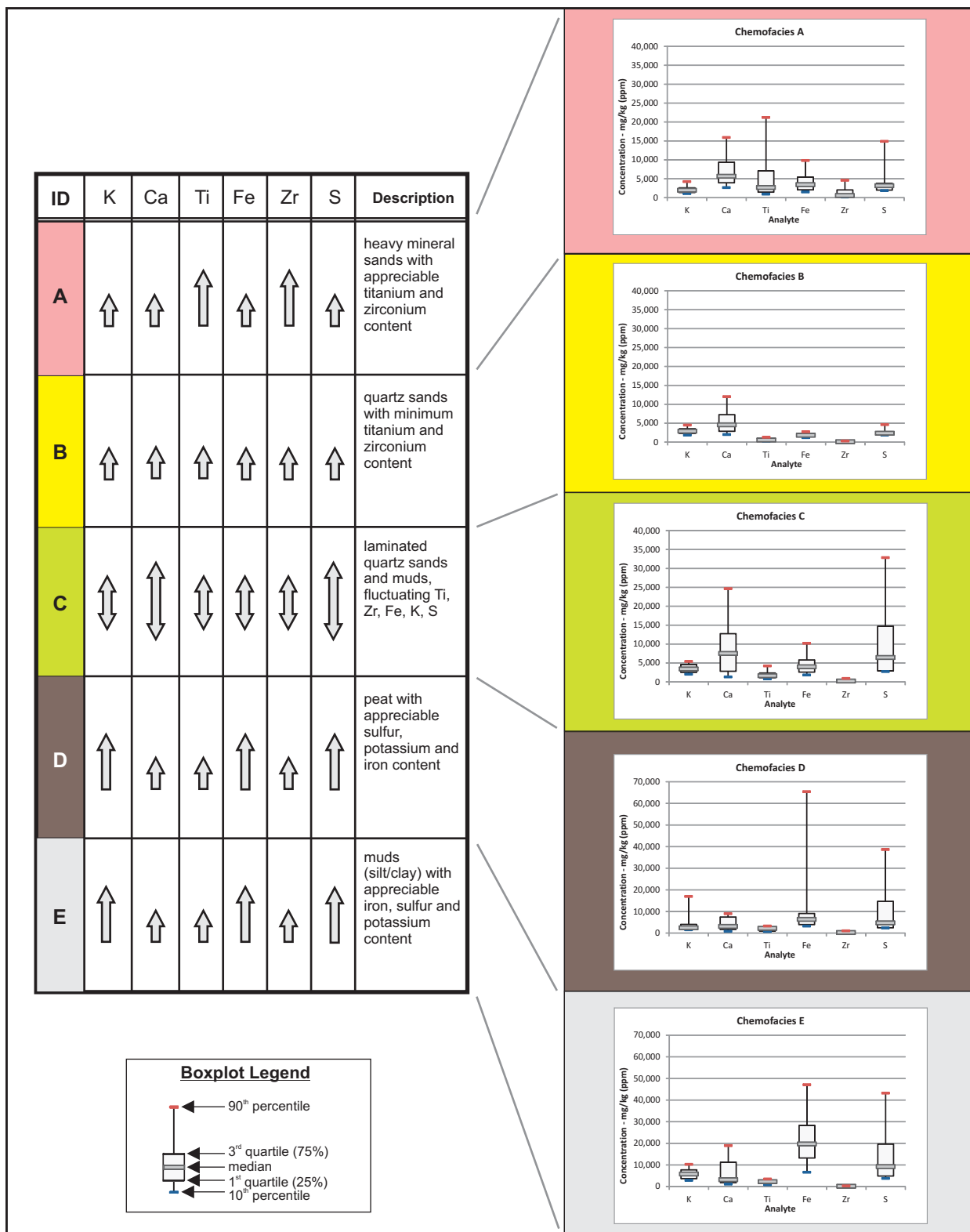


Figure 6-13: A simple graphical representation of the chemofacies groups or designations (A-E) and relative elemental abundances (left) and boxplots for the most commonly detected analytes for Chemofacies A to E (right).

**Table 6:  
Chemofacies, Descriptive Statistics and Lithofacies**

CHEMOFACIES									LITHOFACIES	
Chemofacies ID	Analyte	Min.	10th %	25th %	Median	75th %	90th %	Max.	Lithofacies Description	Depositional Environment/Subenvironment
A	K	550	1,069	1,353	1,962	2,598	4,218	5,994	Quartz sands with appreciable amounts of heavy mineral sands (HMS), HMS containing significant amounts of Ti and Zr bearing minerals (i.e. ilmenite, zircon), horizontal quartz/HMS laminations in backbeach deposits, rippled and horizontal laminations in washover deposits, high angle festoon cross-bedding and quartz/HMS laminations in eolian deposits. Appreciable shells and shell fragments in backbeach deposits.	Backbeach, eolian and washover depositional environments
	Fe	965	1,488	2,071	3,449	5,439	9,810	24,161		
	S	1,817	1,862	2,007	3,155	3,775	14,879	85,422		
	Ca	955	2,639	3,932	5,662	9,369	15,899	100,986		
	Ti	221	920	1,470	2,670	7,086	21,194	80,275		
	Zr	26	149	254	570	2,057	4,583	23,859		
	Ti/Zr	0.98	2.69	3.57	4.40	6.19	8.03	14.00		
	Fe/K	0.28	0.64	0.97	1.60	2.83	5.88	26.60		
B	K	1,086	1,828	2,276	2,864	3,535	4,474	8,063	Quartz sands with minimal amounts of heavy mineral sands (HMS), faint or ghostly laminations where present, whole shells of <i>Mulinia</i> and <i>Donax</i> , some shell fragments. Biofacies include mud-lined ghost shrimp burrows ( <i>Callianassa</i> ) and sand filled burrows.	Forebeach depositional environment
	Fe	692	1,175	1,444	1,813	2,255	2,729	7,726		
	S	1,714	1,862	2,343	2,347	2,751	4,621	28,356		
	Ca	944	1,978	2,857	4,549	7,249	11,987	84,374		
	Ti	83	219	358	563	865	1,276	2,321		
	Zr	27	42	62	96	165	279	556		
	Ti/Zr	2.11	3.38	4.19	5.37	6.92	8.91	17.27		
	Fe/K	0.25	0.45	0.51	0.61	0.77	0.94	1.54		
C	K	558	2,011	2,524	3,401	4,608	5,399	7,975	Laminated quartz sands and mud (silt/clay), moderate concentrations of HMS, intensely bioturbated, with flasers and rip-up clasts and appreciable shell fragments and debris.	Subtidal, tidal creek, dune swale fill and selected high marsh depositional environments
	Fe	458	1,795	2,573	4,003	5,805	10,198	36,282		
	S	2,186	2,715	2,906	6,441	14,714	32,818	88,964		
	Ca	363	1,294	2,806	7,519	12,753	24,618	58,651		
	Ti	211	779	1,106	1,617	2,365	4,196	9,202		
	Zr	29	102	138	231	439	895	2,820		
	Ti/Zr	1.77	3.67	4.47	6.18	8.69	13.44	38.37		
	Fe/K	0.34	0.62	0.80	1.11	1.76	2.52	9.18		
D	K	1,148	1,491	1,706	2,463	4,017	16,946	33,382	Interminated quartz sands and mud (silt/clay), moderate concentrations of HMS, intensely bioturbated, with flasers and rip-up clasts.	Subtidal, tidal creek, dune swale fill and selected high marsh depositional environments
	Fe	2,073	3,190	3,934	6,340	9,062	65,393	124,750		
	S	2,079	2,343	2,472	4,734	14,677	38,623	97,887		
	Ca	274	784	1,711	3,062	7,439	8,970	20,942		
	Ti	580	710	976	2,161	2,818	3,268	5,378		
	Zr	32	79	130	252	449	1,038	1,757		
	Ti/Zr	1.38	3.53	4.25	7.27	10.53	14.46	19.19		
	Fe/K	1.09	1.72	2.03	2.54	3.14	3.78	4.80		
E	K	665	2,853	3,655	5,785	7,749	10,269	21,118	Mud (silt/clay) with little fine to very fine sand, moderate concentrations of HMS, intensely bioturbated, shell debris and whole shells of <i>Ostrea</i> sp. and brackish-salt water foraminifera.	Low marsh and selected high marsh depositional environments
	Fe	2,262	6,601	13,217	19,701	28,268	47,082	136,329		
	S	2,186	3,754	4,865	9,225	19,613	43,191	78,484		
	Ca	223	1,095	1,785	3,162	11,254	18,914	55,489		
	Ti	192	820	1,704	2,267	2,960	3,462	4,564		
	Zr	35	63	87	127	185	283	473		
	Ti/Zr	2.37	6.38	11.22	17.29	21.98	28.13	55.26		
	Fe/K	1.09	2.15	2.91	3.60	4.73	6.27	19.30		

environments. Significant ranges in the levels of the analytes appear to correlate with a variety of lithofacies (muds, sands, muddy sands, etc.).

- Chemofacies D: appreciable sulfur ( $q_1 = 2,472$  ppm), potassium ( $q_1 = 1,706$  ppm), and iron ( $q_1 = 3,934$  ppm) content, associated with peat materials developed on muddy (silt/clay) substrates in marsh depositional environments or developed on a sandy substrate in washover depositional environments.
- Chemofacies E: extremely high levels of iron ( $q_1 = 13,216$  ppm), moderately high levels of potassium ( $q_1 = 3,655$  ppm) and sulfur ( $q_1 = 4,865$  ppm), and associated with muddy lithofacies (silt/clay) developed in marsh or freshwater lacustrine depositional environments.

### 6.3.3 Facies/Depositional Subenvironment Evaluation

Each FPXRF sample was coded in the database with the associated facies and interpreted depositional subenvironments (i.e. upper forebeach, lower forebeach, etc.) and descriptive statistics and box plots were generated for the common depositional environments. The boxplots for the descriptive statistics results from the depositional environments and subenvironments were plotted along with the Chemofacies A-E designations for comparison (Figure 6-14). Similar trends in the minimum, 10<sup>th</sup> percentile, 25<sup>th</sup> percentile (1<sup>st</sup> quartile), median, 75<sup>th</sup> percentile (3<sup>rd</sup> quartile), and 90<sup>th</sup> percentile values may be observed across the various depositional environments/subenvironments within each of the five chemofacies indicating that the cluster analysis of the XRF data has created meaningful groups or chemofacies designations. For example, the boxplots and descriptive statistics results for the depositional subenvironments (upper forebeach and lower forebeach) associated with Chemofacies B display very similar

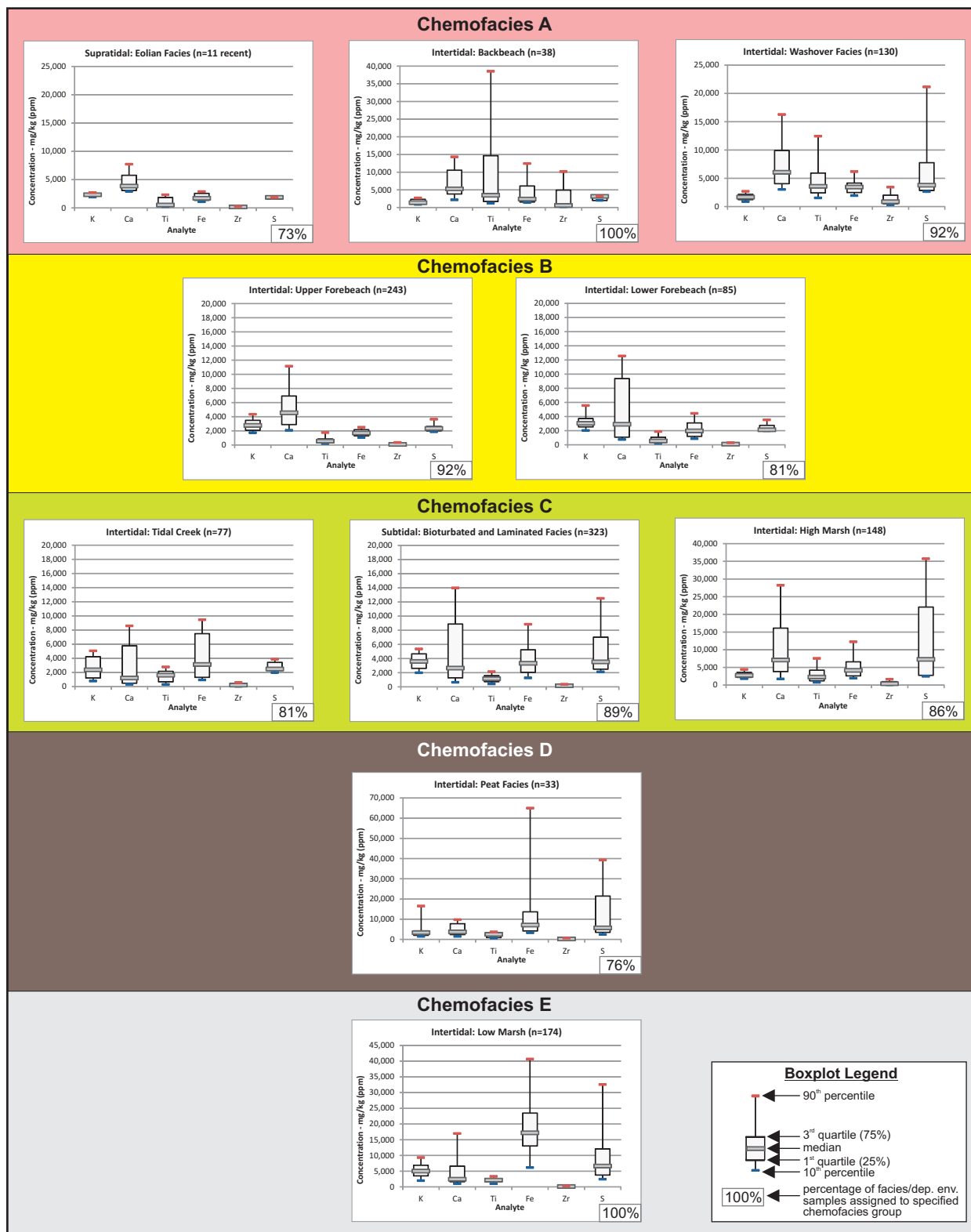


Figure 6-14: A simple graphical representation of the chemofacies designations versus the boxplot results for the most common depositional subenvironments. Multiple subenvironments were associated with Chemofacies A, B and C whereas peat facies were mostly associated with Chemofacies D and the low marsh muddy facies was associated with Chemofacies E.

metrics for the XRF results, graphically illustrating the geochemical similarities that were used to create the groups of samples. While the cluster analysis was successful at grouping the lower and upper forebeach sands into one meaningful group based on the FPXRF results or bulk elemental analysis at a higher level of depositional environment classification, the subsequent separation of the laminated facies (upper forebeach) and burrowed and laminated facies (lower forebeach) is dependent on the recognition of the primary physical and biogenic structures. Similar agreement in statistical measures may be observed across Chemofacies A where the sandy facies associated with the eolian, backbeach and washover processes indicate elevated trends in titanium and zirconium concentrations. As indicated in the Chemofacies B results, the cluster analysis was also successful at grouping the Chemofacies A sediments into one meaningful group based on the bulk elemental analysis at a higher level of classification. The subsequent separation of the eolian, washover and backbeach sediments is dependent on the recognition of the primary physical and biogenic structures. Agreement between the depositional environments/subenvironments and the chemofacies designations was also assessed by calculating a conformance measure of the number of samples from each facies group that occurred within each of the chemofacies designations. These results indicate that 73% to 100% of the samples from each of the major barrier island depositional environments or subenvironments were assigned to a single corresponding chemofacies designation. A conformance rate of 100% was noted for the backbeach samples in being assigned to Chemofacies A and a 100% rate was indicated for the low marsh samples being assigned to Chemofacies E. Conformance rates of greater than 90% were indicated in the washover fan samples (Chemofacies A) and the upper forebeach samples (Chemofacies B). Conformance rates of 73% to 89% were indicated in samples identified as eolian (Chemofacies A), lower



forebeach (Chemofacies B), tidal creek (Chemofacies C), transition zone (Chemofacies C), high marsh (Chemofacies C) and peat (Chemofacies D). Variances in the conformance rates were subsequently evaluated by reviewing the samples with respect to the chemofacies of occurrence and variations in lithology.

The additional level of evaluation to evaluate conformance and variances between the Chemofacies A-E designations and the corresponding facies and was performed by using the corresponding flags (“Chemofacies” vs. “Facies”) in the database and reviewing the vibracore data and a summary of the results are provided as Table 7. Washover facies were identified in 130 of the total samples and associated with Chemofacies A in 92% of the samples (n=119) and associated with Chemofacies B in 8% of the samples (n=11) as a result of relatively lower concentrations of titanium and zirconium or lower HMS content in the eleven samples attributed to heterogeneities in washover fans. The laminated facies of the upper forebeach depositional subenvironment was identified in 243 of the total XRF samples and associated with Chemofacies B in 92% of the samples (n=223) and associated with Chemofacies A in 8% of the samples (n=20) indicating the transitional nature of the backbeach to upper forebeach subenvironments. In addition, it was noted that several of the forebeach samples that were assigned to Chemofacies A were also associated with moderate to low angle crossbedding associated with beach runnels, where HMS is noted to accumulate in ripple troughs. The burrowed and laminated facies of the lower forebeach was indicated in 85 of the total XRF samples and associated with Chemofacies B in 81% of the samples (n=69). The burrowed and laminated facies was also associated with Chemofacies A in 13% of the samples (n=11) and Chemofacies C in 6% of the samples (n=5). The samples that were assigned to Chemofacies A also appear to be associated with HMS accumulation due to beach runnels and the samples assigned to Chemofacies C indicate the

**Table 7:  
Lithofacies and Chemofacies Evaluation  
XRF Results**

Facies and Assoc. Depositional Environment/Subenvironment			Sample Info		Chemofacies Designation				
Tidal Regime	Depositional Environment/ Subenvironment	Facies	No. Samples	% of Total	A	B	C	D	E
Supratidal	Eolian	Eolian Facies	11	1%	<b>73%</b>	27%	0%	0%	0%
Intertidal/Supratidal	Washover	Washover Facies	130	10%	<b>92%</b>	8%	0%	0%	0%
Intertidal	Backbeach	Laminated and Bioturbated	38	3%	<b>100%</b>	0%	0%	0%	0%
Intertidal	Upper Forebeach	Laminated	243	19%	8%	<b>92%</b>	0%	0%	0%
Intertidal	Lower Forebeach	Burrowed and Laminated	85	7%	13%	<b>81%</b>	6%	0%	0%
Subtidal	Transition Zone	Bioturbated and Laminated	323	26%	0%	11%	<b>89%</b>	0%	0%
Intertidal	High Marsh	Sandy Muddy Facies	148	12%	7%	6%	<b>86%</b>	0%	0%
Intertidal	Tidal Creek	Laminated Sands and Muds	77	6%	17%	3%	<b>81%</b>	0%	0%
Intertidal	Low Marsh	Muddy Facies	174	14%	0%	0%	0%	<b>100%</b>	0%
Intertidal	Marsh	Peat facies	33	3%	24%	0%	0%	0%	<b>76%</b>

Notes:

1) Chemofacies Designation = percentage of samples assigned to Chemofacies A-D from each facies and associated depositional environment.

transitional nature of the lower intertidal to subtidal environments. The bioturbated and laminated facies of the subtidal transition zone depositional subenvironment was identified in 323 of the total XRF samples and associated with Chemofacies C in 89% of the samples (n=288) and associated with Chemofacies B in 11% of the samples (n=35) also indicating the transitional nature of the lower intertidal to subtidal conditions. The muddy sand facies and the laminated sand and mud facies of the high marsh was indicated in 148 of the total XRF samples and was associated with Chemofacies C in 86% of the samples (n=128), associated with Chemofacies A in 7% of the samples (n=11), and associated with Chemofacies B in 6% of the samples (n=9). The associations with Chemofacies A and Chemofacies B appear to indicate a probable sand source with appreciable HMS content or may be the result of sorting under the varied hydraulic conditions encountered in the high marsh environment. Sources for sand materials with appreciable HMS content are observed where the high marsh transitions to the island core that is composed of intertidal and supratidal facies associated with HMS content or in areas where the high marsh occurs in the swales within accretional beach ridges that are typically dominated by sandy facies associated with intertidal and supratidal sediments with HMS content. The laminated sand and mud facies and the muddy sand facies associated with tidal creeks were identified in 77 of the total XRF samples and associated with Chemofacies C in 81% of the samples (n=62), associated with Chemofacies A in 17% of the samples (n=13), and associated with Chemofacies B in 3% of the samples (n=2) indicating a sand source with appreciable HMS content. Sources for sand materials with appreciable HMS content would include sands transported via flood tides from the foreshore environments or via washover processes into the tidal creek system as well as upland sources such as the previously described island core and accretional beach ridges. The mud facies associated with the low marsh depositional

subenvironment was identified in 174 of the samples and associated with Chemofacies D in 100% of the samples (n=174). Peat facies that are typically associated with the low marsh depositional subenvironment were grouped into Chemofacies E in 76% of the samples (n=25) and associated with Chemofacies A in 24% of the samples (n=8). A review of the lithofacies and vibracore data indicates that the samples that were assigned to Chemofacies A were associated with inactive washover fans deposited into the low marsh environment, where peat developed on the sandy facies with appreciable HMS content. The chemostratigraphic logs were then synthesized with the lithostratigraphic and radiometric data to construct chemostratigraphic cross-sections that are described in the following sections.

#### 6.3.4 *Quality Assurance/Quality Control*

FPXRF is a valuable screening tool when benchmarked properly against fixed laboratory methods and results (Glanzman and Closs, 2007). Matrix interference, sample heterogeneity, particle size, interfering element spectra, and moisture content may affect FPXRF results. A Quality Control (QC) evaluation was accomplished for the FPXRF results by analyzing duplicate samples on the FPXRF and the GSU Wave Dispersive X-Ray Fluorescence Unit (Rigaku 3270), or WDXRF. A plot of the results for select elements is provided in Figure 6-15 and each plot indicates good correlations between the field and fixed lab results for the target elements. Linear regressions of the data were performed where the slope of the best-fit line provides a conversion factor to estimate fixed laboratory results from the FPXRF results. The results of the regression analyses, slopes of best fit lines (conversion factors) and correlation coefficients for the target elements are: 1)  $Ti = 1.35x$  ( $R^2 = 0.87$ ); 2)  $Zr = 0.763x$  ( $R^2 = 0.95$ ); 3)  $Ca = 1.37x$  ( $R^2 = 0.89$ ); 4)  $Fe = 2.10x$  ( $R^2 = 0.86$ ) and 5)  $K = 2.56x$  ( $R^2 = 0.63$ ). The results of the coefficients of

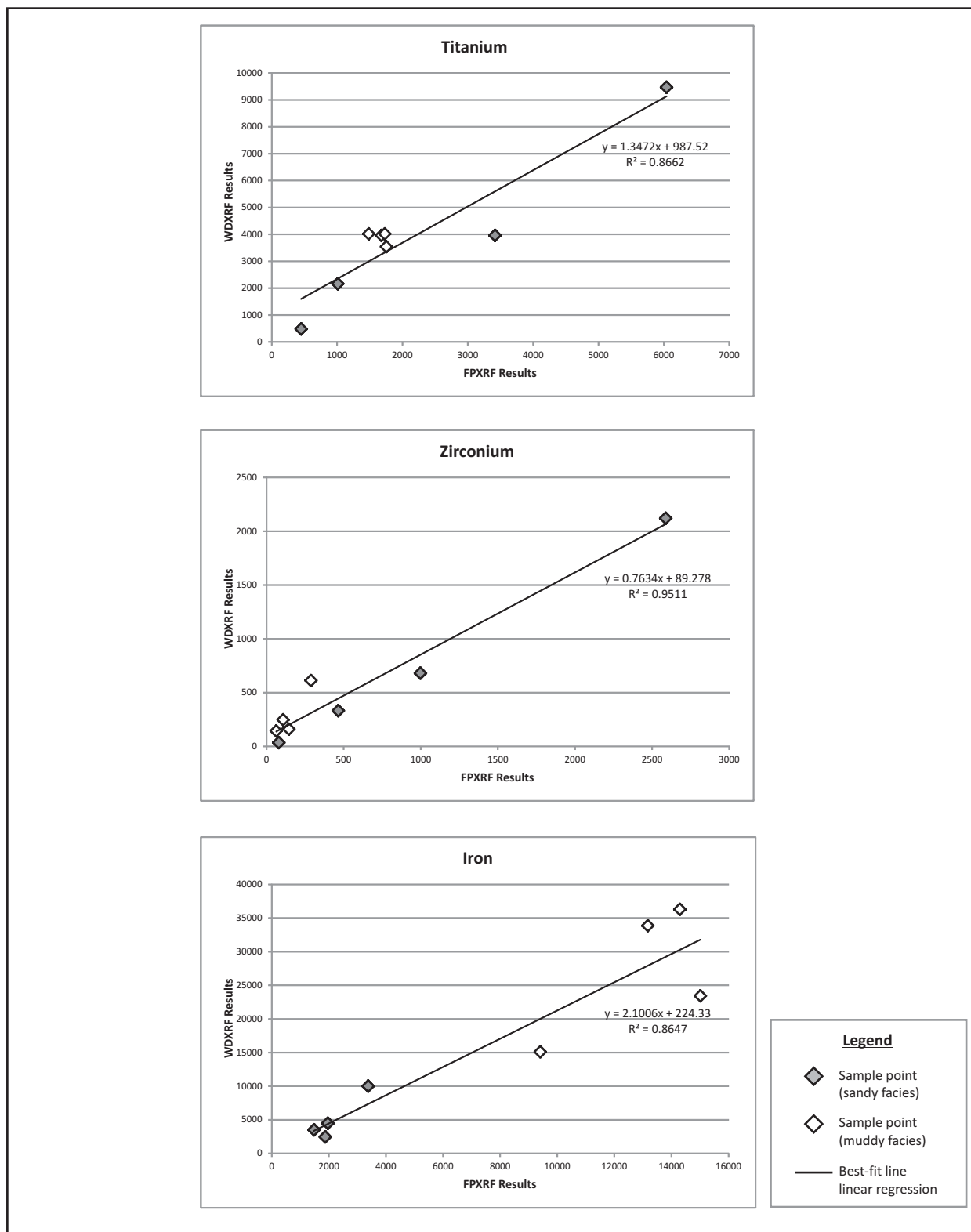


Figure 6-15: Field portable XRF elemental results were evaluated against data from a fixed-laboratory wave-dispersive XRF (Rigaku 3270) unit and indicate a good correlation between field and fixed lab data. Plots of the FPXRF vs. WDXRF results are provided for titanium, zirconium, and iron including linear regression results for the FPXRF and WDXRF data sets.

determination ( $R^2$ ) based on the linear regressions indicates that the regression line fits the data reasonable well indicating linear relationships for the variables. The slope values or conversion factors between the FPXRF and WDXRF results ranged from 0.76x to 2.56x. The FPXRF results are reported in parts per million (ppm) based on the integration of peaks by the Innov-X software using the Compton Normalization (CN) method and may be susceptible to the aforementioned moisture variations, matrix interferences, etc. However, for the purposes of defining chemofacies these slope values or conversion factors are assumed acceptable based on the linear relationship within each element of interest.

The relative standard deviation (RSD) of the sample mean is used to assess method precision. For FPXRF data to be considered adequately precise, the RSD should not be greater than 20 % with the exception of chromium (U.S. EPA, 2007). RSD values were calculated from sandy and muddy facies to evaluate the potential for matrix interference, sample heterogeneity, particle size, interfering element spectra, and moisture content on FPXRF results with respect to the precision of data. Replicate FPXRF analyses (minimum = 10) were performed on select samples and the RSD was determined for each of the target elements. RSD (%) values for titanium ranged from 2.6% to 11.6%; zirconium ranged from 2.8% to 16.9%; calcium ranged from 4.9% to 16.5%; iron ranged from 1.0% to 14.7%; potassium ranged from 3.0% to 12.7%; and sulfur ranged from non-detectable concentrations to 20.5%. The SRD values were all well below the EPA Method 6200 guidance value of 20% with the exception of sulfur at 20.5%.

The results of the FPXRF data QC evaluation indicate reasonable performance with respect to samples that were benchmarked against fixed-laboratory WDXRF analysis. In addition, acceptable precision was indicated from replicate analyses and RSD metrics for the

sandy and muddy matrices indicating FPXRF as a reliable and valuable screening tool for assessing elemental geochemistry in barrier island sediments.

#### **6.4 Stratigraphic and Chemostratigraphic Results**

Compilation of the vibracore, XRF, and radiometric dating results has been performed and lithostratigraphic or interpreted sections have been prepared for the Seaside Spit (A-A'), Beach Pond (B-B'), Flag Lagoon (C-C') and *Mission Santa Catalina de Guale* (D-D') study areas. Chemostratigraphic cross-sections have been produced for the Seaside Spit (A-A'), Beach Pond (B-B'), and Flag Lagoon (C-C') study areas from the chemostratigraphic logs (Appendix D). Interpreted sections that depict the environmental changes observed under the current study from 2009 to 2013 are provided for Seaside Spit (A-A') and Beach Pond (B-B').

##### *6.4.1 Seaside Spit Study Area Stratigraphy*

A series of five vibracores (BKM 112110-01, BKM 112110-02, BKM 050911-01, BKM 050911-02 and BKM 050911-03) were situated across an active washover fan at Seaside Spit and were used in conjunction with field observations to construct a series of cross-sections for the Seaside Spit study area (Figure 6-16). The lower portion of the stratigraphic sequence may be described as being composed of subtidal sediments consisting of laminated sands and muds (bioturbated and laminated facies) extending upward immediately below the modern low mean tide mark at -1.58 meters MSL. The subtidal sediments are immediately overlain by an erosional contact and muddy sands that are attributed to a tidal creek system. The muddy sands associated with the tidal creek are overlain by approximately 2.2 meters of muds associated with the low marsh depositional environment which are overlain by *Spartina* peats that are variable in

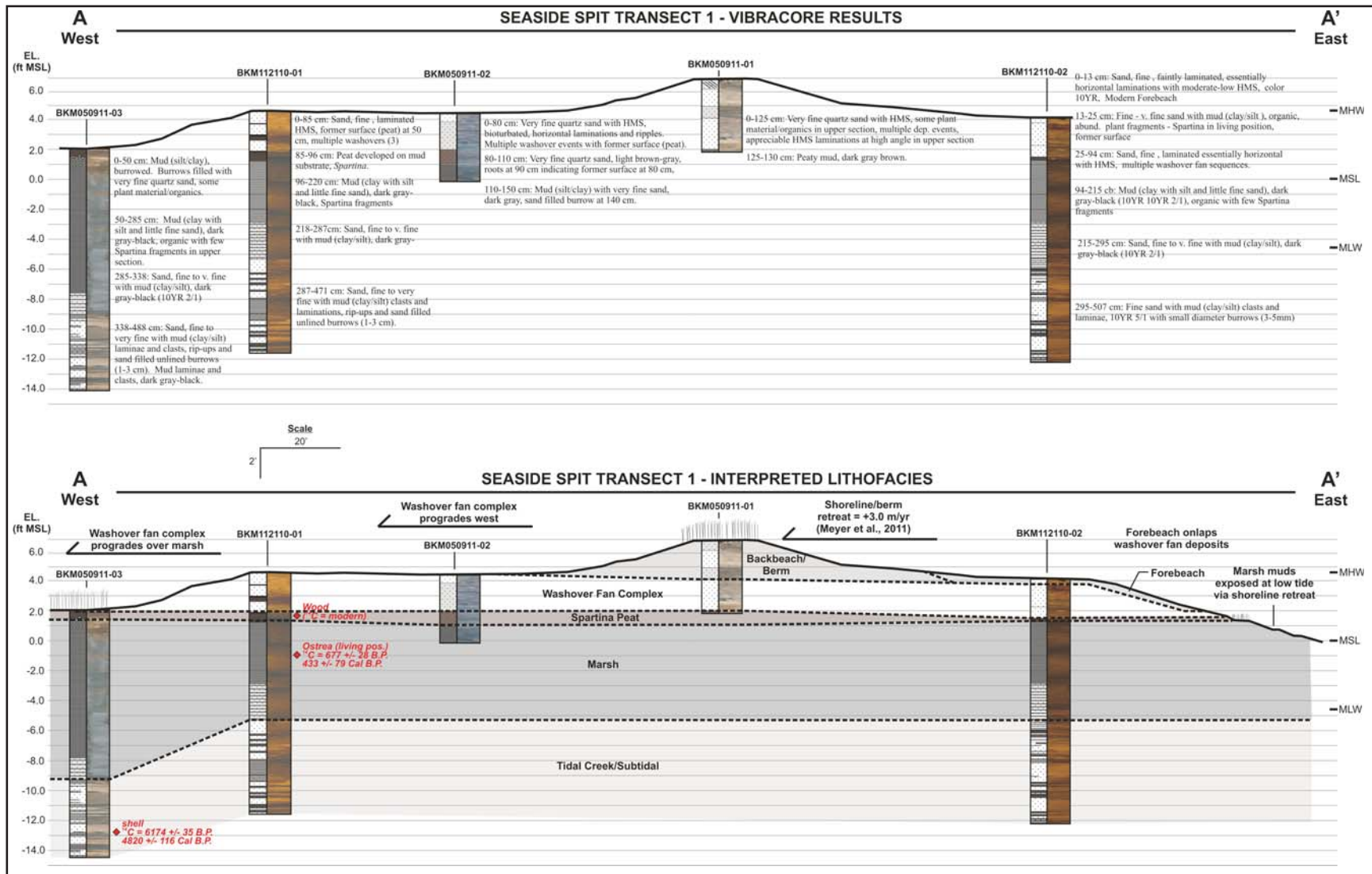


Figure 6-16: Vibracore data (upper) and interpreted section (lower) for the Seaside Spit Study Area. A series of five vibracores (BKM 112110-01, BKM 112110-02, BKM 050911-01, BKM 050911-02 and BKM 050911-03) were situated across an active washover fan and collected from November 2010 to May 2011. The cores indicate a lower subtidal bioturbated and laminated facies (transition zone) overlain by an erosional surface with muddy sands and low marsh sediments.



thickness at +0.6 meters MSL. Washover fan facies are observed in the four eastern cores with several developed peat surfaces, indicating periodic deposition and westward progradation.

A chemostratigraphic section was then prepared to evaluate the chemofacies associated with the Seaside Spit sediments (Figure 6-17). The individual lithologic logs are included in Appendix D and the results are provided in FPXRF mg/kg or ppm. The lower portion of the chemostratigraphic sequence is assigned to Chemofacies C and consists of subtidal bioturbated and laminated sediments and extends upward to near -1.58 meters MSL. Chemofacies C is overlain by approximately 2.2 meters of sediments that were designated as Chemofacies E, consisting of muds associated with the low marsh depositional environment. These sediments are overlain by sediments assigned as Chemofacies D consisting of *Spartina* peats that are variable in thickness at +0.6 meters elevation. Chemofacies A is associated with the washover fan sediments consisting of sandy facies and is observed in the four eastern cores.

#### *6.4.2 Beach Pond Study Area Stratigraphy*

A series of five vibracores (BKM 051011-01, BKM 051011-02, BKM 051011-03, BKM 051111-01 and BKM 072311-01) were situated across an inactive washover fan and used in conjunction with field observations to construct a series of lithostratigraphic and chemostratigraphic sections for the Beach Pond study area (Figure 6-18). The lower portion of the stratigraphic sequence may be described as subtidal sediments consisting of laminated sands and muds (bioturbated and laminated facies) extending upward to -3.7 meters MSL. A sequence of interlapping laminated sands and muds (subtidal environment) and laminated sands (lower forebeach or tidal environment) extends from the top of the subtidal sequence to -1.2 meters MSL. A package of fining upward laminated sands and muds associated with the high marsh or swale fill overlies the subtidal-intertidal sequence and grades at -0.6 meters to 0.0 meters MSL.

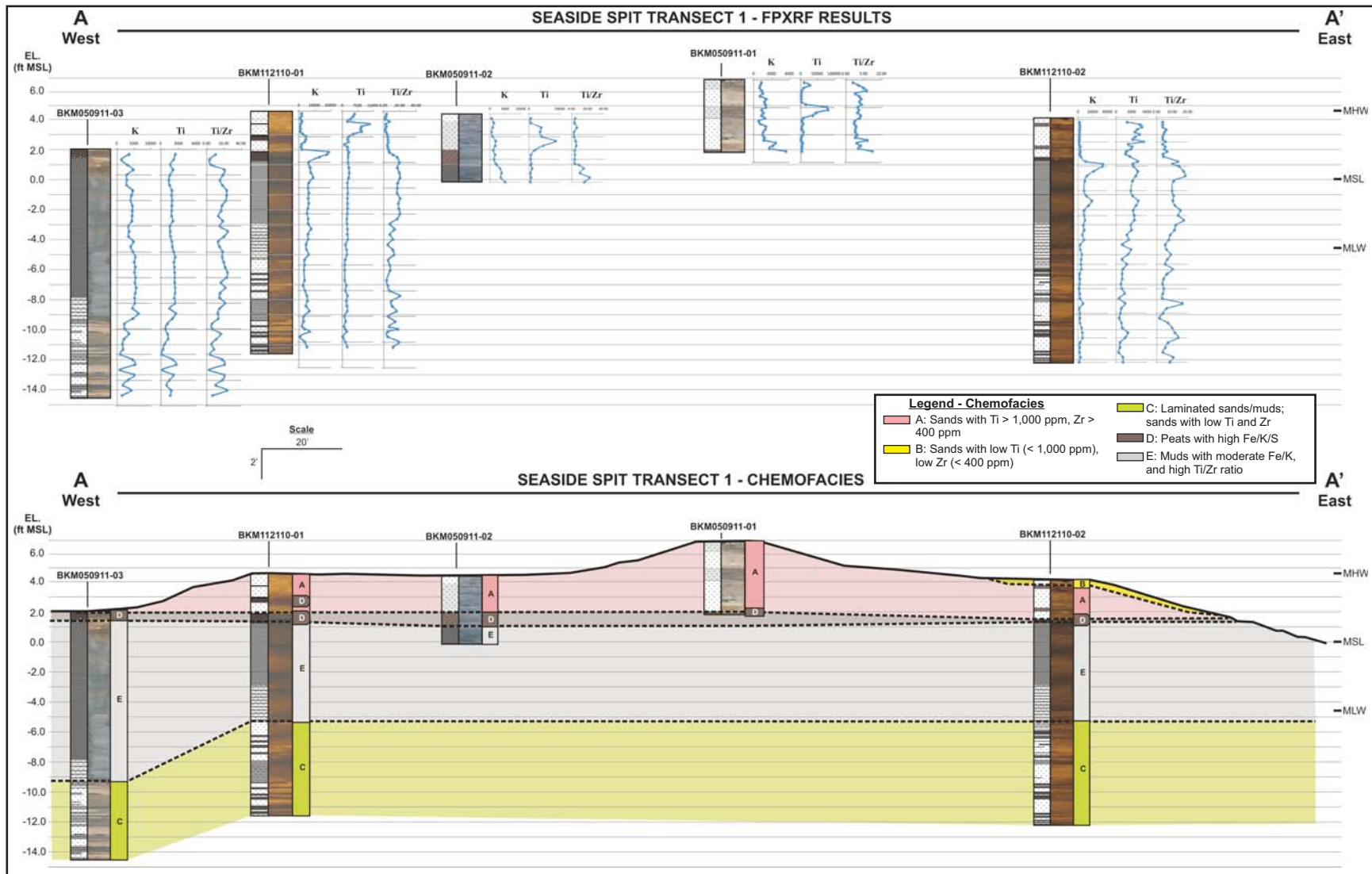
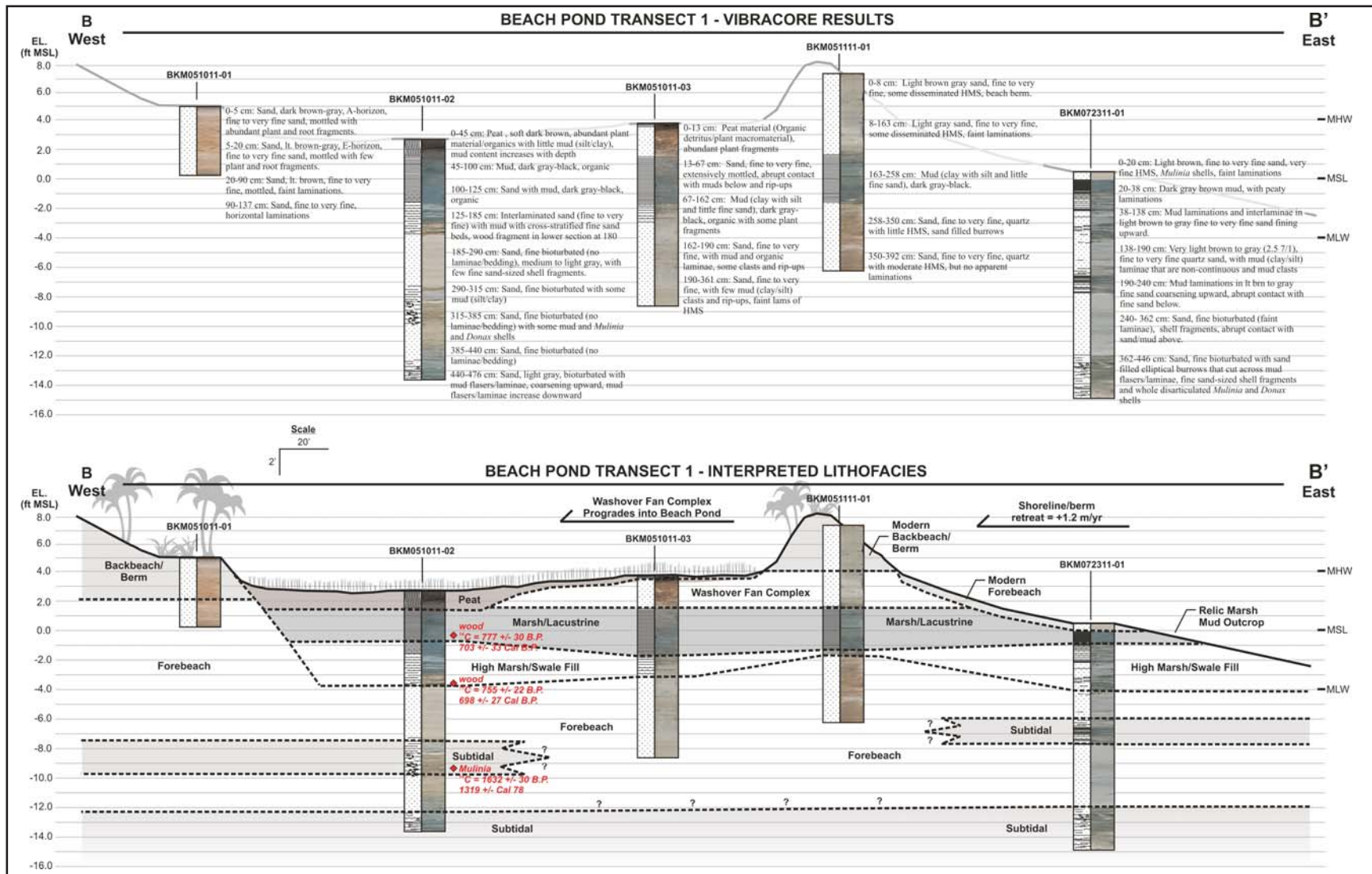


Figure 6-17: Chemostratigraphic cross-section to evaluate the chemofacies associated with the Seaside Spit sediments. The lower portion of the chemostratigraphic sequence is assigned to Chemofacies C (subtidal bioturbated and laminated sediments) and is overlain by approximately 2.2 meters of Chemofacies E (marsh muds) and overlain by Chemofacies D (Spartina peat). Chemofacies A is associated with the washover fan facies observed in the four eastern cores. See Appendix D for individual chemofacies logs.



into muds associated with the modern low environment and an overlying freshwater peat (Booth et al., 1999). Washover fan facies are observed in cores BKM 051011-03 and BKM 051111-01 with several developed peat surfaces, indicating periodic deposition and westward progradation.

A chemostratigraphic section was then prepared to evaluate the chemofacies associated with the Beach Pond sediments (Figure 6-19). The individual lithologic logs are included in Appendix D and the results are provided in FPXRF mg/kg or ppm. The lower portion of the chemostratigraphic sequence may be described as alternating packages of Chemofacies C and Chemofacies B. Sediments associated with Chemofacies C consist of subtidal bioturbated and laminated sediments and Chemofacies B consists of burrowed and laminated facies. An upper unit was designated as Chemofacies C and consists of laminated muds and sands that are interpreted as swale fill that was deposited in between two adjacent beach ridges. This Chemofacies C unit is overlain by sediments associated with Chemofacies E that are interpreted as marsh muds. Chemofacies A is associated with the surficial sediments or washover fan facies and is observed in the upper portions of cores BKM051011-03 and BKM051111-01.

#### *6.4.3 Flag Pond Study Area Stratigraphy*

A series of five vibracores (BKM 052411-01, BKM 052411-02, BKM 052511-01, BKM 052511-02 and BKM 072211-02) were situated across an active flood delta and washover fan complex at Flag Pond, and used in conjunction with field observations to construct a series of lithostratigraphic and chemostratigraphic sections. The lower portion of the stratigraphic sequence may be described as being composed of subtidal sediments consisting of laminated sands and muds (bioturbated and laminated facies) extending upward to -3.0 meters MSL (Figure 6-20). An alternating sequence of bioturbated and laminated sands and muds (subtidal

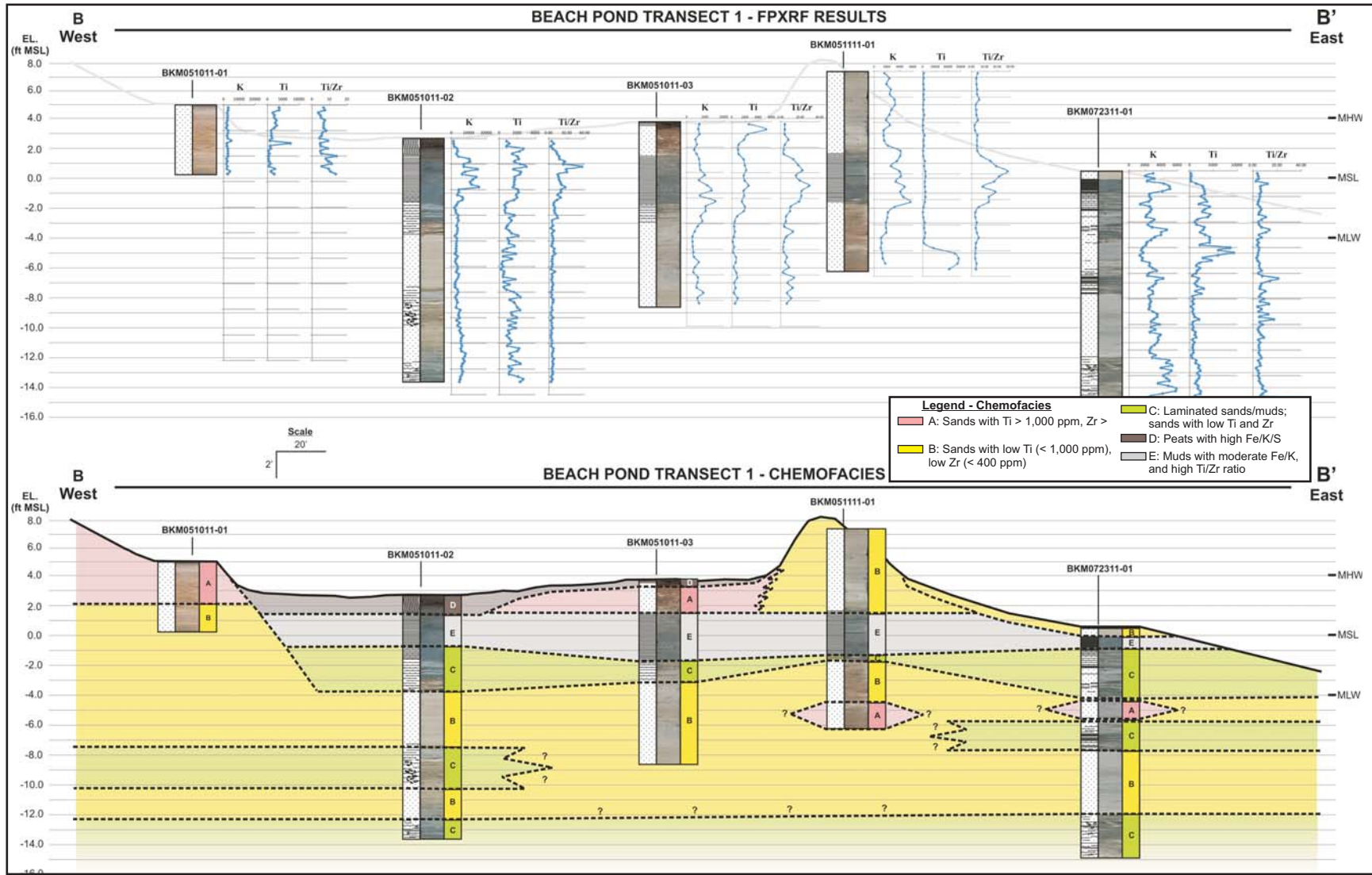


Figure 6-19: Chemostratigraphic cross-section to evaluate the chemofacies associated with the Beach Pond sediments. The lower portion of the chemostratigraphic sequence may be described as alternating packages of Chemofacies C and B. An upper unit was designated as Chemofacies C and consists of laminated muds and sands that are interpreted as swale fill and overlain by Chemofacies E (marsh muds). Chemofacies A is associated with the washover fan facies. See Appendix D for individual chemofacies logs.



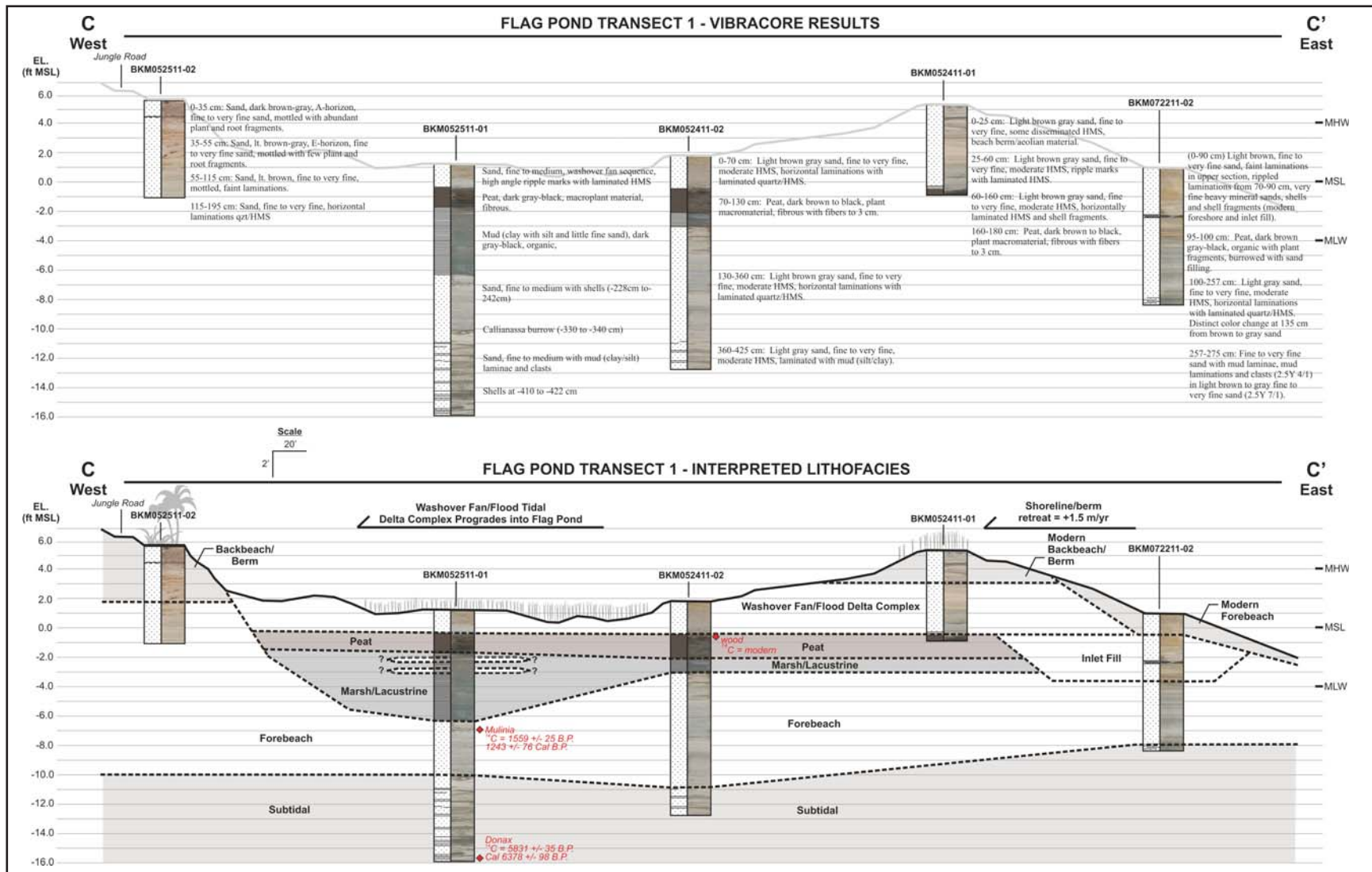


Figure 6-20: A series of five vibracores (BKM 052411-01, BKM 052411-02, BKM 052511-03, BKM 052511-01 and BKM 072211-02) were situated across an active flood delta and washover fan complex and collected from May 2011 to July 2011. The lower sections of the cores indicate cycles of subtidal bioturbated and laminated facies (transition zone) and lower forebeach sands overlain by a gradational swale fill to marsh mud sequence.

environment) and laminated sands (lower forebeach or tidal environment) extends from the top of the subtidal sequence to -1.2 meters MSL with a shell date from the lower penetrated portion of the sequence of 5,831 +/- 35 B.P. The subtidal sediments are overlain by a package of forebeach sands that appear to correlate with the beach ridge that bounds Flag Pond to the west, and yielded a shell date of 1,559 +/- 25 B.P. A package of fining upward laminated sands and muds associated with the high marsh or swale fill overlies the intertidal forebeach sediments and grades at -0.18 meters MSL to 0.9 meters MSL into muds associated with modern marsh muds and an overlying peat surface. A sample of wood from the peat material was dated as modern (> 100 % pMC). Flood delta facies consisting of fine to very fine quartz sands with moderate HMS content and laminations that dip in both a landward and seaward direction due to bimodal flow are observed in cores BKM 052411-01, 052411-02 and 052411-03. Flag Pond was initially a freshwater pond that was breached by the "Storm of The Century" during March 12-13, 1993 (Bishop, et al., 2007). A review of historical imagery for the Flag Pond area indicates that the inlet was initially formed north of the subject vibrocore transect, and migrated south to the current location by 2009. This condition resulted in the deposition of the channel fill sediments including shell debris, rippled laminations and peat materials that are observed in the upper section of core BKM 072211-02 (70 to 135 cm BLS).

A chemostratigraphic section was then prepared to evaluate the chemofacies associated with the Flag Pond sediments (Figure 6-21). The individual lithologic logs are included in Appendix D and the results are provided in FPXRF mg/kg or ppm. The lower portion of the chemostratigraphic sequence may be described as alternating packages of Chemofacies C (bioturbated and laminated facies) and Chemofacies B (burrowed and laminated facies). Sediments associated with Chemofacies C consist of subtidal bioturbated and laminated

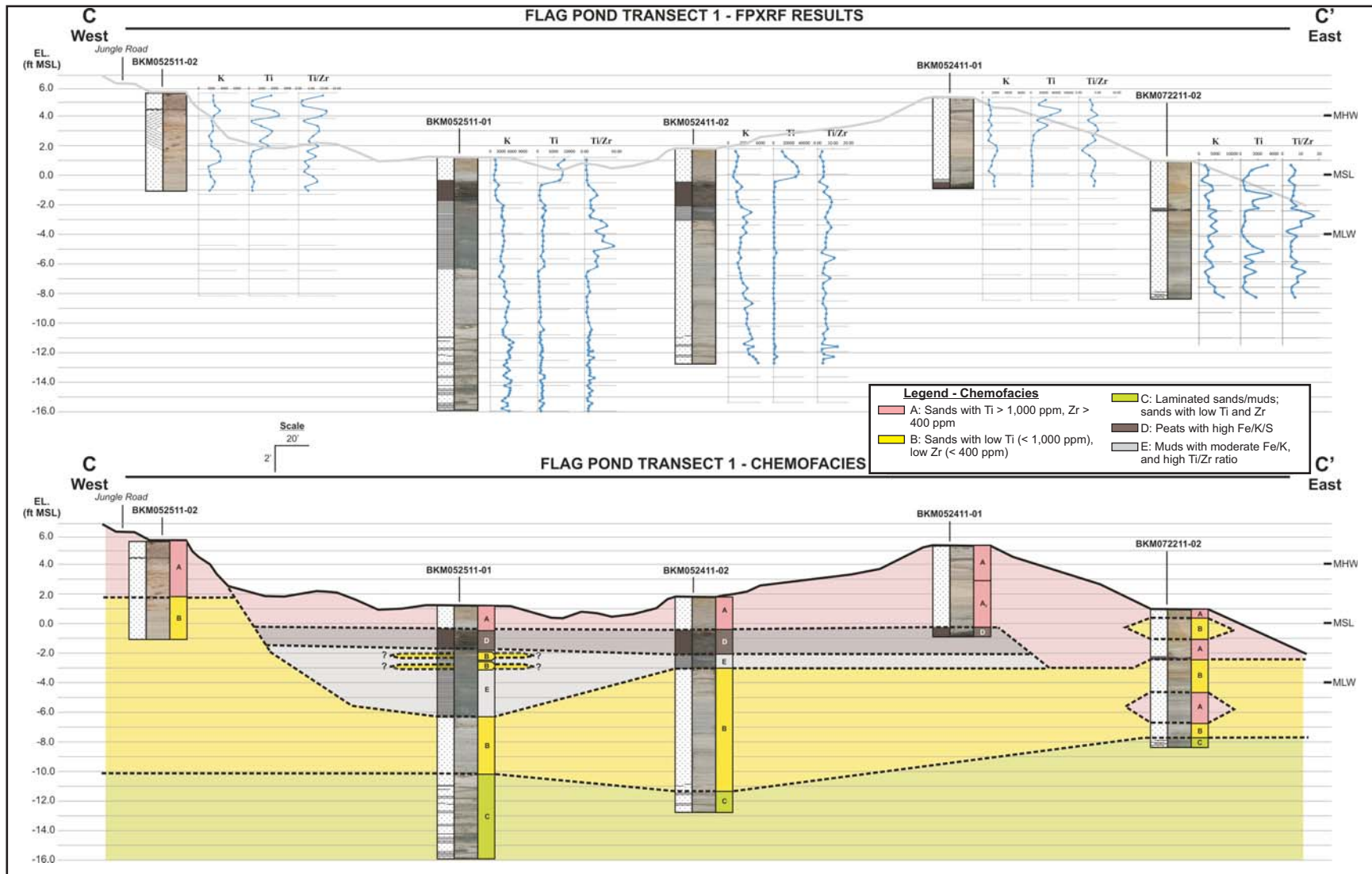


Figure 6-21: Chemostratigraphic cross-section to evaluate the chemofacies associated with the Flag Pond sediments. The lower portion of the chemostratigraphic sequence may be described as alternating packages of Chemofacies C and Chemofacies B. An upper unit was designated as Chemofacies C and consists of laminated muds and sands that are interpreted as swale fill and overlain by Chemofacies E (marsh muds). Chemofacies A is associated with the washover fan and flood delta facies.



sediments, and Chemofacies B consists of laminated and burrowed and laminated facies. An upper Chemofacies C unit consists of laminated muds and sands that are interpreted as swale fill and likely deposited between two adjacent beach ridges. A modern analogue is present in the accretional terrains located on North Beach where interdunal sediments are cumulating in a swale pond at the current time. This Chemofacies C unit is overlain by sediments associated with Chemofacies E that are interpreted as marsh muds (low marsh environment). Chemofacies A is associated with the washover fan and flood delta facies and observed in the upper portions of cores BKM052411-01, BKM052411-02 and BKM052511-01.

#### *6.4.4 North Beach Stratigraphy*

A series of four vibracores (BKM 012112-01, BKM 012112-02, BKM 031712-01, and BKM 031712-02) were situated along North Beach extending from the northern portion of Yellow Banks Bluff to approximately 200 meters north of the Sand Pit Road beach entrance. These cores were used in conjunction with the shoreline model results and field observations to construct an interpreted section across the marine margin or active shoreline of the northeastern accretional terrains (Figure 6-22). The transect was situated such that three vibracores (BKM012112-01, BKM012112-02, and BKM031712-01) are located where shoreline accretion is observed in the northern section of the transect and one core (BKM031712-02) was located along the transect where the shoreline is actively retreating. As a result of the accretional setting in the northern section of the transect, a facies succession is observed where recent or modern subtidal bioturbated and laminated facies are overlain by intertidal laminated facies in a shallowing or progradational sequence. Shoreline accretion rates of +0.61 m/yr to +2.34 m/yr are observed in this section of the island and result in a rapidly prograding sequence as evidenced

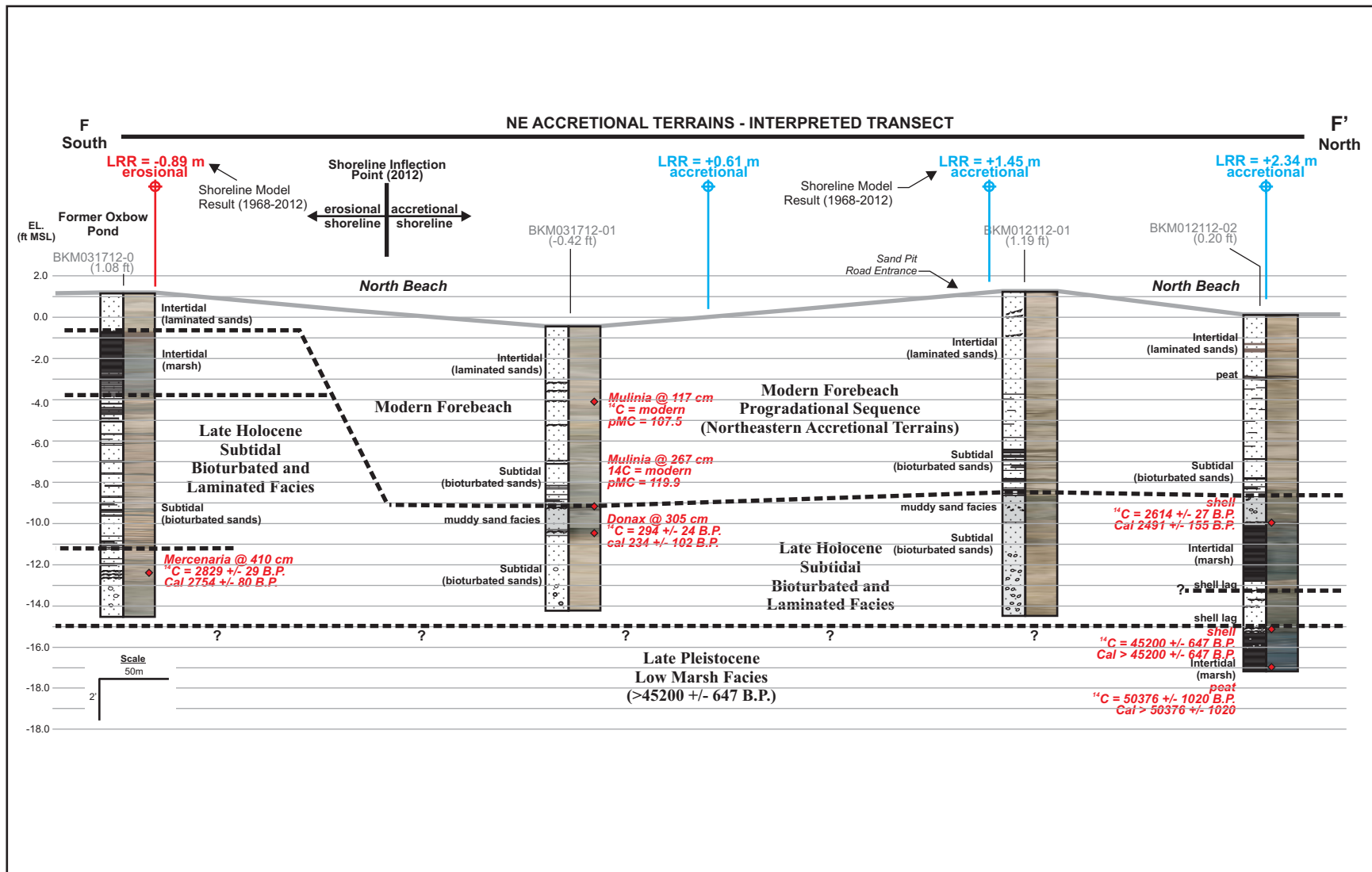


Figure 6-22: A series of four vibracores (BKM 012112-01, BKM 012112-02, BKM 031712-01 and BKM 031712-02) were collected in January and March 2012 on North Beach from the northern terminus of Yellow Banks Bluff extending to the north of the Sand Pit Road entrance to North Beach.

in the subsurface by a low density of *Callianassa* burrows. Howard and Scott (1983) attributed the low density of *Callianassa* burrows in Pleistocene outcrops located on the St. Mary's River as the result of a lack in residency time for colonization and effective burrow establishment due to rapid rates of accretion and burial of substrate. The southern core in the transect (BKM031712-02) was situated where a former oxbow pond or tidal creek was situated in historical imagery and this section of the shoreline is retreating toward the west or into the northern portion of Yellow Banks Bluff at a rate of -0.89 m/yr. A transgressive sequence is observed in core BKM031712-02 where modern upper forebeach sediments overlie the peat and muds associated with the former oxbow pond. This transgressive surface is associated with the modern transgression. The modern forebeach sediments are underlain by a Late Holocene sequence of subtidal bioturbated and laminated sands. A transgressive surface was identified in core BKM012112-02 as an erosional surface with shell lag overlying a marsh mud at approximately -4.6 m MSL, where radiocarbon data indicate that the lower marsh is Late Pleistocene. A *Mulinia* shell was dated from the shell lag material ( $^{14}\text{C} = 45,200 \pm 647$  B.P.) and a peat layer was extracted from the marsh mud and dated at  $^{14}\text{C} = 50,376 \pm 1020$  B.P. Due to the older radiocarbon ages, data calibration was not possible due to impingement associated with the Marine08 database. The older dates of  $45,200 \pm 647$  B.P. and  $50,376 \pm 1020$  B.P. are interpreted as representing radiocarbon infinity and should be considered as minimal ages for the materials. An upper marsh mud (3.0 – 4.0 m BLS) was also observed in core BKM012112-02 and radiocarbon data obtained from an *Ilyanassa* shell indicated a Late Holocene age ( $^{14}\text{C} = 2614 \pm 27$  B.P.,  $2491 \pm 155$  Cal B.P.). The lower shell lag is considered to be the initial transgressive surface of the Holocene and represents sea level reoccupying the eastern portions of St. Catherines Island following the Late Wisconsin glacial event.

#### 6.4.5 Mission Santa Catalina de Guale Stratigraphy

A series of four vibracores (IEP 060411-01, IEP 060411-02, IEP 061111-01, and IEP 061111-02) were collected at *Mission Santa Catalina de Guale* and were situated in the marsh and island core margin to the northwest of Structure 1/Iglesia, and in the unnamed tributary to Wamassee Creek to the east. The lower portion of the stratigraphic sequence as observed in cores IEP 060411-01 and IEP 060411-02 may be described as being composed of subtidal sediments consisting of laminated sands and muds (“bioturbated and laminated facies”) extending upward to -2.7 meters to -3.1 meters MSL. The subtidal sediments are overlain in cores IEP 060411-01 and IEP 060411-02 by intertidal lower forebeach sands composed of fine quartz sands with limited HMS content, and mud lined *Callianassa* burrows that decrease in density in an upward direction in core IEP 060411-02. The intertidal lower forebeach sands are terminated abruptly in core IEP 060411-01 at 3.24 meters BLS and overlain by laminated muds and peats with some sand content that extend to the land surface. In core IEP 060411-02 the lower forebeach sands transition into upper forebeach sands at 1.10 meters BLS and abruptly transition into peaty sands and muds at 0.40 meters BLS. In general, it appears that a subtidal sequence is overlain by a lower forebeach package that is in turn overlain by suspected upper forebeach sediments and capped by modern or recent sediments associated with the freshwater/tidal stream. Core IEP 061112-01 penetrated modern marsh sediments associated with the low marsh environment, and transitioned to a high marsh or tidal creek sequence at 2.05 meters BLS. Cores IEP 060411-01 and 060411-02 bracket Wamassee Scarp and indicate that shallow subtidal marine to intertidal forebeach sediments compose the island core, whereas backbarrier intertidal sediments associated with the marsh depositional environments bound Wamassee Scarp to the south.

An interpreted stratigraphic section (Figure 6-23) has been prepared and indicates that Structure 1/Iglesia is immediately underlain by a marine intertidal to supratidal sequence consisting of lower and upper forebeach sands and probable backbeach to eolian sediments. Although no dateable materials were collected within the marine sands, based on other studies (Linsley, 1993; Bishop et al, 2011) it is assumed that these sediments correlate with the Late Pleistocene. The site is bounded to the immediate west by the Walburg Scarp and low marsh sediments extending to 200 cm BLS. The site is bounded to the southeast by the unnamed tributary to Wamassee Creek and a fluvial-tidal creek sequence that provided a radiocarbon date of  $^{14}\text{C} = 270 \pm 30 \text{ B.P.}$  ( $359 \pm 76 \text{ Cal B.P.}$ ) near the base of the fluvial sequence with the underlying marine sands.

#### *6.4.6 Southeastern Accretional Terrains Stratigraphy*

An evaluation of the sediments that comprise the Southeastern Accretional Terrains (Figure 6-9) was performed by synthesizing information from the current Beach Pond and Flag Pond studies with lithological, palynological and radiometric data from previous studies focused within the Southeastern Accretional Terrains. An interpreted section (Figure 6-24) was constructed using vibracore results from the current study and data from Linsley (1991), Booth et al (1999), Chowns (2011), and Bishop et al (2011).

Facies successions in the cores collected from the causeway located to the west of Cracker Tom Hammock may be described as extremely complex where facies are observed to be out of the expected vertical succession in sediments as predicted by Walther's Law of Facies and the reference or idealized stratigraphic section (Figure 3-8). An example of such a complexity is observed in the lower section of the core "Cracker Tom Scarp" where marsh muds indicate an

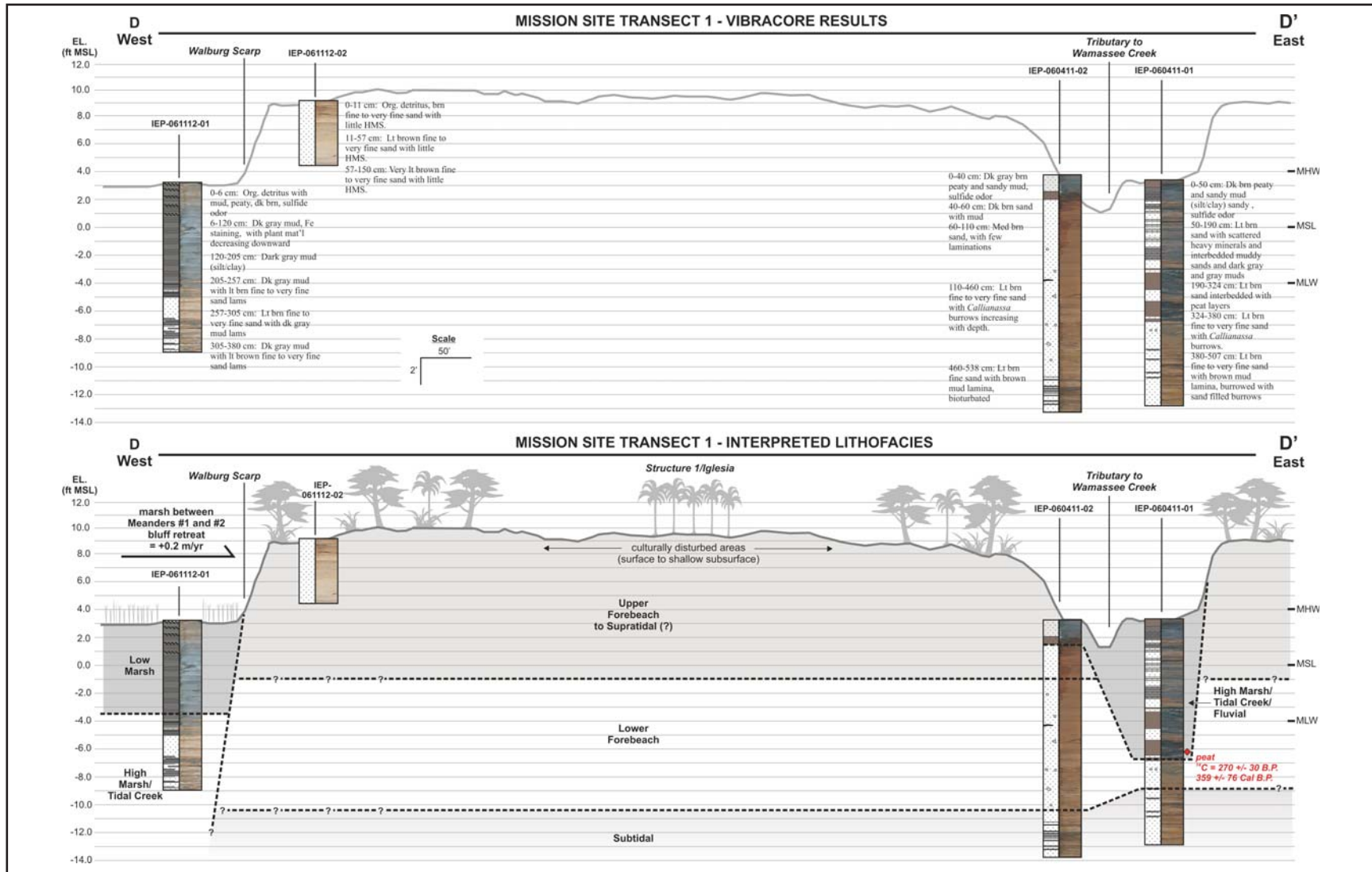


Figure 6-23: The mission site is underlain by a marine intertidal to supratidal sequence of lower and upper forebeach sands and a probable backbeach to eolian sequence. The site is bounded to the immediate west by the Walburg Scarp with low marsh sediments extending to 6 ft. BLS. The site is bounded to the southeast by the unnamed tributary to Wamassee Creek and a fluvial-tidal creek sequence that provided a radiocarbon date of  $^{14}\text{C} = 270 \pm 30 \text{ B.P.}$  near the base of the fluvial sequence.

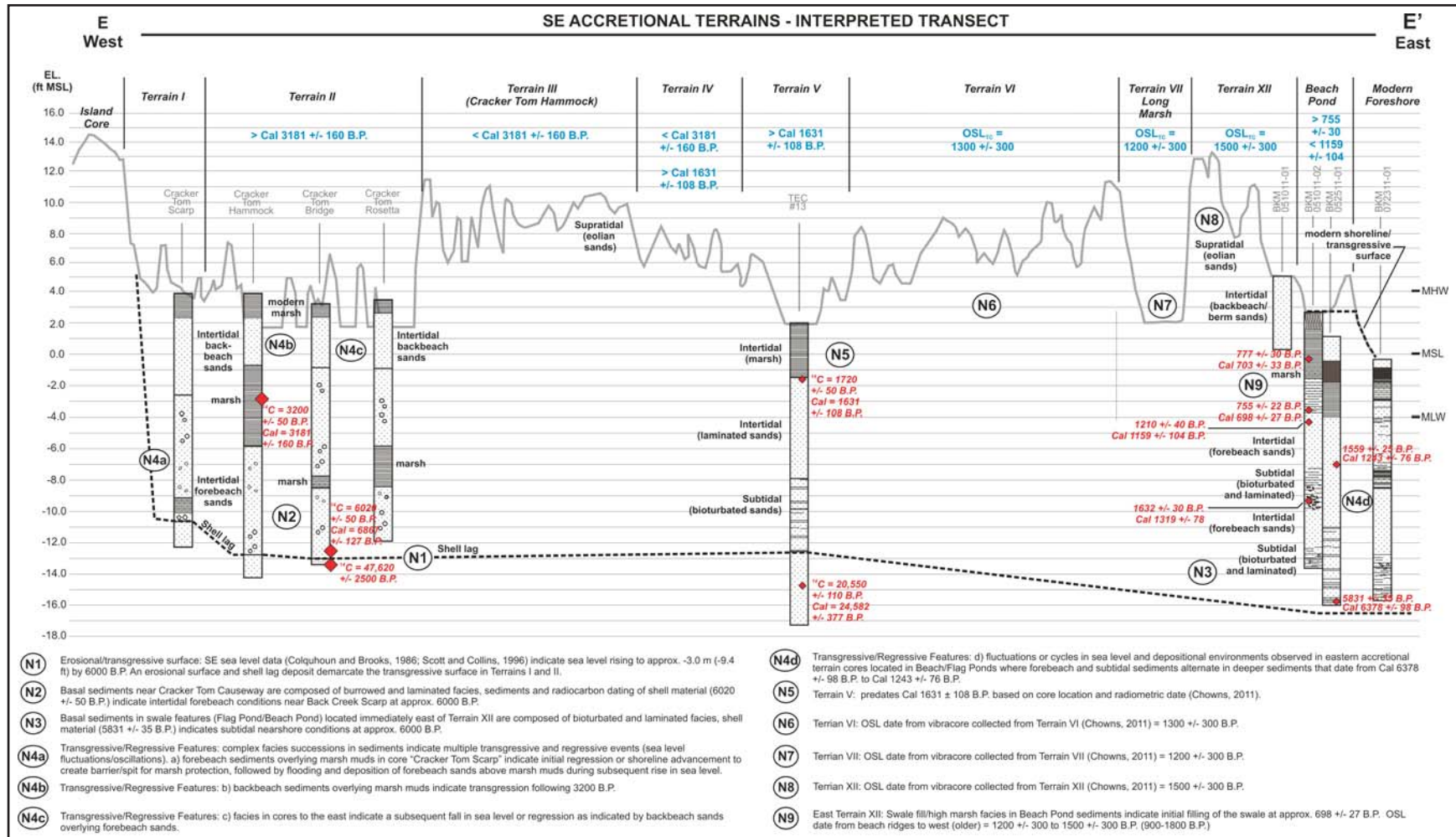


Figure 6-24: Transgressive/regressive sequences are noted in the Cracker Tom transect cores based on multiple erosional surfaces and facies successions. An initial transgressive surface is observed in cores associated with a basal shell lag and additional transgressive surfaces are noted via facies successions where forebeach and backbeach sands are overlying marsh muds. Multiple transgressive/regressive sequences are also noted in the Beach Pond and Flag Pond transect cores based on multiple erosional surfaces and facies successions. Core data from the current study, Linsley (1991), Booth et al (1999), Chowns (2011), and Bishop et al (2011).

initial regression or shoreline advancement creating a barrier or spit necessary for marsh aggradation, followed by flooding and deposition of forebeach sands on top of marsh muds during a subsequent transgression or rise in sea level. The modern processes observed under the current study at Seaside Spit could be considered as a modern analogue for this facies succession, where washover fans are currently prograding over low marsh muds under the modern transgression. A regressional sequence is observed in the upper portion of core “Cracker Tom Scarp” where backbeach sands overlie forebeach sands. This is opposed to a transgressive sequence that is observed in core “Cracker Tom Hammock”, where backbeach and washover sands also overlie a marsh mud yielding a radiocarbon date of 3200 +/- 50 B.P. The cores located to the east also record two regressions of sea level where forebeach sands were initially deposited in the lower sections of the cores and are immediately overlain by marsh muds indicating a prograding shoreline and associated beach ridges. The marsh muds are in turn overlain by forebeach sands indicating an ensuing rise in sea level or retreat of the shoreline as is observed along the modern Seaside Spit where forebeach sands are situated above relic marsh muds.

The transgressive surfaces and regressive or progradational sequences that were observed in the Cracker Tom cores were designated in relative order (i.e. T<sub>1</sub>, T<sub>2</sub>, R<sub>1</sub>, R<sub>2</sub>, etc.) and a sequence of events was constructed (Figure 6-25). An initial transgressive surface (T<sub>1</sub>) is observed in multiple cores from Cracker Tom and associated with a basal shell lag. A minimum of three additional transgressive surfaces (T<sub>2</sub>/ T<sub>3</sub>/ T<sub>4</sub>) are noted as erosional surfaces or as facies successions where forebeach and backbeach sands are overlying marsh muds. Of importance, is that the Cracker Tom cores indicate a vertical distribution of transgressive surfaces or stacked arrangement, indicating an increase in mean sea level from initial to subsequent transgressive



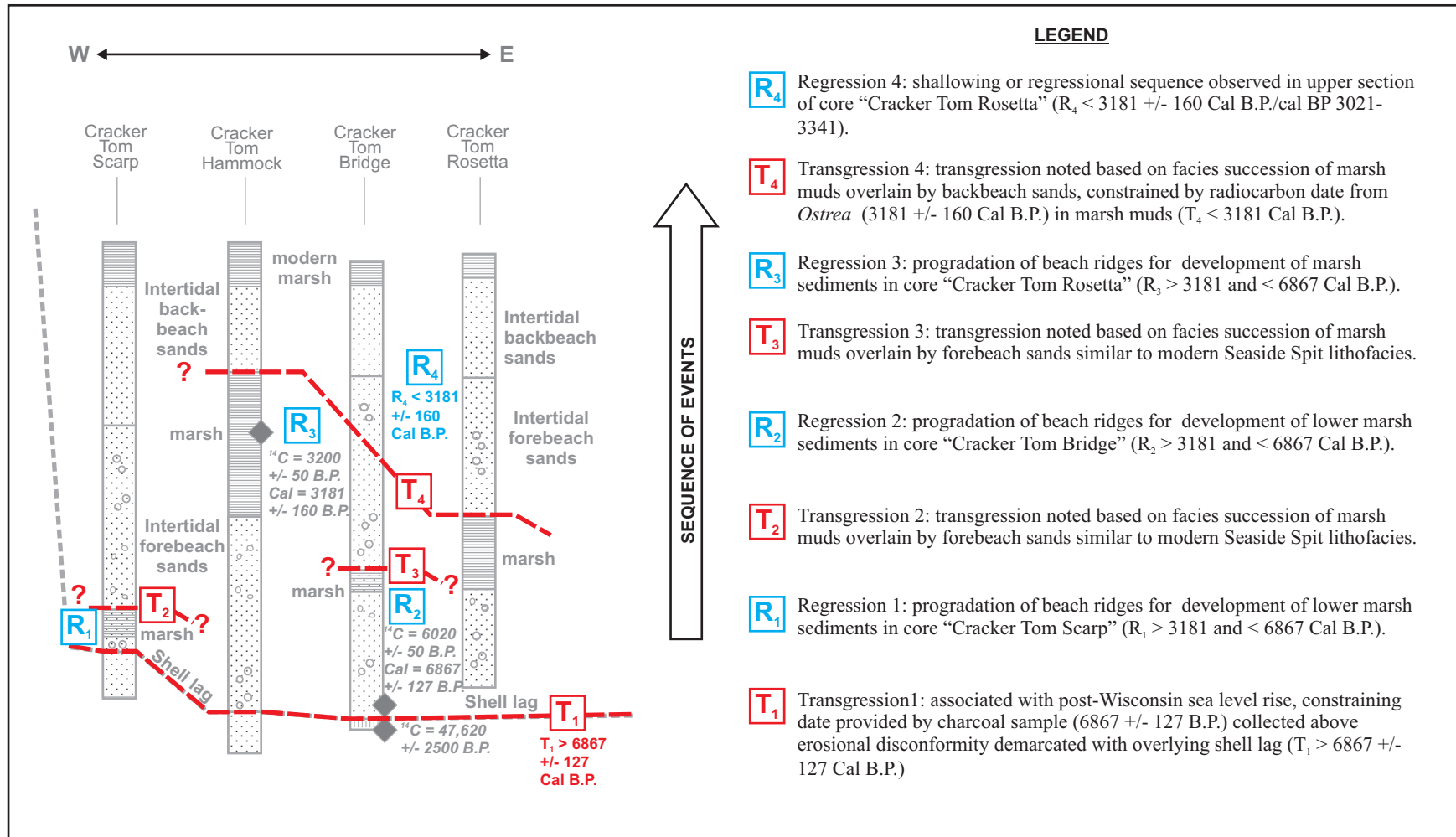


Figure 6-25: Multiple transgressive/regressive sequences are noted in the Cracker Tom transect cores based on multiple erosional surfaces and facies successions. An initial transgressive surface ( $T_1$ ) is observed in multiple cores associated with a basal shell lag, a minimum of three additional transgressive surfaces ( $T_2/T_3/T_4$ ) are noted as facies successions where forebeach and backbeach sands are overlying marsh muds. Constraining dates were provided by radiocarbon data and indicate  $T_1 > 6867 \pm 127$  Cal B.P. and  $T_4 < 3181 \pm 160$  Cal B.P.

events. Constraining dates were provided by radiocarbon data and indicate  $T_1 > 6020$  B.P. and  $T_4 < 3200$  B.P. ( $T_1 > 6867$  Cal B.P. and  $T_4 < 3181$  Cal B.P.).

Fluctuations in sea level are also indicated in facies successions in the Beach Pond and Flag Pond cores. Multiple transgressive/regressive sequences are recognized by erosional surfaces and facies successions. Shallowing or regressive sequences associated with a fall in sea level are observed (Figure 6-26) as forebeach sands overlying subtidal bioturbated and laminated sands ( $R_X$  and  $R_5$ ). The initial Holocene transgressive surface ( $T_1$ ) observed to the west at Cracker Tom is assumed to immediately underlie this transect. Constraining dates were provided by radiocarbon data and indicate  $T_5 > 1632$  B.P. and  $R_4 < 1559$  B.P. ( $T_5 > 1319 \pm 78$  Cal B.P. and  $R_4 < 1243 \pm 76$  Cal B.P.).

Vibracores collected from the sediments situated within the central portions of the southeastern accretional terrains from Terrain III to Terrain VII by Linsley (1993), Booth et al. (1999), and Chowns (2011) provide additional evidence of small transgressions and regressions of sea level through facies successions, erosional transgressive surfaces, and vertical shifts in facies. A core collected by Linsley (1993) in Long Marsh identified an erosional surface and shell lag with shell material that date at  $4370 \pm 120$  B.P. ( $4696 \pm 324$  Cal B.P.) and indicates a transgressive surface that is correlated with transgressions  $T_2$  or  $T_3$ . This transgressive surface will be evaluated with the incorporation of regional sea level information and refined in the discussions. Additional cores collected by Linsley (1993) and Chowns (2011) bracket Terrain III and Terrain V and indicate a vertical shift of approximately one meter in forebeach and subtidal sediments from the older to the younger terrains where Terrain V is constrained by a radiocarbon date of  $> 1720 \pm 50$  B.P. ( $1631 \pm 108$  Cal B.P.). The vertical shift in the transition of facies is

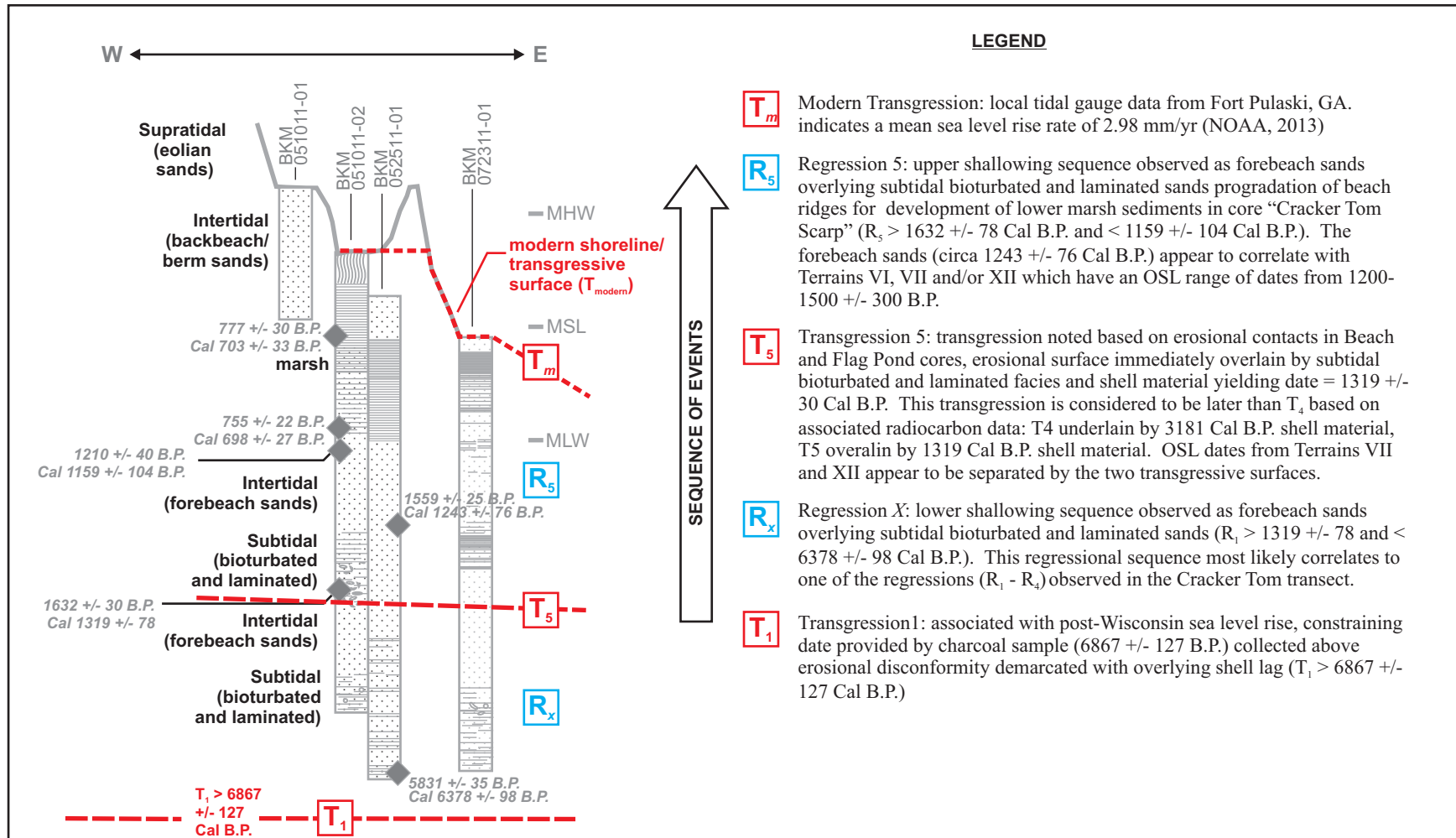


Figure 6-26: Multiple transgressive/regressive sequences are noted in the Beach Pond and Flag Pond transect cores based on multiple erosional surfaces and facies successions. Shallowing sequences associated with a fall in sea level (regression) are observed as forebeach sands overlying subtidal bioturbated and laminated sands (R<sub>x</sub> and R<sub>5</sub>). The initial Holocene transgressive surface (T<sub>1</sub>) is assumed to immediately underlie the transects. Constraining dates were provided by radiocarbon data and indicate T<sub>5</sub> > 1632 Cal B.P. and R<sub>4</sub> < 1559 Cal B.P.

directly attributed to a decrease in relative sea level or the product of a marine regression as opposed to a regressive facies succession that can also be replicated in progradational sequences.

Additional constraining dates for the southeastern accretional terrains were provided by Chowns (2011) through optically stimulated luminescence (OSL) and radiocarbon data from vibracores collected within Terrains V-XII, where Terrain V is constrained by a radiocarbon sample as being  $> 1720 \pm 50$  B.P. ( $> 1631 \pm 108$  Cal B.P.). An OSL sample from Terrain VI along the interpreted transect was dated at  $1300 \pm 300$  B.P., Terrain VII was dated at  $1200 \pm 300$  B.P. and Terrain XII was dated at  $1500 \pm 300$  B.P. utilizing OSL data. Additional constraining dates for the swale located to the east of Terrain XII were provided in the vibracores collected from Beach Pond and Flag Pond under the current study and by Booth et al. (1999). Radiocarbon data from a shell sample (*Donax*, I.D. BKM 052511-01-244) and associated facies indicate upper forebeach sands in the Beach Pond area and a suggested shoreline located to the immediate west at  $1559 \pm 25$  B.P. Sediments consisting of muds and interlaminated mud and sand described as swale fill materials occur in the upper two meters of the Beach Pond and Flag Pond cores. Wood materials collected by Booth et al. (1999) and the current study range from  $1210 \pm 40$  B.P. ( $1159 \pm 104$  Cal B.P.) to  $755 \pm 22$  B.P. ( $697 \pm 28$  Cal B.P.). The facies and associated radiocarbon data indicate that a beach ridge most likely formed to the east circa  $1210 \pm 40$  B.P. ( $1159 \pm 104$  Cal B.P.) thereby creating the swale or topographic low that is currently occupied by Beach Pond and Flag Pond. In addition, Booth et al. (1999) noted an increase in the percentage of terrestrial pollen in sediments immediately underlying the swale or basin fill materials indicating that the island had prograded eastward in close proximity to the current position of Beach Pond circa  $1210 \pm 40$  B.P. ( $1159 \pm 104$  Cal B.P.).

Considering the significance of the numerous transgressive/regressive events as indicated in the vibracore data by the facies successions, vertical shifts in facies, and erosional disconformities or transgressive surfaces, the southeastern Holocene accretional terrains record numerous depositional and erosional events as a result of multiple sea level fluctuations. A conceptual sea level curve may be constructed using the transgressive and regressive sequences with the conditions presented by interpretation of the vibracore data and constrained by radiocarbon data:

- 1) The initial transgressive surface ( $T_1$ ) indicates sea level rising to an elevation of four to five meters below modern sea level at circa 6000 B.P.
- 2) Multiple fluctuations of sea level ( $T_2$ ,  $T_3$ ,  $T_4$  and  $T_5$ ) are observed between 6000 B.P. and 1200 B.P. based on transgressive/regressive sequences.
- 3) The transgressive surfaces occur in a stacked arrangement ( $T_1$  to  $T_4$ ), indicating slightly higher mean sea level conditions for each subsequent transgressive sequence.

A conceptual sea level curve was constructed (Figure 6-27) that captures the initial transgression and four additional fluctuations in sea level of an approximate 1-meter amplitude, culminating in the modern marine transgression. An evaluation of Late Holocene sea level conditions was then performed to test the conceptual sea level curve by specifically evaluating the occurrence of the facies and associated radiocarbon data with respect to relative sea level.

## **6.5 Evaluation of Late Holocene Sea Level Conditions**

A total of eleven samples from the radiocarbon database were selected to evaluate sea level conditions during the Late Holocene (Table 8). Four of the samples used in the current evaluation of sea level are associated with depositional environments that occur above mean sea

**Table 8:  
Evaluation of Late Holocene Sea Level Conditions,  
Radiocarbon Sample Metadata and Age/Depth Relationship Data**

Sample Metadata									AMS Radiocarbon Results		
SL No.	Sample I.D.	Material	ToC EL (ft)	EL (m)	Depth (m) - Compacted	Compaction (%)	Depth (m) - Corrected	EL Sample	<sup>14</sup> C BP (δ <sup>13</sup> C)	1 σ	2 σ
1	Cracker Tom Bridge	charcoal	3.00	0.91	4.79	10.0%	5.27	-4.35	6020	50	100
2	052511-01-496	<i>Donax</i>	1.21	0.37	4.96	10.8%	5.50	-5.13	5831	35	70
3	Cracker Tom Hammock	<i>Crassostrea</i>	2.00	0.61	2.07	10.0%	2.28	-1.67	3200	50	100
4	031712-02-410	<i>Mercenaria</i>	1.08	0.33	4.10	9.4%	4.49	-4.16	2829	29	58
5	012112-02-315	<i>Ilyanassa</i>	0.20	0.06	3.15	8.4%	3.41	-3.35	2614	27	54
6	051011-02-350	<i>Mulinia</i>	2.89	0.88	3.50	15.3%	4.04	-3.15	1632	30	60
7	052511-01-244	<i>Mulinia</i>	1.21	0.37	2.44	10.8%	2.70	-2.33	1559	25	50
8	051011-02-90	wood	2.89	0.88	0.90	15.3%	1.04	-0.16	777	30	60
9	112010-01-155	<i>Crassostrea</i>	3.41	1.04	1.55	10.9%	1.72	-0.68	677	28	56
10	031712-01-305	<i>Mulinia/Donax</i>	-0.42	-0.13	3.05	7.7%	3.28	-3.41	294	24	48
11	112010-01-90	wood	3.41	1.04	0.90	10.9%	1.00	0.04	39	31	62

Sample Metadata		Calibrated Results		Facies/Interpreted Depositional Environment		Relationship to MSL (m)			SL Range	
SL No.	Sample I.D.	Cal. YBP	2 σ	Facies	Dep. Env.	Facies vs. SL	Lower EL (m)	Upper EL (m)	upper	lower
1	Cracker Tom Bridge	6867	127	laminated facies	upper forebeach (intertidal)	upper	0.0	1.1	-4.35	-5.55
2	052511-01-496	6378	98	bioturbated and laminated	transition zone (subtidal)	lower	-4.0	-2.0	-1.13	-3.13
3	Cracker Tom Hammock	3181	160	mud (silt/clay)	tidal creek/low marsh	range	-0.6	1.1	-1.07	-2.77
4	031712-02-410	2754	80	bioturbated and laminated	transition zone (subtidal)	lower	-4.0	-2.0	-0.16	-2.16
5	012112-02-315	2474	138	washover (muddy sand)	low marsh	upper	0.0	1.1	-2.25	-3.35
6	051011-02-350	1319	78	bioturbated and laminated	transition zone (subtidal)	lower	-4.0	-2.0	0.85	-1.15
7	052511-01-244	1243	76	laminated facies	upper forebeach (intertidal)	upper	0.0	1.2	-1.13	-2.33
8	051011-02-90	703	33	mud (silt/clay)	low marsh	upper	0.0	1.1	-0.16	-1.26
9	112010-01-155	433	79	mud (silt/clay)	tidal creek/low marsh	range	-0.6	1.1	-0.08	-1.78
10	031712-01-305	294 (*)	48	bioturbated and laminated	transition zone (subtidal)	lower	-4.0	-2.0	0.59	-1.41
11	112010-01-90	58	26	mud (silt/clay)	low marsh	upper	0.0	1.1	0.04	-1.06

**Notes:**

- 1) SL No. = sea level sample plotted on Figure 48.
- 2) ToC EL (ft) = surface elevation at sample location in feet from LIDAR data.
- 3) Depth (m) - Compacted = sample depth at sample location in meters
- 4) Compaction (%) = compaction of sediment in vibracore based on field measurements
- 5) Depth Corrected (m) = corrected depth of sample based on compaction %
- 6) EL Sample = surface elevation minus (-) the corrected depth of the sample
- 7) <sup>14</sup>C BP (δ<sup>13</sup>C) = radiocarbon results in radiocarbon years corrected for fractionation (δ<sup>13</sup>C)
- 8) Cal. YBP = absolute years from calibrated radiocarbon data, results were calibrated using IntCal08 (terrestrial) and Marine08 (marine samples) and the local reservoir value from SCI (Thomas, 2008)
- 9) Facies/Depositional Environment = interpreted results for facies and corresponding depositional environments
- 10) Relationship to MSL = elevational range of depositional environments relative to mean sea level (Figure 48).
- 11) SL Range = EL Sample +/- Relationship to MSL
- 12) (\*) = sample was outside of the calibration range, estimated result

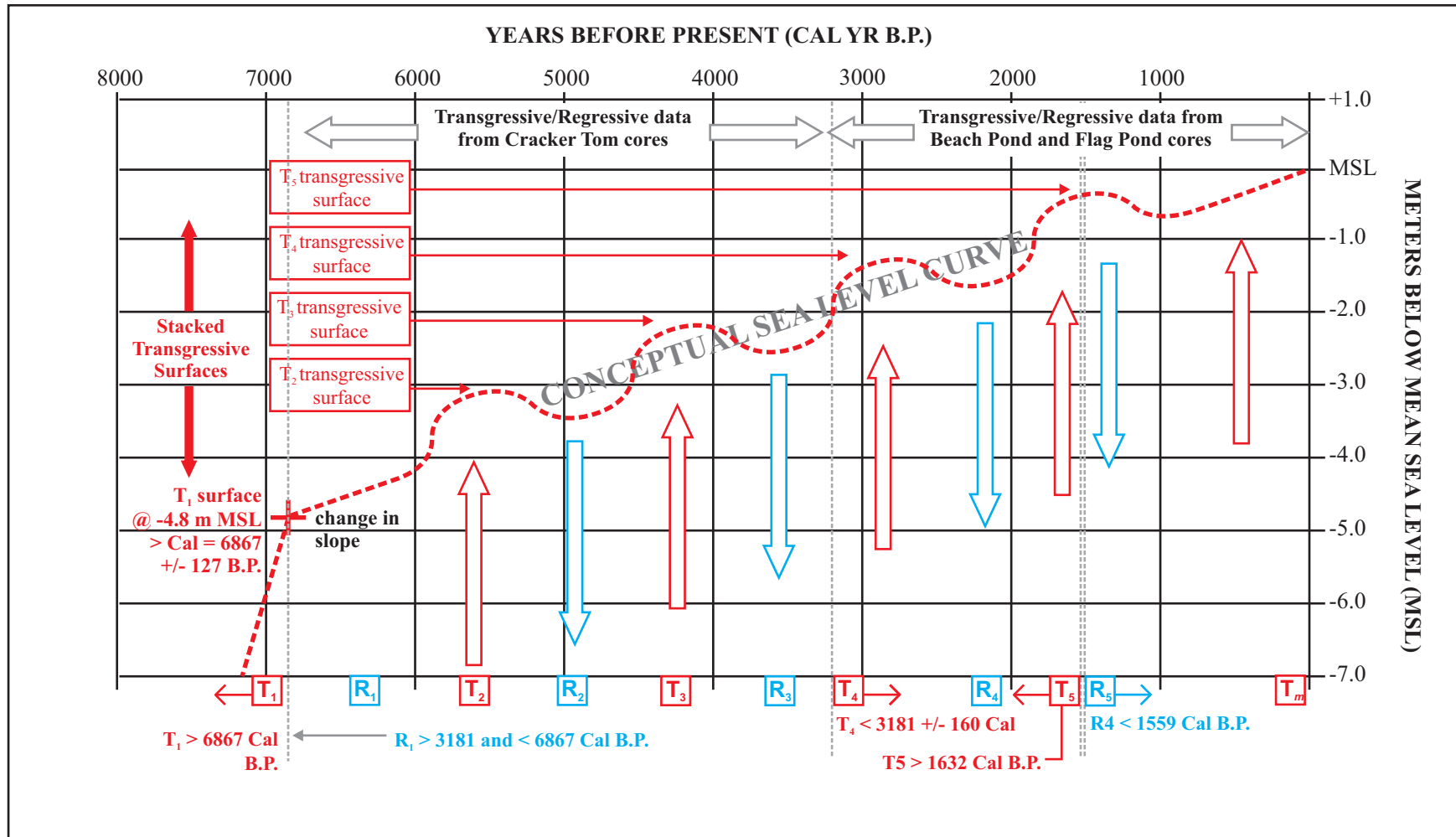


Figure 6-27: One possible scenario for a Late Holocene conceptual sea level curve based on the multiple transgressive/regressive features from the Cracker Tom and Beach/Flag Pond transects. Multiple stacked transgressive surfaces and regressive sequences are noted in the Cracker Tom cores and constraining dates were provided by radiocarbon data and indicate  $T_1 > 6867$  Cal B.P. and  $T_4 < 3181$  Cal B.P. Transgressive/regressive sequences are noted in the Beach/Flag Pond cores based on multiple erosional surfaces and facies successions where constraining dates were provided by radiocarbon data and indicate  $T_5 > 1632$  Cal B.P. and  $R_4 < 1559$  Cal B.P.

level and may be considered as upper constraining points for mean sea level. Five of the samples used in the study are associated with depositional environments that occur below mean sea level and may be considered as lower constraining points for mean sea level. Two additional samples are associated with *Crassostrea virginica* that appeared to be in living position and are plotted as the range in which oysters are observed in the modern environment (-0.6 to +1.1 meters MSL). The samples were processed and the radiocarbon data were calibrated with eight radiocarbon data points being associated with marine samples, and three radiocarbon data points associated with terrestrial samples (i.e. wood). The uncalibrated data and calibrated results are provided in Table 8 with the associated sample information relative to the evaluation of sea level conditions. The radiocarbon data in radiocarbon years and the calibrated data were both used to evaluate Late Holocene sea level conditions, since previous studies of sea level in the southeastern U.S. and proximal regions present data in radiocarbon years B.P. (Depratter and Howard, 1981; Colquhoun and Brooks, 1986) and calibrated years B.P. (Gayes et al., 1992; Scott and Collins, 1995; Balsillie and Donoghue, 2004).

#### 6.5.1 Radiocarbon Data

Sea level data point number 1 (SL No. 1) was obtained from a charcoal sample collected at -4.35 meters MSL and associated with a shell lag and laminated facies, resulting in an upper constraining point of -4.35 meters MSL and a sea level window extending to -5.55 meters MSL at 6020 +/- 100 B.P. SL No. 2 was obtained from a *Donax* specimen collected at -5.13 meters MSL and is associated with the subtidal bioturbated and laminated facies, yielding a lower constraining point of -3.13 meters with respect to modern sea level and extending to -1.13 meters MSL at 5831 +/- 70 B.P. SL No. 3 was obtained from a *Crassostrea* specimen collected in



apparent living position at -1.67 meters elevation and the point was plotted relative to the modern vertical range of the organism (-0.6 to +1.1 meters MSL), yielding a sea level window of -1.07 to -2.77 meters MSL at 3200 +/- 100 B.P. SL No. 4 was obtained from shell material collected at -4.16 meters MSL and is associated with the subtidal bioturbated and laminated facies, yielding a lower constraining point of -2.16 meters with respect to modern sea level and a sea level window extending to -0.16 meters MSL at 2829 +/- 58 B.P. SL No. 5 was obtained from an *Ilyanassa* specimen collected at -3.35 meters MSL and is associated with muddy washover sand assumed to be deposited into the low marsh, resulting in an upper constraining point of -2.25 meters MSL and a sea level window extending to -3.35 meters MSL at 2614 +/- 54 B.P. SL No. 6 was obtained from a *Mulinia* specimen collected at -3.15 meters MSL and is associated with the subtidal bioturbated and laminated facies, yielding a lower constraining point of -1.15 meters MSL and a sea level window extending to +0.85 meters MSL at 1632 +/- 60 B.P. SL No. 7 was obtained from a *Mulinia* specimen collected at -2.33 meters MSL and is associated with the intertidal laminated facies, yielding an upper constraining point of -1.13 meters MSL and a sea level window extending to -2.33 meters MSL at 1559 +/- 50 B.P. SL No. 8 was obtained from a wood sample collected at -0.16 meters MSL and is associated with low marsh sediments, resulting in an upper constraining point of -0.16 meters MSL and a sea level window extending to -1.26 meters MSL at 777 +/- 60 B.P. SL No. 9 was obtained from a *Crassostrea* specimen collected in apparent living position at -0.68 meters MSL and the point was plotted relative to the modern vertical range of the organism (-0.6 to +1.1 meters MSL), yielding a sea level window of -0.08 to -1.78 meters MSL at 677 +/- 56 B.P. SL No. 10 was obtained from shell material collected at -3.41 meters MSL and is associated with the subtidal bioturbated and laminated facies, yielding a lower constraining point of -1.41 meters with respect to modern sea level and a

sea level window extending to +0.59 meters MSL at 294 +/- 48 B.P. SL No. 11 was obtained from a wood sample collected at +0.04 meters MSL and is associated with low marsh sediments, resulting in an upper constraining point of -0.04 meters MSL and a sea level window extending to -1.06 meters MSL at 39 +/- 62 B.P.

The radiocarbon data is clustered in groups associated with three time intervals at approximately 6000 B.P. (n=2), 3200-2800 B.P. (n=3), 1600-1500 B.P. (n=2) but may be considered as reasonably well distributed at less than 1000 B.P. (n=4). The clustering pattern results in data gaps, with a significant data gap from 5831 B.P. to 3200 B.P., a moderate gap from 2614 B.P. to 1632 B.P., and a small gap from 1559 B.P. to 777 B.P. However the data indicates significant changes in the sea level envelope within the clustered data points or windows (Figure 6-28). Data for the time interval between sea level data point number 4 (SL No. 4) and SL No. 5 indicate a negative slope or a regression in sea level 2829 B.P. to 2614 B.P. A second regression is indicated in the data and is associated with the interval between SL No. 6 and SL No. 7 at 1632 B.P. to 1559 B.P. The radiocarbon data indicate sea level reaching approximately three meters below modern sea level at 5831 +/- 70 B.P. with two regressions directly indicated in the sea level envelope for St. Catherines Island that were subsequently evaluated using calibrated radiocarbon data.

### *6.5.2 Calibrated Radiocarbon Data*

The eleven samples from the radiocarbon database selected to evaluate sea level conditions during the Late Holocene were also reviewed using calibrated radiocarbon data and the sample metadata (sample elevation, indicative meaning, etc.).

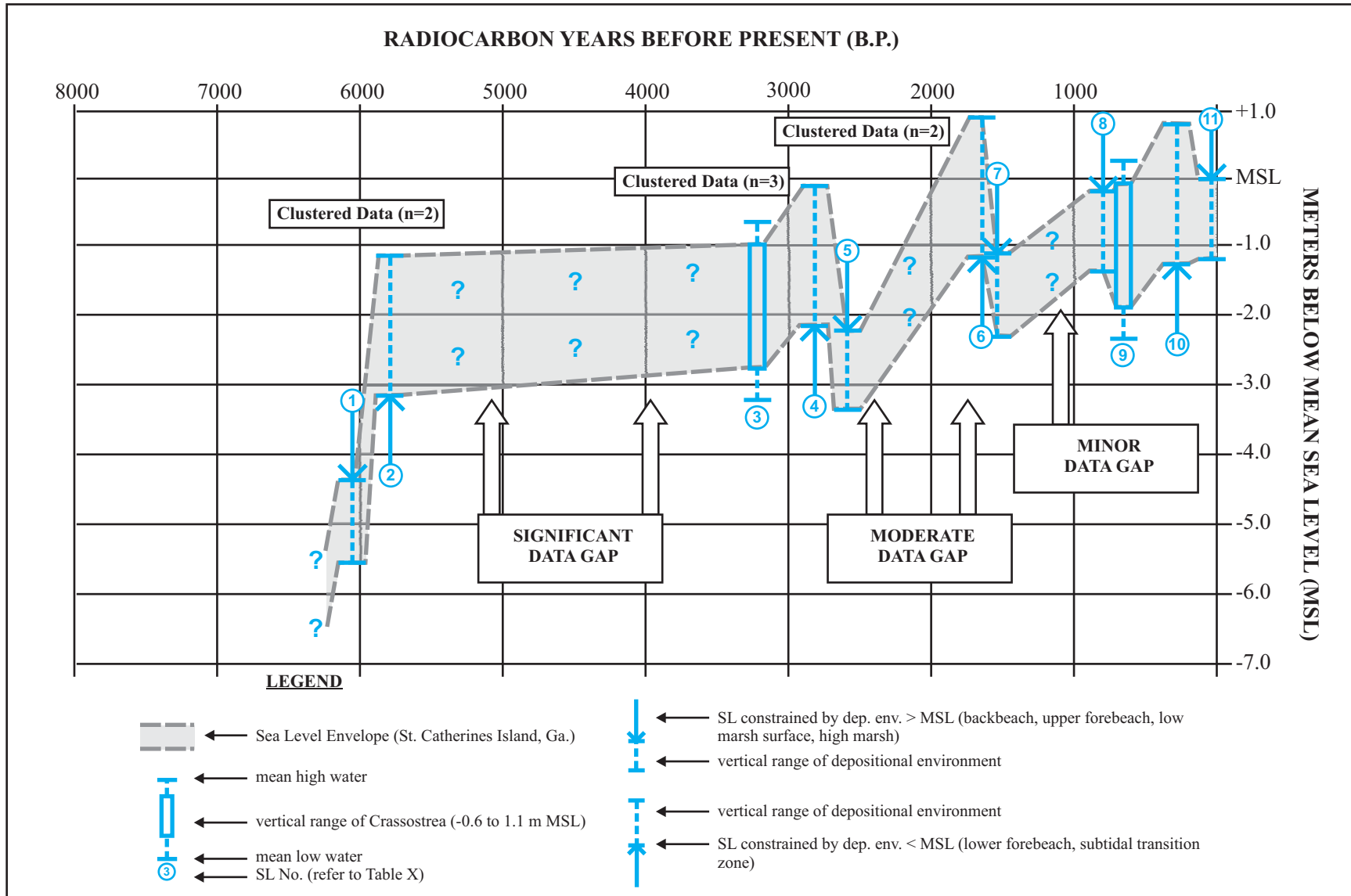


Figure 6-28: Plotted sea level "windows" (ID = SL No. from Table 8) in radiocarbon years before present (B.P.) and corresponding sea level envelope. Data from SL No. 1 and SL No. 2 indicate the initial flooding of the late Pleistocene substrate; SL No. 4 and SL No. 5 indicate a regression or fall in sea level circa 2600-2800 B.P. and another regression is associated with SL No. 6 and SL No. 7 at 1600 B.P.

The calibrated radiocarbon results also indicate a clustering pattern with groups associated with three time intervals at 6867-6378 Cal B.P. (n=2), 3181-2754 Cal B.P. (n=3), 1319-1243 Cal B.P. (n=2) and reasonably well distributed between 1200 Cal B.P., and modern (n=4). The clustering pattern also results in data gaps associated with the calibrated data with a significant data gap from 6378 Cal B.P. to 3181 Cal B.P., a moderate data gap from 2474 Cal B.P. to 1319 Cal B.P., and a minimal data gap from 1243 Cal B.P. to 703 Cal B.P. However, the calibrated data also indicates significant changes in the sea level envelope within the clustered data (Figure 6-29). Data from sea level data point number 4 (SL No. 4) and SL No. 5 indicate a regression or fall in sea level between 2754 Cal B.P. to 2474 Cal B.P. A second regression is indicated in the sea level windows and corresponding sea level envelope and is associated with SL No. 6 and SL No. 7 at 1319 Cal B.P. to 1243 Cal B.P.

The results for the sea level evaluation indicate that mean sea level had risen during the post-Wisconsin transgression during the Holocene to approximately three to four meters below modern sea level by 6000 B.P. Data gaps prohibit a detailed evaluation, however a framework is established where constraints on sea level are adequate for the most recent portion of the record and two regressions are indicated in the data where adjacent upper and constraining points indicate a negative slope or a decrease in mean sea level. This framework for the Late Holocene sea level will be provided with additional structure using indirect evidence from other regional sea level studies and will be tested by evaluating the timing of suspected marine regressions against periods of beach ridge formation.

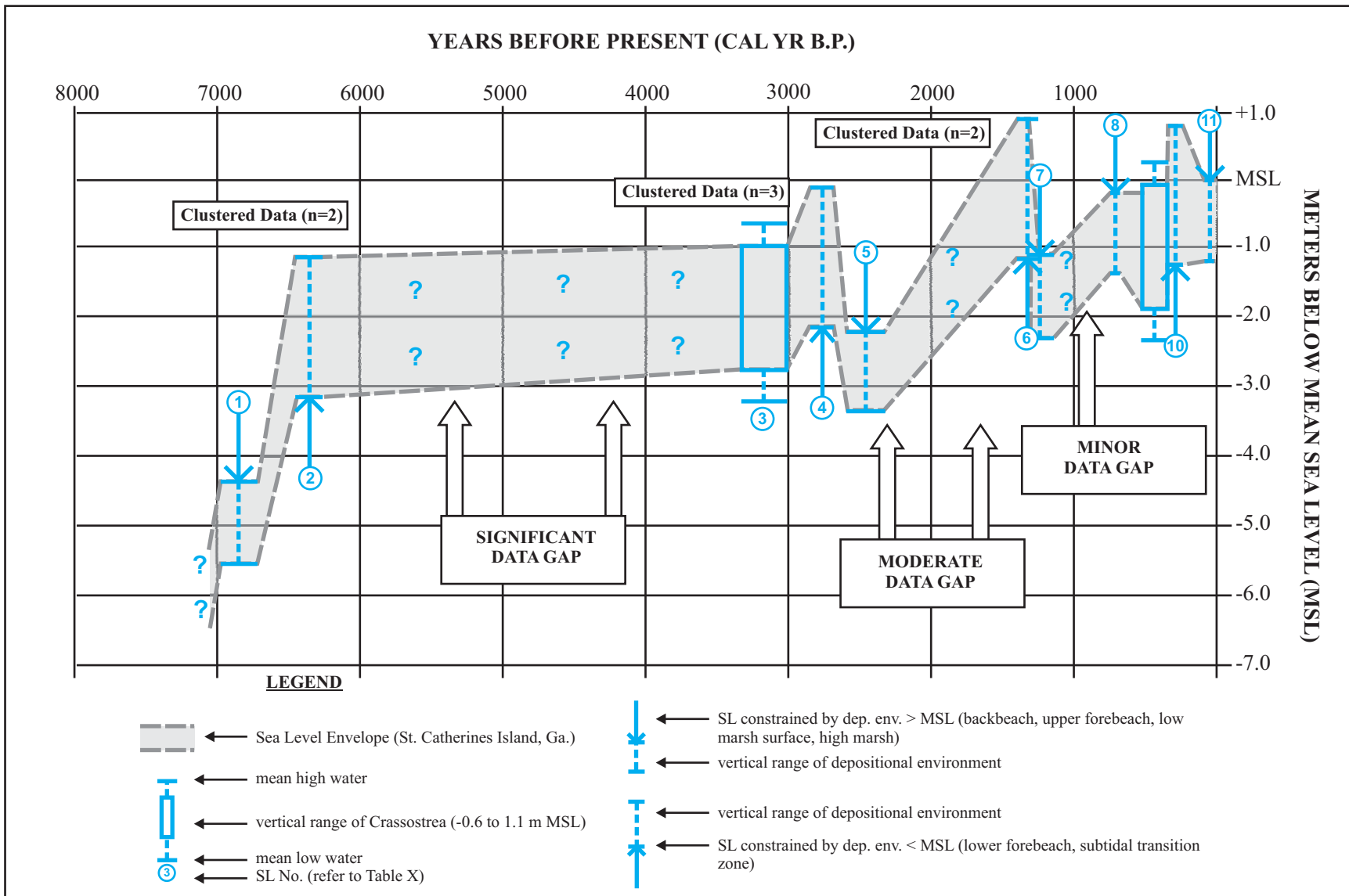


Figure 6-29: Calibration of radiocarbon data was performed using CALIB 6.1.1 software (Reimer et al., 2005) and the results were plotted as sea level "windows" and a corresponding sea level envelope was developed. The effort was performed to compare the SCI sea level envelope to other calibrated sea level data (Gayes et al., 1992; Scott and Collins, 1995; Balsillie and Donoghue, 2004).

## 7 DISCUSSIONS

### 7.1 Chemofacies of Barrier Island Sediments

Titanium (Ti) levels in the FPXRF data for the HMS were controlled by the relative concentrations of ilmenite [(Fe,Mg,Mn,Ti)O<sub>3</sub>], leucoxene (variable chemical comp.) and rutile (TiO<sub>2</sub>) as shown in Table 9 (Pirkle et al., 1991 and Elsner, 1997). Zirconium (Zr) concentrations in the FPXRF data are controlled by the abundance of zircon (ZrSiO<sub>4</sub>). It is apparent that the concentration of Ti is controlled by the three titanium bearing minerals that occur in varying mineral abundance, and that Ti content also varies within ilmenite and leucoxene. Iron (Fe) levels in the FPXRF data were controlled by the relative abundance of ilmenite, leucoxene, staurolite, tourmaline, garnet, epidote and hornblende (Pirkle et al., 1991). Although calcium is most commonly associated with shell debris in marine sediments, contributions to calcium concentrations may also be the result of the occurrence of tourmaline, epidote and hornblende.

A hybrid approach to using cluster analysis was successful in creating meaningful groups or chemofacies designations based on the FPXRF results from the vibracore data. Agreement between the interpreted depositional environments and subenvironments indicated in samples and the chemofacies designations was assessed by calculating a conformance measure of the number of samples from each facies group that occurred within each of the chemofacies designations. These results indicate that 73% to 100% of the samples from each of the major barrier island depositional environments or subenvironments were assigned to a single corresponding chemofacies designation, strongly indicating that the cluster analysis produced meaningful groups or chemofacies designations. A review of the samples that were assigned to

**Table 9:**  
**Mineralogy of Heavy Mineral Sands and FPXRF Results for the Most**  
**Commonly Detected Analytes**

Heavy Minerals		HMS Constituents - Most Commonly Detected Elements					
Mineral Species	Chemical Formula	K	Ca	Ti	Fe	Zr	S
Ilmenite	(Fe,Mg,Mn,Ti)O <sub>3</sub>			X	X		
Leucoxene	variable			X	X		
Rutile	TiO <sub>2</sub>			X			
Zircon	ZrSiO <sub>4</sub>					X	
Kyanite/Sillimanite	Al <sub>2</sub> SiO <sub>5</sub>						
Staurolite	Fe <sup>2+</sup> <sub>2</sub> Al <sub>9</sub> O <sub>6</sub> (SiO <sub>4</sub> ) <sub>4</sub> (O,OH) <sub>2</sub>				X		
Spinel	MgAl <sub>2</sub> O <sub>4</sub>						
Corundum	Al <sub>2</sub> O <sub>3</sub>						
Tourmaline	(Ca,K,Na,[ ])(Al,Fe,Li,Mg,Mn) <sub>3</sub> rep. unit (Al,Cr, Fe,V) <sub>6</sub> (BO <sub>3</sub> ) <sub>3</sub> (Si,Al,B) <sub>6</sub> O <sub>18</sub> (OH,F) <sub>4</sub>		X		X		
Monazite/Xenotime	(Ce,La)PO <sub>4</sub>						
Garnet	The general formula X <sub>3</sub> Y <sub>2</sub> , rep. unit (SiO <sub>4</sub> ) <sup>3</sup>				X		
Epidote	Ca <sub>2</sub> Al <sub>2</sub> (Fe <sup>3+</sup> ;Al)(SiO <sub>4</sub> )(Si <sub>2</sub> O <sub>7</sub> )(OH)		X		X		
Hornblende	(Ca,Na) <sub>2-3</sub> (Mg,Fe,Al) <sub>5</sub> (Al,Si) <sub>8</sub> O <sub>22</sub> (OH,F) <sub>2</sub>		X		X		

non-primary chemofacies groups indicated that the majority of these samples represent transitional conditions between adjacent depositional environments or subenvironments.

Additional samples that were assigned to secondary and tertiary chemofacies groups provided insights into sediment provenance and dynamics associated with the depositional environments. The results of the FPXRF data QC evaluation indicate reasonable performance with respect to samples that were benchmarked against fixed-laboratory WDXRF analysis. In addition, acceptable precision was indicated from replicate analyses and RSD metrics for the sandy and muddy matrices indicating FPXRF as a reliable and valuable screening tool for assessing elemental geochemistry in barrier island sediments.

While the cluster analysis was successful at grouping facies into meaningful groups at a higher level of depositional environment classification based on the bulk elemental analysis, the subsequent separation of the sediments into depositional subenvironments is dependent on the recognition of the primary physical and biogenic structures. These factors indicate that FPXRF offers definite benefits in the rapid assessment of barrier island system sediments from the direct scanning of cores or as a downhole tool to compliment to the full suite of “smart tools” currently being used in direct push technology (DPT) drilling or Geoprobe<sup>TM</sup> systems for rapid data acquisition. Select locations could be continuously sampled to verify the initial results and additional scrutiny of cores could be performed to delineate subenvironments.

## **7.2 Shoreline Dynamics and Anthropogenic Modifications to Sediment Supply**

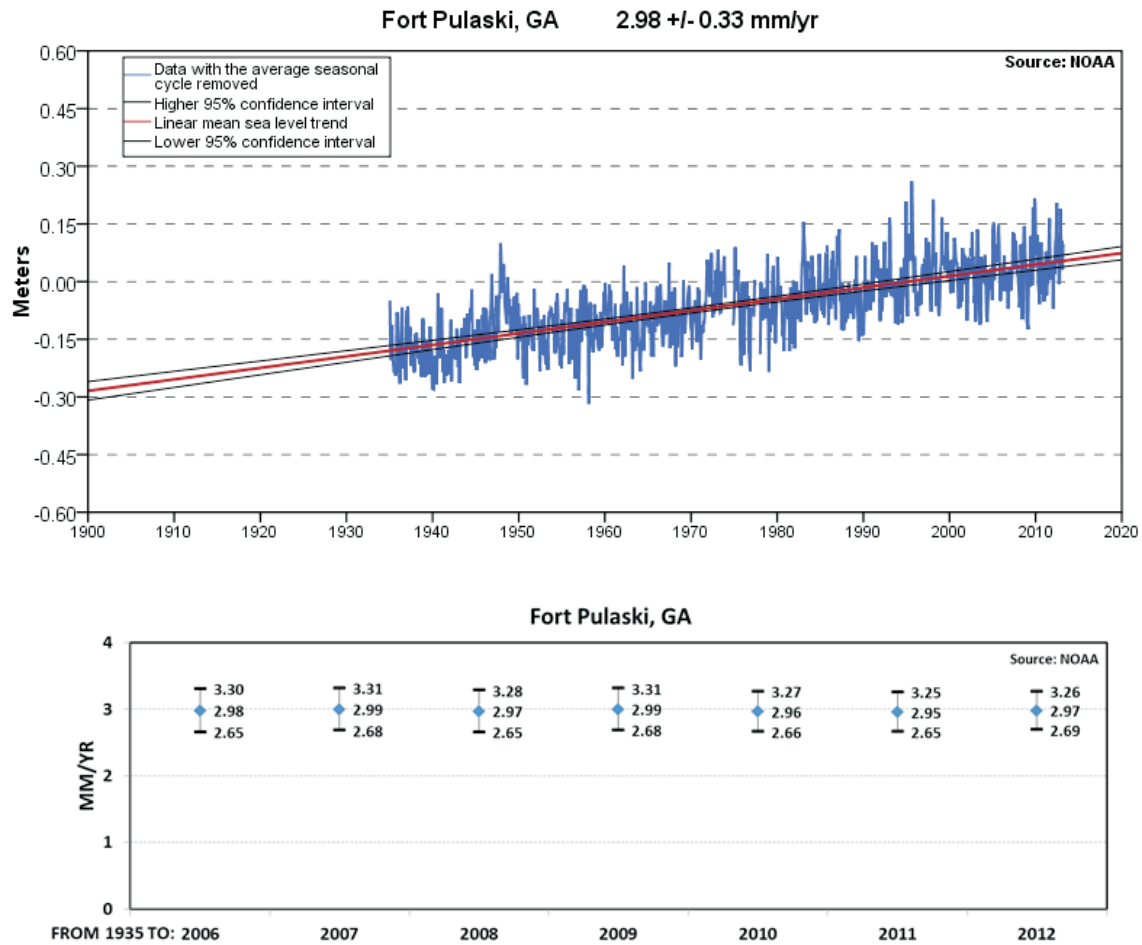
The evaluation of shoreline dynamics at St. Catherines was performed in conjunction with an assessment of the two major controls on barrier island formation and modification processes, the rate of the increase in accommodation space or sea level rise, and the rate of



sediment supply. Data indicate that the rate of sea level rise on the Georgia Coast has been consistent in the 20<sup>th</sup> and 21<sup>st</sup> century based on historical tide gauge data (Figure 7-1). The Savannah River is the closest Piedmont Province river system that discharges to St. Catherines Island, and although sediment transport baseline data is not available since modifications to the river system were made prior to the National Environmental Policy Act (1970), an evaluation of the historical modifications to the river was made under the current study in the form of a timeline (Figure 7-2). The timing of the events specific to producing disruptions in sediment flux were identified and incorporated into the analysis of the shoreline model results.

The magnitude of sediment transport in streams in the southeast U.S. has varied considerably since European settlement as a result of land management practices (Meade and Trimble, 1974; Trimble, 1974; Milliman and Meade, 1983). Colonization and land clearing were initiated in Virginia in 1700 and spread in a southwestern direction to Georgia and Alabama culminating in the mid-1800s. The highest rates of soil erosion, or erosive land use existed in the 1900 to 1920 time interval (Meade and Trimble, 1974) when an estimated 190 mm of soil cover was eroded and transported from the Georgia Piedmont Province (Trimble, 1974).

Modifications in the rate of sediment supply associated with five major streams in the southeastern US have been evaluated in a quantitative manner using the *HydroTrend* hydrological transport numerical model (McCarney-Castle et al., 2010). Changes in suspended sediment flux rates were evaluated during 1) pre-European conditions (1680-1700), 2) pre-dam conditions (1905-1925), and 3) post-dam conditions (1985-2005) for five major watersheds in the southeastern US including the Savannah River and Altamaha River systems. Calibration of the model was performed using modern suspended sediment data for the 1985-2005 time interval and land use/land cover information was integrated for each of the three study periods to model



Images: NOAA Sea Levels On-Line; [http://tidesandcurrents.noaa.gov/sltrends/sltrends\\_states.shtml?region=ga](http://tidesandcurrents.noaa.gov/sltrends/sltrends_states.shtml?region=ga)

Figure 7-1: Tide gauge data from Ft. Pulaski, Georgia indicating a sea level rise rate of 2.98 +/- 0.33 m/yr based on data collected from 1935 to 2011 (upper) with linear mean trends and 95% confidence intervals plotted (lower) that indicate a linear trend in sea level rise.

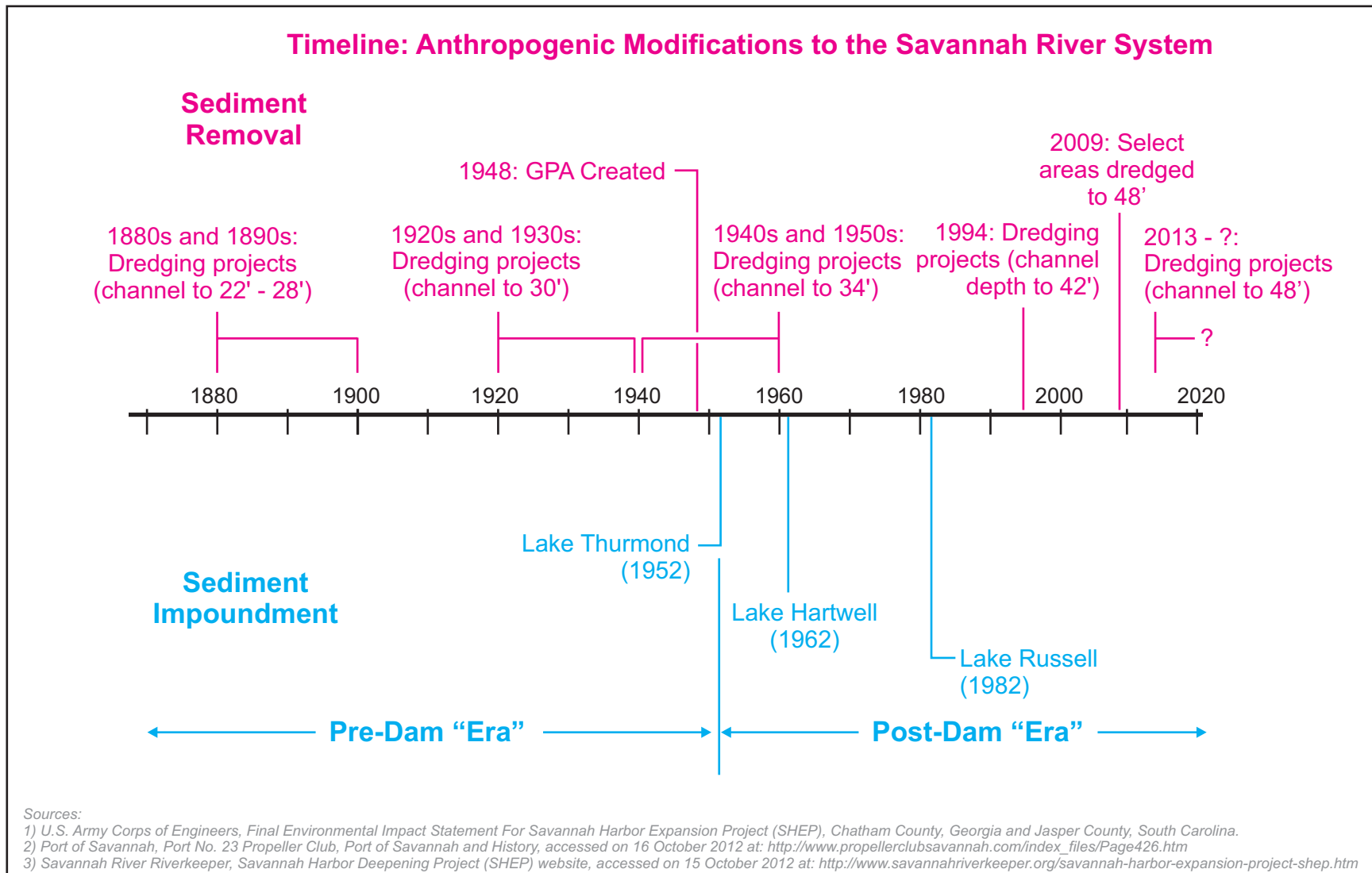


Figure 7-2: Timeline of modification to the Savannah River system including sediment sinks (dredging) and sediment impoundments (dams). The change in shoreline retreat rates appears to correlate with major disruptions in the rate of sediment supply to the coast, specifically the placement of the initial impoundment on the Savannah River in 1952 (Lake Strom Thurmond).

the associated suspended sediment flux in the five watersheds. Results for the Savannah River model indicate a 1.4 megaton per year (Mt/yr) flux of sediment during the pre-European period (1680-1700), a 3.5 Mt/yr rate for the pre-dam period (1905-1925) or the time interval associated with the highest rates of erosive land use, and 1.1 Mt/yr suspended sediment flux for the post-dam era (1985-2005) of the Anthropocene (Figure 7-3). The second closest river to St. Catherines Island with appreciable hydraulic and sediment discharge is the Altamaha River, where model results indicate a 0.9 megaton per year (Mt/yr) flux of sediment during the pre-European period (1680-1700), a 2.3 Mt/yr rate for the pre-dam period (1905-1925), and a 0.9 Mt/yr suspended sediment flux for the post-dam era (1985-2005). Anthropogenic modifications to the Altamaha River may be considered as similar to the timeline for the Savannah River where the initial impoundment was constructed on the river near the southern limits of the Piedmont Province to create Lake Sinclair in 1954. Land clearing and inadequate land management practices contributed to an increase in sediment loads following colonization (pre-dam period), and the effects to landforms and sediment regimes due to increases in sediment flux rates have been documented elsewhere including the rapid expansion of coastal wetlands and marshes in Massachusetts (Kirwan et al., 2011) and sedimentation rates in Chesapeake Bay that increased up to an order of magnitude (Colman and Bratton, 2003; Saenger et al., 2008). The placement of the impoundments on the Savannah River has returned the suspended sediment flux rates to a rate of 20% less than the pre-European land clearance rates. The *HydroTrend* model (McCarney-Castle et al., 2010) confirms and quantifies that modifications to the Savannah River system have resulted in appreciable changes in the rate of sediment transported to the Georgia Coast during the time period that correlates to acceleration in the shoreline retreat rates associated with the spit and berm landforms observed under the current study. The timing of

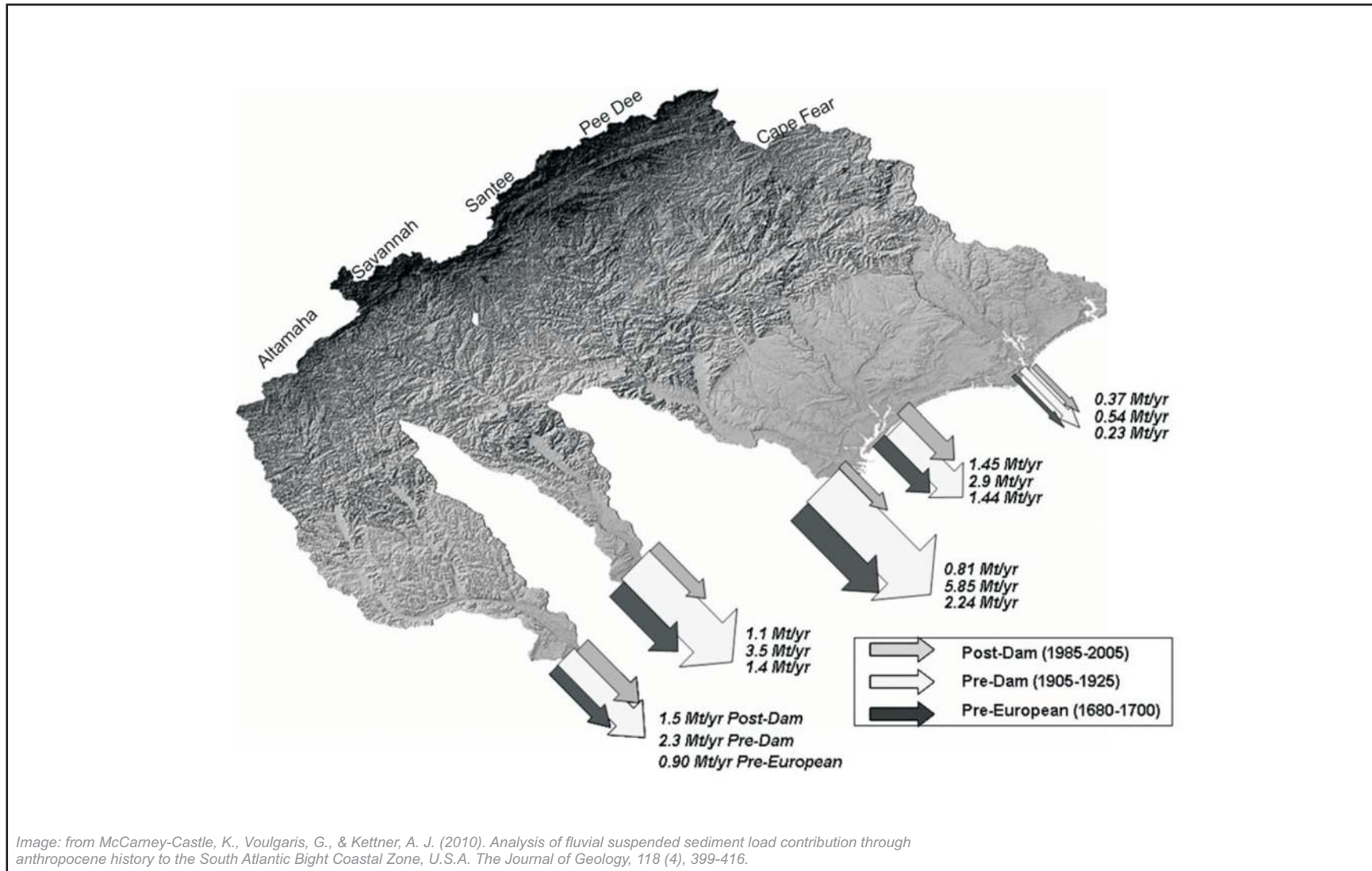


Figure 7-3: Relief map showing pre-European, pre-dam, and post-dam sediment flux rates for five major watersheds in the southeastern U.S. including the Savannah and Altamaha Rivers. Results for the Savannah River model indicate a 1.4 megaton per year (Mt/yr) flux of sediment during the pre-European period (1680-1700), a 3.5 Mt/yr rate for the pre-dam period (1905-1925), and 1.1 Mt/yr suspended sediment flux for the post-dam era (1985-2005) of the Anthropocene (McCarney-Castle et al., 2010).

anthropogenic modifications to sediment flux rates were used to define two time periods (pre-dam and post-dam) in the current study and under this premise the shoreline dynamics modeling was performed for two temporal periods or eras: 1) 1859-1951 (pre-dam conditions including erosive land use), and 2) 1968-2011 (post-dam conditions).

Difficulties would be encountered in trying to determine a quantitative link between the sediment transport rates and the resulting shoreline dynamics. These difficulties would include the potential recovery of sediment flux downstream of the dams and the natural and anthropogenic modifications to downstream fluvial systems and the coast including alterations to estuarine systems.

Results from the shoreline modeling indicate that there is an apparent acceleration in the shoreline retreat rates for the spit and berm landforms on the shoreface portion of the island that is indicated as an inflection point in time-series plots of shoreline displacement and initiated in the specific time interval between the 1951 and 1968 vector data sets (Figure 7-4). The spit and berm landforms are unique with respect to the shoreline at St. Catherines Island where these landforms result from the combination of erosion along the shoreface and deposition via washover processes. Shoreline retreat along the island core and accretional beach ridges results primarily from the erosion and removal of sediments with little to no depositional agent. The change in shoreline retreat rates for the spits and berms appears to correlate with the timing of major disruptions in the rate of sediment supply to the coast of Georgia, specifically the placement of the initial impoundment on the Savannah River in 1952 (Lake Strom Thurmond). A qualitative review of land cover and vegetation in the historical imagery revealed distinct differences in the types of vegetation associated with Seaside Spit and Middle Beach in the older (1951) or pre-dam era imagery versus the modern or post-dam era imagery. Mature vegetation is

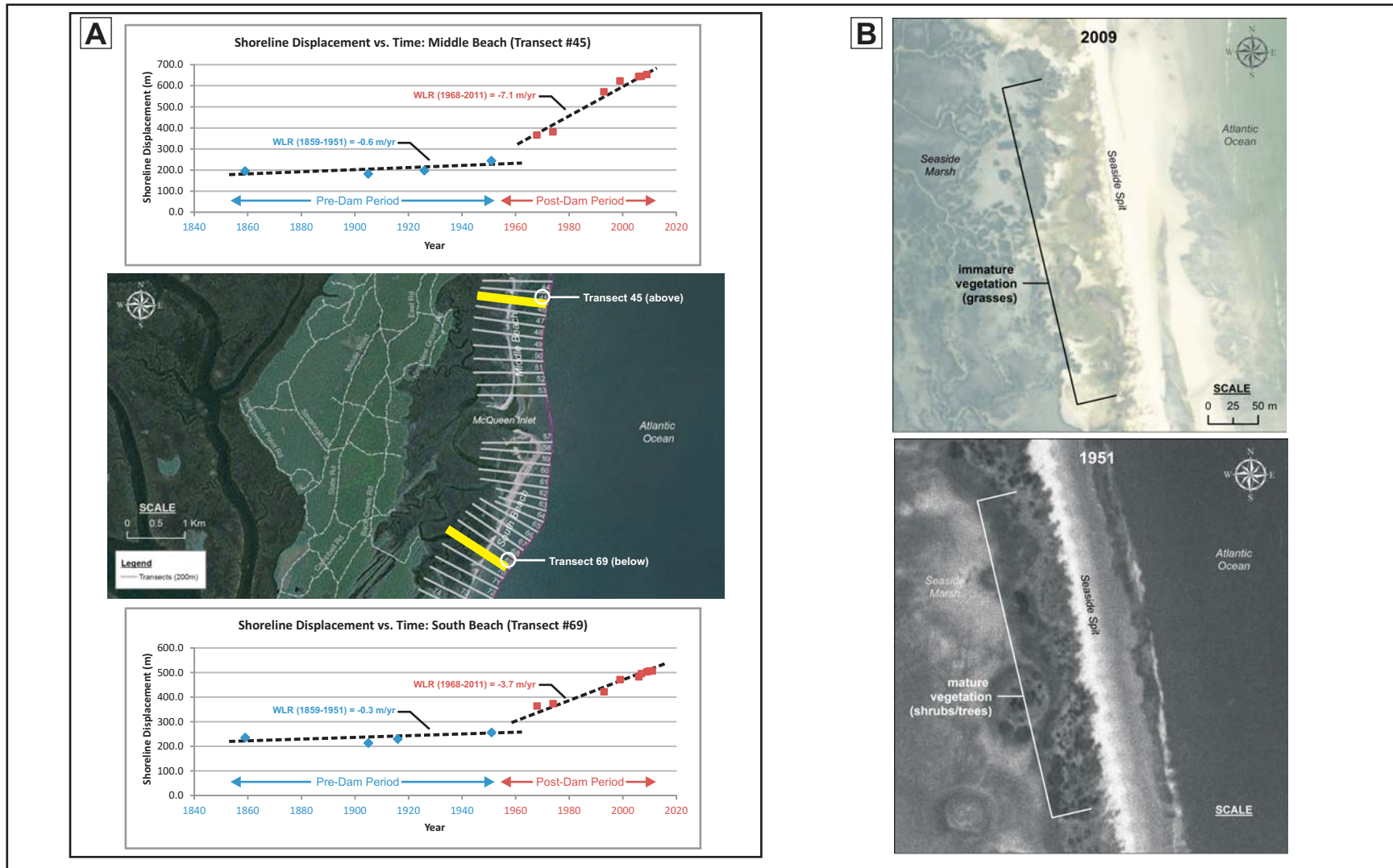


Figure 7-4: Quantitative and qualitative indications of an acceleration in shoreline retreat for the spit/berm landforms associated with Seaside Spit, Middle Beach and South Beach. a) time series plots of shoreline displacement (meters) for Transects 45 (Middle Beach) and Transect 69 (South Beach) for pre-dam and post-dam data series showing an increase in slope or the rate of shoreline retreat. b) the decrease in the maturity of vegetation also indicates an increase in the rate of shoreline retreat where the natural succession of plant types are no longer in balance with the rate of shoreline retreat.

observed in historical imagery on the landward side of the beach berms consisting of shrubs and trees (Figure 7-4). In the modern or post-dam imagery and in field observations performed during the current study period (2010 to 2013) the modern vegetation type appears to be dominated by grasses such as salwort (*Salsola kali*), spike grass (*Distichlis spicata*), beach hogwart (*Croton punctatus*) and limited sea oats (*Uniola paniculata*). This change in the maturity of vegetation is reflective of a less stable landform or a landform that may be retreating at a higher rate where the natural successions of plant types are no longer in balance with the rate of shoreline retreat. There is a potential negative feedback in this process whereby the more immature plants are less efficient at stabilizing the sediment than mature shrubs and trees, thereby accelerating shoreline retreat and landform changes.

The relationship between the relative rates of sediment supply and sea level rise were evaluated for the barrier islands of the Georgia Bight to determine if spatial trends exist. Under the assumption that sea level rise is relatively constant over the Georgia Bight, sediment supply was evaluated as being a function of the distance to major river systems or appreciable sources of sediment supply. The distances from the island center to major rivers located to the north (plotted as “x”) which are the primary sources for sediment and secondary sources for sediment or rivers to the south (plotted as “y”) were determined and plotted with the erosional percentage of the total shoreline (Figure 7-5). The percentage of the total shoreline characterized as erosional using long-term data (1870-2000) is provided as “eLT” and the short-term rates (1970-2000) for shoreline dynamics are provided as “eST”. A significant spatial trend is noted in eST values where the values become greater with increasing distance from the major rivers. The results of the distance to the major river plots indicate that St. Catherines Island is located at the greatest distance to appreciable sediment sources and also exhibits the largest percentage of the



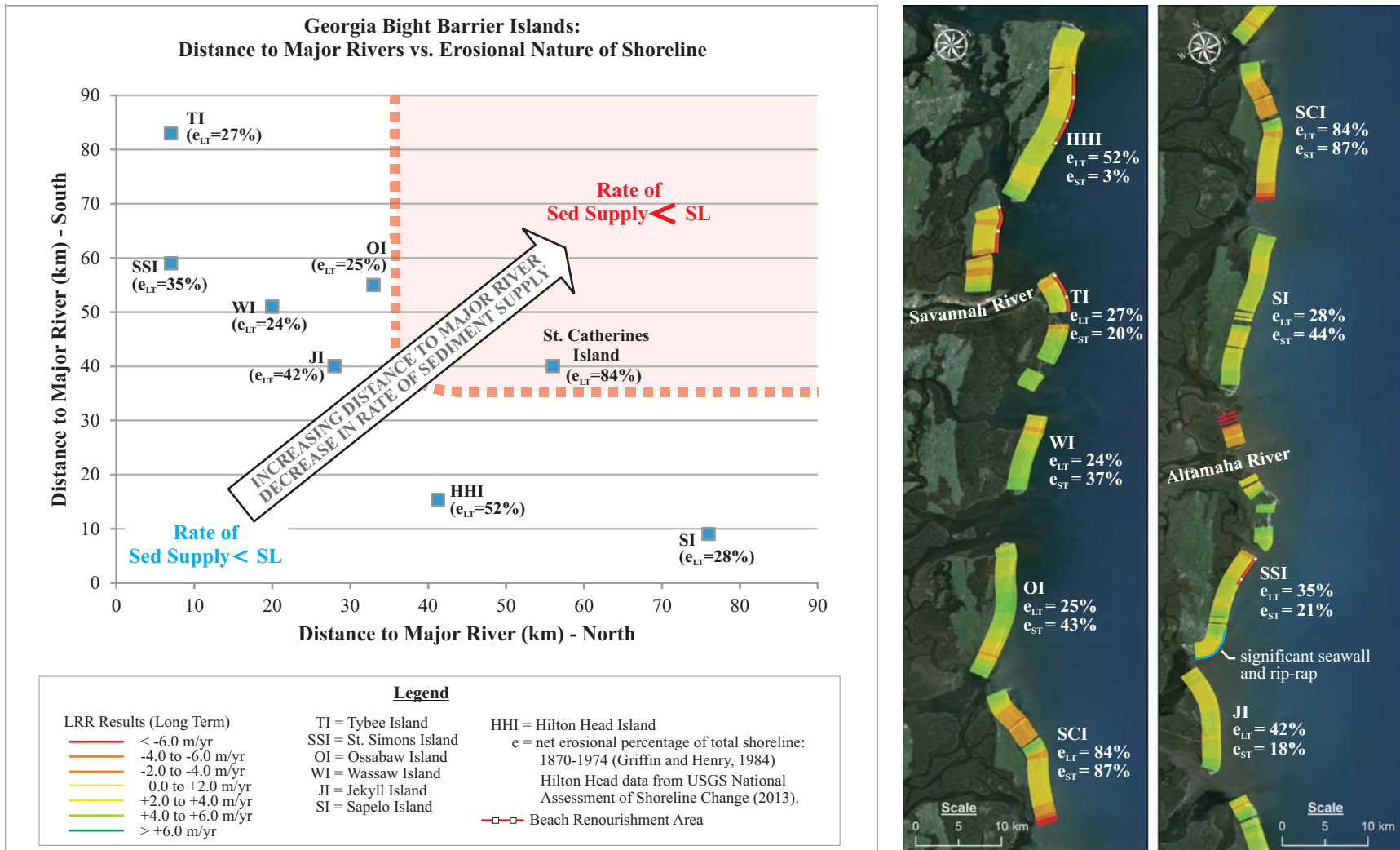


Figure 7-5: Relationship of the Georgia Bight barrier island systems versus the distance to major river systems. The distance from the island center to major rivers located to the north (x) which are the primary sources for sediment and secondary sources for sediment or rivers to the south (y). The percentage of the total shoreline characterized as erosional using long-term data (1870-2000) is provided as “ $e_{LT}$ ” and the short-term rates (1970-2000) for shoreline dynamics are provided as “ $e_{ST}$ ”. The results of  $e_{LT}$  vs.  $e_{ST}$  indicate increases in the percentage of erosional coasts except where anthropogenic modifications have been performed. A spatial trend is noted in  $e_{ST}$  values where the values become greater with increasing distance from the major rivers.

total shoreline. The results of eLT vs. eST indicate increases in the percentage of erosional coasts except where anthropogenic modifications have been performed (Hilton Head Island, Tybee Island, Sea Island, St. Simons Island and Jekyll Island).

A schematic model was developed to conceptualize the major controls on barrier island formation and modification processes. This schematic model borrows from concepts applied to lacustrine environments by Carroll and Bohacs (1999) and builds on the “catch-up”, “keep up”, and “give up” stages of barrier island response where barrier island accretion and significant terrestrial deposits would occur on the left or vertical axis and barrier island drowning or abandonment are indicated on the lower or horizontal axis as end members. If St. Catherines Island is placed onto a schematic model that was developed during this study to conceptualize the major controls on barrier island formation and modification processes (Figure 7-6a) and the model is employed in a predictive manner where the rate of sea level rise is kept as a constant (reflected in 20th and 21<sup>st</sup> century tidal gauge data), a direct relationship is established between the rate of sediment supply and the landforms of St. Catherines Island. Based on the shoreline dynamics study and field observations, the more dynamic landforms such as Seaside Spit and the berms associated with Flag and Beach Ponds should occur in the lower range of the “keep up” stage or near the tipping point with “give up” status. If sediment supply is decreased incrementally, these “sensitive” landforms are predicted to move downward towards the “give up” stage. Based on the timing of events in anthropogenic modifications to sediment supply it is likely that disruptions in the rate of sediment supply to the Georgia Coast, such as the impoundment of rivers and modifications that have impacted longshore transport of sediment, would decrease the rate of sediment supply to longshore processes and ebb deltas, thereby resulting in the rapidly retreating shoreline, an acceleration in the rate of shoreline retreat, and

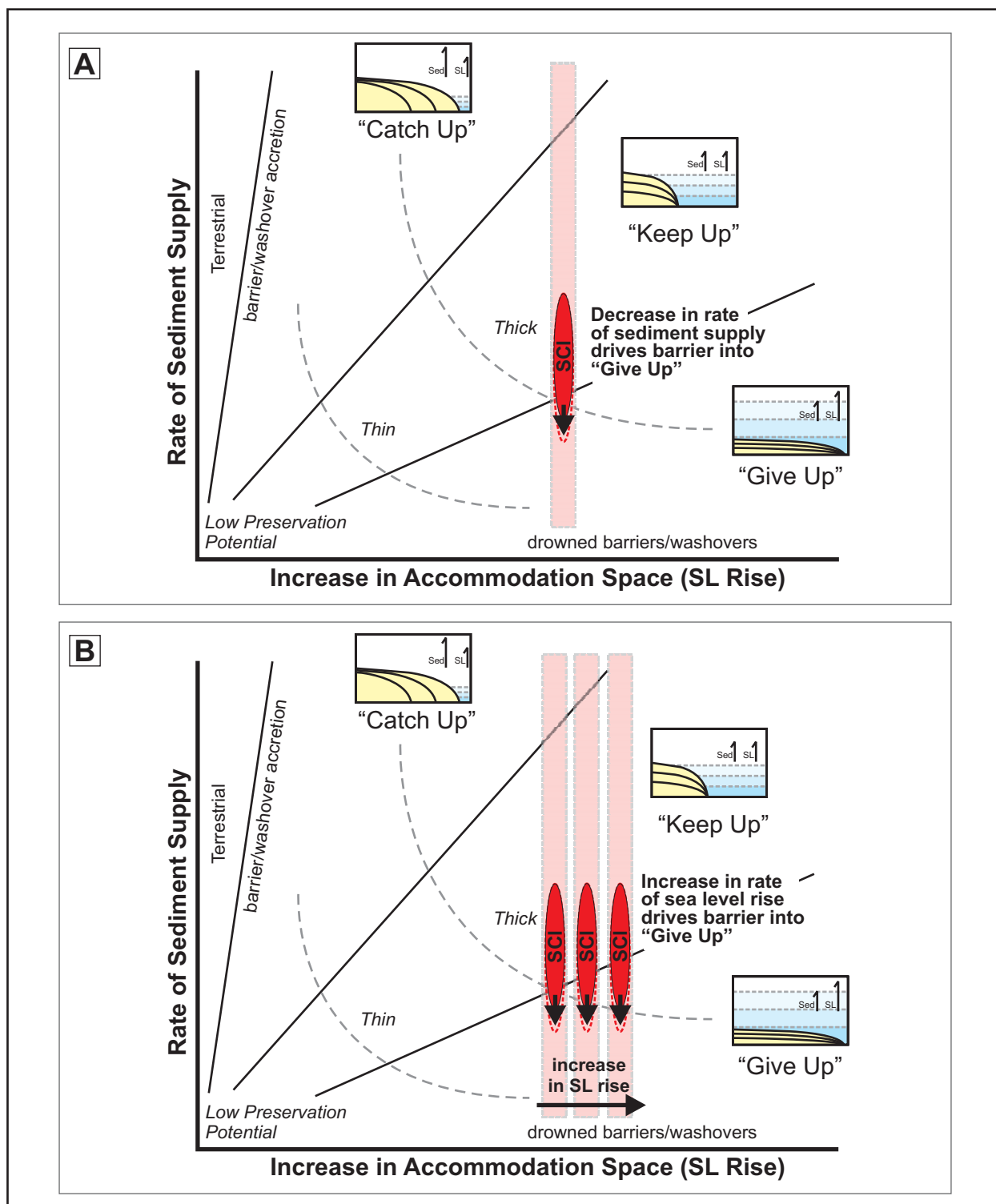


Figure 7-6: Schematic model that borrows from concepts applied to lacustrine environments by Carroll and Bohacs (1999) and builds on the “catch-up”, “keep up”, and “give up” stages of barrier island formation and modification. a) a decrease in sediment supply results in landforms that are sensitive to changes in the rate of sediment supply moving downward into “give up”, and b) current projections for an increase in the rate of sea level rise would result in the barrier system moving to the right or additionally into the “give up” stage.

the landform dynamics observed at St. Catherines Island. The changes in vegetation maturity associated with the spits and berms may be indicative of an initial imbalance between the rates of sediment supply and sea level rise and represent the initial step from “keep-up” to “give-up”. If the rate of sea level rise increases in the 21<sup>st</sup> century as predicted by current climate models, the imbalance in the major controls of barrier island response (rate of sediment supply and rate of sea level rise) will increase resulting in more landform dynamics and driving the island downward into the “give-up” stage in the schematic model at a faster pace (Figure 7-6b).

Local modifications to the rate of sediment supply related to St. Catherines Island were noted in vibracore data collected adjacent to the St. Catherines Shell Ring site (BKM 051311-01) and a core collected from *Mission Santa Catalina de Guale* (IEP 060411-01). Age and depth data from the St. Catherines Shell Ring high marsh core collected at 133 cm BLS indicated a radiocarbon age of 298 +/- 33 B.P. (376 +/- 77 Cal B.P.), or a date that coincides with the mission period or contemporaneous with European colonization and associated land management practices on the island. A sedimentation rate of 0.4 cm/yr is indicated from the age-depth relationship associated with sample collected from 133 cm BLS and this rate greatly exceeds “modern” sedimentation rates (0.1 cm/yr) from the high marsh on Sapelo Island (Letzsch and Frey, 1980). The subject marsh is formed by the confluence of streams that drain the core of the island and is situated on the mainland or western side of the island above the mean high tide line. The increase in the rate of sedimentation is directly attributed to an increase in the local rate of sediment supply based on the historical development of the island. During the “plantation era”, approximately 50% of the island was denuded to cultivate rice and Sea Island cotton (Thomas et al., 2008) resulting in an increase in erosion and availability for sediment transport and corresponding suspended sediment loads. Local anthropogenic controls on sediment flux rates

and sediment controls were also observed in a vibracore collected adjacent to the mission site within the freshwater stream that discharges to Wamassee Creek. A peat sample was collected from core IEP060411-01 at the base of a sandy peat facies that is underlain by intertidal marine sediments that are assumed to be of Late Pleistocene age based on radiocarbon dates in similar sediments. The peat sample was collected at a depth of 310 cm BLS and radiocarbon data indicate an age of 270 +/- 30 B.P. (359 +/- 77 Cal B.P.). A sedimentation rate of 0.9 cm/yr is indicated from the age-depth relationship and is most likely the result of two anthropogenic controls on sediment transport and sediment deposition including the aforementioned land clearing practices that promoted erosion and an increase in sediment flux rates, as well as the impoundment of the stream by a stacked log dam that is periodically exposed in the lower reaches of the unnamed stream. Based on the radiocarbon data and historical accounts, the dam was constructed during the operational period of *Mission Santa Catalina de Guale* (A.D. 1570s-1680s) and served as a freshwater impoundment, tidal barrier and a local sediment impoundment.

Shoreline dynamics have been evaluated at St. Catherines Island, Georgia with attention to the two major controls on barrier island formation and modification processes. These major controls include: a) the increase in accommodation space or the rate of sea level rise for the Georgia Bight, which has remained constant in 20<sup>th</sup> and 21<sup>st</sup> century tide gauge data, and b) dynamically changing rates of sediment supply based on anthropogenic modifications to land cover (Trimble, 1974) and sediment transport (McCarney-Castle et al., 2010). The evaluation of anthropogenic modifications to the rate of sediment supply performed under the current study, indicates that in spite of significant changes in sediment flux rates of +300% (pre-dam era) and -20% (post-dam era), shoreline retreat was continuous during the study period with an

acceleration noted in the rates of shoreline retreat associated with spit and berm landforms in the post-dam or modern era.

### **7.3 Environmental Change**

Environmental change under the modern marine transgression has been monitored along the shoreface in conjunction with the shoreline dynamics study to evaluate spatial modifications in the major depositional subenvironments resulting in alterations to the quality of the associated ecosystems and habitat. Monitoring of Seaside Spit has documented dramatic landform changes resulting from the modern marine transgression and more recently from a significant Spring 2012 nor'easter. This event forced the breaching of the beach berm at Seaside Spit and resulted in the formation of a tidal inlet at the specific location of the Seaside Spit vibrocore transect (A-A') and the conversion of the active washover fan to a flood delta complex (Figure 7-7). The flood delta has prograded an appreciable distance to the west and has converted the low marsh environment to sand flats with little to no vegetation, significantly modifying the depositional environment and associated habitat (Figure 7-8). In addition, the flood delta and inlet have modified the existing hydrologic regime through the capture of tidal creek tributaries that formerly drained to Fish Creek, where the tributaries now discharge to the newly formed tidal inlet at Seaside Spit. A second inlet has recently opened to the north across the beach berm following a Spring 2013 nor'easter, resulting in Seaside Spit currently being separated into three sections. When these landform conditions are evaluated together with the acceleration in shoreline retreat rates, the cumulative effect is a landform that is changing its fundamental nature as the number of inlets increase, resulting in a segmented shoreline. In addition, the understanding of the conversion of these landforms with respect to the shoreline dynamics

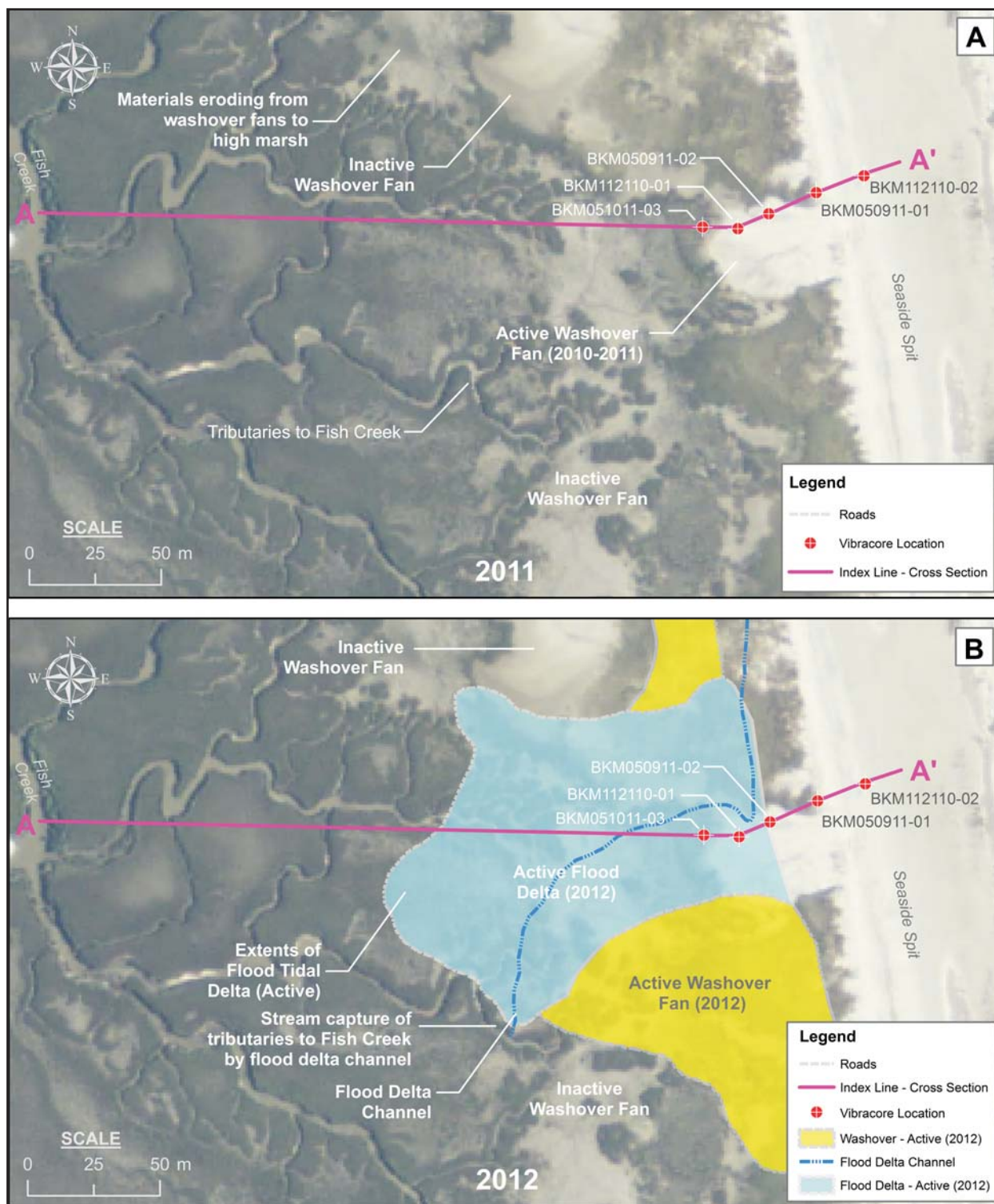


Figure 7-7: Environmental change at Seaside Spit (2011 - 2012). The formation of an inlet and the conversion of a washover fan to a flood tidal delta has been observed during the current study. a) Extents of active and inactive washover fans observed in 2011 and location of vibracore section. b) A new inlet was formed in Spring 2012 bisecting Seaside Spit and resulting in the progradation of a flood delta towards the west and the stream capture of two tributaries to Fish Creek (west).



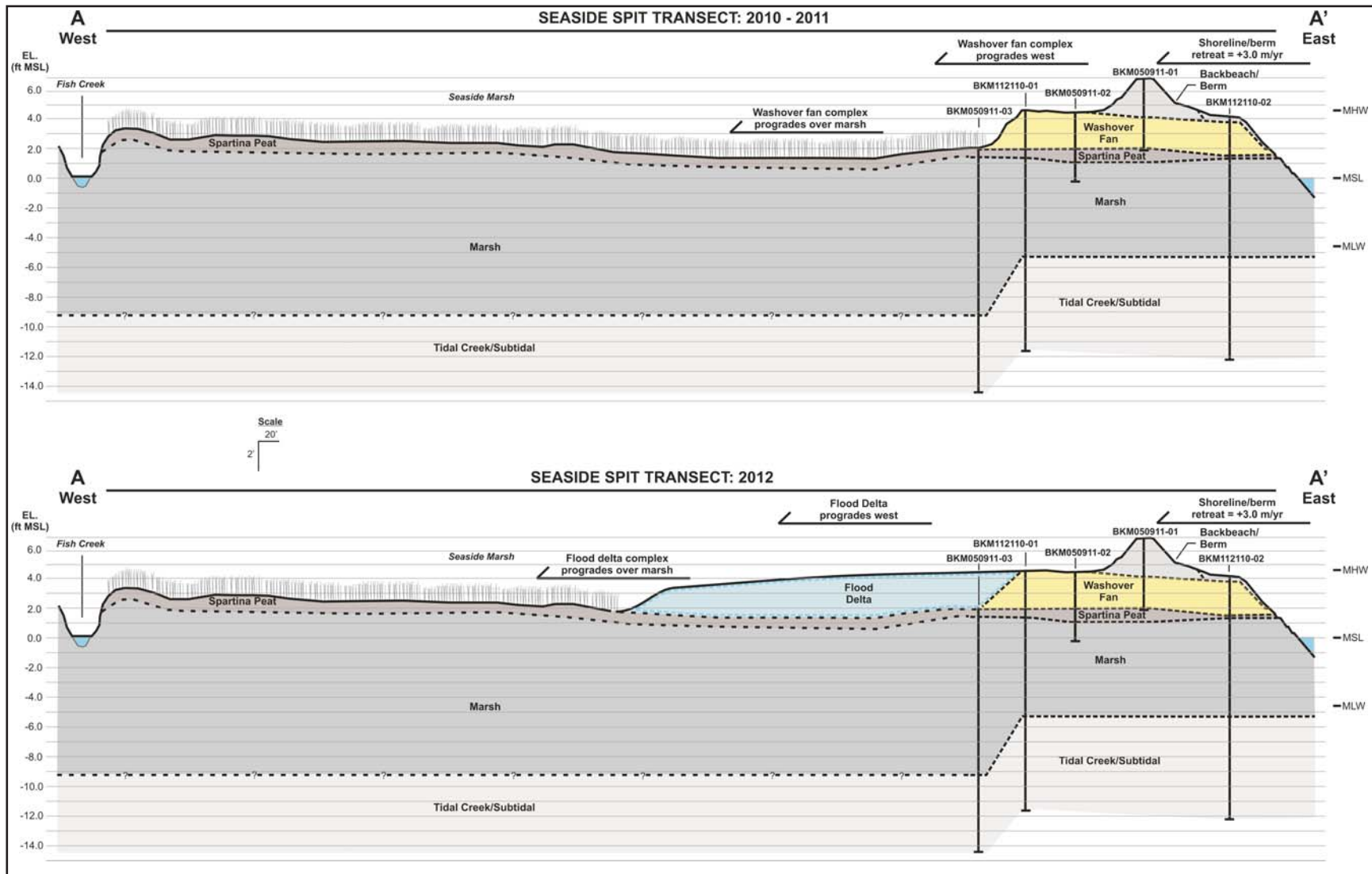


Figure 7-8: Monitoring of Seaside Spit has documented dramatic landform changes resulting from the modern marine transgression and a significant Spring 2012 nor'easter. This storm forced the breaching of the beach berm at Seaside Spit and resulted in the formation of a tidal inlet at the specific location of a vibracore transect and the conversion of the active washover fan to a flood delta complex.



provides insights when interpreting washover fans and flood deltas as lateral equivalents in the rock record.

Documentation for the environmental change at Beach Pond has been produced to capture the dramatic landform and corresponding ecosystem changes resulting from the modern marine transgression and a significant Spring 2012 nor'easter. Data obtained from the National Data Buoy Center for Station 41008 indicate that sustained winds of 25 mph and gusts of 43 mph were realized during the event (NDBC, 2013). This storm also forced the breaching of the beach berm at Beach Pond and has resulted in the formation of a tidal inlet at the specific location of the vibrocore transect where the new inlet has forced the conversion of the active washover fan to a flood delta complex (Figure 7-9). The flood delta has prograded an appreciable distance to the western margin of the pond and converted the freshwater lacustrine environment to a flood delta sand flat with little to no vegetation, greatly altering the hydraulic regime and modifying the depositional environment dramatically (Figure 7-10). As a result of the landform changes, Beach Pond has been altered from a freshwater pond to a tidal lagoon with a tidal exchange volume of approximately 4M gallons during each diurnal cycle. Based on the shoreline dynamics study and the evaluation of the major controls on barrier island processes, it has been observed that in spite of anthropogenic modifications to the rate of sediment supply the shoreline at Beach Pond has continued a steady and unimpeded retreat to the west.

The processes and effects that were documented at Seaside Spit and Beach Pond were previously realized at Flag Pond where environmental change resulted from the modern marine transgression and a significant nor'easter in the Spring of 1993 (March 12, 1993 to March 15, 1993). This "Storm of the Century" culminated on March 13, 1993 with sustained winds of 40 mph and gusts of 67 mph (NCDC, 2013). The continued forcing of shoreline retreat placed the

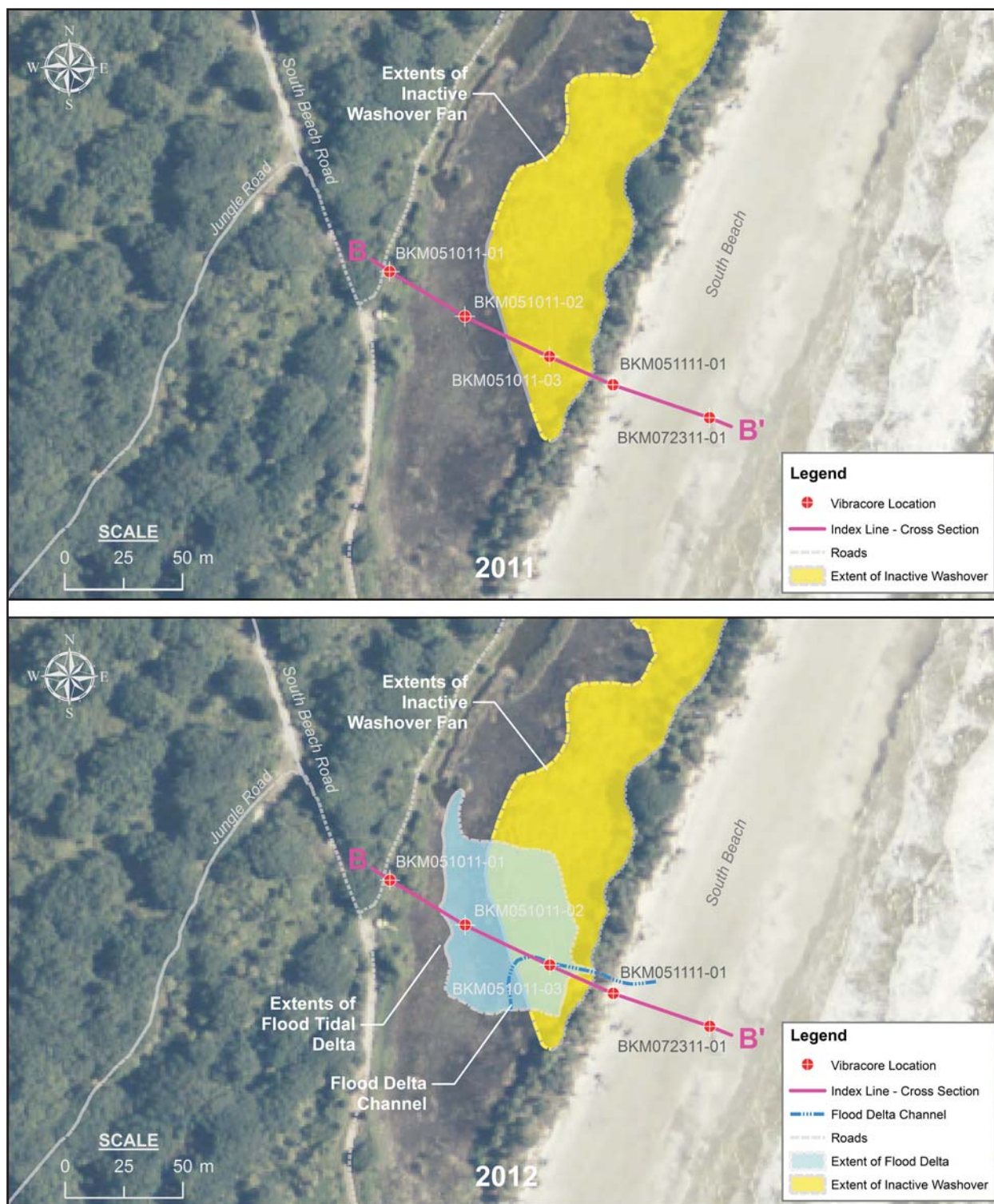


Figure 7-9: Documentation for the environmental change at Beach Pond has been produced to capture the dramatic landform and corresponding ecosystem changes resulting from the modern marine transgression and the significant Spring 2012 nor'easter. This storm forced the breaching of the beach berm at Beach Pond and resulted in the formation of a tidal inlet at the specific location of the vibracore transect. The new inlet has forced the conversion of the active washover fan to a flood delta complex.

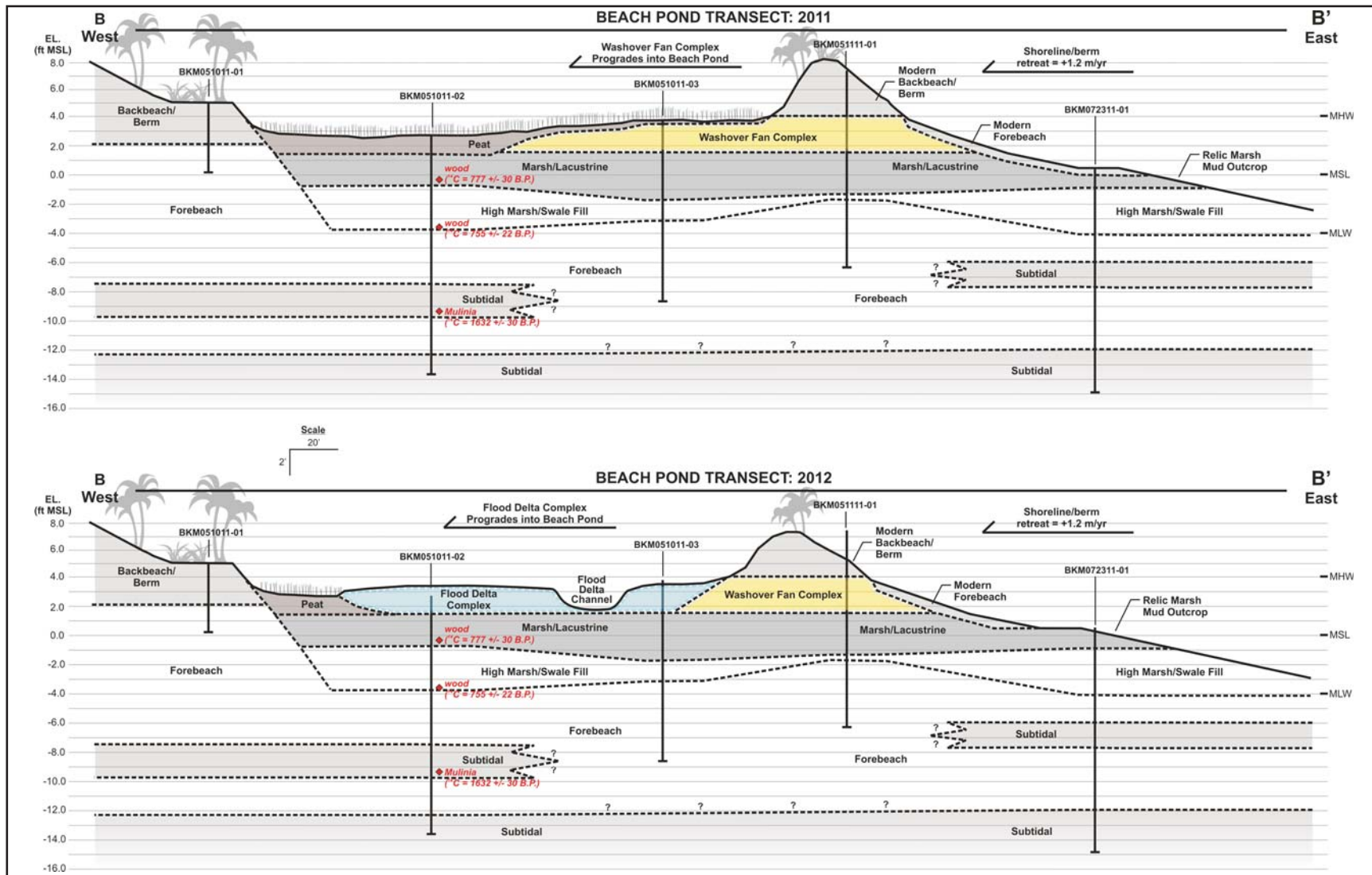


Figure 7-10: The new inlet at Beach Pond has resulted in the conversion of the inactive washover fan to an active flood delta complex. The flood delta has prograded an appreciable distance to the western margin of the pond and converted the freshwater lacustrine environment to a flood delta sand flat with little to no vegetation, greatly altering the hydraulic regime and modifying the depositional environment.

shoreline in close proximity to the pond's eastern berm and the storm forced the breaching of the beach berm at Flag Pond and resulted in the formation of a tidal inlet near the location of the vibracore transect provided in Figure 6-20 and initiated the conversion of a washover fan into a flood delta complex. The distal portion of the flood delta has prograded an appreciable distance to the western margin of the pond and converted the freshwater lacustrine environment to a flood delta sand flat with sparse vegetation consisting of emergent *Spartina*. Similar in nature and landform setting as Beach Pond, the shoreline retreat rates have also been consistent at Flag Pond during local and regional anthropogenic modifications to the rate of sediment supply, resulting in a shoreline that steadily marches to the west under the modern transgression.

To evaluate shoreline dynamics as an agent of environmental change on ecosystems and habitat quality such as sea turtle habitat, the results from the shoreline dynamics study were then evaluated by the landform types that comprise the shoreline and compared to quantitative indicators of loggerhead sea turtle habitat quality. The quantitative metric consists of the 2012 sea turtle rapid habitat assessment scores (G.A. Bishop, personal communication, February 18, 2013) resulting from a systematic habitat quality scoring method (Bishop and Meyer, 2011). This exercise resulted in a strong correlation between landform "stability" and habitat quality and the effects of shoreline dynamics on sea turtle habitat landforms are presented in Figure 7-11. Relatively high scores for sea turtle habitat quality were indicated for the stable and actively accreting Holocene northeastern accretional terrains where a maximum value of 7.0 and a mean value of 3.5 were indicated in the 2012 assessment. The results for the McQueen Dune Field also indicated appreciable habitat quality with a maximum value of 9.0 and a mean value of 3.1. However, these more stable landforms account for only 16% of the total available shoreline for sea turtle nesting habitat. The more erosional landforms (spits/berms, ridge swale topography

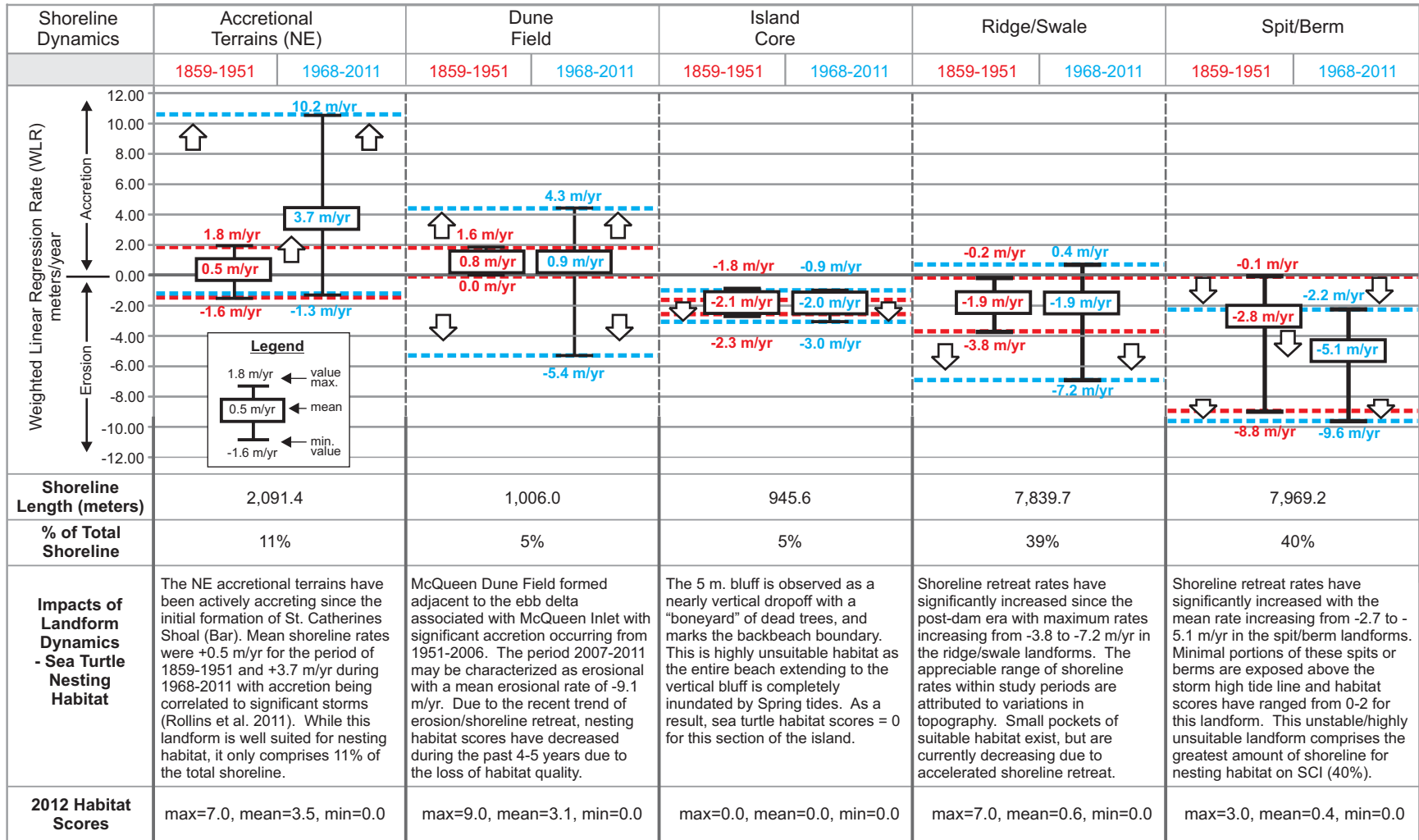


Figure 7-11: The effects of shoreline dynamics as an agent of environmental change on sea turtle habitat are presented. The more stable landforms associated with the NE Accretional Terrains and McQueen Dune Field are shown on the left, and comprise approx. 16% of the total available shoreline for nesting habitat. The more erosional landforms are shown on the right and account for approximately 84% of the shoreline available nesting habitat. In addition, a comparison of Pre-Dam and Post-Dam rates indicate significant accelerations in shoreline retreat associated with the Spit/Berms landforms. These trends in shoreline instability are reflected in the 2012 Habitat Scores as well as an overall decline in the quality of nesting habitat (Bishop and Meyer, 2011).



and island core) account for approximately 84% of the shoreline available for nesting habitat and nesting habitat quality scores are extremely low adjacent to the island core and the spit/berm landforms. In addition, a comparison of Pre-Dam and Post-Dam shoreline retreat rates indicates significant accelerations in shoreline retreat or erosion rates associated with the spit/berm landforms that account for 40% of the available habitat. The trends in shoreline stability and specifically the acceleration in shoreline retreat are reflected in the 2012 Habitat Scores as well as an overall decline in the quality of nesting habitat (Bishop and Meyer, 2011).

A shoreline forecasting exercise was then performed using the most recent and accurate set of data (1999 to 2011 data) to minimize uncertainties and shoreline locations were forecasted at 25, 50 and 100 year intervals under several assumptions and employing multiple scenarios. The purpose of the exercise was to provide shoreline projections for incorporation into the island's long term conservation planning efforts. The results from the shoreline forecasting exercise were provided to the St Catherines Island conservation planning consultant (Enduring Conservation Outcomes, LLC) and reviewed during a briefing in March 2013 and the results are provided in Appendix E. The existing 200 meter transects, the 1999 to 2011 WLR results, and the most recent shoreline (2011) were used as a shoreline forecasting baseline. Distances were then calculated along select transects using the WLR rates at 100, 50 and 25 year time intervals or durations and a projected shoreline point was obtained. A forecasted shoreline was then digitized for each future projection time interval based on the projected shoreline points. The results of the shoreline projection indicate: 1) continued shoreline retreat along St. Catherines Sound with an associated loss of the Holocene northern accretional terrains, 2) continued progradation of the northeast accretional terrains or northeastern lobe of the island towards St. Catherines Shoal/Bar, 3) intense loss of maritime forest along Yellow Banks Bluff, and 4)

significant loss of tidal marsh in Seaside Marsh under one possible scenario for Seaside Spit (Scenario I). Under a second scenario the shorelines of Seaside Spit, Middle Beach and South Beach (berms and spits) would move in tandem or balance due to seasonal reversals in longshore currents and associated longshore drift that could produce a balance among the spit landforms. The results under Scenario II indicate similar modification of depositional subenvironments and ecosystems including the shoreline capture of McQueen Hammock and McQueen Dune Field, and continued shoreline retreat along the northern portion of South Beach. Predicted inlet dynamics include a shift of McQueen Inlet to the north and a potential new inlet that may result from the shoreline capture of an eastern meander of Cracker Tom Creek. Results from the shoreline projections for 25, 50 and 100 year intervals for the central portion of South Beach including Beach Pond and Flag Pond show continued shoreline retreat with significant loss of tidal marsh and accretional dune ridges. The projections indicate the potential shoreline removal of Beach Pond in 25 years, the removal of Flag Pond in 50 years, and the shoreline capture of Long Marsh is indicated in 100 years. Isolated transects were located along the marsh/tidal river boundary and End Point Rates (EPR) were calculated using the imagery and GPS data from 1951 until 2011 to evaluate the shoreline dynamics associated with the margin formed by the marsh and Sapelo Sound. The results show continued shoreline retreat along South Beach with significant loss of island hammocks, and shoreline retreat rates along the southwest marsh/tidal river boundary ranged from 0.1 m/yr. to 1 m/yr.

Shoreline projections have been performed using the most recent or current shoreline data to minimize uncertainties with the 2011 shoreline baseline to evaluate future shoreline locations at 25, 50 and 100-year intervals. The shoreline projections indicate appreciable environmental change under multiple scenarios and the information has been provided for conservation

planning purposes. The shoreline projections predict the future extent or magnitude of the environmental changes that have been observed and documented under the current study and discussed in Section 7.2.

#### **7.4 Stratigraphic Models**

A comparison of the existing stratigraphic models for the generalized facies associated with washover fans in microtidal settings and the models for barrier island/washover response under a rising sea level scenario have been performed against the results from the current study. As expected, the generalized facies model for washover fans under a microtidal setting did not capture the complexities observed in the mesotidal washover fans of St. Catherines Island, specifically the dynamics associated with the development of peat and variability in the location of foreset beds. A preliminary model was constructed and updated as results were generated and is presented as Figure 3-5c. The previous barrier islands and washover fan response models also did not capture the dynamics observed at St. Catherines Island under the modern transgression, specifically the formation of tidal inlets or the fragmentation of coastlines as well as the conversion of washover fans to flood deltas. Transitional stages of barrier islands and washover fan responses from the “keep up” to “give up” stages of Neumann and MacIntyre (1985) have been observed under the current study at St. Catherines Island and were presented as concepts in Figure 3-7. The island developmental model presented as Figure 4-5 was evaluated and updated based on the results of the current study and a revised version follows.

A new stratigraphic model was also constructed that builds on the concepts originally applied by Carroll and Bohacs (1999) to lacustrine environments where the major controls on sedimentation are climate and the rate of sediment supply. This new schematic model was



provided as Figure 7-6 and builds on the “catch-up”, “keep up”, and “give up” stages of barrier island response to sea level rise. The new model incorporates the major controls on barrier island formation and modification processes to conceptualize the effects resulting from changes in the relative rates of the major controls.

## **7.5 Stratigraphy and Development of St. Catherines Island**

### *7.5.1 Southeastern Accretional Terrains*

A developmental model for the sediments of the southeastern Holocene accretional terrains has been developed based on the record of several transgressive and regressive sequences and the incorporation of constraining dates. An initial transgressive surface ( $T_1$ ) is observed in multiple cores from Cracker Tom associated with a basal shell lag. A minimum of three additional transgressive surfaces ( $T_2/ T_3/ T_4$ ) are noted as erosional surfaces or as facies successions where forebeach and backbeach sands are overlying marsh muds. Constraining dates were provided by radiocarbon results from the Cracker Tom study area and indicate  $T_1 > 6020$  B.P. and  $T_4 < 3200$  B.P. ( $T_1 > 6867$  Cal B.P. and  $T_4 < 3181$  Cal B.P.). In addition, an erosive surface with basal shell lag materials was encountered by Linsley (1993) at a depth of 345 cm BLS and was dated via radiocarbon materials at  $4370 \pm 120$  B.P. ( $4696 \pm 324$  Cal B.P.) and is most likely associated with transgression  $T_3$ . An insight into the pattern of sea level is indicated in the sedimentary record from the Cracker Tom cores where the transgressive surfaces occur in a stacked configuration, indicating subsequent transgressions occurred at slightly higher elevations or sea level high stands than the previous transgressions.

Multiple transgressions are also recorded as erosional surfaces and via facies successions in the Beach Pond and Flag Pond cores. Shallowing sequences associated with a fall in sea level

(regression) are observed as forebeach sands overlying subtidal bioturbated and laminated sands. Constraining dates were provided by radiocarbon data and indicate transgression  $T_5 > 1632$  B.P. and regression  $R_4 < 1559$  B.P. ( $T_5 > 1319 \pm 78$  Cal B.P. and  $R_4 < 1243 \pm 76$  Cal B.P.).

A compilation of vibrocore data indicates that the development of the southeastern accretional terrains is recorded in a series of five sequence boundaries consisting of erosional or transgressive surfaces that are most likely the result of a series of sea level fluctuations. Regressive or progradational sequences are observed as facies successions and the vertical shift in facies and appear to coincide with the time intervals between successive transgressive events. The transgressive and regressive sequences were placed into relative order (Figure 7-12) and constrained with radiocarbon data to evaluate the relative and absolute timing of the events and the results were plotted against the absolute age data from the beach ridge terrains to initiate a developmental model for the southeastern accretional terrains. The correlation indicates a strong relationship between the regressive or progradational sequences identified in the subsurface facies and the deposition of beach ridges. A more detailed examination of the regressive or progradational sequences indicates a vertical shift in forebeach/subtidal and forebeach/backbeach sediments indicating a change in sea level as opposed to an actual progradational sequence where facies should maintain a consistent horizontal datum. Additional scrutiny of the sedimentary record is applied with respect to regressive or progradational conditions under the following Late Holocene sea level evaluation.

### *7.5.2 Northern Accretional Terrains*

The model constructed for the southeastern accretional terrains consisting of multiple transgressive/regressive events was applied to the sedimentary record associated with the

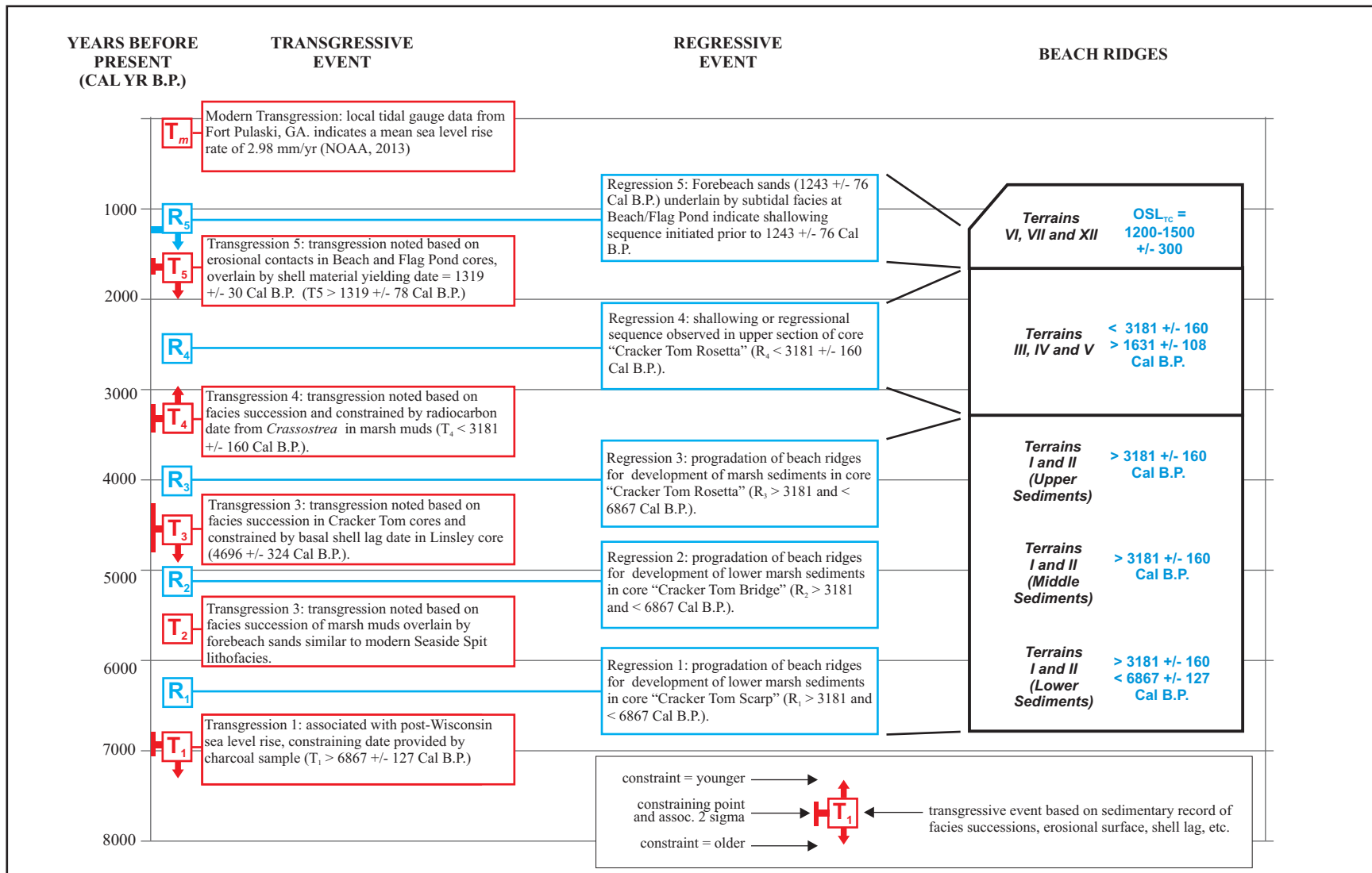


Figure 7-12: Developmental model for the southeastern accretional terrains where transgressive and regressive events were placed in relative sequence and constrained with radiocarbon data. A comparison was then performed with the radiocarbon and OSL data from beach ridges to evaluate the timing of potential regressions and depositional units (beach ridges), the correlation indicates a strong relationship between regressive sequences identified in the subsurface facies and the deposition of beach ridges.

northern accretional terrains. Although the northern accretional terrains are composed of beach ridges that are oriented parallel to St. Catherines Sound and are most likely resulting from inlet processes, increases or decreases in sea level should be replicated as increasing and decreasing forces on the tidal prism associated with the sound or inlet and ultimately reflected in the sedimentary record. Increases in sea level favor erosional conditions as the inlet cross-sectional area expands to accommodate an increase in the tidal prism, and conversely decreases in sea level and the force of the tidal prism will favor deposition of sediment and accretion of beach ridges (Oertel, 1975; Oertel, 1979). This application is made with the understanding that limited vibracoring has been performed in this portion of the island due to logistical challenges associated with surface water occurring in the topographically lower swales and difficulties in the vibracoring technique in penetrating the unsaturated sands on the higher elevations of the dune ridges. Topographic profiles have been generated for the beach ridge systems in the northern terrains to the west of the Northwest Scarp and are located within the northwestern marsh (aka Gator Marsh) and can be compared to the beach ridge systems in the Holocene terrains located east of the King New Ground and Back Creek Scarps in the southeastern accretional terrains. The beach ridges in the northwest marsh are oriented north-northeast with ridge elevations occurring between 1.8 meters to 2.4 meters (6.0 and 8.0 ft) MSL and mimic the elevations observed in Terrains I and II in the southeastern accretional terrains. The beach ridges to the north of Engineers Scarp extend 3.0 meters to 3.6 meters (10.0 to 12.0 ft) MSL and are similar to the topography observed in Terrains III through XII in the southeastern accretional terrains. An OSL date was obtained by Chowns (2011) in the initial beach ridge located north of Engineers Scarp and was dated at 4300 +/- 1400 Cal B.P. indicating that Engineers Scarp is older than 4300 +/- 1400 Cal B.P. Based on cross-cutting relationships, Engineers Scarp cuts across

and is younger than Northwest Scarp. Based on beach ridge topography and the sequencing of events and the model constructed for the development of the southeastern accretional terrains, the beach ridges in the northwest marsh are most likely composed of sediments associated with regressions  $R_1$  or  $R_2$ . Engineers Scarp ( $> 4300 \pm 1400$  Cal B.P.) could correlate to transgressions  $T_2$  and/or  $T_3$  and the beach ridges located north of Engineers Scarp and west of St. Catherines Scarp would correlate with Terrains IV, V, VI, VII and possibly Terrain XII that are considered to be the result of regressions  $R_4$  and  $R_5$ .

A core described by Linsley (1993) from Engineer's Point on the northwestern portion of the island and located within the northern accretional terrains provided organic material that dated at  $4450 \pm 50$  B.P. ( $5015 \pm 137$  Cal B.P.) and was associated with a shell lag or forebeach facies assumed to represent a transgressive surface at 4.94 m to 5.08 m BLS. This transgression apparently correlates with the timing of transgression  $T_3$  as indicated in the southeastern accretional terrains from an erosional surface with shell lag materials that dated at  $4370 \pm 120$  B.P. ( $4696 \pm 324$  Cal B.P.). It should also be noted that the Linsley core (core ID #17) contained lag deposits above (2.90 m to 3.01 m BLS) and below (5.08 m to 5.22 m BLS) the dated lag deposit, which could correlate to transgressions  $T_4$  or  $T_5$  (upper lag deposit) or  $T_1$  or  $T_2$  (lower lag deposit). The shell lag was immediately overlain by "interlaminated to interbedded mud and sand" that is interpreted as the subtidal bioturbated and laminated facies, indicating subtidal water depths of two to four meters below mean sea level near the modern day St. Catherines Sound margin during a time interval that post-dates  $5015 \pm 137$  Cal B.P. The basal subtidal sediments in the northern accretional terrains may correlate with the surficial beach ridges forming after Engineers Scarp and constrained by an OSL date of  $4300 \pm 1400$  Cal B.P. or consistent with the timing for regression  $R_3$ . Multiple stacked erosional surfaces and

the development of a paleosol were also observed by Chowns (personal communication) indicating a minimum of two to three Holocene sediment packages in the northern terrains. In addition, Chowns obtained a radiocarbon date (43,500 B.P. or radiocarbon infinity) from wood material at 4.82 m BLS (compacted depth), indicating that the  $T_1$  transgressive surface is approximately 5 meters below the surface in the northern accretional terrains and at a similar depth to  $T_1$  in the southeastern accretional terrains.

Based on the shoreline dynamics study and a review of historical maps and imagery, the location of St. Catherines Scarp appears to coincide very well with the shoreline demarcated on the 1867 St. Catherines Sound navigational chart that is based on 1859 planimetric data. The 1859 shoreline was located in close proximity to a prominent beach ridge and dunes that extend from Sand Pit Road to St. Catherines Sound, and divide to the north of Sand Pit Road into two sets of dune ridges. The 1926 shoreline appears to demarcate the eastern fork in the linear dune feature indicating that accretion has occurred in the northeastern accretional terrains since the mid-19<sup>th</sup> century or during the modern transgression ( $T_{\text{modern}}$ ) or following transgression  $T_5$  and regression  $R_5$  as indicated in the southeastern accretional terrains developmental model. Based on these conditions and the sequencing of events, it is assumed that St. Catherines Scarp is older than calendar year 1859 and represents a younger transgression than  $T_5$  and regression  $R_5$  which are bracketed with OSL dates in the southeastern accretional terrains (1200-1500 +/- 300 Cal B.P.). Under this premise, it is expected that surficial and shallow sediments associated with the northeastern accretional terrains located to the east of St. Catherines Scarp should post-date calendar year 1859.

### 7.5.3 Northeastern Accretional Terrains

Relatively rapid accretion was noted in the shoreline modeling results from the northeastern accretional terrains that comprise the northern extents of North Beach. Historical imagery and GPS data indicate that 0.7 km of beach dune ridges have prograded since the 1859 data set with weighted linear regression rates ranging up to 9 m/yr. Rapid accretion and progradation are also indicated in the sedimentary record from cores (BKM 012112-01, BKM 012112-02, and BKM 031712-01) collected within this active accretional area. The upper sections of the cores may generally be described as 150 cm to 200 cm of intertidal forebeach sands underlain by 50 cm to 100 cm of subtidal burrowed and laminated facies, indicating a progradational sequence. Radiocarbon samples from the upper sections of the cores date as modern or indicate the percent of modern carbon as greater than 100% (pMC > 100%) and a relatively low density of *Callianassa* burrows indicate the rapid accumulation of sediment within the active accretional terrains. Therefore, the results from the shoreline dynamics modeling and an evaluation of the modern sediments via vibracoring complement each other in documenting the spatial and vertical processes in this rapidly accreting area. The role of storm events in the formation of beach ridges in the northeastern accretional terrains has been proposed as a mechanism for local sedimentation (Rollins et al., 2011). The rapid progradation of three beach ridge sets was documented following Hurricane Hugo in 1989 using aerial imagery and field observations. Rollins et al. attributed the formation of the ridges to a net import of sediment to the shore as a result of the storm interrupting ebb-dominant transport to offshore shoals.

The lower sections of the North Beach cores record the existence of two marsh systems located to the east of St. Catherines Island's current configuration and the presence of multiple transgressive surfaces. Material from a shallow marsh mud (307 cm to 395 cm BLS) was dated

at 2,614 +/- 27 B.P. and a deeper marsh mud occurred from 475 cm to the total depth of the boring (527 cm BLS) and was dated at greater than 45,200 +/- 647 B.P.. The occurrence of the upper marsh deposit indicates the existence of a Holocene marsh located to the northeast of the current shoreline configuration and corroborates the existence of a “lost” barrier island (Guale Island) being previously located to the east of the current island (Bishop et al., 2011). The lower or Late Pleistocene marsh also infers the existence of a protective barrier island being located to the east of the current island configuration at approximately 45,000 B.P. The older marsh mud infers the existence of a Late Pleistocene hypothesized island and will be referred in this narrative as “Coosaponakeesa Island”, with the island taking a place name from the Creek Indian name for Mary Musgrove, who served as a mediator between her Native American people and the settlers of colonial Georgia, and was granted lands on St. Catherines Island. Based on the vibracore results from North Beach, it appears that Holocene marshes and a barrier island (Guale Island) may have reoccupied the former locations of Late Pleistocene marshes and a barrier island (Coosaponakeesa Island). Coosaponakeesa Island would have likely formed due to accretional processes associated with the marine regression or fall in sea level associated with the initiation of the LGM. During the Holocene marine transgression or rise in sea level, Guale Island would have likely reoccupied the topographically higher remnants of Coosaponakeesa Island, with the Holocene marshes reoccupying the topographically lower remnants of the Late Pleistocene Marshes.

A minimum of four transgressive surfaces were identified in the North Beach vibracore data based on erosional surfaces and shell lag sediments. The lower transgressive surface that was observed in core BKM 012112-02 was constrained by radiocarbon data that indicate that the material developed on top of an older Late Pleistocene marsh and based on the chronology and a



similar elevation it is likely associated with the initial transgressive event  $T_1$  as identified in the southeastern and northern accretional terrains. A minimum of two additional shell lag and erosional surfaces were noted as occurring above the lower transgressive surface in the sedimentary record for North Beach and are constrained as  $> 2614 \pm 27$  B.P. ( $2491 \pm 155$  Cal B.P.). The modern transgressive surface ( $T_{\text{modern}}$ ) is represented in the cores by a shallow erosional contact and facies successions where marsh/lacustrine sediments are overlain by forebeach sands in the southern portion of the North Beach study area. Therefore, the shallow sediments of North Beach record the modern transgression in the isolated area of the island where accretion is active whereas the deeper sections of the cores reflect Late Holocene events and chronologies with many similarities to the southeastern and northern accretional terrains.

#### *7.5.5 St. Catherines Island – Holocene Developmental Model*

Information obtained under the current study and corroborating data from other researchers confirms many of the stages or steps in the original island developmental model proposed by Bishop and Meyer (2011). However, several new steps or alterations to the original model are warranted to account for the recent advancements in the understanding of the island stratigraphy.

The probability that the processes of vertical accretion have resulted in the placement of a Holocene sediment cover on the eastern and northern portions of the island has been captured in the revised developmental model. A Holocene veneer of sediments has been recognized and studied in the Yellow Banks Bluff outcrop by previous researchers (Bishop et al., 2011; Martin and Rindsberg, 2011; Vento et al., 2011; Stahlman and Vento, 2012) and has also been evaluated within the Central Depression and other localities on St. Catherines Island by Vento et al. (2011)

and Stahlman and Vento (2012). The basal sediments of Yellow Banks Bluff are marine intertidal forebeach sands and an OSL date of 119,630 B.P. (Figure 7-13a) was obtained at the base of the bluff (Stahlman and Vento, 2012). The date of the marine sediments and associated disconformity are attributed to the Sangamon interglacial sea level high stand. Stahlman and Vento identified eight intervals of “island stability” based on soil A-horizon development on late Pleistocene to Holocene sediments: 1) 42,000 to 39,000 B.P. based on organics recovered by Booth et al. (1999) that represent freshwater accumulation of *Woodwardia* peat on Sangamon interglacial marine sediments; 2) 22,800 to 19,200 B.P. based on organic or A-horizon development from Yellow Banks Bluff (Vento, 2011) and coincident with the Late Wisconsin lowstand of sea level; 3) 15,000 B.P. based on well-developed paleosols that were identified in Crane Yard by Stahlman and Vento (2012); 4) 13,600 B.P. based on buried slough or swale in Yellow Banks Bluff outcrop (Stahlman and Vento, 2012); 5) 10,800 B.P. based on a buried paleosol situated on a thick package of suspected eolian or washover fan materials; 6) 7,200 to 6,200 B.P. based on multiple paleosols that were observed in test pits in the Central Depression and Yellow Banks Bluff; 7) 4,800 to 3,400 B.P. based on radiocarbon data from buried paleosol organic materials in the Central depression; and 8) 1,200 to 1,000 B.P. based on shallow A-horizon development. Stahlman and Vento (2012) correlate many of the periods of island stability with established climate events based on the age relationship where the 1<sup>st</sup> and 2<sup>nd</sup> events are associated with the Wisconsin lowstand and initial topsoil development on the Sangamon age marine sands. The 3<sup>rd</sup> and 4<sup>th</sup> events of stability were associated with the Bolling-Allerod interval (14,700 to 12,700 B.P.) and sediment accumulation is attributed to increased precipitation and runoff processes during the warm and moist conditions. The 5<sup>th</sup> event is correlated to the interval of the Younger Dryas (Vento, 2011) and is attributed to an increase in

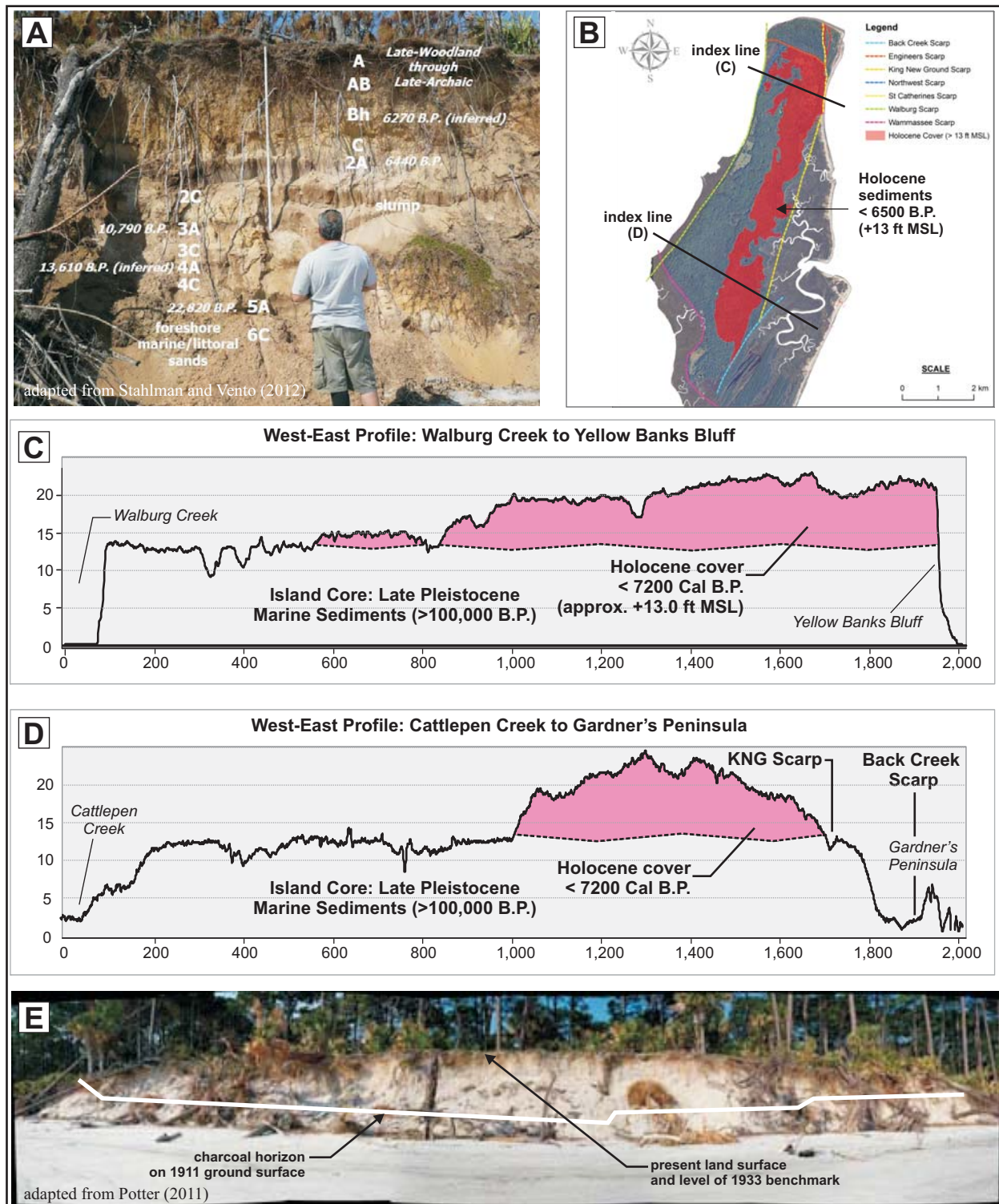


Figure 7-13: a) Yellow Banks Bluff outcrop with late Pleistocene marine sands overlain by Holocene cover sediments, b) under the current study a strong correlation has been noted between the Holocene cover materials and island topography, and specific erosional scarps that represent paleoshorelines (c and d). e) a modern analogue exists for vertical accretion of sediments in the northern portion of the island where Potter (2011) and collaborators documented patterns of 20th century vertical accretion attributed to washover and eolian processes.

eolian deflation due to dryer and colder climate conditions, and the 8<sup>th</sup> event is correlated with the Neo-Atlantic climate phase Stahlman and Vento (2012).

Significant accumulation of sediments in the upper portions of the Yellow Banks Bluff section occurred from 7,200 to 6,200 B.P. and from 4,800 to 3,400 B.P. based on the work of Stahlman and Vento (2011) and the accumulation of these sediments was not directly attributed to climate forcing of sediment transport and deposition. Under the current study a strong correlation has been noted between these Holocene cover materials, island topography and specific erosional scarps that represent marine paleoshorelines associated with the island shoreface or marine conditions. The Holocene cover materials are present and at their greatest thickness adjacent to the scarps that represent paleoshorelines such as the King New Ground Scarp, Northwest Scarp, and Engineers Scarp but the same cover materials are conspicuously absent adjacent to other scarps that represent erosional margins associated with tidal channels or fluvial systems such as Wamassee and Walburg Scarps (Figure 7-13b and 7-13c). There is a limited association or relationship between the occurrence of the Holocene cover sediments and Back Creek Scarp (Figure 7-13d), where the Holocene cover materials are only associated with Back Creek Scarp near the Cracker Tom Causeway in the specific area where the scarp cuts across the King New Ground Scarp and into the island core. The sequencing of events obtained from the southeastern accretional terrain cores and radiocarbon data provide insights into the limited relationship or observation. The King New Ground Scarp is the oldest scarp in the sequencing of events for the southeastern accretional terrains and most likely formed during the initial transgression ( $T_1$ ) and is bounded in the subsurface by sediments that date to approximately 6020 +/- 50 B.P. (6867 +/- 127 Cal B.P.). The Back Creek Scarp cuts across King New Ground Scarp, indicating a relative age younger than transgression  $T_1$ , and is bound

by washover fans and backbeach sediments in Terrains I and II to the immediate east that are constrained as  $< 3200 \pm 50$  B.P. ( $3181 \pm 160$  Cal B.P.) indicating an association with a transgression that post-dates  $T_3$  and is most congruent with transgression  $T_4$ . Although the cover materials are somewhat variable in thickness, a trend is also observed in the island topography with respect to the occurrence of the cover materials in the eastern and northern portions of the island. Absolute dates from Vento et al. (2011) and Stahlman and Vento (2012) were superimposed onto LIDAR topographical profiles for the Holocene materials and the sediments associated with the stability periods of 7,200 to 6,200 B.P. and 4,800 to 3,400 B.P. appear to correlate well with the topographic higher eastern and northern portions of the island with an elevation datum of approximately three to four meters (10.0 to 13.0 feet) MSL (Figure 7-13c and 7-13b). In addition, the accumulation of these Holocene cover materials and multiple soil weathering profiles are not readily apparent in outcrops or vibracores collected in the western portions of the island. These conditions indicate that the  $< 7200$  B.P. cover materials are most likely associated with paleoshorelines or active marine shorelines with the vertical accretion of the sediment occurring as a combination of washover and eolian processes. A modern analogue for this condition exists in the northern portion of the island as described in Section 4.2.2, where Potter (2011) and collaborators have documented patterns of 20<sup>th</sup> century vertical accretion occurring at appreciable rates (approximately 3.5 cm/yr) attributed to washover and eolian processes associated with the active shoreline. By applying the stratigraphic framework that was developed under the current efforts for the southeastern accretional terrains, the sequencing of the scarps, and absolute age data, it appears that the Holocene cover materials that date to 7200 B.P. are associated with vertical accretion processes and the initial transgressive events that are observed in the islands Holocene accretional terrains.

The numerous transgressions and regressions that have been identified and evaluated in the Holocene accretional terrains have been accounted for in the revised island developmental model to capture the concept of multiple shoreline advancements and retreats (Figure 7-14). The revised island developmental model also incorporates the occurrence of the two marsh muds (Late Pleistocene and Late Holocene) in North Beach cores that confirm the existence of two additional or outer doublet barrier islands located east of the current configuration of St. Catherines Island. The relative timing of the scarps that represent paleoshorelines has also been inserted into the chronology where appropriate.

The sedimentary record also indicates that significant dynamics were associated with the Late Holocene shoreline as suggested by the spatial nature of foreshore facies and constraining data. Forebeach sands that range in age from 6020 +/- 50 B.P. (6867 +/- 127 Cal B.P.) to 3200 +/- 50 B.P. (3181 +/- 160 Cal B.P.) occur in the Cracker Tom cores adjacent to the island core and are associated with erosional scarps that represent marine paleoshorelines such as the King New Ground and Back Creek Scarps. The existence of the forebeach facies and distribution of constraining ages indicate that shoreline conditions have occurred adjacent to the island core at multiple times during the Middle and Late Holocene. Upper forebeach laminated facies are also observed in the Beach Pond and Flag Pond cores located 1500 meters to the east and indicate that upper foreshore conditions may have occurred intermittently from 5831 +/- 35 B.P. (6378 +/- 98 Cal B.P.) until 1210 +/- 40 B.P. (1159 +/- Cal 104 B.P.) inferring that the associated shoreline was located in the immediate area to the west of the modern shoreline. These circumstances indicate that a dynamic shoreline existed at St. Catherines Island during the Late Holocene with a range that extended from the eastern margin of the island core in the locations of the King New Ground and Back Creek scarps to areas located one kilometer to the east or

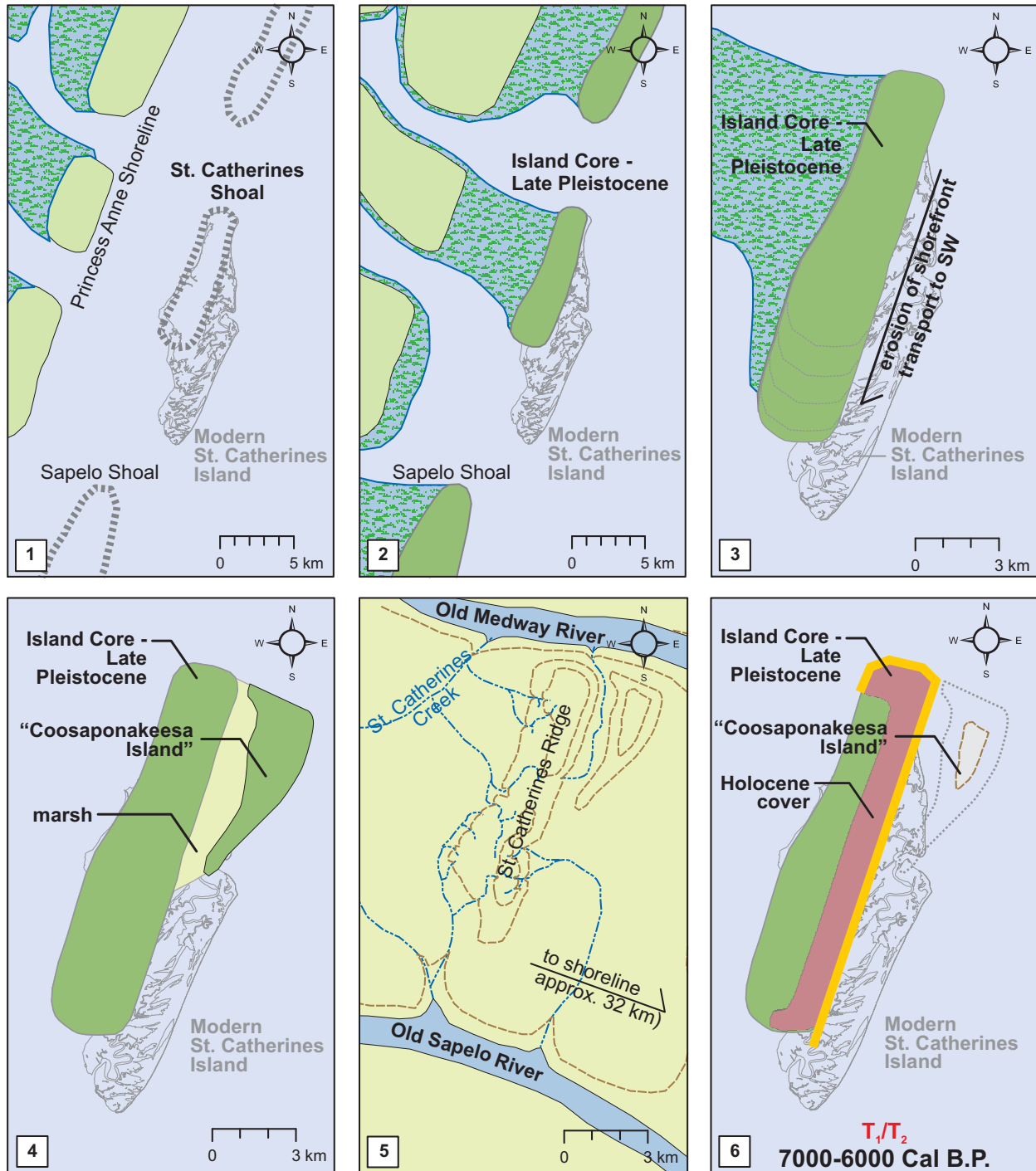


Figure 7-14: Development of St. Catherines Island depicted on background of geomorphogy (Bishop et al. 2007) illustrates one possible scenario of Island evolution. 1) St. Catherines shoal at time of deposition of Princess Anne paleoshoreline; 2) Formation of initial Silver Bluff island; 3) Erosion of older Pleistocene results in long, narrow island and adds sediment to the south; 4) Formation of outer barrier or Coosaponakeesa Island; 5) Wisconsin low-stand, shoreline 32 km east near Grays Reef, island is part of low-relief mainland; 6) Post-Wisconsin transgression brings shoreline to King New Ground Scarp and NW Scarp with Coosaponakeesa Island serving as shoal or emergent barrier and vertical accretion of Holocene cover sediments occurring (cont.),

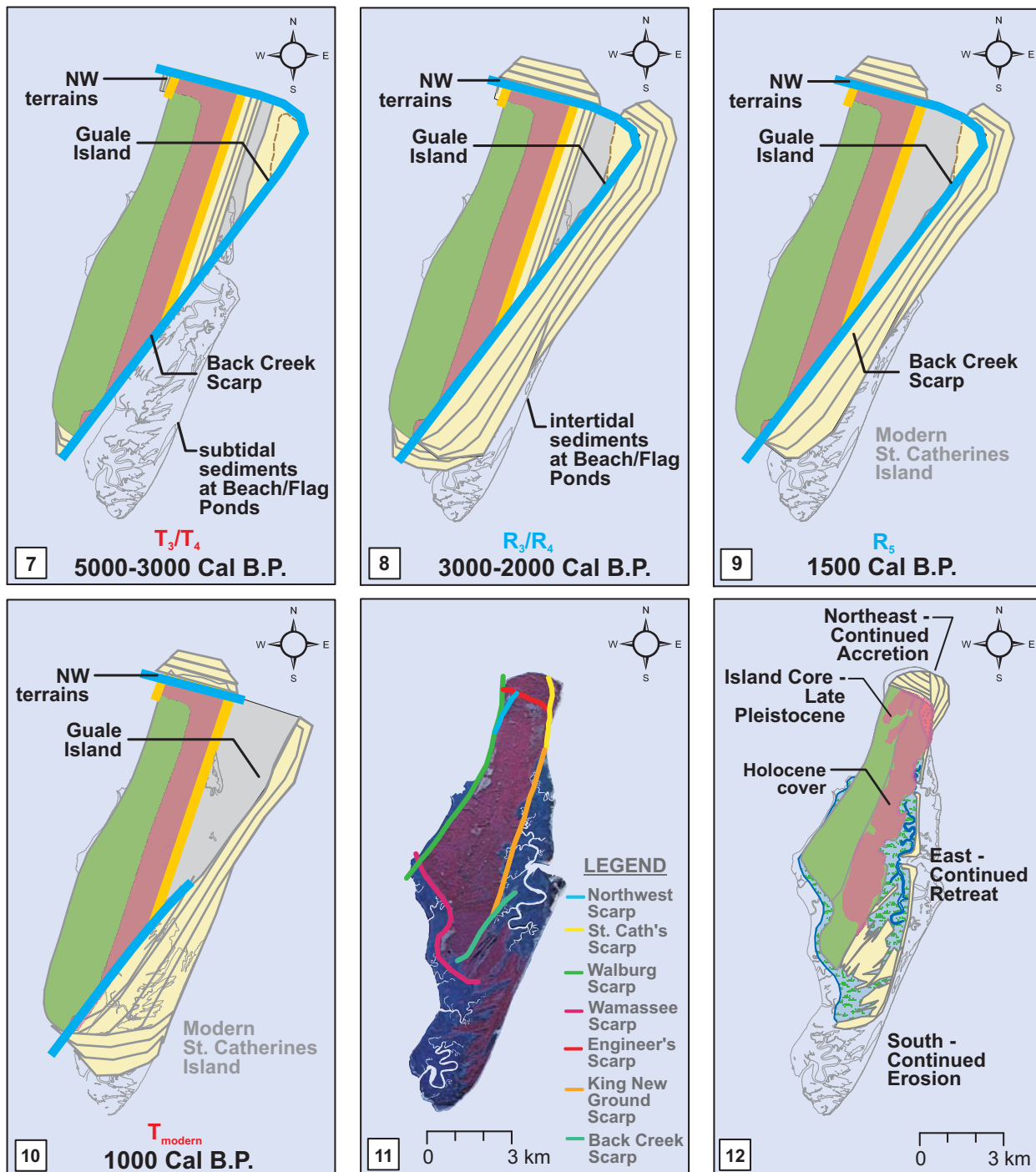


Figure 7-14 (cont.): 7) Transgression  $T_3$  or  $T_4$  results in formation of Back Creek Scarp; 8) Subsequent regression results in regressive package of sediment representing a parasequence with intertidal sediments in the areas of Beach and Flag Pond; 9) Subsequent transgression and regressions result in intertidal to subtidal cycling of sediments at Beach and Flag Pond; 10) Configuration of the island at initiation of modern transgression, subsequent collapse of Guale Island results in source of sediment for accretion of southern terrains adjacent to Sapelo Sound; 11) Present day island with major scarp overlain, and 12) Future configuration of the island using results from the shoreline dynamics study (Appendix A) and shoreline forecasting task (Appendix E).



within several hundreds of meters west of the modern shoreline. Considering the range of the shoreline (1 km) and return intervals on the scale of 1000s of years, the predicted rate of shoreline advance or retreat (< 1 meter/year) is well within the range of shoreline accretion and erosion rates observed under the current shoreline dynamics study.

## **7.6 Evaluation of Late Holocene Sea Level**

Sea level envelopes have been developed for the Late Holocene sediments of St. Catherines Island based on the radiocarbon and calibrated data resulting from the evaluation of facies, radiocarbon samples, the relationship between depositional subenvironments in the sedimentary record, and the association of the modern depositional subenvironments with respect to mean sea level. In addition, the stratigraphic model was refined and additionally tested in conjunction with the evaluation of Late Holocene sea level.

### *7.6.1 Late Holocene Sea Level - Radiocarbon Data (B.P.)*

The sea level envelope based on radiocarbon years for the late Holocene sediments of St. Catherines Island was evaluated against existing sea level curves for the southeastern US that are provided in radiocarbon years (Depratrer and Howard, 1981; Colquhoun and Brooks, 1986). In general, the sea level envelope for St. Catherines Island correlates very well in general trends with the existing sea level curves (Figure 7-15), reflecting an overall increase in sea level for the southeastern US and Gulf of Mexico during the late Holocene with all three sea level data sets indicating sea level rising to a level three meters to four meters below modern sea level by 6000 B.P. However, notable differences exist between the three data sets in terms of the magnitude and timing of one and two meter oscillations in sea level after 6000 B.P. The Colquhoun and

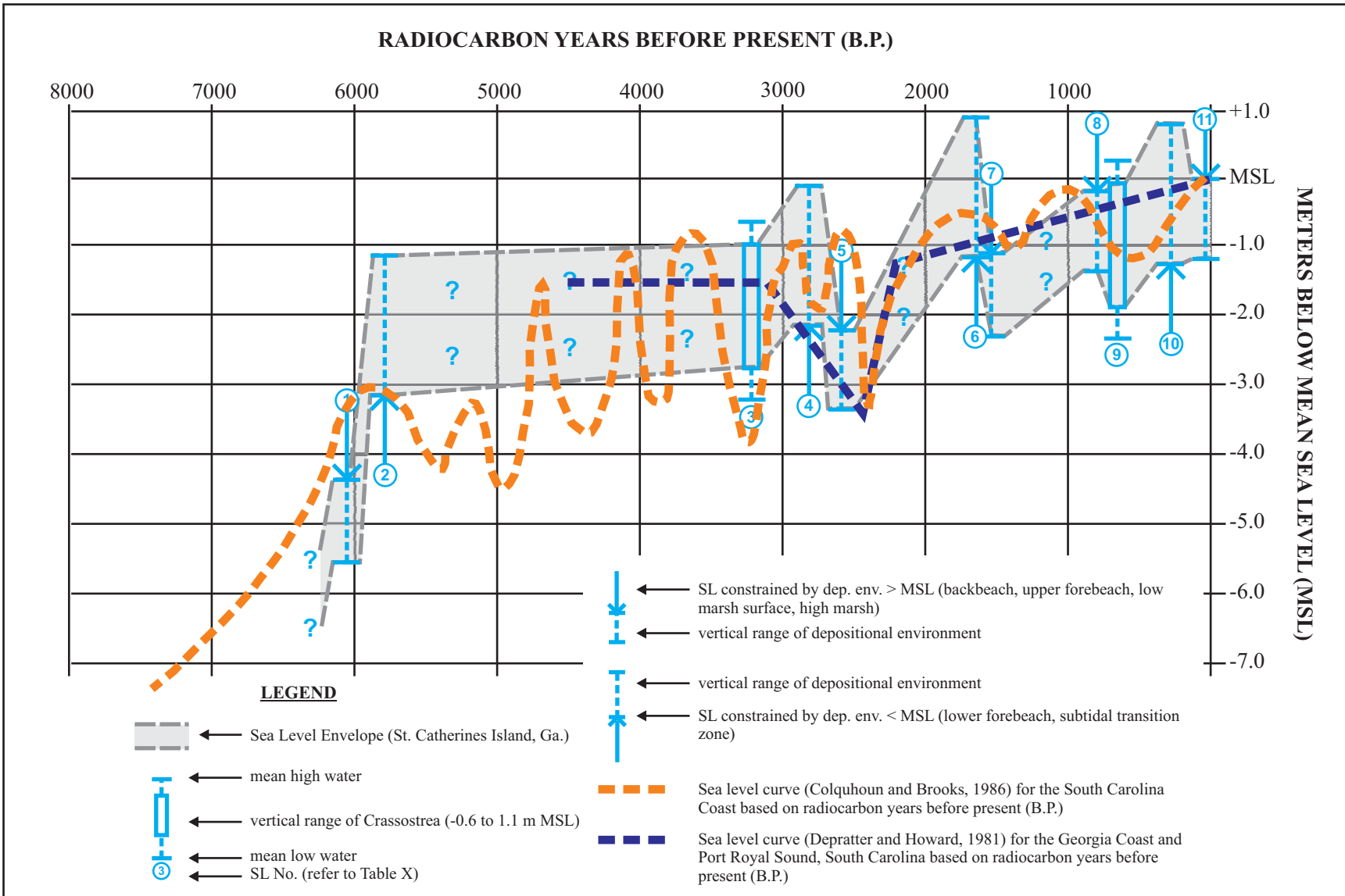


Figure 7-15: Plotted sea level envelope in radiocarbon years before present (B.P.) for St. Catherines Island, Georgia compared to previous radiocarbon sea level curves of Depratrer and Howard (1981) and Colquhoun and Brooks (1986). The sea level envelope compares well in general trends as compared to the previous sea level curves based on radiocarbon data.

Brooks (1986) sea level curve depicts numerous one meter to two meter fluctuations in sea level occurring on roughly 500 year cycles from 6000 B.P. to 2000 B.P. and transgressions/regressions of sea level occurring on 1000-year cycles from 2000 B.P. until present. Many of these fluctuations in sea level are captured in the sea level envelope for St. Catherines Island where data currently exists. The Depratrer and Howard (1981) sea level curve shows sea level rising to 1.5 m to 2.0 m below modern sea level by 4500 B.P. and captures a sea level highstand as occurring until 3000 B.P. with a regression ensuing from 3000 B.P. until 2400 B.P. that is in turn followed by a transgression that brought sea level to modern sea level. The regression indicated in the Depratrer and Howard (1981) sea level curve is reflected in the sea level envelope for St. Catherines Island specifically in sea level data points SL no. 4 and SL No. 5 that indicate a negative slope or fall in sea level from 2829 +/- 29 B.P. until 2614 +/- 27 B.P. Two regressions are noted in the Colquhoun and Brooks (1986) sea level curve as occurring between circa 3000 B.P. and 2400 B.P.; however a moderate data gap exists in the sea level envelope for St. Catherines Island during the second regression.

#### *7.6.2 Late Holocene Sea Level - Calibrated Radiocarbon Data (Cal B.P.)*

The sea level envelope based on calibrated radiocarbon data for the late Holocene sediments of St. Catherines Island was evaluated against existing sea level curves for the southeastern United States that are provided in calibrated years (Gayes et al, 1992; Scott and Collins, 1995; and Balsillie and Donoghue, 2004). As observed in the radiocarbon data sea level evaluation, the calibrated sea level envelope for St. Catherines Island correlates very well in general trends with the existing sea level curves (Figure 7-16), indicating an overall increase in sea level in the southeastern US and Gulf of Mexico during the late Holocene. All three of the

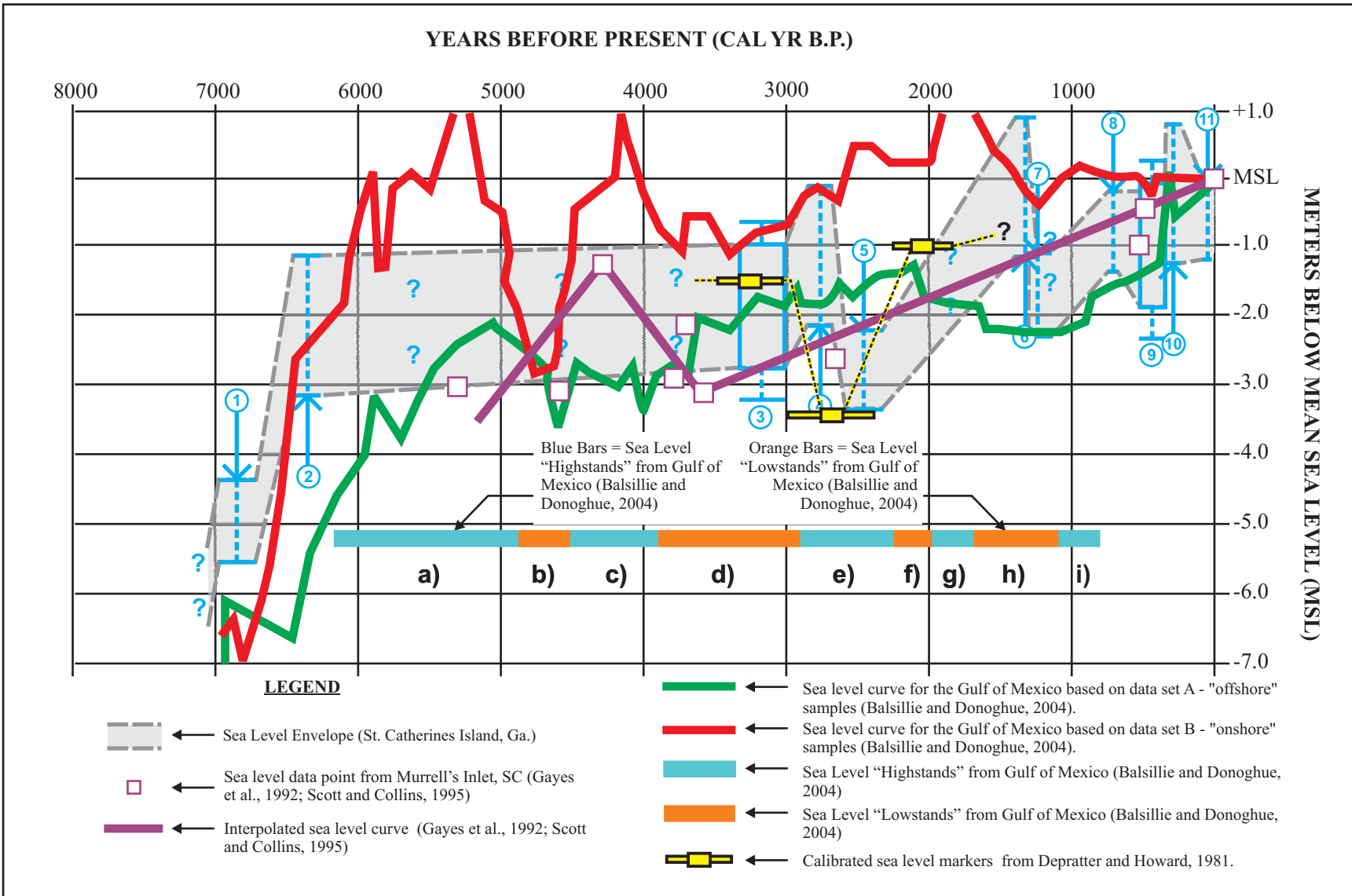


Figure 7-16: Plotted sea level envelope in calibrated years before present (Cal B.P.) for St. Catherines Island, Georgia compared to sea level curves based on calibrated data from Gayes et al. (1992), Scott and Collins (1995), and Balsillie and Donoghue (2004) with Gulf of Mexico highstands/lowstands (Balsillie and Donoghue, 2004) and calibrated sea level markers from Depratrer and Howard (1981).

sea level data sets indicate sea level rising to two to four meters below modern sea level by 6000 Cal B.P. to 6500 Cal B.P. The Gayes et al. (1992) and Scott and Collins (1995) sea level curves from South Carolina indicate sea level rising to approximately one meter below modern sea level by 4200 Cal B.P. followed by a regression of greater than 1.5 meters at 3600 Cal B.P. This regression falls into the data gap in the St. Catherines sea level envelope, however the regression indicated in the South Carolina data is bracketed by two transgressive surfaces ( $T_3$  and  $T_4$ ) in the St. Catherines data providing an indirect association. The sea level envelope from St. Catherines Island indicates a regression or fall in sea level between 2754 Cal B.P. and 2474 Cal B.P and a subsequent regression is indicated from 1319 Cal B.P. to 1243 Cal B.P. It should be noted that the sea level curves from South Carolina have a data gap present from circa 2800 Cal B.P. until 500 Cal B.P. and consequently do not reflect the two regressions indicated in the sea level envelope for St. Catherines Island during this time interval.

The Gulf of Mexico sea level database is based on two primary data sources: 1) on-shore studies using primarily dune ridges and facies occurring above sea level or a dominance of upper constraining points for sea level, and 2) off-shore studies predominately using subtidal sediments and lower constraining points. As a result, the two data sets may be interpreted as constraining curves. The calibrated sea level envelope for St. Catherines Island correlates fairly well with the Gulf of Mexico constraining curves with the exception of the regression observed in the St. Catherines between 2754 Cal B.P. to 2474 Cal B.P. that is not reflected in the Gulf of Mexico data. The subsequent regression in the sea level envelope for St. Catherines Island is reflected in the Gulf of Mexico data. The conformance between the two curves indicates similar forcing of relative sea level due to global or regional controls, whereas the differences in patterns and magnitude of sea level fluctuations indicate local variances in sea level.

In addition, an evaluation was performed using the radiocarbon data from the Depratter and Howard (1981) sea level curve to evaluate the potential effect resulting from the calibration of the data under several scenarios specifically to determine if the Depratter and Howard regression would compare or coincide with the timing of the regression indicated in the South Carolina sea level data. The Depratter and Howard data set references multiple analytical labs that were used over a period of time and it is not apparent that the  $^{14}\text{C}$  data were initially corrected for fractionation of carbon isotopes ( $\delta^{13}\text{C}$ ) by normalizing to  $= -25\text{‰}$  PeeDee Belemnite (PDB) or whether the original analyses used measurement of  $^{14}\text{C}/^{12}\text{C}$  or  $^{14}\text{C}/^{13}\text{C}$ . Depratter and Howard used *Crassostrea* specimens associated with shell midden sites to define a highstand of 1.5 meters below modern sea level that occurred from 3100 to 3000 B.P., followed a regression of three to four meters below modern sea level, and was in turn followed by a transgression that brought sea level to one meter below modern sea level by 2400 B.P. The low stand dates are based on buried tree stumps mostly consisting of cypress and other freshwater species. An initial evaluation of the effects of calibrating data from this time interval and marine matrix was performed using a marine sample from the current study data set at a comparable scale ( $^{14}\text{C} = 2829 \pm 29$  B.P.). The results indicated the potential for a 10% variance in the calibrated age based on whether normalizing with respect to  $\delta^{13}\text{C}$  was performed using results from the various measurement methods. Based on the potential for a 10% variance, an additional evaluation used seven samples of *Crassostrea* from the Depratter and Howard highstand data set (3448-2948 B.P.), and five samples from the lowstand data set consisting of submerged stumps (2522-2949 B.P.). Results indicate a mean calibrated age for the highstand of  $3239 \pm 261$  Cal B.P. and a mean calibrated age for the lowstand of  $2718 \pm 361$  Cal B.P. Depratter and Howard also recognize that the regression has ended by 2400 B.P. based on

*Crassostrea* associated with midden sites on Skidaway Island and a reference sea level at one meter below modern sea level (Depratrer, 1975). A calibration was performed using the 2400 +/- 75 B.P. date obtained from the *Crassostrea* associated with the P.H. Lewis property on Skidaway Island and resulted in a calibrated date of 2061 +/- 201 Cal B.P. The calibration of the Depratrer and Howard sea level data results in three sea level markers associated with the observed highstand to lowstand to highstand pattern in sea level: 1) 3239 +/- 261 Cal B.P. = 1.5 meters below modern sea level; 2) 2718 +/- 361 Cal B.P. = 3.5 meters below modern sea level; and 3) 2061 +/- 201 Cal B.P. = 1.0 meter below modern sea level. The three highstand to lowstand to highstand markers have been plotted to evaluate the timing of the regression and correlate extremely well with the regression noted in the sea level envelope for St. Catherines Island between 2754 +/- 80 Cal B.P. to 2474 +/- 138 Cal B.P.

### 7.6.3 Late Holocene Sea Level - Interpolated Sea Level Curve (Working Model)

A working model for an interpolated sea level curve has been produced using the sea level constraining data based on the calibrated radiocarbon data, incorporating the transgressive/regressive sequences noted in the Holocene accretional terrain cores and utilizing regional and global sea level data to interpolate the timing of events that are not specifically defined in the St. Catherines Island sea level data. This approach specifically addresses the timing of events that fall within the data gaps identified in the sea level envelope for St. Catherines Island including the significant data gap from 6378 Cal B.P. to 3181 Cal B.P., the moderate data gap from 2474 Cal B.P. to 1319 Cal B.P., and the minimal data gap from 1243 Cal B.P. to 703 Cal B.P.

Additional testing and framing of the timing of the regressions of sea level was provided by the radiocarbon data and OSL data that define or constrain the formation of beach ridge systems due to the strong relationship that was observed in the developmental model for the southeastern accretional terrains between the timing of the regressions and beach ridge formation. The relationship between the timing of the regressions and beach ridge formation and the implications from the current shoreline dynamics study regarding the role of sediment supply both complement each other in forming an understanding of the relative roles of the two major controls on a barrier island in this specific physical setting. The evaluation of anthropogenic modifications to sediment transport performed under the shoreline dynamics study indicates significant changes in sediment flux rates. Sediment transport increased by 300% as compared to predevelopment rates during the pre-dam era and was 20% less than predevelopment rates during the post-dam era. Despite these significant modifications to the rate of sediment supply, shoreline retreat was continuous and appears to be unabated during the study period. The two relationships strongly indicate that sediment supply most likely plays a secondary role to the major control of the rate of sea level rise in the formation and modification processes at St. Catherines Island.

Based on the developmental model for the southeastern accretional terrains that was produced by the sequencing of the probable transgressive and regressive events and by the use of the associated constraining radiocarbon data to provide the timing of the events and the Late Holocene sea level evaluation, it is apparent that transgressions  $T_1$ ,  $T_3$ ,  $T_4$  and  $T_5$  were directly indicated and reasonably well constrained from the St. Catherines data. However, the timing of  $T_2$  may be inferred from the Gulf of Mexico sea level data set which may be considered as a high resolution proxy for global sea level since the data set purposely excludes tectonically active



areas such as the Mississippi Delta and should reflect both far-field and near-field variations in sea level due to the propinquity of the data set. Balsillie and Donaghue (2004) delineate a series of highstands and lowstands based on the Gulf of Mexico data sets and these relative sea level designations have been used to verify the transgressions and regressions that have already been constrained by radiocarbon data and also to frame the timing for events that were identified in the sequences of events, but which lacked absolute age information. This framework was then tested and refined by placing the radiocarbon data and OSL data that define or constrain the formation of beach ridge systems into the model to build an interpolated sea level curve for the Late Holocene of St. Catherines Island. Limitations exist in determining the magnitude of the fluctuations in sea level and should be resolved by additional high resolution data collection and subsequent analysis; however, a foundation for an understanding into the nature of the timing of the events may be evaluated. The sea level highstands and lowstands from the Gulf of Mexico data were used to verify the existing framework and the timing of events and used as guides to place the groups of transgressions and regressions into specific time intervals. An obstacle was initially encountered in this approach for regression  $R_1$  which was not correlated immediately with a highstand to lowstand transition representing a regression of sea level in the Gulf of Mexico data presentation. However, a more thorough review of the Balsillie and Donaghue (2004) data set does reveal a small regression (onshore dataset = 1.1 m; offshore dataset = 0.8 m) as occurring at approximately 5900 Cal B.P. to 5700 Cal B.P. The event is not identified as a separate highstand to lowstand transition, most likely due to the scale tolerances used by Balsillie and Donaghue in defining the highstands and lowstands designations. Based on the Gulf of Mexico sea level data regression  $R_2$  was correlated with a significant highstand to lowstand transition observed in the Gulf of Mexico data as occurring from 5300 Cal B.P. and 4700 Cal

B.P. where the onshore dataset indicates four meters of sea level fall or regression and the offshore dataset indicates approximately 1.5 meters of sea level fall or regression. Regression  $R_3$  from the St. Catherines data correlates well with a highstand to lowstand transition in the Balsillie and Donaghue (2004) data set that occurred between 4200 Cal B.P. and 3700 Cal B.P., and it coincides exceptionally well with the regression noted in the Gayes et al. (1992) and Scott and Collins (1995) sea level curves from South Carolina that occurred between 4300 Cal B.P. and 3600 Cal B.P. The small variances in the timing of the regression that has been correlated to  $R_3$  on St. Catherines Island between the Gulf of Mexico and South Carolina sea level curve data is easily explained due to differences in the density or resolution of the two data sets and the errors associated with the generation of vector data from point data. Regression  $R_4$  was indicated in the sea level envelope for St. Catherines Island by sea level data points SL No. 4 and SL No. 5 where the upper and lower constraining points overlap and correlate with a highstand to lowstand transition in the Gulf of Mexico data as well as the calibrated sea level markers that were extrapolated from the Depratrer and Howard (1981) data set. Regression  $R_5$  was indicated in the St. Catherines sea level envelope at 1319 Cal B.P. to 1243 Cal B.P. and appears to correlate with a highstand to lowstand transition in the Gulf of Mexico data from 1700 Cal B.P. to 1100 Cal B.P.

The timing of the sea level regressions were evaluated against the radiocarbon and OSL dates obtained on the beach ridge systems located within the southeastern accretional terrains to provide an additional level of scrutiny to the interpolated sea level curve for St. Catherines Island. Terrains I, II and III are underlain by multiple erosional and shell lag deposits representing transgressive surfaces and a sequential development. Based on the constraining dates from the Cracker Tom cores (Booth et al., 1999) it appears that the deposition of Terrains I,

II and III were initiated following 6867 +/- 127 Cal B.P. and concluded after 3181 +/- 160 Cal B.P., coincidental with regressions R<sub>1</sub>, R<sub>2</sub> and R<sub>3</sub> as indicated in the Gulf of Mexico highstand and lowstand designations. Terrains III, IV and V are constrained by radiometric dates from the Cracker Tom Bridge core (Booth et al, 1999) and Terrain V (Chowns, 2011) with a resulting range of 3181 +/- 160 Cal B.P. to 1631 +/- 108 Cal B.P. This range of dates coincides with the timing of regression R<sub>4</sub> as indicated in the St. Catherines sea level data (2754 +/- 80 Cal B.P. to 2474 +/- 138 Cal B.P.). Terrains VI, VII and XII are constrained by three OSL dates (Chowns, 2011) ranging from 1500 +/- 300 Cal B.P. to 1200 +/- 300 Cal B.P. These dates are consistent with the framework established for regression R<sub>5</sub> from the St. Catherines sea level data (1319 Cal B.P. to 1243 Cal B.P.) and the Gulf of Mexico data (1700 Cal B.P. to 1100 Cal B.P.). The current working version of the interpolated sea level curve or model for St. Catherines Island is presented as Figure 7-17 and should be considered as a working model or a living document where subsequent vibracore data will be used to continue to verify and refine the timing and magnitude of sea level transgressions and regressions.

An additional evaluation was performed by comparing the timing of the regressions from the St. Catherines Island sea level envelope with the Gulf of Mexico sea level data (Balsillie and Donaghue, 2004), global eustatic sea level data from the Red Sea (Siddall et al., 2003) and cyclical Bond events (Bond et al, 1997). The Bond events occur on a cycle of 1470 +/- 500 years and are associated with increases in ice-rafted debris (IRD) as interpreted from sediment cores in the North Atlantic. The mechanisms that control Bond events are unclear, however recent research has focused on solar output and atmospheric-oceanic interactions. The regressions from the St. Catherines Island sea level envelope correlate strongly with regressions in the near-field eustatic sea level data from the Gulf of Mexico as previously described.

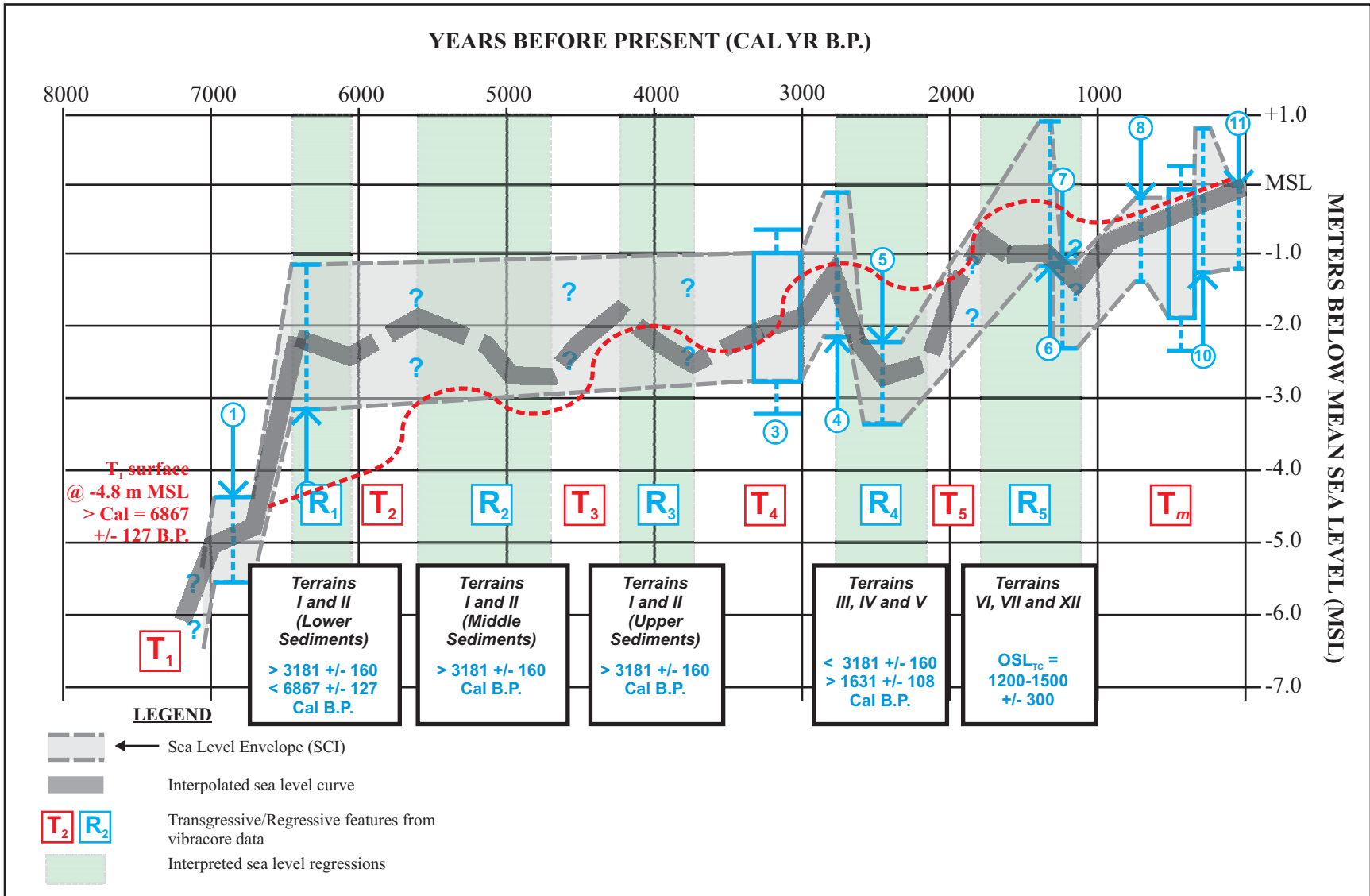


Figure 7-17: Interpolated sea level curve for St. Catherines Island, GA based on the sea level envelope and regional/global sea level data. The transgressions/regressions and radiocarbon data from the current study vibrocore data are synthesized with radiocarbon and OSL beach ridge dates (Chowns, 2011).

Regressions  $R_1$ ,  $R_2$ ,  $R_3$  and  $R_4$  from the St. Catherines Island sea level envelope also correlate well with regressions observed in the far-field or global (Red Sea) sea level data, however regression  $R_5$  from St. Catherines Island is not observed in the Red Sea data (Figure 7-18).

Regressions  $R_1$ ,  $R_3$ ,  $R_4$  and  $R_5$  from the St. Catherines Island sea level envelope are preceded by Bond Events B1 through B4, however regression  $R_2$  is not associated directly with a Bond Event. In summary it appears that the regressions from the St. Catherines Island sea level envelope have a strong association with eustatic controls, however refinement of the model is necessary to advance an understanding of the direct linkages and causes of the apparent cycles in the St. Catherines Island sea level data. This consideration should be taken into account as further testing and refinement of the model is performed.

## **7.7 Limitations and Uncertainties of Data**

A properly designed and implemented study recognizes and manages errors or uncertainties in data collection and the interpretation of results. The current study has assessed uncertainties associated with the shoreline dynamics study, XRF analysis, lithostratigraphic results from the vibracore sample collection and interpretations, and the evaluation of Holocene sea level. The uncertainties associated with the methods employed in the shoreline dynamics study were described and incorporated directly into the rate of change calculations and were provided in Section 5.1.2. Uncertainties associated with the XRF methods and results were assessed by quality assurance and quality control methods and were provided in Section 6.3.4.

Uncertainties are inherent in subsurface drilling and sampling due to the discreet nature of the sampling and are realized as a result of sampling frequency. The uncertainties are generated due to lateral changes in the subsurface lithologies and the ability of the spacing of

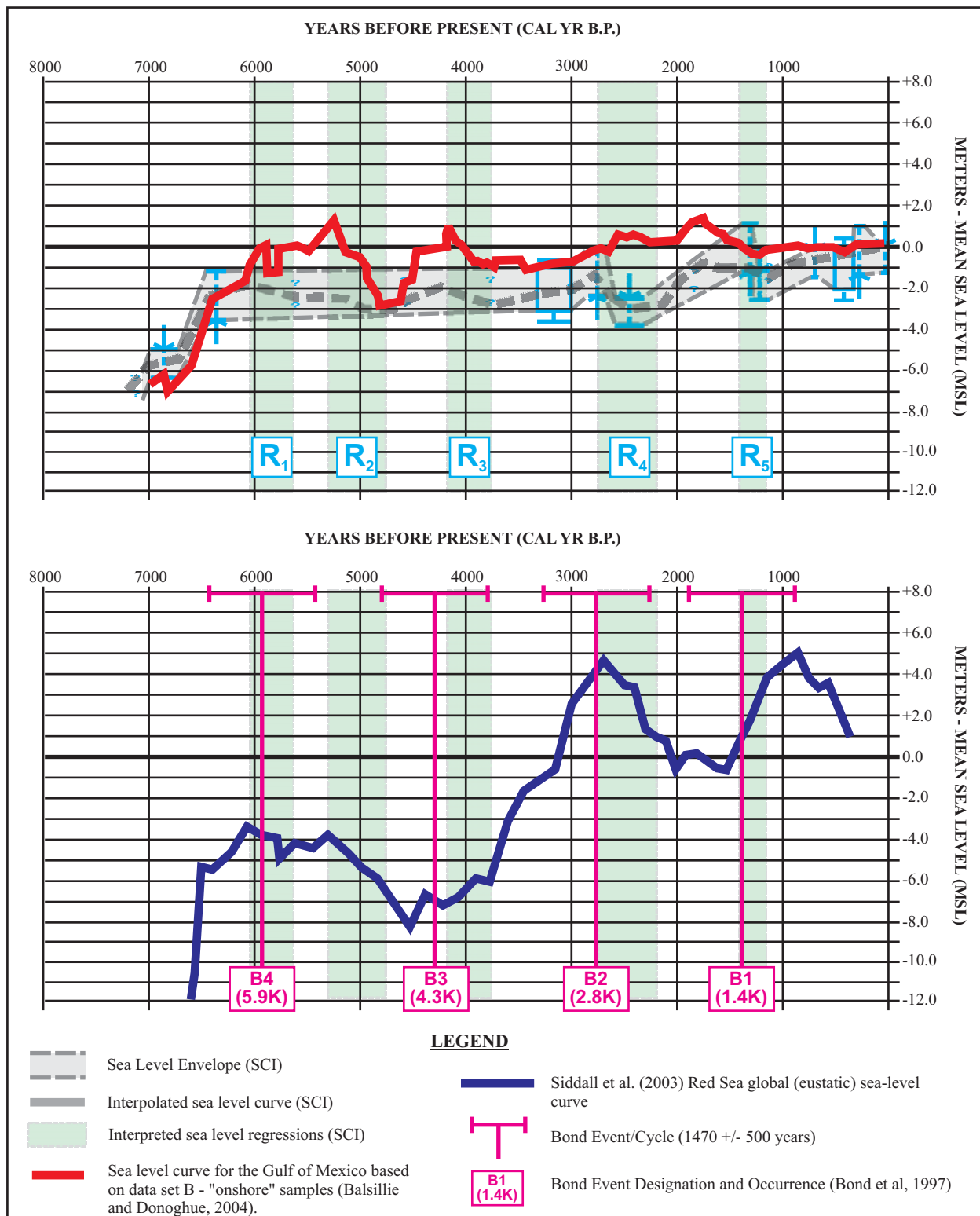


Figure 7-18: A comparison of the interpreted regressions from the St. Catherines Island sea level envelope and Gulf of Mexico sea level data (Balsillie and Donoghue, 2004) versus global eustatic sea level data from the Red Sea (Siddall et al., 2003) and cyclical Bond events (Bond et al, 1997) of 1470 +/- 500 years.

borings to capture these changes where a higher resolution sampling program consisting of closely spaced borings minimizes this uncertainty. An approach was taken under the current study where borings were more closely spaced in study areas with expected small-scale lateral changes in facies. Under the current project vibracore borings were located within the study areas at average spacings of 37 meters at Beach Pond, 45 meters at Flag Pond, and 29 meters at the *Mission Santa Catalina de Guale*. A higher resolution approach was employed in evaluating the stratigraphy of washover fans with expected small-scale lateral changes where an average spacing of 16 meters was used for the borings located at the Seaside Spit study area.

Uncertainties associated with evaluating sea level are the result of errors associated with the age of a sample in the form of radiocarbon calibration and exposure to allochthonous carbon (i.e. penetration by roots), and errors due to the vertical position of the data point. Positional uncertainties include inaccuracies in surveying, depth measurements in cores, inadequate evaluation of induced compaction due to core sampling, and the interpretation of the vertical association of the data (indicative meaning).

Uncertainties in radiocarbon data are typically represented in sea level data presentation as error bars or boxes and should be considered, along with density of data, in determining the frequency or resolution of sea level changes. The radiocarbon data associated with the sea level evaluation was also calibrated using the methods described in Section 5.4.3 to account for variations in the specific activity of  $^{14}\text{C}$  in the atmosphere, fractionation of carbon isotopes ( $\delta^{13}\text{C}$ ), and local radiocarbon reservoir effects. Uncertainties associated with radiometric results have been incorporated as error bars on the sea level envelope plots.

Positional uncertainties have been minimized by determining the horizontal location of borings using global positioning system (GPS) technologies with an estimated Positional

Dilution of Precision (PDOP) error of two to three meters for each boring location. The vertical positions of the borings were determined using the 2009 LIDAR data with an associated error of 10 cm. The borings were located in areas with relatively low relief such that the horizontal uncertainties result in minimal vertical or elevation errors. Uncertainties associated with compaction of the cores were addressed by field measurement of the physical compaction of the cores that were carried into the calculations to determine the vertical position of the radiocarbon samples and associated facies. The uncertainties involved with the interpretation of the vertical association of facies or the indicative meaning of the data were carried from the reference stratigraphic section into the evaluation of Holocene sea level as error bars or “windows” of sea level as demonstrated in Figure 5-5.



## 8 CONCLUSIONS AND RECOMMENDATIONS

### 8.1 Conclusions

Although 20<sup>th</sup> and 21<sup>st</sup> century tide gauge data for the Georgia Bight currently reflects a linear or consistent rate for relative sea level rise, remote sensing data in the form of satellite altimetry from the TOPEX/Poseidon and Jason-1 satellite platforms indicate that acceleration of the rate of sea level rise has taken place over the past 15 years and the current rate of global sea level rise is estimated at 3.1 mm/year (Jevrejeva et al., 2006). The Intergovernmental Panel on Climate Change (IPCC) has projected a sea level rise by the year 2100 of 18 cm to 59 cm (rate of 2 mm/yr to 6.5 mm/yr) depending upon several emission scenarios. Several recent studies (Rahmstorf, 2007; Horton et al., 2008; Siddall et al., 2009; and Grinstead et al., 2010) have indicated that the IPCC study may underestimate sea level rise in the 21<sup>st</sup> century by more than a factor of 2X by not integrating the full contribution of the Greenland and Antarctica ice sheets into estimates. In addition, a more recent study of sea level using tide gauge data in the mid-Atlantic coast of North America has indicated a hot spot of sea level rise due to modifications in the Atlantic Meridional Overturning Current, or AMOC (Sallenger et al, 2012). Warmer and less saline waters in the sub-polar Atlantic Ocean resulting from the melting of ice sheets inhibit the deep convection or sinking of the AMOC, resulting in weakened pressure gradients and the raising of sea level on a regional scale. The current project has evaluated shoreline dynamics and environmental change with attention to the two major controls of barrier island formation and modification processes consisting of a constant rate of sea level rise and changing sediment supply regimes. The current study should serve as a foundation of understanding or a baseline of conditions and continued monitoring should be performed to evaluate responses to the predicted changes in the rate of sea level rise into the future.

Vibracoring data and the incorporation of previous studies provided valuable insights into the stratigraphy and development of St. Catherines Island. A model has been developed for the sediments associated with the Late Holocene accretional terrains where multiple small scale fluctuations in sea level have resulted in the formation of a sedimentary veneer punctuated with transgressive surfaces and regressive sequences that form the Late Holocene beach ridge systems. The initial formation of Holocene cover sediments (10,000 to 12,000 Cal B.P.) that overlap the Late Pleistocene sediments has been correlated with climatic events by previous researchers (Stahlman and Vento, 2011), whereas the bulk of the Late Holocene cover sediments (< 7200 B.P.) were associated with specific erosional scarps and shoreline conditions under the current study where hydraulic (washover) and wind agents (eolian) are considered as likely drivers for vertical accretion as observed in a modern analogue in the northern sound margin of the island (Potter, 2011).

An evaluation of the Late Holocene sea level conditions at St. Catherines Island was performed using evidence from the sedimentary record, absolute age data and creating constraining points on sea level. Although the data does not permit a high-resolution record to be produced, numerous inferences can be made with respect to the Late Holocene sea level conditions of St. Catherines Island. Sea level responded from the Late Wisconsin glaciation and flooded the area immediately to the east of St. Catherines Island by 6000 Cal B.P. Since 6000 Cal B.P. the elevation of mean sea level has increased by approximately four to five meters; however, it appears that this rise in sea level was punctuated by small fluctuations or oscillations in sea level resulting in the occurrence of multiple transgressive surfaces and regressive sequences within the Holocene accretional terrains of St. Catherines Island.

An interpolated sea level curve based on calibrated radiocarbon and OSL data has been constructed using direct evidence of transgressive surfaces and regressive sequences from St. Catherines Island and utilizes indirect evidence from other regional sea level studies to provide additional structure (Figure 7-17). The existence of three transgressive surfaces and regressive sequences were identified in the St. Catherines island sea level evaluation as occurring between 6867 +/- 127 Cal B.P. and 3181 +/- 160 Cal B.P. These three sea level fluctuations ( $R_1$ ,  $R_2$  and  $R_3$ ) were framed into the model using the aforementioned constraining dates and highstand/lowstand information from the Gulf of Mexico sea level data. The regression noted by Gayes et al. (1992) and Scott and Collins (1995) from South Carolina sea level data (4300 Cal B.P. to 3600 Cal B.P.) was used in conjunction with the Gulf of Mexico sea level data to verify and frame regression  $R_3$  in the Late Holocene sea level model for St. Catherines Island. A regression ( $R_4$ ) identified in the St. Catherines data at 2754 +/- 80 Cal B.P. to 2474 +/- 138 Cal B.P. has been correlated with a regression identified from Georgia and South Carolina data by Depratrer and Howard (1981). An additional regression ( $R_5$ ) identified in the St. Catherines data at 1319 Cal B.P. to 1243 Cal B.P. was correlated with a regression in the Gulf of Mexico data at 1700 Cal B.P. to 1100 Cal B.P. Although the exact magnitude of the sea level fluctuations are unknown, an inference can be made for transgressions  $T_1$ ,  $T_2$ ,  $T_3$  and  $T_4$  based on the nature of the stacked transgressive surfaces observed in the Cracker Tom cores. The arrangement of the stacked transgressive surfaces indicates that each transgression was successively higher in relative sea level on a scale approaching one meter in magnitude. Facies were associated with depositional environments, coupled with absolute dating methods and indicate sea level has risen four to five meters over the past 6000 years at St. Catherines Island. Therefore, the sediments of the Holocene accretional terrains at St. Catherines Island provide a record of an overall trend of

rising sea level punctuated by multiple small scale fluctuations of sea level during the Late Holocene.

The relationship between the timing of the regressions versus periods of beach ridge formation and implications from the current shoreline dynamics study regarding the role of sediment supply complement each other. The ages of beach ridge formation strongly correlate to periods that are associated with regressions in sea level based on the sedimentary record and an evaluation of Late Holocene sea level. The evaluation of anthropogenic modifications to the rate of sediment supply performed under the current study indicates that in spite of significant changes in sediment flux rates of +300% (pre-dam era) and -20% (post-dam era), shoreline retreat was continuous during the study period. The two associations indicate strongly that the rate of sediment supply plays a secondary role to the major control of the rate of sea level rise in the formation and modification processes at St. Catherines Island.

## **8.2 Recommendations**

### *8.2.1 Future Scenarios - Implications to the SCISTP and AMNH Archaeology Program*

The SCISTP has demonstrated great innovation and flexibility in managing the loss of habitat during its existence and will face additional challenges based on the current project's future projections and the implications of an increase in the rate of sea level rise. The current projections indicate that the overall shoreline of the island will continue to decrease or shorten with additional shoreline retreat. Acceleration of shoreline retreat has also been noted in the current shoreline dynamics study for the more sensitive landforms that comprise a significant portion of the shoreline, presenting a unique challenge in assessing nest habitat and identifying suitable habitat for the relocation of nests. The McQueen Dune Field has been an area used in

the past as a “nursery” for relocated nests and the current conditions observed in the field (rapid erosion, beach scarps, etc.) and future projections for the area place a greater pressure on the program with the loss of this habitat. An effort has always been employed to minimize the distance that nests are relocated due to sea turtle ecology. To continue this objective, more aggressive and creative conservation measures will need to be initiated and employed.

The geoarchaeology program was presented with the results for the landform dynamics study at the *Mission Santa Catalina de Guale* from the pilot-scale study in 2011 and the final results of the study were presented in 2013. The AMNH reviewed the results from 2011 and implemented immediate actions in the area of Wamassee Creek by opening new excavation units in areas that appear to be at risk of loss to erosion or creek capture in the near future. It is expected that AMNH will utilize the current study results, specifically for the northern, southern and eastern margins of the island, and prioritize other archeological sites for additional research and exploration. At particular risk are the marsh hammocks and accretional terrains in close proximity to the shoreline including McQueen Hammock, where ceramics have been observed and collected along the shore face. If scenarios develop where the eastern marshes collapse, the McQueen Shell Ring would be placed in close proximity to the island shoreface and could also be at risk of shoreline capture. Continued monitoring of shoreline conditions and calibration of the current projections should be maintained to more accurately project shoreline future locations and prioritize archaeological sites.

#### *8.2.2 Opportunities for Research - “Coastal Change” Program*

A robust and successful research program centered on “Coastal Change” should engage all stakeholders in order to provide the maximum benefit to the various research, conservation,

and education programs in existence on the island and in the local region. These stakeholders include the educational institutions (Sewanee University, Georgia Southern University, Georgia State University, etc.), research entities (AMNH and aforementioned institutions), and conservation agencies (SCISTP, SCI Foundation, Georgia DNR, etc.). The “sweet spot” in this program is the overlap in research, conservation, and educational areas where success would be realized by identifying funding opportunities to promote all three objectives in a “Coastal Change” Program.

Several on-going efforts at monitoring shoreline conditions should be maintained into the near future. The SCISTP manages a rapid habitat assessment protocol that should continue to document shoreline conditions as they relate specifically to ecosystem habitat quality. Shoreline monitoring programs are also performed using ground collected data via planimetric surveying methods (Bran Potter, Sewanee), GPS methods (Brian Meyer, Georgia State Univ.), and remote sensing methods (Brian Meyer, Georgia State Univ.). The continuation of these research programs are essential to current and future conservation efforts in assessing current wildlife habitat conditions as well as improving the quality of future shoreline projections and associated habitat conditions.

Monitoring of the marsh habitat should also be a major focus area considering that a significant portion of the total area of this important ecosystem in the eastern U.S. is located in Coastal Georgia. Previous assessments involving sedimentation in marshes have indicated that the rate of vertical accretion was adequate to meet rising sea levels in the late 1970s and early 1980s (Letzsch, 1983). A focus area should be established to monitor the quality of the marshes at SCI with respect to vegetation density and types as well as the physical components including the vertical accretion rate. The previously described future shoreline scenarios were all made

under the assumption that vertical accretion of the marshes is in balance with the current rate of sea level rise. Sewanee University conducts an annual ecology field camp that would be well suited to perform annual vegetation monitoring. Sedimentation in the marshes could be evaluated for temporal trends using cores and various dating techniques ( $^{37}\text{Cs}$ ,  $^{210}\text{Pb}$ ,  $^{14}\text{C}$ ) to evaluate historical rates of sedimentation and a variety of methods are available for evaluating the current rate of sedimentation (settling plates, etc.).

A solid baseline of groundwater quality for the surficial and Floridan Aquifer system has been established through collaborative efforts lead by James Reichard of Georgia Southern University (Reichard et al., 2012). This program, with regional implications, should be expanded and continued to monitor the geochemistry of shallow groundwater with rising sea levels, and monitoring of the Floridan Aquifer should be continued to evaluate the salt water intrusion that was documented in 2011-2012. This condition has consequences that are direct to human receptors through the consumption of groundwater and indirect to ecological receptors via groundwater to surface water discharge. SCI offers a unique setting in that five potable wells tap the Floridan Aquifer with minimal production requirements, making them available for research. The interconnectivity between the aquifer systems has been initially evaluated using Ground Penetrating Radar (GPR) through collaborative efforts lead by R. Kelly Vance of Georgia Southern University (Vance et al., 2011). The interconnectivity of the aquifers should be evaluated additionally through deep drilling/coring, the installation of nested wells, and additional testing (pump testing, packer testing, water quality testing, etc.).

## REFERENCES

- Alexander, C.R. and V.J. Henry, 2007. Wassaw and Tybee Islands - Comparing undeveloped and developed barrier islands, *In* F. J. Rich (ed), *Fieldtrips of the 2007 Annual Meeting, 187-198, Southeastern Section, Geological Society of America*. Georgia Southern University (Statesboro, GA): pp. 187-198.
- Anders, F.J., and Byrnes, M.R., 1991, Accuracy of shoreline change rates as determined from maps and aerial photo-graphs: *Shore and Beach*, v. 59, pp. 17-26.
- Balsillie, J.H., and Donoghue, J.F., 2004. High resolution sea-level history for the Gulf of Mexico since the last glacial maximum. Tallahassee: Florida Geological Survey Report of Investigations 103.
- Bard, E., Hamelin, B., Arnold, M., Montaggioni, L., Cabioch, G., Faure, G. and Rougerie, F., 1996. Deglacial sea-level record from Tahiti corals and the timing of global meltwater discharge. *Nature*, Vol. 382: p. 241-244.
- Behrens, E. W., 1966, Recent emergent beach in eastern Mexico: *Nature*, v. 1952, p. 642-643.
- Bellis, V.J., 1995. Ecology of maritime forests of the southern Atlantic Coast: A community profile. Biological Report 30, U.S. Department of the Interior, National Biological Service, Washington, D.C.
- Bartholomew, M.J. and Rich, F.J., 2013. Pleistocene shorelines and coastal rivers: Sensitive potential indicators of Quaternary tectonism along the Atlantic Coastal Plain of North America. *Geological Society of America Special Papers* 2013; Number 493; pp. 17-36.



- Bishop, G.A., 1990. Modeling heavy mineral accumulation on an evolving barrier island on the southeastern coast. *University System of Georgia, Chancellor's Special Funding Initiative*: 1–12.
- Bishop, G.A., D.H. Thomas, M.C. Sanger, B.K. Meyer, R.K. Vance, R.K. Booth, F.J. Rich, D.B. Potter, and T. Keith-Lucas, 2011a. “Vibracores and Vibracore Transects Constraining the Geological and Cultural History of St. Catherine’s Island, Georgia.” *Geoarchaeology of St. Catherines Island, Georgia, Anthropological Papers of the American Museum of Natural History*, No. 94.
- Bishop, G.A., B.K. Meyer, R.K. Vance, and F.J. Rich, 2011b. “Geoarchaeological Research at St. Catherine’s Island, Georgia: Defining the Geological Foundations.” *Geoarchaeology of St. Catherines Island, Georgia, Anthropological Papers of the American Museum of Natural History*, No. 94.
- Bishop, G.A., and Meyer, B.K., 2011c. Sea Turtle Habitat Deterioration on St. Catherines Island, Georgia: Defining the Modern Transgression. *Geoarchaeology of St. Catherines Island, Georgia, Anthropological Papers of the American Museum of Natural History*, No. 94.
- Bishop, G.A., Hayes, R.H., Meyer, B.K., Rollins, H.E., Rich, F.J., Thomas, D.H., and Vance R.K., 2007, Transgressive Barrier Island Features of St. Catherines Island, Georgia, *In* Rich F.J. (ed), *Fieldtrips of the 2007 Annual Meeting, Southeastern Section, Geological Society of America*. Georgia Southern University (Statesboro, GA), p. 39-85.
- Bishop, G.A., Vance, R.K., and Meyer, B.K., 2007. Evolution of Emerging Electronic Technologies; St. Catherines Island Sea Turtle Conservation Program, in *University System of Georgia Rock Eagle Technology Conference*: pp. 1-11.

- Booth, R.K., F.J. Rich, G.A. Bishop, and N.A. Brannen. 1999. Evolution of a freshwater barrier-island marsh in coastal Georgia, U.S.A. *Wetlands* 19(3): 570-577.
- Carroll, A.R., and Bohacs, K.M., 1999. Stratigraphic classification of ancient lakes: Balancing tectonic and climatic controls. *Geology*; February 1999; v. 27; no. 2; pp. 99–102.
- Booth, R.K., Rich, F.J., and Bishop, G.A., 1999. Palynology and depositional history of Late Pleistocene and Holocene coastal sediments from St. Catherines Island, Georgia, USA. *Palynology* 23: 67–86.
- Carpenter, R.H., and Carpenter, S.F., 1991. Heavy mineral deposits in the Upper Coastal Plain of North Carolina and Virginia. *Economic Geology*, v. 86, p. 1657-1671.
- Carroll, A.M. and Bohacs, K.M., 1999, Stratigraphic classification of ancient lakes: Balancing tectonic and climatic controls: *Geology*, v. 27, p. 99-102.
- Chowns, T.C., 2011. “Drainage changes at Ossabaw, St. Catherines, and Sapelo sounds and their influence on island morphology and spit building on St. Catherines Island”. *Geoarchaeology of St. Catherines Island, Georgia, Anthropological Papers of the American Museum of Natural History*, No. 94.
- Church, J.A., White, N.J., 2006. A 20th century acceleration in global sea level rise. *Geophysical Research Letters*. 33:L01602 doi:10.1029/2005GL024826.
- Clayton, T.D., L.A. Taylor, Jr., W.J. Cleary, P.E. Hosier, P.H., F. Graber, W.J. Neal, and O.H. Pilkey, Sr. 1992. *Living with the Georgia shore*. Durham (NC), Duke University Press.
- Coe, A.L., Bosence, D.W., Church, K.D., Flint, S.S., Howell, J.A., and Wilson, R.C., 2005. *The Sedimentary Record of Sea-Level Change*. Cambridge University Press, Cambridge, UK.

- Collins, E.S., 1976. Quantitative studies of marsh foraminiferal patterns in Southern California and their application to Holocene stratigraphic problems. 1st International Sym. on Benthonic Foraminifera of the Continental Margins, Part A: Ecology and Biology. Maritime Sediments Special Publications 1: 153-170, 1976.
- Colman, S.M., and Bratton, J.F., 2003, Anthropogenically induced changes in sediment and biogenic silica fluxes in Chesapeake Bay: *Geology*, v. 31, p. 71–74.
- Colquhoun, D.J., and Brooks, M.J., 1986. New evidence from the southeastern United States for eustatic components in the late Holocene sea levels. *Geoarchaeology* 1: 275–291.
- Crowell, M., Leatherman, S.P., and Buckley, M.K., 1991, Historical shoreline change— Error analysis and mapping accuracy: *Journal of Coastal Research*, v. 7, pp. 839-852.
- Crowell, M., Douglas, B.C., and Leatherman, S.P., 1997, On forecasting future U.S. shoreline positions— a test of algorithms: *Journal of Coastal Research*, v. 13, n. 4, pp. 1245-1255.
- Curry, J. R., 1960, Sediments and history of Holocene transgression, continental shelf, northwest Gulf of Mexico: In: (F. P. Shepard et al., eds), *Recent Sediments, Northwest Gulf of Mexico*, American Association of Petroleum Geologists, p. 221-226.
- Davies, T. D., 1980. Peat formation in Florida Bay and its significance in interpreting the recent vegetation history of the bay area, Ph.D. Dissertation, College Station: Penn. State University, PA, 338 p.
- de Vries, H., 1958. Variation in the concentration of radiocarbon with time and location on earth. *Proc. Koninkl. Nederl. Akad. Wetenschappen B61*, 1-9.
- Deery, J.R., and J.D. Howard, 1977. Origin and character of washover fans on the Georgia coast, U.S.A. *Transactions of the Gulf Coast Association of Geological Societies* 27: 259-271.

- DePratter, C.B. and J.D. Howard, 1981. Evidence for a sea level low stand between 4500 and 2400 years B.P. on the Southeast Coast of the United States. *Journal of Sedimentary Petrology*, 51:1287-1295.
- Dolan, R., B. P. Hayden, S. May, P. May, and H. Lins, 1980. The Reliability of Shoreline Change Measurements from Aerial Photographs. *Shore and Beach*. 48(4): 22-29.
- Dolan, R., Fenster, M.S., and Holme, S.J., 1991. Temporal analysis of shoreline recession and accretion: *Journal of Coastal Research*, v. 7, pp. 723-744.
- Drever, J.I., and Vance, G.F., 1994. Role of soil organic acids in mineral weathering processes: in *Organic Acids in Geological processes*, Pittman, E.D. and Lewan, M.D., eds., Springer Verlag, berlin, p. 138-161.
- Elsner, H., 1997. Economic geology of the heavy mineral placer deposits in northeastern Florida. Florida Geological Survey Open File Report No. 71, 98 p.
- Engelhart, S.E., B.P. Horton, and A.C. Kemp. 2011. Holocene sea level changes along the United States' Atlantic Coast. *Oceanography* 24(2):70–79.
- Fairbanks, R.G., 1989. A 17,000-year glacio-eustatic sea level record: influence of glacial melting rates on the Younger Dryas event and deep-ocean circulation. *Nature*, Vol. 342:p. 637-642.
- Fairbridge, R. W., 1961, Eustatic change in sea-level: In: (L. H. Ahrens et al., ed.), *Physics and Chemistry of the Earth*, v. 4, New York: Pergamon Press, p. 99-185.
- Fairbridge, R. W., 1974, The Holocene sea-level record in south Florida: In: (P. J. Gleason, ed.), *Environments of South Florida: Present and Past*, Miami Geological Survey, Memoir No. 2, p. 223-232.

- Faught, M. K., and Donoghue, J. F., 1997, Marine inundated archaeological sites and paleofluvial systems: examples from a karst-controlled continental shelf setting in Apalachee Bay, northeastern Gulf of Mexico: *Geoarchaeology*, v. 12, p. 416-458.
- Ferguson, S.M., Rich, F.J., and Vance, R.K., 2010. A palynological investigation of the Central Depression on St. Catherines Island, Georgia. Geological Society of America Abstracts with Programs, Vol. 42, No. 1, p. 175.
- Fletcher, C.H.; Rooney, J.J.B.; Barbee, M.; Lim, S.C., and Richmond, B.M., 2003. Mapping shoreline change using digital orthophotogrammetry on Maui, Hawaii. *Journal of Coastal Research*, Special Issue No. 38, pp. 106–124.
- Force, E.R., 1976. Metamorphic source rocks of titanium placer deposits – a geochemical cycle. U.S. Geological Survey Professional Paper 959-B, pp. B1-B16.
- Force, E.R. and Rich, F.J., 1989. Geologic evolution of Trail Ridge eolian heavy-mineral sand and underlying peat, northern Florida. U.S. Geological Survey Professional Paper 1499, 16 p.
- Frazier, D. E., 1974, Depositional episodes: their relationship to the Quaternary framework in the northwestern portion of the Gulf Basin: Texas Bureau of Economic Geology, Geological Circular 74-1, 28 p.
- Frey, R.W. and Basan, P.B. 1985, Taphonomy of relict saltmarsh deposits, Cabretta Island, Georgia. *Senckenbergiana maritima*. 13, 111-155.
- Garnar and Stanaway, 1994. Titanium minerals. In Carr, D.D. (editor), *Industrial Minerals and Rocks*, 6<sup>th</sup> Edition, Society for Mining, Metallurgy, and Exploration, Inc., Littleton, CO, pp. 1071-1089.

- Gayes, P.T., D.B. Scott, E.S. Collins, and D.D. Nelson. 1992. A Late Holocene sea-level irregularity in South Carolina; Society of Economic Paleontologists and Mineralogists, Special Publication 48: 154–160.
- Genz, A.S.; Fletcher, C.H.; Dunn, R.A.; Frazer, L.N., and Rooney, J.J., 2007. The predictive accuracy of shoreline change rate methods and alongshore beach variation on Maui, Hawaii. *Journal of Coastal Research*, 23(1), 87–105. West Palm Beach (Florida), ISSN 0749-0208.
- Glanzman, R.K. and Closs, L.G., 2007. Field Portable X-Ray Fluorescence Geochemical Analysis – Its Contribution to Onsite Real-time Project Evaluation. In Milkereit (Editor), Proceedings of Exploration 07: Fifth Decennial International Conference on Mineral Exploration, p. 291-301.
- Goldberg, E.D., Griffin, J.J., Hodge, V., Koide, M. and Windom, H., 1979. Pollution history of the Savannah River estuary. *Environmental Science Technology*, 13: pp. 588-594.
- Griffin, M.M. and V.J. Henry, Jr., 1984. Historical Changes in the Mean High Water Shoreline of Georgia. *Georgia Geological Survey, Bulletin 98*, 96p.
- Grinsted A, Moore JC, Jevrejeva S (2010) Reconstructing sea level from paleo and projected temperatures 200 to 2100 AD. *Climate Dynamics*, 34:4.
- Hails, J.R. and J.H. Hoyt, 1969. An Appraisal of the Evolution of the Lower Atlantic Coastal Plain of Georgia, U. S. A. *Transactions of the Institute of British Geographers*, No. 46: 53-68.
- Haq B, Hardenbol J, Vail P (1987) Chronology of fluctuating sea levels since the Triassic. *Science*, 235:1156–1167.

- Hargett, K.S., Vance, R.K., Meyer, B.K, Rich, F.J., and Bishop, G.A. Investigation of Holocene Accretionary Terrain on St. Catherines Island, Georgia. Southeastern Section Geological Society of America, 60th Annual Meeting, Wilmington, N.C.
- Hayes, M.O., 1975. Morphology of sand accumulations in estuaries. In: L.E. Cronin (Editor), *Estuarine Research*, V.2. Academic Press, New York, N.Y., pp.3--22.
- Hayes, R.H., and D.H. Thomas, 2008. Hydrology of St. Catherines Island. In D.H. Thomas, *Native American Landscapes of St. Catherines Island, Georgia: The Theoretical Framework*. Anthropological Papers of the American Museum of Natural History 88 (1): 56–58.
- Himmelstoss, E.A., 2009. DSAS 4.2 Installation Instructions and User Guide. U.S. Geological Survey Open-File Report 2008-1278, updated for DSAS Version 4.2.
- Horton R, Herweijer C, Rosenzweig C, Liu J, Gornitz V, Ruane AC (2008) Sea level rise projections for current generation CGCMs based on the semi-empirical method. *Geophysical Research Letters*, 35.
- Howard, J.D., and R.M. Scott, 1983. Comparison of Pleistocene and Holocene barrier island beach-to-offshore sequence, Georgia and northeast Florida coasts. *Sedimentary Geology* 34: 167–183.
- Howard, J.D., and J. Dörjes, 1972. Animal-sediment relationships in two beach-related tidal flats, Sapelo Island, Georgia. *Journal of Sedimentary Petrology* 42: 608–623.
- Howard, J.D, and R.W. Frey, 1975. Estuaries of the Georgia coast, United States: sedimentology and biology: II. Regional animal-sediment characteristics of Georgia estuaries. *Senckenbergiana Maritima* 7: 33–103.

- Howard, J.D., and R.W. Frey, 1980. Holocene depositional environments of the Georgia coast and continental shelf. In J.D. Howard, C.B. DePratter, and R.W. Frey (editors), *Excursions in southeastern geology: the archaeology- geology of the Georgia coast*. Georgia Geological Survey, Guidebook 20: 66–134.
- Howard, J.D., and R.W. Frey, 1985. Physical and biogenic aspects of backbarrier sedimentary sequences, Georgia coast, U.S.A. *Marine Geology* 63: 77–127.
- Howard, J.D., and H.E. Reineck, 1972. Georgia coastal region, Sapelo Island, U.S.A.: sedimentology and biology. IV. Physical and biogenic sedimentary structures of the nearshore shelf. *Senckenbergiana Maritima* 4: 81–123.
- Howard, J.D., and R.M. Scott, 1983. Comparison of Pleistocene and Holocene barrier island beach-to-offshore sequence, Georgia and northeast Florida coasts. *Sedimentary Geology* 34: 167–183.
- Hoyt, J.H., 1967. Barrier island formation. *Geological Society of America Bulletin* 78: 1125–1136.
- Hoyt, J.H., 1968. Geology of the Golden Isles and lower Georgia coastal plain. In D.S. Maney (editor), *The future of the marshlands and sea islands of Georgia*: 18–32. Georgia Natural Areas Council and Coastal Planning and Development Commission.
- Hoyt, J.H., and J.R. Hails. 1967. Pleistocene shoreline sediments in coastal Georgia: depositional and modification. *Science* 155: 1541–1543.
- Hoyt, J.H., V.J. Henry, Jr., and R.J. Weimer, 1968. Age of late-Pleistocene shoreline deposits, coastal Georgia. In R.B. Morrison, and H.E. Wright (editors), *Means of correlation of Quaternary successions* 8: 381–393. Salt Lake City: University of Utah Press.



- Hoyt, W. H. & J. M. Demarest, 1981. Vibracoring in coastal environments: a description of equipment and procedures. DEL-SG-01-81, Sea Grant College Program, University of Delaware, Newark, 20-31.
- Huddleston, P.F., 1988. A revision of the lithostratigraphic units of the Coastal Plain of Georgia—Miocene through Holocene. Georgia Geological Survey Bulletin 104. Atlanta, GA.
- Hughen, K.A., Baillie, M.G.L. , Bard, E. , Beck, J.W. , Bertrand, C.J.H. , Blackwell, P.G. , Buck, C.E. , Burr, G.S. , Cutler, K.B. , Damon, P.E. , Edwards, R.L. , Fairbanks, R.G. , Friedrich, M. , Guilderson, T.P. , Kromer, B., McCormac, G., Manning, S., Ramsey, C., Reimer, P.J., Reimer, R.W., Remmele, S., Southon, J.R., Stuiver, M., Talamo, S., Taylor, F.W., Plicht, J. van der, Weyhenmeyer, C. E., 2004. Marine04 Marine Radiocarbon Age Calibration, 0-26 Cal kyr BP. *Radiocarbon*, Volume 46, Number 3, p 1059-1086.
- Innov-X Systems, 2007. User Instructional Manual, Alpha Series™, Revision B. Innov-X Systems, Inc., Olympus Corporation, USA Headquarters, Waltham, MA.
- Intergovernmental Panel for Climate Change (IPCC), 2000. Emissions Scenarios. Nebojsa Nakicenovic and Rob Swart (Eds.), Cambridge University Press, UK. pp 570.
- Jarrett, J.T., 1976. Tidal prism-inlet area relationships. U.S. Army, GITI Rep.3, 55 pp.
- Jevrejeva S., Grinsted A., Moore J.C., Holgate S (2006) Nonlinear trends and multiyear cycles in sea level records. *Journal of Geophysical Research*, V. 111. doi:10.1029/2005JC003229
- Johnson, A.S., Hillestad, H.O., Shanholtzer, S.F., and Shanholtzer, G.F., 1974. An ecological survey of the coastal region of Georgia. U.S. National Park Service, Monograph 3, 233 p.
- Kachigan, S.K., 1991. Multivariate Statistical Analysis: A Conceptual Introduction. Radius Press, June 1, 1991.

- Kelley, J. T., Gehrels, W. R., and Belknap, D. F. (1995). Late Holocene relative sea-level rise and the geological development of tidal marshes at Wells, Maine, U.S.A. *Journal of Coastal Research*, 11, 136–153.
- Kemp, A.C., Horton, B.P., Corbett, D.R., Culver, S.J., Edwards, R.J. and van de Plassche, O., 2009. The relative utility of foraminifera and diatoms for reconstructing late Holocene sea-level change in North Carolina, USA. *Quaternary Research* 71, p. 9–21.
- Kirwan, M.L., Murray, A.B., Donnelly, J.P. and Corbett, D.R., 2011. Rapid wetland expansion during European settlement and its implication for marsh survival under modern sediment delivery rates. *Geology*, v. 39, no. 5, p. 507-510.
- Kochel, R.C., Dolan, R., 1986. The role of overwash on a mid-Atlantic coast barrier island. *Journal of Geology*, Volume 94, p. 902-906.
- Kuehn, D. W., 1980, Offshore transgressive peat deposits of southwest Florida: Evidence for a late Holocene rise of sea-level: M. S. Thesis, Department of Geology, Pennsylvania University, 104 p.
- Kumar, N. and Sanders, J.E., 1974. Inlet sequence: a vertical succession of sedimentary structures and textures created by the lateral migration of tidal inlets. *Sedimentology*, 21: 491-532.
- LaForge, L., and Cooke, C.W., 1925. *Physical Geology of Georgia*, Georgia Geological Survey Bulletin 42, 189 pp.
- Langley, S.K., Alexander, C.R., Bush, D.M., and Jackson, C.W., 2003. Modernizing shoreline change analysis in Georgia using topographic survey sheets in a GIS environment. *Journal of Coastal Research*, Special Issue 38: 168-177.

- Leatherman, S.P. (editor), 1977. Barrier Islands: From the Gulf of St. Lawrence to the Gulf of Mexico. Academic Press, Harcourt Brace Jovanovich Publishers.
- Leatherman, S.P., Williams, A.T., 1977. Lateral textural grading in overwash sediments. *Earth Surface Processes and Landforms* 2, pp. 333-341.
- Leatherman, S.P., Williams, A.T., 1983. Vertical sedimentation units in a barrier island washover fan. *Earth Surface Processes and Landforms*, University of Pittsburgh, PA: 186 p.
- Lener, E.F., 1997. Mineral chemistry of heavy minerals in the Old Hickory Deposit, Sussex and Dinwiddie Counties, Virginia. Masters Thesis, Virginia Polytechnic Institute and State University, Blacksburg, VA, 92 p.
- Letzsch, W. S. 1983. Seven year's measurement of deposition and erosion, Holocene salt marsh, Sapelo Island, Georgia. *Senckenbergiana Maritima* 15:157–165.
- Letzsch, W.S., and Frey, R.W., 1980. Deposition and erosion in a Holocene salt marsh, Sapelo Island, Georgia. *Journal of Sedimentary Research*, June 1980, v. 50 no. 2, p. 529-542.
- Linsley, D.M., 1993. Depositional environments of St. Catherines Island: their relationship to late Quaternary sea-level change and application to late Paleozoic cyclic stratigraphy. Ph.D. dissertation, University of Pittsburgh.
- Linsley, D.M., G.A. Bishop, and H.B. Rollins, 2008. Stratigraphy and geologic evolution of St. Catherines Island. In D.H. Thomas, *Native American Landscapes of St. Catherines Island: I. Theoretical framework*. Anthropological Papers of the American Museum of Natural History 88 (1): 26–41.
- MacNeil, F.S., 1950. Pleistocene Shore Lines in Florida and Georgia. United States Geological Survey Professional Paper No 221-F, 107 p.

- Martin, A.J., and Rindsberg, A.K., 2011. Ichnological diagnosis of ancient storm-washover fans, Yellow Banks Bluff, St. Catherines Island, Georgia. *Geoarchaeology of St. Catherines Island, Georgia, Anthropological Papers of the American Museum of Natural History*, No. 94.
- McBride, R. A., 1997, Seafloor morphology, geologic framework, and sedimentary processes of a sand-rich shelf offshore Alabama and northwest Florida, northeastern Gulf of Mexico: Ph.D. Dissertation, Department of Oceanography and Coastal Sciences, Louisiana State University, 509 p.
- McFarlan, E., Jr., 1961, Radiocarbon dating of late Quaternary deposits, South Louisiana: *Geological Society of America Bulletin*, v. 72, p. 129-158.
- Meade, R.H., 1969. Landward Transport of Bottom Sediments in Estuaries of the Atlantic Coastal Plain. *Journal of Sedimentary Petrology*, Vol. 39, No. 1, pp. 222-234.
- Meade, R.H., and Trimble, S.W., 1974. Changes in sediment loads in rivers of the Atlantic drainage of the United States since 1900. In *Effects of man on the interface of the hydrological cycle with the physical environment*. International Association of Hydrological Sciences Publication 113, pp. 99-104.
- Meyer, B.K., 2012. Shoreline Dynamics and Environmental Change Under the Modern Transgression: St. Catherines Island, Georgia, Research Proposal.
- Meyer, B.K, Bishop, G.A, and Vance, R.K., 2011. An Evaluation of Shoreline Dynamics at St. Catherines Island, Georgia Utilizing the Digital Shoreline Analysis System (USGS). Southeastern Section Geological Society of America, 60th Annual Meeting, Wilmington, N.C.

- Meyer, B.K., Keith-Lucas, T., Bishop, G.A., Thomas, D.H., Hayes, R.H., Sanger, M., and Vance, R.K., 2009. Digital Atlas of St. Catherines Island, Georgia. St. Catherines Research Consortium Publication CD-1.
- Miller K.G., Kominz M.A., Browning J.V., Wright .JD., Mountain G.S., Katz M.E., Sugarman P.J., Cramer B.S., Christie-Blic N., Pekar S.F., 2005. The Phanerozoic record of global sea level change. *Science*, 310:1293–1298.
- Milliman, J. D., and Meade, R. H. 1983. World-wide delivery of river sediments to the oceans. *Journal of Geology*, Vol. 91, pp. 1–21.
- Montero-Serrano, J.C., Palarea-Albaladejo, J., Martín-Fernández, J.A., Martínez-Santana, M., Gutiérrez-Martín, J.V., 2010. Sedimentary chemofacies characterization by means of multivariate analysis. *Sedimentary Geology*, V. 228, 218–228.
- NCDC, 2013. National Climatic Data Center, data accessed online (26 July 2013) at <http://www.ncdc.noaa.gov/cdo-web/>
- NDBC, 2013. National Data Buoy Center, data accessed online (26 July 2013) at <http://www.ndbc.noaa.gov/>
- Neumann, A.C., and MacIntyre, I., 1985. Reef response to sea level rise: keep-up, catch-up or give-up. Proceedings of the 5th International Coral Reef Congress, Tahiti, pp. 105-110.
- Neiheisel, J, and Weaver, C.E., 1967. Transport and Deposition of Clay Minerals, Southeastern United States. *Journal of Sedimentary Petrology*, Vol. 37, No. 4, pp. 1084-1116.
- Nelson, H. R., and Bray, E. E., 1970, Stratigraphy and history of the Holocene sediments in the Sabine-High Island area, Gulf of Mexico: In: (Morgan, J. P., ed.), Deltaic Sedimentation, Modern and Ancient, Society of Economic Paleontologists and Mineralogists Special Publication 15, p. 48-77.

NOAA, 2013. Sea Levels Online, NOAA Tides and Currents webpage.

<http://tidesandcurrents.noaa.gov/sltrends/sltrends.shtml>

- O'Brien, M.P., 1969. Equilibrium flow areas of inlets on sandy coasts. Proceedings of the American Society of Civil Engineers, *Journal of the Waterways, Harbors and Coastal Engineering Division*, WWI: pp. 43-52.
- Oertel, G.F., 1972. Sediment transport on estuary entrance shoals and the formation of swash platforms. *Journal of Sedimentary Petrology*, 42: pp. 858-863.
- Oertel, G.F., 1973. A sedimentary framework of the substrate adjacent to Georgia tidal inlets. In: R. Frey (Editor), *The Neogene of the Georgia Coast*. University of Georgia, Athens, Ga., pp. 59-66.
- Oertel, G.F., 1975. Post Pleistocene island and inlet adjustment along the Georgia coast. J. *Journal of Sedimentary Petrology*, 45: pp. 150-159.
- Oertel, G.F., and Larsen, M., 1976. Developmental sequences in coastal dunes and distribution of dune plants. *Bulletin of the Georgia Academy of Science*, v. 34, pp. 35-48.
- Oertel, G.F., 1979. Barrier Island development during the Holocene recession, southeastern United States. In: S.P. Leatherman (Editor), *Barrier Islands*. Academic Press, New York, N.Y.
- Oertel, G.F., 1985. The Barrier Island System. In: G.F. Oertel and S.P. Leatherman (Editors), *Barrier Islands*. *Marine Geology*, 63: 1-18.
- Pearce, T.J., Besly, B.M., Wray, D.S., Wright, D.K., 1999. Chemostratigraphy: a method to improve interwell correlation in barren sequences — a case study using onshore Duckmantian/Stephanian sequences (West Midlands, U.K.). *Sedimentary Geology* 124, 197–220.

- Pevear, D., 1988. Clay Minerals for Petroleum Geologists and Engineers. Society of Economic Paleontologists and Mineralogists, SEPM Short Course 22, Tulsa, Oklahoma.
- Pickering, S.M., Jr. and J.B. Murray. 1976. Geologic map of Georgia. Georgia Geological Survey.
- Pinet, P.R., and Morgan, W.P., 1979. Implications of Clay-Provenance Studies in Two Georgia Estuaries. *Journal of Sedimentary Petrology*, Volume 49, Number 2, p. 575-580.
- Pirazzoli, P.A., 1991. World Atlas of Holocene Sea-level Changes, Elsevier Oceanography Series 58, Amsterdam: Elsevier, 300 p.
- Pirkle, F.L., F.J. Rich, J.G. Reynolds, T.A. Zayac, W.A. Pirkle, and R.W. Portel. 2007. The geology, stratigraphy, and paleontology of Reids, Bells, and Roses Bluffs in northeastern Florida. In F.J. Rich (editor), *Guide to field trips, 56th Annual Meeting Southeastern Section of the Geological Society of America, Savannah, GA*: 137–151. Georgia Southern University Department of Geology and Geography, Contribution Series 1.
- Pirkle, W.A. and Pirkle, F.L., 2007. An introduction to heavy mineral sand deposits of the Florida and Georgia Atlantic Coastal Plain. In F.J. Rich (editor), *Guide to field trips, 56th Annual Meeting Southeastern Section of the Geological Society of America, Savannah, GA*: 129-136. Georgia Southern University Department of Geology and Geography, Contribution Series 1.
- Pirkle, F.L., E.C. Pirkle, and J.G. Reynolds, 1991. Heavy mineral deposits of the southeastern Atlantic coastal plain: Georgia Geological Survey Bulletin 120: 15–41.
- Pirkle, E.C., and Yoho, W.H., 1970. The heavy mineral orebody of Trail Ridge, Florida. *Economic Geology*, v. 65, pp. 17-30.
- Pohl, M.E., 1946. Ecological Observations on *Callianassa Major* (Say 1818) at Beaufort, North

- Carolina. *Ecology*, Vol. 27, No. 1, pp. 71-80.
- Potter, D.B., 2011. Recent shoreline erosion and vertical accretion patterns, St. Catherines Island. *Geoarchaeology of St. Catherines Island, Georgia, Anthropological Papers of the American Museum of Natural History*, No. 94.
- Pryor, W.A., 1975. Biogenic sedimentation and alteration of argillaceous sediments in shallow marine environments. *Geological Society of America Bulletin* 86, pp. 1244-1254.
- Rahmstorf S (2007) A semi-empirical approach to predicting future sea level rise. *Science* 315:368–370.
- Reátegui, K., Martínez, M., Esteves, I., Gutiérrez, J.V., Martínez, A., Meléndez, W., Urbani, F., 2005. Geochemistry of the Mirador Formation (Late Eocene-Early Oligocene), southwestern Venezuela: chemostratigraphic constraints on provenance and the influence of the sea level. *Geochem. J.* 39 (3), 213–226.
- Reichard, J.S., Nelson, B.R., Meyer, B.K., Vance, R.K., and Van Stan, J.T., 2012. Saltwater intrusion in the Upper Floridan Aquifer on St. Catherines Island, Georgia. *Geological Society of America, Abstracts with Programs* 44 (7), p. 616.
- Reimer, P. J., Baillie, M. G. L., Bard, E., Bayliss, A., Beck, J. W., Bertrand, C. J. H., Blackwell, P. G., Buck, C. E., Burr, G. S., Cutler, K. B., Damon, P. E., Edwards, R. L., Fairbanks, R. G., Friedrich, M., Guilderson, T. P., Hogg, A. G., Hughen, K. A., Kromer, B., McCormac, F. G., Manning, S. W., Ramsey, C. B., Reimer, R. W., Remmele, S., Southon, J. R., Stuiver, M., Talamo, S., Taylor, F. W., van der Plicht, J., and Weyhenmeyer, C. E., 2004. IntCal04 Terrestrial radiocarbon age calibration, 26 - 0 ka BP. *Radiocarbon* 46, 1029-1058.
- Robbin, D. M., 1984, A new Holocene sea-level curve for the upper Florida Keys and Florida reef tract: *Miami Geological Society Memoir* No. 2, p. 437-458.



- Rohling EJ, Grant K, Bolshaw M, Roberts AP, Siddall M, Hemleben C, Kucera M (2009) Antarctic temperature and global sea level closely coupled over the past five glacial cycles. *Nature Geoscience*, 2:500–504.
- Roep, B. and Beets, B.J., 1988. Sea level rise and paleotidal levels from sedimentary structures in the coastal barriers in the western Netherlands since 5,600 BP. *Geologie en Mijnbouw* 67, pp. 53-60.
- Rollins, H.B., Beratan, K., and Pottinger, J.E., 2011. Role of storm events in beach ridge formation, St. Catherines Island. *Geoarchaeology of St. Catherines Island, Georgia, Anthropological Papers of the American Museum of Natural History*, No. 94.
- Romine, B.M., Fletcher, C.H., Frazer, L.N., Genz, A.S., and Barbee, M.M., 2009. Historical Shoreline Change, Southeast Oahu, Hawaii; Applying Polynomial Models to Calculate Shoreline Change Rates. *Journal of Coastal Research*, Vol. 25, pp. 1236–1253.
- Rooney, J.J.B.; Fletcher, C.H.; Barbee, M.; Eversole, D.; Lim, S.-C.; Richmond, B.M., and Gibbs, A., 2003. Dynamics of sandy shorelines in Maui, Hawaii: consequences and causes. *Coastal Sediments 2003 Proceedings*, (Clearwater Beach, Florida).
- Rutherford, S., and D'Hondt, S., 2000. Early onset and tropical forcing of 100,000-year Pleistocene glacial cycles. *Nature*, 408:72–75.
- Saenger, C., Cronin, T.M., Willard, D., Halka, J., and Kerhin, R., 2008. Increased terrestrial to ocean sediment and carbon fluxes in the northern Chesapeake Bay associated with twentieth century land alteration: *Estuaries and Coasts*, v. 31, p. 492–500.
- Sallenger, A.H., Doran, K.S., and Howd, P.A., 2012. Hotspot of accelerated sea-level rise on the Atlantic coast of North America. *Nature Climate Change*, Volume 2, pp. 884–888.

- Schnable, J. E., and Goodell, H. G., 1968. Pleistocene-Recent stratigraphy, evolution, and development of the Apalachicola coast, Florida: Geological Society of America Special Paper No. 112, 72 p.
- Scholl, D. W., and Stuiver, M., 1967. Recent submergence of southern Florida: A comparison with adjacent coasts and other eustatic data: Geological Society of America Bulletin, v. 78, p.437-454.
- Schroeder, W. W., Shultz, A. W., and Pilkey, O. H., 1995. Late Quaternary oyster shells and sea-level history, inner shelf, northeast Gulf of Mexico: *Journal of Coastal Research*, v. 11, no. 3, p. 664-674.
- Scott, D. B., 1976. 1st Int. Symp. Benthonic Foraminifera of Continental Margins Special Publications 1, pp. 153–170, Halifax, Nova Scotia.
- Scott, D.B., and E.S. Collins, 1995. Late Mid-Holocene sea-level oscillation: A possible cause, *Quaternary Science Reviews* 15: 851–856.
- Sedgewick, P.E., and R.A. Davis, Jr., 2003. Stratigraphy of washover deposits in Florida: Implications for recognition in the stratigraphic record. *Marine Geology*, 200: 31–48.
- Shepard, F. P., 1960, Rise of sea-level along northwest Gulf of Mexico: In: (F. P. Shepard et al., eds), Recent Sediments, Northwest Gulf of Mexico, American Association of Petroleum Geologists, p. 338-344.
- Shier, D. E., 1969, Vermetid reefs and coastal development in the Ten Thousand Islands, southwest Florida: Geological Society of America Bulletin, v. 80, p. 485-508.
- Siddall M, Stocker TF, Clark PU (2009) Constraints on future sea level rise from past sea level change. *Nature Geoscience* 2:571–575.

- Siddall, M., Rohling, E. J., Almogi-Labin, A., Hemleben, Ch., Meischner, D., Schmetzer, I., and Smeed, D. A., 2003, Sea-level fluctuations during the last glacial cycle: *Nature*, v. 423, p. 853-858.
- Smith, D. G., 1984. Vibracoring fluvial and deltaic sediments: tips on improving penetration and recovery. *Journal of Sedimentary Petrology*, 54: 660–663.
- Smith, J.M. and Frey, R.W., 1985. Biodeposition by the ribbed mussel *Geukensia demissa* in a salt marsh, Sapelo Island, Georgia. *Journal of Sedimentary Petrology*, 55: 817-828.
- Smith, J.W., S.M. Pickering, and J.R. Landrum, 1968. Heavy-mineral-bearing sand of the coastal region of Georgia. Geological Society of America Special Paper: 500 p.
- Snyder, J.P., 1987. Map Projections: A Working Manual. USGS Professional Paper: 1395.
- Spackman, W., Dolsen, C. P. and Riegel, W., 1966, Phytogenic organic sediments and sedimentary environments in the Everglades-mangrove-complex. Part I. Evidence of a transgressing sea and its effect on environments of the Shark River area of southwest Florida: *Palaeontographica*, v. B117, p. 135-152.
- SPSS Statistics Base 17.0 User's Guide, SPSS Inc., Chicago, IL.
- Stahlman, P.A., and Vento, F.J., 2012. Early Prehistoric Site Potential on Atlantic Coast Barrier Islands: St. Catherines Island, Georgia – A Proxy Study. Southeastern Archaeology Conference Abstracts with Programs.
- Stapor, F.W., Jr., and T.D. Mathews, 1983. Higher than present Holocene sea-level events recorded in wave cut terraces and scarps: Old Island, Beaufort County, South Carolina. *Marine Geology* 52: pp. 53–60.
- Stapor, F. W., and Tanner, W. F., 1977, Late Holocene mean sea-level data from St. Vincent Island, and the shape of the late Holocene sea-level curve: *In*: (W. F. Tanner, ed.),

- Coastal Sedimentology, Tallahassee, FL: Department of Geology, Florida State University, p. 35-68.
- Stuiver, M. and Daddario, J.J., 1963. Submergence of the New Jersey coast. *Science*, 142: 951.
- Tan, P.N., Steinbach, M., and Kumar, V., 2005. Introduction to Data Mining. Addison-Wesley, May 2, 2005, 1<sup>st</sup> Edition.
- Thieler, E.R., and Danforth, W.W., 1994, Historical shore-line mapping: Improving techniques and reducing positioning errors: *Journal of Coastal Research*, v. 10, p. 549-563.
- Thomas, D.H., 2011. 1. Why this archaeologist cares about geoarchaeology: some pasts and futures of St. Catherines Island: In: (G.A. Bishop, H.R. Rollins, and D.H. Thomas, ed.) *Geoarchaeology of St. Catherines Island, Georgia*. Anthropological Papers of the American Museum of Natural History, Number 94, ISSN 0065-9452.
- Thomas, D.H. 2008. Native American landscapes of St. Catherines Island, Georgia. *Anthropological Papers of the American Museum of Natural History* 88, parts I–III: pp 1136.
- Thomsen, V., and Schatzlein, D., 2002. Advances in Field-Portable XRF, *Spectroscopy* 17 (7) July 2002, pp 14-20.
- Trimble, S. W. 1974. Man-induced soil erosion on the southern Piedmont 1700–1970. Ankeny, IA, Soil Conservation Society of America, 180 p.
- U.S. Army Corps of Engineers, 1991. Savannah Harbor, Georgia comprehensive study: Draft feasibility report and environmental impact statement. U.S. Army Corps of Engineers, Savannah District, Savannah, Georgia, 565 p.

- U.S. Army Corps of Engineers, 1996. Savannah Harbor long-term management strategy study, harbor operation and maintenance, Chatham County, Georgia, and Jasper County, South Carolina (EPA Number 960398F), 765 p.
- U.S. EPA, 2007. Field Portable X-Ray Fluorescence Spectrometry for the Determination of Elemental Concentrations in Soil and Sediment. USEPA Office of Solid Waste, Test Methods for Evaluating Solid Waste, Physical/Chemical Methods.
- Vance, R.K., Bishop, G.A, Meyer, B.K, Rich, F.J., and Reichard, J.S., 2011. St. Catherines Island, Georgia: Sag Structures, Hydrology, and Sea Level Rise. Southeastern Section Geological Society of America, 60th Annual Meeting, Wilmington, N.C.
- Vance, R.K., and Pirkle, F.L., 2007. An overview of titanium concentration in heavy mineral sand ore deposits. In F.J. Rich (editor), Guide to field trips, 56th Annual Meeting Southeastern Section of the Geological Society of America, Savannah, GA: 177-185. Georgia Southern University Department of Geology and Geography, Contribution Series 1.
- van de Plassche, O., 1986. Sea-level Research: A Manual for the Collection and Evaluation of Data. Kluwer Academic Publishers, 618 pp.
- van de Plassche, O., 1989. Submergence of Coastal Connecticut 6000-3000 (14C) Years B.P. Marine Geology, 86, p. 349-354.
- van de Plassche, O., 1990. Mid-Holocene Sea-level Change on the Eastern Shore of Virginia. Marine Geology, 91, p. 149-154
- Vento, F.J., and Stahlman, P.A., 2011. Development of a late Pleistocene-Holocene genetic stratigraphic framework for St. Catherines Island, Georgia: implications in archaeology.

Geoarchaeology of St. Catherines Island, Georgia, Anthropological Papers of the American Museum of Natural History, No. 94.

Wadsworth, J.R., 1981. Structural control of drainage morphology of salt marshes on St.

Catherines Island, Georgia. Georgia Marine Science Center, Univ. System of Georgia, Skidaway Island, GA., 43 p.

Weimer, R.J. and Hoyt, J.H. 1964, Burrows of *Callianassa major* (Say), geologic indicators of littoral and shallow neritic environments. *Journal of Paleontology* 38, pp. 761-767.

Winchester, J., Max, M., 1996. Chemostratigraphic correlation, structure and sedimentary environments in the Dalradian of the NW County Mayo inlier, NW Ireland. *Journal of the Geological Society of London*, Volume 153, pp. 779–801.

Winker, C.D., and J.D. Howard, 1977. Correlation of tectonically deformed shorelines on the southern Atlantic coastal plain. *Geology*, No. 5: pp. 123–127.

## APPENDICES

## Appendix A: Shoreline Dynamics Model Results

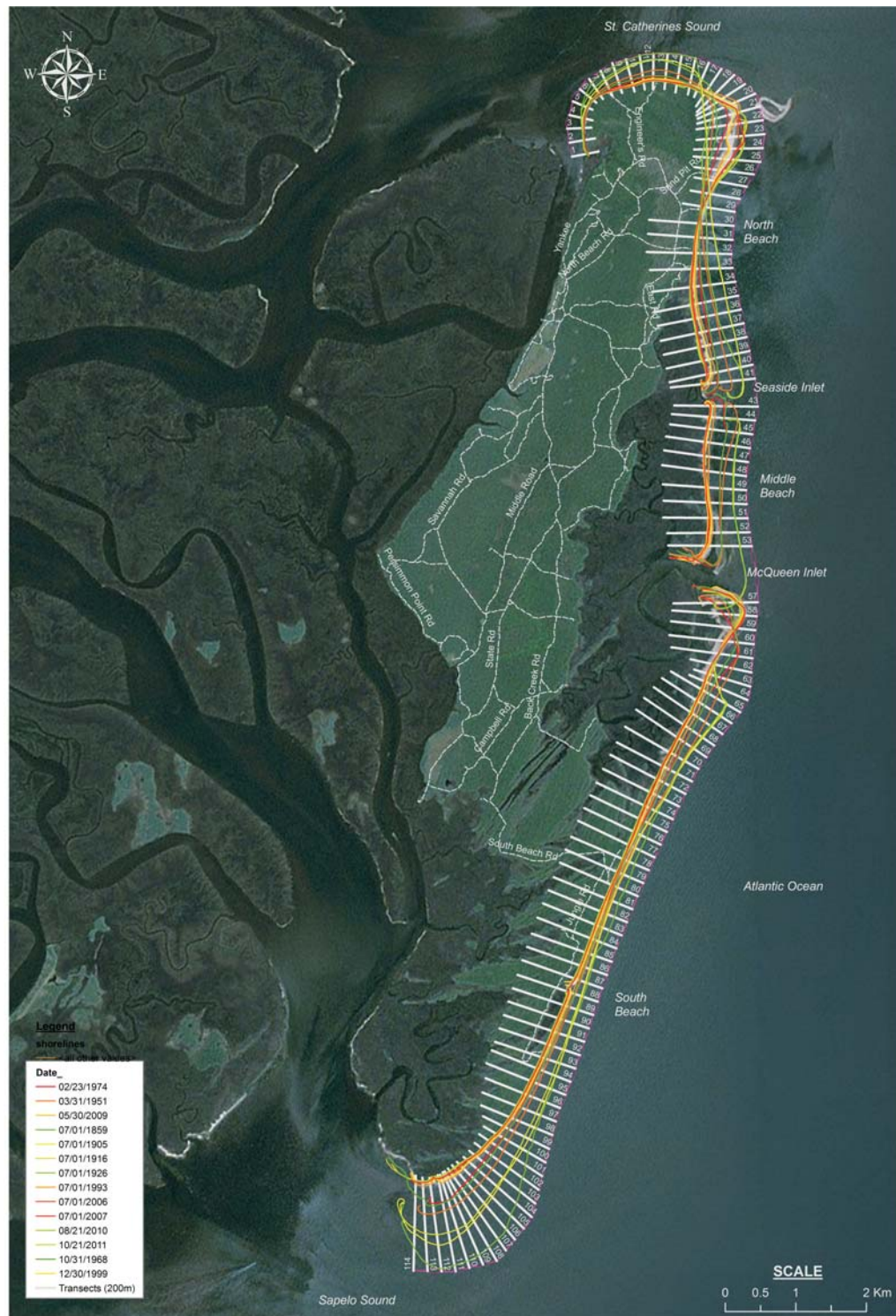


Figure A-1: Time series data for 2011, 2010, 2009, 2007, 2006, 1999, 1993, 1974, 1968, 1951, 1916, and 1859 were obtained from historical aerial imagery, historical maps and GPS sources. Transects were cast every 200 meters and statistics of shoreline change were generated. Basemap USDA NAIP (2009).



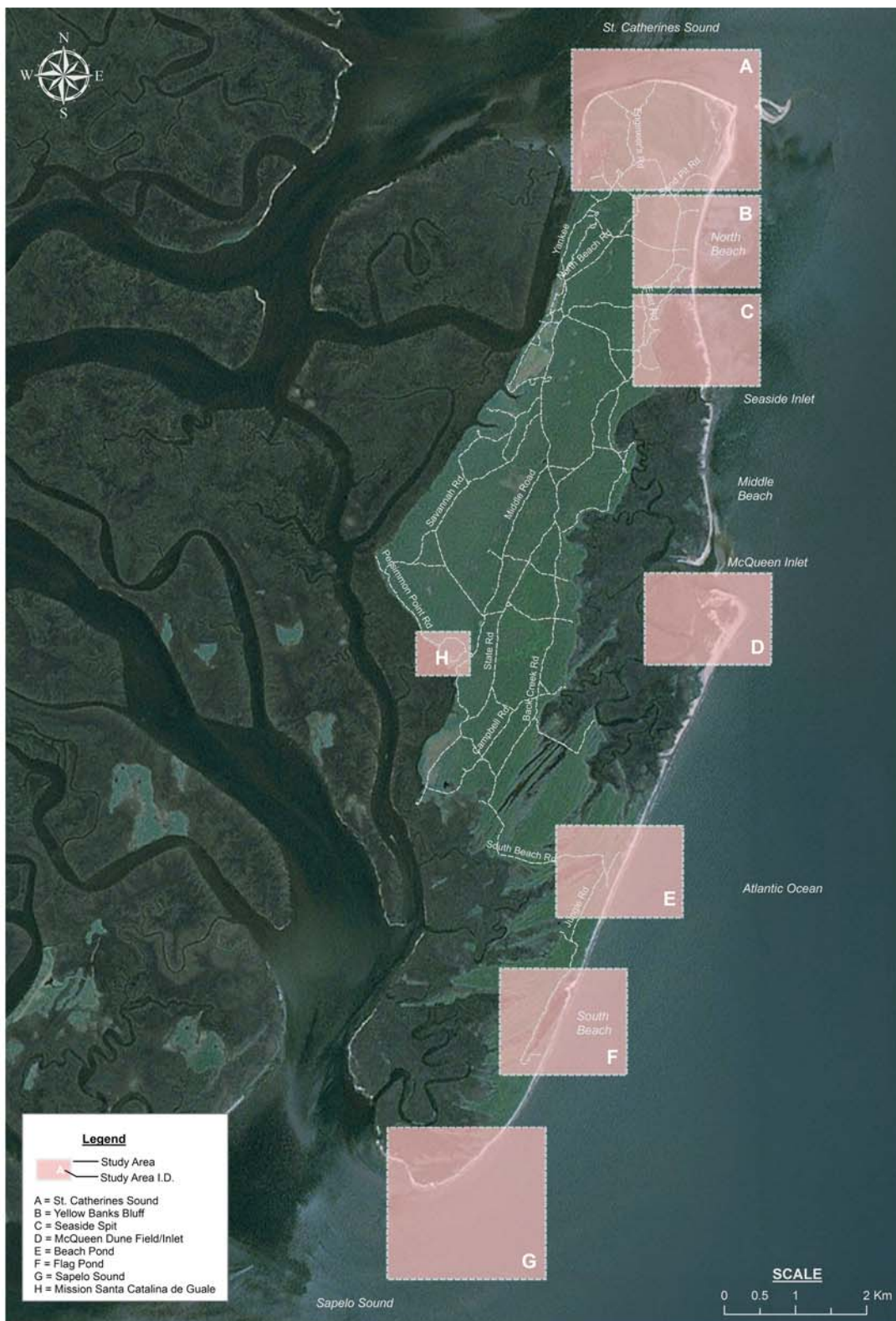


Figure A-2: Index map to detailed study areas for DSAS results and landform changes. Study areas include the northern end of the island (A), Yellow Banks Bluff (B), Seaside Spit (C), McQueen Inlet (D), Beach Pond (E), Flag Pond (F), and the southern end of the island (G). Basemap USDA NAIP (2009).



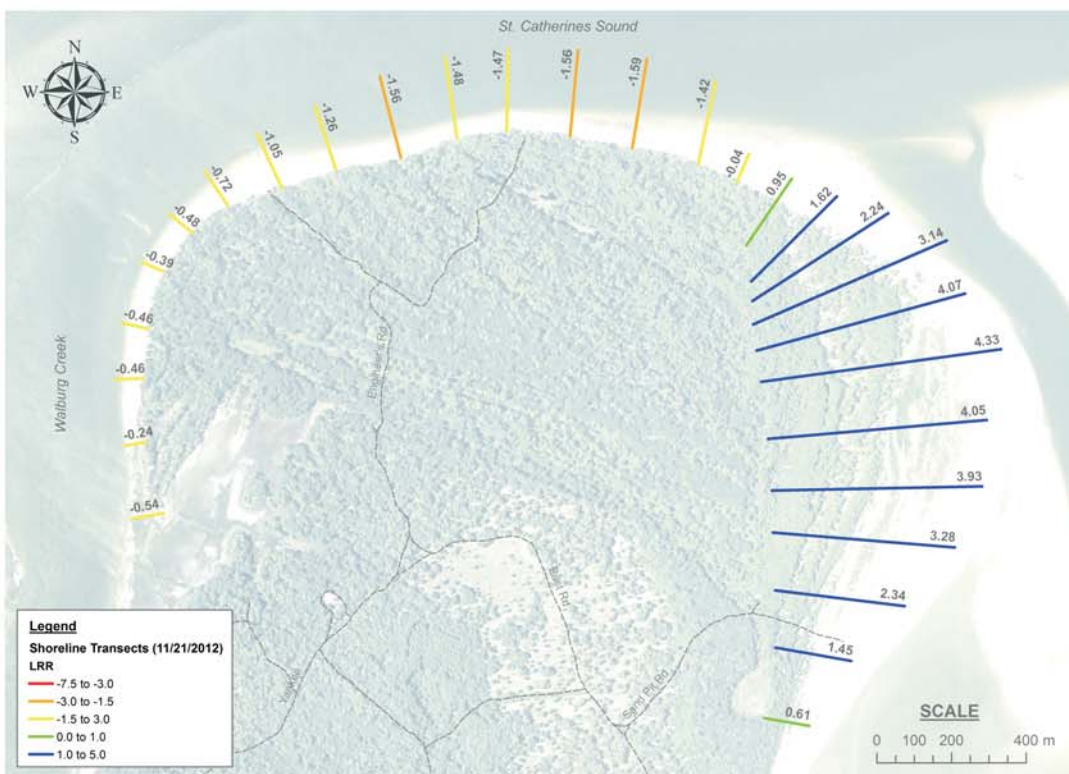
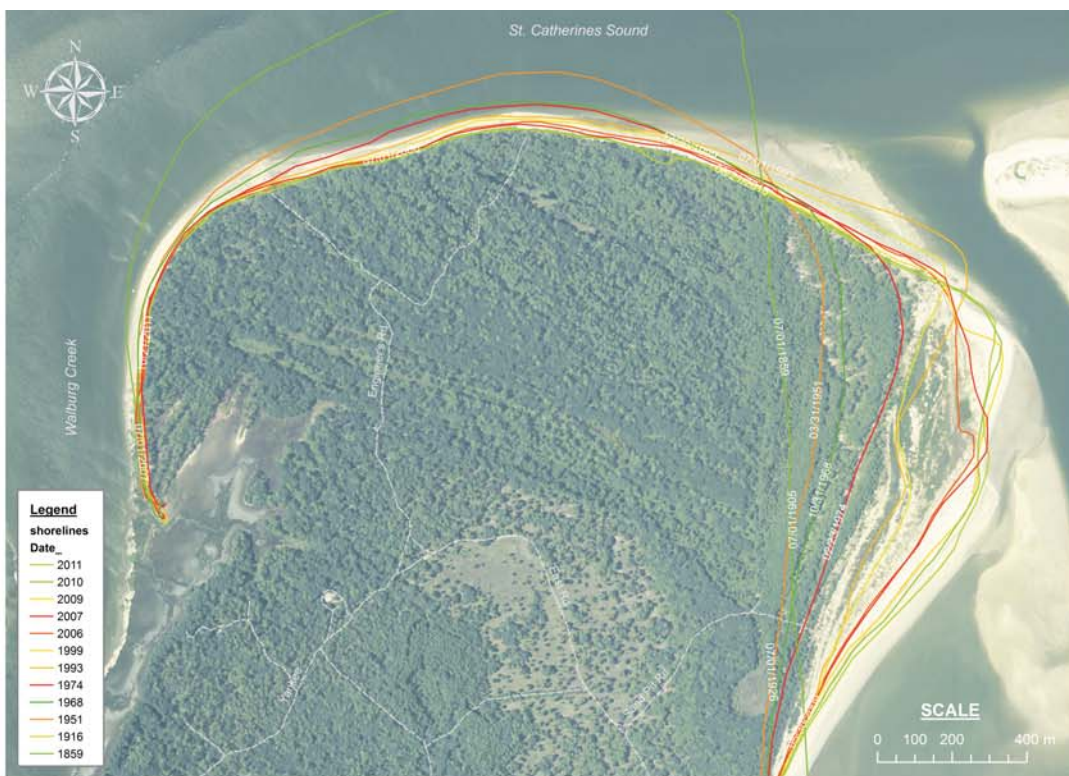


Figure A-3: Shoreline dynamics modeling results for the north end of St. Catherines Island, GA. Results showing moderate erosion on the northwest and northern portion of the island and significant accretion on the northeastern lobe of the island. Basemap image from USDA NAIP Imagery (2009).

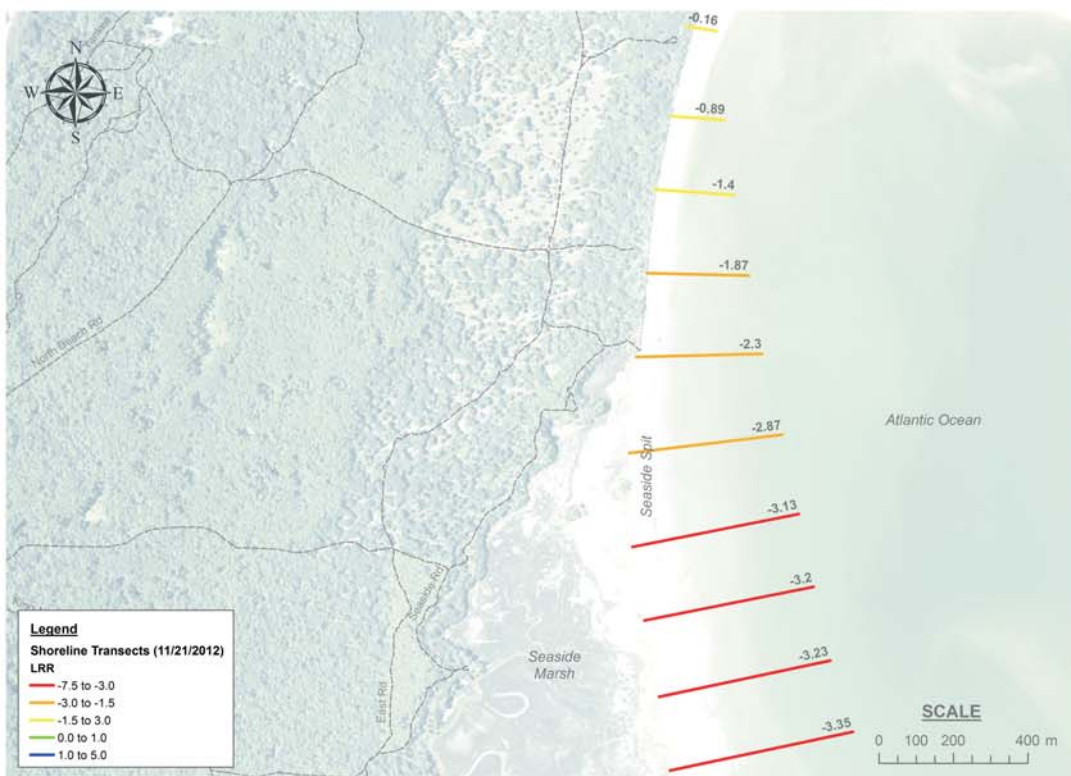
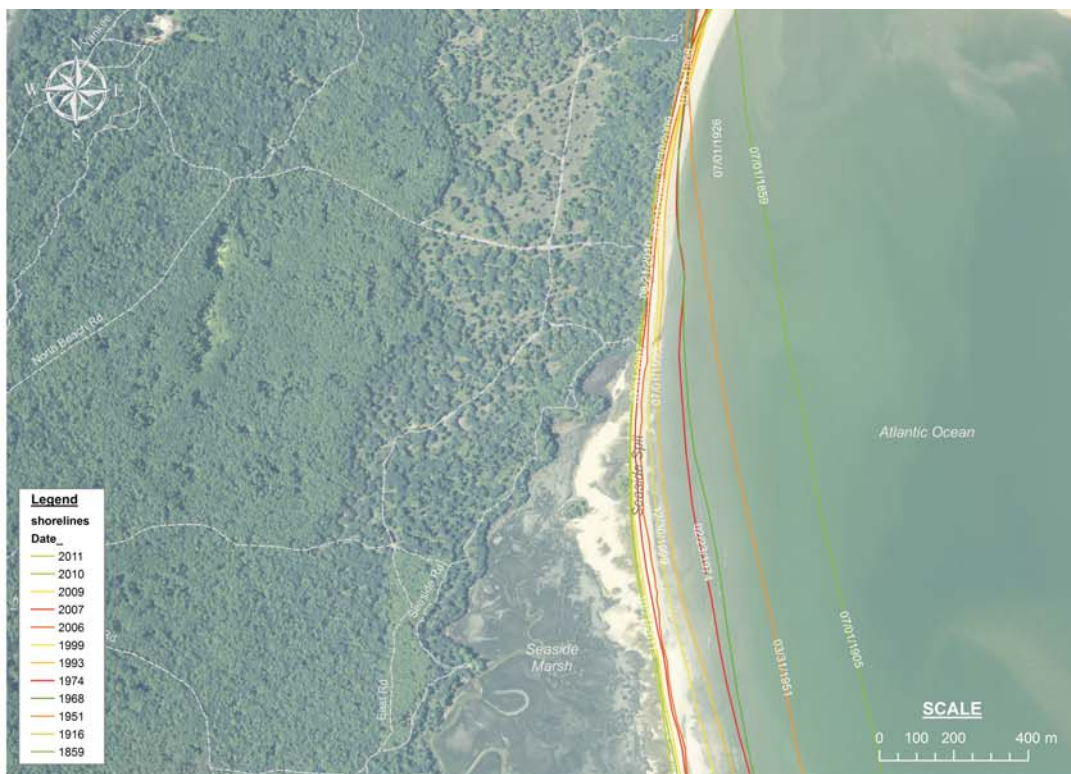


Figure A-4: Shoreline dynamics modeling results for the Yellow Bnaks Bluff area indicating moderate erosion or shoreline retreat rates of approx. 1 to 2 m/yr with rates increasing to the south on Seaside Spit of > 3 m/yr. Basemap image from USDA NAIP Imagery (2009).



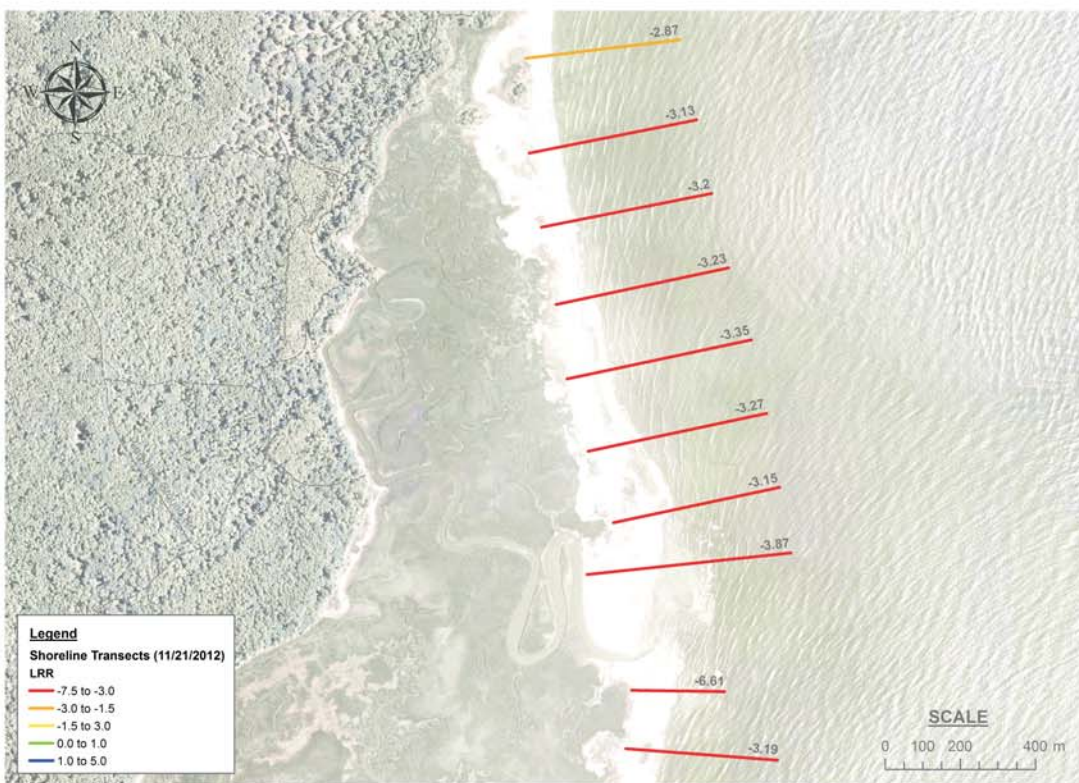


Figure A-5: Shoreline dynamics modeling results for the south end of Seaside Spit. Results indicate erosion rates of > 3.0 m/yr along Seaside Spit. Basemap image from USDA NAIP (2009).





Figure A-6: Shoreline dynamics modeling results for the area located to the south of McQueen Inlet, results indicate net accretion immediately south of the inlet and appreciable rates of erosion to the south. Basemap image USDA NAIP (2009).



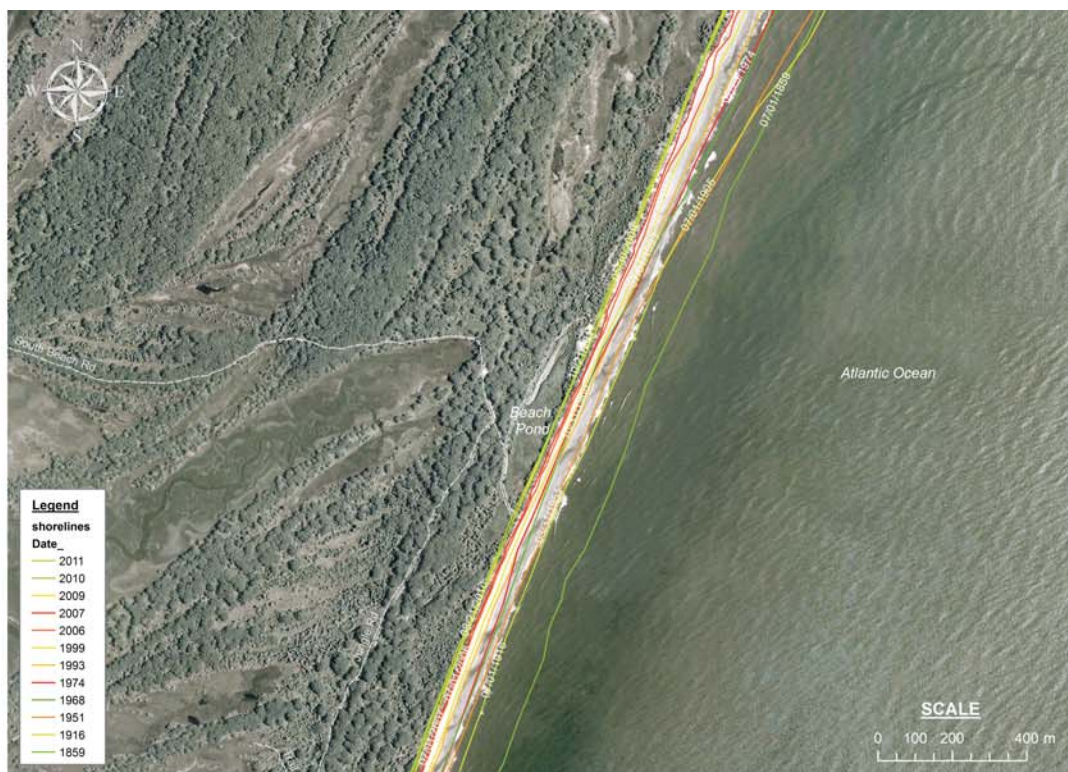


Figure A-7: Shoreline dynamics modeling results for the area located near Beach Pond. Results indicate erosional rates of  $> 1.2$  m/yr in the South Beach area near Beach Pond. Basemap image from USDA NAIP Imagery (2007).



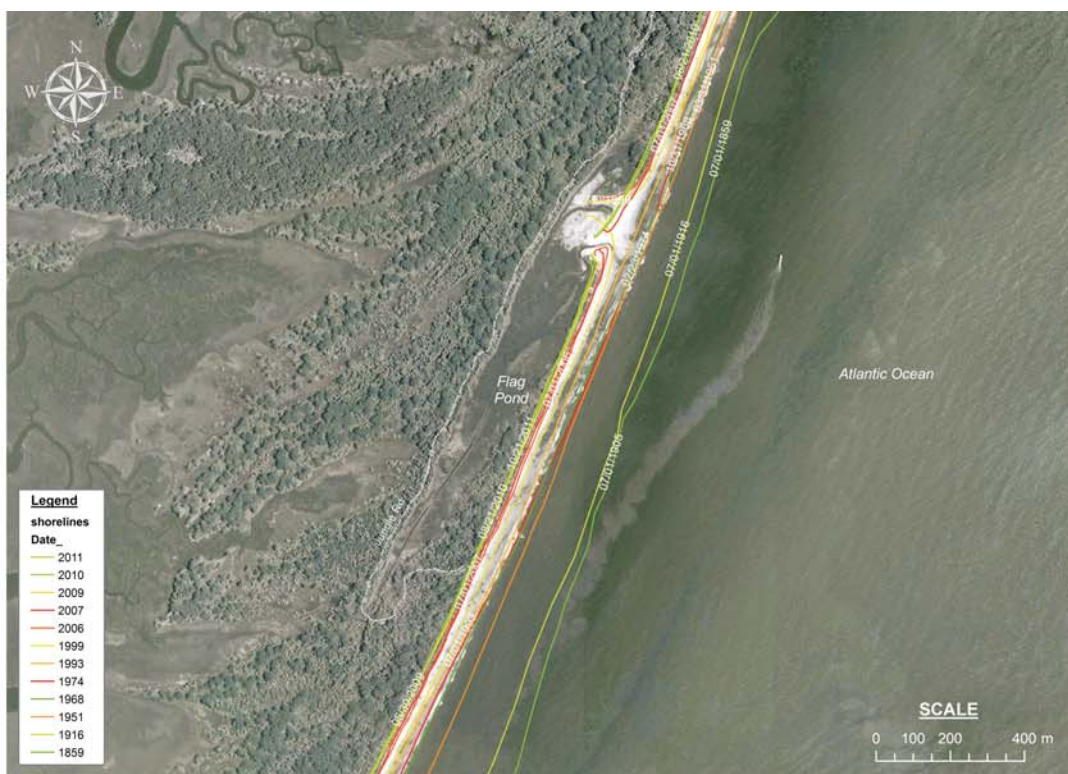


Figure A-8: Shoreline dynamics modeling results for the area located near Flag Pond. Results indicate erosional rates of approx. 2-3 m/yr in the South Beach area near Flag Pond. Basemap image from USDA NAIP Imagery (2007).

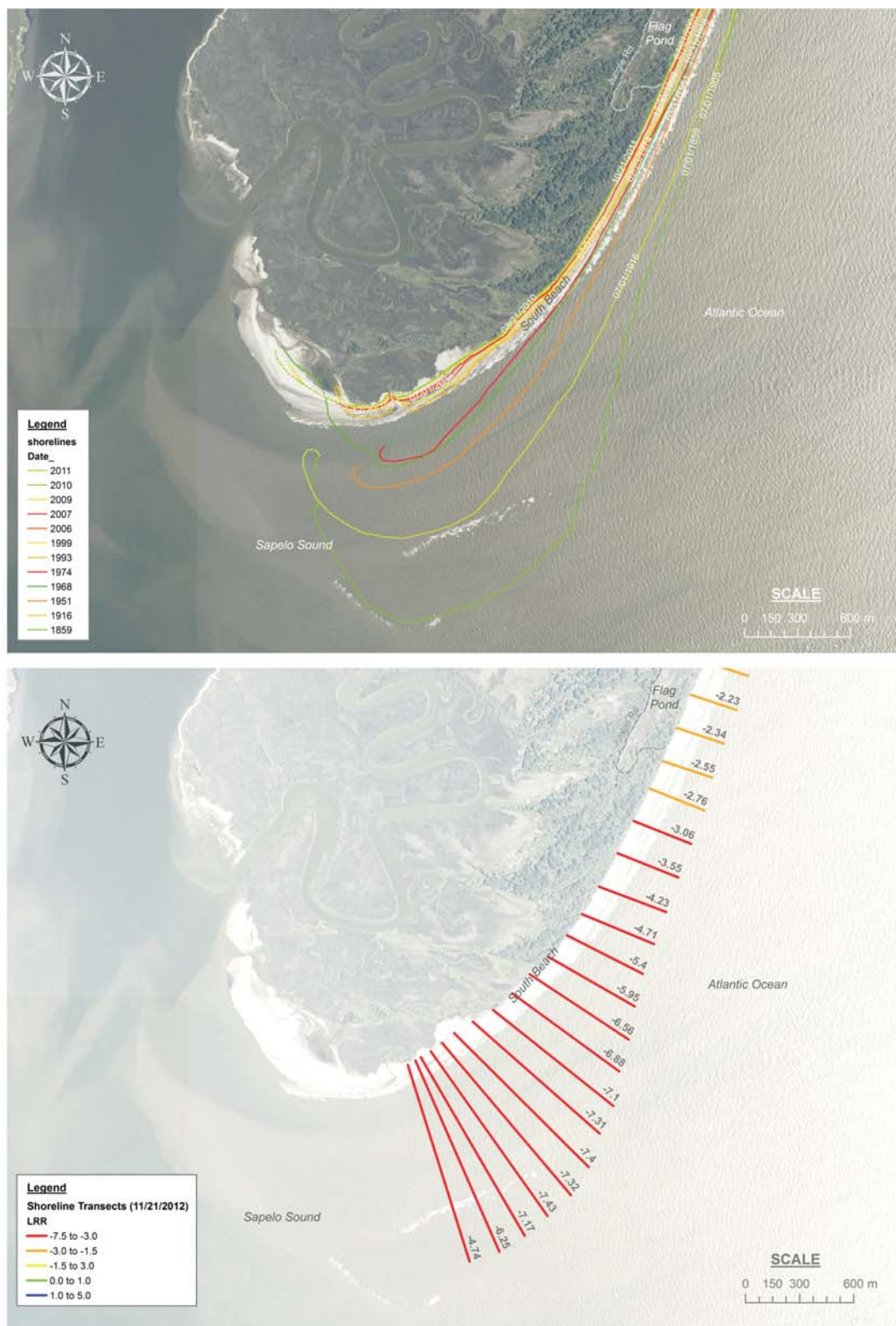







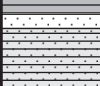
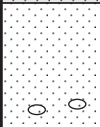
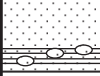


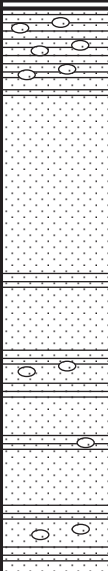



















Figure A-9: Shoreline dynamics modeling results for the south end of St. Catherines Island, GA. Results showing moderate erosion to the south of Flag Pond (2-3 m/yr) and appreciable shoreline retreat adjacent to Sapelo Sound ( $>7$  m/yr). Basemap image from USDA NAIP Imagery (2009).

### Appendix B: Vibracore Boring Logs

 <b>VIBRACORE BORING LOG</b> 		<b>LOCATION NUMBER: BKM 112010-01</b>		
		<b>PAGE NO. 1 OF 2</b>		
PROJECT NAME: PALEOTEMPESTOLOGY/STRATIGRAPHY RESEARCH		TOTAL DEPTH: 4.78 METERS (COMPACTED)/5.36 METERS (ORIGINAL)		
W.O. NUMBER: N/A		NORTHING: 486,918.23		
LOCATION: SEASIDE SPIT/MARSH, NORTH BEACH, SCI		EASTING: 3,503,920.19		
DRILLERS: MEYER, SKAGGS, AND VANCE		GROUND SURFACE ELEVATION: 6.05 ft MSL		
DRILL RIG TYPE: SCI VIBRACORE RIG		DEPTH TO TOP OF CORE: 50" BTOP		
DRILLING METHOD: VIBRACORE		HEIGHT ABOVE LAND SURFACE: 27" BTOP		
SAMPLING METHOD: 3-INCH I.D. ALUMINUM PIPE		COMPACTION (%): 10.9%		
LOGGED BY: B. MEYER WEATHER: COOL, CLOUDY		BOREHOLE DIAMETER: 3- INCH BOREHOLE		
DATE BEGUN: 11/20/10 DATE COMPLETED: 11/20/10		LOGGER SIGNATURE: _____		
DEPTH (m)	LITHOLOGIC DESCRIPTION	GRAPHIC LOG	PHOTOGRAPHIC LOG	COMMENTS
0	GROUND SURFACE DEVOID OF VEGETATION Sand, fine to very fine, quartz laminated with HMS, color 10YR 7/1 to 10YR 5/1, washover fan sequence unit, ripple marks in lower section overlain by more horizontal laminations, abrupt contact with underlying washover unit, no vegetation at surface or A horizon development.			land surface
	Sand, fine to very fine, quartz laminated with HMS, 10YR 2/1, washover fan sequence unit, ripple marks in lower section overlain by more horizontal laminations, weakly developed A horizon with peaty layer near top underlain by mottled interval, abrupt transition to upper washover unit.			Washover fan sequence
1.0	Peat with mud (clay with silt and little fine sand), dark gray-black, organic			BKM 112010-01-90, wood @ 90 cm
	Mud (clay with silt and little fine sand), dark gray-black, organic, oyster shells at 1.48-1.58 m BLS			BKM 112010-01-155, ostrea @ 155 cm
2.0				Intertidal Sequence Low Marsh Facies
	Sand, fine to very fine laminated with mud (clay/silt)			
	Mud (clay with silt and little fine sand), dark gray-black, organic			
	Sand, fine to very fine with mud (clay/silt) clasts, ripples and sand filled unlined burrows (1-3 cm)			Subtidal Sequence Transition Zone Bioturbated and Laminated Facies
3.0	Mud (clay with silt and little fine sand), dark gray-black, intensely burrowed interval at 3.10-3.35m BLS, sand filled and unlined burrows			



	<h2 style="margin: 0;">VIBRACORE BORING LOG</h2>		<b>LOCATION NUMBER: BKM 112010-01</b>	
			<b>PAGE NO. 2 OF 2</b>	
PROJECT NAME: <u>PALEOTEMPESTOLOGY/STRATIGRAPHY RESEARCH</u>		TOTAL DEPTH: <u>4.78 METERS (COMPACTED)/5.36 METERS (ORIGINAL)</u>		
W.O. NUMBER: <u>N/A</u>		NORTHING: <u>486,918.23</u>		
LOCATION: <u>SEASIDE SPIT/MARSH, NORTH BEACH, SCI</u>		EASTING: <u>3,503,920.19</u>		
DRILLERS: <u>MEYER, SKAGGS, AND VANCE</u>		GROUND SURFACE ELEVATION: <u>6.05 ft MSL</u>		
DRILL RIG TYPE: <u>SCI VIBRACORE RIG</u>		DEPTH TO TOP OF CORE: <u>50" BTOP</u>		
DRILLING METHOD: <u>VIBRACORE</u>		HEIGHT ABOVE LAND SURFACE: <u>27" BTOP</u>		
SAMPLING METHOD: <u>3-INCH I.D. ALUMINUM PIPE</u>		COMPACTION (%): <u>10.9%</u>		
LOGGED BY: <u>B. MEYER</u> WEATHER: <u>COOL, CLOUDY</u>		BOREHOLE DIAMETER: <u>3- INCH BOREHOLE</u>		
DATE BEGUN: <u>11/20/10</u> DATE COMPLETED: <u>11/20/10</u>		LOGGER SIGNATURE: _____		
DEPTH (m)	LITHOLOGIC DESCRIPTION	GRAPHIC LOG	PHOTOGRAPHIC LOG	COMMENTS
3.0	Fine to very fine sand with mud (clay with silt) laminae, dark gray-black, intensely burrowed interval at 3.10-3.35m BLS			<i>unlined and sand filled burrows 3.10-3.35m</i>
4.0	Sand, fine to very fine with mud (clay/silt) laminae, burrowed			<i>Subtidal Sequence Transition Zone Bioturbated and Laminated Facies</i>
	Sand, fine to medium with mud (clay/silt) laminae and clasts, coarse sand (1-2 mm) lag at 4.57-4.58 m BLS			<i>fine gravel - coarse sand lag (4.57m)</i>
	BORING TERMINATED AT 4.78 METERS BLS			
5.0				
6.0				

 <b>VIBRACORE BORING LOG</b> 		<b>LOCATION NUMBER: BKM 112110-01</b>		
		<b>PAGE NO. 1 OF 2</b>		
PROJECT NAME: <u>PALEOTEPESTOLOGY/STRATIGRAPHY RESEARCH</u>		TOTAL DEPTH: <u>4.71 METERS (COMPACTED)</u>		
W.O. NUMBER: <u>N/A</u>		NORTHING: <u>3,503,630.37</u>		
LOCATION: <u>SEASIDE SPIT, SCI</u>		EASTING: <u>486,975.32</u>		
DRILLERS: <u>MEYER, VANCE, SKAGGS</u>		GROUND SURFACE ELEVATION: <u>3.41 FT MSL</u>		
DRILL RIG TYPE: <u>SCI VIBRACORE RIG</u>		DEPTH TO TOP OF CORE: <u>41.75" BTOP</u>		
DRILLING METHOD: <u>VIBRACORE</u>		HEIGHT ABOVE LAND SURFACE: <u>26" BTOP</u>		
SAMPLING METHOD: <u>3-INCH I.D. ALUMINUM PIPE</u>		COMPACTION (%): <u>7.5%</u>		
LOGGED BY: <u>B. MEYER</u> WEATHER: <u>COOL, CLEAR</u>		BOREHOLE DIAMETER: <u>3- INCH BOREHOLE</u>		
DATE BEGUN: <u>11/21/10</u> DATE COMPLETED: <u>11/21/10</u>		LOGGER SIGNATURE: _____		
DEPTH (m)	LITHOLOGIC DESCRIPTION	GRAPHIC LOG	PHOTOGRAPHIC LOG	COMMENTS
0	GROUND SURFACE SPARSELY VEGETATED Sand, fine , laminated essentially horizontal (0-29cm) with some HMS, color 10YR 7/1 to 10YR 5/1, subangular			<i>land surface</i>
	Sand, fine , laminated ripple marks (29-51cm) with moderate HMS, color 10YR 3/1, subangular			<i>Washover fan sequence</i>
	Fine - v. fine sand with mud (clay/silt) , 10YR 2/1, organic, abund. plant fragments - Spartina (51-67cm)			<i>Spartina peat</i>
	Sand, fine , laminated essentially horizontal (67-85cm) with HMS, color 10YR 7/1 to 10YR 5/1			<i>Spartina peat</i>
1.0	Mud (clay with silt and little fine sand), dark gray-black (10YR 10YR 2/1), organic with Spartina fragments (85cm-96cm) former surface at 85cm?			
	Mud (clay with silt and little fine sand), dark gray-black (10YR 10YR 2/1), organic with few Spartina fragments (96-220cm)			<i>Intertidal Sequence Low Marsh Facies</i>
2.0				
	Sand, fine to v. fine with mud (clay/silt), dark gray-black (10YR 2/1)			
3.0	Sand, fine to very fine with mud (clay/silt) clasts, ripples and sand filled unlined burrows (1-3 cm), 10YR 5/1			<i>Subtidal Sequence Transition Zone Bioturbated and Laminated Facies</i>





## VIBRACORE BORING LOG











**LOCATION NUMBER:  
BKM 112110-02**






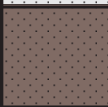

**PAGE NO. 1 OF 2**



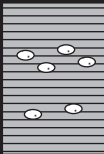





PROJECT NAME: PALEOTEMPESTOLOGY/STRATIGRAPHY RESEARCH W.O. NUMBER: N/A LOCATION: SEASIDE SPIT/MARSH, NORTH BEACH, SCI DRILLERS: MEYER, SKAGGS, AND VANCE DRILL RIG TYPE: SCI VIBRACORE RIG DRILLING METHOD: VIBRACORE SAMPLING METHOD: 3-INCH I.D. ALUMINUM PIPE LOGGED BY: B. MEYER WEATHER: COOL, CLEAR DATE BEGUN: 11/21/10 DATE COMPLETED: 11/21/10	TOTAL DEPTH: 5.07 METERS (COMPACTED) NORTHING: 3,503,650.41 EASTING: 487,023.08 GROUND SURFACE ELEVATION: 3.89 FT MLS DEPTH TO TOP OF CORE: 40" BTOP HEIGHT ABOVE LAND SURFACE: 29" BTOP COMPACTION (%): 5.1% BOREHOLE DIAMETER: 3- INCH BOREHOLE LOGGER SIGNATURE:
---	---

DEPTH (m)	LITHOLOGIC DESCRIPTION	GRAPHIC LOG	PHOTOGRAPHIC LOG	COMMENTS
0	Sand, fine , laminated essentially horizontal (0-13cm) with moderate HMS, color 10YR, Modern Beach			<i>land surface</i> <i>Intertidal Sequence</i> <i>Modern Upper Forebeach</i> <i>Laminated Facies</i>
	Fine - v. fine sand with mud (clay/silt ), 10YR ??, organic, abund. plant fragments - Spartina (13-25cm) in living position, former surface			<i>Spartina peat</i> <i>Washover fan sequence</i>
	Sand, fine , laminated ripple marks (27-47cm) with moderate HMS, color 10YR 3/1, subangular			
1.0	Sand, fine , laminated essentially horizontal (65-83cm) with HMS, color 10YR 7/1 to 10YR 5/1, subangular to subrounded, washover fan sequence			<i>Spartina peat</i>
	Mud (clay with silt and little fine sand), dark gray-black (10YR 10YR 2/1), organic with Spartina fragments (83cm-94cm) former surface at 79cm?			
	Mud (clay with silt and little fine sand), dark gray-black (10YR 10YR 2/1), organic with few Spartina fragments (94-215cm)		<i>Intertidal Sequence</i> <i>Low Marsh</i> <i>Facies</i>	
2.0				
	215-295 cm: Sand, fine to v. fine with mud (clay/silt), dark gray-black (10YR 2/1)			
3.0	Fine sand with mud (clay/silt) clasts and laminae, 10YR 5/1 with small diameter burrows (3-5mm)		<i>Subtidal Sequence</i> <i>Transition Zone</i> <i>Bioturbated and Laminated</i> <i>Facies</i>	





	<b>VIBRACORE BORING LOG</b>		<b>LOCATION NUMBER: BKM 050911-01</b>	
			<b>PAGE NO. 1 OF 1</b>	
PROJECT NAME: PALEOTEMPESTOLOGY/STRATIGRAPHY RESEARCH		TOTAL DEPTH: 1.30 METERS (COMPACTED)/1.30 METERS (ORIGINAL)		
W.O. NUMBER: N/A		NORTHING: 3,503,644		
LOCATION: SEASIDE SPIT, SCI		EASTING: 487,005		
DRILLERS: MEYER, SHOREDITS, SMITH		GROUND SURFACE ELEVATION: 5.35 ft MSL		
DRILL RIG TYPE: SCI VIBRACORE RIG		DEPTH TO TOP OF CORE: 28" BTOP		
DRILLING METHOD: VIBRACORE		HEIGHT ABOVE LAND SURFACE: 28" BTOP		
SAMPLING METHOD: 3-INCH I.D. ALUMINUM PIPE		COMPACTION (%): 0.0%		
LOGGED BY: B. MEYER WEATHER: HOT, HUMID		BOREHOLE DIAMETER: 3- INCH BOREHOLE		
DATE BEGUN: 05/09/11 DATE COMPLETED: 05/09/11		LOGGER SIGNATURE: _____		
DEPTH (m)	LITHOLOGIC DESCRIPTION	GRAPHIC LOG	PHOTOGRAPHIC LOG	COMMENTS
0	0-20 cm: Very fine quartz sand with HMS, some plant material/organics, HMS laminations at high angle.			<i>land surface</i>
	20-47 cm: Very fine quartz sand with little HMS.			<i>Intertidal Sequence Backbeach/Berm Laminated and Burrowed Facies</i>
	47-70 cm: Very fine quartz sand with appreciable HMS, medium-dark gray, horizontal laminations.			<i>Washover fan sequence</i>
1.0	70-113 cm: Very fine quartz sand with some HMS, light-medium gray, faint horizontal laminations.			<i>Intertidal Sequence Low Marsh Facies</i>
	113-130 cm: Very fine quartz sand with some HMS and mud, light-medium brown gray.			
	BORING REFUSAL AT 1.30 METERS BLS			
2.0				
3.0				


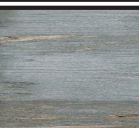
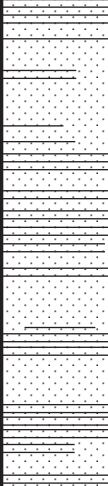

 <b>VIBRACORE BORING LOG</b> 		<b>LOCATION NUMBER: BKM 050911-02</b>		
		<b>PAGE NO. 1 OF 2</b>		
PROJECT NAME: PALEOTEMPESTOLOGY/STRATIGRAPHY RESEARCH		TOTAL DEPTH: 1.50 METERS (COMPACTED)/1.50 METERS (ORIGINAL)		
W.O. NUMBER: N/A		NORTHING: 3,503,636		
LOCATION: SEASIDE SPIT, SCI		EASTING: 486,987		
DRILLERS: MEYER, SHOREDITS, SMITH		GROUND SURFACE ELEVATION: 5.35 ft MSL		
DRILL RIG TYPE: SCI VIBRACORE RIG		DEPTH TO TOP OF CORE: 28" BTOP		
DRILLING METHOD: VIBRACORE		HEIGHT ABOVE LAND SURFACE: 28" BTOP		
SAMPLING METHOD: 3-INCH I.D. ALUMINUM PIPE		COMPACTION (%): 0.0%		
LOGGED BY: B. MEYER WEATHER: HOT, HUMID		BOREHOLE DIAMETER: 3- INCH BOREHOLE		
DATE BEGUN: 05/09/11 DATE COMPLETED: 05/09/11		LOGGER SIGNATURE: _____		
DEPTH (m)	LITHOLOGIC DESCRIPTION	GRAPHIC LOG	PHOTOGRAPHIC LOG	TBD RESULTS COMMENTS
0	0-20 cm: Very fine quartz sand with HMS, bioturbated, no apparent bedding.			<i>land surface</i>
	20-80 cm: Very fine quartz sand, light gray, near horizontal laminations, burrowed, with appreciable			<i>Washover Fan Sequence</i>
1.0	80-110 cm: Very fine quartz sand, light brown-gray, roots at 90 cm indicating former surface at 80 cm, near			
	110-150 cm: Mud (silt/clay) with very fine sand, dark gray (N), sand filled burrow at 140 cm.			<i>Intertidal Sequence Low Marsh Facies</i>
	BORING TERMINATED AT 1.50 METERS BLS			
2.0				
3.0				

 <b>VIBRACORE BORING LOG</b> 		<b>LOCATION NUMBER: BKM 050911-03</b>		
		<b>PAGE NO. 1 OF 2</b>		
PROJECT NAME: PALEOTEMPESTOLOGY/STRATIGRAPHY RESEARCH		TOTAL DEPTH: 4.88 METERS (COMPACTED)/5.18 METERS (ORIGINAL)		
W.O. NUMBER: N/A		NORTHING: 3,503,631		
LOCATION: SEASIDE SPIT, SCI		EASTING: 486,962		
DRILLERS: MEYER, SHOREDITS, SMITH		GROUND SURFACE ELEVATION: 2.33 ft MSL		
DRILL RIG TYPE: SCI VIBRACORE RIG		DEPTH TO TOP OF CORE: 38" BTOP		
DRILLING METHOD: VIBRACORE		HEIGHT ABOVE LAND SURFACE: 26" BTOP		
SAMPLING METHOD: 3-INCH I.D. ALUMINUM PIPE		COMPACTION (%): 5.9%		
LOGGED BY: B. MEYER WEATHER: HOT, HUMID		BOREHOLE DIAMETER: 3- INCH BOREHOLE		
DATE BEGUN: 05/09/11 DATE COMPLETED: 05/09/11		LOGGER SIGNATURE: _____		
DEPTH (m)	LITHOLOGIC DESCRIPTION	GRAPHIC LOG	PHOTOGRAPHIC LOG	COMMENTS
0	0-50 cm: Mud (silt/clay), burrowed. Burrows filled with very fine quartz sand, some plant material/organics.			<i>land surface</i>
1.0	50-285 cm: Mud (clay with silt and little fine sand), dark gray-black (10YR 10YR 2/1), organic with few Spartina fragments in upper section.			<i>Intertidal Sequence Low Marsh Facies</i>
2.0				
3.0	285-338: Sand, fine to v. fine with mud (clay/silt), dark gray-black (10YR 2/1)			
f:\misc documents\sci_logs\BKM050911_03.cdr				









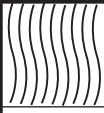



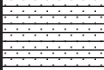

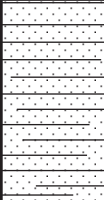


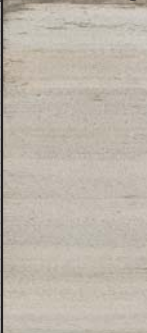
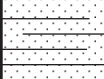

	<h2 style="margin: 0;">VIBRACORE BORING LOG</h2>		<b>LOCATION NUMBER: BKM 050911-03</b>
			<b>PAGE NO. 2 OF 2</b>
PROJECT NAME: PALEOTEMPESTOLOGY/STRATIGRAPHY RESEARCH		TOTAL DEPTH: 4.88 METERS (COMPACTED)/5.18 METERS (ORIGINAL)	
W.O. NUMBER: N/A		NORTHING: 3,503,631	
LOCATION: BEACH POND, SCI		EASTING: 486,962	
DRILLERS: MEYER, SHOREDITS, SMITH		GROUND SURFACE ELEVATION: 2.33 ft MSL	
DRILL RIG TYPE: SCI VIBRACORE RIG		DEPTH TO TOP OF CORE: 38" BTOP	
DRILLING METHOD: VIBRACORE		HEIGHT ABOVE LAND SURFACE: 26" BTOP	
SAMPLING METHOD: 3-INCH I.D. ALUMINUM PIPE		COMPACTION (%): 5.9%	
LOGGED BY: B. MEYER WEATHER: HOT, HUMID		BOREHOLE DIAMETER: 3- INCH BOREHOLE	
DATE BEGUN: 05/10/11 DATE COMPLETED: 05/10/11		LOGGER SIGNATURE: _____	



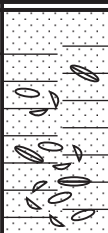

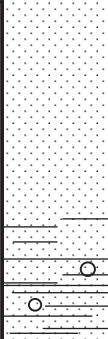

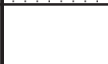

  





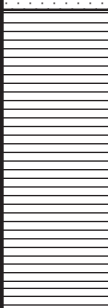

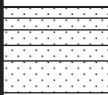



DEPTH (m)	LITHOLOGIC DESCRIPTION	GRAPHIC LOG	PHOTOGRAPHIC LOG	COMMENTS
3.0	285-338: Sand, fine to v. fine with mud (clay/silt), dark gray-black (10YR 2/1)			<i>Intertidal Sequence Low Marsh Facies</i>
4.0	338-488 cm: Sand, fine to very fine with mud (clay/silt) laminae and clasts, rip-ups and sand filled unlined burrows (1-3 cm), 10YR 5/1. Mud laminae and clasts (clay with silt and little fine sand), dark gray-black (10YR 2/1).			<i>Subtidal Sequence Transition Zone Bioturbated and Laminated Facies</i>  BKM 050911-03-440, shell @ 440 cm
5.0	BORING REFUSAL AT 4.88 METERS BLS			
6.0				





f:\misc documents\sci\_logs\BKM050911\_03.cdr







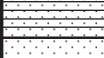



	<h2 style="margin: 0;">VIBRACORE BORING LOG</h2>		<b>LOCATION NUMBER: BKM 051011-01</b>	
			<b>PAGE NO. 1 OF 2</b>	
PROJECT NAME: <u>PALEOTEMPESTOLOGY/STRATIGRAPHY RESEARCH</u>		TOTAL DEPTH: <u>1.37 METERS (COMPACTED)</u>		
W.O. NUMBER: <u>N/A</u>		NORTHING: <u>3,495,895 m</u>		
LOCATION: <u>BEACH POND, SCI</u>		EASTING: <u>485,792 m</u>		
DRILLERS: <u>MEYER, SMITH, SHOREDITS</u>		GROUND SURFACE ELEVATION: <u>6.95 ft MSL</u>		
DRILL RIG TYPE: <u>SCI VIBRACORE RIG</u>		DEPTH TO TOP OF CORE: <u>24" BTOP</u>		
DRILLING METHOD: <u>VIBRACORE</u>		HEIGHT ABOVE LAND SURFACE: <u>20" BTOP</u>		
SAMPLING METHOD: <u>3-INCH I.D. ALUMINUM PIPE</u>		COMPACTION (%): <u>6.9%</u>		
LOGGED BY: <u>B. MEYER</u> WEATHER: <u>HOT, HUMID</u>		BOREHOLE DIAMETER: <u>3-INCH BOREHOLE</u>		
DATE BEGUN: <u>05/10/11</u> DATE COMPLETED: <u>05/10/11</u>		LOGGER SIGNATURE: _____		
DEPTH (m)	LITHOLOGIC DESCRIPTION	GRAPHIC LOG	PHOTOGRAPHIC LOG	COMMENTS
0	GROUND SURFACE VEGETATED - PALMETTO			<i>land surface</i>
	0-5 cm: Sand, dark brown-gray, A-horizon, fine to very fine sand, mottled with abundant plant and			<i>Intertidal Sequence Backbeach/Berm Laminated and Bioturbated Facies</i>
	5-20 cm: Sand, lt. brown-gray, E-horizon, fine to very fine sand, mottled with few plant and root			
	20-90 cm: Sand, lt. brown, fine to very fine,			
1.0	90-137 cm: Sand, fine to very fine, horizontal			<i>Intertidal Sequence Upper Forebeach Laminated Facies</i>
	BORING REFUSAL AT 1.37 METERS BLS			
2.0				
3.0				





 <b>VIBRACORE BORING LOG</b> 		<b>LOCATION NUMBER: BKM 051011-02</b>		
		<b>PAGE NO. 1 OF 2</b>		
PROJECT NAME: PALEOTEMPESTOLOGY/STRATIGRAPHY RESEARCH		TOTAL DEPTH: 4.76 METERS (COMPACTED)/5.47 METERS (ORIGINAL)		
W.O. NUMBER: N/A		NORTHING: 3,495,876		
LOCATION: BEACH POND, SCI		EASTING: 485,824		
DRILLERS: MEYER, SHOREDITS, SMITH		GROUND SURFACE ELEVATION: 2.48 ft MSL		
DRILL RIG TYPE: SCI VIBRACORE RIG		DEPTH TO TOP OF CORE: 52" BTOP		
DRILLING METHOD: VIBRACORE		HEIGHT ABOVE LAND SURFACE: 18" BTOP		
SAMPLING METHOD: 3-INCH I.D. ALUMINUM PIPE		COMPACTION (%): 15.3%		
LOGGED BY: B. MEYER WEATHER: HOT, HUMID		BOREHOLE DIAMETER: 3- INCH BOREHOLE		
DATE BEGUN: 05/10/11 DATE COMPLETED: 05/10/11		LOGGER SIGNATURE: _____		
DEPTH (m)	LITHOLOGIC DESCRIPTION	GRAPHIC LOG	PHOTOGRAPHIC LOG	COMMENTS
0	Peat (0-45 cm), soft dark brown, abundant plant material/organics with little mud (silt/clay), mud content increases with depth (5YR 2/1).			land surface Freshwater peat Spartina peat
	Mud (clay and silt and very little fine sand), dark gray-black (N3 to 10YR 2/1), organic (45 cm to 100 cm)			Intertidal Sequence Low Marsh Facies  BKM 051011-02-90, wood @ 90 cm
1.0	Sand with mud (clay and silt), dark gray-black (10YR 2/1), organic (100 cm to 125 cm)			
	Interlaminated sand (fine to very fine) with mud with cross-stratified fine sand beds (125 cm to 185 cm), wood fragment in lower section at 180 cm.			Intertidal Sequence High Marsh/Swale Fill (Sand/Mud Laminated Facies)  BKM 051011-02-185, wood @ 185 cm
2.0	Sand, fine bioturbated (no laminae/bedding), medium to light gray (5Y 8/1), with few fine sand-sized shell fragments (185 cm to 290 cm).			Foreshore Sequence (Laminated Facies)
3.0	Sand, fine bioturbated with some mud (silt/clay), 290 cm to 315 cm			Subtidal Sequence Transition Zone Bioturbated and Laminated Facies

 <b>VIBRACORE BORING LOG</b> 		<b>LOCATION NUMBER: BKM 051011-02</b>		
		<b>PAGE NO. 2 OF 2</b>		
PROJECT NAME: <u>PALEOTEMPESTOLOGY/STRATIGRAPHY RESEARCH</u>		TOTAL DEPTH: <u>4.76 METERS (COMPACTED)/5.47 METERS (ORIGINAL)</u>		
W.O. NUMBER: <u>N/A</u>		NORTHING: <u>3,495,876</u>		
LOCATION: <u>BEACH POND, SCI</u>		EASTING: <u>485,824</u>		
DRILLERS: <u>MEYER, SHOREDITS, SMITH</u>		GROUND SURFACE ELEVATION: <u>2.48 ft MSL</u>		
DRILL RIG TYPE: <u>SCI VIBRACORE RIG</u>		DEPTH TO TOP OF CORE: <u>52" BTOP</u>		
DRILLING METHOD: <u>VIBRACORE</u>		HEIGHT ABOVE LAND SURFACE: <u>18" BTOP</u>		
SAMPLING METHOD: <u>3-INCH I.D. ALUMINUM PIPE</u>		COMPACTION (%): <u>15.3%</u>		
LOGGED BY: <u>B. MEYER</u> WEATHER: <u>HOT, HUMID</u>		BOREHOLE DIAMETER: <u>3- INCH BOREHOLE</u>		
DATE BEGUN: <u>05/10/11</u> DATE COMPLETED: <u>05/10/11</u>		LOGGER SIGNATURE: _____		
DEPTH (m)	LITHOLOGIC DESCRIPTION	GRAPHIC LOG	PHOTOGRAPHIC LOG	COMMENTS
3.0	Sand, fine bioturbated (no laminae/bedding) with some mud (silt/clay) and <i>Mulinia</i> shells (whole and fragmented), 315 cm to 385 cm			<i>Subtidal Sequence Transition Zone Bioturbated and Laminated Facies</i>  BKM 051011-02-350, <i>Mulinia</i> @ 350 cm
4.0	385-440 cm: Sand, fine bioturbated (no laminae/bedding), small shell fragments  Sand, light gray (N7), fine bioturbated with mud flasers/laminae, coarsening upward, mud flasers/laminae increase downward, fine sand-sized shell fragments (440 cm to 476 cm)			<i>Intertidal Sequence Lower Forebeach Burrowed and Laminated Facies</i>  <i>Subtidal Sequence Transition Zone Bioturbated and Laminated Facies</i>
5.0	Sand, fine bioturbated with sand filled burrows at 450 cm and 460 cm, burrows ( <i>Thalassinoides</i> ) are slightly elliptical (2 cm x 1.5 cm) and cut across mud flasers/laminae, fine sand-sized shell fragments (440 cm to 476 cm).			
6.0	BORING REFUSAL AT 4.76 METERS BLS			



	<h2 style="margin: 0;">VIBRACORE BORING LOG</h2>		<b>LOCATION NUMBER: BKM 051011-03</b>	
			<b>PAGE NO. 1 OF 2</b>	
PROJECT NAME: <u>PALEOTEMPESTOLOGY RESEARCH</u>		TOTAL DEPTH: <u>3.61 METERS (COMPACTED)/3.61 METERS (ORIGINAL)</u>		
W.O. NUMBER: <u>N/A</u>		NORTHING: <u>3,495,859</u>		
LOCATION: <u>BEACH POND, SCI</u>		EASTING: <u>485,860</u>		
DRILLERS: <u>MEYER, SHOREDITS, SMITH</u>		GROUND SURFACE ELEVATION: <u>3.71 ft MSL</u>		
DRILL RIG TYPE: <u>SCI VIBRACORE RIG</u>		DEPTH TO TOP OF CORE: <u>96" BTOP</u>		
DRILLING METHOD: <u>VIBRACORE</u>		HEIGHT ABOVE LAND SURFACE: <u>96" BTOP</u>		
SAMPLING METHOD: <u>3-INCH I.D. ALUMINUM PIPE</u>		COMPACTION (%): <u>0%</u>		
LOGGED BY: <u>B. MEYER</u> WEATHER: <u>HOT, HUMID</u>		BOREHOLE DIAMETER: <u>3- INCH BOREHOLE</u>		
DATE BEGUN: <u>05/10/11</u> DATE COMPLETED: <u>05/10/11</u>		LOGGER SIGNATURE: _____		
DEPTH (m)	LITHOLOGIC DESCRIPTION	GRAPHIC LOG	PHOTOGRAPHIC LOG	COMMENTS
0	GROUND SURFACE DEVOID OF VEGETATION 0-13 cm: Peat material (Organic detritus/plant macromaterial), abundant plant fragments  13-67 cm: Sand, fine to very fine, extensively mottled with organic detritus, some heavy minerals, abrupt contact with muds below including rip-ups, washover fan material			<i>land surface</i> <i>Freshwater peat</i>  <i>Washover fan sequence</i>
1.0	67-162 cm: Mud (clay with silt and little fine sand), dark gray-black, organic with some plant fragments			<i>Intertidal Sequence</i> <i>Low Marsh Facies</i>
2.0	Sand, fine to very fine, with mud (clay/silt) and organic laminae, some clasts and rip-ups			<i>Intertidal Sequence</i> <i>High Marsh/Swale Fill</i> <i>(Sand/Mud Laminated Facies)</i>
3.0	Sand, fine to very fine, with few mud (clay/silt) clasts and rip-ups, faint laminations of quartz/heavy minerals			<i>Intertidal Sequence</i> <i>Upper Forebeach</i> <i>Laminated Facies</i>
F:\misc documents\sci_logs\BKM051011_03.cdr				

	<h2 style="margin: 0;">VIBRACORE BORING LOG</h2>		<b>LOCATION NUMBER: BKM 051011-03</b>	
			<b>PAGE NO. 2 OF 2</b>	
PROJECT NAME: <u>PALEOTEMPESTOLOGY RESEARCH</u>		TOTAL DEPTH: <u>3.61 METERS (COMPACTED)/3.61 METERS (ORIGINAL)</u>		
W.O. NUMBER: <u>N/A</u>		NORTHING: <u>3,495,859</u>		
LOCATION: <u>BEACH POND, SCI</u>		EASTING: <u>485,860</u>		
DRILLERS: <u>MEYER, SHOREDITS, SMITH</u>		GROUND SURFACE ELEVATION: <u>3.71 ft MSL</u>		
DRILL RIG TYPE: <u>SCI VIBRACORE RIG</u>		DEPTH TO TOP OF CORE: <u>96" BTOP</u>		
DRILLING METHOD: <u>VIBRACORE</u>		HEIGHT ABOVE LAND SURFACE: <u>96" BTOP</u>		
SAMPLING METHOD: <u>3-INCH I.D. ALUMINUM PIPE</u>		COMPACTION (%): <u>0%</u>		
LOGGED BY: <u>B. MEYER</u> WEATHER: <u>HOT, HUMID</u>		BOREHOLE DIAMETER: <u>3- INCH BOREHOLE</u>		
DATE BEGUN: <u>05/10/11</u> DATE COMPLETED: <u>05/10/11</u>		LOGGER SIGNATURE: _____		
DEPTH (m)	LITHOLOGIC DESCRIPTION	GRAPHIC LOG	PHOTOGRAPHIC LOG	COMMENTS
3.0	Sand, fine to very fine, quartz with little heavy minerals, few shell fragments			<i>Intertidal Sequence Upper Forebeach Laminated Facies</i>
	BORING REFUSAL AT 3.61 METERS BLS			
4.0				
5.0				
6.0				









	<h2 style="margin: 0;">VIBRACORE BORING LOG</h2>		<b>LOCATION NUMBER: BKM 051111-01</b>	
			<b>PAGE NO. 1 OF 2</b>	
PROJECT NAME: <u>PALEOTEMPESTOLOGY/STRATIGRAPHY RESEARCH</u>		TOTAL DEPTH: <u>3.92 METERS (COMPACTED)/4.03 METERS (ORIGINAL)</u>		
W.O. NUMBER: <u>N/A</u>		NORTHING: <u>3,495,847</u>		
LOCATION: <u>BEACH POND, SCI</u>		EASTING: <u>485,887</u>		
DRILLERS: <u>MEYER, SHOREDITS, SMITH</u>		GROUND SURFACE ELEVATION: <u>7.56 ft MSL</u>		
DRILL RIG TYPE: <u>SCI VIBRACORE RIG</u>		DEPTH TO TOP OF CORE: <u>67" BTOP</u>		
DRILLING METHOD: <u>VIBRACORE</u>		HEIGHT ABOVE LAND SURFACE: <u>62.5" BTOP</u>		
SAMPLING METHOD: <u>3-INCH I.D. ALUMINUM PIPE</u>		COMPACTION (%): <u>2.8%</u>		
LOGGED BY: <u>B. MEYER</u> WEATHER: <u>HOT, HUMID</u>		BOREHOLE DIAMETER: <u>3- INCH BOREHOLE</u>		
DATE BEGUN: <u>05/11/11</u> DATE COMPLETED: <u>05/11/11</u>		LOGGER SIGNATURE: _____		
DEPTH (m)	LITHOLOGIC DESCRIPTION	GRAPHIC LOG	PHOTOGRAPHIC LOG	COMMENTS
0	GROUND SURFACE DEVOID OF VEGETATION 0-8 cm: Light brown gray sand, fine to very fine, some disseminated HMS, beach berm.  8-163 cm: Light gray sand, fine to very fine, some disseminated HMS, faint laminations.			<i>land surface</i>  <i>Intertidal Sequence Modern Upper Forebeach Laminated Facies</i>
1.0				
2.0	163-243 cm: Mud (clay with silt and little fine sand), dark gray-black.			<i>Intertidal Sequence Low Marsh Facies</i>
2.5	243-250 cm: Sand, fine to very fine, quartz with mud laminae			<i>Intertidal Sequence High Marsh/Swale Fill (Sand/Mud Laminated Facies)</i>
3.0	250-350 cm: Sand, fine to very fine, quartz with little HMS, burrowed, sand filled			<i>Intertidal Sequence Upper Forebeach Laminated Facies</i>
F:\misc documents\sci_logs\BKM051111_01.cdr				

	<h2 style="margin: 0;">VIBRACORE BORING LOG</h2>		<b>LOCATION NUMBER: BKM 051111-01</b>	
			<b>PAGE NO. 2 OF 2</b>	
PROJECT NAME: PALEOTEMPESTOLOGY/STRATIGRAPHY RESEARCH		TOTAL DEPTH: 3.92 METERS (COMPACTED)/4.03 METERS (ORIGINAL)		
W.O. NUMBER: N/A		NORTHING: 3,495,847		
LOCATION: BEACH POND, SCI		EASTING: 485,887		
DRILLERS: MEYER, SHOREDITS, SMITH		GROUND SURFACE ELEVATION: 7.56 ft MSL		
DRILL RIG TYPE: SCI VIBRACORE RIG		DEPTH TO TOP OF CORE: 67" BTOP		
DRILLING METHOD: VIBRACORE		HEIGHT ABOVE LAND SURFACE: 62.5" BTOP		
SAMPLING METHOD: 3-INCH I.D. ALUMINUM PIPE		COMPACTION (%): 2.8%		
LOGGED BY: B. MEYER WEATHER: HOT, HUMID		BOREHOLE DIAMETER: 3- INCH BOREHOLE		
DATE BEGUN: 05/11/11 DATE COMPLETED: 05/11/11		LOGGER SIGNATURE: _____		
DEPTH (m)	LITHOLOGIC DESCRIPTION	GRAPHIC LOG	PHOTOGRAPHIC LOG	COMMENTS
3.0	258-350 cm: Sand, fine to very fine, quartz with little HMS, burrowed with sand filled burrows			<i>Intertidal Sequence Upper Forebeach Laminated Facies</i>
	350-392 cm: Sand, fine to very fine, quartz with moderate HMS, but no apparent laminations			<i>Intertidal Sequence Lower Forebeach Burrowed and Laminated Facies</i>
4.0	BORING REFUSAL AT 3.92 METERS BLS			
5.0				
6.0				











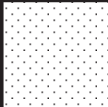




	<h2 style="margin:0;">VIBRACORE BORING LOG</h2>		<b>LOCATION NUMBER: BKM 051311-01</b>
			<b>PAGE NO. 1 OF 2</b>
PROJECT NAME: <u>PALEOTEMPESTOLOGY/STRATIGRAPHY RESEARCH</u>		TOTAL DEPTH: <u>4.57 METERS (COMPACTED)/5.29 METERS (ORIGINAL)</u>	
W.O. NUMBER: <u>N/A</u>		NORTHING: <u>3,502,226</u>	
LOCATION: <u>ST CATHERINES SHELL RING, SCI</u>		EASTING: <u>483,989</u>	
DRILLERS: <u>MEYER, SHOREDITS AND SMITH</u>		GROUND SURFACE ELEVATION: <u>3.81 ft MSL</u>	
DRILL RIG TYPE: <u>SCI VIBRACORE RIG</u>		DEPTH TO TOP OF CORE: <u>51" BTOP</u>	
DRILLING METHOD: <u>VIBRACORE</u>		HEIGHT ABOVE LAND SURFACE: <u>26" BTOP</u>	
SAMPLING METHOD: <u>3-INCH I.D. ALUMINUM PIPE</u>		COMPACTION (%): <u>12.2%</u>	
LOGGED BY: <u>B. MEYER</u> WEATHER: <u>HOT, HUMID</u>		BOREHOLE DIAMETER: <u>3- INCH BOREHOLE</u>	
DATE BEGUN: <u>05/13/11</u> DATE COMPLETED: <u>05/13/11</u>		LOGGER SIGNATURE: _____	





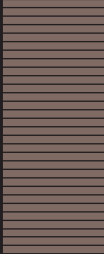
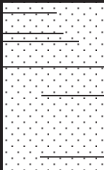

  





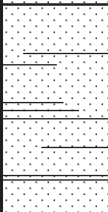

DEPTH (m)	LITHOLOGIC DESCRIPTION	GRAPHIC LOG	PHOTOGRAPHIC LOG	COMMENTS
0	GROUND SURFACE VEGETATED - SPARTINA.			<i>land surface</i>
1.0	Gray sand, fine to very fine, with mud laminae (dark gray clay/silt) and clasts, laminae are discontinuous and horizontal to gently dipping and vary in thickness from 2 to 20+mm, sands have little HMS.			<i>Intertidal Sequence High Marsh/Tidal Creek (Sand/Mud Laminated Facies)</i>
2.0	Gray sand, fine to very fine, quartz sand with appreciable HMS content, laminations near horizontal. HMS content decreases with depth.			BKM 051311-01-133, peat/wood @ 133 cm,
3.0	Brown sand, fine to very fine, with mud laminae (dark brown clay/silt) and clasts, laminae are discontinuous and horizontal to gently dipping and vary in thickness from 2 to 20+mm, sands have little HMS.			Holocene Pleistocene <i>Intertidal Sequence High Marsh/Tidal Creek (Sand/Mud Laminated Facies)</i>





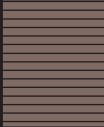


F:\misc documents\sci\_logs\BKM052511\_01.cdr





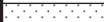


 <b>VIBRACORE BORING LOG</b> 		<b>LOCATION NUMBER: BKM 051311-01</b>		
		<b>PAGE NO. 2 OF 2</b>		
PROJECT NAME: <u>PALEOTEMPESTOLOGY/STRATIGRAPHY RESEARCH</u>		TOTAL DEPTH: <u>4.57 METERS (COMPACTED)/5.29 METERS (ORIGINAL)</u>		
W.O. NUMBER: <u>N/A</u>		NORTHING: <u>3,502,226</u>		
LOCATION: <u>ST CATHERINES SHELL RING, SCI</u>		EASTING: <u>483,989</u>		
DRILLERS: <u>MEYER, SHOREDITS AND SMITH</u>		GROUND SURFACE ELEVATION: <u>3.81 ft MSL</u>		
DRILL RIG TYPE: <u>SCI VIBRACORE RIG</u>		DEPTH TO TOP OF CORE: <u>51" BTOP</u>		
DRILLING METHOD: <u>VIBRACORE</u>		HEIGHT ABOVE LAND SURFACE: <u>26" BTOP</u>		
SAMPLING METHOD: <u>3-INCH I.D. ALUMINUM PIPE</u>		COMPACTION (%): <u>12.2%</u>		
LOGGED BY: <u>B. MEYER</u> WEATHER: <u>HOT, HUMID</u>		BOREHOLE DIAMETER: <u>3- INCH BOREHOLE</u>		
DATE BEGUN: <u>05/13/11</u> DATE COMPLETED: <u>05/13/11</u>		LOGGER SIGNATURE: _____		
DEPTH (m)	LITHOLOGIC DESCRIPTION	GRAPHIC LOG	PHOTOGRAPHIC LOG	COMMENTS
3.0	Brown sand, fine to very fine, with mud laminae (dark brown clay/silt) and clasts, laminae are discontinuous and horizontal to gently dipping and vary in thickness from 2 to 20+mm, sands have little HMS.			<i>Intertidal Sequence High Marsh/Tidal Creek (Sand/Mud Laminated Facies)</i>
4.0				Brown to dark brown sand, fine to very fine with intensive burrowing, burrows are filled with light brown sand, no apparent bedding structures due to high degree of bioturbation
5.0	BORING REFUSAL AT 4.57 METERS BLS			
6.0				



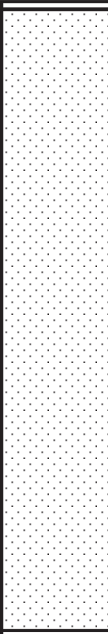

	<h2 style="margin: 0;">VIBRACORE BORING LOG</h2>		<b>LOCATION NUMBER: BKM 052411-01</b>	
			<b>PAGE NO. 1 OF 1</b>	
PROJECT NAME: <u>PALEOTEPESTOLOGY/STRATIGRAPHY RESEARCH</u>		TOTAL DEPTH: <u>1.80 METERS (COMPACTED)/1.80 METERS (ORIGINAL)</u>		
W.O. NUMBER: <u>N/A</u>		NORTHING: <u>3,494,292</u>		
LOCATION: <u>FLAG POND, SCI</u>		EASTING: <u>485,240</u>		
DRILLERS: <u>MEYER, LEGGETT, AND SARAJILIC</u>		GROUND SURFACE ELEVATION: <u>3.30 ft MSL</u>		
DRILL RIG TYPE: <u>SCI VIBRACORE RIG</u>		DEPTH TO TOP OF CORE: <u>14" BTOP</u>		
DRILLING METHOD: <u>VIBRACORE</u>		HEIGHT ABOVE LAND SURFACE: <u>14" BTOP</u>		
SAMPLING METHOD: <u>3-INCH I.D. ALUMINUM PIPE</u>		COMPACTION (%): <u>0.0%</u>		
LOGGED BY: <u>B. MEYER</u> WEATHER: <u>HOT, HUMID</u>		BOREHOLE DIAMETER: <u>3- INCH BOREHOLE</u>		
DATE BEGUN: <u>05/24/11</u> DATE COMPLETED: <u>0524/11</u>		LOGGER SIGNATURE: _____		
DEPTH (m)	LITHOLOGIC DESCRIPTION	GRAPHIC LOG	PHOTOGRAPHIC LOG	COMMENTS
0	GROUND SURFACE VEGETATED WITH DUNE GRASSES 0-25 cm: Light brown gray sand, fine to very fine, some disseminated HMS, beach berm/aeolian material.			<i>land surface</i>
	25-60 cm: Light brown gray sand, fine to very fine, moderate HMS, ripple marks with laminated HMS.			<i>Intertidal Sequence Modern Upper Forebeach Laminated Facies</i>
	60-85 cm: Light brown gray sand, fine to very fine, moderate HMS, horizontally laminated HMS.			
1.0	85-110 cm: Light brown gray sand, fine to very fine, moderate HMS, ripple marks with laminated HMS and shell fragments.			
	110-160 cm: Light brown gray sand, fine to very fine, moderate HMS, horizontally laminated HMS and shell fragments.			<i>Washover fan sequence</i>
	160-180 cm: Peat, dark brown to black, plant macromaterial, fibrous with fibers to 3 cm.			<i>peat</i>
2.0	BORING REFUSAL AT 1.80 METERS BLS			
3.0				

 <b>VIBRACORE BORING LOG</b> 		<b>LOCATION NUMBER: BKM 052411-02</b>			
		<b>PAGE NO. 1 OF 2</b>			
PROJECT NAME: <u>PALEOTEMPESTOLOGY/STRATIGRAPHY RESEARCH</u>		TOTAL DEPTH: <u>4.25 METERS (COMPACTED)/4.33 METERS (ORIGINAL)</u>			
W.O. NUMBER: <u>N/A</u>		NORTHING: <u>3,494,308</u>			
LOCATION: <u>SEASIDE SPIT/MARSH, NORTH BEACH, SCI</u>		EASTING: <u>485,195</u>			
DRILLERS: <u>MEYER, SARAJILIC, LEGGETT, McCARVILLE, VANCE</u>		GROUND SURFACE ELEVATION: <u>2.92 ft MSL</u>			
DRILL RIG TYPE: <u>SCI VIBRACORE RIG</u>		DEPTH TO TOP OF CORE: <u>62" BTOP</u>			
DRILLING METHOD: <u>VIBRACORE</u>		HEIGHT ABOVE LAND SURFACE: <u>59" BTOP</u>			
SAMPLING METHOD: <u>3-INCH I.D. ALUMINUM PIPE</u>		COMPACTION (%): <u>1.8%</u>			
LOGGED BY: <u>B. MEYER</u> WEATHER: <u>HOT, HUMID</u>		BOREHOLE DIAMETER: <u>3- INCH BOREHOLE</u>			
DATE BEGUN: <u>05/24/11</u> DATE COMPLETED: <u>05/24/11</u>		LOGGER SIGNATURE: _____			
DEPTH (m)	LITHOLOGIC DESCRIPTION	GRAPHIC LOG	PHOTOGRAPHIC LOG	COMMENTS	
0	GROUND SURFACE VEGETATED WITH SPARSE SALICORNIA			<i>land surface</i>	
	0-70 cm: Light brown gray sand, fine to very fine, moderate HMS, horizontal laminations with laminated quartz/HMS.			<i>Washover/Flood Delta Sequence</i>	
1.0	70-130 cm: Peat, dark brown to black, plant macromaterial, fibrous with fibers to 3 cm.			BKM 052411-02-79, wood @ 79 cm	<i>Intertidal Sequence Low Marsh Facies  Lacustrine Sequence</i>
				<i>Intertidal Sequence High Marsh/Swale Fill (Sand/Mud Laminated Facies)</i>	
2.0					
	130-360 cm: Light brown gray sand, fine to very fine, moderate HMS, horizontal laminations with laminated quartz/HMS.			<i>Intertidal Sequence Upper Forebeach Laminated Facies</i>	
3.0					





 <b>VIBRACORE BORING LOG</b> 		<b>LOCATION NUMBER: BKM 052411-02</b>		
		<b>PAGE NO. 2 OF 2</b>		
PROJECT NAME: <u>PALEOTEMPESTOLOGY/STRATIGRAPHY RESEARCH</u>		TOTAL DEPTH: <u>4.25 METERS (COMPACTED)/4.33 METERS (ORIGINAL)</u>		
W.O. NUMBER: <u>N/A</u>		NORTHING: <u>3,494,308</u>		
LOCATION: <u>SEASIDE SPIT/MARSH, NORTH BEACH, SCI</u>		EASTING: <u>485,195</u>		
DRILLERS: <u>MEYER, SARAJILIC, LEGGETT, McCARVILLE, VANCE</u>		GROUND SURFACE ELEVATION: <u>2.92 ft MSL</u>		
DRILL RIG TYPE: <u>SCI VIBRACORE RIG</u>		DEPTH TO TOP OF CORE: <u>62" BTOP</u>		
DRILLING METHOD: <u>VIBRACORE</u>		HEIGHT ABOVE LAND SURFACE: <u>59" BTOP</u>		
SAMPLING METHOD: <u>3-INCH I.D. ALUMINUM PIPE</u>		COMPACTION (%): <u>1.8%</u>		
LOGGED BY: <u>B. MEYER</u> WEATHER: <u>HOT, HUMID</u>		BOREHOLE DIAMETER: <u>3- INCH BOREHOLE</u>		
DATE BEGUN: <u>05/24/11</u> DATE COMPLETED: <u>05/24/11</u>		LOGGER SIGNATURE: _____		
DEPTH (m)	LITHOLOGIC DESCRIPTION	GRAPHIC LOG	PHOTOGRAPHIC LOG	COMMENTS
3.0	130-360 cm: Light brown gray sand, fine to very fine, moderate HMS, horizontal laminations with laminated quartz/HMS.			<i>Intertidal Sequence Upper Forebeach Laminated Facies</i>
4.0	360-425 cm: Light gray sand, fine to very fine, moderate HMS, laminated with mud (silt/clay).			<i>Subtidal Sequence Transition Zone Bioturbated and Laminated Facies</i>
5.0	BORING REFUSAL AT 4.25 METERS BLS			
6.0				





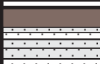




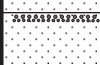
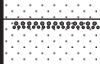
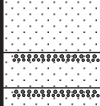
	<h2 style="margin:0;">VIBRACORE BORING LOG</h2>		<b>LOCATION NUMBER: BKM 052511-01</b>	
			<b>PAGE NO. 1 OF 2</b>	
PROJECT NAME: <u>PALEOTEMPESTOLOGY/STRATIGRAPHY RESEARCH</u>		TOTAL DEPTH: <u>5.01 METERS (COMPACTED)/5.62 METERS (ORIGINAL)</u>		
W.O. NUMBER: <u>N/A</u>		NORTHING: <u>3,494,332</u>		
LOCATION: <u>FLAG LAGOON, SCI</u>		EASTING: <u>485,158</u>		
DRILLERS: <u>MEYER, LEGGETT AND SARJELIC</u>		GROUND SURFACE ELEVATION: <u>1.21 ft MSL</u>		
DRILL RIG TYPE: <u>SCI VIBRACORE RIG</u>		DEPTH TO TOP OF CORE: <u>44" BTOP</u>		
DRILLING METHOD: <u>VIBRACORE</u>		HEIGHT ABOVE LAND SURFACE: <u>20" BTOP</u>		
SAMPLING METHOD: <u>3-INCH I.D. ALUMINUM PIPE</u>		COMPACTION (%): <u>10.8%</u>		
LOGGED BY: <u>B. MEYER</u> WEATHER: <u>HOT, HUMID</u>		BOREHOLE DIAMETER: <u>3- INCH BOREHOLE</u>		
DATE BEGUN: <u>05/25/11</u> DATE COMPLETED: <u>0525/11</u>		LOGGER SIGNATURE: _____		
DEPTH (m)	LITHOLOGIC DESCRIPTION	GRAPHIC LOG	PHOTOGRAPHIC LOG	COMMENTS
0	GROUND SURFACE SPARSELY VEGETATED - SALICORNIA AND EMERGENT SPARTINA. Sand, fine to medium, washover fan sequence, high angle ripple marks with laminated HMS			<i>land surface</i>  <i>Washover/Flood Delta Sequence</i>
	Peat, dark gray-black, macroplant material, fibrous.			<i>peat</i>
1.0	Mud (clay with silt and little fine sand), dark gray-black, organic,			<i>Intertidal Sequence Low Marsh Facies</i>  <i>Lacustrine Sequence</i>
2.0	Sand, fine to medium with shells (-228cm to- 242cm)			BKM 052511-01-244 <i>Mulinia</i> shell @ 244 cm  <i>Intertidal Sequence Upper Forebeach Laminated Facies</i>
3.0				





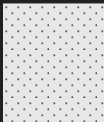












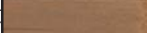


	<h2 style="margin:0;">VIBRACORE BORING LOG</h2>		<b>LOCATION NUMBER: BKM 052511-01</b>	
			<b>PAGE NO. 2 OF 2</b>	
PROJECT NAME: <u>PALEOTEMPESTOLOGY/STRATIGRAPHY RESEARCH</u>		TOTAL DEPTH: <u>5.01 METERS (COMPACTED)/5.62 METERS (ORIGINAL)</u>		
W.O. NUMBER: <u>N/A</u>		NORTHING: <u>3,494,332</u>		
LOCATION: <u>FLAG LAGOON, SCI</u>		EASTING: <u>485,158</u>		
DRILLERS: <u>MEYER, LEGGETT AND SARAJILIC</u>		GROUND SURFACE ELEVATION: <u>1.21 ft MSL</u>		
DRILL RIG TYPE: <u>SCI VIBRACORE RIG</u>		DEPTH TO TOP OF CORE: <u>44" BTOP</u>		
DRILLING METHOD: <u>VIBRACORE</u>		HEIGHT ABOVE LAND SURFACE: <u>20" BTOP</u>		
SAMPLING METHOD: <u>3-INCH I.D. ALUMINUM PIPE</u>		COMPACTION (%): <u>10.8%</u>		
LOGGED BY: <u>B. MEYER</u> WEATHER: <u>HOT, HUMID</u>		BOREHOLE DIAMETER: <u>3- INCH BOREHOLE</u>		
DATE BEGUN: <u>05/25/11</u> DATE COMPLETED: <u>0525/11</u>		LOGGER SIGNATURE: _____		
DEPTH (m)	LITHOLOGIC DESCRIPTION	GRAPHIC LOG	PHOTOGRAPHIC LOG	COMMENTS
3.0	<p><i>Callianassa</i> burrow (-330 to -340 cm)</p>			<p><i>Intertidal Sequence Upper Forebeach Laminated Facies</i></p>
	<p>Sand, fine to medium with mud (clay/silt)</p>			<p><i>Intertidal Sequence Lower Forebeach Burrowed and Laminated Facies</i></p>
4.0	<p>Shells at -410 to -425 cm</p>			<p><i>Subtidal Sequence Transition Zone Bioturbated and Laminated Facies</i></p>
5.0	<p>BORING REFUSAL AT 5.01 METERS BLS</p>			<p>BKM 052511-01-496 <i>Donax</i> shell @ 496 cm</p>
6.0				
f:\misc documents\sci_logs\BKM052511_01.cdr				




	<h2 style="margin: 0;">VIBRACORE BORING LOG</h2>		<b>LOCATION NUMBER: BKM 052511-02</b>	
			<b>PAGE NO. 1 OF 1</b>	
PROJECT NAME: <u>PALEOTEMPESTOLOGY/STRATIGRAPHY RESEARCH</u>		TOTAL DEPTH: <u>1.95 METERS (COMPACTED)/2.02 METERS (ORIGINAL)</u>		
W.O. NUMBER: <u>N/A</u>		NORTHING: <u>3,494,377m</u>		
LOCATION: <u>FLAG LAGOON (JUNGLE ROAD), SCI</u>		EASTING: <u>485,129m</u>		
DRILLERS: <u>MEYER, LEGGETT AND SARAJILIC</u>		GROUND SURFACE ELEVATION: <u>5.61 ft (1.71 m) MSL</u>		
DRILL RIG TYPE: <u>SCI VIBRACORE RIG</u>		DEPTH TO TOP OF CORE: <u>19" BTOP</u>		
DRILLING METHOD: <u>VIBRACORE</u>		HEIGHT ABOVE LAND SURFACE: <u>16.25" BTOP</u>		
SAMPLING METHOD: <u>3-INCH I.D. ALUMINUM PIPE</u>		COMPACTION (%): <u>3.5%</u>		
LOGGED BY: <u>B. MEYER</u> WEATHER: <u>HOT, HUMID</u>		BOREHOLE DIAMETER: <u>3- INCH BOREHOLE</u>		
DATE BEGUN: <u>05/25/11</u> DATE COMPLETED: <u>05/25/11</u>		LOGGER SIGNATURE: _____		
DEPTH (m)	LITHOLOGIC DESCRIPTION	GRAPHIC LOG	PHOTOGRAPHIC LOG	COMMENTS
0	GROUND SURFACE VEGETATED - PALMETTO			<i>land surface</i>
	0-35 cm: Sand, dark brown-gray, A-horizon, fine to very fine sand, mottled with abundant plant and root fragments.			<i>Intertidal Sequence Backbeach/Berm Laminated and Bioturbated Facies</i>
	35-55 cm: Sand, lt. brown-gray, E-horizon, fine to very fine sand, mottled with few plant and root fragments.			
	55-115 cm: Sand, lt. brown, fine to very fine, mottled, faint laminations.			
1.0	115-195 cm: Sand, fine to very fine, horizontal laminations qzt/HMS			<i>Intertidal Sequence Upper Forebeach Laminated Facies</i>
2.0	BORING REFUSAL AT 1.95 METERS BLS			
3.0				















  <b>VIBRACORE BORING LOG</b>  		<b>LOCATION NUMBER: IEP 060411-01</b>			
		<b>PAGE NO. 1 OF 2</b>			
PROJECT NAME: <u>MISSION GEOARCHAEOLOGY</u>		TOTAL DEPTH: <u>5.07 METERS (COMPACTED)/5.69 METERS (ORIGINAL)</u>			
W.O. NUMBER: <u>N/A</u>		NORTHING: <u>3,498,850.66</u>			
LOCATION: <u>MISSION SITE, SCI</u>		EASTING: <u>483,638.52</u>			
DRILLERS: <u>IEP (KEITH-LUCAS, POTTER AND STUDENTS)</u>		GROUND SURFACE ELEVATION: <u>3.23 FT MLS</u>			
DRILL RIG TYPE: <u>SCI VIBRACORE RIG</u>		DEPTH TO TOP OF CORE: <u>41.9" BTOP</u>			
DRILLING METHOD: <u>VIBRACORE</u>		HEIGHT ABOVE LAND SURFACE: <u>17.7" BTOP</u>			
SAMPLING METHOD: <u>3-INCH I.D. ALUMINUM PIPE</u>		COMPACTION (%): <u>10.8%</u>			
LOGGED BY: <u>BISHOP/MEYER</u> WEATHER: <u>HOT, CLEAR</u>		BOREHOLE DIAMETER: <u>3- INCH BOREHOLE</u>			
DATE BEGUN: <u>6/4/2011</u> DATE COMPLETED: <u>6/4/2011</u>		LOGGER SIGNATURE: _____			
DEPTH (m)	LITHOLOGIC DESCRIPTION	GRAPHIC LOG	PHOTOGRAPHIC LOG	COMMENTS	
0	0-20 cm: Mud (silt/clay) sandy and peaty, dark brown, sulfide odor			<i>land surface</i>	
	20-50 cm: Mud peaty above, black, tacky and waxy near bottom, lower contact mottled/grading into underlying sand				
	50-62 cm: Sand, tan to dark brown, scattered heavy minerals				
	62-70 cm: Sand, mottled with black, wood material				
1.0	70-112 cm: Sand, mud flasers, sand layers 10 cm thick, 1 cm muddy sand flasers, mottled, 2 cm peat at 100 cm				
	112-119 cm: Mud (silt/clay) with sand				
	119-164 cm: Sand, fine to med., mottled				
	164-190 cm: Sand, muddy, black, some peat chips				
2.0	190-227 cm: Sand, fine to med., mottled peat stringer				
	227-245 cm: Peat, coarse, dark				
	245-271 cm: Sand, light brown with black mud				
	271-305 cm: Peat, coarse, dark				
3.0	305-324 cm: Dark gray peat underlain by with sand, med. to coarse, gray-tan, with sharp contact below.				GAB20110607-009, peat @ 310 cm ( <sup>14</sup> C = 270 +/- 30 B.P.)





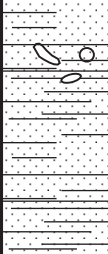

  <b>VIBRACORE BORING LOG</b>  		<b>LOCATION NUMBER: IEP 060411-01</b>		
		<b>PAGE NO. 2 OF 2</b>		
PROJECT NAME: <u>MISSION GEOARCHAEOLOGY</u>		TOTAL DEPTH: <u>5.07 METERS (COMPACTED)/5.69 METERS (ORIGINAL)</u>		
W.O. NUMBER: <u>N/A</u>		NORTHING: <u>3,498,850.66</u>		
LOCATION: <u>MISSION SITE, SCI</u>		EASTING: <u>483,638.52</u>		
DRILLERS: <u>IEP (KEITH-LUCAS, POTTER AND STUDENTS)</u>		GROUND SURFACE ELEVATION: <u>3.23 FT MLS</u>		
DRILL RIG TYPE: <u>SCI VIBRACORE RIG</u>		DEPTH TO TOP OF CORE: <u>41.9" BTOP</u>		
DRILLING METHOD: <u>VIBRACORE</u>		HEIGHT ABOVE LAND SURFACE: <u>17.7" BTOP</u>		
SAMPLING METHOD: <u>3-INCH I.D. ALUMINUM PIPE</u>		COMPACTION (%): <u>10.8%</u>		
LOGGED BY: <u>BISHOP/MEYER</u> WEATHER: <u>HOT, CLEAR</u>		BOREHOLE DIAMETER: <u>3- INCH BOREHOLE</u>		
DATE BEGUN: <u>6/4/2011</u> DATE COMPLETED: <u>6/4/2011</u>		LOGGER SIGNATURE: _____		
DEPTH (m)	LITHOLOGIC DESCRIPTION	GRAPHIC LOG	PHOTOGRAPHIC LOG	COMMENTS
3.0	300-324 cm: Dark gray peat underlain by with sand, med. to coarse, gray-tan, with sharp contact below.			<i>Intertidal Sequence High Marsh/Tidal Creek/Fluvial Facies</i>
	324-380 cm: Light brown fine sand with ghost shrimp burrows (lined with dk. brown mud, filled with lt. brown fine sand)			GAB20110607-009, peat @ 310 cm  <i>Intertidal Sequence Lower Forebeach Burrowed and Laminated Facies</i>
4.0	coarse sand			
	coarse sand			
	coarse sand			
	coarse sand			
5.0	380-507 cm: Light brown fine sand with coarse sand layers, and discontinuous mud layers			<i>Subtidal Sequence Transition Zone Bioturbated and Laminated Facies</i>
	BORING TERMINATED AT 5.07 METERS BLS (COMPACTED)			
6.0				

  <b>VIBRACORE BORING LOG</b>  				<b>LOCATION NUMBER: IEP 060411-02</b>	
				<b>PAGE NO. 1 OF 2</b>	
PROJECT NAME: <u>MISSION GEOARCHAEOLOGY</u>			TOTAL DEPTH: <u>5.38 METERS (COMPACTED)/5.68 METERS (ORIGINAL)</u>		
W.O. NUMBER: <u>N/A</u>			NORTHING: <u>3,498,877.25</u>		
LOCATION: <u>MISSION SITE, SCI</u>			EASTING: <u>483,647.10</u>		
DRILLERS: <u>IEP (KEITH-LUCAS, POTTER AND STUDENTS)</u>			GROUND SURFACE ELEVATION: <u>2.68 FT MLS</u>		
DRILL RIG TYPE: <u>SCI VIBRACORE RIG</u>			DEPTH TO TOP OF CORE: <u>29.3" BTOP</u>		
DRILLING METHOD: <u>VIBRACORE</u>			HEIGHT ABOVE LAND SURFACE: <u>17.3" BTOP</u>		
SAMPLING METHOD: <u>3-INCH I.D. ALUMINUM PIPE</u>			COMPACTION (%): <u>5.3%</u>		
LOGGED BY: <u>BISHOP/MEYER</u> WEATHER: <u>HOT, CLEAR</u>			BOREHOLE DIAMETER: <u>3- INCH BOREHOLE</u>		
DATE BEGUN: <u>6/4/2011</u> DATE COMPLETED: <u>6/4/2011</u>			LOGGER SIGNATURE: _____		
DEPTH (m)	LITHOLOGIC DESCRIPTION	GRAPHIC LOG	PHOTOGRAPHIC LOG	COMMENTS	
0				<i>land surface</i>	
0-40 cm	Sand, medium-fine, dark chocolate brown - dark gray, some mottling. No apparent primary sedimentary structures.			<i>Intertidal Sequence High Marsh/Tidal Creek/Fluvial Facies</i>	
40-60 cm	Sand with some mud (clay/silt), fine to med. sand, dark brown				
60-110 cm	Sand with little mud (clay/silt), fine to med. sand, medium brown, horizontal laminations are few and faint.			<i>Intertidal Sequence Upper Forebeach Laminated Facies</i>	
110-460 cm	Sand with little mud (clay/silt), fine to med. sand, medium brown, horizontal laminations are few and faint, with increasing ghost shrimp burrows with depth.				
170 cm	circular/elliptical lined burrow, burrow lined with mud/sand and filled with sand, ghost shrimp burrow				
220 cm	circular/elliptical lined burrow, burrow lined with mud/sand and filled with sand, ghost shrimp burrow				
240 cm	mud flaser			<i>Intertidal Sequence Lower Forebeach Burrowed and Laminated Facies</i>	
270 cm	triangular lined burrow, lined with mud/sand and sand filled				
3.0					







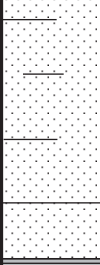

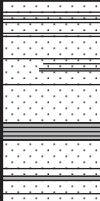



  <b>VIBRACORE BORING LOG</b> 		<b>LOCATION NUMBER: IEP 060411-02</b>		
		<b>PAGE NO. 2 OF 2</b>		
PROJECT NAME: <u>MISSION GEOARCHAEOLOGY</u>		TOTAL DEPTH: <u>5.38 METERS (COMPACTED)/5.68 METERS (ORIGINAL)</u>		
W.O. NUMBER: <u>N/A</u>		NORTHING: <u>3,498,877.25</u>		
LOCATION: <u>MISSION SITE, SCI</u>		EASTING: <u>483,647.10</u>		
DRILLERS: <u>IEP (KEITH-LUCAS, POTTER AND STUDENTS)</u>		GROUND SURFACE ELEVATION: <u>2.68 FT MLS</u>		
DRILL RIG TYPE: <u>SCI VIBRACORE RIG</u>		DEPTH TO TOP OF CORE: <u>29.3" BTOP</u>		
DRILLING METHOD: <u>VIBRACORE</u>		HEIGHT ABOVE LAND SURFACE: <u>17.3" BTOP</u>		
SAMPLING METHOD: <u>3-INCH I.D. ALUMINUM PIPE</u>		COMPACTION (%): <u>5.3%</u>		
LOGGED BY: <u>BISHOP/MEYER</u> WEATHER: <u>HOT, CLEAR</u>		BOREHOLE DIAMETER: <u>3- INCH BOREHOLE</u>		
DATE BEGUN: <u>6/4/2011</u> DATE COMPLETED: <u>6/4/2011</u>		LOGGER SIGNATURE: _____		
DEPTH (m)	LITHOLOGIC DESCRIPTION	GRAPHIC LOG	PHOTOGRAPHIC LOG	COMMENTS
3.0	170-460 cm: Sand with little mud (clay/silt), fine to med. sand, medium brown, horizontal laminations are few and faint, with increasing ghost shrimp burrows with depth.			<i>Intertidal Sequence Lower Forebeach Burrowed and Laminated Facies</i>
	340-360 cm: circular lined burrows, burrows lined with mud/sand and filled with sand, ghost shrimp burrows			
	380-390 cm: elliptical lined burrow, burrow lined with mud/sand and filled with sand, ghost shrimp burrow			
4.0	420-425 cm: circular lined burrow, burrow lined with mud/sand and filled with sand, ghost shrimp burrow			
5.0	460-538 cm: Sand, medium to coarse, little HMS, interbedded with muddy sand, muddy sands are bioturbated.			<i>Subtidal Sequence Transition Zone Bioturbated and Laminated Facies</i>
	BORING REFUSAL AT 5.38 METERS BLS			
6.0				

 <b>VIBRACORE BORING LOG</b> 		<b>LOCATION NUMBER: BKM 072211-02</b>		
		<b>PAGE NO. 1 OF 2</b>		
PROJECT NAME: PALEOTEMPESTOLOGY/STRATIGRAPHY RESEARCH		TOTAL DEPTH: 2.75 METERS (COMPACTED)/LOST 2.74 METERS ON RETRIEVAL		
W.O. NUMBER: N/A		NORTHING: 3,494,271		
LOCATION: FLAG POND, SCI		EASTING: 485,273		
DRILLERS: MEYER, VANCE, SKILES, HUCKINS, NELSON		GROUND SURFACE ELEVATION: 1.71 ft MSL		
DRILL RIG TYPE: SCI VIBRACORE RIG		DEPTH TO TOP OF CORE: 39" BTOP		
DRILLING METHOD: VIBRACORE		HEIGHT ABOVE LAND SURFACE: 24" BTOP		
SAMPLING METHOD: 3-INCH I.D. ALUMINUM PIPE		COMPACTION (%): 6.5%		
LOGGED BY: B. MEYER WEATHER: WARM/CLEAR		BOREHOLE DIAMETER: 3- INCH BOREHOLE		
DATE BEGUN: 07/22/11 DATE COMPLETED: 07/22/11		LOGGER SIGNATURE: _____		
DEPTH (m)	LITHOLOGIC DESCRIPTION	GRAPHIC LOG	PHOTOGRAPHIC LOG	COMMENTS
0				land surface
0-0.095	(0-95 cm) Light brown, fine to very fine sand (2.5Y 8/2) , faint laminations in upper section, rippled laminations from 70-90 cm, very fine heavy mineral sands, shells and shell fragments (modern foreshore and inlet fill).			Modern Intertidal Sequence Upper Forebeach Laminated Facies
0.095-1.0	95-100 cm: Peat, dark brown gray-black (10YR 10YR 2/1), organic with plant fragments, burrowed with sand filling.			Inlet Fill Sequence
1.0-2.57	100-257 cm: Light gray sand, fine to very fine, moderate HMS, horizontal laminations with laminated quartz/HMS. Distinct color change at 135 cm from brown to gray sand			Intertidal Sequence Lower Forebeach Burrowed and Laminated Facies
2.57-2.75	257-275 cm: Fine to very fine sand with mud laminae, mud laminations and clasts (2.5Y 4/1) in light brown to gray fine to very fine sand (2.5Y 7/1).			Subtidal Sequence Transition Zone Bioturbated and Laminated Facies
	BORING RECOVERED = 2.75 METERS BLS			
3.0				



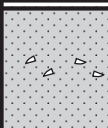

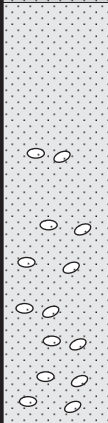

 <b>VIBRACORE BORING LOG</b> 		<b>LOCATION NUMBER: BKM 072311-01</b>		
		<b>PAGE NO. 1 OF 2</b>		
PROJECT NAME: STRATIGRAPHY/PALEOTEMPESTOLOGY RESEARCH		TOTAL DEPTH: 4.46 METERS (COMPACTED)/5.22 METERS (ORIGINAL)		
W.O. NUMBER: N/A		NORTHING: 3,495,833		
LOCATION: BEACH POND, SCI		EASTING: 485,928		
DRILLERS: MEYER, HUCKINS, SKILES, VANCE		GROUND SURFACE ELEVATION: 1.09 ft MSL		
DRILL RIG TYPE: SCI VIBRACORE RIG		DEPTH TO TOP OF CORE: 53" BTOP		
DRILLING METHOD: VIBRACORE		HEIGHT ABOVE LAND SURFACE: 23" BTOP		
SAMPLING METHOD: 3-INCH I.D. ALUMINUM PIPE		COMPACTION (%): 14.6%		
LOGGED BY: B. MEYER WEATHER: HOT/CLEAR		BOREHOLE DIAMETER: 3- INCH BOREHOLE		
DATE BEGUN: 07/23/11 DATE COMPLETED: 07/23/11		LOGGER SIGNATURE: _____		
DEPTH (m)	LITHOLOGIC DESCRIPTION	GRAPHIC LOG	PHOTOGRAPHIC LOG	COMMENTS
0	GROUND SURFACE DEVOID OF VEGETATION (0-20 cm) Lt brown, fine to very fine sand (2.5Y 8/2), very fine HMS, <i>Mulinia</i> shells and shell fragments, faint horiz. lams			land surface Intertidal Sequence Modern Upper Forebeach Laminated Facies
	20-38 cm: Dark gray brown mud (2.5Y 3/1) stiff, with peaty laminations			Intertidal Sequence Low Marsh Facies
1.0	38-138 cm: Mud laminations and interlaminae in light brown to gray fine to very fine sand fining upward.			Intertidal Sequence High Marsh/Swale Fill (Sand/Mud Laminated Facies)
	138-190 cm: Very light brown to gray (2.5 7/1), fine to very fine quartz sand, with mud (clay/silt) laminae that are non-continuous and mud clasts (2.5Y 2.5/1)			Upper Foreshore Sequence (Laminated Facies)
2.0	190-240 cm: Mud laminations and interlaminae in light brown to gray fine to very fine sand coarsening upward, abrupt contact with fine sand below.			Subtidal Sequence Transition Zone Bioturbated and Laminated Facies
3.0	240- 362 cm: Sand, fine bioturbated (faint laminae/bedding of HMS), shell fragments, abrupt contact with sand/mud above.			Upper Foreshore Sequence (Laminated Facies)



 <b>VIBRACORE BORING LOG</b> 		<b>LOCATION NUMBER: BKM 072311-01</b>		
		<b>PAGE NO. 2 OF 2</b>		
PROJECT NAME: STRATIGRAPHY/PALEOTEMPESTOLOGY RESEARCH		TOTAL DEPTH: 4.46 METERS (COMPACTED)/5.22 METERS (ORIGINAL)		
W.O. NUMBER: N/A		NORTHING: 3,495,833		
LOCATION: BEACH POND, SCI		EASTING: 485,928		
DRILLERS: MEYER, HUCKINS, SKILES, VANCE		GROUND SURFACE ELEVATION: 1.09 ft MSL		
DRILL RIG TYPE: SCI VIBRACORE RIG		DEPTH TO TOP OF CORE: 53" BTOP		
DRILLING METHOD: VIBRACORE		HEIGHT ABOVE LAND SURFACE: 23" BTOP		
SAMPLING METHOD: 3-INCH I.D. ALUMINUM PIPE		COMPACTION (%): 14.6%		
LOGGED BY: B. MEYER WEATHER: HOT/CLEAR		BOREHOLE DIAMETER: 3- INCH BOREHOLE		
DATE BEGUN: 07/23/11 DATE COMPLETED: 07/23/11		LOGGER SIGNATURE: _____		
DEPTH (m)	LITHOLOGIC DESCRIPTION	GRAPHIC LOG	PHOTOGRAPHIC LOG	COMMENTS
3.0	240- 362 cm: Sand, fine bioturbated (faint laminae/bedding of HMS), shell fragments, abrupt contact with sand/mud above.			<i>Foreshore Sequence (Laminated Facies)</i>  <i>Intertidal Sequence Lower Forebeach Burrowed and Laminated Facies</i>
4.0	362-446 cm: Sand, fine bioturbated with sand filled burrows at 370 cm and 380 cm, burrows are slightly elliptical (2 cm x 1.5 cm) and cut across mud flasers/laminae, fine sand-sized shell fragments and whole disarticulated <i>Mulinia</i> and <i>Donax</i> shells			<i>Subtidal Sequence Transition Zone Bioturbated and Laminated Facies</i>
5.0	BORING REFUSAL AT 4.46 METERS BLS			
6.0				





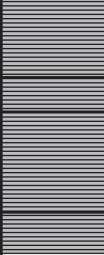



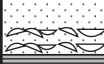

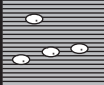

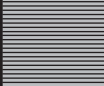









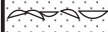


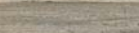


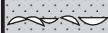



 <b>VIBRACORE BORING LOG</b> 		<b>LOCATION NUMBER:</b> <b>BKM 012112-01</b>		
		<b>PAGE NO. 1 OF 2</b>		
PROJECT NAME: STRATIGRAPHY/PALEOTEMPESTOLOGY RESEARCH		TOTAL DEPTH: 5.26 METERS (COMPACTED)/5.77 METERS (ORIGINAL)		
W.O. NUMBER: N/A		NORTHING: 3,505,686		
LOCATION: NORTH BEACH, SCI		EASTING: 487,431		
DRILLERS: MEYER, VANCE, KENNEDY AND MEHMET		GROUND SURFACE ELEVATION: 1.19 ft MSL		
DRILL RIG TYPE: SCI VIBRACORE RIG		DEPTH TO TOP OF CORE: 33.0" BTOP		
DRILLING METHOD: VIBRACORE		HEIGHT ABOVE LAND SURFACE: 13.0" BTOP		
SAMPLING METHOD: 3-INCH I.D. ALUMINUM PIPE		COMPACTION (%): 8.8%		
LOGGED BY: B. MEYER WEATHER: COOL/CLOUDY/WINDY		BOREHOLE DIAMETER: 3- INCH BOREHOLE		
DATE BEGUN: 01/21/12 DATE COMPLETED: 01/21/12		LOGGER SIGNATURE: _____		
DEPTH (m)	LITHOLOGIC DESCRIPTION	GRAPHIC LOG	PHOTOGRAPHIC LOG	TBD RESULTS COMMENTS
0	GROUND SURFACE DEVOID OF VEGETATION (0-20 cm) Light brown gray, fine to very fine sand (2.5Y 8/2) , rippled laminations, very fine disseminated heavy mineral sands, <i>Mulinia</i> shells and shell fragments (modern foreshore) (20-80 cm) Light brown gray, fine to very fine sand (2.5Y 7/1), rippled laminations, very fine disseminated heavy mineral sands, <i>Mulinia</i> shells and shell fragments (modern foreshore)			land surface  <i>Modern Intertidal Sequence Upper Forebeach Laminated Facies</i>
1.0	(80-150 cm): Light brown to gray (2.5 7/1), fine to very fine quartz sand, light horizontal laminations of quartz/heavy mineral sands, firm, little to traces of shell fragments (modern foreshore)			<i>Intertidal Sequence Lower Forebeach Burrowed and Laminated Facies</i>
2.0	Very light brown to gray (2.5 7/1), fine to very fine quartz sand, with mud (clay/silt) laminae that are non-continuous and mud clasts (2.5Y 2.5/1)			<i>Subtidal Sequence Transition Zone Bioturbated and Laminated Facies</i>
	Mud laminations and clasts (2.5Y 4/1) in light brown to gray fine to very fine sand (2.5Y 7/1), coarsening upward.			
3.0	Muddy sand, dark gray brown sand (2.5Y 4/1), with shell fragments			<i>Intertidal Sequence Tidal Creek (Muddy Sand)</i>




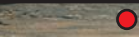
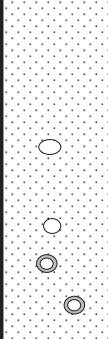









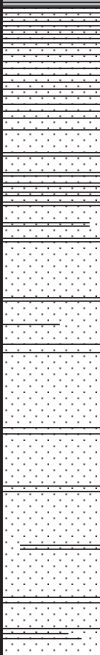
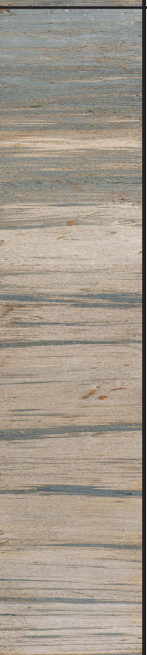
	<h2 style="margin: 0;">VIBRACORE BORING LOG</h2>		<b>LOCATION NUMBER: BKM 012112-01</b>	
			<b>PAGE NO. 2 OF 2</b>	
PROJECT NAME: <u>STRATIGRAPHY/PALEOTEMPESTOLOGY RESEARCH</u>		TOTAL DEPTH: <u>5.26 METERS (COMPACTED)/5.77 METERS (ORIGINAL)</u>		
W.O. NUMBER: <u>N/A</u>		NORTHING: <u>3,505,686</u>		
LOCATION: <u>NORTH BEACH, SCI</u>		EASTING: <u>487,431</u>		
DRILLERS: <u>MEYER, VANCE, KENNEDY AND MEHMET</u>		GROUND SURFACE ELEVATION: <u>1.19 ft MSL</u>		
DRILL RIG TYPE: <u>SCI VIBRACORE RIG</u>		DEPTH TO TOP OF CORE: <u>33.0" BTOP</u>		
DRILLING METHOD: <u>VIBRACORE</u>		HEIGHT ABOVE LAND SURFACE: <u>13.0" BTOP</u>		
SAMPLING METHOD: <u>3-INCH I.D. ALUMINUM PIPE</u>		COMPACTION (%): <u>8.8%</u>		
LOGGED BY: <u>B. MEYER</u> WEATHER: <u>COOL/CLOUDY/WINDY</u>		BOREHOLE DIAMETER: <u>3- INCH BOREHOLE</u>		
DATE BEGUN: <u>01/21/12</u> DATE COMPLETED: <u>01/21/12</u>		LOGGER SIGNATURE: _____		
DEPTH (m)	LITHOLOGIC DESCRIPTION	GRAPHIC LOG	PHOTOGRAPHIC LOG	COMMENTS
3.0	Muddy sand, dark gray brown sand (2.5Y 4/1), with shell fragments			<i>Intertidal Sequence Tidal Creek (Muddy Sand)</i>
4.0	Dark gray brown fine to very fine sand (2.5Y 5/1), with some to little mud, extensively burrowed with sand filled burrows, degree of bioturbation increases with depth			<i>Subtidal Sequence Transition Zone Bioturbated and Laminated Facies</i>
5.0	BORING TERMINATED AT 5.26 m BOTTOM OF CORE LOST ON RETRIEVAL (521 cm)			
6.0				



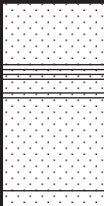
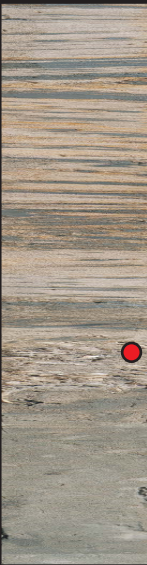
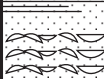
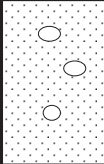
 <b>VIBRACORE BORING LOG</b> 		<b>LOCATION NUMBER: BKM 012112-02</b>			
		<b>PAGE NO. 1 OF 2</b>			
PROJECT NAME: <u>STRATIGRAPHY/PALEOTEMPESTOLOGY RESEARCH</u>		TOTAL DEPTH: <u>5.27 METERS (COMPACTED)/5.75 METERS (ORIGINAL)</u>			
W.O. NUMBER: <u>N/A</u>		NORTHING: <u>3,505,804</u>			
LOCATION: <u>NORTH BEACH, SCI</u>		EASTING: <u>487,549</u>			
DRILLERS: <u>MEYER, VANCE, KENNEDY AND MEHMET</u>		GROUND SURFACE ELEVATION: <u>0.20 ft MSL</u>			
DRILL RIG TYPE: <u>SCI VIBRACORE RIG</u>		DEPTH TO TOP OF CORE: <u>33.5" BTOP</u>			
DRILLING METHOD: <u>VIBRACORE</u>		HEIGHT ABOVE LAND SURFACE: <u>14.5" BTOP</u>			
SAMPLING METHOD: <u>3-INCH I.D. ALUMINUM PIPE</u>		COMPACTION (%): <u>8.4%</u>			
LOGGED BY: <u>B. MEYER</u> WEATHER: <u>COOL/CLOUDY/WINDY</u>		BOREHOLE DIAMETER: <u>3- INCH BOREHOLE</u>			
DATE BEGUN: <u>01/21/12</u> DATE COMPLETED: <u>01/21/12</u>		LOGGER SIGNATURE: _____			
DEPTH (m)	LITHOLOGIC DESCRIPTION	GRAPHIC LOG	PHOTOGRAPHIC LOG	TBD RESULTS	COMMENTS
0	(0-53 cm) Light brown, fine to very fine sand (2.5Y 8/2) , rippled laminations, very fine heavy mineral sands, <i>Mulinia</i> shells and shell fragments (modern foreshore)				land surface
	Organic peat layers at 43 cm, 52 cm, 53-54 cm, and 55-56 cm below land surface, macroplant material (peat)				Modern foreshore sequence
	Light brown to gray (2.5 7/1), fine to very fine quartz sand, light horizontal laminations of quartz/heavy mineral sands, firm, <i>Mulinia</i> shells and shell fragments				peat
1.0	Dark brown (2.5Y 3/1) organic peat layers, macroplant material (peat), slightly sloping/dipping (10-15d).				
	Very light brown to gray (2.5 7/1), fine to very fine quartz sand, with mud (clay/silt) laminae that are non-continuous and mud clasts (2.5Y 2.5/1)				Tidal Creek/Subtidal Sequence (laminated to burrowed facies)
2.0	Mud laminations and interlaminae in light brown to gray fine to very fine sand coarsening upward.				
	Dark gray to brown fine to very fine sand with organics (2.5Y 3/1), burrowed contact surface, burrows (1-2 cm)				
3.0	Lower sand/mud contact shell lag of whole and fragmented <i>Mulinia</i> and <i>Littoraria</i> and wood debris.			BKM 012112-02-315, <i>Ilyanassa</i> @ 315 cm (2614 +/- 27 B.P. )	Marsh and Washover Sequence
	Dk gray brn mud (2.5Y 3/1) stiff, with peaty lams				

 <b>VIBRACORE BORING LOG</b> 		<b>LOCATION NUMBER: BKM 012112-02</b>			
		<b>PAGE NO. 2 OF 2</b>			
PROJECT NAME: STRATIGRAPHY/PALEOTEMPESTOLOGY RESEARCH		TOTAL DEPTH: 5.27 METERS (COMPACTED)/5.75 METERS (ORIGINAL)			
W.O. NUMBER: N/A		NORTHING: 3,505,804			
LOCATION: NORTH BEACH, SCI		EASTING: 487,549			
DRILLERS: MEYER, VANCE, KENNEDY AND MEHMET		GROUND SURFACE ELEVATION: 0.20 ft MSL			
DRILL RIG TYPE: SCI VIBRACORE RIG		DEPTH TO TOP OF CORE: 33.5" BTOP			
DRILLING METHOD: VIBRACORE		HEIGHT ABOVE LAND SURFACE: 14.5" BTOP			
SAMPLING METHOD: 3-INCH I.D. ALUMINUM PIPE		COMPACTION (%): 8.4%			
LOGGED BY: B. MEYER WEATHER: COOL/CLOUDY/WINDY		BOREHOLE DIAMETER: 3- INCH BOREHOLE			
DATE BEGUN: 01/21/12 DATE COMPLETED: 01/21/12		LOGGER SIGNATURE:			
DEPTH (m)	LITHOLOGIC DESCRIPTION	GRAPHIC LOG	PHOTOGRAPHIC LOG	TBD RESULTS	COMMENTS
3.0	Lower sand/mud contact shell lag of whole and fragmented <i>Mulinia</i> and <i>Littoraria</i> and wood debris			BKM 012112-02-315, <i>Ilyanassa</i> @ 315 cm (2614 +/- 27 B.P.)	<i>Marsh Sequence</i>
	Dark gray brown mud (2.5Y 3/1) stiff, with peaty laminations			<i>Holocene</i>	
4.0	Medium gray (2.5 6/1), fine to very fine quartz sand, with mud (clay/silt) clasts, sand burrowed heavily, shell fragments in layers			<i>Pleistocene</i>	<i>Sound Margin/Washover Sequence</i>
	(457-449 cm) Abundant shell fragments lag			BKM 012112-02-470, <i>Donax</i> @ 465 cm (39,124 +/- 377 B.P.)	
5.0	475 cm: Burrows ( <i>Uca</i> ?) filled with fine sand from above, matrix is dark gray brown mud (2.5Y 3/1), stiff.			BKM 012112-02-470, <i>Mulinia</i> @ 470 cm (45,200 +/- 647 B.P.)	<i>Marsh Sequence</i>
	Fine sand laminations (2.5Y 7/1): 1) 5 mm, 2) 8 mm, and 3) 7 mm.			BKM 012112-02-520, peat @ 520 cm, (50,376 +/- 1020 B.P.)	
	Peat lamination (2.5Y 2.5/1) 7-9 mm thick, plant macromaterial				
	BORING TERMINATED AT 5.27 m				
6.0					






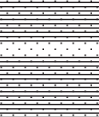

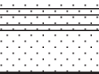
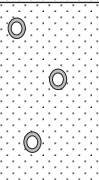
 <b>VIBRACORE BORING LOG</b> 		<b>LOCATION NUMBER: BKM 031712-01</b>		
		<b>PAGE NO. 1 OF 2</b>		
PROJECT NAME: PALEOTEMPESTOLOGY/STRATIGRAPHY RESEARCH		TOTAL DEPTH: 4.18 METERS (COMPACTED)/LOST 33" ON RETRIEVAL		
W.O. NUMBER: N/A		NORTHING: 3,505,426		
LOCATION: NORTH BEACH, SCI		EASTING: 487,230		
DRILLERS: MEYER, VANCE, RICH, KENNEDY		GROUND SURFACE ELEVATION: -0.42 ft MSL		
DRILL RIG TYPE: SCI VIBRACORE RIG		DEPTH TO TOP OF CORE: 43" BTOP		
DRILLING METHOD: VIBRACORE		HEIGHT ABOVE LAND SURFACE: 27" BTOP		
SAMPLING METHOD: 3-INCH I.D. ALUMINUM PIPE		COMPACTION (%): 7.7%		
LOGGED BY: B. MEYER WEATHER: WARM/CLEAR		BOREHOLE DIAMETER: 3- INCH BOREHOLE		
DATE BEGUN: 03/17/12 DATE COMPLETED: 03/17/12		LOGGER SIGNATURE: _____		
DEPTH (m)	LITHOLOGIC DESCRIPTION	GRAPHIC LOG	PHOTOGRAPHIC LOG	COMMENTS
0	0-50 cm: Sand, fine to very fine, little to no mud content, little HMS, faint horizontal laminations.			land surface
1.0				Intertidal Sequence Modern Upper Forebeach Laminated Facies
2.0	50-264 cm: Sand, fine to very fine with abundant shell fragments, whole disarticulated shells in layers at -94 cm, -100 cm, -117 cm, -145 cm and -200 cm, mud content increases downward from 230 cm to 264 cm.			Intertidal Sequence Modern Upper Forebeach Laminated Facies
3.0	264-310 cm: Muddy sand, fine to very fine with abundant shell fragments, whole disarticulated shells ( <i>Mulinia</i> , <i>Donax</i> and <i>Littoraria</i> ) in layers at -267 cm and -305 cm.			BKM 031712-01-117, <i>Mulinia</i> @ 117 cm ( <sup>14</sup> C = modern)
				BKM 031712-01-267, <i>Mulinia</i> @ 267 cm ( <sup>14</sup> C = modern)
				BKM 031712-01-305, <i>Donax</i> @ 305 cm

	<h2 style="margin:0;">VIBRACORE BORING LOG</h2>		<b>LOCATION NUMBER: BKM 031712-01</b>	
			<b>PAGE NO. 2 OF 2</b>	
PROJECT NAME: PALEOTEMPESTOLOGY/STRATIGRAPHY RESEARCH		TOTAL DEPTH: 4.18 METERS (COMPACTED)/LOST 33" ON RETRIEVAL		
W.O. NUMBER: N/A		NORTHING: 3,505,426		
LOCATION: NORTH BEACH, SCI		EASTING: 487,230		
DRILLERS: MEYER, VANCE, RICH, KENNEDY		GROUND SURFACE ELEVATION: -0.42 ft MSL		
DRILL RIG TYPE: SCI VIBRACORE RIG		DEPTH TO TOP OF CORE: 43" BTOP		
DRILLING METHOD: VIBRACORE		HEIGHT ABOVE LAND SURFACE: 27" BTOP		
SAMPLING METHOD: 3-INCH I.D. ALUMINUM PIPE		COMPACTION (%): 7.7%		
LOGGED BY: B. MEYER WEATHER: WARM/CLEAR		BOREHOLE DIAMETER: 3- INCH BOREHOLE		
DATE BEGUN: 03/17/12 DATE COMPLETED: 03/17/12		LOGGER SIGNATURE: _____		
DEPTH (m)	LITHOLOGIC DESCRIPTION	GRAPHIC LOG	PHOTOGRAPHIC LOG	COMMENTS
3.0				BKM 031712-01-305, <i>Donax</i> @ 305 cm
	310-418 cm: Sand, fine to very fine, little mud content, heavily burrowed, with sand filled burrows (Skolithos).			<i>Subtidal Sequence Transition Zone Bioturbated and Laminated Facies</i>
4.0				
	BORING RECOVERED = 4.18 METERS BLS			
5.0				
6.0				
f:\misc documents\sci_logs\BKM031712_01.cdr				








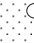




 <b>VIBRACORE BORING LOG</b> 		LOCATION NUMBER: <b>BKM 031712-02</b>		
		PAGE NO. 1 OF 2		
PROJECT NAME: PALEOTEMPESTOLOGY/STRATIGRAPHY RESEARCH		TOTAL DEPTH: 4.77 METERS (COMPACTED)/LOST 33" ON RETRIEVAL		
W.O. NUMBER: N/A		NORTHING: 3,505,135		
LOCATION: NORTH BEACH, SCI		EASTING: 487,099		
DRILLERS: MEYER, VANCE, RICH, KENNEDY		GROUND SURFACE ELEVATION: 1.08 ft MSL		
DRILL RIG TYPE: SCI VIBRACORE RIG		DEPTH TO TOP OF CORE: 38" BTOP		
DRILLING METHOD: VIBRACORE		HEIGHT ABOVE LAND SURFACE: 17" BTOP		
SAMPLING METHOD: 3-INCH I.D. ALUMINUM PIPE		COMPACTION (%): 9.4%		
LOGGED BY: B. MEYER WEATHER: WARM/CLEAR		BOREHOLE DIAMETER: 3- INCH BOREHOLE		
DATE BEGUN: 03/17/12 DATE COMPLETED: 03/17/12		LOGGER SIGNATURE: _____		
DEPTH (m)	LITHOLOGIC DESCRIPTION	GRAPHIC LOG	PHOTOGRAPHIC LOG	COMMENTS
0				land surface
	(0-55 cm) Light brown, fine to very fine sand (2.5Y 8/2) , faint laminations in upper section, rippled laminations from 20-30 cm, very fine heavy mineral sands, shells and shell fragments (modern foreshore).			<i>Intertidal Sequence Modern Upper Forebeach Laminated Facies</i>
1.0	55-120 cm: Mud (clay with silt and little fine sand), dark gray-black (10YR 10YR 2/1), organic with plant fragments in upper dark brown section.			<i>Freshwater Peat  Intertidal Sequence Low Marsh Facies</i>
2.0				<i>Intertidal Sequence High Marsh Facies</i>
3.0	120-425 cm: Fine to very fine sand with mud laminae, mud laminations and clasts (2.5Y 4/1) in light brown to gray fine to very fine sand (2.5Y 7/1), mud content increases upward from 180 cm to 120			<i>Subtidal to Intertidal Sequence Transition Zone/Channel Fill Bioturbated and Laminated Facies</i>





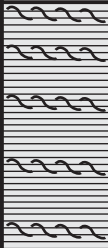



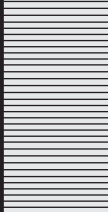



 <b>VIBRACORE BORING LOG</b> 		<b>LOCATION NUMBER: BKM 031712-02</b>		
		<b>PAGE NO. 2 OF 2</b>		
PROJECT NAME: <u>PALEOTEMPESTOLOGY/STRATIGRAPHY RESEARCH</u>		TOTAL DEPTH: <u>4.77 METERS (COMPACTED)/LOST 33" ON RETRIEVAL</u>		
W.O. NUMBER: <u>N/A</u>		NORTHING: <u>3,505,135</u>		
LOCATION: <u>NORTH BEACH, SCI</u>		EASTING: <u>487,099</u>		
DRILLERS: <u>MEYER, VANCE, RICH, KENNEDY</u>		GROUND SURFACE ELEVATION: <u>1.08 ft MSL</u>		
DRILL RIG TYPE: <u>SCI VIBRACORE RIG</u>		DEPTH TO TOP OF CORE: <u>38" BTOP</u>		
DRILLING METHOD: <u>VIBRACORE</u>		HEIGHT ABOVE LAND SURFACE: <u>17" BTOP</u>		
SAMPLING METHOD: <u>3-INCH I.D. ALUMINUM PIPE</u>		COMPACTION (%): <u>9.4%</u>		
LOGGED BY: <u>B. MEYER</u> WEATHER: <u>WARM/CLEAR</u>		BOREHOLE DIAMETER: <u>3- INCH BOREHOLE</u>		
DATE BEGUN: <u>03/17/12</u> DATE COMPLETED: <u>03/17/12</u>		LOGGER SIGNATURE: _____		
DEPTH (m)	LITHOLOGIC DESCRIPTION	GRAPHIC LOG	PHOTOGRAPHIC LOG	TBD RESULTS COMMENTS
3.0	120-425 cm: Fine to very fine sand with mud laminae, mud laminations and clasts (2.5Y 4/1) in light brown to gray fine to very fine sand (2.5Y 7/1), mud content increases upward from 180 cm to 120			<i>Subtidal to Intertidal Sequence Transition Zone/Channel Fill Bioturbated and Laminated Facies</i>
4.0	410-425 cm: Appreciable shell fragments in fine to medium sand, shell/sand channel lag.			BKM 031712-02-410, <i>Mercenaria @ 410 cm</i>
	425-477 cm: Dark gray brown fine to very fine sand (2.5Y 5/1), with some to little mud, extensively burrowed with sand filled burrows.			<i>Subtidal Sequence Transition Zone Bioturbated and Laminated Facies</i>
5.0	BORING RECOVERED = 4.77 METERS BLS			
6.0				





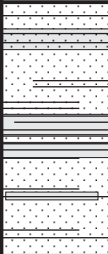



 <b>VIBRACORE BORING LOG</b> 		<b>LOCATION NUMBER: BKM 031812-01</b>		
		<b>PAGE NO. 1 OF 2</b>		
PROJECT NAME: PALEOTEMPESTOLOGY/STRATIGRAPHY RESEARCH		TOTAL DEPTH: 4.66 METERS (COMPACTED)/LOST 1" ON RETRIEVAL		
W.O. NUMBER: N/A		NORTHING: 3,504,460		
LOCATION: NORTH BEACH, SCI		EASTING: 486,985		
DRILLERS: MEYER, RICH, KENNEDY		GROUND SURFACE ELEVATION: 0.0 ft MSL		
DRILL RIG TYPE: SCI VIBRACORE RIG		DEPTH TO TOP OF CORE: 20.5" BTOP		
DRILLING METHOD: VIBRACORE		HEIGHT ABOVE LAND SURFACE: 13.5" BTOP		
SAMPLING METHOD: 3-INCH I.D. ALUMINUM PIPE		COMPACTION (%): 3.7%		
LOGGED BY: B. MEYER WEATHER: WARM/CLEAR		BOREHOLE DIAMETER: 3- INCH BOREHOLE		
DATE BEGUN: 03/18/12 DATE COMPLETED: 03/18/12		LOGGER SIGNATURE: _____		
DEPTH (m)	LITHOLOGIC DESCRIPTION	GRAPHIC LOG	PHOTOGRAPHIC LOG	TBD RESULTS COMMENTS
0				<i>land surface</i>
	0-65 cm: Dark brown, peat with fine to very fine sand (2.5Y 8/2) with interbedded sand layers of fine to very fine sand with organic material.			
	65-130 cm: Dark brown, peat with some fine to very fine sand (2.5Y 8/2).			BKM 031712-02-95, macroplant mat'l @ 95
	130-170 cm: Sand with mud (clay and silt), dark gray-black (10YR 2/1), organic.			<i>Freshwater Peat</i>
	170-235 cm: Mud (clay and silt and very little fine sand), dark gray-black (N3 to 10YR 2/1), organic with sand stringer at 200 cm.			<i>Marsh/Lacustrine Sequence</i>
	235-260 cm: Fine to very fine sand with mud laminae, mud laminations and clasts (2.5Y 4/1) in light brown to gray fine to very fine sand (2.5Y 7/1).			<i>Intertidal Sequence High Marsh Facies</i>
	260-322 cm: Fine to very fine sand, medium to light gray (5Y 8/1), with brown mud-lined <i>Callianassa</i> burrows		<i>Intertidal Sequence Lower Forebeach Burrowed and Laminated Facies</i>	
3.0				



	<h2 style="margin: 0;">VIBRACORE BORING LOG</h2>		<b>LOCATION NUMBER: BKM 031812-01</b>	
			<b>PAGE NO. 2 OF 2</b>	
PROJECT NAME: PALEOTEMPESTOLOGY/STRATIGRAPHY RESEARCH		TOTAL DEPTH: 4.66 METERS (COMPACTED)/LOST 1" ON RETRIEVAL		
W.O. NUMBER: N/A		NORTHING: 3,504,460		
LOCATION: NORTH BEACH, SCI		EASTING: 486,985		
DRILLERS: MEYER, RICH, KENNEDY		GROUND SURFACE ELEVATION: 0.0 ft MSL		
DRILL RIG TYPE: SCI VIBRACORE RIG		DEPTH TO TOP OF CORE: 20.5" BTOP		
DRILLING METHOD: VIBRACORE		HEIGHT ABOVE LAND SURFACE: 13.5" BTOP		
SAMPLING METHOD: 3-INCH I.D. ALUMINUM PIPE		COMPACTION (%): 3.7%		
LOGGED BY: B. MEYER WEATHER: WARM/CLEAR		BOREHOLE DIAMETER: 3- INCH BOREHOLE		
DATE BEGUN: 03/18/12 DATE COMPLETED: 03/18/12		LOGGER SIGNATURE: _____		
DEPTH (m)	LITHOLOGIC DESCRIPTION	GRAPHIC LOG	PHOTOGRAPHIC LOG	COMMENTS
3.0	260-322 cm: Fine to very fine sand, medium to light gray (5Y 8/1), with brown mud-lined <i>Callianassa</i> burrows			<i>Intertidal Sequence Lower Forebeach Burrowed and Laminated Facies</i>
4.0	322-466 cm: Dark gray brown fine to very fine sand (2.5Y 5/1), with some to little mud, extensively burrowed with sand filled burrows.	      		<i>Subtidal Sequence Transition Zone Bioturbated and Laminated Facies</i>
5.0	BORING TERMINATED = 4.66 METERS BLS			
6.0				

  <b>VIBRACORE BORING LOG</b>  		<b>LOCATION NUMBER: IEP 061112-01</b>		
		<b>PAGE NO. 1 OF 2</b>		
PROJECT NAME: <u>MISSION GEOARCHAEOLOGY</u>		TOTAL DEPTH: <u>3.80 METERS (COMPACTED)</u>		
W.O. NUMBER: <u>N/A</u>		NORTHING: <u>3,498,963.7</u>		
LOCATION: <u>MISSION SITE, SCI</u>		EASTING: <u>483,425.6</u>		
DRILLERS: <u>JEP (KEITH-LUCAS, POTTER AND STUDENTS)</u>		GROUND SURFACE ELEVATION: <u>2.78 FT MLS</u>		
DRILL RIG TYPE: <u>SCI VIBRACORE RIG</u>		DEPTH TO TOP OF CORE: <u>64.9" BTOP</u>		
DRILLING METHOD: <u>VIBRACORE</u>		HEIGHT ABOVE LAND SURFACE: <u>N/A BTOP</u>		
SAMPLING METHOD: <u>3-INCH I.D. ALUMINUM PIPE</u>		COMPACTION (%): <u>30.3%</u>		
LOGGED BY: <u>BISHOP/MEYER</u> WEATHER: <u>HOT, CLEAR</u>		BOREHOLE DIAMETER: <u>3- INCH BOREHOLE</u>		
DATE BEGUN: <u>6/11/2012</u> DATE COMPLETED: <u>6/11/2012</u>		LOGGER SIGNATURE: _____		
DEPTH (m)	LITHOLOGIC DESCRIPTION	GRAPHIC LOG	PHOTOGRAPHIC LOG	COMMENTS
0	0-6 cm: Organic detritus with mud (silt/clay) sandy and peaty, dark brown, sulfide odor  6-120 cm: Dark gray mud (silt/clay), iron staining, with plant material decreasing downward			<i>land surface</i>  <i>Intertidal Sequence Low Marsh Facies</i>
1.0	120-205 cm: Dark gray mud (silt/clay)			
2.0	205-257 cm: Dark gray mud (silt/clay) with light brown fine to very fine sand laminations			
3.0	257-305 cm: Light brown fine to very fine sand with dark gray mud (silt/clay) laminations  305-380 cm: Dark gray mud (silt/clay) with light brown fine to very fine sand laminations			<i>Intertidal Sequence High Marsh/Tidal Creek Facies</i>
F:\misc documents\sci_logs\IEP060411_01.cdr				

		<h2 style="margin:0;">VIBRACORE BORING LOG</h2>			<b>LOCATION NUMBER: IEP 061112-01</b>
					<b>PAGE NO. 2 OF 2</b>
PROJECT NAME: <u>MISSION GEOARCHAEOLOGY</u>			TOTAL DEPTH: <u>3.80 METERS (COMPACTED)</u>		
W.O. NUMBER: <u>N/A</u>			NORTHING: <u>3,498,963.7</u>		
LOCATION: <u>MISSION SITE, SCI</u>			EASTING: <u>483,425.6</u>		
DRILLERS: <u>JEP (KEITH-LUCAS, POTTER AND STUDENTS)</u>			GROUND SURFACE ELEVATION: <u>2.78 FT MLS</u>		
DRILL RIG TYPE: <u>SCI VIBRACORE RIG</u>			DEPTH TO TOP OF CORE: <u>64.9" BTOP</u>		
DRILLING METHOD: <u>VIBRACORE</u>			HEIGHT ABOVE LAND SURFACE: <u>N/A BTOP</u>		
SAMPLING METHOD: <u>3-INCH I.D. ALUMINUM PIPE</u>			COMPACTION (%): <u>30.3%</u>		
LOGGED BY: <u>BISHOP/MEYER</u> WEATHER: <u>HOT, CLEAR</u>			BOREHOLE DIAMETER: <u>3- INCH BOREHOLE</u>		
DATE BEGUN: <u>6/11/2012</u> DATE COMPLETED: <u>6/11/2012</u>			LOGGER SIGNATURE: _____		
DEPTH (m)	LITHOLOGIC DESCRIPTION	GRAPHIC LOG	PHOTOGRAPHIC LOG	COMMENTS	
3.0	305-380 cm: Dark gray mud (silt/clay) with light			<i>Intertidal Sequence High Marsh/Tidal Creek Facies</i>	
4.0	BORING TERMINATED AT 3.80 METERS BLS (COMPACTED)				
5.0					
6.0					



## Appendix C: XRF Results

ID	DEPTH	BORING_ID	DEP_ENV	Chemo-facies	Date	Reading	Mode	S	S +/-	Cl	Cl +/-	K	K +/-	Ca	Ca +/-	Ti	Ti +/-	Cr	Cr +/-	Mn	Mn +/-	Fe	Fe +/-	Sr	Sr +/-	Zr	Zr +/-	Ti/Zr	Fe/K
2	5.0	BKM 112010-01	washover	A	28-Mar-12	2	Soil	<LOD	3775	12037	565	1579	151	6398	191	7419	185	<LOD	16	159	10	3891	64	91	3	2057	25	3.61	2.46
3	10.0	BKM 112010-01	washover	A	28-Mar-12	3	Soil	<LOD	3665	6892	491	1273	155	10300	263	15142	319	<LOD	22	283	13	6250	102	96	4	3264	40	4.64	4.91
4	15.0	BKM 112010-01	washover	A	28-Mar-12	4	Soil	<LOD	2657	3394	340	1034	127	5979	175	3380	112	22	5	80	8	2490	42	82	3	1080	13	3.13	2.41
5	20.0	BKM 112010-01	washover	A	28-Mar-12	5	Soil	4485	1296	4279	427	1229	154	11833	287	13193	287	<LOD	21	222	12	5887	96	97	4	2559	31	5.16	4.79
6	25.0	BKM 112010-01	washover	A	28-Mar-12	6	Soil	<LOD	3554	6739	460	1312	149	8534	228	6696	177	21	6	196	11	3763	64	114	4	3940	49	1.70	2.87
7	30.0	BKM 112010-01	washover	A	28-Mar-12	7	Soil	<LOD	2517	2493	307	1739	141	2422	112	2530	93	<LOD	13	108	8	1771	32	65	3	663	9	3.82	1.02
8	35.0	BKM 112010-01	washover	A	28-Mar-12	8	Soil	<LOD	2379	771	771	1323	134	4325	147	5765	151	24	6	111	8	3041	50	64	3	2422	29	2.38	2.30
9	40.0	BKM 112010-01	washover	A	28-Mar-12	9	Soil	<LOD	3008	6387	421	2210	159	3995	145	3108	110	<LOD	15	74	8	3915	63	63	3	452	7	6.88	1.77
10	45.0	BKM 112010-01	washover	A	28-Mar-12	10	Soil	<LOD	3095	5298	411	2031	160	6089	183	5984	162	<LOD	17	117	9	4290	70	73	3	857	11	6.98	2.11
11	50.0	BKM 112010-01	washover	A	28-Mar-12	11	Soil	<LOD	3345	9030	487	2239	162	4261	151	4558	134	<LOD	16	86	8	4120	67	67	3	609	8	7.48	1.84
12	55.0	BKM 112010-01	washover	A	28-Mar-12	12	Soil	<LOD	3423	8347	467	2598	169	6191	182	4734	138	<LOD	15	90	8	4031	65	83	3	1180	15	4.01	1.55
13	60.0	BKM 112010-01	washover	A	28-Mar-12	13	Soil	<LOD	3381	13575	572	2484	166	5524	170	3270	112	<LOD	15	75	8	4128	66	77	3	669	9	4.89	1.66
14	65.0	BKM 112010-01	washover	A	28-Mar-12	14	Soil	<LOD	3400	11778	539	2588	169	6065	180	2745	102	<LOD	15	79	8	3723	61	70	3	529	7	5.19	1.44
15	70.0	BKM 112010-01	washover	A	28-Mar-12	15	Soil	<LOD	3502	11075	517	2025	153	3370	132	2175	90	<LOD	15	39	7	3618	59	56	2	489	7	4.45	1.79
16	75.0	BKM 112010-01	washover	A	28-Mar-12	16	Soil	<LOD	2330	1766	291	1589	141	3967	141	2160	88	<LOD	13	51	7	2194	38	55	2	349	5	6.19	1.38
17	80.0	BKM 112010-01	washover	A	28-Mar-12	17	Soil	<LOD	2629	3206	329	1967	149	4349	147	1792	80	<LOD	13	51	7	1995	35	52	2	695	9	2.58	1.01
18	85.0	BKM 112010-01	washover	A	28-Mar-12	18	Soil	4365	1051	5863	387	1783	140	1762	98	1424	70	<LOD	12	34	6	1646	30	41	2	360	5	3.96	0.92
19	90.0	BKM 112010-01	washover	A	28-Mar-12	19	Soil	4900	1206	10913	504	1188	128	3008	123	1618	74	<LOD	12	46	7	2071	36	32	2	521	7	3.11	1.74
20	95.0	BKM 112010-01	washover	A	28-Mar-12	20	Soil	<LOD	2477	2343	286	1130	120	3569	128	1761	75	<LOD	12	36	6	1698	30	48	2	371	6	4.75	1.50
21	100.0	BKM 112010-01	washover	A	28-Mar-12	21	Soil	<LOD	2383	1546	278	1265	130	2074	105	1190	65	<LOD	13	<LOD	17	1193	24	38	2	185	4	6.43	0.94
22	105.0	BKM 112010-01	low marsh peat	D	28-Mar-12	22	Soil	28221	3888	139670	3007	4374	257	3074	158	2099	114	<LOD	23	206	14	13657	241	81	3	285	6	7.36	3.12
23	120.0	BKM 112010-01	low marsh	E	28-Mar-12	23	Soil	<LOD	17755	417846	8413	1266	196	256	256	302	69	<LOD	24	54	12	11824	228	68	3	83	3	6.34	9.34
24	130.0	BKM 112010-01	low marsh	E	28-Mar-12	24	Soil	<LOD	17681	378270	7871	1838	220	252	252	338	66	<LOD	24	61	12	8704	175	74	3	88	3	3.84	4.74
25	140.0	BKM 112010-01	low marsh	E	28-Mar-12	25	Soil	43321	5663	310526	6219	1585	199	750	110	363	69	<LOD	23	109	13	13728	254	67	3	153	4	2.37	8.66
26	150.0	BKM 112010-01	low marsh	E	28-Mar-12	26	Soil	<LOD	18192	375670	8226	1007	216	4025	205	358	66	<LOD	23	56	11	3886	88	43	3	53	3	6.75	3.86
27	160.0	BKM 112010-01	low marsh	E	28-Mar-12	27	Soil	<LOD	15825	309513	6620	3042	259	3049	176	915	88	<LOD	23	70	12	8941	180	55	3	66	3	13.86	2.94
29	170.0	BKM 112010-01	low marsh	E	28-Mar-12	29	Soil	<LOD	17895	437863	8530	665	167	223	223	192	50	<LOD	20	61	10	2793	60	36	2	66	3	2.91	4.20
30	180.0	BKM 112010-01	low marsh	E	28-Mar-12	30	Soil	<LOD	19150	427420	9125	966	208	3130	182	204	55	<LOD	22	<LOD	30	3656	82	56	3	54	3	3.78	3.78
31	190.0	BKM 112010-01	low marsh	E	28-Mar-12	31	Soil	<LOD	18160	390747	8490	1293	220	269	269	444	68	<LOD	22	100	13	4144	93	34	2	56	3	7.93	3.20
32	200.0	BKM 112010-01	low marsh	E	28-Mar-12	32	Soil	<LOD	18493	452441	9155	956	190	1064	123	404	59	<LOD	19	64	10	2262	53	49	3	60	3	6.73	2.37
33	210.0	BKM 112010-01	low marsh	E	28-Mar-12	33	Soil	<LOD	16804	376195	7436	1104	188	9066	287	353	55	<LOD	19	43	10	3179	67	92	3	90	3	3.92	2.88
34	220.0	BKM 112010-01	low marsh	E	28-Mar-12	34	Soil	43158	6134	340064	7055	1733	228	22958	570	725	80	<LOD	20	54	11	6115	124	126	4	75	3	9.67	3.53
35	230.0	BKM 112010-01	low marsh	E	28-Mar-12	35	Soil	<LOD	17235	424263	8098	166	970	112	303	50	<LOD	18	77	10	2528	54	88	3	69	3	4.39	3.15	
36	240.0	BKM 112010-01	low marsh	E	28-Mar-12	36	Soil	<LOD	4027	20197	690	3437	184	1380	94	1288	72	<LOD	15	59	8	4558	72	39	2	281	5	4.58	1.33
37	250.0	BKM 112010-01	low marsh	E	28-Mar-12	37	Soil	17242	5097	317037	6128	4357	258	439	101	1209	93	<LOD	24	81	12	12934	232	74	3	154	4	7.85	2.97
38	260.0	BKM 112010-01	low marsh	E	28-Mar-12	38	Soil	9330	3099	115361	2496	5999	280	1067	110	1855	105	<LOD	23	64	11	12708	217	64	3	160	4	11.59	2.12
39	270.0	BKM 112010-01	bioturbated and laminated	C	28-Mar-12	39	Soil	7182	1653	36290	927	3008	166	872	80	804	56	<LOD	13	<LOD	18	2760	45	52	2	278	5	2.89	0.92
40	280.0	BKM 112010-01	bioturbated and laminated	C	28-Mar-12	40	Soil	6897	1990	44635	1183	3668	208	2073	119	2169	99	<LOD	17	59	9	5600	93	48	2	522	8	4.16	1.53
41	290.0	BKM 112010-01	bioturbated and laminated	C	28-Mar-12	41	Soil	<LOD	3181	9983	470	2644	158	1901	101	1506	71	<LOD	13	41	7	2749	45	40	2	226	4	6.66	1.04
42	300.0	BKM 112010-01	bioturbated and laminated	C	28-Mar-12	42	Soil	6350	1923	45178	1162	2246	169	4842	166	828	62	<LOD	14	<LOD	19	2106	39	38	2	233	4	3.55	0.94
43	310.0	BKM 112010-01	bioturbated and laminated	C	28-Mar-12	43	Soil	16847	2689	80369	1755	2620	185	9304	247	1181	74	<LOD	15	<LOD	21	3300	58	50	2	283	5	4.17	1.26
44	320.0	BKM 112010-01	bioturbated and laminated	C	28-Mar-12	44	Soil	6965	2025	50518	1254	4384	217	1733	110	1195	74	<LOD	16	33	8	6099	99	49	2	297	5	4.02	1.39
45	330.0	BKM 112010-01	bioturbated and laminated	C	28-Mar-12	45	Soil	11597	2085	43632	1138	5043	231	2683	130	1869	90	<LOD	18	53	9	7684	122	49	2	136	3	13.74	1.52
46	340.0	BKM 112010-01	bioturbated and laminated	C	28-Mar-12	46	Soil	7153	1174	4338	357	2314	155	793	79	1053	64	<LOD	13	<LOD	18	2438	42	39	2	238	4	4.42	1.05
47	350.0	BKM 112010-01	bioturbated and laminated	C	28-Mar-12	47	Soil	<LOD	2752	3052	341	2929	178	1092	91	1413	74	<LOD	15	21	7	4021	66	38	2	154	4	9.18	1.37
48	360.0	BKM 112010-01	bioturbated and laminated	C	28-Mar-12	48	Soil	3531	932	2828	310	2483	157	598	73	792	54	<LOD	12	19	6	1779	32	31	2	174	4	4.55	0.72
49	370.0	BKM 112010-01	bioturbated and laminated	C	28-Mar-12	49	Soil	<LOD	4009	20528	706	1521	141	953	84	694	52	<LOD	13	<LOD	17	1074	23	22	2	118	3	5.88	0.71
50	380.0	BKM 112010-01	bioturbated and laminated	C	28-Mar-12	50	Soil	11764	2049	43125	1115	5109	229	2088	116	1833	9												

ID	DEPTH	BORING_ID	DEP_ENV	Chemo-facies	Date	Reading	Mode	S	S +/-	Cl	Cl +/-	K	K +/-	Ca	Ca +/-	Ti	Ti +/-	Cr	Cr +/-	Mn	Mn +/-	Fe	Fe +/-	Sr	Sr +/-	Zr	Zr +/-	Ti/Zr	Fe/K
9	160.0	BKM112110-02	low marsh	E	26-Mar-12	9	Soil	19158	4019	141066	3237	10921	426	3157	178	3116	166	41	12	215	19	39350	721	126	4	286	6	10.90	3.60
10	170.0	BKM112110-02	low marsh	E	26-Mar-12	10	Soil	30644	2760	14925	735	18559	532	2449	159	4189	180	48	13	198	18	53918	901	159	4	402	7	10.42	2.91
11	180.0	BKM112110-02	low marsh	E	26-Mar-12	11	Soil	23007	2294	11529	615	14002	422	4363	180	3819	155	<LOD	31	280	17	41200	653	148	4	325	6	11.75	2.94
12	190.0	BKM112110-02	low marsh	E	26-Mar-12	12	Soil	14469	1793	7780	500	8144	301	3127	146	3238	133	42	9	175	13	22316	346	85	3	212	4	15.27	2.74
13	200.0	BKM112110-02	low marsh	E	26-Mar-12	13	Soil	33048	2344	8585	506	8292	294	2243	126	3446	135	<LOD	26	197	14	27694	413	79	3	250	4	13.78	3.34
14	210.0	BKM112110-02	low marsh	E	26-Mar-12	14	Soil	11618	1811	9150	556	9318	337	1268	115	3478	148	36	10	184	15	32341	517	95	3	200	4	17.39	3.47
15	220.0	BKM112110-02	low marsh	E	26-Mar-12	15	Soil	11882	1626	6183	455	7039	276	4210	162	2768	118	27	8	85	11	16493	255	85	3	225	4	12.30	2.34
16	230.0	BKM112110-02	low marsh	E	26-Mar-12	16	Soil	10091	1543	7921	482	8149	290	1902	117	2917	118	34	8	116	11	17701	267	85	3	254	5	11.48	2.17
17	240.0	BKM112110-02	low marsh	E	26-Mar-12	17	Soil	10872	1549	5673	438	5672	248	2408	126	2038	102	<LOD	21	106	11	14285	222	67	3	233	5	8.75	2.52
18	250.0	BKM112110-02	bioturbated and laminated	C	26-Mar-12	18	Soil	11515	1609	8791	504	7975	288	2806	134	2424	108	30	7	82	10	13532	207	82	3	314	5	7.72	1.70
19	260.0	BKM112110-02	bioturbated and laminated	C	26-Mar-12	19	Soil	3694	1010	2408	321	2880	176	1839	106	1178	69	<LOD	14	26	7	3590	60	39	2	214	4	5.50	1.25
20	270.0	BKM112110-02	bioturbated and laminated	C	26-Mar-12	20	Soil	7057	1191	1854	310	3101	181	2963	128	2779	104	<LOD	15	66	8	4338	70	44	2	439	7	6.33	1.40
21	280.0	BKM112110-02	bioturbated and laminated	C	26-Mar-12	21	Soil	5471	1244	6786	441	4012	222	3458	140	2261	96	<LOD	17	110	9	6528	102	63	3	250	5	9.04	1.33
22	290.0	BKM112110-02	bioturbated and laminated	C	26-Mar-12	22	Soil	8320	1333	5792	416	4117	205	2331	118	1130	70	<LOD	16	35	7	4024	66	48	2	166	4	6.81	0.98
23	300.0	BKM112110-02	bioturbated and laminated	C	26-Mar-12	23	Soil	3870	1120	7059	432	3750	191	1977	109	2030	88	<LOD	15	40	7	4750	75	59	2	370	6	5.49	1.27
24	310.0	BKM112110-02	bioturbated and laminated	C	26-Mar-12	24	Soil	4418	1109	6737	414	4389	200	1094	88	1270	71	<LOD	15	71	8	5555	84	54	2	124	3	10.24	1.27
25	320.0	BKM112110-02	bioturbated and laminated	C	26-Mar-12	25	Soil	3917	1027	5335	376	2070	148	2612	115	1128	61	<LOD	13	32	6	2057	36	37	2	172	4	6.56	0.99
27	330.0	BKM112110-02	bioturbated and laminated	C	26-Mar-12	27	Soil	3535	1118	10113	487	2453	158	847	81	1152	65	<LOD	14	35	7	2431	42	42	2	263	5	4.38	0.99
28	340.0	BKM112110-02	bioturbated and laminated	C	26-Mar-12	28	Soil	<LOD	2624	4695	363	2142	151	1655	97	1098	56	<LOD	13	<LOD	17	1398	27	39	2	245	4	3.71	0.65
29	350.0	BKM112110-02	bioturbated and laminated	C	26-Mar-12	29	Soil	<LOD	2369	2675	304	1654	137	1086	83	1092	60	<LOD	11	27	6	1300	25	29	2	238	4	4.59	0.79
30	360.0	BKM112110-02	bioturbated and laminated	C	26-Mar-12	30	Soil	2997	928	3865	337	2372	153	1023	83	1629	75	<LOD	12	31	6	1699	31	35	2	415	6	3.93	0.72
31	370.0	BKM112110-02	bioturbated and laminated	C	26-Mar-12	31	Soil	2734	904	3469	326	2741	162	817	78	528	48	<LOD	13	22	6	1943	34	40	2	143	3	3.69	0.71
32	380.0	BKM112110-02	bioturbated and laminated	C	26-Mar-12	32	Soil	13157	2049	26503	898	6536	278	2876	143	1700	103	<LOD	24	76	11	16124	260	62	3	103	3	16.50	2.47
33	390.0	BKM112110-02	bioturbated and laminated	C	26-Mar-12	33	Soil	<LOD	3777	15555	587	1612	135	730	75	987	57	<LOD	12	21	6	1369	26	28	2	150	3	6.58	0.85
34	400.0	BKM112110-02	bioturbated and laminated	C	26-Mar-12	34	Soil	<LOD	2713	10777	473	2618	152	929	78	811	51	<LOD	12	<LOD	16	1085	22	38	2	202	4	4.01	0.41
35	410.0	BKM112110-02	bioturbated and laminated	C	26-Mar-12	35	Soil	<LOD	2584	5602	369	2274	148	716	74	586	47	<LOD	12	18	6	1451	27	38	2	331	5	1.77	0.64
36	420.0	BKM112110-02	bioturbated and laminated	C	26-Mar-12	36	Soil	<LOD	3389	11578	517	2596	162	1380	92	1010	64	<LOD	14	40	7	3339	54	45	2	139	3	7.27	1.29
37	430.0	BKM112110-02	bioturbated and laminated	C	26-Mar-12	37	Soil	15297	2683	77434	1755	4728	237	2136	125	1182	80	<LOD	19	38	9	7730	128	61	3	119	3	9.93	1.63
38	440.0	BKM112110-02	bioturbated and laminated	C	26-Mar-12	38	Soil	14714	2352	42755	1209	5619	265	4496	175	2218	112	<LOD	23	121	12	12747	211	82	3	189	4	11.74	2.27
39	450.0	BKM112110-02	bioturbated and laminated	C	26-Mar-12	39	Soil	9866	1901	24801	872	6087	271	1609	116	1713	99	27	8	50	10	12263	202	71	3	123	3	13.93	2.01
40	460.0	BKM112110-02	bioturbated and laminated	C	26-Mar-12	40	Soil	<LOD	2173	1457	241	2496	144	724	71	738	50	<LOD	11	<LOD	15	1305	24	34	2	101	3	7.31	0.52
41	470.0	BKM112110-02	bioturbated and laminated	C	26-Mar-12	41	Soil	2632	839	3651	308	2180	139	363	63	711	48	<LOD	11	<LOD	16	1142	22	31	2	128	3	5.55	0.52
42	480.0	BKM112110-02	bioturbated and laminated	C	26-Mar-12	42	Soil	3971	981	6828	381	2005	135	1646	90	451	41	<LOD	10	<LOD	16	1116	22	36	2	113	3	3.99	0.56
43	490.0	BKM112110-02	bioturbated and laminated	C	26-Mar-12	43	Soil	7229	1553	18927	706	3115	189	1502	102	1288	73	<LOD	16	31	7	4224	71	47	2	122	3	10.56	1.36
44	500.0	BKM112110-02	bioturbated and laminated	C	26-Mar-12	44	Soil	6274	1100	3477	330	1573	136	2052	104	1327	68	<LOD	12	<LOD	17	1630	30	36	2	158	3	8.40	1.04
55	5.0	BKM 050911-01	backbeach	A1	5-May-12	55	Soil	<LOD	3024	<LOD	858	850	135	9140	235	10132	230	<LOD	19	154	10	5679	90	124	5	5220	66	1.94	6.68
56	10.0	BKM 050911-01	backbeach	A1	5-May-12	56	Soil	<LOD	3645	<LOD	1096	740	160	15301	360	27263	529	<LOD	27	516	18	11256	185	140	5	7819	105	3.49	15.21
57	15.0	BKM 050911-01	backbeach	A1	5-May-12	57	Soil	<LOD	2536	<LOD	832	659	127	8980	230	8871	206	22	6	156	10	4391	71	102	3	1793	22	4.95	6.66
58	20.0	BKM 050911-01	backbeach	A1	5-May-12	58	Soil	<LOD	2151	<LOD	753	906	121	3061	124	3299	108	<LOD	13	76	7	1853	33	43	2	572	8	5.77	2.05
59	25.0	BKM 050911-01	backbeach	A2	5-May-12	59	Soil	<LOD	1854	<LOD	641	1005	115	2606	111	1586	73	<LOD	13	29	6	1238	24	51	2	607	8	2.61	1.23
60	30.0	BKM 050911-01	backbeach	A2	5-May-12	60	Soil	<LOD	2399	1359	266	706	112	3939	137	1724	78	<LOD	13	35	6	1791	32	49	2	462	7	3.73	2.54
61	35.0	BKM 050911-01	backbeach	A2	5-May-12	61	Soil	<LOD	1943	<LOD	682	1399	127	2496	109	1635	73	<LOD	12	31	6	1429	27	44	2	382	6	4.28	1.02
62	40.0	BKM 050911-01	backbeach	A2	5-May-12	62	Soil	<LOD	2077	<LOD	653	1187	123	2340	108	2465	91	<LOD	13	50	7	1906	33	31	2	655	8	3.76	1.61
63	45.0	BKM 050911-01	backbeach	A3	5-May-12	63	Soil	<LOD	2908	3440	394	1281	148	4952	170	15297	314	<LOD	21	224	12	5530	89	51	3	3520	42	4.35	4.32
64	50.0	BKM 050911-01	backbeach	A3	5-May-12	64	Soil	<LOD	6513	5347	737	1372	241	17325	469	78054	1556	<LOD	50	1321	38	24161	453	117	10	23859	484	3.27	17.61
65	55.0	BKM 050911-01	backbeach	A3	5-May-12	65	Soil	<LOD	5881	4072	693	872	220	15696	430	80275	1564	<LOD	48	1258	36	23194	427	94	10	22235	447	3.61	26.60
66	60.0	BKM 050911-01	backbeach	A3	5-May-12	66	Soil	<LOD	5083	8688	655	1088	188	13900	358	45373	857	<LOD	34	727	23	14160	242	116	7	13906	217	3.26	13.01
67	65.0	BKM 050911-01	backbeach	A3	5-May-12	67	Soil	<LOD	3981	3699	495	88																	

ID	DEPTH	BORING_ID	DEP_ENV	Chemo-facies	Date	Reading	Mode	S	S +/-	Cl	Cl +/-	K	K +/-	Ca	Ca +/-	Ti	Ti +/-	Cr	Cr +/-	Mn	Mn +/-	Fe	Fe +/-	Sr	Sr +/-	Zr	Zr +/-	Ti/Zr	Fe/K	
70	70.0	BKM 050911-02	washover	A	6-Jun-12	8	Soil	<LOD	3617	1202	362	1720	164	9473	247	23095	432	31	8	432	16	8297	130	79	4	4054	49	5.70	4.82	
80	80.0	BKM 050911-02	washover	A	6-Jun-12	9	Soil	<LOD	2828	2177	341	1056	138	6802	196	9262	216	22	6	171	10	4577	74	64	3	2434	29	3.81	4.33	
90	90.0	BKM 050911-02	washover	A	6-Jun-12	10	Soil	<LOD	2703	2068	307	1690	146	8936	222	3559	116	28	6	88	8	2949	49	70	3	920	12	3.87	1.74	
100	100.0	BKM 050911-02	washover	A	6-Jun-12	11	Soil	<LOD	2415	1744	300	1308	137	5731	174	3057	108	<LOD	15	94	8	2694	46	65	3	834	10	3.67	2.06	
110	110.0	BKM 050911-02	washover	A	6-Jun-12	12	Soil	<LOD	2434	1754	276	1926	141	5529	161	3889	117	<LOD	14	84	7	2555	42	60	3	1031	12	3.77	1.33	
112	112.0	BKM 050911-02	low marsh peat	D	6-Jun-12	13	Soil	<LOD	2703	4547	358	2114	150	4185	143	2569	97	<LOD	14	55	7	3600	57	61	2	292	5	8.80	1.70	
120	120.0	BKM 050911-02	low marsh peat	D	6-Jun-12	14	Soil	<LOD	3218	7527	432	3244	176	3817	138	5185	144	<LOD	18	90	9	9447	136	50	2	349	5	14.86	2.91	
130	130.0	BKM 050911-02	low marsh peat	D	6-Jun-12	15	Soil	<LOD	4249	1230	10158	485	3779	188	2887	122	2495	104	24	7	65	10	19266	271	45	2	244	4	10.23	5.10
140	140.0	BKM 050911-02	low marsh peat	D	6-Jun-12	16	Soil	5078	1275	11454	500	3480	178	4542	148	3355	116	<LOD	20	94	10	21267	291	64	2	152	3	22.07	6.11	
150	150.0	BKM 050911-02	low marsh peat	D	6-Jun-12	17	Soil	11804	1601	10594	505	4901	215	2373	116	2327	112	<LOD	24	59	12	33664	473	51	2	149	3	15.62	6.87	
82	10.0	BKM 050911-03	low marsh	E	5-May-12	82	Soil	6483	1250	11173	477	3476	170	3557	127	2433	95	21	6	65	9	13717	185	52	2	239	4	10.18	3.95	
83	20.0	BKM 050911-03	low marsh	E	5-May-12	83	Soil	<LOD	2743	4488	359	1245	129	3852	137	2158	86	<LOD	14	66	7	2655	44	70	3	661	9	3.26	2.13	
84	30.0	BKM 050911-03	low marsh	E	5-May-12	84	Soil	<LOD	2966	7691	413	2917	161	2222	105	1582	76	<LOD	15	62	7	5882	85	45	2	332	5	4.77	2.02	
85	40.0	BKM 050911-03	low marsh	E	5-May-12	85	Soil	8335	1447	11398	511	4680	207	3565	135	2038	103	<LOD	23	62	11	27813	387	51	2	100	3	20.38	5.94	
86	50.0	BKM 050911-03	low marsh	E	5-May-12	86	Soil	3730	1000	10483	410	2806	137	1068	73	1547	74	<LOD	17	74	8	17471	211	47	2	83	2	18.64	6.23	
87	60.0	BKM 050911-03	low marsh	E	5-May-12	87	Soil	<LOD	2844	11894	428	2894	135	1029	71	1342	68	20	5	76	8	13139	159	45	2	88	2	15.25	4.54	
88	70.0	BKM 050911-03	low marsh	E	5-May-12	88	Soil	4360	1017	10931	413	2793	134	1133	73	1466	72	18	6	46	8	16880	202	49	2	81	2	18.10	6.04	
89	80.0	BKM 050911-03	low marsh	E	5-May-12	89	Soil	2823	919	6997	352	4528	172	1187	79	1861	79	33	6	65	8	15780	195	47	2	81	2	22.98	3.48	
90	90.0	BKM 050911-03	low marsh	E	5-May-12	90	Soil	<LOD	2774	7977	374	4191	168	1002	76	1801	79	18	6	83	8	16175	201	43	2	79	2	22.80	3.86	
91	100.0	BKM 050911-03	low marsh	E	5-May-12	91	Soil	<LOD	2867	7667	373	3970	166	1333	82	1916	84	28	6	69	9	17621	221	46	2	88	2	21.77	4.44	
92	110.0	BKM 050911-03	low marsh	E	5-May-12	92	Soil	2942	953	8083	376	4460	172	1827	90	1857	80	28	6	67	8	15148	188	64	2	106	3	17.52	3.40	
93	120.0	BKM 050911-03	low marsh	E	5-May-12	93	Soil	<LOD	2750	7092	360	4442	174	2631	104	1847	82	22	6	68	8	14983	188	65	2	111	3	16.64	3.37	
94	130.0	BKM 050911-03	low marsh	E	5-May-12	94	Soil	3293	983	8325	386	4382	173	2236	98	1818	82	19	6	101	9	14626	184	67	2	137	3	13.27	3.34	
95	140.0	BKM 050911-03	low marsh	E	5-May-12	95	Soil	<LOD	2809	8435	386	4295	170	1674	88	2040	83	31	6	94	9	16071	201	54	2	111	3	18.38	3.74	
96	150.0	BKM 050911-03	low marsh	E	5-May-12	96	Soil	<LOD	2539	9977	402	3272	146	1267	78	1536	72	<LOD	16	61	8	14705	180	50	2	101	3	15.21	4.49	
97	160.0	BKM 050911-03	low marsh	E	5-May-12	97	Soil	3016	949	9370	387	3500	149	2136	92	1593	73	<LOD	17	48	8	16241	195	42	2	66	2	24.14	4.64	
98	170.0	BKM 050911-03	low marsh	E	5-May-12	98	Soil	4417	1006	8448	380	3313	150	1711	87	1637	76	25	6	75	8	14576	180	54	2	82	2	19.96	4.40	
99	180.0	BKM 050911-03	low marsh	E	5-May-12	99	Soil	<LOD	2957	9124	411	4809	185	2237	100	1871	85	<LOD	18	65	8	14773	189	72	2	144	3	12.99	3.07	
100	190.0	BKM 050911-03	low marsh	E	5-May-12	100	Soil	4992	1105	8962	411	3959	170	2466	104	1955	86	<LOD	19	2048	35	15618	201	61	2	132	3	14.81	3.94	
101	200.0	BKM 050911-03	low marsh	E	5-May-12	101	Soil	5661	1081	6972	367	4643	181	2172	99	2172	87	<LOD	17	259	11	14858	190	60	2	119	3	18.25	2.26	
2	210.0	BKM 050911-03	low marsh	E	18-May-12	2	Soil	6463	1182	5411	362	5356	208	5207	156	2434	95	25	6	116	10	15837	214	70	2	137	3	17.77	2.90	
3	220.0	BKM 050911-03	low marsh	E	18-May-12	3	Soil	5441	1090	5463	348	5005	194	2741	113	2215	93	21	6	135	10	16716	219	57	2	113	3	19.60	3.34	
4	230.0	BKM 050911-03	low marsh	E	18-May-12	4	Soil	4840	1013	5057	324	5330	192	2280	101	2299	90	25	6	131	9	16673	211	59	2	109	3	21.09	3.13	
5	240.0	BKM 050911-03	low marsh	E	18-May-12	5	Soil	4351	1014	5464	336	5073	189	2796	110	2352	91	<LOD	18	120	9	17014	217	58	2	98	3	24.00	3.35	
6	250.0	BKM 050911-03	low marsh	E	18-May-12	6	Soil	7089	1139	5664	345	5403	197	2076	100	2362	94	22	6	111	9	16943	218	56	2	103	3	22.93	3.14	
7	260.0	BKM 050911-03	low marsh	E	18-May-12	7	Soil	3432	991	6223	357	5210	194	2997	115	2348	91	36	6	104	9	14463	187	65	2	143	3	16.42	2.78	
8	270.0	BKM 050911-03	low marsh	E	18-May-12	8	Soil	3763	1034	5656	355	5572	206	1877	99	2415	97	24	7	131	10	18404	242	60	2	113	3	21.37	3.30	
9	280.0	BKM 050911-03	low marsh	E	18-May-12	9	Soil	6840	1167	5313	351	5323	203	1444	92	2417	98	<LOD	19	107	10	19057	252	54	2	156	3	15.49	3.58	
10	290.0	BKM 050911-03	low marsh	E	18-May-12	10	Soil	4662	1077	6239	368	5118	197	1977	100	2281	95	21	6	107	9	16796	221	62	2	151	3	15.11	3.28	
11	300.0	BKM 050911-03	low marsh	E	18-May-12	11	Soil	5712	1092	4742	333	5195	198	2299	105	2415	96	31	7	114	10	17378	228	54	2	115	3	21.00	3.35	
12	310.0	BKM 050911-03	low marsh	E	18-May-12	12	Soil	5835	1076	5134	342	4512	186	1785	96	1486	75	<LOD	17	81	8	10335	140	53	2	99	3	15.01	2.29	
13	320.0	BKM 050911-03	low marsh	E	18-May-12	13	Soil	6421	1130	5928	358	6206	215	2279	105	2507	95	22	6	116	9	14535	191	70	2	197	4	12.73	2.34	
14	330.0	BKM 050911-03	low marsh	E	18-May-12	14	Soil	3364	985	5177	351	4642	192	2001	101	1964	85	23	6	113	9	9910	136	47	2	148	3	13.27	2.13	
15	340.0	BKM 050911-03	bioturbated and laminated	C	18-May-12	15	Soil	4559	907	1307	242	2162	139	3854	129	1110	58	<LOD	11	31	6	2011	33	44	2	182	4	6.10	0.93	
16	350.0	BKM 050911-03	bioturbated and laminated	C	18-May-12	16	Soil	3820	883	1219	247	2264	145	3866	132	747	50	<LOD	12	<LOD	16	1135	22	36	2	119	3	6.28	0.50	
17	360.0	BKM 050911-03	bioturbated and laminated	C	18-May-12	17	Soil	14485	1425	5226	349	3442	168	9252	210	1139	67	<LOD	15	38	7	7686	105	37	2	71	2	16.04	2.23	
18	370.0	BKM 050911-03	bioturbated and laminated	C	18-May-12	18	Soil	<LOD	1892	1830	248	2009	131	518	65	1211	59	<LOD	10	18	5	815	17	27	2	111	3	10.91	0.41	
19	380.0	BKM 050911-03	bioturbated and laminated	C	18-May-12	19	Soil	<LOD	1898	1481	244	1574	124	892	74	619	46	<LOD	10	<LOD	15	862	18	28	2	113	3	5.48	0.55	
20	390.0	BKM 05091																												

ID	DEPTH	BORING_ID	DEP_ENV	Chemo-facies	Date	Reading	Mode	S	S +/-	Cl	Cl +/-	K	K +/-	Ca	Ca +/-	Ti	Ti +/-	Cr	Cr +/-	Mn	Mn +/-	Fe	Fe +/-	Sr	Sr +/-	Zr	Zr +/-	Ti/Zr	Fe/K
11	50.0	BKM051011-01	backbeach	A	14-May-12	11	Soil	<LOD	2117	<LOD	665	2932	168	5397	164	1131	68	<LOD	13	27	6	1488	28	79	3	142	3	7.96	0.51
12	55.0	BKM051011-01	backbeach	A	14-May-12	12	Soil	<LOD	1963	<LOD	633	2647	157	4864	151	1242	66	<LOD	13	36	6	1350	25	74	3	219	4	5.67	0.51
13	60.0	BKM051011-01	backbeach	A	14-May-12	13	Soil	<LOD	1913	<LOD	650	2136	147	4256	142	1288	66	14	5	38	6	1495	28	64	2	236	4	5.46	0.70
14	65.0	BKM051011-01	backbeach	A	14-May-12	14	Soil	<LOD	1981	<LOD	663	2590	157	5129	156	1470	70	<LOD	13	27	6	1461	27	78	3	342	5	4.30	0.56
15	70.0	BKM051011-01	backbeach	A	14-May-12	15	Soil	<LOD	1671	<LOD	604	4622	194	3784	133	757	51	<LOD	12	23	6	1283	24	77	2	84	3	9.01	0.28
16	75.0	BKM051011-01	backbeach	A	14-May-12	16	Soil	<LOD	2643	<LOD	775	2036	158	11494	265	7221	181	<LOD	18	126	9	3991	64	118	3	1522	18	4.74	1.96
17	80.0	BKM051011-01	backbeach	A	14-May-12	17	Soil	<LOD	1499	<LOD	602	2064	137	3100	116	832	52	<LOD	12	<LOD	15	1197	23	61	2	169	3	4.92	0.58
18	85.0	BKM051011-01	backbeach	A	14-May-12	18	Soil	<LOD	1994	<LOD	657	2660	158	4650	148	1052	60	<LOD	12	23	6	1453	27	69	2	117	3	8.99	0.55
19	90.0	BKM051011-01	upper forebeach	B	14-May-12	19	Soil	<LOD	2007	<LOD	588	2732	153	2357	105	278	36	<LOD	12	<LOD	16	1221	23	49	2	59	2	4.71	0.45
20	95.0	BKM051011-01	upper forebeach	B	14-May-12	20	Soil	<LOD	1816	<LOD	595	2685	155	6074	167	576	48	<LOD	12	<LOD	15	1402	26	79	3	106	3	5.43	0.52
21	100.0	BKM051011-01	upper forebeach	B	14-May-12	21	Soil	<LOD	1887	<LOD	667	2783	156	2418	107	364	42	<LOD	12	<LOD	15	990	20	56	2	26	2	14.00	0.36
22	105.0	BKM051011-01	upper forebeach	B	14-May-12	22	Soil	<LOD	1797	<LOD	550	1865	131	4735	142	330	37	<LOD	10	16	5	965	19	61	2	42	2	7.86	0.52
23	110.0	BKM051011-01	upper forebeach	B	14-May-12	23	Soil	<LOD	1864	<LOD	583	2227	144	4892	148	477	44	<LOD	12	<LOD	16	1187	23	58	2	51	2	9.35	0.53
24	115.0	BKM051011-01	upper forebeach	B	14-May-12	24	Soil	<LOD	2274	<LOD	655	1723	142	9434	225	956	60	<LOD	13	26	6	1719	31	85	3	86	3	11.12	1.00
25	120.0	BKM051011-01	upper forebeach	B	14-May-12	25	Soil	<LOD	1963	<LOD	632	2379	149	4030	136	371	41	<LOD	11	26	6	1146	23	63	2	68	3	5.46	0.48
26	125.0	BKM051011-01	upper forebeach	B	14-May-12	26	Soil	<LOD	2376	<LOD	662	2041	148	10219	234	2328	88	<LOD	14	51	7	2494	41	114	3	246	4	9.46	1.22
27	130.0	BKM051011-01	upper forebeach	B	14-May-12	27	Soil	3155	869	<LOD	672	3889	185	5125	157	1109	64	<LOD	12	23	6	2179	37	78	3	106	3	10.46	0.56
28	135.0	BKM051011-01	upper forebeach	B	14-May-12	28	Soil	4626	997	<LOD	690	2571	161	9986	233	2081	85	<LOD	14	44	7	2751	45	83	3	155	3	13.43	1.07
13	5.0	BKM 051011-02	Freshwater pond	A	17-Mar-12	13	Soil	11612	1162	12115	397	1148	90	9933	182	797	43	<LOD	10	25	5	3186	40	81	2	183	3	4.36	2.78
14	10.0	BKM 051011-02	Freshwater pond	A	17-Mar-12	14	Soil	4550	905	8845	358	1275	95	3498	106	1085	51	<LOD	10	23	5	3548	46	51	2	133	3	8.16	2.78
15	15.0	BKM 051011-02	Freshwater pond	A	17-Mar-12	15	Soil	4917	852	8252	325	1609	95	1905	78	811	46	12	4	46	5	4018	49	45	2	266	4	3.05	2.50
16	20.0	BKM 051011-02	Freshwater pond	A	17-Mar-12	16	Soil	3491	979	5097	352	3328	167	2401	107	2634	96	26	6	71	8	6986	99	48	2	405	6	6.50	2.10
17	25.0	BKM 051011-02	Freshwater pond	A	17-Mar-12	17	Soil	<LOD	2625	5357	340	3503	163	2600	108	2223	87	26	5	62	7	7123	97	46	2	188	3	11.82	2.03
18	30.0	BKM 051011-02	Freshwater pond	A	17-Mar-12	18	Soil	3921	845	4839	289	2916	134	1453	78	1439	65	18	5	42	6	7010	87	38	2	105	3	13.70	2.40
19	35.0	BKM 051011-02	Freshwater pond	A	17-Mar-12	19	Soil	4213	969	4826	330	3931	172	2397	105	2001	81	22	5	41	7	6295	87	39	2	116	3	17.25	1.60
20	40.0	BKM 051011-02	low marsh	E	17-Mar-12	20	Soil	23487	1917	5619	401	10089	306	2540	124	2145	108	<LOD	24	<LOD	33	33341	467	48	2	122	3	17.58	3.30
21	45.0	BKM 051011-02	low marsh	E	17-Mar-12	21	Soil	32648	2513	5649	459	10448	350	2528	138	1664	133	<LOD	36	<LOD	49	71695	1099	54	2	63	2	26.41	6.86
22	50.0	BKM 051011-02	low marsh	E	17-Mar-12	22	Soil	70773	3856	6592	570	7239	330	28438	607	2289	147	<LOD	37	84	18	64737	1085	155	4	95	3	24.09	8.94
23	55.0	BKM 051011-02	low marsh	E	17-Mar-12	23	Soil	71221	4584	8845	729	7065	383	7517	284	2984	220	<LOD	56	<LOD	81	1E+05	2622	92	3	54	3	25.56	19.30
24	60.0	BKM 051011-02	low marsh	E	17-Mar-12	24	Soil	78484	5026	6399	696	14865	579	11878	398	1557	202	<LOD	60	<LOD	86	1E+05	2665	123	3	54	3	28.83	8.87
25	65.0	BKM 051011-02	low marsh	E	17-Mar-12	25	Soil	39057	2695	5091	454	7768	304	6145	203	2362	139	<LOD	34	91	17	63472	981	102	3	79	3	29.90	8.17
26	70.0	BKM 051011-02	low marsh	E	17-Mar-12	26	Soil	31761	2186	3867	370	6177	243	15386	321	2245	112	<LOD	26	118	12	33934	477	93	3	150	3	14.97	5.49
27	75.0	BKM 051011-02	low marsh	E	17-Mar-12	27	Soil	57815	3489	5845	533	14061	452	15856	392	1687	149	<LOD	41	<LOD	56	79688	1316	185	4	104	3	16.22	5.67
28	80.0	BKM 051011-02	low marsh	E	17-Mar-12	28	Soil	58431	3347	5185	490	12158	399	19855	439	1699	138	<LOD	37	<LOD	51	72937	1155	164	4	101	3	16.82	6.00
29	85.0	BKM 051011-02	low marsh	E	17-Mar-12	29	Soil	63368	3707	4566	517	10649	398	18076	436	1638	150	<LOD	42	<LOD	58	84992	1433	147	4	86	3	19.05	7.98
30	90.0	BKM 051011-02	low marsh	E	17-Mar-12	30	Soil	54844	3477	4822	517	11462	412	14501	374	1654	155	<LOD	43	<LOD	59	88909	1496	169	4	80	3	20.68	7.76
31	95.0	BKM 051011-02	low marsh	E	17-Mar-12	31	Soil	77094	4319	5354	583	15612	520	22094	534	1519	164	<LOD	47	<LOD	66	1E+05	1809	273	5	56	3	27.13	6.54
32	100.0	BKM 051011-02	high marsh	C1	17-Mar-12	32	Soil	27372	2037	3164	354	4285	209	18523	366	2049	102	<LOD	22	111	11	21588	308	74	3	102	3	20.09	5.04
2	105.0	BKM 051011-02	high marsh	C1	18-Mar-12	2	Soil	32445	2116	2482	327	4255	202	19677	373	2120	100	<LOD	21	99	10	20747	288	79	3	107	3	19.81	4.88
3	110.0	BKM 051011-02	high marsh	C1	18-Mar-12	3	Soil	42701	2432	2711	349	3374	192	32145	552	1857	93	<LOD	19	81	9	13695	196	86	3	128	3	14.51	4.06
4	115.0	BKM 051011-02	high marsh	C1	18-Mar-12	4	Soil	35664	2341	2981	369	6413	257	20648	408	1953	101	<LOD	23	87	11	21813	320	146	3	101	3	19.34	3.40
5	120.0	BKM 051011-02	high marsh	C1	18-Mar-12	5	Soil	32792	2247	2842	362	6183	252	16826	352	1626	96	<LOD	23	82	11	21821	321	119	3	121	3	13.44	3.53
6	125.0	BKM 051011-02	high marsh	C1	18-Mar-12	6	Soil	11043	1386	2256	317	3655	193	8161	214	851	63	<LOD	15	45	8	5452	85	56	2	102	3	8.34	1.49
7	130.0	BKM 051011-02	high marsh	C1	18-Mar-12	7	Soil	35563	2218	1416	311	2921	182	22574	426	597	55	<LOD	13	22	6	2923	49	77	3	76	3	7.86	1.00
8	135.0	BKM 051011-02	high marsh	C1	18-Mar-12	8	Soil	29765	2030	1597	308	1754	153	21205	403	705	57	<LOD	13	32	7	2679	45	66	2	72	3	9.79	1.53
9	140.0	BKM 051011-02	high marsh	C1	18-Mar-12	9	Soil	22414	1762	2308	311	2497	163	14708	304	614	52	<LOD	13	49	7	2267	39	64	2	67	3	9.16	0.91
10	145.0	BKM 051011-02	high marsh	C1	18-Mar-12	10	Soil	21841	1777	2707	329	2588	169	16728	336	686	54	<LOD	13	25	6	1915	34	68	2	70	3	9.80	0.74
11	150.0	BKM 051011-02	high marsh	C1	18-Mar-12	11	Soil	13933	1461	2217	303	4041	193	10215	237	1679	81	21	6	65	8	7676	112	71</					



ID	DEPTH	BORING_ID	DEP_ENV	Chemo-facies	Date	Reading	Mode	S	S +/-	Cl	Cl +/-	K	K +/-	Ca	Ca +/-	Ti	Ti +/-	Cr	Cr +/-	Mn	Mn +/-	Fe	Fe +/-	Sr	Sr +/-	Zr	Zr +/-	Ti/Zr	Fe/K	
31	255.0	BKM 051011-02	upper forebeach	B1	18-Mar-12	31	Soil	<LOD	2482	1751	266	3449	172	3966	136	193	34	<LOD	12	<LOD	16	1204	23	59	2	56	2	3.45	0.35	
32	260.0	BKM 051011-02	upper forebeach	B1	18-Mar-12	32	Soil	<LOD	2778	904	1682	275	2778	163	5006	156	528	48	<LOD	12	<LOD	16	1345	26	63	2	55	2	9.60	0.48
33	265.0	BKM 051011-02	upper forebeach	B1	18-Mar-12	33	Soil	3693	981	2409	305	4219	197	5423	166	477	48	<LOD	13	35	6	2244	39	76	3	97	3	4.92	0.53	
34	270.0	BKM 051011-02	upper forebeach	B1	18-Mar-12	34	Soil	<LOD	2590	2506	296	3962	187	4591	149	423	45	<LOD	13	19	6	1699	31	69	2	75	3	5.64	0.43	
35	275.0	BKM 051011-02	upper forebeach	B1	18-Mar-12	35	Soil	<LOD	2687	1667	291	3152	178	8712	218	1770	82	<LOD	15	59	7	2698	45	80	3	420	6	4.21	0.86	
36	280.0	BKM 051011-02	upper forebeach	B1	18-Mar-12	36	Soil	<LOD	2498	1349	270	2270	155	4129	143	491	47	<LOD	12	<LOD	17	1351	26	43	2	89	3	5.52	0.60	
37	285.0	BKM 051011-02	upper forebeach	B1	18-Mar-12	37	Soil	<LOD	2615	1817	294	2020	153	4440	150	1097	65	<LOD	13	25	6	1521	29	48	2	157	4	6.99	0.75	
38	290.0	BKM 051011-02	upper forebeach	B1	18-Mar-12	38	Soil	<LOD	2602	1771	278	2117	149	5499	163	493	47	<LOD	11	19	6	1329	26	51	2	94	3	5.24	0.63	
39	295.0	BKM 051011-02	upper forebeach	B1	18-Mar-12	39	Soil	3314	904	1553	267	3455	175	5356	159	795	55	<LOD	13	29	6	1966	34	68	2	142	3	5.60	0.57	
40	300.0	BKM 051011-02	upper forebeach	B1	18-Mar-12	40	Soil	<LOD	2803	2352	310	3914	194	6245	181	1620	78	<LOD	14	56	7	3141	52	81	3	476	7	3.40	0.80	
41	305.0	BKM 051011-02	upper forebeach	B1	18-Mar-12	41	Soil	4560	1014	1167	273	3108	176	6073	177	1996	85	<LOD	14	38	7	2085	37	71	3	392	6	5.09	0.67	
42	310.0	BKM 051011-02	bioturbated and laminated	C2	18-Mar-12	42	Soil	8725	1258	2234	311	2207	158	9951	237	2319	91	<LOD	13	40	7	2075	37	58	3	563	8	4.12	0.94	
43	315.0	BKM 051011-02	bioturbated and laminated	C2	18-Mar-12	43	Soil	11310	1544	2128	338	2983	193	37491	648	1163	70	<LOD	13	33	7	2094	38	98	3	158	4	7.36	0.70	
44	320.0	BKM 051011-02	bioturbated and laminated	C2	18-Mar-12	44	Soil	6149	1181	2810	330	3442	188	10064	243	1634	78	<LOD	15	52	7	3383	56	70	3	251	4	6.51	0.98	
46	330.0	BKM 051011-02	bioturbated and laminated	C2	18-Mar-12	46	Soil	11517	1374	1247	285	2714	170	10927	253	1990	85	<LOD	13	29	6	2601	44	108	3	423	6	4.70	0.96	
47	335.0	BKM 051011-02	bioturbated and laminated	C2	18-Mar-12	47	Soil	24041	1938	2064	337	5078	230	19584	392	2269	99	<LOD	18	88	9	6648	103	112	3	413	6	5.49	1.31	
48	340.0	BKM 051011-02	bioturbated and laminated	C2	18-Mar-12	48	Soil	46186	2601	1549	343	4356	222	35572	625	1289	78	<LOD	16	65	8	4148	68	118	3	396	6	3.26	0.95	
49	345.0	BKM 051011-02	bioturbated and laminated	C2	18-Mar-12	49	Soil	24361	2270	1563	407	3991	251	23913	526	1439	88	72	8	57	9	3707	71	100	3	372	6	3.87	0.93	
50	350.0	BKM 051011-02	bioturbated and laminated	C2	18-Mar-12	50	Soil	20510	1940	1984	361	4563	234	30226	569	1939	94	<LOD	17	55	8	4881	81	155	4	284	5	6.83	1.07	
51	355.0	BKM 051011-02	bioturbated and laminated	C2	18-Mar-12	51	Soil	36150	2297	1405	325	2998	190	28897	525	936	69	<LOD	15	46	7	3705	61	85	3	286	5	3.27	1.24	
52	360.0	BKM 051011-02	bioturbated and laminated	C2	18-Mar-12	52	Soil	10415	1363	1514	297	4734	213	13355	290	1827	84	21	5	70	8	4255	67	100	3	386	6	4.73	0.90	
53	365.0	BKM 051011-02	bioturbated and laminated	C2	18-Mar-12	53	Soil	46448	2510	1253	316	3519	196	34081	584	1096	69	<LOD	15	27	6	2752	46	123	3	242	4	4.53	0.78	
54	370.0	BKM 051011-02	bioturbated and laminated	C2	18-Mar-12	54	Soil	17539	1666	1764	315	5309	228	18965	374	1827	84	<LOD	13	49	7	3428	56	126	3	291	5	6.28	0.65	
55	375.0	BKM 051011-02	bioturbated and laminated	C2	18-Mar-12	55	Soil	33071	2170	1075	306	4625	218	26202	480	977	68	<LOD	14	47	7	3326	55	120	3	282	5	3.46	0.72	
56	380.0	BKM 051011-02	bioturbated and laminated	C2	18-Mar-12	56	Soil	23617	1876	1907	319	5364	229	23156	433	1121	71	<LOD	15	40	7	3308	54	135	3	251	5	4.47	0.62	
57	385.0	BKM 051011-02	lower forebeach	B2	18-Mar-12	57	Soil	4283	1050	1844	292	6572	242	11330	256	819	61	<LOD	14	43	7	3345	53	135	3	260	5	3.15	0.51	
58	390.0	BKM 051011-02	lower forebeach	B2	18-Mar-12	58	Soil	3875	1031	810	810	5560	229	10971	256	1081	69	<LOD	15	44	7	3248	53	130	3	288	5	3.75	0.58	
59	395.0	BKM 051011-02	lower forebeach	B2	18-Mar-12	59	Soil	5235	1090	843	268	5472	225	11959	267	1309	72	<LOD	15	57	7	3094	51	132	3	262	5	5.00	0.57	
60	400.0	BKM 051011-02	lower forebeach	B2	18-Mar-12	60	Soil	<LOD	2857	1626	298	5545	231	9371	234	1210	70	<LOD	15	45	7	3139	52	130	3	241	4	5.02	0.57	
61	405.0	BKM 051011-02	lower forebeach	B2	18-Mar-12	61	Soil	3574	1005	1090	277	5969	236	10105	242	893	62	<LOD	14	37	7	2872	48	132	3	238	4	3.75	0.48	
62	410.0	BKM 051011-02	lower forebeach	B2	18-Mar-12	62	Soil	3396	1012	810	820	5415	227	11073	258	2165	92	<LOD	15	60	8	3883	62	128	3	304	5	7.12	0.72	
63	415.0	BKM 051011-02	lower forebeach	B2	18-Mar-12	63	Soil	3120	1022	1121	285	5160	235	12453	280	1981	89	<LOD	15	60	8	3825	62	140	4	284	5	6.98	0.66	
64	420.0	BKM 051011-02	lower forebeach	B2	18-Mar-12	64	Soil	<LOD	2827	1653	302	8063	278	14397	310	1151	74	<LOD	16	42	7	4192	67	183	4	223	4	5.16	0.52	
65	425.0	BKM 051011-02	lower forebeach	B2	18-Mar-12	65	Soil	<LOD	3075	1585	296	7663	267	12662	281	1432	77	<LOD	16	47	7	4309	68	172	4	271	5	5.28	0.56	
66	430.0	BKM 051011-02	lower forebeach	B2	18-Mar-12	66	Soil	<LOD	3042	810	820	6666	252	13781	300	1185	70	<LOD	14	56	7	3713	60	154	4	148	4	8.01	0.56	
67	435.0	BKM 051011-02	lower forebeach	B2	18-Mar-12	67	Soil	<LOD	3062	1655	300	7480	265	13964	301	1823	85	<LOD	16	75	8	4544	71	150	4	311	5	5.86	0.61	
68	440.0	BKM 051011-02	lower forebeach	B2	18-Mar-12	68	Soil	3449	1095	1541	305	6338	249	14884	318	2321	98	60	7	101	9	7726	117	152	4	338	6	6.87	1.22	
69	445.0	BKM 051011-02	bioturbated and laminated	C3	18-Mar-12	69	Soil	43169	2463	810	919	5760	242	35928	617	1031	68	<LOD	15	43	7	3748	60	157	4	162	4	6.36	0.65	
70	450.0	BKM 051011-02	bioturbated and laminated	C3	18-Mar-12	70	Soil	43826	2548	1836	351	5794	249	38367	664	1414	79	<LOD	16	70	8	4281	69	164	4	304	5	4.65	0.74	
71	455.0	BKM 051011-02	bioturbated and laminated	C3	18-Mar-12	71	Soil	35740	2324	1921	345	6434	259	32292	578	1156	76	<LOD	17	65	8	4732	76	157	4	185	4	6.25	0.74	
72	460.0	BKM 051011-02	bioturbated and laminated	C3	18-Mar-12	72	Soil	41586	2441	1191	324	6069	249	38176	650	1069	71	<LOD	15	55	7	4137	66	186	4	180	4	5.94	0.68	
73	465.0	BKM 051011-02	bioturbated and laminated	C3	18-Mar-12	73	Soil	23933	1935	1274	318	5239	234	24847	468	2055	93	<LOD	17	52	8	4650	74	133	4	532	7	3.86	0.89	
74	470.0	BKM 051011-02	bioturbated and laminated	C3	18-Mar-12	74	Soil	39011	2386	2432	356	4975	229	35538	613	2616	104	<LOD	17	84	8	6326	97	148	4	466	7	5.61	1.27	
75	475.0	BKM 051011-02	bioturbated and laminated	C3	18-Mar-12	75	Soil	48282	2710	1514	356	4546	231	39207	689	2303	99	<LOD	17	73	8	4318	71	109	3	708	9	3.25	0.95	
8	5.0	BKM 051011-03	washover peat	A	29-Feb-12	8	Soil	7232	1598	30840	833	3391	175	7794	198	2567	96	21	5	108	8	3682	57	100	4	630	9	4.07	1.09	
9	15.0	BKM 051011-03	washover	A	29-Feb-12	9	Soil	<LOD	3742	18415	642	3104	172	5131	161	5138	141	21	6	150	9	4351	67	101	3	1257	15	4.09	1.40	
10	25.0	BKM 051011-03	washover	A	29-Feb-12	10	Soil	<LOD	2595	7448	408	3424	171	4577	146	2382	91	23	5	80	7	3164	49	74	3	599	8	3.98	0.92	
11	35.0	BKM 051011-03	washover	A	29-Feb-12	11	Soil	<LOD	2084																					

ID	DEPTH	BORING_ID	DEP_ENV	Chemo-facies	Date	Reading	Mode	S	S +/-	Cl	Cl +/-	K	K +/-	Ca	Ca +/-	Ti	Ti +/-	Cr	Cr +/-	Mn	Mn +/-	Fe	Fe +/-	Sr	Sr +/-	Zr	Zr +/-	Ti/Zr	Fe/K
31	235.0	BKM 051011-03	upper forebeach	B	29-Feb-12	31	Soil	<LOD	1452	<LOD	543	1557	120	989	74	96	26	<LOD	11	26	5	995	20	31	2	29	2	3.31	0.64
32	245.0	BKM 051011-03	upper forebeach	B	29-Feb-12	32	Soil	<LOD	1662	<LOD	527	1654	125	3440	121	305	39	<LOD	12	45	6	1410	25	76	3	117	3	2.61	0.85
33	255.0	BKM 051011-03	upper forebeach	B	29-Feb-12	33	Soil	<LOD	1740	<LOD	543	1767	126	1028	76	132	32	<LOD	12	37	6	1168	22	35	2	45	2	2.93	0.66
34	265.0	BKM 051011-03	upper forebeach	B	29-Feb-12	34	Soil	<LOD	2025	<LOD	615	1927	132	2071	98	596	45	<LOD	12	38	6	1377	25	55	2	94	3	6.34	0.71
35	275.0	BKM 051011-03	upper forebeach	B	29-Feb-12	35	Soil	3310	811	<LOD	598	3212	161	4918	146	549	46	<LOD	12	36	6	1787	30	76	3	119	3	4.61	0.56
36	285.0	BKM 051011-03	upper forebeach	B	29-Feb-12	36	Soil	<LOD	1907	<LOD	567	2234	137	1716	90	247	35	<LOD	11	39	6	1450	26	43	2	30	2	8.23	0.65
37	295.0	BKM 051011-03	upper forebeach	B	29-Feb-12	37	Soil	<LOD	1949	<LOD	617	1799	131	2882	113	646	48	17	4	48	6	1684	29	61	2	306	5	2.11	0.94
38	305.0	BKM 051011-03	upper forebeach	B	29-Feb-12	38	Soil	<LOD	1973	<LOD	613	3013	157	2762	111	779	52	<LOD	12	47	6	1732	29	54	2	58	2	13.43	0.57
39	315.0	BKM 051011-03	upper forebeach	B	29-Feb-12	39	Soil	<LOD	1897	<LOD	638	2895	155	2651	109	338	39	<LOD	12	36	6	1623	28	38	2	50	2	6.76	0.56
40	325.0	BKM 051011-03	upper forebeach	B	29-Feb-12	40	Soil	2380	769	<LOD	631	2642	152	3638	128	508	47	16	5	40	6	2165	36	52	2	42	2	12.10	0.82
41	335.0	BKM 051011-03	upper forebeach	B	29-Feb-12	41	Soil	<LOD	2009	790	229	4443	189	2854	116	286	41	19	5	35	6	2393	39	83	3	45	2	6.36	0.54
42	345.0	BKM 051011-03	upper forebeach	B	29-Feb-12	42	Soil	<LOD	2363	940	233	2893	157	4969	148	837	55	<LOD	13	40	6	2332	38	73	2	80	3	10.46	0.81
43	355.5	BKM 051011-03	upper forebeach	B	29-Feb-12	43	Soil	<LOD	2155	1608	253	3292	165	2165	103	442	45	<LOD	13	38	6	1787	31	63	2	73	3	6.05	0.54
45	3.5	BKM 051111-01	upper forebeach	B	29-Feb-12	45	Soil	<LOD	1822	738	237	1548	132	3307	124	845	55	<LOD	13	38	6	1530	28	78	3	181	4	4.67	0.99
46	13.5	BKM 051111-01	upper forebeach	B	29-Feb-12	46	Soil	<LOD	1878	<LOD	642	2305	148	5057	152	850	55	<LOD	13	62	7	1784	31	82	3	236	4	3.60	0.77
47	25.0	BKM 051111-01	upper forebeach	B	29-Feb-12	47	Soil	<LOD	1939	<LOD	635	1886	135	3339	122	600	49	32	5	40	6	1393	26	66	2	160	3	3.75	0.74
48	35.0	BKM 051111-01	upper forebeach	B	29-Feb-12	48	Soil	<LOD	1895	<LOD	638	2550	150	4260	137	981	59	<LOD	13	44	6	1776	30	76	3	229	4	4.28	0.70
49	45.0	BKM 051111-01	upper forebeach	B	29-Feb-12	49	Soil	<LOD	1792	<LOD	641	2409	148	4177	137	687	51	<LOD	13	40	6	1913	32	92	3	163	3	4.21	0.79
50	55.0	BKM 051111-01	upper forebeach	B	29-Feb-12	50	Soil	<LOD	1964	<LOD	640	3125	164	6805	178	948	59	<LOD	13	54	7	2212	36	104	3	163	3	5.82	0.71
51	65.0	BKM 051111-01	upper forebeach	B	29-Feb-12	51	Soil	<LOD	1921	<LOD	614	3224	165	4269	139	524	48	<LOD	12	56	7	2100	35	90	3	162	3	3.23	0.65
52	75.0	BKM 051111-01	upper forebeach	B	29-Feb-12	52	Soil	<LOD	1846	<LOD	593	2652	148	5531	154	485	46	15	4	55	6	2028	33	103	3	139	3	3.49	0.76
53	85.0	BKM 051111-01	washover	B	29-Feb-12	53	Soil	<LOD	1891	<LOD	649	2348	151	5838	167	1226	69	<LOD	14	77	7	2363	39	98	3	337	5	3.64	1.01
54	95.0	BKM 051111-01	washover	B	29-Feb-12	54	Soil	<LOD	1795	<LOD	566	1832	129	2361	103	397	41	<LOD	12	40	6	1262	23	55	2	83	3	4.78	0.69
55	105.0	BKM 051111-01	washover	B	29-Feb-12	55	Soil	<LOD	1680	<LOD	610	2425	144	2829	112	258	37	<LOD	12	44	6	1638	28	74	3	110	3	2.35	0.68
56	115.0	BKM 051111-01	washover	B	29-Feb-12	56	Soil	<LOD	1577	<LOD	541	1472	117	1475	84	224	36	<LOD	12	30	6	1319	24	44	2	88	3	2.55	0.90
57	125.0	BKM 051111-01	washover	B	29-Feb-12	57	Soil	<LOD	1645	<LOD	628	1476	122	2863	112	1356	66	<LOD	13	54	6	1359	25	61	2	306	5	4.43	0.92
58	135.0	BKM 051111-01	washover	B	29-Feb-12	58	Soil	<LOD	1905	<LOD	613	1555	127	3524	125	646	51	<LOD	13	47	6	1727	30	74	3	158	3	4.09	1.11
59	145.0	BKM 051111-01	washover	B	29-Feb-12	59	Soil	<LOD	1864	<LOD	619	2129	139	3409	122	923	58	<LOD	13	58	7	1853	31	64	2	221	4	4.18	0.87
60	155.0	BKM 051111-01	washover	B	29-Feb-12	60	Soil	<LOD	2090	<LOD	740	4015	196	5228	165	357	48	<LOD	14	64	7	2658	45	107	3	80	3	4.46	0.66
61	165.0	BKM 051111-01	washover	B	29-Feb-12	61	Soil	<LOD	2018	<LOD	636	3986	179	4853	148	501	48	17	5	69	7	3987	59	105	3	69	3	7.26	1.00
62	175.0	BKM 051111-01	low marsh	E	29-Feb-12	62	Soil	9517	1214	1228	248	3506	171	11399	241	1561	78	20	6	171	10	11791	158	74	2	108	3	14.45	3.36
63	185.0	BKM 051111-01	low marsh	E	29-Feb-12	63	Soil	32350	2328	<LOD	997	2580	198	55489	921	1200	86	<LOD	19	110	10	9766	149	211	4	63	3	19.05	3.79
64	195.0	BKM 051111-01	low marsh	E	29-Feb-12	64	Soil	7971	1253	1679	277	3897	187	17260	329	2007	93	28	7	157	11	17511	237	118	3	72	3	27.88	4.49
65	205.0	BKM 051111-01	low marsh	E	29-Feb-12	65	Soil	7606	1200	1897	275	4082	186	11402	244	2218	95	33	7	184	11	19229	257	98	3	104	3	21.33	4.71
66	215.0	BKM 051111-01	low marsh	E	29-Feb-12	66	Soil	20918	1766	2108	307	3318	183	24054	430	1732	90	24	7	147	11	17839	247	69	2	100	3	17.32	5.38
67	225.0	BKM 051111-01	low marsh	E	29-Feb-12	67	Soil	3732	968	1165	261	4671	201	5265	160	1729	83	21	6	86	9	8710	125	101	3	201	4	8.60	1.86
68	235.0	BKM 051111-01	low marsh	E	29-Feb-12	68	Soil	5251	1091	2684	299	4015	186	3897	136	2052	94	34	7	98	10	18209	249	69	2	112	3	18.32	4.54
69	245.0	BKM 051111-01	low marsh	E	29-Feb-12	69	Soil	15150	1564	1531	288	4462	204	16924	332	2088	99	25	7	114	11	22118	305	82	3	156	3	13.38	4.96
70	255.0	BKM 051111-01	low marsh	C	29-Feb-12	70	Soil	26066	2102	1584	335	5559	246	33782	599	1730	104	30	8	74	11	25868	377	87	3	131	3	13.21	4.65
71	265.0	BKM 051111-01	upper forebeach	B	29-Feb-12	71	Soil	2822	840	2056	266	3142	161	3249	120	709	52	<LOD	13	41	6	2898	45	80	3	130	3	5.45	0.92
72	275.0	BKM 051111-01	upper forebeach	B	29-Feb-12	72	Soil	<LOD	1866	1829	246	2134	134	1705	90	193	36	<LOD	12	29	6	1805	30	56	2	66	2	2.92	0.85
73	285.0	BKM 051111-01	upper forebeach	B	29-Feb-12	73	Soil	<LOD	1629	1566	244	2043	135	2218	100	571	48	<LOD	12	42	6	1926	32	55	2	198	4	2.88	0.94
74	295.0	BKM 051111-01	upper forebeach	B	29-Feb-12	74	Soil	<LOD	2259	3973	312	1825	130	3004	114	1554	71	<LOD	13	64	7	2339	37	62	2	400	6	3.89	1.28
75	305.0	BKM 051111-01	upper forebeach	B	29-Feb-12	75	Soil	<LOD	2189	2595	285	1824	134	3545	126	1183	63	<LOD	13	40	6	1442	26	66	2	380	6	3.11	0.79
76	315.0	BKM 051111-01	upper forebeach	B	29-Feb-12	76	Soil	<LOD	1978	1755	251	1832	129	2904	113	1918	76	<LOD	12	52	6	1585	27	66	2	468	6	4.10	0.87
77	325.0	BKM 051111-01	upper forebeach	B	29-Feb-12	77	Soil	<LOD	1912	1872	259	1086	113	3208	118	1370	66	<LOD	13	45	6	1424	26	63	2	253	4	5.42	1.31
78	335.0	BKM 051111-01	upper forebeach	B	29-Feb-12	78	Soil	<LOD	1858	1069	231	1145	113	2141	99	855	52	<LOD	12	32	6	832	18	46	2	254	4	3.37	0.73
79	345.0	BKM 051111-01	upper forebeach	A	29-Feb-12	79	Soil	<LOD	2132	<LOD	766	1031	119	2639	114	8389	186	<LOD	16	183	9	3695	57	48	3	2683	31	3.13	3.58
80	355.0	BKM 051111-01	lower forebeach	A	29-Feb-12	80																							

ID	DEPTH	BORING_ID	DEP_ENV	Chemo-facies	Date	Reading	Mode	S	S +/-	Cl	Cl +/-	K	K +/-	Ca	Ca +/-	Ti	Ti +/-	Cr	Cr +/-	Mn	Mn +/-	Fe	Fe +/-	Sr	Sr +/-	Zr	Zr +/-	Ti/Zr	Fe/K
51	80.0	BKM 051311-01	high marsh	C2	16-Mar-12	51	Soil	33784	2230	1768	343	3002	189	21821	423	6132	165	20	6	130	9	5805	91	93	3	1471	18	4.17	1.93
52	85.0	BKM 051311-01	high marsh	C2	16-Mar-12	52	Soil	13427	1504	2338	328	4180	205	9443	235	2305	97	<LOD	16	61	8	5854	91	84	3	531	7	4.34	1.40
53	90.0	BKM 051311-01	high marsh	C2	16-Mar-12	53	Soil	22037	1813	1881	320	2776	177	18950	372	3316	113	<LOD	16	79	8	3704	60	104	3	964	12	3.44	1.33
54	95.0	BKM 051311-01	high marsh	C2	16-Mar-12	54	Soil	9877	1294	1486	289	3343	182	7207	195	2365	95	16	5	85	8	4152	65	93	3	644	9	3.67	1.24
55	100.0	BKM 051311-01	high marsh	C2	16-Mar-12	55	Soil	7042	1206	1452	300	4347	205	8962	225	5407	148	<LOD	17	137	9	4496	71	109	3	1542	18	3.51	1.03
56	105.0	BKM 051311-01	high marsh	C2	16-Mar-12	56	Soil	6615	1123	1348	276	5669	222	6046	175	2757	102	<LOD	15	114	8	4424	68	102	3	699	9	3.94	0.78
57	110.0	BKM 051311-01	high marsh	C2	16-Mar-12	57	Soil	7996	1228	1673	297	5624	227	6825	191	2930	107	<LOD	16	78	8	4521	71	90	3	699	9	4.19	0.80
58	115.0	BKM 051311-01	high marsh	C2	16-Mar-12	58	Soil	6904	1201	1445	298	6802	253	5439	172	3838	125	22	6	108	9	6986	106	95	3	745	10	5.15	1.03
59	120.0	BKM 051311-01	high marsh	C2	16-Mar-12	59	Soil	6441	1142	1248	285	4615	210	5779	176	2523	100	<LOD	15	100	8	3549	58	86	3	511	7	4.94	0.77
60	125.0	BKM 051311-01	high marsh	C2	16-Mar-12	61	Soil	5870	1080	1631	281	5652	220	5022	158	2988	103	<LOD	15	89	8	4217	65	88	3	580	8	5.15	0.75
61	130.0	BKM 051311-01	high marsh	C2	16-Mar-12	62	Soil	4259	1335	1746	411	3667	238	4467	183	8153	230	<LOD	22	189	13	7024	127	75	3	1826	24	4.46	1.92
62	135.0	BKM 051311-01	high marsh	C2	16-Mar-12	63	Soil	7809	1305	928	928	4987	231	6895	204	5200	155	30	7	137	10	5442	89	87	3	1224	15	4.25	1.09
63	140.0	BKM 051311-01	high marsh	C2	16-Mar-12	64	Soil	12149	1385	1757	290	3991	190	6048	174	2949	109	19	6	124	10	11732	166	82	3	475	7	6.21	2.94
64	145.0	BKM 051311-01	high marsh	C2	16-Mar-12	65	Soil	17370	1635	2585	331	4085	200	10942	254	3309	114	<LOD	17	131	9	6523	98	82	3	706	9	4.69	1.60
65	150.0	BKM 051311-01	high marsh	C2	16-Mar-12	66	Soil	21659	1727	1731	294	2937	171	9402	226	977	70	25	6	128	9	8384	122	58	2	135	3	7.24	2.85
68	155.0	BKM 051311-01	high marsh	C2	16-Mar-12	68	Soil	5606	1157	2256	326	3379	192	5965	183	1168	73	<LOD	16	45	8	4193	69	74	3	93	3	12.56	1.24
69	160.0	BKM 051311-01	high marsh	C2	16-Mar-12	69	Soil	3834	984	2633	311	2426	159	3856	139	990	62	<LOD	14	30	6	2352	40	55	2	204	4	4.85	0.97
70	165.0	BKM 051311-01	high marsh	C2	16-Mar-12	70	Soil	9552	1400	2665	353	4537	223	6776	202	1476	84	<LOD	17	41	8	4699	78	81	3	109	3	13.54	1.04
71	170.0	BKM 051311-01	high marsh	C2	16-Mar-12	71	Soil	6735	1111	2065	289	2533	158	6074	172	1214	67	<LOD	13	61	7	2608	43	60	2	110	3	11.04	1.03
72	175.0	BKM 051311-01	high marsh	C2	16-Mar-12	72	Soil	10738	1432	1909	330	3440	197	9346	240	3076	114	<LOD	18	100	9	5889	94	120	3	233	5	13.20	1.71
73	180.0	BKM 051311-01	high marsh	C2	16-Mar-12	73	Soil	9144	1270	2922	319	2606	162	8788	215	2236	90	<LOD	15	68	8	4919	75	101	3	307	5	7.28	1.89
74	185.0	BKM 051311-01	high marsh	C2	16-Mar-12	74	Soil	6089	1046	1878	275	2799	160	4525	145	678	51	<LOD	14	17	17	2338	39	65	2	67	3	10.12	0.84
75	190.0	BKM 051311-01	high marsh	C2	16-Mar-12	75	Soil	4878	1013	1766	282	3589	182	3910	139	643	52	<LOD	13	17	18	2474	42	62	2	80	3	8.04	0.69
76	195.0	BKM 051311-01	high marsh	A2	16-Mar-12	76	Soil	9165	1734	2191	457	2002	196	21067	452	34038	631	<LOD	30	643	21	16234	261	124	4	1061	14	32.08	8.11
77	200.0	BKM 051311-01	high marsh	A2	16-Mar-12	77	Soil	6901	1280	2296	339	2136	166	12688	287	6365	171	<LOD	19	138	10	6896	106	147	4	803	11	7.93	3.23
78	205.0	BKM 051311-01	high marsh	A2	16-Mar-12	78	Soil	22172	2573	3633	607	2264	239	27279	618	52491	1017	<LOD	39	979	29	22563	397	199	6	6318	87	8.31	9.97
79	210.0	BKM 051311-01	high marsh	A2	16-Mar-12	79	Soil	21332	2211	2570	467	1707	194	26962	552	26959	528	47	11	518	19	17890	291	235	6	3587	47	7.52	10.48
80	215.0	BKM 051311-01	high marsh	A2	16-Mar-12	80	Soil	13925	1637	2951	375	1850	164	15269	330	10201	233	<LOD	21	274	13	9272	142	150	4	1625	20	6.28	5.01
81	220.0	BKM 051311-01	high marsh	A2	16-Mar-12	81	Soil	19276	2275	2743	517	2167	218	23176	517	34520	681	<LOD	34	634	22	19285	329	201	6	7280	102	4.74	8.90
82	225.0	BKM 051311-01	high marsh	A2	16-Mar-12	82	Soil	21559	2147	2574	452	1938	192	21431	456	26044	505	<LOD	26	420	17	14239	230	154	5	4051	52	6.43	7.35
83	230.0	BKM 051311-01	high marsh	C3	16-Mar-12	83	Soil	24353	1988	1964	350	2011	170	18747	385	5780	163	21	7	137	10	7007	110	124	4	1094	14	5.28	3.48
84	235.0	BKM 051311-01	high marsh	C3	16-Mar-12	84	Soil	7448	1171	1957	299	3556	186	4501	152	1062	64	<LOD	13	22	6	2131	38	57	2	76	3	13.97	0.60
85	240.0	BKM 051311-01	high marsh	C3	16-Mar-12	85	Soil	10849	1337	2199	306	2437	161	8547	214	1799	83	<LOD	14	54	7	3591	57	93	3	115	3	15.64	1.47
86	245.0	BKM 051311-01	high marsh	C3	16-Mar-12	86	Soil	15583	1650	1775	335	3060	189	8976	235	5631	162	<LOD	20	148	11	9311	144	109	3	1012	13	5.56	3.04
87	250.0	BKM 051311-01	high marsh	C3	16-Mar-12	87	Soil	26250	2162	2983	402	2111	182	15950	357	7420	200	26	8	161	12	14384	226	136	4	674	9	11.01	6.81
88	255.0	BKM 051311-01	high marsh	C3	16-Mar-12	88	Soil	18982	1733	2740	346	2606	174	8375	221	2385	100	<LOD	17	68	8	5979	94	82	3	76	3	31.38	2.29
89	260.0	BKM 051311-01	high marsh	C3	16-Mar-12	89	Soil	13562	1507	3271	349	3380	189	5466	173	321	48	<LOD	15	33	7	4826	77	65	2	37	2	8.68	1.43
90	265.0	BKM 051311-01	high marsh	C3	16-Mar-12	90	Soil	32086	2237	1914	351	1839	167	16564	356	3301	122	22	7	89	9	8106	128	113	3	478	7	6.91	4.41
91	270.0	BKM 051311-01	high marsh	C3	16-Mar-12	91	Soil	33003	2419	2754	414	1990	185	15776	363	8110	216	<LOD	21	144	11	11589	188	104	4	2056	26	3.94	5.82
92	275.0	BKM 051311-01	high marsh	C3	16-Mar-12	92	Soil	35852	2449	2339	391	2659	195	11858	294	6795	191	<LOD	22	184	12	14368	228	111	4	1438	18	4.73	5.40
93	280.0	BKM 051311-01	high marsh	C3	16-Mar-12	93	Soil	15659	1582	2712	334	4390	208	6138	183	1846	67	21	6	47	8	6806	104	76	3	251	4	7.35	1.55
94	285.0	BKM 051311-01	high marsh	C3	16-Mar-12	94	Soil	23138	1852	2474	337	4952	221	6026	183	2659	106	<LOD	17	41	8	7891	120	91	3	779	10	3.41	1.59
95	290.0	BKM 051311-01	high marsh	C3	16-Mar-12	95	Soil	22999	1890	2066	341	2781	181	11669	272	5905	164	<LOD	19	131	10	9524	144	122	4	1366	17	4.32	3.42
96	292.5	BKM 051311-01	high marsh	C3	16-Mar-12	96	Soil	23884	2128	1538	382	3014	211	12149	309	6754	195	<LOD	21	119	11	10124	169	116	4	1112	15	6.07	3.36
97	295.0	BKM 051311-01	high marsh	C4	16-Mar-12	97	Soil	11064	1291	2579	298	3289	171	7071	185	1200	72	17	5	60	7	3901	59	94	3	138	3	8.70	1.19
99	300.0	BKM 051311-01	high marsh	C4	16-Mar-12	99	Soil	3492	961	2548	311	2859	168	2941	123	1830	82	<LOD	14	47	7	2359	40	65	2	293	5	6.25	0.83
100	302.0	BKM 051311-01	high marsh	C4	16-Mar-12	100	Soil	3407	922	3516	312	3950	180	2091	102	1266	69	15	5	94	8	2946	46	81	3	174	4	7.28	0.75
101	304.0	BKM 051311-01	high marsh	C4	16-Mar-12	101	Soil	<LOD	2428	2569	297</																		

ID	DEPTH	BORING_ID	DEP_ENV	Chemo-facies	Date	Reading	Mode	S	S +/-	Cl	Cl +/-	K	K +/-	Ca	Ca +/-	Ti	Ti +/-	Cr	Cr +/-	Mn	Mn +/-	Fe	Fe +/-	Sr	Sr +/-	Zr	Zr +/-	Ti/Zr	Fe/K
121	395.0	BKM 051311-01	high marsh	C4	16-Mar-12	121	Soil	3915	967	2994	313	2249	150	2001	103	2138	85	<LOD	13	70	7	2755	45	53	2	381	6	5.61	1.22
122	400.0	BKM 051311-01	high marsh	C4	16-Mar-12	122	Soil	3339	947	2895	319	1783	141	1133	87	3755	117	<LOD	15	66	7	2373	40	45	2	789	10	4.76	1.33
2	405.0	BKM 051311-01	high marsh	C4	17-Mar-12	2	Soil	<LOD	2399	2695	319	1651	139	1211	89	5820	152	<LOD	16	104	8	2914	48	33	2	1417	17	4.11	1.76
3	410.0	BKM 051311-01	high marsh	C4	17-Mar-12	3	Soil	<LOD	2236	1836	286	1352	129	927	81	4189	122	<LOD	14	49	7	2471	41	26	2	1103	13	3.80	1.83
4	415.0	BKM 051311-01	high marsh	C4	17-Mar-12	4	Soil	6357	1089	2891	313	1683	136	2187	106	3532	114	<LOD	14	52	7	2956	48	22	2	1146	13	3.08	1.76
5	420.0	BKM 051311-01	high marsh	C4	17-Mar-12	5	Soil	3035	927	3280	325	1497	132	1119	84	4210	124	<LOD	15	53	7	2515	42	27	2	975	12	4.32	1.68
6	425.0	BKM 051311-01	high marsh	C4	17-Mar-12	6	Soil	3488	1062	3709	371	1824	153	1943	109	6749	175	<LOD	18	109	9	3970	65	23	3	2820	34	2.39	2.18
7	430.0	BKM 051311-01	high marsh	A3	17-Mar-12	7	Soil	4542	1143	5247	401	2066	154	2192	113	9278	210	21	6	165	10	6095	93	42	3	4167	50	2.23	2.95
8	435.0	BKM 051311-01	high marsh	A3	17-Mar-12	8	Soil	14879	1559	2478	342	1674	150	8271	216	7817	188	<LOD	16	123	9	3810	62	27	2	2235	26	3.50	2.28
9	440.0	BKM 051311-01	high marsh	A3	17-Mar-12	9	Soil	3685	1214	4368	426	1921	163	2761	135	21194	399	<LOD	23	274	13	7251	113	41	3	3818	45	5.55	3.77
10	445.0	BKM 051311-01	high marsh	C5	17-Mar-12	10	Soil	32214	2226	4702	417	2194	172	23534	448	7798	191	<LOD	17	124	9	5237	83	40	3	2316	27	3.37	2.39
11	450.0	BKM 051311-01	high marsh	C5	17-Mar-12	11	Soil	32818	2210	6143	438	1960	162	21546	412	6201	162	<LOD	16	99	8	4314	68	45	3	1669	20	3.72	2.20
12	455.0	BKM 051311-01	high marsh	C5	17-Mar-12	12	Soil	10026	1308	12936	481	2692	144	6816	168	1343	63	<LOD	12	44	6	4038	57	67	2	276	4	4.87	1.50
2	5.0	BKM 052411-01	backbeach	A	1-Mar-12	2	Soil	<LOD	3200	<LOD	982	979	148	10685	267	23159	438	51	9	409	15	8610	135	101	5	7815	103	2.96	8.79
3	15.0	BKM 052411-01	backbeach	A	1-Mar-12	3	Soil	<LOD	2425	<LOD	793	1005	130	7329	199	12735	260	23	7	292	12	5645	86	93	4	3502	41	3.64	5.62
4	25.0	BKM 052411-01	backbeach	A	1-Mar-12	4	Soil	<LOD	4071	<LOD	1320	1240	180	13789	342	46437	837	63	12	794	24	15699	256	122	7	13841	226	3.36	12.66
5	35.0	BKM 052411-01	backbeach	A	1-Mar-12	5	Soil	<LOD	3344	<LOD	1089	1282	165	15899	354	30819	560	64	10	631	20	11699	183	168	5	6421	83	4.80	9.13
6	45.0	BKM 052411-01	backbeach	A	1-Mar-12	6	Soil	<LOD	2925	<LOD	839	967	140	12522	288	10110	232	37	7	234	12	5426	87	161	5	4054	50	2.49	5.61
7	55.0	BKM 052411-01	backbeach	A	1-Mar-12	7	Soil	<LOD	3527	<LOD	1071	1393	171	13470	325	25855	496	29	9	539	18	10466	169	146	5	5934	77	4.36	7.51
8	65.0	BKM 052411-01	backbeach	A	1-Mar-12	8	Soil	<LOD	2731	<LOD	781	859	130	10132	244	12256	257	<LOD	20	260	12	6228	95	131	4	2446	29	5.01	7.25
9	75.0	BKM 052411-01	washover	A2	1-Mar-12	9	Soil	<LOD	1961	<LOD	627	1291	123	4583	144	4094	118	<LOD	14	107	8	2491	40	60	3	1110	13	3.69	1.93
10	85.0	BKM 052411-01	washover	A2	1-Mar-12	10	Soil	<LOD	1869	<LOD	631	924	113	2871	115	3645	112	16	5	90	7	2324	38	40	2	832	10	4.38	2.52
11	95.0	BKM 052411-01	washover	A2	1-Mar-12	11	Soil	<LOD	1588	<LOD	592	2057	135	1692	90	992	58	17	4	57	6	1761	30	48	2	420	6	2.36	0.86
12	105.0	BKM 052411-01	washover	A2	1-Mar-12	12	Soil	<LOD	1691	<LOD	574	2261	142	4841	145	290	38	<LOD	12	37	6	1453	26	59	2	296	5	0.98	0.64
13	115.0	BKM 052411-01	washover	A2	1-Mar-12	13	Soil	<LOD	1702	<LOD	637	1892	131	3181	117	920	56	<LOD	13	62	6	1600	28	61	2	329	5	2.80	0.85
14	125.0	BKM 052411-01	washover	A2	1-Mar-12	14	Soil	<LOD	1810	<LOD	675	1509	127	3625	128	2703	95	15	5	75	7	2414	39	53	2	631	8	4.28	1.60
15	135.0	BKM 052411-01	washover	A2	1-Mar-12	15	Soil	<LOD	1950	768	234	1367	123	1934	98	2245	87	<LOD	13	94	7	1898	32	38	2	525	7	4.28	1.39
16	145.0	BKM 052411-01	washover	A2	1-Mar-12	16	Soil	<LOD	1834	<LOD	656	951	113	3821	131	2670	95	<LOD	13	83	7	2256	37	46	2	711	9	3.76	2.37
17	155.0	BKM 052411-01	washover	A2	1-Mar-12	17	Soil	<LOD	1950	<LOD	649	1835	132	3079	117	1444	69	<LOD	13	62	7	2018	33	64	2	438	6	3.30	1.10
18	165.0	BKM 052411-01	low marsh	D	1-Mar-12	18	Soil	<LOD	1967	1811	222	1718	112	1767	84	1745	68	<LOD	12	64	6	3070	43	58	2	407	5	4.29	1.79
19	175.0	BKM 052411-01	low marsh	D	1-Mar-12	19	Soil	<LOD	2190	1682	233	1844	122	3291	113	2326	81	<LOD	13	66	6	3433	49	54	2	589	7	3.95	1.86
3	5.0	BKM 052411-02	washover	A	2-Mar-12	3	Soil	<LOD	2834	5182	403	1368	140	7037	195	11499	243	29	7	255	12	5405	83	93	4	3813	45	3.02	3.95
4	15.0	BKM 052411-02	washover	A	2-Mar-12	4	Soil	<LOD	2754	4239	404	1851	158	6372	191	15705	315	<LOD	21	295	13	6349	99	95	5	9176	124	1.71	3.43
5	25.0	BKM 052411-02	washover	A	2-Mar-12	5	Soil	<LOD	3300	3313	429	1563	166	7726	226	24485	467	34	9	475	17	9170	146	101	5	6889	89	3.55	8.77
6	35.0	BKM 052411-02	washover	A	2-Mar-12	6	Soil	<LOD	3268	2696	423	1493	164	9809	257	30746	555	<LOD	27	592	19	10556	165	114	5	7985	106	3.85	7.07
7	45.0	BKM 052411-02	washover	A	2-Mar-12	7	Soil	<LOD	3489	2442	424	1130	157	8636	240	32551	585	<LOD	30	605	19	11260	176	100	5	8107	110	4.02	9.96
8	55.0	BKM 052411-02	washover	A	2-Mar-12	8	Soil	<LOD	3266	2200	410	944	152	10740	273	28837	528	50	9	622	19	10415	164	112	5	7621	102	3.78	11.03
9	65.0	BKM 052411-02	low marsh	D	2-Mar-12	9	Soil	<LOD	2288	2862	292	1636	129	3385	123	2327	86	16	5	52	6	2073	34	68	3	1691	20	1.38	1.27
10	75.0	BKM 052411-02	low marsh	D	2-Mar-12	10	Soil	14448	1411	6713	362	2525	144	20942	348	1813	77	<LOD	14	73	7	7850	101	80	2	288	4	6.30	3.11
11	85.0	BKM 052411-02	low marsh	D	2-Mar-12	11	Soil	<LOD	1936	6345	277	1534	89	277	46	580	38	<LOD	10	22	5	4029	47	39	2	140	3	4.14	2.63
12	95.0	BKM 052411-02	low marsh	D	2-Mar-12	12	Soil	<LOD	1903	5945	272	1670	93	274	47	604	41	12	4	28	5	5401	62	39	2	76	2	7.95	3.23
13	105.0	BKM 052411-02	low marsh	D	2-Mar-12	13	Soil	2496	737	6529	298	1880	103	537	55	704	45	<LOD	12	18	5	6572	77	42	2	77	2	9.14	3.50
14	115.0	BKM 052411-02	low marsh	D	2-Mar-12	14	Soil	3420	827	4298	285	2491	130	1062	72	991	57	21	5	35	6	6385	82	53	2	120	3	8.26	2.56
15	125.0	BKM 052411-02	low marsh	E	2-Mar-12	15	Soil	<LOD	2548	2433	277	4241	182	2150	102	1910	84	24	6	67	8	8178	113	68	2	295	5	6.47	1.93
16	135.0	BKM 052411-02	low marsh	E	2-Mar-12	16	Soil	2810	923	2271	296	2806	166	3170	126	703	60	<LOD	16	50	8	6166	92	67	2	138	3	5.09	2.20
17	145.0	BKM 052411-02	low marsh	E	2-Mar-12	17	Soil	2874	861	2398	281	3445	170	1940	99	464	48	16	5	42	7	3768	57	68	2	68	2	6.82	1.09
18	155.0	BKM 052411-02	high marsh	B	2-Mar-12	18	Soil	<LOD	2013	1199	245	2744	156	2764	114	530	48	<LOD	14	33	6	2777	44	66	2	60	2	8.83	1.01
19	165.0	BKM 052411-02	high marsh	B	2-Mar-12	19	Soil	2701	825	2042	262	3319	163	2538	108	574	49	<LOD	14	56	7	3797	56	77	3	93	3	6.17	1.14
20	175.0	BKM 052411-02	high marsh	B	2-Mar-12	20																							

ID	DEPTH	BORING_ID	DEP_ENV	Chemo-facies	Date	Reading	Mode	S	S +/-	Cl	Cl +/-	K	K +/-	Ca	Ca +/-	Ti	Ti +/-	Cr	Cr +/-	Mn	Mn +/-	Fe	Fe +/-	Sr	Sr +/-	Zr	Zr +/-	Ti/Zr	Fe/K
40	365.0	BKM 052411-02	bioturbated and laminated	B	2-Mar-12	40	Soil	<LOD	2293	1514	250	4072	180	4500	142	361	44	21	5	47	6	2189	36	112	3	98	3	3.68	0.54
41	375.0	BKM 052411-02	bioturbated and laminated	B	2-Mar-12	41	Soil	<LOD	2273	1687	257	4425	188	4413	142	449	46	28	5	45	6	2236	36	119	3	95	3	4.73	0.51
42	385.0	BKM 052411-02	bioturbated and laminated	B	2-Mar-12	42	Soil	<LOD	2384	1055	254	2975	167	7377	191	1151	66	<LOD	14	53	7	2551	42	136	3	361	6	3.19	0.86
47	390.0	BKM 052411-02	bioturbated and laminated	C	2-Mar-12	47	Soil	5544	1152	7988	406	4683	190	7235	182	2627	99	19	6	109	9	11886	159	75	2	205	4	12.81	2.54
43	395.0	BKM 052411-02	bioturbated and laminated	C	2-Mar-12	43	Soil	2906	887	1323	259	3684	179	7269	188	1339	70	<LOD	13	56	7	2993	47	131	3	438	6	3.06	0.81
44	405.0	BKM 052411-02	bioturbated and laminated	C	2-Mar-12	44	Soil	<LOD	2437	1881	265	3917	179	8710	205	1142	62	<LOD	13	57	7	2870	44	137	3	275	5	4.15	0.73
48	410.0	BKM 052411-02	bioturbated and laminated	C	2-Mar-12	48	Soil	5316	1213	5861	396	4642	205	11627	258	4574	135	31	7	132	10	10725	153	99	3	442	6	10.35	2.31
45	415.0	BKM 052411-02	bioturbated and laminated	C	2-Mar-12	45	Soil	<LOD	2441	1388	252	5105	202	9689	220	918	59	<LOD	14	59	7	3378	51	140	3	230	4	3.99	0.66
46	422.5	BKM 052411-02	bioturbated and laminated	C	2-Mar-12	46	Soil	<LOD	2458	2005	280	5540	216	11311	248	806	60	<LOD	13	59	7	3193	50	166	4	233	4	3.46	0.58
24	5.0	BKM 052511-01	washover	A	3-Mar-12	24	Soil	<LOD	2534	4140	356	1353	131	5853	170	8358	191	<LOD	17	186	10	4268	65	87	3	2768	32	3.02	3.15
25	15.0	BKM 052511-01	washover	A	3-Mar-12	25	Soil	<LOD	2531	4879	364	1566	134	5180	157	6423	159	<LOD	16	138	9	3699	57	89	3	2149	25	2.99	2.36
26	25.0	BKM 052511-01	washover	A	3-Mar-12	26	Soil	<LOD	2425	3610	348	1447	137	6474	181	7799	185	<LOD	18	156	9	4396	68	96	3	2818	33	2.77	3.04
27	35.0	BKM 052511-01	washover	A	3-Mar-12	27	Soil	<LOD	2171	2586	305	1070	120	4324	142	7813	177	18	6	140	9	3703	57	90	3	1862	21	4.20	3.46
28	45.0	BKM 052511-01	washover	A	3-Mar-12	28	Soil	<LOD	2338	2033	298	1223	128	6029	172	6910	167	<LOD	16	150	9	3465	54	84	3	1814	21	3.81	2.83
29	55.0	BKM 052511-01	freshwater pond/low marsh	D	3-Mar-12	29	Soil	5712	1087	8622	393	2311	134	8114	184	1207	67	<LOD	15	60	7	8571	111	65	2	194	4	6.22	3.71
30	65.0	BKM 052511-01	freshwater pond/low marsh	D	3-Mar-12	30	Soil	<LOD	2064	8273	315	1464	89	1981	77	767	42	<LOD	10	26	5	4225	49	36	2	53	2	14.47	2.89
31	75.0	BKM 052511-01	freshwater pond/low marsh	D	3-Mar-12	31	Soil	<LOD	1973	6822	297	1486	92	753	57	614	40	<LOD	10	17	5	3222	40	34	2	32	2	19.19	2.17
32	85.0	BKM 052511-01	freshwater pond/low marsh	D	3-Mar-12	32	Soil	2309	728	7109	304	2027	104	1109	65	931	48	14	4	27	5	5092	60	52	2	99	2	9.40	2.51
33	95.0	BKM 052511-01	low marsh	E	3-Mar-12	33	Soil	<LOD	2750	6664	387	3668	175	3030	119	2350	94	<LOD	17	66	8	7840	110	81	3	235	4	10.00	2.14
59	100.0	BKM 052511-01	storm layer	B	3-Mar-12	59	Soil	<LOD	2318	2470	284	3271	167	5608	161	1703	75	<LOD	13	48	6	2542	41	120	3	179	4	9.51	0.78
34	105.0	BKM 052511-01	low marsh	E	3-Mar-12	34	Soil	4747	1091	6824	386	3324	166	6037	165	2497	93	21	6	53	8	9805	134	58	2	180	3	13.87	2.93
35	115.0	BKM 052511-01	low marsh	E	3-Mar-12	35	Soil	2244	1797	6777	407	3155	174	24052	420	1718	83	<LOD	16	46	7	7035	100	70	2	210	4	8.18	2.25
60	118.5	BKM 052511-01	storm layer	B	3-Mar-12	60	Soil	<LOD	2631	5168	364	3213	170	1033	83	1436	74	<LOD	16	41	7	6397	94	46	2	149	3	9.64	1.99
36	125.0	BKM 052511-01	low marsh	E	3-Mar-12	36	Soil	<LOD	2982	8914	413	3828	169	2006	97	2052	88	34	6	68	9	16186	210	45	2	79	2	25.97	4.23
37	135.0	BKM 052511-01	low marsh	E	3-Mar-12	37	Soil	4133	1991	7927	405	3671	172	1618	92	1946	87	<LOD	19	74	9	18858	249	44	2	56	2	34.75	5.14
38	145.0	BKM 052511-01	low marsh	E	3-Mar-12	38	Soil	11528	1370	7368	388	3318	164	16984	309	1481	75	<LOD	16	70	8	11532	151	76	2	83	2	17.84	3.48
39	155.0	BKM 052511-01	low marsh	E	3-Mar-12	39	Soil	4234	1047	8199	394	3643	164	3260	117	1736	80	22	6	82	9	14719	190	65	2	58	2	29.93	4.04
40	165.0	BKM 052511-01	low marsh	E	3-Mar-12	40	Soil	3335	1000	7469	377	3859	167	1762	91	1773	83	<LOD	18	70	9	18557	236	43	2	63	2	28.14	4.41
41	175.0	BKM 052511-01	low marsh	E	3-Mar-12	41	Soil	18122	1509	7108	369	3544	161	11264	226	1591	75	<LOD	16	67	8	13127	166	53	2	35	2	45.46	3.70
44	185.0	BKM 052511-01	low marsh	E	3-Mar-12	44	Soil	16264	1558	6275	380	3330	170	15881	302	1763	84	27	6	58	8	15114	201	61	2	117	3	15.07	4.54
45	195.0	BKM 052511-01	low marsh	E	3-Mar-12	45	Soil	19764	1775	8614	442	2945	172	32641	530	1067	74	<LOD	17	74	9	14104	191	74	2	51	2	20.92	4.79
46	205.0	BKM 052511-01	low marsh	E	3-Mar-12	46	Soil	4324	1072	8332	403	2899	152	3749	126	1997	85	18	6	88	9	14749	192	47	2	115	3	17.37	5.09
58	215.0	BKM 052511-01	low marsh	E	3-Mar-12	58	Soil	9749	1414	7601	426	3732	185	10470	239	2058	94	<LOD	20	71	10	18535	256	77	3	104	3	19.79	4.97
47	225.0	BKM 052511-01	upper forebeach	B	3-Mar-12	47	Soil	<LOD	2322	1803	260	3344	167	3214	121	253	39	<LOD	12	36	6	2975	46	67	2	47	2	5.38	0.89
48	235.0	BKM 052511-01	upper forebeach	B	3-Mar-12	48	Soil	<LOD	2988	1691	282	2519	163	21457	394	204	38	<LOD	13	<LOD	17	1795	32	126	3	80	3	2.55	0.71
49	245.0	BKM 052511-01	upper forebeach	B	3-Mar-12	49	Soil	<LOD	2133	1499	252	3874	179	6072	167	524	47	<LOD	12	37	6	2301	38	89	3	93	3	5.63	0.59
50	255.0	BKM 052511-01	upper forebeach	B	3-Mar-12	50	Soil	<LOD	2263	2289	279	3835	179	4355	142	555	50	<LOD	13	30	6	2054	34	101	3	96	3	5.78	0.54
51	265.0	BKM 052511-01	upper forebeach	B	3-Mar-12	51	Soil	<LOD	2159	2163	260	4475	183	4552	140	400	42	<LOD	13	31	6	2036	33	97	3	49	2	8.16	0.45
52	275.0	BKM 052511-01	upper forebeach	B	3-Mar-12	52	Soil	<LOD	2106	2075	265	3906	176	6631	173	718	52	<LOD	12	42	6	2354	38	106	3	205	4	3.50	0.60
53	285.0	BKM 052511-01	upper forebeach	B	3-Mar-12	53	Soil	<LOD	2398	2509	288	5158	206	7243	187	673	53	<LOD	12	31	6	2388	39	108	3	173	4	3.89	0.46
54	295.0	BKM 052511-01	upper forebeach	B	3-Mar-12	54	Soil	<LOD	2524	2235	278	4845	198	5674	162	785	55	<LOD	12	31	6	2422	39	104	3	174	3	4.51	0.50
55	305.0	BKM 052511-01	upper forebeach	B	3-Mar-12	55	Soil	<LOD	2478	3629	314	4391	189	7429	187	1002	62	<LOD	13	39	6	2628	42	106	3	314	5	3.19	0.60
56	315.0	BKM 052511-01	upper forebeach	B	3-Mar-12	56	Soil	<LOD	2288	2792	297	4121	186	5781	165	976	61	<LOD	13	28	6	2236	37	103	3	191	4	5.11	0.54
57	325.0	BKM 052511-01	lower forebeach	B	3-Mar-12	57	Soil	<LOD	2434	3255	301	4578	191	5872	164	481	47	<LOD	12	30	6	2260	37	91	3	74	3	6.50	0.49
2	340.0	BKM 052511-01	lower forebeach	C	16-Mar-12	2	Soil	9564	1416	8164	454	3476	186	11148	256	1907	86	<LOD	16	29	7	5001	77	104	3	175	4	10.90	1.44
3	345.0	BKM 052511-01	lower forebeach	C	16-Mar-12	3	Soil	7761	1207	3562	332	3546	181	10076	234	912	59	<LOD	13	32	6	1967	34	90	3	105	3	8.69	0.55
4	350.0	BKM 052511-01	lower forebeach	C	16-Mar-12	4	Soil	13472	1456	2448	313	3595	187	12624	276	841	57	<LOD	13	31	6	1795	32	92	3	103	3	8.17	0.50
5	355.0	BKM 052511-01	lower forebeach	C	16-Mar-12	5	Soil	5092	1069	2648	307	4314	197	9431	225	710	54	<LOD	13	20	6	2175	37	98	3	123	3	5.77	0.50
6	360.0	BKM 052511-0																											

ID	DEPTH	BORING_ID	DEP_ENV	Chemo-facies	Date	Reading	Mode	S	S +/-	Cl	Cl +/-	K	K +/-	Ca	Ca +/-	Ti	Ti +/-	Cr	Cr +/-	Mn	Mn +/-	Fe	Fe +/-	Sr	Sr +/-	Zr	Zr +/-	Ti/Zr	Fe/K
25	450.0	BKM 052511-01	bioturbated and laminated	C	16-Mar-12	25	Soil	7819	1265	4639	368	3953	193	10892	250	1670	80	<LOD	14	42	7	3086	50	87	3	340	5	4.91	0.78
26	455.0	BKM 052511-01	bioturbated and laminated	C	16-Mar-12	26	Soil	10039	1369	5433	384	5504	221	11898	263	1352	71	17	5	44	7	4460	68	106	3	183	4	7.39	0.81
27	460.0	BKM 052511-01	bioturbated and laminated	C	16-Mar-12	27	Soil	7084	1285	8770	442	5452	214	9487	222	1642	83	<LOD	17	88	9	10941	152	96	3	139	3	11.81	2.01
28	465.0	BKM 052511-01	bioturbated and laminated	C	16-Mar-12	28	Soil	7572	1327	8261	445	5295	217	12964	277	1305	74	<LOD	16	76	8	6817	100	113	3	175	4	7.46	1.29
29	470.0	BKM 052511-01	bioturbated and laminated	C	16-Mar-12	29	Soil	11183	1430	5531	389	5010	214	14177	296	1420	74	<LOD	14	39	7	4692	72	98	3	163	4	8.71	0.94
30	475.0	BKM 052511-01	bioturbated and laminated	C	16-Mar-12	30	Soil	4374	1087	4130	354	4109	196	8999	222	1560	76	<LOD	14	26	6	3128	51	85	3	356	5	4.38	0.76
31	480.0	BKM 052511-01	bioturbated and laminated	C	16-Mar-12	31	Soil	10536	1348	3708	340	3335	179	11652	259	709	55	<LOD	13	43	7	2472	41	82	3	140	3	5.06	0.74
32	485.0	BKM 052511-01	bioturbated and laminated	C	16-Mar-12	32	Soil	<LOD	3449	11547	499	4714	201	8320	206	1956	88	26	6	81	9	11863	165	100	3	170	3	11.51	2.52
33	490.0	BKM 052511-01	bioturbated and laminated	C	16-Mar-12	33	Soil	6859	1262	6993	415	4747	206	11375	253	1413	77	<LOD	15	63	8	6679	98	113	3	196	4	7.21	1.41
34	495.0	BKM 052511-01	bioturbated and laminated	C	16-Mar-12	34	Soil	9555	1285	3361	331	3243	177	8878	218	741	55	<LOD	12	32	6	1632	30	65	2	128	3	5.79	0.50
35	500.0	BKM 052511-01	bioturbated and laminated	C	16-Mar-12	35	Soil	8718	1322	6405	402	5221	214	12764	273	1076	66	<LOD	15	39	7	4262	65	110	3	180	4	5.98	0.82
2	5.0	BKM 052511-02	washover	A	3-Mar-12	2	Soil	<LOD	1845	<LOD	637	2317	146	5209	154	1730	77	21	5	110	8	2885	45	51	2	181	4	9.56	1.25
3	15.0	BKM 052511-02	washover	A	3-Mar-12	3	Soil	<LOD	1700	<LOD	580	2315	142	3856	129	2888	39	16	4	60	6	1704	29	60	2	193	4	1.49	0.74
4	25.0	BKM 052511-02	washover	A	3-Mar-12	4	Soil	<LOD	1645	<LOD	579	2557	151	3971	134	276	40	24	5	49	6	1695	30	71	2	148	3	1.86	0.66
5	35.0	BKM 052511-02	washover	A	3-Mar-12	5	Soil	<LOD	1982	<LOD	617	3312	167	7712	190	1947	80	15	5	85	7	2827	44	90	3	179	4	10.88	0.85
6	45.0	BKM 052511-02	washover	A	3-Mar-12	6	Soil	<LOD	2275	<LOD	602	2418	150	8632	205	2304	87	<LOD	14	72	7	2325	38	89	3	259	4	8.90	0.96
7	55.0	BKM 052511-02	washover	A	3-Mar-12	7	Soil	<LOD	1553	<LOD	613	2056	137	3233	119	221	34	16	4	42	6	1081	21	68	2	104	3	2.13	0.53
8	65.0	BKM 052511-02	washover	A	3-Mar-12	8	Soil	<LOD	1968	<LOD	645	2239	146	4990	151	952	57	<LOD	12	51	6	1587	28	82	3	128	3	7.44	0.71
9	75.0	BKM 052511-02	washover	A	3-Mar-12	9	Soil	<LOD	1769	<LOD	700	2218	150	6376	177	1791	78	<LOD	14	47	7	2277	38	95	3	223	4	8.03	1.03
10	85.0	BKM 052511-02	washover	A	3-Mar-12	10	Soil	<LOD	1939	687	229	1643	131	7018	180	1431	68	<LOD	13	56	7	1984	33	114	3	251	4	5.70	1.21
13	95.0	BKM 052511-02	washover	A	3-Mar-12	13	Soil	<LOD	1622	743	217	2033	134	4034	131	873	55	<LOD	12	53	6	1301	24	90	3	214	4	4.08	0.64
14	105.0	BKM 052511-02	washover	A	3-Mar-12	14	Soil	<LOD	2184	<LOD	675	2020	142	5342	158	1514	71	<LOD	13	48	6	1606	29	85	3	199	4	7.61	0.80
15	115.0	BKM 052511-02	upper forebeach	B	3-Mar-12	15	Soil	<LOD	1949	<LOD	629	3068	158	2714	111	357	41	<LOD	12	31	6	922	19	84	3	99	3	3.61	0.30
16	125.0	BKM 052511-02	upper forebeach	B	3-Mar-12	16	Soil	<LOD	1398	706	210	3417	162	2205	100	188	33	<LOD	12	26	5	1188	22	67	2	28	2	6.71	0.35
17	135.0	BKM 052511-02	upper forebeach	B	3-Mar-12	17	Soil	<LOD	1784	724	213	3296	160	1592	89	83	83	<LOD	11	23	5	834	18	60	2	32	2	2.59	0.25
18	145.0	BKM 052511-02	upper forebeach	B	3-Mar-12	18	Soil	<LOD	1686	<LOD	604	1599	120	1760	89	182	31	<LOD	11	27	5	692	15	50	2	45	2	4.04	0.43
19	155.0	BKM 052511-02	upper forebeach	B	3-Mar-12	19	Soil	<LOD	1573	889	216	1750	125	1818	91	90	27	<LOD	12	32	6	821	17	58	2	39	2	2.31	0.47
20	165.0	BKM 052511-02	upper forebeach	B	3-Mar-12	20	Soil	<LOD	1579	913	211	1917	127	2024	94	236	33	<LOD	10	34	5	834	17	52	2	41	2	5.76	0.44
21	175.0	BKM 052511-02	upper forebeach	B	3-Mar-12	21	Soil	<LOD	1871	1070	225	2527	144	2426	104	403	40	13	4	29	6	1146	22	66	2	55	2	7.33	0.45
22	185.0	BKM 052511-02	upper forebeach	B	3-Mar-12	22	Soil	<LOD	1978	1151	228	2206	137	1947	95	258	34	<LOD	12	32	6	942	19	58	2	96	3	2.69	0.43
23	192.5	BKM 052511-02	upper forebeach	B	3-Mar-12	23	Soil	<LOD	1604	842	209	1741	123	1537	85	286	34	12	4	23	5	991	19	58	2	75	2	3.81	0.57
2	10.0	IEP 20110604-01	High Marsh/Tidal Creek	C	5-Jun-12	2	Soil	3845	955	5653	354	2382	142	661	71	2002	79	34	5	23	6	3428	51	28	2	266	4	7.53	1.44
3	20.0	IEP 20110604-01	High Marsh/Tidal Creek	C	5-Jun-12	3	Soil	4786	884	5758	301	2724	127	1277	74	1773	69	<LOD	13	41	6	8482	101	45	2	150	3	11.82	3.11
4	30.0	IEP 20110604-01	High Marsh/Tidal Creek	C	5-Jun-12	4	Soil	<LOD	2811	5850	351	3970	173	869	76	2204	92	<LOD	18	60	8	15195	198	43	2	159	3	13.86	3.83
5	40.0	IEP 20110604-01	High Marsh/Tidal Creek	C	5-Jun-12	5	Soil	13240	1466	5676	364	3412	170	2877	116	2190	100	<LOD	23	49	11	33258	437	41	2	107	3	20.47	9.75
6	50.0	IEP 20110604-01	High Marsh/Tidal Creek	C	5-Jun-12	6	Soil	<LOD	2365	2305	301	808	115	182	182	3463	111	<LOD	14	52	7	3402	55	11	2	353	5	9.81	4.21
7	60.0	IEP 20110604-01	High Marsh/Tidal Creek	C	5-Jun-12	7	Soil	2849	629	7630	268	750	59	352	42	176	19	<LOD	6	34	4	627	11	35	2	152	3	1.16	0.84
8	70.0	IEP 20110604-01	High Marsh/Tidal Creek	C	5-Jun-12	8	Soil	<LOD	3153	1808	351	933	134	1487	105	18961	362	39	8	216	11	5456	87	18	5	10020	148	1.89	5.85
9	80.0	IEP 20110604-01	High Marsh/Tidal Creek	C	5-Jun-12	9	Soil	2819	788	3202	277	620	92	393	58	886	53	<LOD	12	20	5	1980	32	26	2	287	4	3.09	3.19
10	90.0	IEP 20110604-01	High Marsh/Tidal Creek	C	5-Jun-12	10	Soil	<LOD	2421	1679	285	1092	123	337	66	4364	127	<LOD	14	79	7	1565	29	13	2	1503	18	2.90	1.43
11	93.0	IEP 20110604-01	High Marsh/Tidal Creek	C	5-Jun-12	11	Soil	2345	663	5989	272	1022	77	873	58	815	44	10	3	32	4	1208	18	34	2	249	4	3.27	1.18
12	96.0	IEP 20110604-01	High Marsh/Tidal Creek	C	5-Jun-12	12	Soil	<LOD	1952	1752	262	1295	121	164	164	1009	56	<LOD	12	24	6	718	17	18	2	62	2	16.27	5.55
13	100.0	IEP 20110604-01	High Marsh/Tidal Creek	C	5-Jun-12	13	Soil	<LOD	3007	1433	361	1088	145	1583	113	20357	396	<LOD	23	233	12	5584	92	26	3	5574	68	3.65	5.13
14	110.0	IEP 20110604-01	High Marsh/Tidal Creek	C	5-Jun-12	14	Soil	<LOD	2425	3582	307	1815	131	218	58	1822	75	<LOD	13	25	6	2870	45	17	2	258	4	7.06	1.58
15	120.0	IEP 20110604-01	High Marsh/Tidal Creek	C	5-Jun-12	15	Soil	<LOD	2105	2517	289	1907	138	162	162	1596	73	<LOD	13	31	6	1893	33	15	2	230	4	6.94	0.99
16	130.0	IEP 20110604-01	High Marsh/Tidal Creek	C	5-Jun-12	16	Soil	<LOD	2304	3577	304	2138	137	374	64	1755	75	<LOD	13	<LOD	17	4003	59	18	2	242	4	7.25	1.87
17	140.0	IEP 20110604-01	High Marsh/Tidal Creek	C	5-Jun-12	17	Soil	<LOD	1876	1202	266	1308	129	181	181	2390	89	<LOD	12	21	6	1150	23	13	2	219	4	10.91	0.88
18	150.0	IEP 20110604-01	High Marsh/Tidal Creek	C	5-Jun-12	18	Soil	<LOD	2573	4040	316	2923	154	474	67	2302	86	15	5	36	7	4812	69	19	2	145	3	15.88	1.65
19	160.0	IEP 20110604-01	High Marsh/Tidal Creek	C	5-Jun-12	1																							

ID	DEPTH	BORING_ID	DEP_ENV	Chemo-facies	Date	Reading	Mode	S	S +/-	Cl	Cl +/-	K	K +/-	Ca	Ca +/-	Ti	Ti +/-	Cr	Cr +/-	Mn	Mn +/-	Fe	Fe +/-	Sr	Sr +/-	Zr	Zr +/-	Ti/Zr	Fe/K
38	320.0	IEP 20110604-01	High Marsh/Tidal Creek	C	5-Jun-12	38	Soil	<LOD	1885	2094	263	3768	173	996	79	566	47	<LOD	12	<LOD	16	1468	26	51	2	79	3	7.16	0.39
39	330.0	IEP 20110604-01	lower forebeach	B	5-Jun-12	39	Soil	<LOD	2110	2493	274	3323	163	672	71	407	42	<LOD	12	23	6	1650	29	44	2	73	3	5.58	0.50
40	340.0	IEP 20110604-01	lower forebeach	B	5-Jun-12	40	Soil	3349	988	6158	383	3350	171	632	74	1114	64	<LOD	14	32	6	3641	56	43	2	72	2	15.47	1.09
41	350.0	IEP 20110604-01	lower forebeach	B	5-Jun-12	41	Soil	<LOD	2130	3724	319	2464	151	316	64	188	35	<LOD	12	<LOD	16	1772	31	30	2	55	2	3.42	0.72
42	360.0	IEP 20110604-01	lower forebeach	B	5-Jun-12	42	Soil	<LOD	2997	6363	425	2472	168	530	75	235	37	<LOD	14	<LOD	19	2092	38	30	2	47	2	5.00	0.85
44	370.0	IEP 20110604-01	lower forebeach	B	5-Jun-12	44	Soil	<LOD	1944	2406	271	2796	152	424	65	807	51	<LOD	11	16	5	1629	28	30	2	112	3	7.21	0.58
45	380.0	IEP 20110604-01	lower forebeach	B	5-Jun-12	45	Soil	<LOD	2228	2077	273	1815	135	169	185	33	<LOD	12	<LOD	17	2829	45	21	2	45	2	4.11	1.56	
46	390.0	IEP 20110604-01	bioturbated and laminated	C	5-Jun-12	46	Soil	3154	885	2396	280	2626	153	647	71	400	48	<LOD	14	<LOD	20	6958	99	37	2	105	3	3.81	2.65
47	400.0	IEP 20110604-01	bioturbated and laminated	C	5-Jun-12	47	Soil	<LOD	2104	1491	257	2185	144	172	172	339	38	<LOD	11	<LOD	16	844	19	17	2	36	2	9.42	0.39
48	405.0	IEP 20110604-01	bioturbated and laminated	C	5-Jun-12	48	Soil	3315	941	5264	353	2527	150	710	73	518	49	<LOD	13	24	6	3310	51	31	2	69	2	7.51	1.31
49	410.0	IEP 20110604-01	bioturbated and laminated	C	5-Jun-12	49	Soil	2390	778	2001	257	3046	156	404	65	401	41	<LOD	12	<LOD	16	2378	38	36	2	49	2	8.18	0.78
50	420.0	IEP 20110604-01	bioturbated and laminated	C	5-Jun-12	50	Soil	<LOD	1851	2045	261	2833	154	480	66	270	36	<LOD	12	<LOD	14	1160	22	27	2	29	2	9.31	0.41
51	430.0	IEP 20110604-01	bioturbated and laminated	C	5-Jun-12	51	Soil	4256	997	3270	319	2511	157	258	65	377	48	<LOD	15	<LOD	20	6505	97	28	2	48	2	7.85	2.59
52	440.0	IEP 20110604-01	bioturbated and laminated	C	5-Jun-12	52	Soil	<LOD	2786	2789	314	5434	221	865	85	646	59	<LOD	16	<LOD	22	9015	132	46	2	89	3	7.26	1.66
53	450.0	IEP 20110604-01	bioturbated and laminated	C	5-Jun-12	53	Soil	2549	850	2153	280	5144	206	583	75	729	53	<LOD	14	20	6	3148	50	38	2	94	3	7.76	0.61
54	460.0	IEP 20110604-01	bioturbated and laminated	C	5-Jun-12	54	Soil	<LOD	2102	1345	255	2147	145	164	97	31	<LOD	13	<LOD	16	1193	24	13	2	24	2	4.04	0.56	
55	470.0	IEP 20110604-01	bioturbated and laminated	C	5-Jun-12	55	Soil	<LOD	2571	2659	297	2876	163	495	69	187	39	<LOD	14	<LOD	19	5536	83	36	2	39	2	4.79	1.92
56	480.0	IEP 20110604-01	bioturbated and laminated	C	5-Jun-12	56	Soil	3986	908	2531	281	2455	147	722	72	299	43	15	5	19	6	4017	60	25	2	52	2	5.75	1.64
57	490.0	IEP 20110604-01	bioturbated and laminated	C	5-Jun-12	57	Soil	5117	1008	4426	327	2705	151	659	71	286	44	<LOD	13	<LOD	19	6290	89	37	2	59	2	4.85	2.33
2	10.0	IEP 20110604-02	High Marsh/Tidal Creek	A	5-May-12	2	Soil	<LOD	2233	3830	324	1707	130	1216	84	5985	148	<LOD	16	111	8	3409	52	24	2	2229	25	2.69	2.00
3	20.0	IEP 20110604-02	High Marsh/Tidal Creek	A	5-May-12	3	Soil	<LOD	1726	2389	269	1889	130	388	64	2009	79	<LOD	12	25	6	1799	30	20	2	528	7	3.80	0.95
4	30.0	IEP 20110604-02	High Marsh/Tidal Creek	A	5-May-12	4	Soil	<LOD	1835	1877	249	1305	113	693	68	2277	83	<LOD	11	32	6	1431	25	28	2	631	8	3.61	1.10
5	40.0	IEP 20110604-02	High Marsh/Tidal Creek	A	5-May-12	5	Soil	<LOD	1910	1510	247	1326	117	636	68	2661	90	<LOD	12	43	6	1308	24	29	2	739	9	3.60	0.99
6	50.0	IEP 20110604-02	High Marsh/Tidal Creek	B	5-May-12	6	Soil	<LOD	2269	2021	278	2295	149	1274	87	995	58	<LOD	13	36	6	994	21	42	2	135	3	7.37	0.43
7	60.0	IEP 20110604-02	High Marsh/Tidal Creek	B	5-May-12	7	Soil	<LOD	2110	2768	263	2198	130	1275	79	623	44	<LOD	11	24	5	851	17	48	2	53	2	11.75	0.39
8	70.0	IEP 20110604-02	upper forebeach	B	5-May-12	8	Soil	<LOD	1923	1638	239	2940	151	1206	80	299	34	13	4	<LOD	15	591	14	46	2	25	2	11.96	0.20
9	80.0	IEP 20110604-02	upper forebeach	B	5-May-12	9	Soil	<LOD	2118	1256	243	2843	156	1101	81	384	40	<LOD	12	<LOD	16	629	15	41	2	52	2	7.38	0.22
10	90.0	IEP 20110604-02	upper forebeach	B	5-May-12	10	Soil	<LOD	1764	1376	233	2967	152	1002	76	386	40	16	4	19	5	663	15	41	2	62	2	6.23	0.22
11	100.0	IEP 20110604-02	upper forebeach	B	5-May-12	11	Soil	<LOD	1848	2559	257	4565	178	906	74	139	30	<LOD	11	110	7	539	13	55	2	21	2	6.62	0.12
12	110.0	IEP 20110604-02	upper forebeach	B	5-May-12	12	Soil	<LOD	2102	1474	270	4605	202	2722	118	395	42	<LOD	13	23	6	840	19	60	2	40	2	9.88	0.18
13	120.0	IEP 20110604-02	lower forebeach	B	5-May-12	13	Soil	<LOD	1570	1079	243	3718	178	1466	91	245	38	<LOD	13	<LOD	16	684	16	50	2	39	2	6.28	0.18
14	130.0	IEP 20110604-02	lower forebeach	B	5-May-12	14	Soil	<LOD	1865	1441	259	2426	152	900	79	160	32	<LOD	12	<LOD	16	521	14	31	2	56	2	2.86	0.21
15	140.0	IEP 20110604-02	lower forebeach	B	5-May-12	15	Soil	<LOD	1966	1540	249	3027	159	1422	87	386	40	<LOD	12	<LOD	16	735	17	47	2	47	2	8.21	0.24
16	150.0	IEP 20110604-02	lower forebeach	B	5-May-12	16	Soil	<LOD	1962	1446	237	3035	154	1271	82	689	50	<LOD	12	33	6	990	19	53	2	180	3	3.83	0.33
17	160.0	IEP 20110604-02	lower forebeach	B	5-May-12	17	Soil	<LOD	1975	1029	241	2475	151	1077	81	446	45	<LOD	13	25	6	662	16	48	2	53	2	8.42	0.27
18	170.0	IEP 20110604-02	lower forebeach	B	5-May-12	18	Soil	<LOD	1984	1528	239	3826	169	1618	90	894	54	14	4	36	6	1206	22	58	2	149	3	6.00	0.32
19	180.0	IEP 20110604-02	lower forebeach	B	5-May-12	19	Soil	<LOD	1860	1266	230	3298	159	1685	90	430	44	21	4	20	5	1065	20	50	2	107	3	4.02	0.32
20	190.0	IEP 20110604-02	lower forebeach	B	5-May-12	20	Soil	<LOD	1840	1018	226	2859	151	1101	79	793	54	<LOD	12	29	6	1174	22	57	2	148	3	5.36	0.41
21	200.0	IEP 20110604-02	lower forebeach	B	5-May-12	21	Soil	<LOD	1715	867	222	3442	165	1356	85	260	37	<LOD	12	17	5	800	17	49	2	56	2	4.64	0.23
22	210.0	IEP 20110604-02	lower forebeach	B	5-May-12	22	Soil	<LOD	1957	975	223	3252	159	1400	85	502	44	<LOD	12	28	6	919	19	57	2	83	3	6.05	0.28
23	220.0	IEP 20110604-02	lower forebeach	B	5-May-12	23	Soil	<LOD	1808	1132	226	2076	133	875	73	486	43	<LOD	12	25	5	957	19	43	2	66	2	7.36	0.46
24	230.0	IEP 20110604-02	lower forebeach	B	5-May-12	24	Soil	<LOD	1894	1085	236	2630	152	1375	87	243	35	<LOD	12	28	6	862	18	49	2	37	2	6.57	0.33
25	240.0	IEP 20110604-02	lower forebeach	B	5-May-12	25	Soil	<LOD	1758	1187	231	2959	154	902	75	395	42	<LOD	12	<LOD	16	865	18	52	2	88	3	4.49	0.29
26	250.0	IEP 20110604-02	lower forebeach	B	5-May-12	26	Soil	<LOD	1806	1339	245	2920	157	1668	92	953	59	<LOD	13	30	6	1176	23	60	2	202	4	4.72	0.40
27	260.0	IEP 20110604-02	lower forebeach	B	5-May-12	27	Soil	<LOD	1824	1068	228	2894	153	1169	80	415	42	19	4	33	6	969	19	49	2	71	2	5.85	0.33
28	270.0	IEP 20110604-02	lower forebeach	B	5-May-12	28	Soil	<LOD	2162	3534	301	2292	141	1379	85	619	50	<LOD	13	111	8	2368	38	43	2	76	3	8.14	1.03
29	280.0	IEP 20110604-02	lower forebeach	B	5-May-12	29	Soil	<LOD	2166	1357	258	2088	144	1328	85	322	39	15	4	<LOD	17	805	18	38	2	76	3	4.24	0.39
30	290.0	IEP 20110604-02	lower forebeach	B	5-May-12	30	Soil	<LOD	2042	1237	245	3162	163	1095	82	761	51	<LOD	13	23	6	1083	21	43	2	72	3	10.57	0.34
31	300.0																												

ID	DEPTH	BORING_ID	DEP_ENV	Chemo-facies	Date	Reading	Mode	S	S +/-	Cl	Cl +/-	K	K +/-	Ca	Ca +/-	Ti	Ti +/-	Cr	Cr +/-	Mn	Mn +/-	Fe	Fe +/-	Sr	Sr +/-	Zr	Zr +/-	Ti/Zr	Fe/K
50	490.0	IIEP 20110604-02	bioturbated and laminated	C	5-May-12	50	Soil	9862	1252	4300	341	2703	158	1144	84	357	47	18	5	34	7	4536	69	33	2	67	2	5.33	1.68
51	500.0	IIEP 20110604-02	bioturbated and laminated	C	5-May-12	51	Soil	12599	1311	2650	292	1270	121	755	73	111	111	20	5	<LOD	18	4012	61	25	2	37	2	3.00	3.16
52	510.0	IIEP 20110604-02	bioturbated and laminated	C	5-May-12	52	Soil	8415	1213	2080	297	2725	166	1284	90	296	50	<LOD	16	<LOD	21	7732	115	45	2	52	2	5.69	2.84
53	520.0	IIEP 20110604-02	bioturbated and laminated	C	5-May-12	53	Soil	<LOD	2353	1928	266	2087	140	381	64	490	44	<LOD	12	<LOD	16	1663	29	23	2	100	3	4.90	0.80
30	10.0	BKM 072211-02	upper forebeach	A	18-May-12	30	Soil	<LOD	2089	904	246	1840	138	6720	178	3087	103	23	5	87	7	2242	37	70	3	678	9	4.55	1.22
31	20.0	BKM 072211-02	upper forebeach	A	18-May-12	31	Soil	<LOD	2101	<LOD	726	2773	163	4286	144	1295	67	<LOD	12	21	6	1540	28	56	2	189	4	6.85	0.56
32	30.0	BKM 072211-02	upper forebeach	B	18-May-12	32	Soil	<LOD	2143	1084	257	2591	160	4406	146	887	57	<LOD	13	28	6	1687	31	51	2	147	3	6.03	0.65
33	40.0	BKM 072211-02	upper forebeach	B	18-May-12	33	Soil	<LOD	2676	967	275	856	134	28537	503	308	45	<LOD	12	<LOD	15	954	21	58	2	87	3	3.54	1.11
34	50.0	BKM 072211-02	upper forebeach	B	18-May-12	34	Soil	<LOD	1883	960	249	3622	181	6524	180	421	45	<LOD	12	<LOD	17	1917	34	82	3	64	2	6.58	0.53
35	60.0	BKM 072211-02	upper forebeach	B	18-May-12	35	Soil	<LOD	2411	1115	283	4112	205	18089	362	686	56	<LOD	13	27	7	2700	46	130	3	111	3	6.18	0.66
36	70.0	BKM 072211-02	inlet fill	A	18-May-12	36	Soil	<LOD	2200	948	261	1864	144	6412	179	3515	112	19	5	76	7	2249	38	74	3	603	8	5.83	1.21
37	80.0	BKM 072211-02	inlet fill	A	18-May-12	37	Soil	<LOD	2147	964	255	2862	166	5294	161	1462	72	<LOD	13	47	7	2007	35	62	2	309	5	4.73	0.70
38	90.0	BKM 072211-02	inlet fill	A	18-May-12	38	Soil	<LOD	1974	<LOD	656	2980	163	2622	112	1551	71	<LOD	12	21	6	1664	30	43	2	209	4	7.42	0.56
39	95.0	BKM 072211-02	inlet fill	A	18-May-12	39	Soil	<LOD	2723	4521	338	2840	157	2444	109	2038	83	<LOD	14	45	7	3470	53	47	2	405	6	5.03	1.22
40	100.0	BKM 072211-02	inlet fill	B	18-May-12	40	Soil	<LOD	2088	996	245	5075	206	3877	136	654	52	<LOD	12	<LOD	17	2203	37	82	3	65	2	10.06	0.43
41	110.0	BKM 072211-02	lower forebeach	B	18-May-12	41	Soil	<LOD	2169	<LOD	681	3136	164	3737	130	471	45	<LOD	12	<LOD	16	1496	27	57	2	28	2	16.82	0.48
42	120.0	BKM 072211-02	lower forebeach	B	18-May-12	42	Soil	<LOD	2124	980	235	5084	200	4108	137	541	49	<LOD	12	23	6	2199	36	84	3	54	2	10.02	0.43
43	130.0	BKM 072211-02	lower forebeach	B	18-May-12	43	Soil	<LOD	2029	1050	246	3588	177	2909	119	302	38	<LOD	11	<LOD	16	1676	30	55	2	30	2	10.07	0.47
44	140.0	BKM 072211-02	lower forebeach	B	18-May-12	44	Soil	<LOD	2425	996	265	5211	218	21820	402	125	125	<LOD	12	<LOD	18	2808	46	122	3	51	2	2.45	0.54
45	150.0	BKM 072211-02	lower forebeach	B	18-May-12	45	Soil	<LOD	1973	<LOD	684	2859	161	4475	145	349	40	<LOD	12	<LOD	16	1539	28	54	2	46	2	7.59	0.54
46	160.0	BKM 072211-02	lower forebeach	B	18-May-12	46	Soil	<LOD	2149	798	229	3239	165	5997	165	825	52	<LOD	12	27	6	1982	33	84	3	165	3	5.00	0.61
47	170.0	BKM 072211-02	lower forebeach	A	18-May-12	47	Soil	<LOD	2225	799	244	4084	188	6734	181	1452	72	<LOD	12	36	6	2357	39	87	3	320	5	4.54	0.58
48	180.0	BKM 072211-02	lower forebeach	A	18-May-12	48	Soil	<LOD	2512	1162	270	2248	156	13511	285	2588	97	<LOD	14	70	7	2998	48	130	3	527	7	4.91	1.33
49	190.0	BKM 072211-02	lower forebeach	A	18-May-12	49	Soil	<LOD	1996	713	226	1912	137	5089	151	542	47	<LOD	12	<LOD	16	1649	29	65	2	120	3	4.52	0.86
51	200.0	BKM 072211-02	lower forebeach	A	18-May-12	51	Soil	<LOD	2028	<LOD	687	3380	169	5142	153	1434	67	<LOD	12	22	6	1974	33	79	3	189	4	7.59	0.58
52	210.0	BKM 072211-02	lower forebeach	A	18-May-12	52	Soil	<LOD	1938	956	239	4115	185	4540	145	502	45	<LOD	13	<LOD	16	1685	30	63	2	98	3	5.12	0.41
53	220.0	BKM 072211-02	lower forebeach	A	18-May-12	53	Soil	<LOD	1698	<LOD	695	1843	137	6120	168	1691	73	<LOD	12	39	6	1848	32	69	2	141	3	11.99	1.00
54	230.0	BKM 072211-02	lower forebeach	B	18-May-12	54	Soil	<LOD	1825	<LOD	660	2909	158	3054	118	490	44	<LOD	12	<LOD	16	1597	28	54	2	61	2	8.03	0.55
74	240.0	BKM 072211-02	lower forebeach	B	18-May-12	74	Soil	<LOD	1691	<LOD	677	2930	159	2814	114	538	44	<LOD	12	<LOD	16	1502	27	57	2	65	2	8.28	0.51
75	250.0	BKM 072211-02	lower forebeach	B	18-May-12	75	Soil	<LOD	1984	976	244	4770	200	6971	184	268	39	<LOD	12	18	6	2041	35	85	3	53	2	5.06	0.43
76	260.0	BKM 072211-02	bioturbated and laminated	C	18-May-12	76	Soil	2970	892	1796	266	4800	197	6525	175	743	56	<LOD	13	30	6	4147	62	87	3	144	3	5.16	0.86
77	270.0	BKM 072211-02	bioturbated and laminated	C	18-May-12	77	Soil	4588	1195	4276	363	7312	258	19726	377	1768	87	<LOD	17	111	9	8049	118	162	4	264	4	6.70	1.10
2	5.0	BKM 072311-01	upper forebeach	B	4-May-12	2	Soil	<LOD	2530	3199	306	2951	162	3442	127	274	39	<LOD	13	30	6	2168	36	53	2	76	3	3.61	0.73
3	10.0	BKM 072311-01	upper forebeach	B	4-May-12	3	Soil	<LOD	2183	3242	296	2022	137	2787	112	368	39	<LOD	12	<LOD	16	1515	27	43	2	84	3	4.38	0.75
4	15.0	BKM 072311-01	upper forebeach	B	4-May-12	4	Soil	<LOD	1898	953	240	3088	165	3720	131	226	36	<LOD	12	37	6	1457	27	52	2	48	2	4.71	0.47
5	20.0	BKM 072311-01	upper forebeach	B	4-May-12	5	Soil	<LOD	2741	1305	345	2219	189	4734	177	266	48	<LOD	15	<LOD	20	1519	33	52	2	103	3	2.58	0.68
6	25.0	BKM 072311-01	low marsh	E	4-May-12	6	Soil	78144	3894	8465	603	4269	264	55016	1021	1380	102	<LOD	22	41	11	15608	261	311	6	115	4	12.00	3.66
7	30.0	BKM 072311-01	low marsh	E	4-May-12	7	Soil	43224	2711	5829	474	4948	246	27188	530	2740	122	<LOD	23	69	11	16969	264	150	4	440	7	6.23	3.43
8	35.0	BKM 072311-01	low marsh	E	4-May-12	8	Soil	3306	1009	1949	295	5019	213	4248	147	2974	111	22	7	81	9	12993	185	90	3	473	7	6.29	2.59
9	40.0	BKM 072311-01	low marsh	E	4-May-12	9	Soil	<LOD	3122	1181	322	4101	220	5380	183	3115	122	<LOD	20	93	10	8118	132	74	3	468	7	6.66	1.98
10	45.0	BKM 072311-01	high marsh	C	4-May-12	10	Soil	<LOD	2985	945	290	2524	173	9740	243	3186	113	<LOD	15	65	8	4148	68	101	3	572	8	5.57	1.64
11	50.0	BKM 072311-01	high marsh	C	4-May-12	11	Soil	4707	1095	<LOD	849	2516	174	8319	222	2361	100	29	6	64	8	4426	72	99	3	407	6	5.80	1.76
12	55.0	BKM 072311-01	high marsh	C	4-May-12	12	Soil	3183	1016	<LOD	823	2708	178	9806	245	3196	114	<LOD	16	101	9	4134	68	105	3	625	9	5.11	1.53
13	60.0	BKM 072311-01	high marsh	C	4-May-12	13	Soil	<LOD	2704	<LOD	894	2412	176	8499	229	3626	123	<LOD	16	77	8	3779	64	108	3	809	11	4.48	1.57
14	65.0	BKM 072311-01	high marsh	C	4-May-12	14	Soil	<LOD	2364	<LOD	766	1354	144	6755	196	1922	89	38	6	54	8	2566	46	86	3	493	7	3.90	1.90
15	70.0	BKM 072311-01	high marsh	C	4-May-12	15	Soil	<LOD	2490	<LOD	793	2559	169	7519	204	4204	129	<LOD	16	73	8	4829	76	101	3	735	10	5.72	1.89
16	75.0	BKM 072311-01	high marsh	C	4-May-12	16	Soil	3246	993	<LOD	807	2743	174	8397	217	3194	113	<LOD	17	96	9	6188	95	99	3	465	7	6.87	2.26
17	80.0	BKM 072311-01	high marsh	C	4-May-12	17	Soil	3721	989	<LOD	768	2566	167	6943	192	2687	102	<LOD	16	63	8	5498	85	98	3	489	7	5.49	2.14
18	85.0	BKM 072311-																											



ID	DEPTH	BORING_ID	DEP_ENV	Chemo-facies	Date	Reading	Mode	S	S +/-	Cl	Cl +/-	K	K +/-	Ca	Ca +/-	Ti	Ti +/-	Cr	Cr +/-	Mn	Mn +/-	Fe	Fe +/-	Sr	Sr +/-	Zr	Zr +/-	Ti/Zr	Fe/K
37	180.0	BKM 072311-01	bioturbated and laminated	C	4-May-12	37	Soil	<LOD	2186	1557	280	2547	162	6821	187	2053	86	<LOD	14	45	7	2140	37	82	3	376	6	5.46	0.84
38	185.0	BKM 072311-01	bioturbated and laminated	C	4-May-12	38	Soil	<LOD	2236	1312	270	2487	160	6405	180	1401	69	<LOD	13	28	6	1938	34	75	3	274	5	5.11	0.78
39	190.0	BKM 072311-01	bioturbated and laminated	C	4-May-12	39	Soil	<LOD	2682	2216	313	2883	176	8108	212	2160	90	<LOD	15	57	7	3413	56	94	3	389	6	5.55	1.18
40	195.0	BKM 072311-01	bioturbated and laminated	C	4-May-12	40	Soil	<LOD	2622	1760	288	3401	182	6237	179	1581	79	16	5	58	8	4631	72	60	2	226	4	7.00	1.36
41	200.0	BKM 072311-01	bioturbated and laminated	C	4-May-12	41	Soil	<LOD	2330	1533	268	2436	154	5478	162	1344	68	<LOD	13	28	6	2067	35	65	2	317	5	4.24	0.85
42	205.0	BKM 072311-01	bioturbated and laminated	C	4-May-12	42	Soil	<LOD	2498	1532	277	2272	156	6205	177	522	49	<LOD	13	39	7	2463	42	43	2	67	3	7.79	1.08
43	210.0	BKM 072311-01	bioturbated and laminated	C	4-May-12	43	Soil	4717	989	2035	270	4204	184	3354	124	1921	85	21	6	54	8	11200	152	61	2	92	3	20.88	2.66
44	215.0	BKM 072311-01	bioturbated and laminated	C	4-May-12	44	Soil	3795	972	1747	270	3333	172	5996	168	1545	79	20	6	60	8	10766	150	66	2	110	3	14.05	3.23
45	220.0	BKM 072311-01	bioturbated and laminated	C	4-May-12	45	Soil	<LOD	2557	1123	259	3282	175	4748	152	1081	67	16	5	36	7	6146	91	71	2	156	3	6.93	1.87
46	225.0	BKM 072311-01	bioturbated and laminated	C	4-May-12	46	Soil	4025	1050	2267	313	2932	176	5127	165	1577	81	27	6	25	7	7005	107	76	3	255	4	6.18	2.39
47	230.0	BKM 072311-01	bioturbated and laminated	C	4-May-12	47	Soil	<LOD	2757	1350	284	2417	162	4858	158	2927	105	<LOD	15	61	8	3849	62	61	2	520	7	5.63	1.59
48	235.0	BKM 072311-01	bioturbated and laminated	C	4-May-12	48	Soil	<LOD	2803	1304	291	2903	179	7248	202	1190	70	<LOD	14	28	7	3091	52	73	3	117	3	10.17	1.06
49	240.0	BKM 072311-01	bioturbated and laminated	C	4-May-12	49	Soil	<LOD	2710	1292	288	2923	177	7928	210	2465	96	<LOD	14	74	8	4168	67	76	3	358	5	6.89	1.43
50	245.0	BKM 072311-01	upper forebeach	B	4-May-12	50	Soil	<LOD	2404	1515	272	2403	157	9514	226	543	49	30	5	21	6	1612	30	69	2	104	3	5.22	0.67
51	250.0	BKM 072311-01	upper forebeach	B	4-May-12	51	Soil	<LOD	2262	1265	263	2548	160	11711	256	865	56	<LOD	12	27	6	1798	32	73	2	95	3	9.11	0.71
52	255.0	BKM 072311-01	upper forebeach	B	4-May-12	52	Soil	<LOD	2059	933	247	2688	160	7156	187	533	48	<LOD	12	25	6	1589	29	76	3	90	3	5.92	0.59
53	260.0	BKM 072311-01	upper forebeach	B	4-May-12	53	Soil	<LOD	1974	734	243	2523	157	3289	127	826	54	<LOD	12	31	6	1328	26	54	2	63	3	13.11	0.53
54	265.0	BKM 072311-01	upper forebeach	B	4-May-12	54	Soil	<LOD	2277	1220	264	2554	160	4385	147	331	40	<LOD	12	<LOD	17	1316	26	52	2	85	3	3.89	0.52
55	270.0	BKM 072311-01	upper forebeach	B	4-May-12	55	Soil	<LOD	2087	1095	250	2430	153	4178	141	739	55	18	5	24	6	1511	28	56	2	104	3	7.11	0.62
56	275.0	BKM 072311-01	upper forebeach	B	4-May-12	56	Soil	<LOD	2358	954	270	2951	176	6714	191	587	53	<LOD	14	36	7	1947	35	82	3	129	3	4.55	0.66
57	280.0	BKM 072311-01	upper forebeach	B	4-May-12	57	Soil	<LOD	2370	1289	274	3472	184	4734	155	841	56	15	5	<LOD	18	1935	35	68	2	67	3	12.55	0.56
58	285.0	BKM 072311-01	upper forebeach	B	4-May-12	58	Soil	<LOD	2298	855	252	3443	179	7950	203	1034	62	<LOD	13	46	7	2136	37	99	3	193	4	5.36	0.62
59	290.0	BKM 072311-01	upper forebeach	B	4-May-12	59	Soil	15710	1614	1088	303	3037	188	13729	307	1952	87	<LOD	15	66	8	2234	41	75	3	113	3	17.27	0.74
61	295.0	BKM 072311-01	upper forebeach	B	4-May-12	61	Soil	<LOD	2584	1303	282	2707	171	7536	202	691	54	<LOD	13	20	6	1702	32	85	3	128	3	5.40	0.63
62	300.0	BKM 072311-01	upper forebeach	B	4-May-12	62	Soil	<LOD	2706	1324	273	3752	189	12177	268	544	51	<LOD	12	<LOD	17	1910	34	83	3	67	3	8.12	0.51
63	305.0	BKM 072311-01	upper forebeach	B	4-May-12	63	Soil	<LOD	2497	1025	263	2686	166	8030	206	798	53	<LOD	12	18	6	1811	33	69	3	159	4	5.02	0.67
64	310.0	BKM 072311-01	upper forebeach	B	4-May-12	64	Soil	<LOD	2599	2464	307	3223	178	8240	210	603	50	<LOD	14	22	6	1813	33	85	3	150	3	4.02	0.56
65	315.0	BKM 072311-01	upper forebeach	B	4-May-12	65	Soil	<LOD	2404	2198	306	2576	166	8592	217	1218	69	15	5	48	7	2070	37	101	3	239	4	5.10	0.80
66	320.0	BKM 072311-01	lower forebeach	B	4-May-12	66	Soil	<LOD	2778	3044	336	3847	197	9160	230	1104	67	18	5	92	8	2255	40	94	3	167	4	6.61	0.59
67	325.0	BKM 072311-01	lower forebeach	B	4-May-12	67	Soil	<LOD	2821	2037	300	3570	187	10777	250	1378	71	<LOD	14	37	7	2256	39	107	3	154	3	8.95	0.63
68	330.0	BKM 072311-01	lower forebeach	B	4-May-12	68	Soil	<LOD	2676	2460	309	3599	187	6862	190	549	51	<LOD	13	24	6	1736	32	75	3	122	3	4.50	0.48
69	335.0	BKM 072311-01	lower forebeach	B	4-May-12	69	Soil	<LOD	2516	2813	322	3474	185	7249	197	1007	63	<LOD	13	29	6	1762	32	70	2	169	4	5.96	0.51
70	340.0	BKM 072311-01	lower forebeach	B	4-May-12	70	Soil	<LOD	2328	1480	266	3121	170	7146	188	706	53	<LOD	13	32	6	1705	30	76	3	146	3	4.84	0.55
71	345.0	BKM 072311-01	lower forebeach	B	4-May-12	71	Soil	<LOD	2535	2155	304	2702	169	5876	175	605	51	<LOD	13	<LOD	18	1538	29	65	2	120	3	5.04	0.57
72	350.0	BKM 072311-01	lower forebeach	B	4-May-12	72	Soil	<LOD	2681	2685	308	2543	160	5309	162	763	54	<LOD	13	25	6	1677	31	64	2	141	3	5.41	0.66
73	355.0	BKM 072311-01	lower forebeach	B	4-May-12	73	Soil	<LOD	3050	2482	333	2558	176	17082	354	792	62	<LOD	14	<LOD	19	1648	32	106	3	163	4	4.86	0.64
74	360.0	BKM 072311-01	bioturbated and laminated	B	4-May-12	74	Soil	<LOD	2873	2491	311	3271	181	9169	225	386	44	<LOD	12	<LOD	17	1499	29	72	3	66	3	5.85	0.46
75	365.0	BKM 072311-01	bioturbated and laminated	B	4-May-12	75	Soil	4661	993	2935	305	2848	162	4629	147	490	44	<LOD	12	19	6	1245	24	47	2	69	3	7.10	0.44
76	370.0	BKM 072311-01	bioturbated and laminated	C	4-May-12	76	Soil	<LOD	2770	2936	327	4939	215	8153	212	1367	76	20	5	42	7	3892	62	96	3	305	5	4.48	0.79
77	375.0	BKM 072311-01	bioturbated and laminated	C	4-May-12	77	Soil	<LOD	3022	3919	345	4581	204	8081	207	1243	69	<LOD	15	38	7	4964	76	91	3	224	4	5.55	1.08
78	380.0	BKM 072311-01	bioturbated and laminated	C	4-May-12	78	Soil	4402	1195	3215	368	5305	239	9610	248	1975	94	23	6	70	9	7027	112	110	3	318	5	6.21	1.32
79	385.0	BKM 072311-01	bioturbated and laminated	C	4-May-12	79	Soil	<LOD	3048	2993	349	3939	205	9262	237	1840	88	17	5	49	8	3692	61	107	3	718	10	2.56	0.94
80	390.0	BKM 072311-01	bioturbated and laminated	C	4-May-12	80	Soil	3453	1052	3219	335	5189	219	10530	246	2228	93	<LOD	16	78	8	5133	79	123	3	537	7	4.15	0.99
81	395.0	BKM 072311-01	bioturbated and laminated	C	4-May-12	81	Soil	<LOD	3129	2744	335	4836	220	10141	247	1591	82	26	6	82	8	4649	74	111	3	325	5	4.90	0.96
82	400.0	BKM 072311-01	bioturbated and laminated	C	4-May-12	82	Soil	4730	1130	3762	353	4210	202	8799	223	2042	91	18	6	63	8	5312	82	102	3	470	7	4.34	1.26
83	405.0	BKM 072311-01	bioturbated and laminated	C	4-May-12	83	Soil	4917	1163	2897	348	4608	219	8324	223	1915	90	<LOD	17	57	8	5462	87	92	3	354	6	5.41	1.19
84	410.0	BKM 072311-01	bioturbated and laminated	C	4-May-12	84	Soil	3983	1079	2415	313	4952	215	14097	298	1499	78	<LOD	15	66	8	4798	74	107	3	300	5	5.00	0.97
85	415.0	BKM 072311-01	bioturbated and laminated	C	4-May-12	85	Soil	<LOD	2553	2537	297	3563	179	6418	178	1200	65	15	5	37	7	3292	52	74	3	190	4	6.32	0.92
86																													

ID	DEPTH	BORING_ID	DEP_ENV	Chemo-facies	Date	Reading	Mode	S	S +/-	Cl	Cl +/-	K	K +/-	Ca	Ca +/-	Ti	Ti +/-	Cr	Cr +/-	Mn	Mn +/-	Fe	Fe +/-	Sr	Sr +/-	Zr	Zr +/-	Ti/Zr	Fe/K
17	70.0	BKM 012112-01	upper forebeach	B	11-Mar-12	15	Soil	<LOD	2539	1427	274	3576	184	14100	293	455	47	<LOD	13	27	6	1619	30	74	3	88	3	5.17	0.45
18	75.0	BKM 012112-01	upper forebeach	B	11-Mar-12	16	Soil	<LOD	1551	<LOD	666	2068	139	2109	100	180	34	<LOD	12	<LOD	15	1066	21	42	2	41	2	4.39	0.52
19	80.0	BKM 012112-01	upper forebeach	A	11-Mar-12	17	Soil	<LOD	1838	938	246	1348	127	3256	124	1193	64	<LOD	13	24	6	1427	27	40	2	184	4	6.48	1.06
20	85.0	BKM 012112-01	upper forebeach	A	11-Mar-12	18	Soil	<LOD	1742	<LOD	698	1462	132	3406	128	1718	76	<LOD	14	26	6	1626	30	46	2	192	4	8.95	1.11
21	90.0	BKM 012112-01	upper forebeach	A	11-Mar-12	19	Soil	<LOD	2298	<LOD	740	1779	140	5404	161	2799	99	<LOD	14	47	7	2269	38	68	2	355	5	7.88	1.28
22	95.0	BKM 012112-01	upper forebeach	A	11-Mar-12	20	Soil	<LOD	2458	<LOD	734	2552	162	8338	210	2243	90	<LOD	15	52	7	2767	46	95	3	334	5	6.72	1.08
23	100.0	BKM 012112-01	upper forebeach	B	11-Mar-12	21	Soil	<LOD	1987	769	242	2949	165	4243	142	832	55	<LOD	12	18	6	1719	31	73	2	93	3	8.95	0.58
3	102.5	BKM 012112-01	upper forebeach	B	12-Mar-12	3	Soil	<LOD	1927	1058	243	3012	163	5143	154	660	50	<LOD	12	<LOD	17	1830	32	84	3	88	3	7.50	0.61
4	105.0	BKM 012112-01	upper forebeach	B	12-Mar-12	4	Soil	<LOD	2380	859	249	3261	174	10820	243	584	51	<LOD	13	25	6	2269	38	90	3	52	2	11.23	0.70
5	110.0	BKM 012112-01	upper forebeach	B	12-Mar-12	5	Soil	<LOD	2044	<LOD	674	4701	197	3484	129	564	47	<LOD	11	28	6	1964	34	72	2	40	2	14.10	0.42
6	115.0	BKM 012112-01	upper forebeach	B	12-Mar-12	6	Soil	<LOD	2274	1085	249	4827	200	5895	168	577	49	<LOD	12	<LOD	17	2119	36	82	3	47	2	12.28	0.44
7	120.0	BKM 012112-01	upper forebeach	A	12-Mar-12	7	Soil	<LOD	2374	<LOD	738	3517	184	5777	172	920	60	<LOD	13	20	6	1909	34	77	3	100	3	9.20	0.54
8	125.0	BKM 012112-01	upper forebeach	A	12-Mar-12	8	Soil	<LOD	2335	1099	275	3808	193	6858	192	1491	73	20	5	26	6	2305	40	87	3	134	3	11.13	0.61
9	130.0	BKM 012112-01	upper forebeach	A	12-Mar-12	9	Soil	<LOD	1990	<LOD	707	3087	169	5453	162	1067	60	<LOD	12	39	6	2003	35	73	2	136	3	7.85	0.65
10	135.0	BKM 012112-01	upper forebeach	A	12-Mar-12	10	Soil	<LOD	2386	1026	252	4490	197	7913	200	784	58	<LOD	13	25	6	2586	42	88	3	120	3	6.53	0.58
11	140.0	BKM 012112-01	upper forebeach	A	12-Mar-12	11	Soil	<LOD	2545	<LOD	751	4342	197	8576	212	2462	90	<LOD	14	47	7	2970	48	88	3	430	6	5.73	0.68
12	145.0	BKM 012112-01	upper forebeach	A	12-Mar-12	12	Soil	<LOD	2253	<LOD	724	3868	186	4626	150	578	50	<LOD	13	30	6	2223	38	77	3	107	3	5.40	0.57
13	150.0	BKM 012112-01	bioturbated and laminated	B	12-Mar-12	13	Soil	<LOD	2494	2790	291	3798	177	5203	154	998	61	<LOD	15	32	7	6016	86	68	2	122	3	8.18	1.58
14	155.0	BKM 012112-01	bioturbated and laminated	B	12-Mar-12	14	Soil	<LOD	4942	<LOD	1785	3560	329	3916	218	794	91	<LOD	21	42	11	1886	53	62	3	105	4	7.56	0.53
15	160.0	BKM 012112-01	bioturbated and laminated	B	12-Mar-12	15	Soil	<LOD	1976	916	234	3587	172	5222	153	852	55	<LOD	12	<LOD	17	2070	34	76	3	139	3	6.13	0.58
16	165.0	BKM 012112-01	bioturbated and laminated	B	12-Mar-12	16	Soil	<LOD	2067	<LOD	702	3539	179	4651	151	739	57	<LOD	13	20	6	2213	38	63	2	129	3	5.73	0.63
17	170.0	BKM 012112-01	bioturbated and laminated	B	12-Mar-12	17	Soil	<LOD	2346	1200	246	3081	163	3873	133	640	49	<LOD	12	<LOD	17	2087	35	62	2	132	3	4.85	0.68
18	175.0	BKM 012112-01	bioturbated and laminated	B	12-Mar-12	18	Soil	2987	877	1676	266	3324	170	3851	134	919	60	<LOD	14	19	6	3449	53	56	2	77	3	11.94	1.04
19	180.0	BKM 012112-01	bioturbated and laminated	B	12-Mar-12	19	Soil	<LOD	2041	1498	250	3474	169	4177	136	669	50	<LOD	13	19	6	2551	41	66	2	114	3	5.87	0.73
20	185.0	BKM 012112-01	bioturbated and laminated	B	12-Mar-12	20	Soil	<LOD	1873	924	235	2821	157	3136	120	389	42	<LOD	12	<LOD	16	1570	28	51	2	77	3	5.05	0.56
21	190.0	BKM 012112-01	bioturbated and laminated	B	12-Mar-12	21	Soil	<LOD	2317	1353	251	3180	165	4278	140	451	46	<LOD	12	<LOD	17	2752	44	58	2	51	2	8.84	0.87
22	195.0	BKM 012112-01	bioturbated and laminated	B	12-Mar-12	22	Soil	<LOD	2674	1902	331	3272	198	4412	161	1002	69	<LOD	16	34	8	4204	72	52	2	58	3	17.28	1.28
23	200.0	BKM 012112-01	bioturbated and laminated	B	12-Mar-12	23	Soil	<LOD	1702	<LOD	699	2516	154	3178	123	568	47	<LOD	12	<LOD	16	1361	26	46	2	101	3	5.62	0.54
24	205.0	BKM 012112-01	bioturbated and laminated	B	12-Mar-12	24	Soil	<LOD	2284	1370	248	3152	163	3336	122	640	49	<LOD	12	<LOD	16	2321	38	59	2	88	3	7.27	0.74
25	210.0	BKM 012112-01	bioturbated and laminated	B	12-Mar-12	25	Soil	<LOD	2034	1491	246	2766	152	2874	113	726	50	<LOD	12	19	6	2303	37	50	2	62	2	11.71	0.83
26	215.0	BKM 012112-01	bioturbated and laminated	B	12-Mar-12	26	Soil	<LOD	1891	730	232	2588	153	2564	111	538	46	<LOD	12	<LOD	16	1662	29	44	2	101	3	5.33	0.64
27	220.0	BKM 012112-01	bioturbated and laminated	B	12-Mar-12	27	Soil	<LOD	1901	1059	237	2510	149	1931	97	375	41	<LOD	12	<LOD	16	1276	24	43	2	127	3	2.95	0.51
28	225.0	BKM 012112-01	bioturbated and laminated	B	12-Mar-12	28	Soil	<LOD	2151	<LOD	722	2211	152	1601	95	178	34	<LOD	12	<LOD	16	1233	25	33	2	54	2	3.30	0.56
29	230.0	BKM 012112-01	bioturbated and laminated	B	12-Mar-12	29	Soil	<LOD	2175	1273	247	2986	160	2782	114	777	53	<LOD	13	<LOD	17	2471	40	48	2	89	3	8.73	0.83
30	235.0	BKM 012112-01	tidal creek	C	12-Mar-12	30	Soil	2764	895	3302	302	3533	170	3859	131	1177	68	<LOD	15	34	7	6726	95	51	2	54	2	21.80	1.90
31	240.0	BKM 012112-01	tidal creek	C	12-Mar-12	31	Soil	<LOD	2297	1149	240	2047	138	2301	104	558	44	<LOD	12	<LOD	17	2044	34	34	2	76	2	7.34	1.00
32	245.0	BKM 012112-01	tidal creek	C	12-Mar-12	32	Soil	<LOD	2158	1448	254	2678	155	1956	99	456	45	<LOD	13	<LOD	17	2844	45	44	2	42	2	10.86	1.06
33	250.0	BKM 012112-01	tidal creek	C	12-Mar-12	33	Soil	<LOD	2150	1504	256	1973	139	1780	95	316	38	<LOD	13	<LOD	17	1829	32	32	2	34	2	9.29	0.93
34	255.0	BKM 012112-01	tidal creek	C	12-Mar-12	34	Soil	<LOD	2452	2446	290	2871	162	2009	101	662	55	<LOD	14	<LOD	19	5224	78	40	2	35	2	18.91	1.82
35	260.0	BKM 012112-01	tidal creek	C	12-Mar-12	35	Soil	<LOD	1962	955	228	2078	137	1234	82	283	36	<LOD	12	<LOD	15	1789	31	41	2	21	2	13.48	0.86
36	265.0	BKM 012112-01	tidal creek	C	12-Mar-12	36	Soil	<LOD	1598	747	226	2381	147	1520	90	236	35	<LOD	12	<LOD	16	1473	27	35	2	43	2	5.49	0.62
37	270.0	BKM 012112-01	tidal creek	C	12-Mar-12	37	Soil	<LOD	1821	1033	235	2910	157	1401	87	231	35	<LOD	11	<LOD	15	1224	23	41	2	30	2	7.70	0.42
38	275.0	BKM 012112-01	tidal creek	C	12-Mar-12	38	Soil	3485	982	3943	318	4337	186	4799	146	1474	79	19	6	62	8	13318	179	60	2	56	2	26.32	3.07
39	280.0	BKM 012112-01	tidal creek	C	12-Mar-12	39	Soil	3938	982	4202	316	4023	176	4180	134	1536	77	<LOD	16	66	8	13014	172	61	2	49	2	31.35	3.23
40	285.0	BKM 012112-01	tidal creek	C	12-Mar-12	40	Soil	<LOD	1942	870	229	2259	143	876	76	111	30	<LOD	12	<LOD	14	1036	21	23	2	42	2	2.64	0.46
41	290.0	BKM 012112-01	tidal creek	C	12-Mar-12	41	Soil	<LOD	2510	3394	302	3204	163	4666	144	1269	71	<LOD	16	71	8	10319	140	51	2	50	2	25.38	3.22
42	295.0	BKM 012112-01	tidal creek	C	12-Mar-12	42	Soil	<LOD	1867	<LOD	707	2990	166	1209	86	120	30	<LOD	12	<LOD	15	937	20	30	2	33	2	3.64	0.31
43	300.0	BKM 012112-01	tidal creek	C	12-Mar-12	43	Soil	<LOD	2937	3083	321	4574	203	9066	220	1855	87	19	6	89	9	8624	125	103	3	448	6		

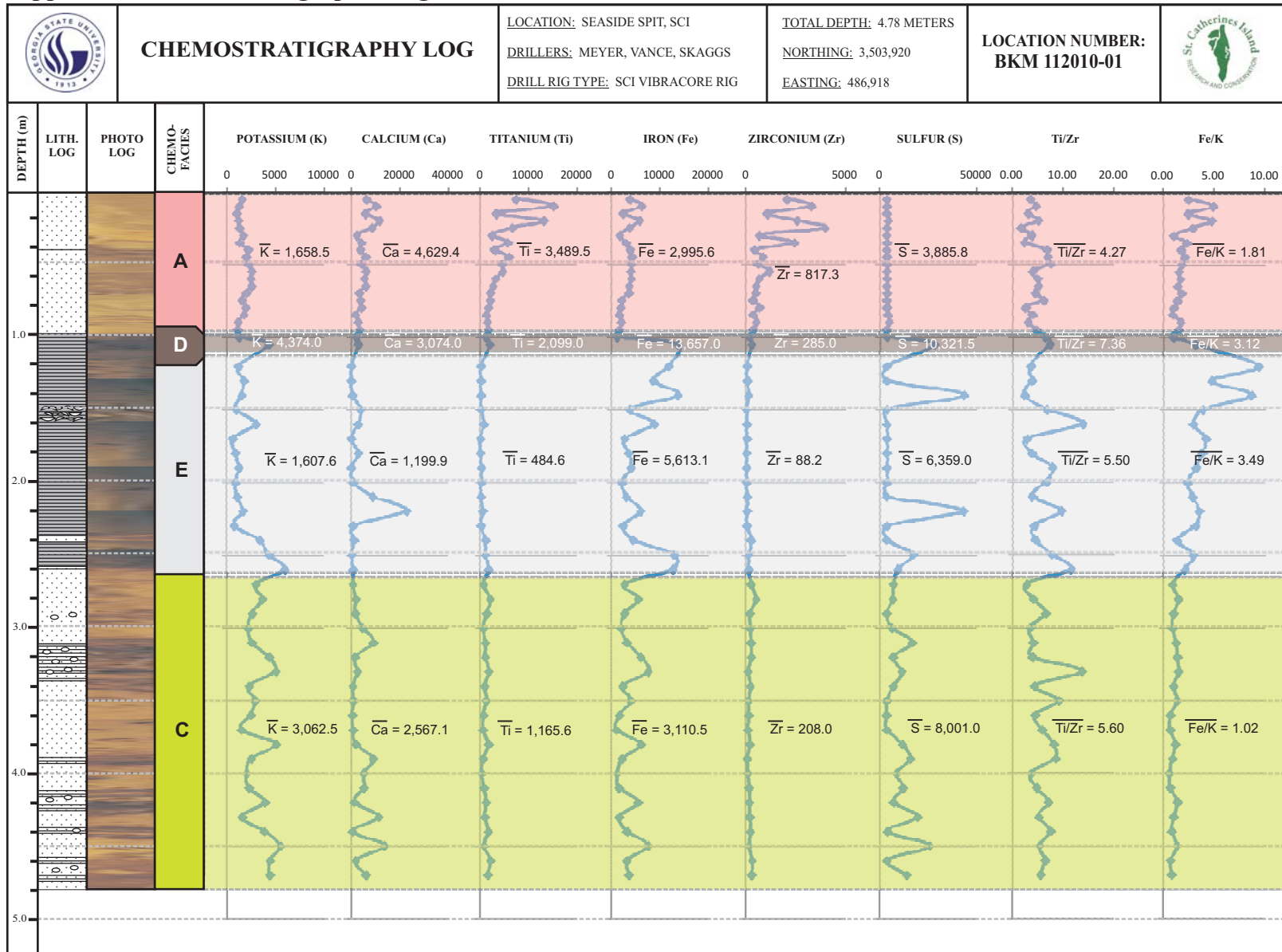
ID	DEPTH	BORING_ID	DEP_ENV	Chemo-facies	Date	Reading	Mode	S	S +/-	Cl	Cl +/-	K	K +/-	Ca	Ca +/-	Ti	Ti +/-	Cr	Cr +/-	Mn	Mn +/-	Fe	Fe +/-	Sr	Sr +/-	Zr	Zr +/-	Ti/Zr	Fe/K
65	400.0	BKM 012112-01	bioturbated and laminated	C	12-Mar-12	65	Soil	3420	895	<LOD	735	4072	191	2126	107	1217	68	<LOD	14	24	6	2738	45	160	4	296	5	4.11	0.67
66	405.0	BKM 012112-01	bioturbated and laminated	C	12-Mar-12	66	Soil	<LOD	2231	960	243	3730	178	1545	93	787	55	<LOD	13	25	6	2732	44	175	4	220	4	3.58	0.73
67	410.0	BKM 012112-01	bioturbated and laminated	C	12-Mar-12	67	Soil	4290	903	1053	241	3834	177	1524	92	942	59	<LOD	14	28	6	3176	49	228	4	203	4	4.64	0.83
68	415.0	BKM 012112-01	bioturbated and laminated	C	12-Mar-12	68	Soil	5044	953	<LOD	691	3518	176	1419	91	1154	65	<LOD	14	20	6	2446	40	153	4	192	4	6.01	0.70
69	420.0	BKM 012112-01	bioturbated and laminated	C	12-Mar-12	69	Soil	2766	823	<LOD	697	3736	178	1731	97	1090	64	<LOD	13	31	6	2692	43	155	4	325	5	3.35	0.72
70	425.0	BKM 012112-01	bioturbated and laminated	C	12-Mar-12	70	Soil	2606	820	748	238	4001	184	1396	91	982	61	<LOD	13	36	6	2810	45	163	4	223	4	4.40	0.70
71	430.0	BKM 012112-01	bioturbated and laminated	C	12-Mar-12	71	Soil	3220	827	755	226	3509	168	1807	95	1279	65	<LOD	13	27	6	3238	49	179	4	339	5	3.77	0.92
72	435.0	BKM 012112-01	bioturbated and laminated	C	12-Mar-12	72	Soil	2916	837	<LOD	713	4003	185	1296	89	1048	64	<LOD	14	29	6	2587	42	136	3	218	4	4.81	0.65
73	440.0	BKM 012112-01	bioturbated and laminated	C	12-Mar-12	73	Soil	3842	881	<LOD	684	4098	186	1674	96	928	60	<LOD	13	33	6	2815	45	159	4	220	4	4.22	0.69
74	445.0	BKM 012112-01	bioturbated and laminated	C	12-Mar-12	74	Soil	4086	885	<LOD	676	4863	197	1771	97	1200	64	<LOD	13	<LOD	18	2866	45	134	3	168	3	7.14	0.59
75	450.0	BKM 012112-01	bioturbated and laminated	C	12-Mar-12	75	Soil	4117	955	<LOD	744	5284	219	1617	101	1041	65	<LOD	15	40	7	3447	56	131	3	162	4	6.43	0.65
76	455.0	BKM 012112-01	bioturbated and laminated	C	12-Mar-12	76	Soil	2478	824	729	241	4386	193	1807	100	1371	71	<LOD	14	41	7	3285	52	140	3	262	4	5.23	0.75
77	460.0	BKM 012112-01	bioturbated and laminated	C	12-Mar-12	77	Soil	3112	852	<LOD	691	4284	190	1843	100	1116	66	<LOD	15	40	7	3831	59	133	3	199	4	5.61	0.89
78	465.0	BKM 012112-01	bioturbated and laminated	C	12-Mar-12	78	Soil	<LOD	2468	1190	251	5261	207	1888	101	1503	74	<LOD	14	48	7	4130	62	136	3	178	4	8.44	0.79
79	470.0	BKM 012112-01	bioturbated and laminated	C	12-Mar-12	79	Soil	3118	871	<LOD	710	3841	188	1439	94	1164	68	16	5	<LOD	19	3203	52	123	3	112	3	10.39	0.83
2	5.0	BKM 012112-02	upper forebeach	B	14-Mar-12	2	Soil	6344	1070	2360	286	3422	172	6961	183	419	43	<LOD	11	34	6	1551	28	80	3	56	2	7.48	0.45
3	10.0	BKM 012112-02	upper forebeach	B	14-Mar-12	3	Soil	2820	927	1909	285	2467	159	10463	240	114	33	<LOD	12	<LOD	17	1174	23	56	2	42	2	2.71	0.48
4	15.0	BKM 012112-02	upper forebeach	B	14-Mar-12	4	Soil	<LOD	2069	1972	271	3469	173	4158	139	329	40	<LOD	12	33	6	1645	29	73	2	92	3	3.58	0.47
5	20.0	BKM 012112-02	upper forebeach	B	14-Mar-12	5	Soil	<LOD	2086	983	246	3354	173	3220	125	427	44	<LOD	11	<LOD	17	1497	28	64	2	57	2	7.49	0.45
6	25.0	BKM 012112-02	upper forebeach	B	14-Mar-12	6	Soil	<LOD	2583	1170	288	4658	218	3658	144	377	48	<LOD	14	<LOD	18	1985	37	80	3	71	3	5.31	0.43
7	30.0	BKM 012112-02	upper forebeach	B	14-Mar-12	7	Soil	<LOD	1992	1136	259	1876	144	2387	111	324	39	<LOD	12	<LOD	16	1069	22	36	2	42	2	7.71	0.57
8	35.0	BKM 012112-02	upper forebeach	B	14-Mar-12	8	Soil	<LOD	1953	<LOD	714	3510	177	3427	129	384	41	<LOD	12	<LOD	17	1672	30	65	2	38	2	10.11	0.48
9	40.0	BKM 012112-02	upper forebeach	B	14-Mar-12	9	Soil	3440	921	1054	262	2227	154	5020	159	242	38	<LOD	12	<LOD	16	1071	22	48	2	47	2	5.15	0.48
10	45.0	BKM 012112-02	upper forebeach	B	14-Mar-12	10	Soil	<LOD	2105	871	242	3503	176	3726	133	285	39	<LOD	13	<LOD	17	1679	30	65	2	31	2	9.19	0.48
11	50.0	BKM 012112-02	upper forebeach	B	14-Mar-12	11	Soil	11382	1370	1389	283	3776	192	16214	327	190	38	<LOD	12	<LOD	17	1526	29	81	3	27	2	7.04	0.40
12	55.0	BKM 012112-02	upper forebeach	B	14-Mar-12	12	Soil	18764	1704	1906	315	4759	218	17490	355	216	43	<LOD	13	<LOD	18	2421	42	102	3	38	2	5.68	0.51
13	60.0	BKM 012112-02	upper forebeach	B	14-Mar-12	13	Soil	<LOD	2884	1059	280	5319	227	12005	274	683	57	<LOD	13	27	7	2505	43	127	3	77	3	8.87	0.47
14	65.0	BKM 012112-02	upper forebeach	B	14-Mar-12	14	Soil	<LOD	2505	1354	268	4691	203	6787	185	897	58	<LOD	13	29	6	2300	39	96	3	97	3	9.25	0.49
15	70.0	BKM 012112-02	upper forebeach	B	14-Mar-12	15	Soil	<LOD	2242	1471	277	3235	178	3494	133	342	40	<LOD	12	<LOD	17	1533	29	59	2	71	3	4.82	0.47
16	75.0	BKM 012112-02	upper forebeach	B	14-Mar-12	16	Soil	<LOD	2253	1200	286	4399	211	5510	174	202	38	<LOD	13	<LOD	18	1880	35	85	3	34	2	5.94	0.43
17	80.0	BKM 012112-02	upper forebeach	B	14-Mar-12	17	Soil	<LOD	2237	1328	267	4968	209	10189	236	428	46	<LOD	12	<LOD	17	1979	34	85	3	35	2	12.23	0.40
18	85.0	BKM 012112-02	upper forebeach	B	14-Mar-12	18	Soil	8924	1386	1432	320	4199	219	17585	373	193	45	<LOD	15	<LOD	19	1994	38	129	3	33	2	5.85	0.47
19	90.0	BKM 012112-02	upper forebeach	B	14-Mar-12	19	Soil	18420	2105	2773	417	3684	240	84374	1396	199	58	<LOD	15	<LOD	20	2254	42	186	4	45	3	4.42	0.61
20	92.5	BKM 012112-02	peat	D	14-Mar-12	20	Soil	29707	1862	8386	403	1716	129	18972	328	405	47	<LOD	13	37	7	8647	113	74	2	59	2	6.86	0.54
21	94.5	BKM 012112-02	upper forebeach	B	14-Mar-12	21	Soil	28356	1889	2196	299	3156	172	20887	378	391	43	<LOD	11	20	6	2066	35	95	3	54	2	7.24	0.65
22	95.5	BKM 012112-02	peat	D	14-Mar-12	22	Soil	37415	2083	7511	397	2173	143	25304	413	473	50	<LOD	13	42	7	8279	110	76	2	40	2	11.83	3.81
23	100.0	BKM 012112-02	upper forebeach	B	14-Mar-12	23	Soil	18220	1647	1620	299	4472	208	14777	311	451	49	<LOD	13	<LOD	18	2008	36	84	3	62	3	7.27	0.45
24	105.0	BKM 012112-02	upper forebeach	B	14-Mar-12	24	Soil	24207	1814	1425	289	4140	198	17735	347	518	47	<LOD	12	24	6	1903	34	70	2	52	2	9.96	0.46
25	110.0	BKM 012112-02	upper forebeach	B	14-Mar-12	25	Soil	<LOD	2476	1595	264	3856	181	7782	195	967	59	<LOD	13	32	6	2235	37	83	3	149	3	6.49	0.58
26	115.0	BKM 012112-02	upper forebeach	B	14-Mar-12	26	Soil	<LOD	2430	2366	299	4096	193	6900	188	751	57	<LOD	14	<LOD	18	2319	39	82	3	165	4	4.55	0.57
27	120.0	BKM 012112-02	upper forebeach	B	14-Mar-12	27	Soil	10713	1277	1783	279	2995	167	9433	222	662	52	<LOD	12	<LOD	17	1631	29	65	2	109	3	6.07	0.54
28	125.0	BKM 012112-02	upper forebeach	B	14-Mar-12	28	Soil	11581	1330	2038	288	2893	166	12355	264	608	48	<LOD	11	23	6	1971	34	72	2	91	3	6.68	0.68
29	130.0	BKM 012112-02	upper forebeach	B	14-Mar-12	29	Soil	<LOD	2418	2950	304	3048	166	4860	151	751	52	<LOD	12	24	6	2118	36	63	2	108	3	6.95	0.69
30	135.0	BKM 012112-02	upper forebeach	B	14-Mar-12	30	Soil	<LOD	2341	1897	284	2604	161	4936	155	949	59	<LOD	13	20	6	2014	35	68	2	121	3	7.84	0.77
31	140.0	BKM 012112-02	upper forebeach	B	14-Mar-12	31	Soil	<LOD	2281	1696	272	3716	181	2849	119	684	53	<LOD	12	18	6	1682	30	63	2	164	3	4.17	0.45
32	145.0	BKM 012112-02	upper forebeach	B	14-Mar-12	32	Soil	<LOD	2354	2211	281	2863	161	3240	123	478	45	<LOD	12	22	6	1698	30	57	2	82	3	5.83	0.59
33	150.0	BKM 012112-02	upper forebeach	B	14-Mar-12	33	Soil	<LOD	2503	1493	274	2445	158	2766	119	716	53	<LOD	12	<LOD	17	1426	27	47	2	118	3	6.07	0.58
34	155.0	BKM 012112-02	upper forebeach	B	14-Mar-12	34	Soil	8168	1162	2734	298	2524	154	7410	189	659	50	<LOD	12	<LOD	17	2088	35	56	2	124			

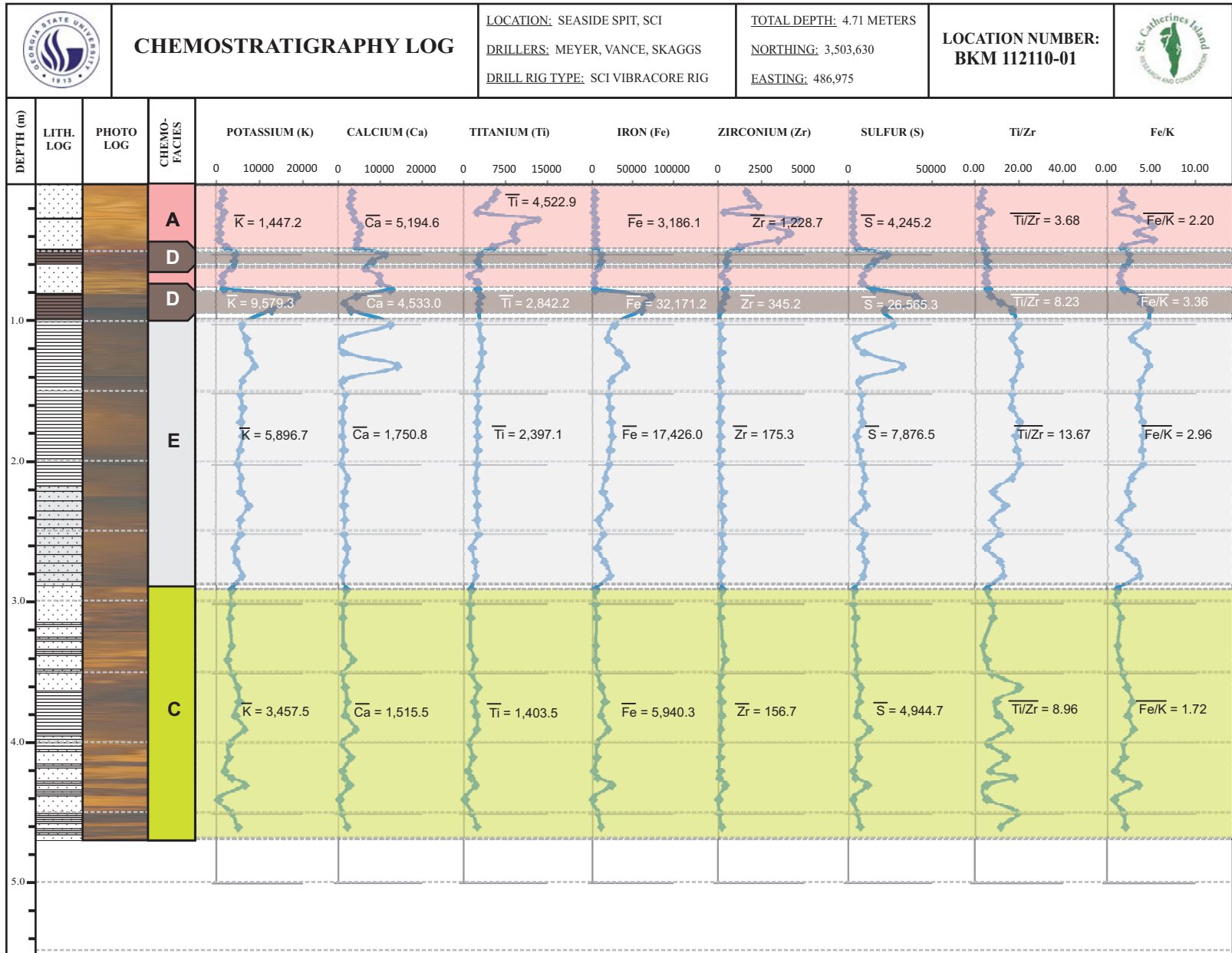
ID	DEPTH	BORING_ID	DEP_ENV	Chemo-facies	Date	Reading	Mode	S	S +/-	Cl	Cl +/-	K	K +/-	Ca	Ca +/-	Ti	Ti +/-	Cr	Cr +/-	Mn	Mn +/-	Fe	Fe +/-	Sr	Sr +/-	Zr	Zr +/-	Ti/Zr	Fe/K
17	247.5	BKM 012112-02	bioturbated and laminated	B	21-Mar-12	17	Soil	<LOD	2283	2213	274	2728	155	3694	129	563	48	<LOD	13	<LOD	17	2548	41	49	2	71	2	7.93	0.93
18	250.0	BKM 012112-02	bioturbated and laminated	B	21-Mar-12	18	Soil	<LOD	2363	1011	249	2433	154	1809	98	211	36	<LOD	12	<LOD	16	1253	24	40	2	42	2	5.02	0.52
19	255.0	BKM 012112-02	bioturbated and laminated	B	21-Mar-12	19	Soil	<LOD	1911	1494	253	3232	166	2143	103	301	38	<LOD	12	<LOD	16	1853	32	45	2	62	2	4.85	0.57
20	260.0	BKM 012112-02	bioturbated and laminated	B	21-Mar-12	20	Soil	<LOD	2228	1077	246	2854	161	2198	105	288	37	<LOD	11	<LOD	16	1410	26	46	2	67	2	4.30	0.49
21	265.0	BKM 012112-02	bioturbated and laminated	B	21-Mar-12	21	Soil	<LOD	2588	3039	294	3389	167	3841	131	825	58	<LOD	14	39	7	5236	75	65	2	72	2	11.46	1.54
22	270.0	BKM 012112-02	bioturbated and laminated	B	21-Mar-12	22	Soil	<LOD	2389	2068	260	2723	150	3488	123	700	49	<LOD	12	21	6	2960	45	55	2	76	3	9.21	1.09
23	275.0	BKM 012112-02	tidal creek	A	21-Mar-12	23	Soil	4118	1041	3941	335	4320	193	6412	177	2348	93	21	6	65	8	7987	114	94	3	303	5	7.75	1.85
24	280.0	BKM 012112-02	tidal creek	A	21-Mar-12	24	Soil	3542	1018	4041	337	5047	207	6558	179	1953	86	<LOD	16	79	8	7895	113	96	3	304	5	6.42	1.56
25	285.0	BKM 012112-02	tidal creek	A	21-Mar-12	25	Soil	<LOD	2989	4691	346	4485	193	7385	189	1979	87	<LOD	16	74	8	9217	129	88	3	191	4	10.36	2.06
26	290.0	BKM 012112-02	tidal creek	A	21-Mar-12	26	Soil	<LOD	3121	3335	353	4569	215	7314	204	1926	90	<LOD	16	76	8	6429	100	97	3	434	6	4.44	1.41
27	295.0	BKM 012112-02	tidal creek	A	21-Mar-12	27	Soil	3602	1036	4593	345	4736	198	8501	205	2120	90	<LOD	17	91	8	9443	131	91	3	281	5	7.54	1.99
28	300.0	BKM 012112-02	tidal creek	A	21-Mar-12	28	Soil	4443	1031	3812	326	4407	193	6104	170	1194	67	<LOD	15	44	7	5770	84	92	3	216	4	5.53	1.31
29	305.0	BKM 012112-02	tidal creek	A	21-Mar-12	29	Soil	6347	1167	5175	358	4742	198	8761	208	2167	89	22	6	103	9	10030	139	96	3	357	5	6.07	2.12
30	310.0	BKM 012112-02	tidal creek	A	21-Mar-12	30	Soil	3421	1072	5312	380	5186	215	6140	177	1956	90	<LOD	17	97	9	9068	132	93	3	202	4	9.68	1.75
31	315.0	BKM 012112-02	tidal creek	A	21-Mar-12	31	Soil	<LOD	5155	7048	506	4128	246	85131	1386	1925	103	<LOD	19	125	10	8271	131	280	5	181	4	10.64	2.00
35	320.0	BKM 012112-02	low marsh Holocene	E	21-Mar-12	35	Soil	7066	1468	4760	417	5966	257	28784	539	2088	101	23	7	88	10	10441	161	126	3	175	4	11.93	1.75
36	325.0	BKM 012112-02	low marsh Holocene	E	21-Mar-12	36	Soil	6214	1186	5770	377	5336	211	2697	117	2319	96	27	7	138	10	15983	220	55	2	119	3	19.49	3.00
37	330.0	BKM 012112-02	low marsh Holocene	E	21-Mar-12	37	Soil	5243	1083	5458	345	5370	200	2206	103	2368	95	28	7	92	9	18344	239	51	2	85	2	27.86	3.42
38	335.0	BKM 012112-02	low marsh Holocene	E	21-Mar-12	38	Soil	5653	1090	4728	330	5475	202	1962	99	2625	100	<LOD	19	102	10	19513	253	51	2	82	2	32.01	3.56
39	340.0	BKM 012112-02	low marsh Holocene	E	21-Mar-12	39	Soil	7788	1207	5198	347	5791	210	1650	95	2687	101	34	7	121	10	21131	277	53	2	97	3	27.70	3.65
40	345.0	BKM 012112-02	low marsh Holocene	E	21-Mar-12	40	Soil	5878	1108	3615	310	5884	212	3167	122	2551	101	21	7	155	11	19889	261	58	2	107	3	23.84	3.18
41	350.0	BKM 012112-02	low marsh Holocene	E	21-Mar-12	41	Soil	6755	1187	4432	344	5778	218	2353	111	2700	105	26	7	110	10	18186	247	57	2	97	3	27.84	3.35
42	355.0	BKM 012112-02	low marsh Holocene	E	21-Mar-12	42	Soil	5217	1133	4184	338	6611	232	2683	117	3109	114	34	7	126	11	21844	295	54	2	105	3	29.61	3.30
43	360.0	BKM 012112-02	low marsh Holocene	E	21-Mar-12	43	Soil	49169	3072	6261	514	6008	283	20276	445	2425	139	<LOD	33	139	16	50995	813	53	2	111	3	21.85	8.49
44	365.0	BKM 012112-02	low marsh Holocene	E	21-Mar-12	44	Soil	6109	1252	3930	361	6598	249	2133	114	3255	125	24	8	102	11	22831	328	60	2	168	3	19.38	3.46
45	370.0	BKM 012112-02	low marsh Holocene	E	21-Mar-12	45	Soil	6799	1214	3911	335	6893	240	1784	103	3144	115	43	8	84	10	24200	329	57	2	137	3	22.95	3.51
46	375.0	BKM 012112-02	low marsh Holocene	E	21-Mar-12	46	Soil	7476	1283	4362	356	7134	249	1852	106	3373	123	46	8	124	11	26359	363	58	2	135	3	24.99	3.69
47	380.0	BKM 012112-02	low marsh Holocene	E	21-Mar-12	47	Soil	7337	1205	3942	329	6840	234	1859	102	3012	113	31	7	133	11	22234	298	63	2	144	3	20.92	3.25
48	385.0	BKM 012112-02	low marsh Holocene	E	21-Mar-12	48	Soil	13226	1605	4873	394	7362	267	1847	112	3427	130	36	9	171	13	30364	439	59	2	153	3	22.40	4.12
49	390.0	BKM 012112-02	low marsh Holocene	E	21-Mar-12	49	Soil	5630	1228	3826	352	7231	257	1656	105	3363	128	36	8	196	13	26184	369	71	2	223	4	15.08	3.62
50	395.0	BKM 012112-02	low marsh Holocene	E	21-Mar-12	50	Soil	6307	1162	3916	328	6440	228	2078	106	2706	108	39	8	163	11	22044	295	52	2	101	3	26.79	3.42
51	400.0	BKM 012112-02	low marsh Holocene	E	21-Mar-12	51	Soil	12591	1398	4613	343	5590	211	1776	99	2559	102	36	7	125	10	20461	273	50	2	91	3	28.12	3.66
52	405.0	BKM 012112-02	washover	A	21-Mar-12	52	Soil	4010	910	1572	260	5389	207	1607	95	1297	67	<LOD	14	35	6	3030	47	51	2	254	4	5.11	0.56
53	410.0	BKM 012112-02	washover	A	21-Mar-12	53	Soil	<LOD	2669	1826	300	3655	192	2348	116	1024	67	<LOD	15	32	7	2572	45	48	2	232	4	4.41	0.70
54	415.0	BKM 012112-02	washover	A	21-Mar-12	54	Soil	11398	1365	2549	314	4218	198	5279	165	1036	66	<LOD	16	<LOD	20	5454	83	33	2	202	4	5.13	1.29
55	420.0	BKM 012112-02	washover	A	21-Mar-12	55	Soil	3536	971	2034	292	4097	193	5517	166	1417	74	<LOD	14	44	7	3964	62	52	2	231	4	6.13	0.97
56	425.0	BKM 012112-02	washover	A	21-Mar-12	56	Soil	<LOD	2568	1575	279	5768	225	4730	154	2008	87	<LOD	15	51	7	3973	62	79	3	344	5	5.84	0.69
57	430.0	BKM 012112-02	washover	A	21-Mar-12	57	Soil	<LOD	2346	1015	260	5716	224	3579	136	1403	72	<LOD	14	74	7	3034	49	80	3	266	5	5.27	0.53
58	435.0	BKM 012112-02	washover	A	21-Mar-12	58	Soil	4086	933	1527	262	5994	219	3131	123	1941	81	<LOD	14	47	7	3675	56	71	2	296	5	6.56	0.61
59	440.0	BKM 012112-02	washover	A	21-Mar-12	59	Soil	4225	964	2076	282	4535	195	3342	127	1529	75	<LOD	14	39	7	3167	50	64	2	349	5	4.38	0.70
60	445.0	BKM 012112-02	washover	A	21-Mar-12	60	Soil	6522	1077	1194	261	3903	185	4445	146	1013	63	<LOD	14	30	7	3921	60	59	2	259	4	3.91	1.00
61	450.0	BKM 012112-02	washover	A	21-Mar-12	61	Soil	<LOD	2563	2108	281	4358	192	3525	129	1338	70	<LOD	14	40	7	3912	60	70	2	226	4	5.92	0.90
62	455.0	BKM 012112-02	washover	A	21-Mar-12	62	Soil	5268	1008	1838	275	4719	199	2845	118	1101	65	<LOD	13	32	6	3602	56	64	2	149	3	7.39	0.76
63	460.0	BKM 012112-02	washover	A	21-Mar-12	63	Soil	6311	1102	1684	286	4195	197	3383	132	933	63	<LOD	14	31	7	3631	58	60	2	152	3	6.14	0.87
64	465.0	BKM 012112-02	washover	A	21-Mar-12	64	Soil	3249	968	1621	286	4004	194	6658	186	1397	75	<LOD	15	42	7	3989	63	77	3	173	4	8.08	1.00
65	470.0	BKM 012112-02	washover	A	21-Mar-12	65	Soil	37291	2684	1406	399	3377	240	1E+05	1639	520	71	<LOD	16	25	7	3751	65	306	6	139	4	3.74	1.11
66	475.0	BKM 012112-02	washover	A	21-Mar-12	66	Soil	7780	2011	2248	472	5169	306	90770	1666	909	89	<LOD	20	57	10	5926	109	281	6	98	4	9.28	1.15
67	480.0	BKM 012112-02	low marsh Pleistocene	E	21-Mar-12	67	Soil	9658	1495	3385	365	8476	291	13549	301	3549	132	31	8	171	13								

ID	DEPTH	BORING_ID	DEP_ENV	Chemo-facies	Date	Reading	Mode	S	S +/-	Cl	Cl +/-	K	K +/-	Ca	Ca +/-	Ti	Ti +/-	Cr	Cr +/-	Mn	Mn +/-	Fe	Fe +/-	Sr	Sr +/-	Zr	Zr +/-	Ti/Zr	Fe/K	
66	90.0	BKM031712-01	upper forebeach	B	18-May-12	66	Soil	<LOD	1812	899	232	1920	136	2816	113	645	48	<LOD	11	17	5	1268	24	50	2	95	3	6.79	0.66	
67	100.0	BKM031712-01	upper forebeach	B	18-May-12	67	Soil	<LOD	1869	<LOD	725	1939	144	5078	156	614	49	<LOD	13	<LOD	17	1109	23	37	2	104	3	5.90	0.57	
68	110.0	BKM031712-01	upper forebeach	B	18-May-12	68	Soil	<LOD	1791	<LOD	664	2021	140	2464	108	464	43	<LOD	11	<LOD	16	1070	21	41	2	59	2	7.86	0.53	
69	120.0	BKM031712-01	upper forebeach	B	18-May-12	69	Soil	<LOD	1921	<LOD	660	2410	152	2879	117	475	44	<LOD	11	<LOD	17	1238	24	44	2	84	3	5.65	0.51	
70	130.0	BKM031712-01	upper forebeach	B	18-May-12	70	Soil	<LOD	1770	<LOD	648	2588	148	3530	124	442	41	<LOD	12	<LOD	15	1237	23	57	2	81	3	5.46	0.48	
71	140.0	BKM031712-01	upper forebeach	B	18-May-12	71	Soil	<LOD	1880	<LOD	651	4472	192	3843	134	456	45	<LOD	12	<LOD	17	1826	32	63	2	53	2	8.60	0.41	
72	150.0	BKM031712-01	upper forebeach	B	18-May-12	72	Soil	<LOD	2120	985	240	4662	195	4741	148	1223	62	<LOD	12	32	6	2337	38	72	2	139	3	8.80	0.50	
73	160.0	BKM031712-01	upper forebeach	B	18-May-12	73	Soil	<LOD	2122	1222	262	3418	176	5869	169	2541	93	<LOD	13	48	7	2378	40	82	3	569	7	4.47	0.70	
2	170.0	BKM031712-01	upper forebeach	B	21-May-12	2	Soil	<LOD	1646	680	225	1962	137	2092	100	276	34	<LOD	11	<LOD	16	1009	21	39	2	80	3	3.45	0.51	
3	180.0	BKM031712-01	upper forebeach	B	21-May-12	3	Soil	<LOD	1594	<LOD	656	1566	128	4365	139	668	47	<LOD	11	<LOD	16	1362	25	57	2	73	2	9.15	0.87	
4	190.0	BKM031712-01	upper forebeach	B	21-May-12	4	Soil	<LOD	1980	910	246	2946	166	4512	147	382	42	<LOD	13	<LOD	17	1272	25	61	2	64	2	5.97	0.43	
5	200.0	BKM031712-01	upper forebeach	B	21-May-12	5	Soil	<LOD	1996	1039	240	2835	158	7584	190	757	53	<LOD	11	20	6	1882	32	68	2	125	3	6.06	0.66	
6	210.0	BKM031712-01	upper forebeach	B	21-May-12	6	Soil	<LOD	1945	<LOD	658	1941	136	4966	148	562	45	<LOD	11	<LOD	16	1529	27	62	2	168	3	3.35	0.79	
7	220.0	BKM031712-01	upper forebeach	B	21-May-12	7	Soil	<LOD	2058	817	236	4210	187	6132	169	623	52	<LOD	12	25	6	2119	35	92	3	111	3	5.61	0.50	
8	230.0	BKM031712-01	upper forebeach	B	21-May-12	8	Soil	<LOD	1777	<LOD	705	3735	181	3675	133	368	42	14	<LOD	17	1744	31	57	2	70	2	5.26	0.47		
9	240.0	BKM031712-01	upper forebeach	B	21-May-12	9	Soil	<LOD	2386	1153	254	4338	193	8688	210	1270	9	7	3430	53	111	3	389	6	3.26	0.79				
10	250.0	BKM031712-01	upper forebeach	B	21-May-12	10	Soil	<LOD	2892	3140	313	5264	209	15300	300	2934	105	<LOD	17	172	10	9853	136	136	3	693	8	4.23	1.87	
11	260.0	BKM031712-01	upper forebeach	B	21-May-12	11	Soil	<LOD	2804	1897	293	5929	229	13342	282	2676	101	<LOD	16	130	9	6113	90	134	3	911	11	2.94	1.03	
12	270.0	BKM031712-01	tidal creek	C	21-May-12	12	Soil	<LOD	3170	2038	331	5154	233	11087	269	2893	114	<LOD	19	117	10	7439	117	133	4	549	8	5.27	1.44	
13	280.0	BKM031712-01	tidal creek	C	21-May-12	13	Soil	<LOD	4531	1087	3726	331	5899	222	11011	243	2577	98	18	6	108	9	9009	126	126	3	632	8	4.08	1.53
14	290.0	BKM031712-01	tidal creek	C	21-May-12	14	Soil	<LOD	2964	2071	290	6388	230	13792	282	3455	112	<LOD	15	120	9	6542	94	144	4	802	10	4.31	1.02	
15	300.0	BKM031712-01	tidal creek	C	21-May-12	15	Soil	<LOD	3345	985	2279	285	4250	189	16247	310	1671	77	<LOD	15	88	8	5452	78	155	4	401	6	4.17	1.28
16	310.0	BKM031712-01	tidal creek	C	21-May-12	16	Soil	<LOD	2057	1761	255	4544	188	2332	105	926	59	15	5	35	6	2462	39	144	3	198	4	4.68	0.54	
17	320.0	BKM031712-01	bioturbated and laminated	C	21-May-12	17	Soil	<LOD	1893	1899	249	4703	184	2191	100	1566	69	15	5	39	6	3694	53	70	2	311	5	5.04	0.79	
18	330.0	BKM031712-01	bioturbated and laminated	C	21-May-12	18	Soil	<LOD	1648	2004	239	3499	156	1262	80	682	49	14	4	18	5	2051	32	54	2	152	3	4.49	0.59	
19	340.0	BKM031712-01	bioturbated and laminated	C	21-May-12	19	Soil	<LOD	1751	1068	226	4653	186	973	79	629	48	<LOD	11	20	5	1437	25	51	2	159	3	3.96	0.31	
20	350.0	BKM031712-01	bioturbated and laminated	C	21-May-12	20	Soil	<LOD	1924	2170	254	3818	167	1267	83	752	53	<LOD	12	<LOD	16	2056	33	61	2	111	3	6.77	0.54	
21	360.0	BKM031712-01	bioturbated and laminated	C	21-May-12	21	Soil	<LOD	1709	<LOD	677	3601	172	1738	95	1192	62	<LOD	12	31	6	1637	29	49	2	312	5	3.82	0.45	
22	370.0	BKM031712-01	bioturbated and laminated	C	21-May-12	22	Soil	<LOD	1856	1139	230	4135	177	1199	83	837	52	<LOD	12	23	5	1448	26	53	2	148	3	5.66	0.35	
23	380.0	BKM031712-01	bioturbated and laminated	C	21-May-12	23	Soil	<LOD	1783	918	227	3752	172	1118	82	542	45	<LOD	11	<LOD	15	1142	22	58	2	99	3	5.47	0.30	
24	390.0	BKM031712-01	bioturbated and laminated	C	21-May-12	24	Soil	<LOD	1647	1248	228	4078	173	1274	83	700	49	<LOD	12	19	5	1327	24	56	2	128	3	5.47	0.33	
25	400.0	BKM031712-01	bioturbated and laminated	C	21-May-12	25	Soil	<LOD	1735	1294	241	3273	163	1358	87	981	57	<LOD	13	20	6	1738	30	51	2	136	3	7.21	0.53	
26	410.0	BKM031712-01	bioturbated and laminated	C	21-May-12	26	Soil	<LOD	1773	1508	232	4433	177	1524	87	814	52	<LOD	12	22	5	2002	32	51	2	189	3	4.31	0.45	
31	10.0	BKM031712-02	upper forebeach	B	21-May-12	31	Soil	<LOD	1971	996	233	2352	145	3258	121	451	44	<LOD	11	24	6	1369	25	50	2	112	3	4.03	0.58	
32	20.0	BKM031712-02	upper forebeach	B	21-May-12	32	Soil	<LOD	1867	818	231	4038	182	1761	96	654	48	<LOD	12	<LOD	16	855	18	31	2	97	3	6.74	0.21	
33	30.0	BKM031712-02	upper forebeach	B	21-May-12	33	Soil	<LOD	1800	881	232	1736	132	3596	127	553	43	<LOD	11	33	6	1236	23	41	2	119	3	4.65	0.71	
34	40.0	BKM031712-02	upper forebeach	B	21-May-12	34	Soil	<LOD	1934	1012	238	2938	160	4305	140	415	44	<LOD	12	<LOD	16	1624	29	69	2	64	2	6.48	0.55	
35	50.0	BKM031712-02	peat	D	21-May-12	35	Soil	<LOD	2113	<LOD	676	3576	174	3986	135	183	34	<LOD	11	<LOD	16	1224	23	53	2	30	2	6.10	0.34	
36	60.0	BKM031712-02	peat	D	21-May-12	36	Soil	<LOD	744	5499	255	1324	82	549	51	718	40	<LOD	10	14	5	5529	61	22	2	52	2	13.81	4.18	
37	70.0	BKM031712-02	low marsh	E	21-May-12	37	Soil	<LOD	709	4912	255	2243	106	499	53	1012	50	<LOD	12	26	5	7789	87	32	2	49	2	20.65	3.47	
38	80.0	BKM031712-02	low marsh	E	21-May-12	38	Soil	<LOD	963	4349	296	4421	171	991	75	2108	86	19	6	74	8	18243	224	43	2	89	2	23.69	4.13	
39	90.0	BKM031712-02	low marsh	E	21-May-12	39	Soil	<LOD	849	3531	275	3971	162	780	70	2080	83	27	6	63	8	14775	183	48	2	117	3	17.78	3.72	
40	100.0	BKM031712-02	low marsh	E	21-May-12	40	Soil	<LOD	2243	3318	263	4077	161	574	65	2006	81	24	6	70	8	13246	162	42	2	72	2	27.86	3.25	
41	110.0	BKM031712-02	low marsh	E	21-May-12	41	Soil	<LOD	948	2219	261	4567	182	806	76	2310	90	23	6	49	8	11571	152	55	2	124	3	18.63	2.53	
42	120.0	BKM031712-02	low marsh	E	21-May-12	42	Soil	<LOD	893	2651	258	4476	174	660	69	2248	89	34	6	59	8	16203	202	47	2	86	2	26.14	3.62	
43	130.0	BKM031712-02	high marsh	E	21-May-12	43	Soil	<LOD	895	1982	258	4412	182	815	76	2003	84	26	6	41	7	10519	141	54	2	129	3	15.53	2.38	
44	140.0	BKM031712-02	high marsh	E	21-May-12	44	Soil	<LOD	768	787	221	3423	164	686	71	985	60	<LOD	14	<LOD	18	5270	75	40	2	68	2	14.49	1.54	
45	150.0	BKM031712-02	high marsh	E	21-May-12	45	Soil	<LOD	764	807	220	3537	164	730	72	1442	69	<LOD	14	<LOD	18	4498	64	40	2	132	3	10.92	1.27	
46	160.0	BKM031712-02	high marsh	E	21-May-12	46	Soil	<LOD	1925	701	231																			

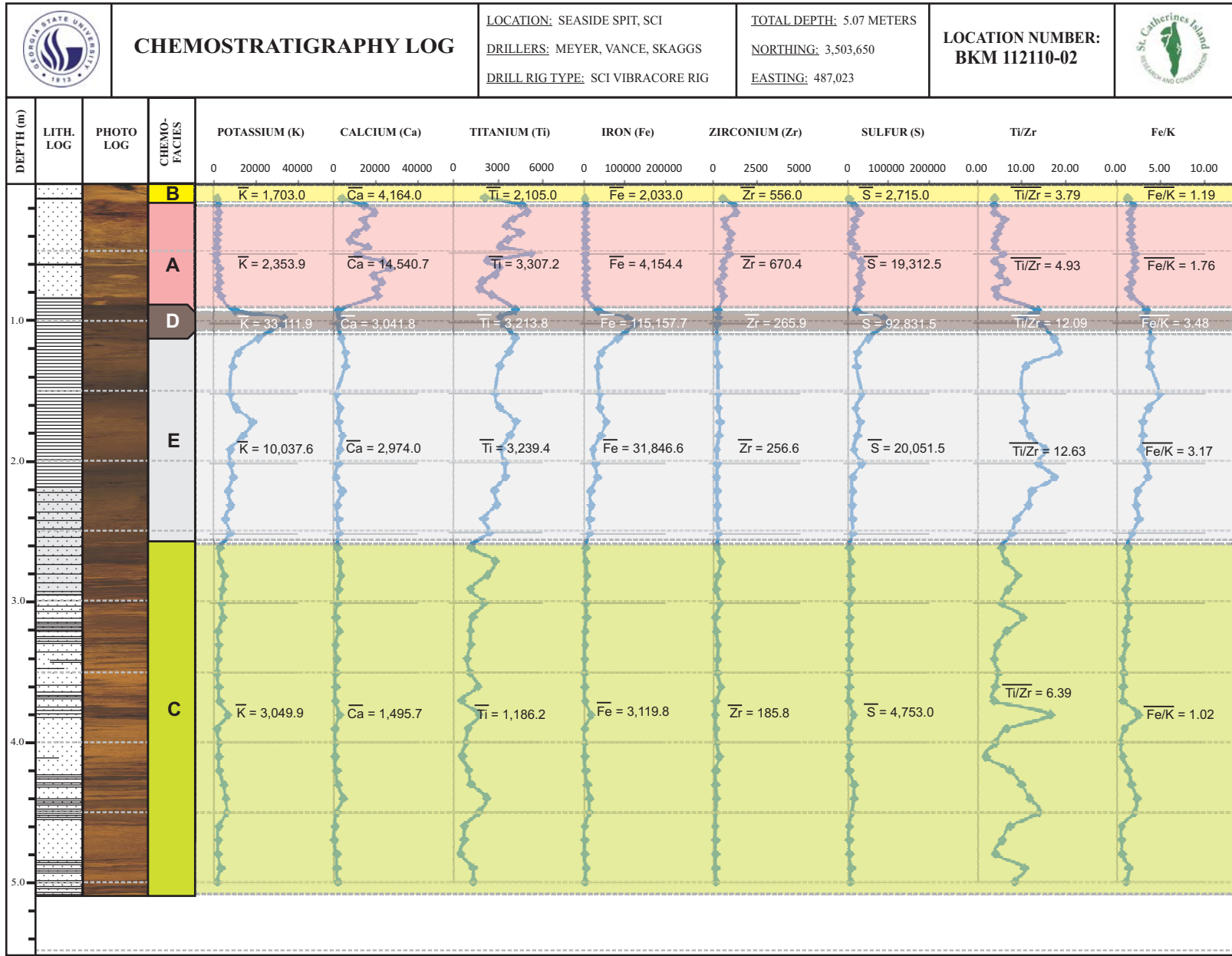
ID	DEPTH	BORING_ID	DEP_ENV	Chemo-facies	Date	Reading	Mode	S	S +/-	Cl	Cl +/-	K	K +/-	Ca	Ca +/-	Ti	Ti +/-	Cr	Cr +/-	Mn	Mn +/-	Fe	Fe +/-	Sr	Sr +/-	Zr	Zr +/-	Ti/Zr	Fe/K
13	350.0	BKM031712-02	bioturbated and laminated	C	23-May-12	13	Soil	<LOD	1801	<LOD	638	1637	130	408	64	701	49	<LOD	12	<LOD	17	2006	34	23	2	77	2	9.10	1.23
14	360.0	BKM031712-02	bioturbated and laminated	C	23-May-12	14	Soil	<LOD	1797	<LOD	673	1280	123	153	153	735	49	<LOD	12	<LOD	16	657	16	15	2	213	4	3.45	0.51
15	370.0	BKM031712-02	bioturbated and laminated	C	23-May-12	15	Soil	7968	1059	<LOD	612	1872	134	4510	141	487	45	<LOD	12	<LOD	17	2106	35	20	2	82	3	5.94	1.13
16	380.0	BKM031712-02	bioturbated and laminated	C	23-May-12	16	Soil	4306	861	<LOD	590	1534	125	1789	93	700	51	<LOD	12	64	7	2889	45	15	2	84	3	8.33	1.88
17	390.0	BKM031712-02	bioturbated and laminated	C	23-May-12	17	Soil	<LOD	1480	<LOD	588	1650	125	175	56	695	47	<LOD	11	<LOD	16	1005	20	22	2	46	2	15.11	0.61
18	400.0	BKM031712-02	bioturbated and laminated	C	23-May-12	18	Soil	3114	859	<LOD	674	4026	183	2782	116	1719	79	29	6	38	7	5676	82	46	2	125	3	13.75	1.41
19	410.0	BKM031712-02	bioturbated and laminated	C	23-May-12	19	Soil	<LOD	3370	1317	375	1033	176	30028	617	868	69	<LOD	16	28	7	1252	29	81	3	142	4	6.11	1.21
20	420.0	BKM031712-02	bioturbated and laminated	C	23-May-12	20	Soil	<LOD	3138	<LOD	797	3238	189	29360	518	1364	71	<LOD	14	34	7	2611	44	108	3	221	4	6.17	0.81
21	430.0	BKM031712-02	bioturbated and laminated	C	23-May-12	21	Soil	<LOD	2106	<LOD	605	2371	143	1888	95	870	55	<LOD	13	18	6	2284	37	33	2	220	4	3.95	0.96
22	440.0	BKM031712-02	bioturbated and laminated	C	23-May-12	22	Soil	<LOD	2188	<LOD	635	4661	192	3378	124	1666	76	<LOD	14	35	6	3746	56	66	2	303	5	5.50	0.80
23	450.0	BKM031712-02	bioturbated and laminated	C	23-May-12	23	Soil	<LOD	2157	<LOD	645	4503	191	2939	118	1498	71	<LOD	13	27	6	2304	38	56	2	221	4	6.78	0.51
24	460.0	BKM031712-02	bioturbated and laminated	C	23-May-12	24	Soil	<LOD	1778	<LOD	577	4188	178	2361	105	1266	63	<LOD	13	27	6	2096	34	59	2	242	4	5.23	0.50
25	470.0	BKM031712-02	bioturbated and laminated	C	23-May-12	25	Soil	<LOD	2046	<LOD	661	4307	189	4029	137	1161	65	15	5	32	6	3863	59	63	2	213	4	5.45	0.90

### Appendix D: Chemostratigraphic Logs







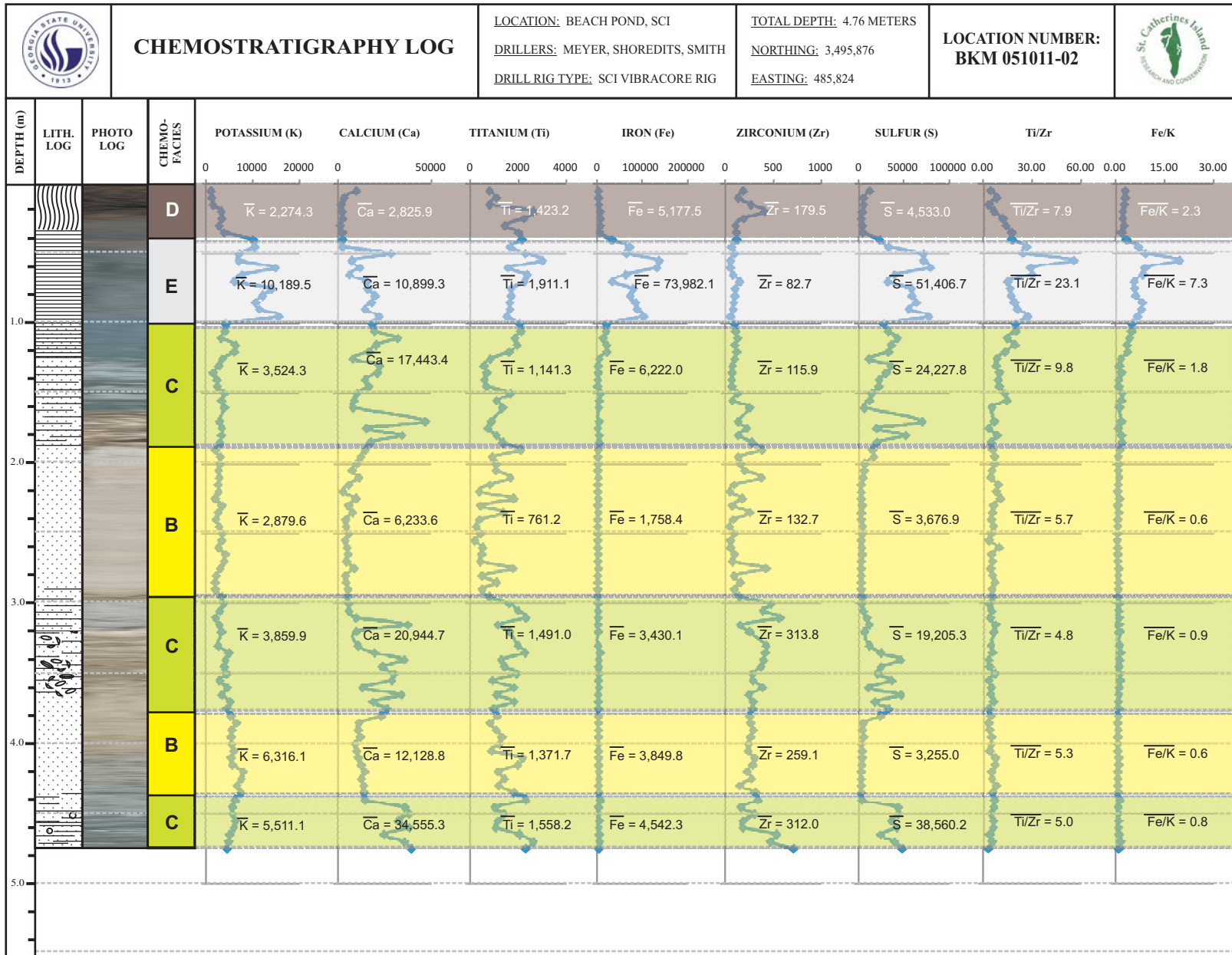




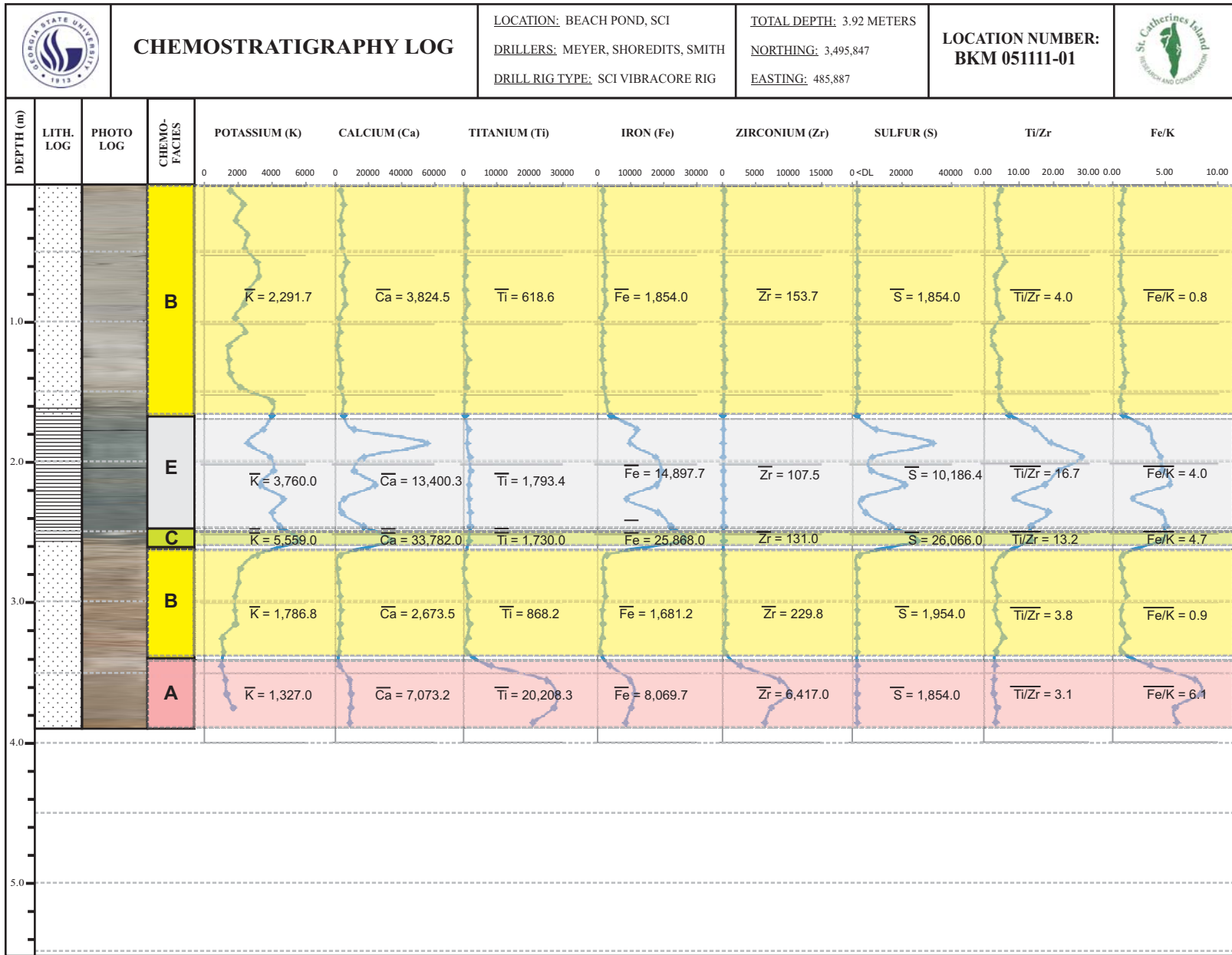














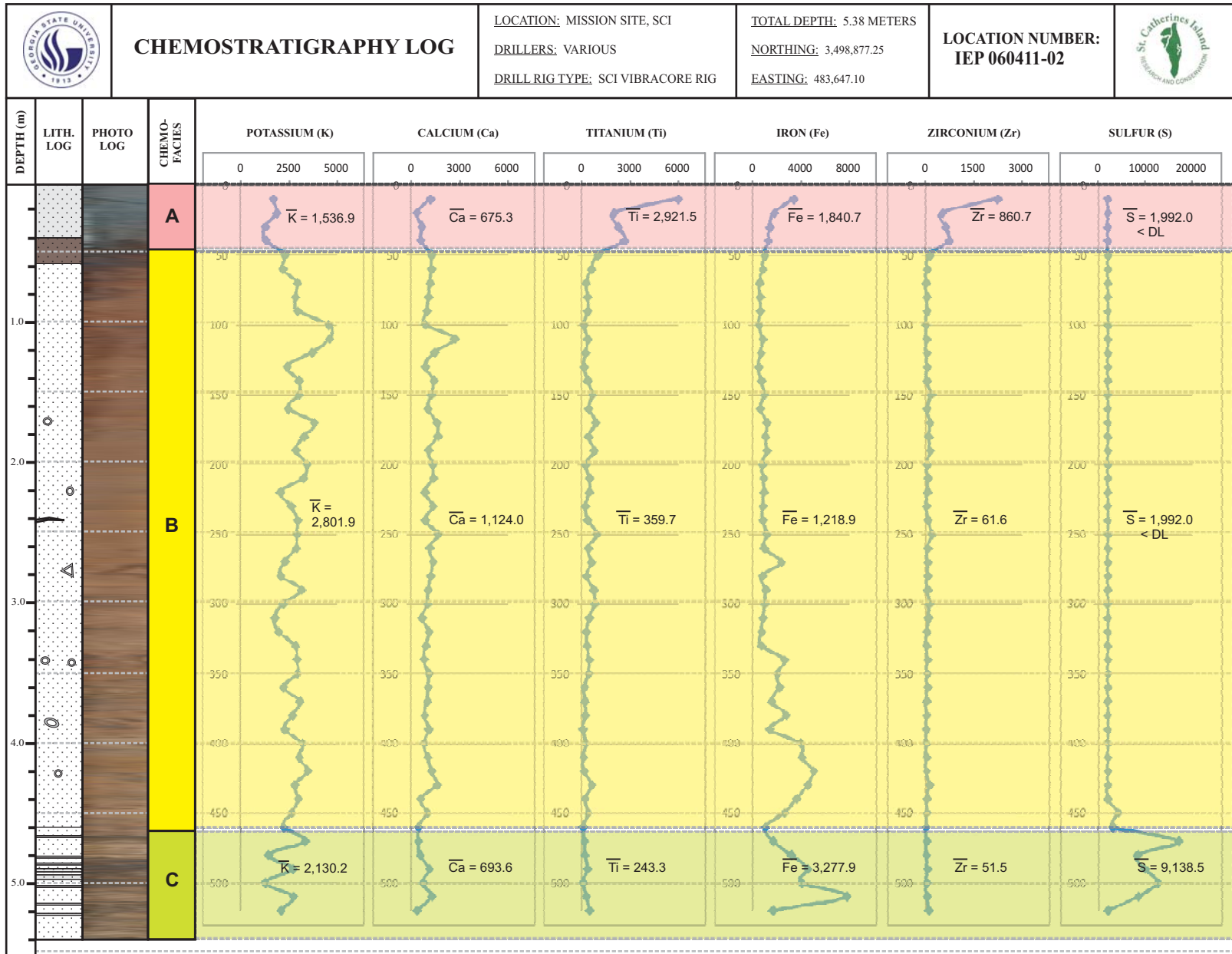






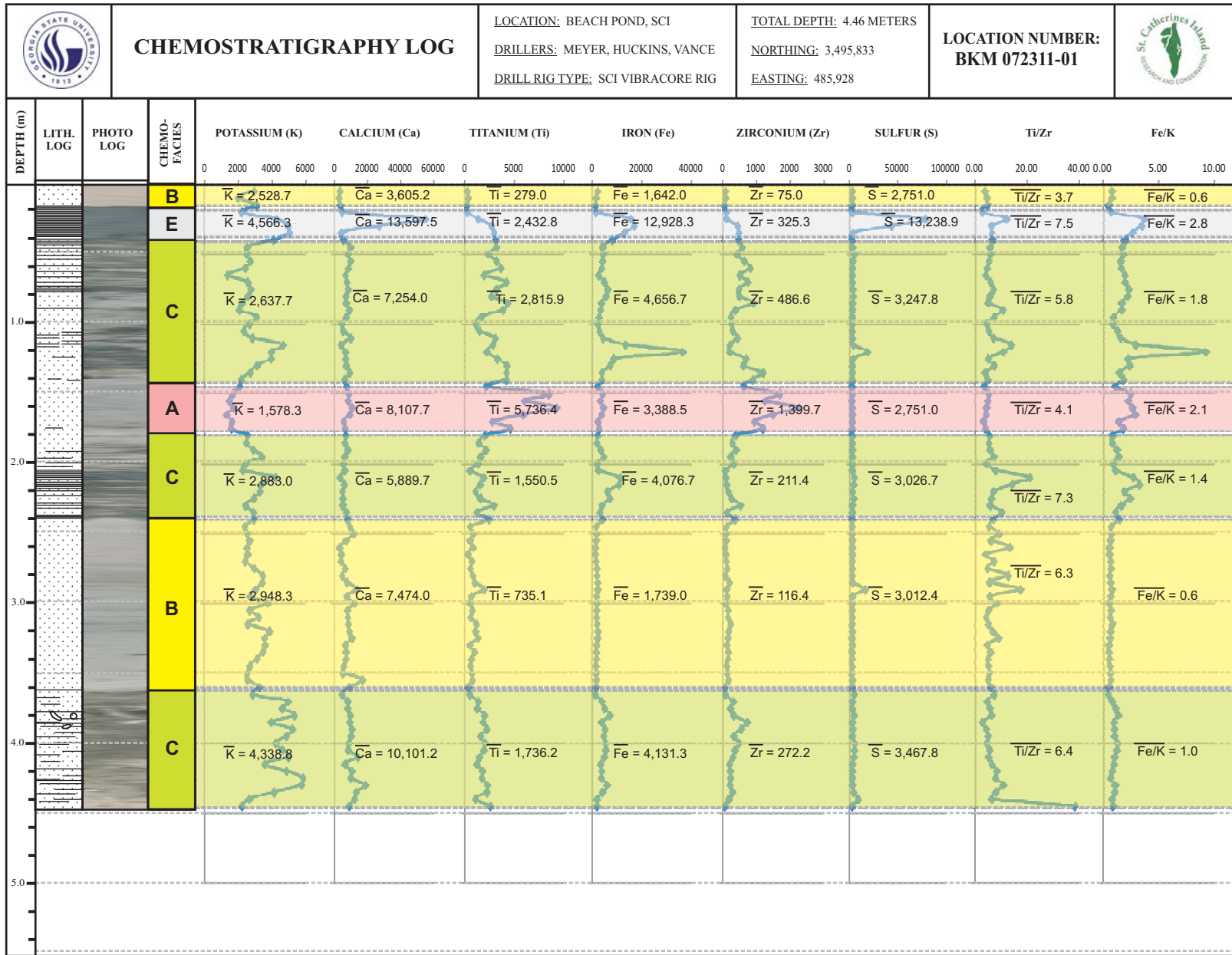




















Appendix E: Shoreline Forecasting Results



**Figure E-1**  
**Shoreline Forecasting Exercise Results**  
**North - Scenario I**















